

*Wiley Series of Practical Construction Guides*

*Wiley Series of Practical Construction Guides*

M.D. MORRIS, P.E., EDITOR

Jacob Feld  
CONSTRUCTION FAILURE

William G. Rapp  
CONSTRUCTION OF STRUCTURAL STEEL BUILDING  
FRAMES, Second Edition

Ben C. Gerwick, Jr.  
CONSTRUCTION OF PRESTRESSED CONCRETE STRUCTURES

S. Peter Volpe  
CONSTRUCTION MANAGEMENT PRACTICE

Robert Crimmins, Reuben Samuels, and Bernard Monahan  
CONSTRUCTION ROCK WORK GUIDE

B. Austin Barry  
CONSTRUCTION MEASUREMENTS

D.A. Day  
CONSTRUCTION EQUIPMENT GUIDE

Gordon A. Fletcher and Vernon A. Smoots  
CONSTRUCTION GUIDE FOR SOILS AND FOUNDATIONS

Walter Podolny, Jr. and John B. Scalzi  
CONSTRUCTION AND DESIGN OF CABLE-STAYED BRIDGES

John P. Cook  
COMPOSITE CONSTRUCTION METHODS

John E. Traister  
CONSTRUCTION ELECTRICAL CONTRACTING

William R. Park  
CONSTRUCTION BIDDING FOR PROFIT

J. Stewart Stein  
CONSTRUCTION GLOSSARY: AN ENCYCLOPEDIA REFERENCE  
AND MANUAL

Howard J. Rosen and Phillip M. Bennett  
CONSTRUCTION MATERIALS EVALUATION AND SELECTION:  
A SYSTEMATIC APPROACH

C.R. Tumblin  
CONSTRUCTION COST ESTIMATES

Harvey V. Debo and Leo Diatnant  
CONSTRUCTION SUPERINTENDENTS JOB GUIDE

Robert M. Koerner and Joseph P. Welsh  
CONSTRUCTION AND GEOTECHNICAL ENGINEERING  
USING SYNTHETIC FABRICS

J. Patrick Powers  
CONSTRUCTION DEWATERING: A GUIDE TO THEORY AND  
PRACTICE

Harold J. Rosen  
CONSTRUCTION SPECIFICATIONS WRITING:  
PRINCIPLES AND PROCEDURES, Second Edition

Walter Podolny, Jr. and Jean M. Müller  
CONSTRUCTION AND DESIGN OF PRESTRESSED  
CONCRETE SEGMENTAL BRIDGES

Ben C. Gerwick, Jr. and John C. Woolery  
CONSTRUCTION AND ENGINEERING MARKETING  
FOR MAJOR PROJECT SERVICES

James E. Clyde  
CONSTRUCTION INSPECTION: A FIELD GUIDE TO PRACTICE.  
Second Edition

Julian R. Panek and John Philip Cook  
CONSTRUCTION SEALANTS AND ADHESIVES, Second Edition

Courtland A. Collier and Don A. Halperin  
CONSTRUCTION FUNDING: WHERE THE MONEY COMES  
FROM, Second Edition

James B. Fullman  
CONSTRUCTION SAFETY, SECURITY, AND LOSS PREVENTION

Harold J. Rosen  
CONSTRUCTION MATERIALS FOR ARCHITECTURE

William B. Kays  
CONSTRUCTION OF LININGS FOR RESERVOIRS, TANKS,  
AND POLLUTION CONTROL FACILITIES, Second Edition

Walter Podolny and John B. Scalzi  
CONSTRUCTION OF CABLE-STAYED BRIDGES, Second Edition

Edward J. Monahan  
CONSTRUCTION OF AND ON COMPACTED FILLS

**CH**  
castiñeira

**castiñeira**

**LIBROS DE TECNICA**

EMPRESA EDITADORA 748/82

C/ Santiago Rusiñol, 4

Teléfono 233 82 01 - 234 16 64

Madrid

14570

*Construction and Design of Cable-Stayed Bridges*  
*Second Edition*

*Walter Podolny, Jr., Ph.D.*

*and*

*John B. Scalzi, Sc.D.*

*A Wiley-Interscience Publication*

JOHN WILEY & SONS

New York Chichester Brisbane Toronto Singapore

## *Series Preface*

The Wiley Series of Practical Construction Guides provides the working constructor with up-to-date information that can help to increase the job profit margin. These guidebooks, which are scaled mainly for practice, but include the necessary theory and design, should aid a construction contractor in approaching work problems with more knowledgeable confidence. The guides should be useful also to engineers, architects, planners, specification writers, project managers, superintendents, materials and equipment manufacturers and, the source of all these callings, instructors and their students.

Construction in the United States alone will reach \$250 billion a year in the early 1980s. In all nations, the business of building will continue to grow at a phenomenal rate, because the population proliferation demands new living, working, and recreational facilities. This construction will have to be more substan-

tial, thus demanding a more professional performance from the contractor. Before science and technology had seriously affected the ideas, job plans, financing, and erection of structures, most contractors developed their know-how by field trial-and-error. Wheels, small and large, were constantly being reinvested in all sectors, because there was no interchange of knowledge. The current complexity of construction, even in more rural areas, has revealed a clear need for more proficient, professional methods and tools in both practice and learning.

Because construction is highly competitive, some practical technology is necessarily proprietary. But most practical day-to-day problems are common to the whole construction industry. These are the subjects for the Wiley Practical Construction Guides.

M. D. MORRIS, P. E.

## *Preface to First Edition*

The reconstruction of bridges in Europe destroyed during World War II provided engineers with the opportunity to apply new technology to an old concept in bridge design, the cable-stayed bridge. The impetus came in the 1950s, in Germany, when many of the bridges spanning the Rhine River were replaced with various types of cable-stayed bridges.

The original concept of the cable-stayed bridge dates back to 1784 but was "shelved" by engineers because of the many collapses of the early bridges. The need to build bridges more economically combined with modern methods of analysis, construction methods, and more reliable construction materials provided bridge engineers with the impetus to develop the present-day cable-stayed bridge.

Economic studies have indicated that the cable-stayed bridge may fill the void between long-span girder bridges and suspension bridges. Some European engineers feel that the cable-stayed bridge may also replace the suspension bridge in many applications. In addition to the potential economies, some engineers believe the cable-stayed bridge adds a new dimension to the aesthetics of bridge design.

Engineers in the United States are planning and designing cable-stayed structures for pedestrian overpasses, highway bridges, and bridges for pipe lines, despite the paucity of design and construction data in the American technical literature.

The objective of this book is to bring together in one volume the current state of the art of design and construction methods for all types of cable-stayed bridges so that engineering faculties, practicing engineers, local, state, and federal bridge engineers can have a ready reference source of construction details and design data.

The book discusses the general principles of cable-stayed bridges, relating to all facets of technical design, construction details and methods, and potential economies.

The book delves into the historical development of the cable-stayed bridge from its first application to the widespread use in Germany after the war and the extensions into other countries around the world. The principal features used in modern bridges receive a thorough description, including geometrical configurations, the types and styles of the towers, and the various types of roadway decks made of different materials and methods.

Illustrations of bridges from various countries are discussed and accompanied by appropriate detail sketches and photographs of the special features of each bridge.

For the uninitiated design and construction engineer, a discussion of the manufacturing and production processes of making structural wires, rope, and strand is presented.

Among the most important aspects of cable-stayed bridges are the types and methods of making the connections between the cables and the deck and/or the towers. A discussion of the various methods is presented to enable construction and design engineers to evaluate the techniques in terms of American practices and, we hope, to improve upon them.

The theory of cables and structures and methods of analysis are contained in other textbooks, and only a discussion of the special considerations for analysis and design are included here. Such items include a summary of the general behavior of cables, a detailed explanation of the use of an equivalent modulus of elasticity for the cable as a substitute member, and a discussion of wind and aerodynamic effects. All of these factors affect the design of the cable-stayed bridge.

Because the methods of fabrication and erection influence design characteristics and construction methods, a discussion of several possible techniques is presented. These discussions may assist engineers in developing their concepts and may lead to more efficient and economical methods.

1001

## *Preface*

When the first edition of this book was published, in 1976, there was only one completed contemporary vehicular cable-stay bridge in the United States, the Sitka Harbor Bridge in Alaska. Shortly thereafter construction began on the Pasco-Kennewick Intercity Bridge in the state of Washington and the design of the Luling Bridge in Louisiana had commenced. Of necessity, the first edition relied very heavily on European experience and illustrated many of the European bridges. As of this writing, there are in the United States approximately 18 cable-stayed bridges either completed, under construction, or in design.

In the last decade there has been considerable evolution in the state of the art of cable-stayed bridges. In this time period we have seen the emergence of multi-cable-stay systems, segmental concrete construc-

tion, composite steel and concrete superstructures, parallel strand stays, and the utilization of the concept of alternate designs. All of this activity has provided the impetus to prepare this second edition. Although much of the data of the first edition has been retained, the second edition has been reorganized and updated to reflect the emerging state of the art and to present, as much as possible, the evolving American experience.

WALTER PODOLNY, JR.  
JOHN B. SCALZI

*Burke, Virginia*  
*Arlington, Virginia*

*March 1986*

*Preface to First Edition*

Most of the material presented in this book is not original, and though individual acknowledgment of the many sources is not possible, full credit is noted wherever the specific source can be identified.

Every effort has been made to eliminate errors, but should errors be found, the authors would appreciate such notification from the readers.

The authors hope that this book will enable other

engineers to design and construct cable-stayed bridges in their own country with economy and confidence.

WALTER PODOLNY, JR.  
JOHN B. SCALZI

*Burke, Virginia*  
*Arlington, Virginia*

*February 1976*



## Contents

|          |   |           |  |
|----------|---|-----------|--|
| <b>1</b> | <b><i>Cable-Stayed Bridges</i></b>                        | <b>1</b>  |  |
| 1.1      | Introduction, 1   |           |  |
| 1.2      | Historical Evolution, 3                                   |           |  |
| 1.3      | Contemporary Implementation, 8                            |           |  |
| 1.4      | Early Applications in the United States, 8                |           |  |
| 1.5      | Recent Applications in the United States, 10              |           |  |
| 1.6      | Projects in Design or Under Consideration, 18             |           |  |
|          | References, 20  |           |  |
| <b>2</b> | <b><i>Bridge Component Configurations</i></b>             | <b>21</b> |  |
| 2.1      | General Description, 21                                   |           |  |
| 2.2      | Transverse Cable Arrangement, 21                          |           |  |
| 2.2.1    | Single-Plane System, 22                                   |           |  |
| 2.2.2    | Double-Plane System, 25                                   |           |  |
| 2.2.3    | Triple-Plane System, 25                                   |           |  |
| 2.3      | Longitudinal Cable Arrangements, 25                       |           |  |
| 2.4      | Towers, 27  |           |  |
| 2.5      | Cable System Summary, 28                                  |           |  |
| 2.6      | Superstructure Types, 31                                  |           |  |
|          | References, 34  |           |  |
| <b>3</b> | <b><i>Economic Evaluation</i></b>                         | <b>36</b> |  |
| 3.1      | Introduction, 36  |           |  |
| 3.2      | Bidding Procedures, 36                                    |           |  |
| 3.2.1    | Single Design, 37   |           |  |
| 3.2.2    | Design and Build, 37                                      |           |  |
| 3.2.3    | Value Engineering, 37                                     |           |  |
| 3.2.4    | Alternate Designs, 38                                     |           |  |
| 3.2.5    | Summary Remarks on Bidding Procedures, 39                 |           |  |
| 3.3      | Economic Studies, 40                                      |           |  |
| 3.4      | Economic Comparisons in the United States, 44             |           |  |
| 3.4.1    | Sitka Harbor Bridge, 44                                   |           |  |
| 3.4.2    | Luling Bridge, 46   |           |  |
| 3.4.3    | Pasco-Kennewick Bridge, 46                                |           |  |
| 3.5      | Results of Alternate Bidding in the United States, 49     |           |  |
|          | References, 50  |           |  |
| <b>4</b> | <b><i>Concrete Superstructures</i></b>                    | <b>51</b> |  |
| 4.1      | Introduction, 51  |           |  |
| 4.1.1    | Historical Review, 51                                     |           |  |
| 4.1.2    | Advantages of Concrete Cable-Stayed Bridges, 54           |           |  |
| 4.1.3    | Structural Style and Arrangement, 54                      |           |  |
| 4.2      | Lake Maracaibo Bridge, Venezuela, 57                      |           |  |
| 4.3      | Wadi Kuf Bridge, Libya, 59                                |           |  |
| 4.4      | Chaco/Corrientes Bridge, Argentina, 59                    |           |  |
| 4.5      | Mainbrücke, West Germany, 60                              |           |  |
| 4.6      | Tiel Bridge, The Netherlands, 61                          |           |  |
| 4.7      | Pasco-Kennewick Bridge, U.S.A., 64                        |           |  |
| 4.8      | Brotonne Bridge, France, 66                               |           |  |
| 4.9      | Danube Canal Bridge, Austria, 70                          |           |  |
| 4.10     | Sunshine Skyway Bridge, U.S.A., 72                        |           |  |
| 4.11     | Neches River Bridge, U.S.A., 74                           |           |  |
| 4.12     | Barrios de Luna Bridge, Spain, 75                         |           |  |
| 4.13     | Notable Examples of Concepts, 77                          |           |  |
| 4.13.1   | Danish Great Belt Bridge Competition, 77                  |           |  |
| 4.13.2   | Proposed Dame Point Bridge, U.S.A., 78                    |           |  |
| 4.13.3   | Proposed Ruck-A-Chucky Bridge, U.S.A., 79                 |           |  |
| 4.13.4   | James River and Proposed Cooper River Bridges, U.S.A., 82 |           |  |
|          | References, 84  |           |  |

**5 Steel Superstructures**

- 5.1 Introduction, 85
- 5.2 Strömsund Bridge, Sweden, 85
- 5.3 Theodor Heuss Bridge, West Germany, 86
- 5.4 Severin Bridge, West Germany, 88
- 5.5 Norderelbe Bridge, West Germany, 89
- 5.6 Rhine River Bridge at Maxau, West Germany, 89
- 5.7 Wye River Bridge, Great Britain, 90
- 5.8 Rhine River Bridge at Rees, West Germany, 92
- 5.9 Friedrich-Ebert Bridge, West Germany, 93
- 5.10 Elevated Highway Bridge at Ludwigshafen, West Germany, 93
- 5.11 Onomichi Bridge, Japan, 94
- 5.12 Duisburg-Neuenkamp Bridge, West Germany, 94
- 5.13 Kniebrücke Bridge, West Germany, 96
- 5.14 Papineau-Leblanc Bridge, Canada, 98
- 5.15 Toyosato-Ohashi Bridge, Japan, 99
- 5.16 Arakawa River Bridge, Japan, 100
- 5.17 Erskine Bridge, Scotland, 100
- 5.18 Batman Bridge, Australia, 101
- 5.19 Bridge over the Danube at Bratislava, Czechoslovakia, 102
- 5.20 Nordbrücke Mannheim-Ludwigshafen Bridge, West Germany, 103
- 5.21 Köhlbrand High-Level Bridge, West Germany, 105
- 5.22 Oberkassel Bridge, West Germany, 105
- 5.23 Zarate-Brazo Largo Bridges, Argentina, 107
- 5.24 Sacramento River Bridge, U.S.A., 108
- 5.25 Luling Bridge, U.S.A., 113
- 5.26 West Gate Bridge, Australia, 116
- 5.27 Saint Nazaire Bridge, France, 117

**6 Composite Superstructures**

- 6.1 Introduction, 119
- 6.2 Sitka Harbor Bridge, U.S.A., 119

- 85 6.3 East Huntington Bridge, U.S.A., 122
- 6.4 Sunshine Skyway Alternate, U.S.A., 122
- 6.5 Weirton-Steubenville Bridge, U.S.A., 124
- 6.6 Quincy Bridge, U.S.A., 125
- 6.7 James River Bridge Alternate, U.S.A., 128
- References, 128

**7 Pedestrian Bridges**

129

- 7.1 Introduction, 129
- 7.2 Footbridge at the West German Pavilion, Brussels Exhibition, 1958, 129
- 7.3 Volta-Steg Bridge at Stuttgart-Münster, 130
- 7.4 Bridge over the Schillerstrasse, Stuttgart, 131
- 7.5 The Glacischaussee Bridge, Hamburg, 131
- 7.6 Lodemann Bridge, Hanover, West Germany, 132
- 7.7 Raxstrasse Footbridge, Austria, 132
- 7.8 Pont de la Bourse, Le Havre, France, 133
- 7.9 Canal du Centre, Obourg, Belgium, 134
- 7.10 River Barwon Footbridge, Australia, 135
- 7.11 Mount Street Footbridge, Australia, 136
- 7.12 Menomonee Falls Pedestrian Bridge, U.S.A., 136
- 7.13 Prince's Island Pedestrian Bridge, Canada, 139
- 7.14 Footbridge Liebrüti, Kaiseraugst, Switzerland, 139
- 7.15 Horikoshi Bridge, Hachioji City, Japan, 140
- 7.16 Footbridge over Motorway M-30, Madrid, Spain, 141
- References, 142

**8 Erection and Fabrication**

143

119

- 8.1 Introduction, 143
- 8.2 Methods of Erection, 143
- 8.3 Staging Method, 144

|          |   |           |  |            |
|----------|---|-----------|--|------------|
| 8.3.1    | Rhine River Bridge at Maxau, West Germany, 144        | 9.6       | Parallel Bars, 197   |            |
| 8.3.2    | Toyosato-Ohhashi Bridge, Japan, 145                   | 9.7       | Parallel Wire, 197   |            |
| 8.4      | Push-Out Method, 146                                  | 9.8       | Parallel Strand, 198   |            |
| 8.4.1    | Jülicher Strasse Bridge, West Germany, 146            | 9.9       | Comparison of Various Types of Stays, 198                      |            |
| 8.4.2    | Paris-Masséna Bridge, France, 149                     | 9.10      | Corrosion Protection, 198                                      |            |
| 8.4.3    | Oberkassel Bridge, West Germany, 152                  | 9.11      | Handling, 199  |            |
| 8.5      | Cantilever Method, 156                                |           | References, 200  |            |
| 8.5.1    | Strömsund Bridge, Sweden, 156                         | <b>10</b> | <b><i>Cable-Stay Anchorages and Connections</i></b>            | <b>201</b> |
| 8.5.2    | Papineau-Leblanc Bridge, Canada, 158                  | 10.1      | Introduction, 201  |            |
| 8.5.3    | Severin Bridge, West Germany, 159                     | 10.2      | General Considerations, 201                                    |            |
| 8.5.4    | Batman Bridge, Australia, 163                         | 10.3      | End Anchorages, 202  |            |
| 8.5.5    | Kniebrücke Bridge, West Germany, 165                  | 10.3.1    | Swaged and Zinc-Poured Anchorages, 203                         |            |
| 8.5.6    | Lake Maracaibo Bridge, Venezuela, 169                 | 10.3.2    | HiAm Anchorages, 205   |            |
| 8.5.7    | Chaco/Corrientes Bridge, Argentina, 174               | 10.3.3    | VSL Anchorages, 206  |            |
| 8.5.8    | Pasco-Kennewick Intercity Bridge, U.S.A., 176         | 10.3.4    | Stronghold Anchorages, 209                                     |            |
| 8.5.9    | East Huntington Bridge, U.S.A., 180                   | 10.3.5    | Frcyssinct Anchorages, 213                                     |            |
| 8.6      | Fabrication, 184                                      | 10.3.6    | Considerations in the Selection of Stay Anchorage Systems, 214 |            |
| 8.6.1    | General Structural Steel Fabrication and Welding, 185 | 10.4      | Saddles, 214   |            |
| 8.6.2    | Structural Steel Superstructures, 186                 | 10.5      | Connection of Cable Stays to Pylon, 215                        |            |
| 8.6.3    | Structural Steel Pylons, 188                          | 10.6      | Connection of Cable Stays to Girder, 222                       |            |
| 8.6.4    | Concrete Fabrication, 189                             |           | References, 226  |            |
|          | References, 189                                       | <b>11</b> | <b><i>Structural Behavior of Cables</i></b>                    | <b>227</b> |
| <b>9</b> | <b><i>Cable Data</i></b>                              | 11.1      | Introduction, 227  |            |
| 9.1      | Introduction, 191                                     | 11.2      | Catenary Curve, 227  |            |
| 9.2      | Development of Cable Applications, 191                | 11.3      | Parabolic Curve, 228   |            |
| 9.3      | Manufacturing Process, 193                            | 11.4      | Catenary versus Parabola, 228                                  |            |
| 9.4      | Structural Strand and Rope, 194                       | 11.5      | Assumptions for Analysis, 230                                  |            |
| 9.4.1    | Prestretching, 195                                    | 11.6      | General Cable Theorem, 231                                     |            |
| 9.4.2    | Modulus of Elasticity, 195                            | 11.7      | Cable with Inclined Chord, 232                                 |            |
| 9.4.3    | Strand and Rope Compared, 197                         | 11.8      | Equivalent Modulus of Elasticity, 234                          |            |
| 9.5      | Locked-Coil Strand, 197                               |           | References, 236  |            |
|          |   | <b>12</b> | <b><i>Design Considerations and Analysis</i></b>               | <b>237</b> |
|          |   | 12.1      | Introduction, 237  |            |
|          |   | 12.2      | Multicable-Stay Systems, 238                                   |            |
|          |   | 12.3      | Longitudinal Stay Arrangement, 238                             |            |
|          |   | 12.4      | Transverse Stay Arrangement, 239                               |            |

- 12.5 Span Proportions, 239
  - 12.6 Proportion of Pylon Height to Center Span, 240
  - 12.7 Loads and Forces, 241
  - 12.8 Structure Anchorage, 242
  - 12.9 Multispan Stayed Girder Bridges, 245
  - 12.10 Preliminary Manual Calculations, 249
  - 12.11 Methods of Analysis, 252
  - 12.12 Stiffness Parameter, 252
  - 12.13 Mixed Method of Analysis—Single Plane, 255
    - 12.13.1 Cable-Stayed Bridge Behavior, 255
    - 12.13.2 Fundamental Analysis, 256
    - 12.13.3 Multicable Structure—Radiating System, 259
    - 12.13.4 Multicable Structure—Harp System, 259
    - 12.13.5 Axial Force in the Girder, 261
    - 12.13.6 Fixed Base Tower, 261
    - 12.13.7 Multitower Continuous Girder Cable-Stayed Bridge, 262
    - 12.13.8 Cable Attached to Rigid Supports, 262
  - 12.14 Mixed Method of Analysis—Double Plane, 263
    - 12.14.1 Structural Behavior, 263
    - 12.14.2 Basic Analysis, 264
    - 12.14.3 Effects of Other Actions, 266
    - 12.14.4 Double-Plane Structure with an A-Frame Tower, 267
    - 12.14.5 Double-Plane Structure with a Portal Frame, 267
    - 12.14.6 Multitower Continuous Girder—Double-Plane Configuration, 268
  - 12.15 Summary of the Mixed Method, 269
  - 12.16 Nonlinearity, 269
  - 12.17 Influence Lines, 269
  - 12.18 Live Load Stresses, 281
  - 12.19 Other Methods of Analysis, 282
  - References, 283
- 
- 13 Design Considerations—Wind Effects 284**
    - 13.1 Introduction, 284
      - 13.1.1 Description of Bridge Failures, 284
      - 13.1.2 Adverse Vibrations in Other Bridges, 288
      - 13.1.3 Lessons from History, 289
    - 13.2 Wind Environment, 289
      - 13.2.1 The Natural Wind, 290
      - 13.2.2 Design Wind Velocity, 291
      - 13.2.3 Funnclling Factor, 291
      - 13.2.4 Design Wind Vclocity at Structure Altitude, 291
      - 13.2.5 Effect of Structure Length on Design Wind Velocity, 291
      - 13.2.6 Effect of Structure Height on Design Wind Velocity, 292
      - 13.2.7 Wind Force and Angle of Attack, 293
    - 13.3 Wind Effects—Static, 294
      - 13.3.1 Lateral Buckling, 295
      - 13.3.2 Torsional Divergence, 295
      - 13.3.3 Turbulence Effects, 297
    - 13.4 Vibration, 297
      - 13.4.1 Free Vibrations, 298
      - 13.4.2 Forced Vibrations, 298
      - 13.4.3 Self-Excited Vibrations, 298
      - 13.4.4 Damping, 299
    - 13.5 Wind Effects—Aerodynamic, 300
      - 13.5.1 Vortex Shedding, 300
      - 13.5.2 Flutter, 302
      - 13.5.3 Turbulence, 302
    - 13.6 Wind Tunnel Testing, 303
      - 13.6.1 Boundary Layer Full Model Test, 303
      - 13.6.2 Sectional Model l'est, 303
      - 13.6.3 Dynamic Similarity, 303
      - 13.6.4 Aerodynamic Similarity, 304
    - 13.7 Stability of Staycd-Girder Bridges, 304
    - 13.8 Deck Stability, 305
    - 13.9 Stability During Erection, 306
    - 13.10 Wind Tunnel Investigations, 307

|         |  |                   |  |            |
|---------|--|-------------------|--|------------|
| 13.10.1 | Long's Creek Bridge,<br>Canada, 307                    | 13.10.6           | Luling Bridge, U.S.A ,<br>313            |            |
| 13.10.2 | Kniebrücke, West<br>Germany, 308                       | 13.11             | Motion Tolerance, 313<br>References, 315 |            |
| 13.10.3 | Proposed New Burrard<br>Inlet Crossing, Canada,<br>308 |                   |  |            |
| 13.10.4 | Pasco-Kennewick<br>Intercity Bridge,<br>U.S.A., 309    | <i>Appendix A</i> | <i>Chronological Bibliography</i>        | <i>318</i> |
| 13.10.5 | The Narrows Bridge,<br>Canada, 310                     | <i>Appendix B</i> | <i>Author Vitae</i>                      | <i>327</i> |
|         |  |                   | <i>Index of Bridges</i>                  | <i>329</i> |
|         |  |                   | <i>Index of Personal Names</i>           | <i>331</i> |
|         |  |                   | <i>Index of Firms and Organizations</i>  | <i>333</i> |
|         |  |                   | <i>Index of Subjects</i>                 | <i>335</i> |

# 1

## *Cable-Stayed Bridges*

|     |   |    |
|-----|---|----|
| 1.1 | INTRODUCTION                              | 1  |
| 1.2 | HISTORICAL EVOLUTION                      | 3  |
| 1.3 | CONTEMPORARY IMPLEMENTATION               | 8  |
| 1.4 | EARLY APPLICATIONS IN THE UNITED STATES   | 8  |
| 1.5 | RECENT APPLICATIONS IN THE UNITED STATES  | 10 |
| 1.6 | PROJECTS IN DESIGN OR UNDER CONSIDERATION | 18 |
|     | REFERENCES                                | 20 |

### *1.1 Introduction*

The cable-stayed bridge is an innovative structure that is both old and new in concept. It is old in the sense that it has been evolving over a period of approximately 400 years and new in that its modern-day implementation began in the 1950s in Germany and started to seriously attract the attention of bridge engineers in the United States only as recently as 1970.

The selection of the proper type of bridge for a particular site with a given set of conditions must take into account many parameters. The process of evaluating these parameters for various types of bridges under consideration is certainly more of an art than a science. The process of choosing the type or types of bridges for a particular site could very well be the subject of a book in itself. This book provides the information necessary for the reader to intelligently assess and evaluate cable-stayed bridges with other types.

Bridges that depend on high-strength steel cables as major structural elements may be classified as suspension bridges, specifically as cable-suspended or cable-stayed bridges—the fundamental difference is the manner in which the bridge deck is supported by the cables.

In the cable-suspended bridges the deck is supported at relatively short intervals by vertical hangers, which are in turn suspended from a main cable, Fig. 1.1(a). The main cables are relatively flexible and thus

take a profile shape that is a function of the magnitude and position of loading. A typical example is the classical suspension bridge. No one will deny the graceful beauty of the silhouette of cables and deck against the sky. In this type of structure even the uninitiated can relate to form following function

Inclined cables of the cable-stayed bridge, Fig. 1.1(b), support the bridge deck directly with relatively taut cables which, compared to the classical suspension bridge, provide relatively inflexible supports at several points along the span. This type of structure also easily relates the concept of form following function and presents an equally graceful and aesthetically pleasing appearance.

Having defined or classified a cable-stayed bridge, the obvious next question is why should a cable-stayed bridge be considered? To answer this question, the Luling Bridge (Hale Boggs Memorial Bridge), which crosses the Mississippi River in the state of Louisiana, will be cited as an example. For the central, high-level bridge over the navigation channel, the superstructure system selected by the Louisiana Department of Highways incorporates cable-stayed trapezoidal box girders of structural steel. Early in the design phase of the project the system included the main span of 1235 ft (376 m) and two anchor spans of 495 ft (151 m) each. Subsequently, it was found desirable to extend the deck of this structure past the anchor piers by incorporating a 260-ft (79-m) approach span at either end of the main bridge. This was done principally with the idea of enhancing the aesthetics of the highly exposed central structure. An additional design revision moved the main expansion joints required for the roadway away from the anchorage points of the principal back stays. Consequently, final design called for a five-span continuous girder with the three central spans supported by cable stays.

Why was a cable-stayed system selected for this

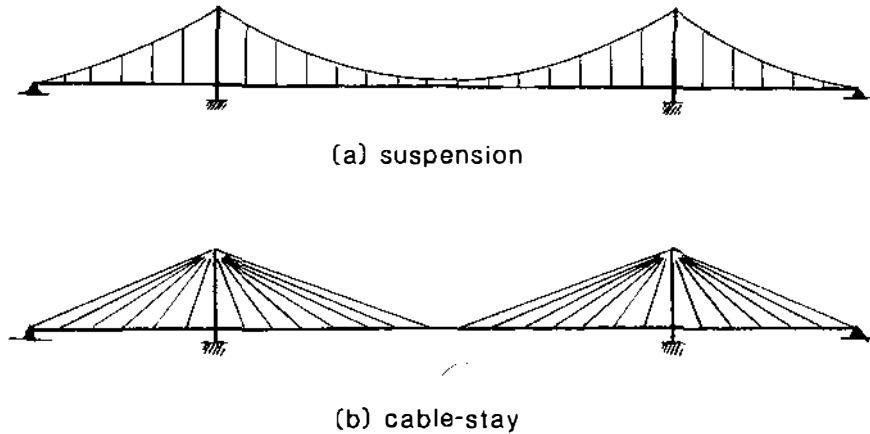


FIGURE 1.1 Cable-suspended bridge systems, (a) suspension and (b) cable-stayed.

crossing? Certainly there are other structural systems suitable for the given span range that are more familiar to builders of bridges across the Mississippi River. Foremost in this respect is the venerable cantilever truss, so very common on the Mississippi River below St. Louis. However, the cantilever truss and its variations require large and thus heavy amounts of steel for spans over 1000 ft (305 m) in length. Moreover, maintenance and inspection costs of long-span truss bridges are high because of their numerous structural components, many of which are not easily accessible.

In contrast, a cable-stayed system employing deck girders for stiffening of the bridge floor offers immediate advantages in terms of weight alone. The reason for this advantage is clearly evident in Fig. 1.2.<sup>1</sup> It shows a comparison of bending moments in a five-span unstayed design and a cable-stayed girder structure selected for the Luling Bridge. The ratio of these moments is close to 1/10 in favor of the stayed system. Moreover, these moments can be controlled to make them more uniformly distributed along the girder length. In the process, material utilization is more ef-

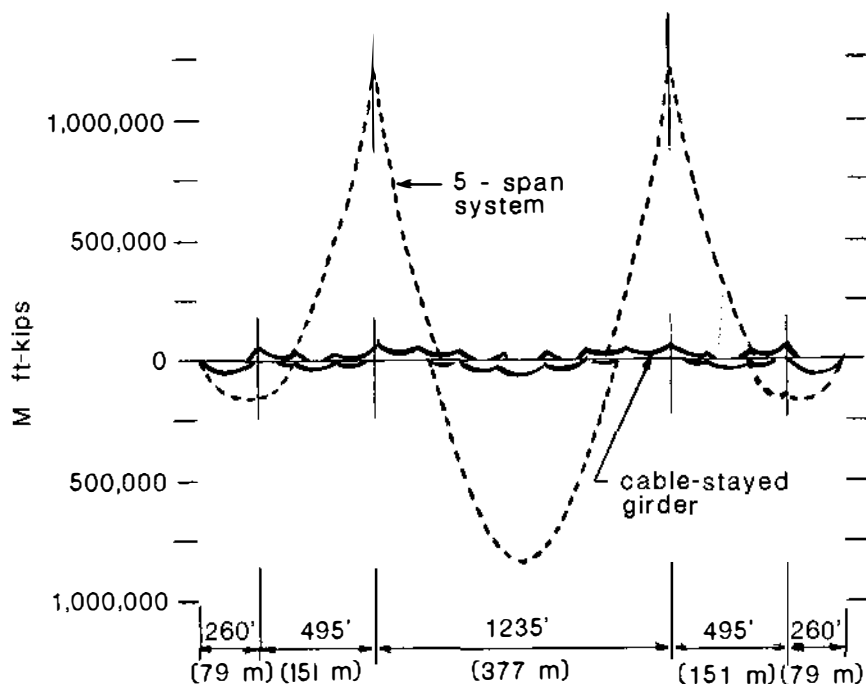


FIGURE 1.2 Moment diagram comparison, cable-stayed versus five-span system. (Courtesy of Stanley Jarosz, Frankland & Lienhard.)

ficant, even with a very low depth-to-span ratio of 1/90 as in the case of the Luling Bridge. This factor, along with the anticipated low cost of maintenance compared with trusses, had a significant effect on the selection of a cable-stayed system.

## 1.2 Historical Evolution

The concept and practical application of the cable-stayed bridge date back to the 1600s, when a Venetian engineer named Verantius built a bridge with several diagonal chain stays.<sup>2,3</sup> The concept was attractive to engineers and builders for many centuries, and experimentation and development continued until its modern-day version evolved in 1950 in Germany.

The early stayed bridges used chains or bars for the stays. The advent of the various types of structural cables, with their inherent high carrying capacity and ease of installation, led engineers and contractors to replace the chains and bars. As a result, the more specific descriptive term, "cable-stayed bridges," entered the literature. However, cable-stayed today is used in a generic sense. The stays are not necessarily limited to a cold-drawn wire product. There are a few modern cable-stayed bridges that actually utilize a high-strength bar for the composition of the stays.

Although the concept of a bridge partially suspended by inclined stays dates back to seventeenth-century Venice, the concept of a bridge suspended only by inclined stays is credited to C. J. Löscher, a carpenter from Fribourg, Switzerland who built a completely timber bridge including stays and tower in

1784, Fig. 1.3, with a span of 105 ft (32 m). Apparently the stayed-bridge concept was not used again until 1817, when two British engineers, Redpath and Brown, built the King's Meadow footbridge, which had an approximate span of 110 ft (33.6 m), using sloping wire cable-stay suspension members attached to a cast iron tower.

Communication of technical information among engineers must have been very good following the English design because in 1821 the French architect, Poyet, suggested a bridge using steel bar stays suspended from high towers, Fig. 1.4.

The stayed bridge might have become a conventional form of construction had it not been for the bad publicity that followed the collapse of two bridges. One was the 259-ft (79-m) pedestrian bridge crossing the Tweed River near Dryburgh-Abbey, England, which collapsed in 1818 when wind oscillation caused the chain stays to break at the joints.<sup>4</sup> The other bridge credited with delaying the use of cable-stayed bridges collapsed in 1824; it had a 256-ft (78-m) span and crossed the Saale River near Nienburg West Germany.<sup>5</sup>

We can only assume that the technical knowledge of analysis and behavior of materials was insufficient for the successful design and construction of these ill-fated bridges. The inclined members were forged tie bars or chain links made of looped wires. The reason for the failure of the Nienburg bridge was not reported, although the technical literature of the period attributed the collapse to the overloading. Apparently, a crowd of people who gathered on the bridge structure to watch a river festival or boat race caused the col-

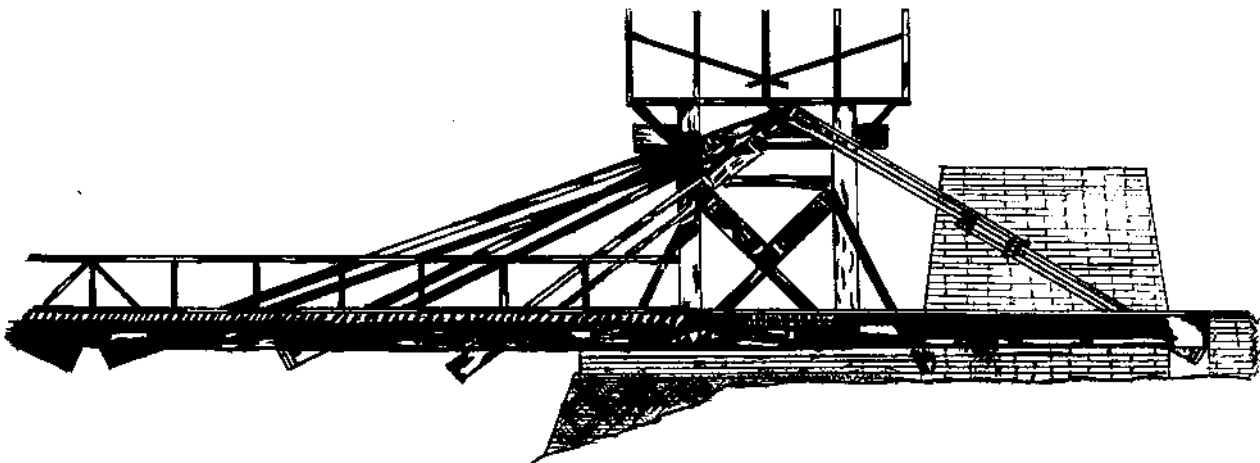


FIGURE 1.3 Löscher-type timber bridge. (Courtesy of the British Constructional Steelwork Association, Ltd.)



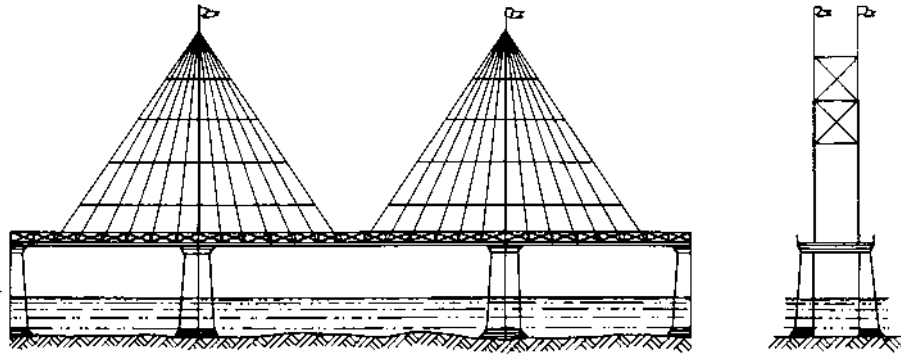


FIGURE 1.4 Poyet-type bridge. (Courtesy of the British Constructional Steelwork Association, Ltd.)

lapse, but unfortunately the exact reason was not recorded. The famous French engineer, Navier, discussed these failures with his colleagues, and his adverse comments are assumed to have condemned the stay-bridge concept to relative obscurity. Whatever the reason, engineers turned to the suspension bridge, which was also emerging, as the preferred type of bridge for river crossings.

The principle of using stays to support a bridge superstructure did not die completely in the minds of engineers. John Roebling incorporated the concept in

his suspension bridges, such as the one near Niagara Falls, Fig. 1.5; the Old St. Clair Bridge in Pittsburgh, Fig. 1.6; the Cincinnati Bridge across the Ohio River, Fig. 1.7; and the Brooklyn Bridge in New York, Fig. 1.8. The stays were used in addition to the vertical hangers to support the bridge superstructure. Observations of performance indicated that the stays and hangers were not efficient partners. Consequently, although the stays were comforting safety measures in the early bridges, in the later developments of the suspension bridge the stays were omitted. Evidence of the

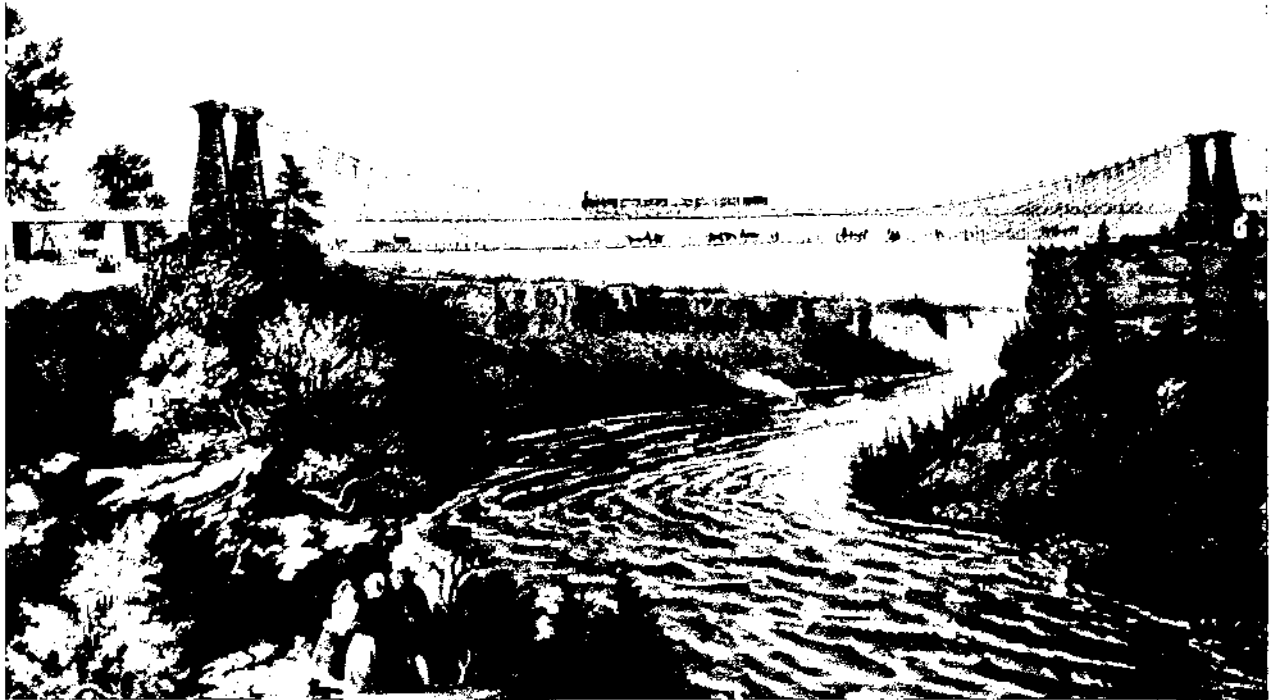


FIGURE 1.5 Niagara Falls Bridge.

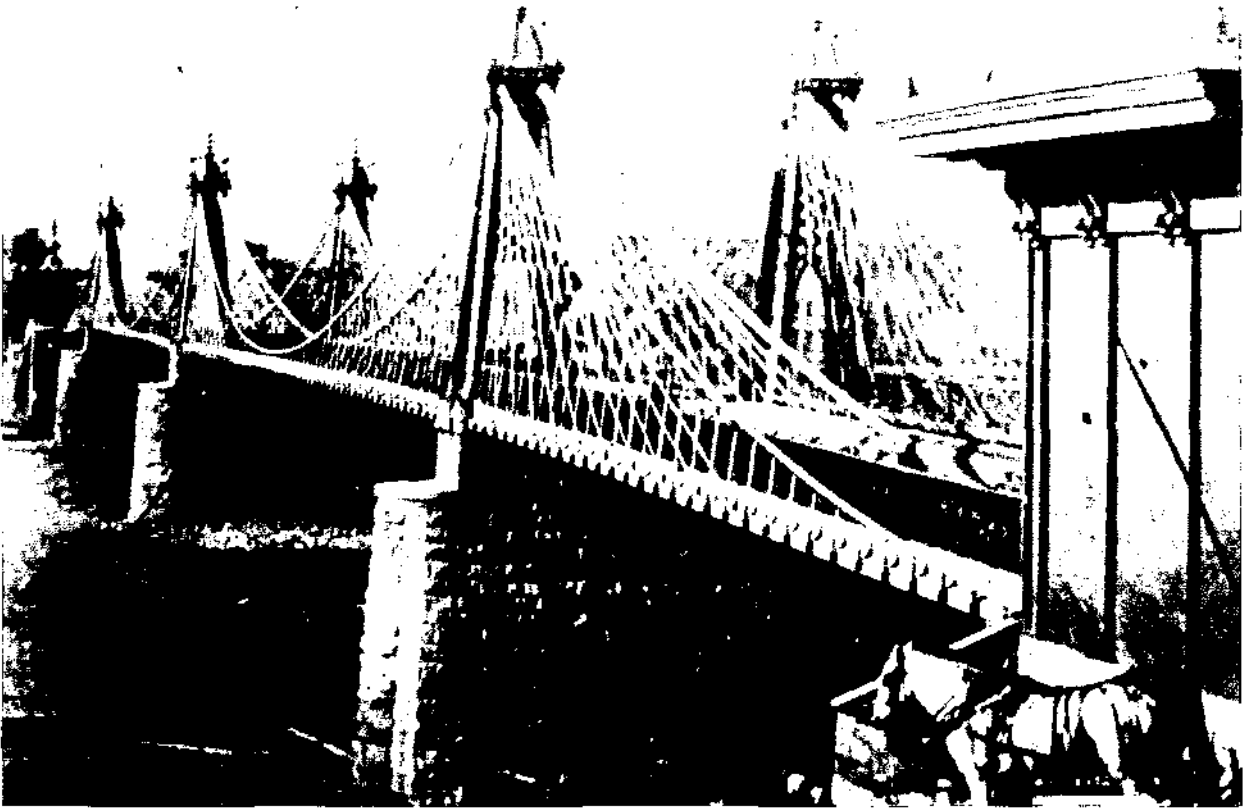


FIGURE 1.6 Old St. Clair Bridge, Pittsburgh, Pennsylvania.

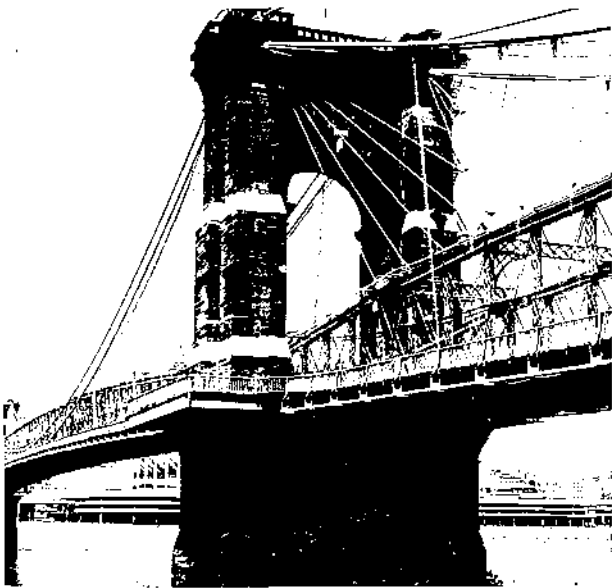
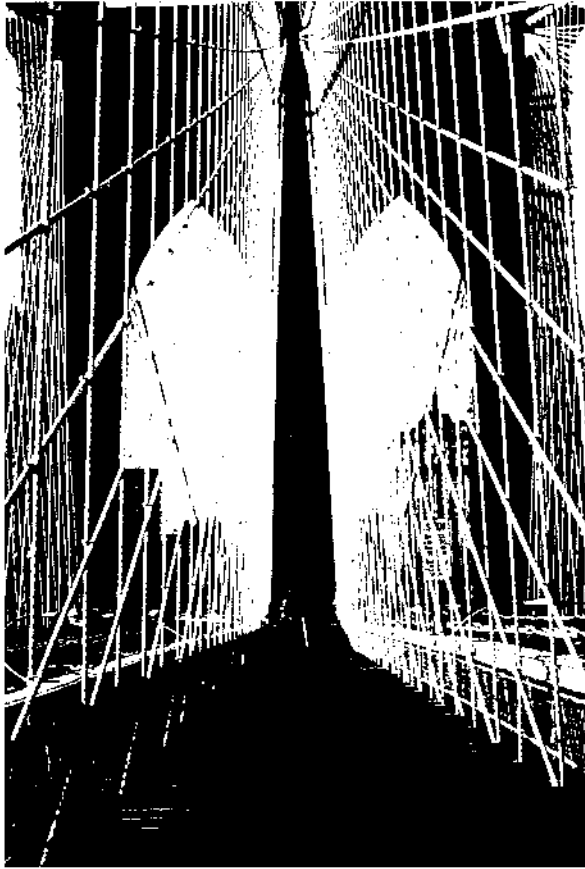


FIGURE 1.7 The Cincinnati Bridge across the Ohio River.

dual system is also present in the bridge at Wheeling, West Virginia, Fig. 1.9. This bridge was designed and rebuilt by Ellet, without stays. Stays were added later by others, who were influenced by Roebing.

It should be noted that the stays used by Roebing in his suspension bridges were used as an addition to the classical suspension bridge with the main catenary cable and its suspenders. During Roebing's time the suspension-bridge concept was suffering with failures resulting from wind forces. The Wheeling, West Virginia bridge was a notable failure during this era. In many respects Roebing was before his time. He knew that by incorporating the diagonal stays he could minimize the susceptibility of his structures to adverse wind loading. However, it is not clear whether he used the two suspension systems compositely, or more likely, that the stays were used as an independent secondary back-up system with the primary catenary suspension system taking all the static load.

Despite Navier's adverse criticism of the stayed bridge, a few more bridges were built shortly after the fatal collapses of the bridges in England and Germany.



**FIGURE 1.8** The Brooklyn Bridge in New York.



**FIGURE 1.9** Ellet's bridge Wheeling, West Virginia.

The Gisclard-Arnodin cable bridge, Fig. 1.10, used multiple sloping cables hung from two masonry towers. In 1840, Hatley, an Englishman, used chain stays in a parallel configuration, Fig. 1.11, resembling harp strings. He maintained the parallel spacing of the main stays by using a closely spaced subsystem anchored to the deck and perpendicular to the principal load-carrying cables.

Constructed in 1873, the Albert Bridge over the Thames River, Fig. 1.12, with a main span of 400 ft (122 m), affords a good example of catenary suspension combined with stays. In this structure the suspen-

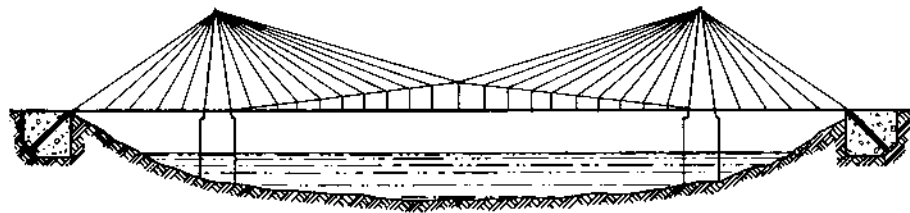


**FIGURE 1.10** Gisclard-Arnodin-type sloping-cable bridge. (Courtesy of the British Constructional Steelwork Association, Ltd.)

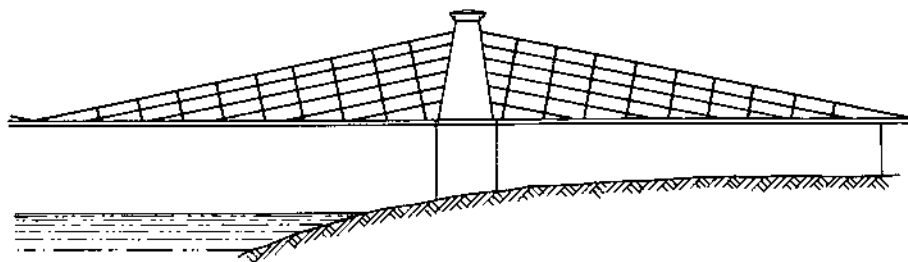


**FIGURE 1.11** Hatley chain bridge. (Courtesy of the British Constructional Steelwork Association, Ltd.)

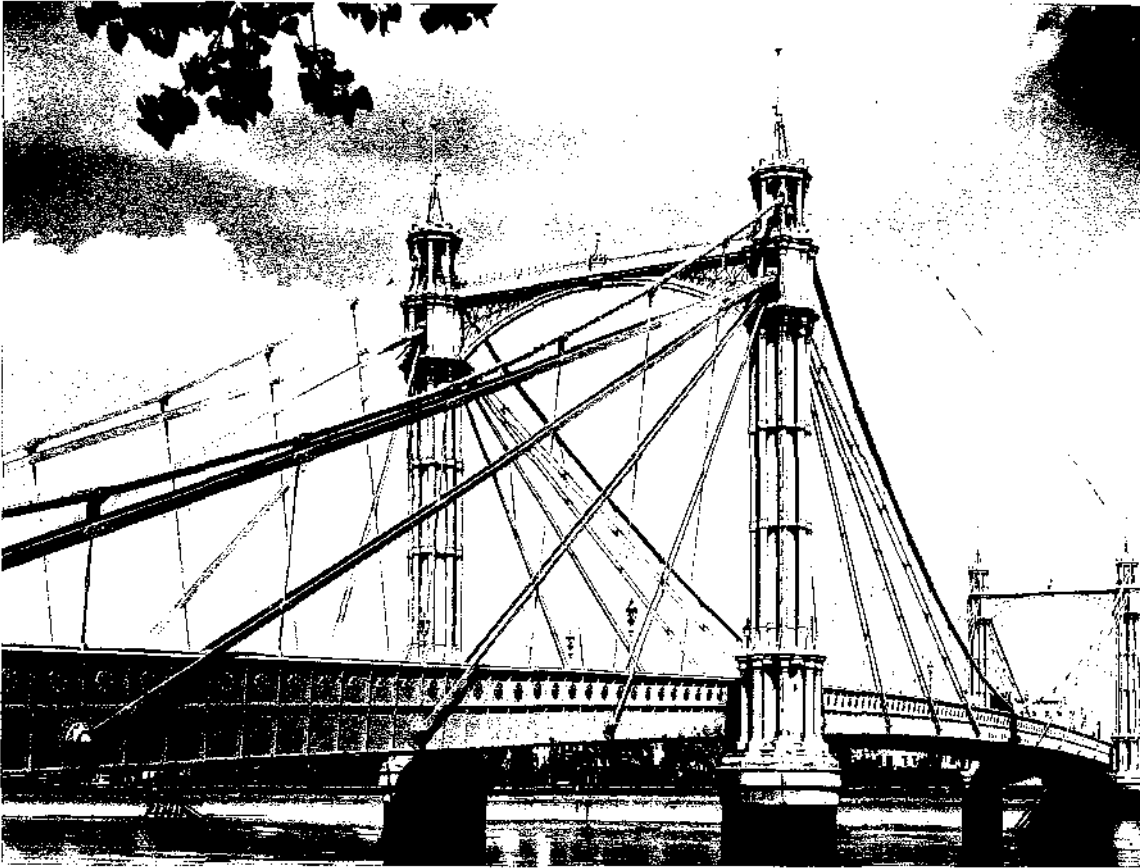


**FIGURE 1.12** The Albert Bridge. (Courtesy of the British Constructional Steelwork Association, Ltd.)

sion system consisted of stays converging at the tops of the towers. There were three inclined stays on each side of the center span and four stays on each side of the end spans.<sup>5,6</sup>

The virtual banishment of the stayed bridge during the eighteenth and nineteenth centuries can be attributed to the lack of technical knowledge of the theoretical analyses for the internal forces of the total system. The lack of understanding of the behavior of the stayed system and the methods of controlling the equilibrium and compatibility of the various highly indeterminate systems appears to have been the major drawback to the rapid development of the concept. Not only was the theory lacking but the materials of the period were not suitable for stayed bridges. Materials such as timber, round bars, and chains of various types are not the most desirable for the tension forces acting in the stays. These materials exhibit low strengths and cannot be pretensioned to avoid the slack condition resulting from asymmetrical loadings. For the stays to participate in tension at all times without prestressing,

it was necessary for the superstructure to have substantial deformations, which endangered the structure as a whole. Perhaps the early collapses were the result of this unsuitable stress condition.

Against this background of a lack of theoretical knowledge and less than adequate materials, the German engineer, F. Dischinger,<sup>7</sup> appears to have rediscovered the stayed bridge in 1938. While designing a suspension bridge to cross the Elbe River near Hamburg, Dischinger determined that the vertical deflection of the bridge under railroad loading could be reduced considerably by incorporating cable stays into the suspension system, Fig. 1.13. From these studies and his later design of the Strömsund Bridge in Sweden evolved the modern-day cable-stayed bridge.

Roebbling's revived concept of utilizing stays with hangers is reflected in Steinman's bridge across the Tagus River in Portugal, Fig. 1.14. At the top is the present structure, a conventional suspension bridge. At the bottom is the future structure, when cable stays will be added to accommodate additional rail traffic.

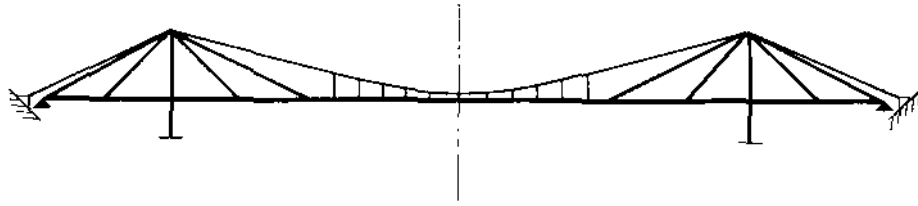


FIGURE 1.13 Bridge system proposed by Dischinger.

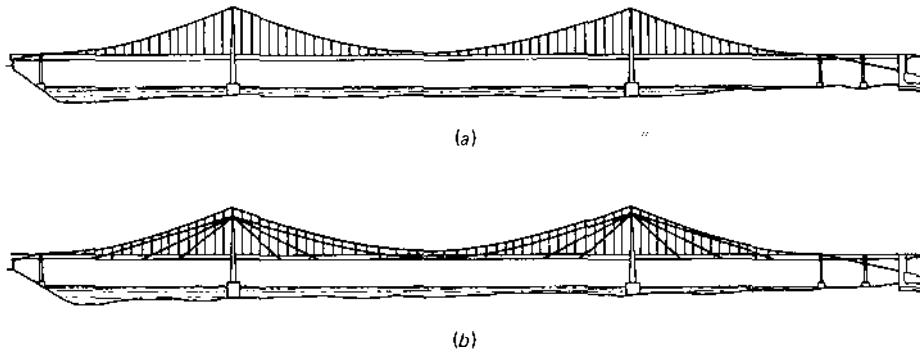


FIGURE 1.14 The Salazar Bridge: (a) elevation of present bridge, (b) elevation of future bridge.

### 1.3 Contemporary Implementation

Following World War II, West Germany determined that approximately 15,000 bridges had been destroyed during the conflict. Therefore, the postwar period of rebuilding these crossings provided the opportunity for engineers, builders, and contractors to apply new concepts of design and construction. During this period steel was in short supply and a great emphasis was placed on minimum weight design. As a result of this emphasis, orthotropic plate design developed, which provided a marriage with cable-stayed design to produce bridges that were in some cases 40% lighter than their prewar counterparts. Efficient use of materials and speed of erection made cable-stayed bridges the most economical type of structure to use for replacements.

The first modern cable-stayed bridge, The Strömsund Bridge, Fig. 1.15, was completed in Sweden in 1955. It is interesting to note that the bridge was built by a German contractor, Demag, in collaboration with a German engineer, F. Dischinger.

A comprehensive search of the literature from the time of the Strömsund Bridge in 1955 to approximately 1972 produced references to some 43 bridges that had been built or were being contemplated, incorporating a system of cable stays.<sup>8</sup> Thirteen were in Germany, with the balance distributed in 16 other

countries throughout the world. Four were in the United States, two were actually constructed and two were abandoned. Two years later (1974) the total number had grown to 50; in the United States two had been constructed and four were proposed.<sup>9</sup> A 1977 report<sup>10</sup> indicated 62 cable-stayed bridges distributed among 19 countries. West Germany had 19, followed by Japan with eight, the United States with six, and France with five. As of 1985 in the United States there are seven cable-stayed bridges completed, six under construction, four in design, and four under study.

The rapid growth in the number of applications of the cable-stayed bridge concept implies that these bridges are satisfying many needs, such as economy, ease of fabrication, erection, and aesthetics. Bridge engineers are becoming acquainted with the many advantages of cable-stayed bridges and are planning many more applications. There appears to be no doubt that the cable-stayed bridge with its many geometrical configurations will be applied in great numbers in the future in the United States.

### 1.4 Early Applications in the United States

Although contemporary cable-stayed bridges began in the United States in 1972, bridges employing the gen-

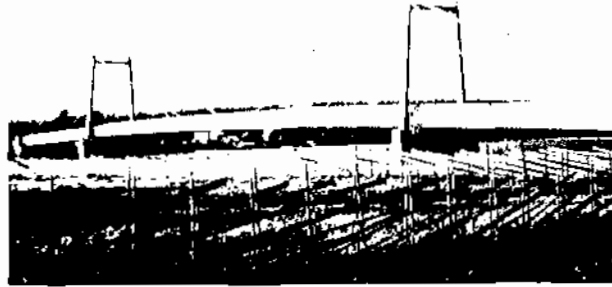
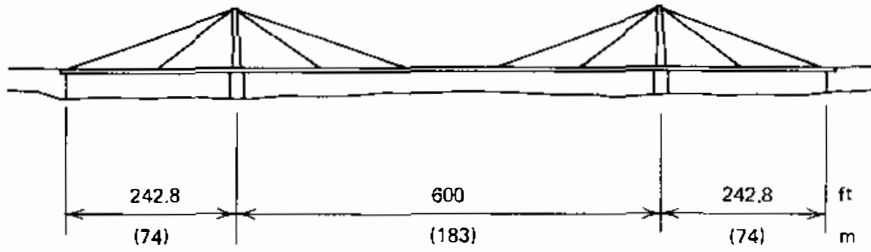


FIGURE 1.15 The Strömsund Bridge (Sweden).

eral concept had been previously constructed in the United States.

A three-span cable-stay bridge was constructed in 1889 across the Whitewater River at Richmond, Indiana.<sup>11</sup> It had an overall length of 200 ft (61 m) between anchorages with a center span of 150 ft (45.7 m). It was constructed in 30 days by the Mitchell Bridge Company at a total cost of \$2150. It had a life span of eight years, being washed away in 1897. Figure 1.16 shows a stayed swing span in Louisiana, circa 1929. The stayed girder concept is not unfamiliar to the Pacific Northwest as indicated by Figs. 1.17 and 1.18.

In 1953 the Aloha Lumber Company built a cable-stayed logging bridge across the Quinault River in the

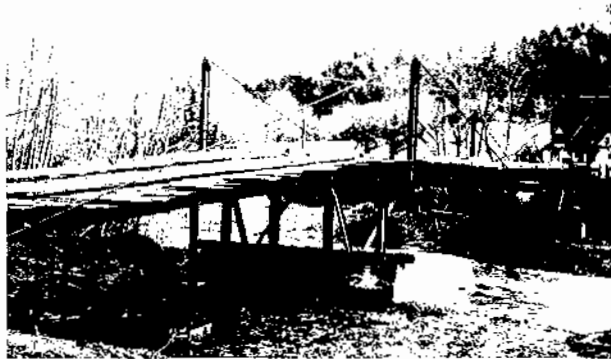


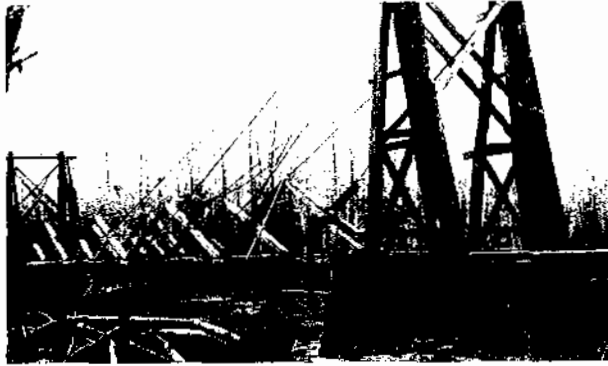
FIGURE 1.17 South Myrtle Creek Bridge, Washington. (Courtesy of John H. Garren, FHWA Washington Division.)



FIGURE 1.16 Louisiana stayed bridge. (Courtesy of Sidney L. Poleynard, Raymond Technical Facilities, Inc.)



FIGURE 1.18 Coos River Bridge, Washington. (Courtesy of John H. Garren, FHWA Washington Division.)



**FIGURE 1.19** Quinault River Bridge. (Courtesy of Arvid Grant, Arvid Grant and Associates, Inc.)

state of Washington, Fig. 1.19. This structure was built in 1953 and designed by Frank Milward, Aloha Company logging superintendent. The structure collapsed on September 24, 1964 as a result of a failure of one of the 2 $\frac{1}{4}$ -in. (57-mm) diameter cables and was rebuilt. The structure collapsed again in August of 1973 and has been revamped. It has a center span of 256 ft (78 m).

On July 5, 1957 a stayed structure, Fig. 1.20, crossing the Yakima River at Benton City (10 miles west of Richland, Washington) was opened to traffic. Designed by Homer M. Hadley, the structure has a total length of 400 ft (122-m) with a center span of 170 ft (52-m). A 60-ft (18-m) central drop-in or suspended span of 33-in. (0.84-m) wide flange beams is supported by transverse concrete beams, which in turn are supported by the 10-in. (254-mm), 112-lb (50.8-kg) wide flange stays. Continuous longitudinal concrete beams



**FIGURE 1.20** Benton City Bridge, Washington. (Courtesy of John H. Garren, FHWA Washington Division.)

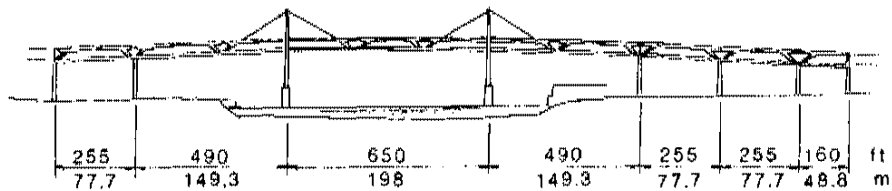
comprise the remainder of the structure and receive support at their extremity in the center span from the transverse concrete beams and stays. The 10-in. (254-mm), 112-lb (50.8-kg) wide flange sections were also used for the pylon legs and were encased in concrete. The stays were set with their flanges vertical to match the flanges of the pylon legs. Stays were connected to the pylon by plates and high-tensile bolts in single shear.<sup>12</sup>

### 1.5 Recent Applications in the United States

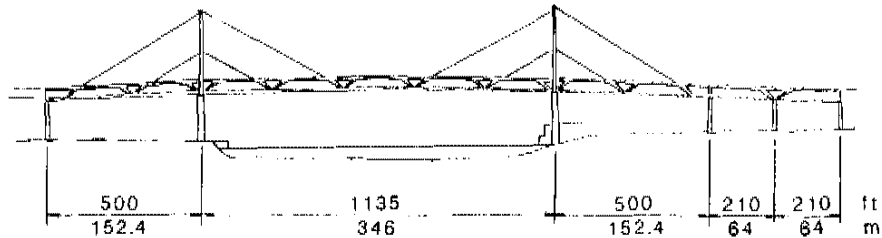
Although serious consideration of cable-stayed bridges in the United States did not begin until about 1970, there were earlier attempts. In August of 1964, the firm of Parsons Brinkerhoff Quade & Douglas was conducting studies to select the type bridge for the Fremont Bridge crossing the Willamette River in Portland, Oregon. Two cable-stayed alternate bridges were given consideration, Fig. 1.21. The first cable-stayed alternate bridge considered had a main span of 650 ft (198 m) with 490-ft (149-m) side spans and both pylon piers in the river. It was to be a two-level, or double-deck, structure and have two vertical planes of stays with single stays emanating from each side of the portal pylons. The other alternative was essentially the same except that it included a center span of 1135 ft (346 m) with side spans of 500 ft (152 m), piers out of the water, and two stays emanating from each side of the pylon.

In about 1965 the Danish Government sponsored an "International Contest of Idcas" for the Great Belt Crossing in Denmark. One of the first-prize winners was an entry by Sverdrup & Parcel and Associates, Inc., Fig. 1.22. It contained a 1476-ft (450-m) center span and flanking spans of 633 ft (193 m). It had a truss-type stiffening girder to support two decks, six vehicular lanes carried on the top, and two sets of railroad tracks on the lower deck.

In 1969 the California State Division of Bay Toll Crossings was designing the proposed Southern Crossing in the San Francisco Bay area, Fig. 1.23.<sup>13,14</sup> The symmetrical stayed portion of this crossing included a 1300-ft (396-m) center span and 450-ft (137-m) side spans. The transverse cable geometry was two sloping planes. In elevation two stays would have emanated from each side of the tower in each plane. The deck girder would have been composed of a continuous three-span orthotropic deck with twin trapezoidal box girders interconnected at cable anchorage points by



Alternate I



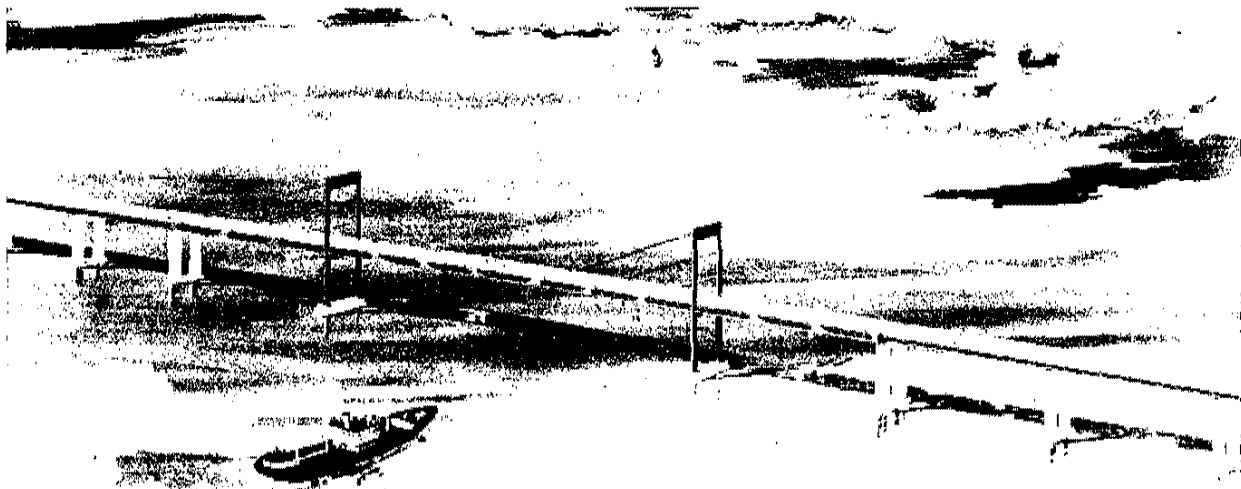
Alternate II

**FIGURE 1.21** Freemont Bridge.

rectangular transverse anchorage beams. Because a vertical navigation clearance of 220 ft (67 m) was required, a diamond-shaped tower configuration was selected and would have been 466 ft (142 m) high. If the legs had been extended below the roadway to form an A-frame, because of the height the base would have been awkwardly wide and would have required an expensive substructure. This structure was never constructed because of environmental considerations.

The Menomonee Falls, Wisconsin, pedestrian bridge, built in 1971, is the first contemporary cable-stayed bridge to be constructed in the United States,

Fig. 1.24. Based on preliminary designs by Stanley W. Woods, the bridge was designed by the Wisconsin Division of Highways Bridge Section.<sup>15</sup> It is a symmetrical three-span structure with a center span of 217 ft (66 m) and end spans of 72 ft (22 m). It has A-frame towers 56 ft 6 in. (17.2 m) tall. The transverse stay arrangement is two sloping planes. In elevation a single stay emanates from the top of the pylon on each side and in each plane. The American Institute of Steel Construction, in their Prize Bridge Contest, awarded this structure the 1971 Award of Merit in the "Special Type" category.

**FIGURE 1.22** Danish Great Belt Bridge Competition. (Courtesy of ASCE—Civil Engineering.)



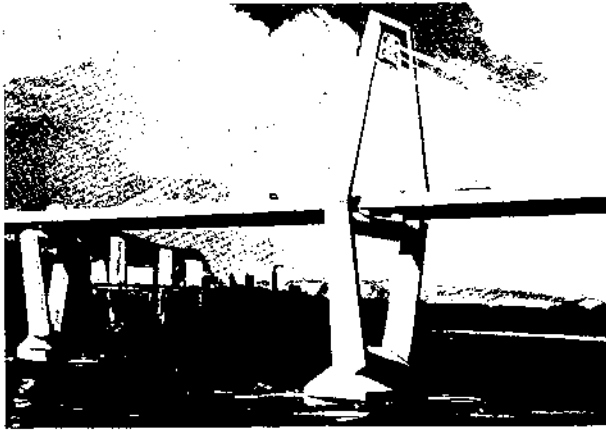


**FIGURE 1.23** Southern Crossing, San Francisco Bay. (Courtesy of C. Seim.)

In 1972 the first vehicular cable-stayed bridge, the John O'Connell Memorial Bridge at Sitka, Alaska, was constructed, Fig. 1.25. The bridge was designed by the State of Alaska Department of Highways under the direction of William L. Gute.<sup>16</sup> The symmetrical

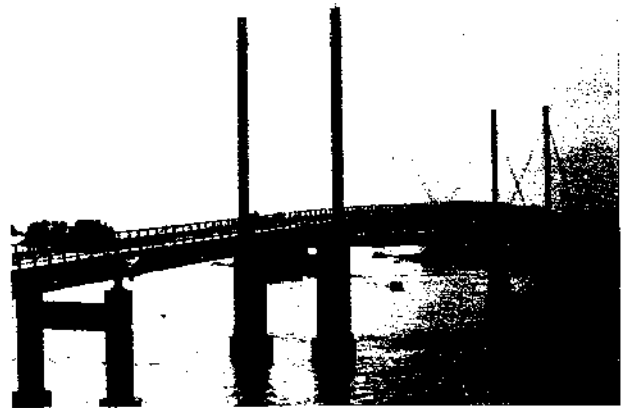


**FIGURE 1.25** Sitka Harbor Bridge.

bridge has a center span of 450 ft (137 m) and side spans of 150 ft (45.7 m). The geometry of the stays transverse to the longitudinal axis of the bridge is in two vertical planes. In elevation only one stay emanates from each side of the pylon. Each stay consists of three galvanized structural strands oriented in a vertical plane.

In 1973 the West Seattle Freeway was being designed by the firm of Knoerle, Bender, Stone & Associates, Inc., Fig. 1.26. It had a single concrete portal-type pylon with two stay planes and one stay emanating from each side of the pylon in each plane. There was one straight stayed span at 507 ft (154.5 m) and one horizontally curved span at 528 ft (161 m) with a radius of 1162 ft (354 m). The project was abandoned because of funding problems.

In 1973 a 1200-ft (366-m) center-span structure designed by Maddigan and Prager was contemplated to cross Long Island Sound connecting the city of Rye with Oak Neck Point across the Sound, Fig. 1.27. It was abandoned because of environmental objections.

In 1974 the State of Alaska Department of Highways completed the Captain William Moore Bridge located about 12 miles (19.3-km) north of Skagway, Fig. 1.28. Studies of long-span alternatives for this site were especially concerned with problems of access and erection from one side of the canyon. This consideration led to the single-tower cable-stayed bridge with a major span of 271 ft (82.6 m).

The Meridian California, a swing-span, cable-stayed bridge, was completed in 1977. Designed by the State of California Division of Highways, this structure has symmetrical spans of 179.7 ft (54.8 m), Fig. 1.29.

The Pasco-Kennewick Bridge in the state of Washington, designed by Arvid Grant and Associates, Inc.

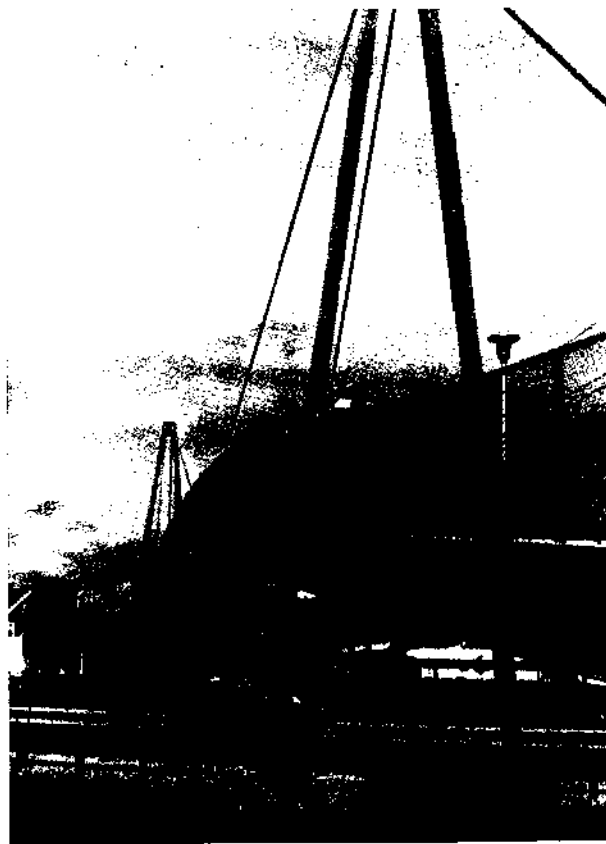


**FIGURE 1.24** Menomonee Falls, Wisconsin, pedestrian bridge. (Courtesy of the Wisconsin Division of Highways.)



**FIGURE 1.26** West Seattle freeway bridge. (Courtesy of J. E. Arnberg, City of Seattle Department of Engineering.)



**FIGURE 1.27** Long Island Sound, N.Y. Bridge. (Courtesy of Jerome S. B. Iffland, Iffland Kavanagh Waterbury, P.C.)

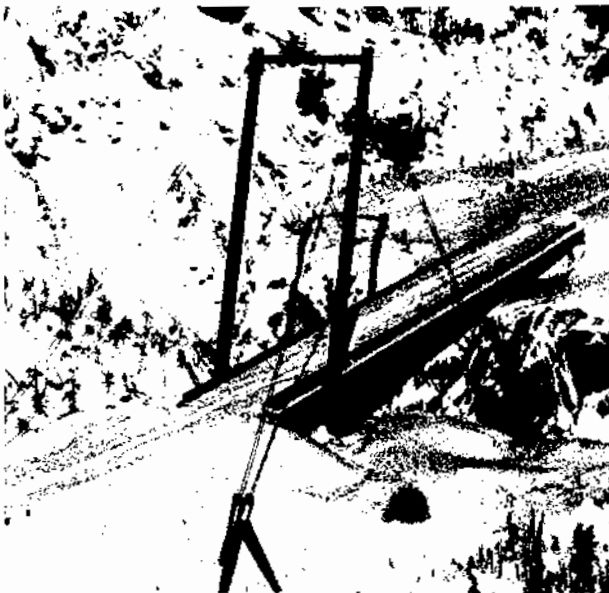


**FIGURE 1.28** Capt. William Moore Bridge. (Courtesy of Donald Halsted, Alaska Department of Highways.)

in professional collaboration with Leonhardt and Andra, represents the first concrete cable-stayed bridge in the United States, Fig. 1.30. Construction began in August 1975 and was completed in May 1978. It has a center cable-stayed span of 981 ft (299 m), and the stayed flanking spans are 406.5 ft (124 m).

An independent group proposed that a cable-stayed bridge, Fig. 1.31, be built across the Bering Straits linking Alaska and Siberia and, thus, providing a transportation route that would connect five continents.<sup>17</sup> The proposed concept was a combined highway and railway bridge 50 miles (80.5 km) in length, requiring approximately 260 spans of 1000 ft (304.8 m) each. The project has never progressed past the conceptual stage because of a lack of interest.

A design by T. Y. Lin International to cross the middle fork of the American River, Auburn, California, is a cable-stayed, hanging horizontal-arc bridge, The Ruck-a-Chucky Bridge,<sup>18</sup> with a span of 1300 ft (396 m) on a curve of a 1500-ft (457-m) radius with a subtended central angle of 45 degrees, Fig. 1.32. This



**FIGURE 1.29** Cable-stay swing span; Meridian, California. (Courtesy Department of Transportation, Division of Highways, Office of Structures, State of California.)

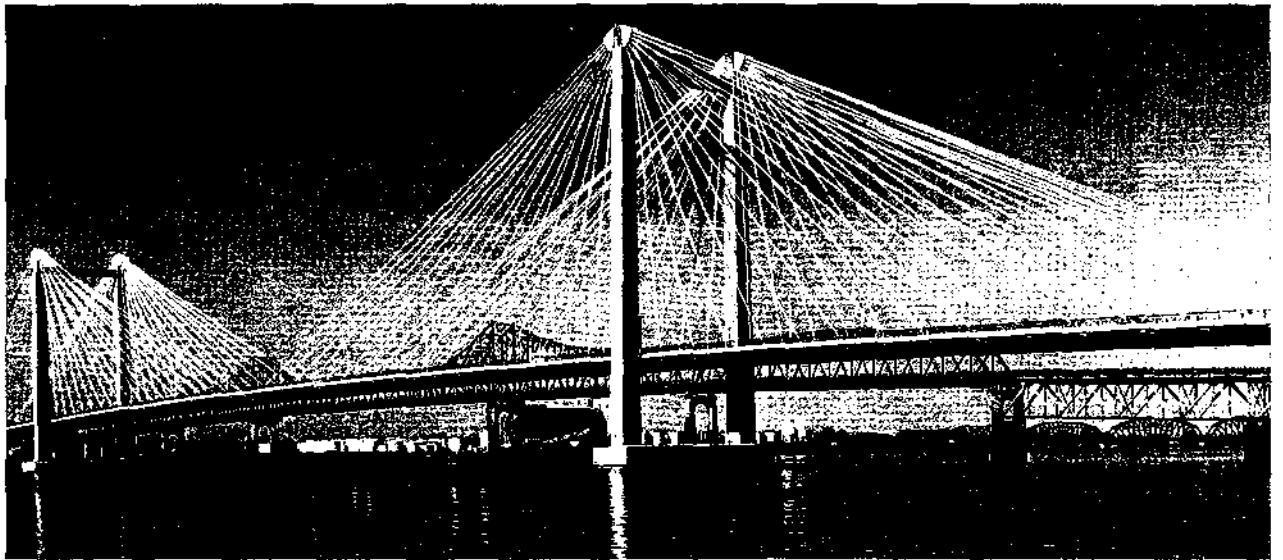


**FIGURE 1.30** Pasco-Kennewick Intercity Bridge. (Courtesy of Arvid Grant, Arvid Grant and Associates, Inc.)

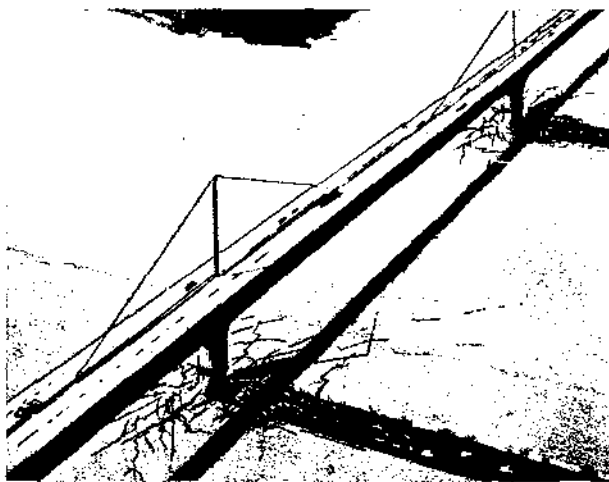


**FIGURE 1.31** Artist's rendering, Inter-Continental Peace Bridge. (Courtesy of T. Y. Lin.)

bridge was conceived to fit the particular site requirements by eliminating 350-ft (107-m) high piers, which would have to resist heavy hydroseismic forces. The 40-degree slopes of the canyon walls would have demanded tunnel approaches at both ends if the bridge were designed as a straight one. This hanging arc minimizes approach cutting and utilizes the steep walls of the canyon to suspend the entire span. The project was abandoned because of a lack of funding.

Construction of the Luling Bridge crossing the Mississippi River in the state of Louisiana began in spring 1975 and was completed in 1983, Fig. 1.33. The design of this structure originally proposed a center span of 1235 ft (377 m) with flanking stayed side spans of 495 ft (151 m), Fig. 1.2. During construction of the foundations for the pylons, a caisson shifted 13 ft (4 m) toward the river, necessitating span modifications

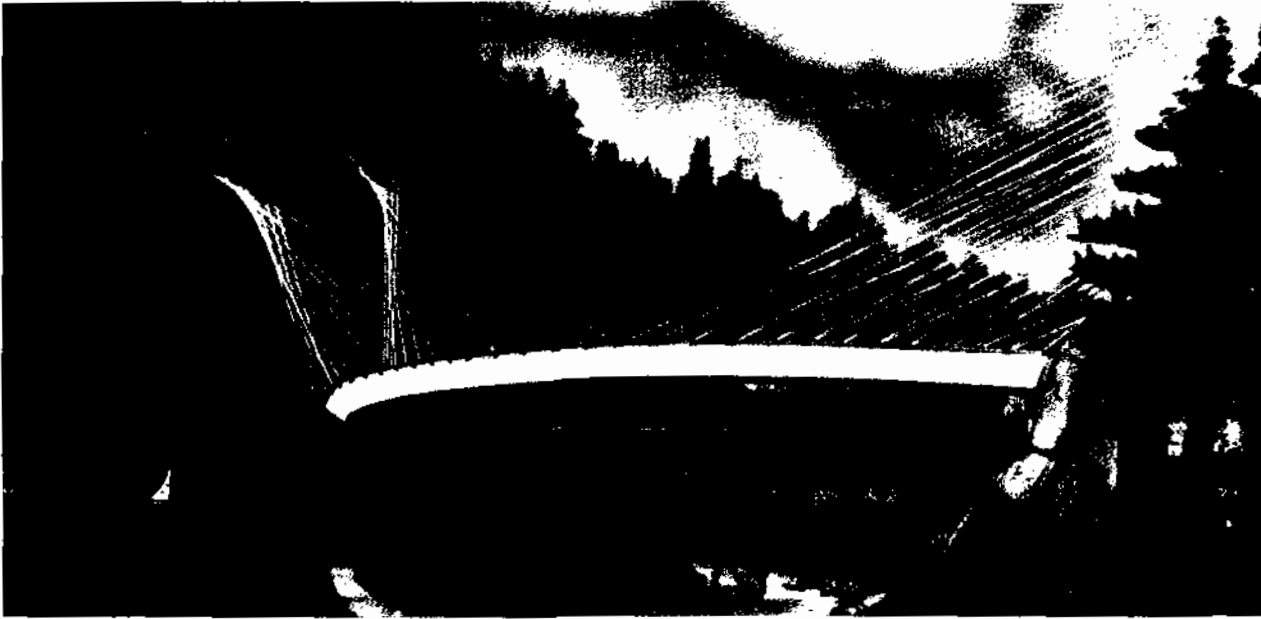


FIGURE 1.32 Ruck-A-Chucky Bridge, artist's rendering. (Courtesy of T. Y. Lin.)

to 508, 1222, and 495 ft (155, 373, and 151 m). This structure represents the longest cable-stayed bridge in the United States and is also the only cable-stayed bridge with an orthotropic steel deck. Designers are the joint venture of Frankland & Lienhard/Modjeski and Masters. Construction of the substructure was by the joint venture of Massman Construction Company and Al Johnson Construction Company. Williams Brothers Construction Company was the general contractor for the superstructure, and the steel erection subcontractor was Melbourne Brothers Construction Company.

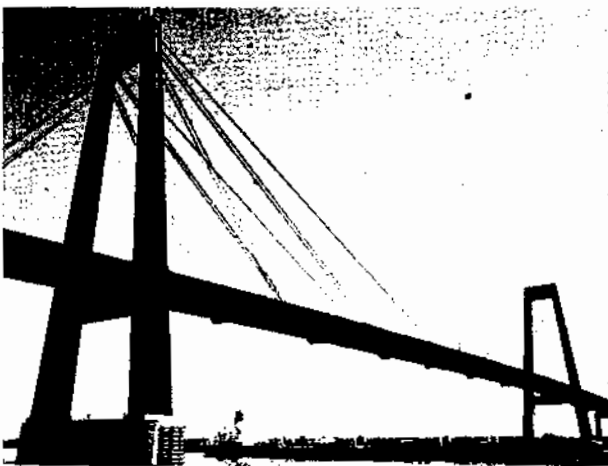


FIGURE 1.33 Luling Bridge.

An asymmetrical cable-stayed structure crossing the Ohio River, Fig. 1.34, between East Huntington, West Virginia and Proctorville, Ohio was completed in 1985. It has a major span of 900 ft (274 m) and a minor span of 608 ft (185 m). The cross section consists of two solid rectangular concrete edge beams with transverse structural steel floor beams and a composite concrete deck. The designer is Arvid Grant and Associates, Inc. and Leonhardt and Andra.

Another asymmetric structure currently under construction (1985) is the Ohio River bridge between Weirton, West Virginia and Steubenville, Ohio, Fig. 1.35. Designed by Michael Baker, Jr., Inc., it will have a major span of 820-ft (250-m) and a minor span of 688-ft (210-m). It has structural steel edge girders and floor beams with a composite concrete deck.

A monumental structure under construction (1985) is the Sunshine Skyway replacement bridge crossing Tampa Bay in Florida. The main navigation spans will feature a cable-stayed unit with a center span of 1200 ft (366-m) and side spans of 540 ft (164.5 m). This 2280-ft (695-m) long portion of the bridge will be supported by a single central plane of stays at 24 ft (7.3 m) on center, Fig. 1.36, and will be constructed with a single-cell concrete box girder 95 ft 3 in. (29 m) wide. Design is by Figg and Muller Engineers, Inc.

The Quincy Bridge crossing the Mississippi River between Illinois and Missouri, also under construction (1985), is a symmetric three-span cable-stayed bridge with a center span of 900-ft (274-m) and side spans of

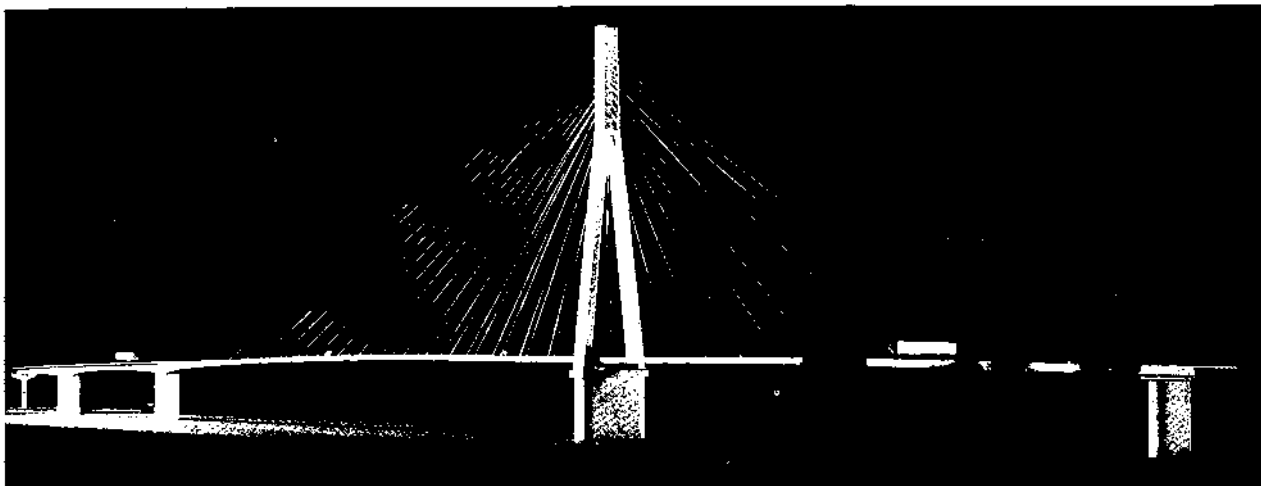


**FIGURE 1.34** East Huntington Bridge, artist's rendering. (Courtesy of Arvid Grant, Arvid Grant and Associates, Inc.)

440-ft (134-m). It has two vertical planes of stays with portal-type pylons, Fig. 1.37. The deck structure consists of structural steel I-shaped edge girders, floor beams, and stringers with a precast composite deck slab. Designer is Modjeski and Masters.

Another project under construction (1985) is the Neches River Bridge in Texas, Fig. 1.38. It will have a main span of 640 ft (195 m) and side spans of 280 ft (85 m). Designer is Figg and Muller Engineers, Inc.

The Dame Point Bridge in Jacksonville, Florida, Fig. 1.39, will have a main span of 1300 ft (396-m) and side spans of 650 ft (198 m). It was bid in 1980 with a concrete and a steel alternate. The concrete alternate was the low bid at \$64.8 million. However, work on the project was never started because of a lack of funds. A revised concrete alternate was bid in late 1984 with the following design changes: vertical navigation channel clearance increased from 152-ft (46-m)

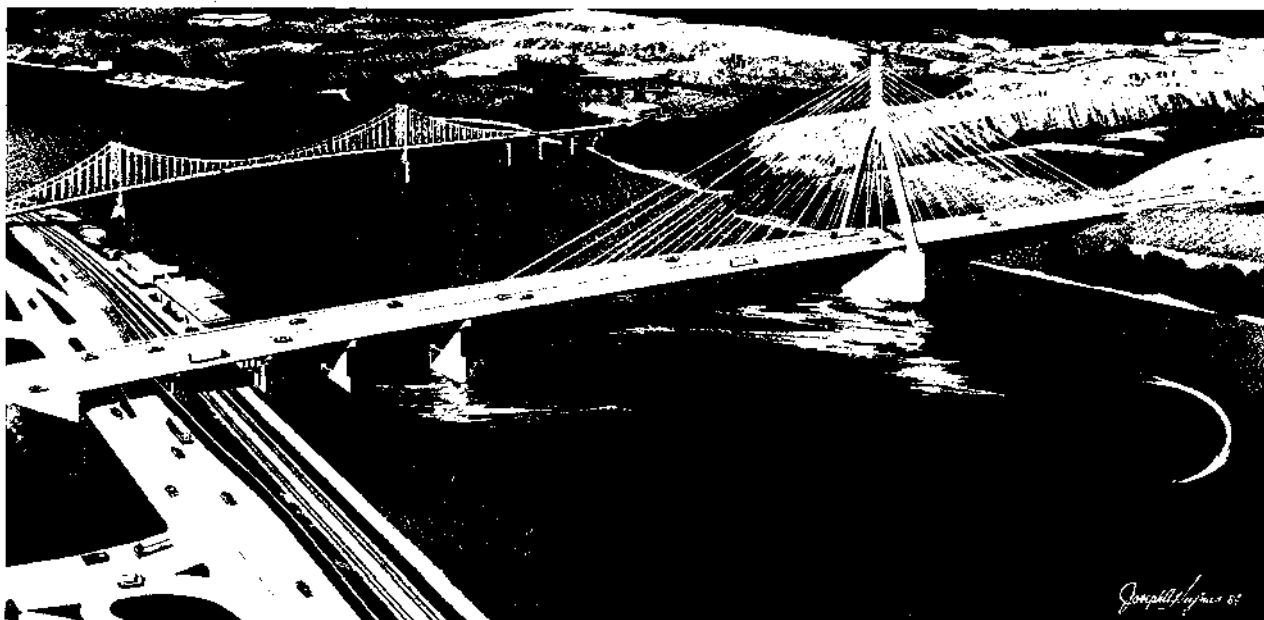


**FIGURE 1.35** Weirton-Stebenville Bridge, artist's rendering. (Courtesy of Michael Baker, Jr., Inc.)



**FIGURE 1.36** Sunshine Skyway Bridge model. (Courtesy of Figg and Muller Engineers, Inc.)

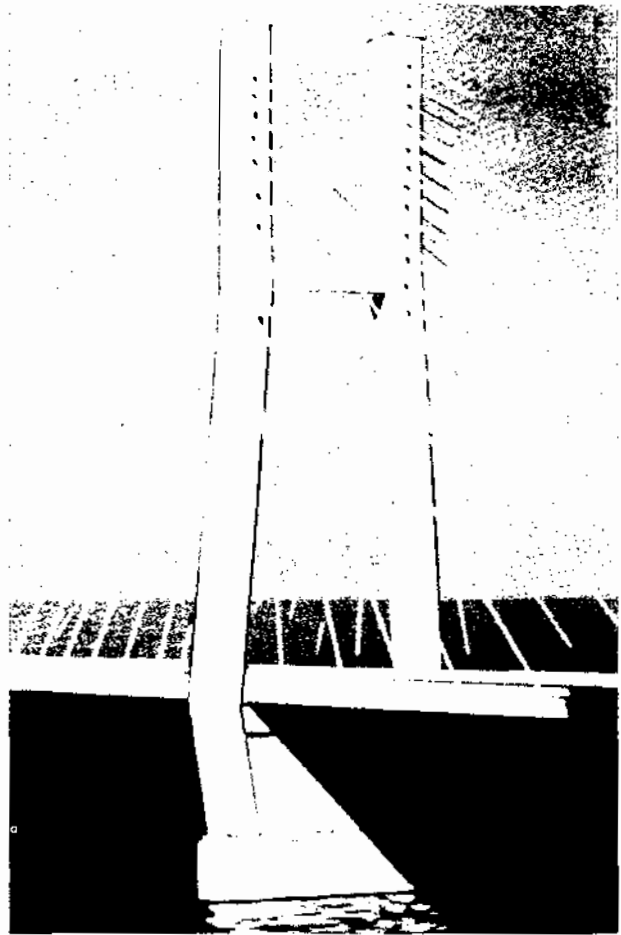


**FIGURE 1.37** Quincy, Illinois Bridge. (Courtesy of John M. Kulicki, Modjeski and Masters.)

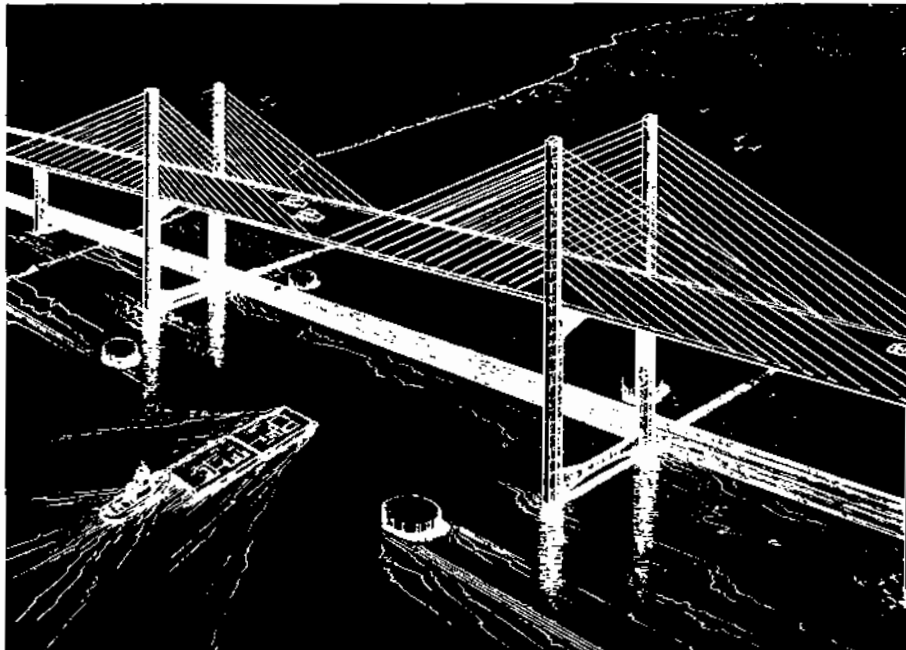


**FIGURE 1.38** Neches River Bridge, Texas. (Courtesy of Figg and Muller Engineers, Inc.)

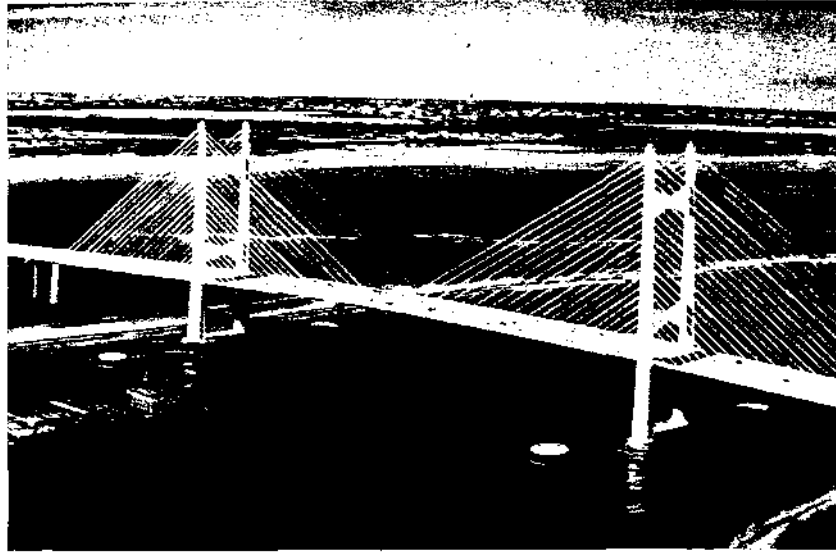


**FIGURE 1.39** Dame Point Bridge, Florida, artist's rendering. (Courtesy of Howard Needles Tammen & Bergendoff)

to 174-ft (53-m) and modifications to the pile foundations. In addition, contractor-sponsored alternative designs were allowed.

A concrete cable-stay bridge with a main span of 630 ft (192 m) is under construction (1985) for the I-295 James River Bridge near Richmond, Virginia, Fig. 1.40.

#### *1.6 Projects in Design or Under Consideration*

As of 1985 there are four cable-stayed bridges in design and four under study in the United States. Concrete and composite steel alternative designs are being prepared for the Talmadge Memorial Bridge at Savannah, Georgia, Fig. 1.41; and the Cochrane Bridge at

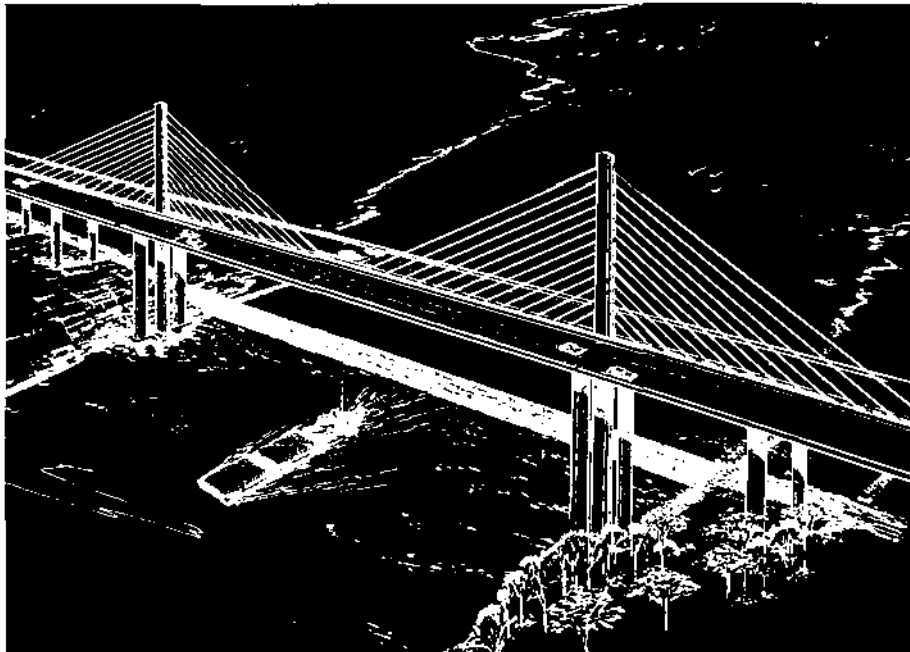


**FIGURE 1.40** James River Bridge, Virginia, artist's rendering. (Courtesy of Figg and Muller Engineers, Inc.)

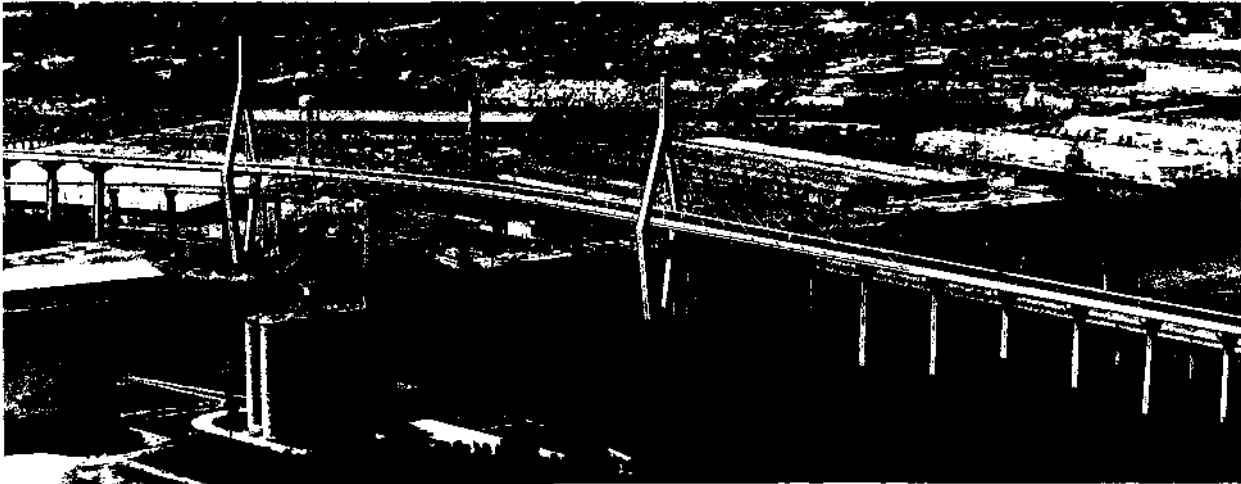


**FIGURE 1.41** Talmadge Memorial Bridge, artist's rendering. (Courtesy of Mr. Wendell B. Lawing, Georgia DOT.)

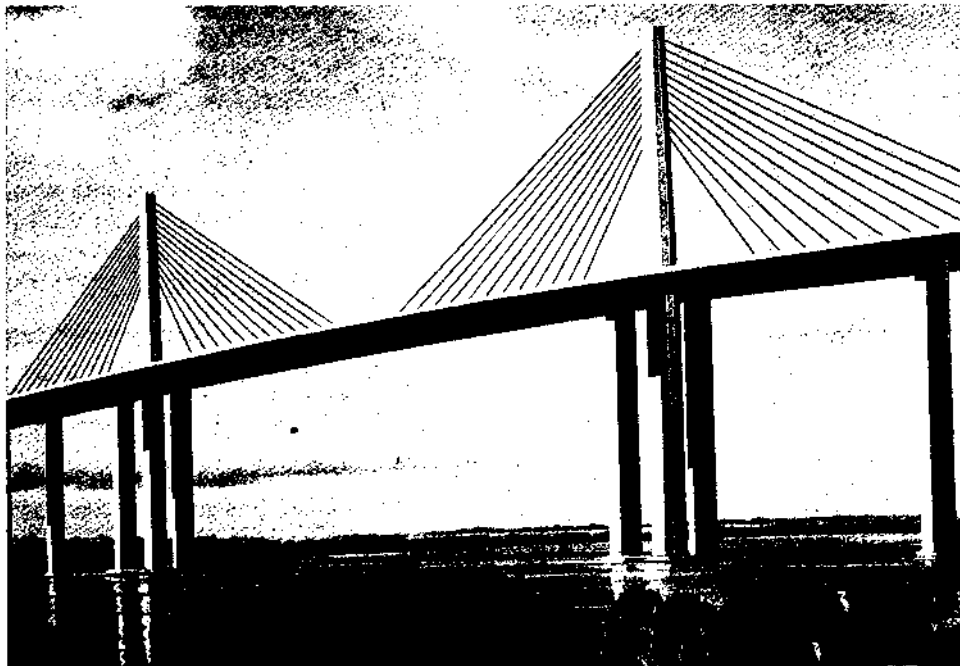


**FIGURE 1.42** Cooper River Bridge, South Carolina, artist's rendering. (Courtesy of Figg and Muller Engineers, Inc.)





FIGURE 1.43 Houston Ship Channel, Baytown Bridge, Texas. (Courtesy of Ben G. Christopher, Greiner Engineering Sciences, Inc.)

Mobile, Alabama. The I-526, Cooper River Bridge, Fig. 1.42, near Charleston, South Carolina is being designed as a concrete cable-stayed bridge alternative to a steel truss. A cable-stayed bridge is under design for a crossing of the Houston Ship Channel at Baytown, Texas, Fig. 1.43.

#### References

- Jaros, S. E., "Luling Bridge," *Cable-Stayed Bridges, Structural Engineering Series No. 4*, June 1978, Bridge Division, Federal Highway Administration, Washington, D.C.
- Hopkins, H. J., *A Span of Bridges: An Illustrated History*, Praeger, 1970. New York and Washington.
- Kavanagh, T. C., Discussion of "Historical Developments of Cable-Stayed Bridges" by Podolny and Fleming, *Journal of the Structural Division*, ASCE, Vol. 99, No. ST 7, July 1973, Proc. Paper 9826.
- Leonhardt, F. and Zellner, W., "Cable-Stayed Bridges: Report on Latest Developments," Canadian Structural Engineering Conference, 1970, Canadian Steel Industries Construction Council, Toronto, Ontario, Canada.
- Feige, A., "The Evolution of German Cable-Stayed Bridges—An Overall Survey," *Acier-Stahl-Steel* (English version), No. 12, December 1966, reprinted *AISC Engineering Journal*, July 1967.
- Thul, H., "Cable-Stayed Bridges in Germany," *Proceedings of the British Constructional Steelwork Association Conference on Structural Steelwork*, held at the Institution of Civil Engineers, September 26-28, 1966, the British Constructional Steelwork Association Ltd., London, England.
- Dischinger, F., "Hängebrücken für Schwerste Verkehrslasten," *Der Bauingenieur*, March 1949.
- Podolny, W., Jr. and Fleming, J. F., "Historical Developments of Cable-Stayed Bridges," *Journal of the Structural Division*, ASCE, Vol. 98, No. ST 9, September 1972, Proc. Paper 9201.
- Podolny, W., Jr., "Cable-Stayed Bridges," *Engineering Journal*, American Institute of Steel Construction, First Quarter 1974.
- "Bibliography and Data on Cable-Stayed Bridges," Subcommittee on Cable-Stayed Bridges, *Journal of the Structural Division*, ASCE, Vol. 103, No. ST 10, October 1977.
- "Bridges over the Whitewater River at Richmond, Ind.," *Engineering News*, Vol. XLI, No. 25, June 22, 1899.
- Hadley, H. M., "Tied-Cantilever Bridge—Pioneer Structure in U.S.," *Civil Engineering*, ASCE, January 1958.
- Seim, C., Larsen, S. and Dang, A., "Design of the Southern Crossing Cable Stayed Girder," Preprint Paper 1352, ASCE National Water Resources Engineering Meeting, Phoenix, Arizona, January 11-15, 1971.
- Seim, C., Larsen, S. and Dang, A., "Analysis of Southern Crossing Cable Stayed Girder," Preprint Paper 1402, ASCE National Structural Engineering Meeting, Baltimore, Maryland, April 19-23, 1971.
- Woods, S. W., Discussion of "Historical Developments of Cable-Stayed Bridges," by Podolny and Fleming, *Journal of the Structural Division*, ASCE, Vol. 99, No. ST 4, April 1973.
- Gute, W. L., "First Vehicular Cable-Stayed Bridge in the U.S.," *Civil Engineering*, ASCE, Vol. 43, No. 11, November 1973.
- Anon., "Intercontinental Peace Bridge," ICPB, Inc., San Francisco, 1970.
- Lin, T. Y., Yang, Y. C., Lu, H. K. and Redfield, C. M., "Design of Ruck-A-Chucky Bridge," *Cable-Stayed Bridges, Structural Engineering Series No. 4*, June 1978, Bridge Division, Federal Highway Administration, Washington, D.C.

# 2

## *Bridge Component Configurations*

|       |                                 |    |
|-------|---------------------------------|----|
| 2.1   | GENERAL DESCRIPTION             | 21 |
| 2.2   | TRANSVERSE CABLE ARRANGEMENT    | 21 |
| 2.2.1 | Single-Plane System             | 22 |
| 2.2.2 | Double-Plane System             | 25 |
| 2.2.3 | Triple-Plane System             | 25 |
| 2.3   | LONGITUDINAL CABLE ARRANGEMENTS | 25 |
| 2.4   | TOWERS                          | 24 |
| 2.5   | CABLE SYSTEM SUMMARY            | 28 |
| 2.6   | SUPERSTRUCTURE TYPES            | 31 |
|       | REFERENCES                      | 34 |

### *2.1 General Description*

The cables extending from one or more towers of the cable-stayed bridge support the superstructure at many points along the span. The cable system is ideal for spanning natural barriers of wide rivers, deep valleys, or ravines, and for vehicular and pedestrian bridges crossing wide interstate highways because there are no piers that will form obstructions. For the most part, cable-stayed bridges have been built across navigable rivers where navigation requirements have dictated the dimensions of the spans and clearance above the main water level.

In general, span arrangements are of three basic types: two spans, symmetrical or asymmetrical, three spans, or multiple spans, Fig. 2.1.

In an economical stayed bridge design the span proportions, tower height, number and inclination of cables, and type of superstructure must be evaluated in conjunction with each other. For the two-span asymmetrical bridge structure, a partial survey of the existing bridges, Table 2.1, indicates that the longer span ranges from 60 to 70% of the total length. Two exceptions are the Batman and Bratislava bridges, Fig. 2.2, whose longer spans are 80% of the total length of the bridge structure. The reason for the longer spans is the fact that the back stays are concentrated into a single back stay anchored to the abutment, rather than

being distributed along the short span. In some instances the back stays may anchor into "dead-man" anchorage blocks, and only one span is supported by stays as in the Captain William Moore Bridge, Fig. 1.28, or the Ebro River Bridge, Fig. 2.3.

A similar survey of numerous three-span cable-stayed bridge structures, Table 2.2, indicates that the center span is approximately 55% of the total length of bridge. The remainder is usually equally divided between the two end spans. An investigation of bridges with multiple spans indicates that the spans are normally of equal length, with the exception of the flanking spans, which are adjusted to connect with the approach span or abutments. In this type of bridge the cables are arranged symmetrically on both sides of the towers. For convenience of fabrication and erection, the bridge structure has "drop-in" sections for the center portions of the span. The ratio of drop-in span length to total span length ranges from 20%, when a single stay emanates from each side of the tower, to 8%, where multiple stays emanate from each side of the tower.

The versatile cable-stayed-bridge concept lends itself to a large variety of geometrical configurations. The arrangement of the cables, type of superstructure, and style of the towers can be easily adjusted to suit the numerous requirements of site conditions and aesthetics for highway and pedestrian bridges. A detailed description and discussion of the advantages and disadvantages of the many geometrical forms for cable arrangement and type of towers is presented in this chapter.

### *2.2 Transverse Cable Arrangement*

In the transverse direction to the longitudinal axis of the bridge, the cables may lie in either a single or a

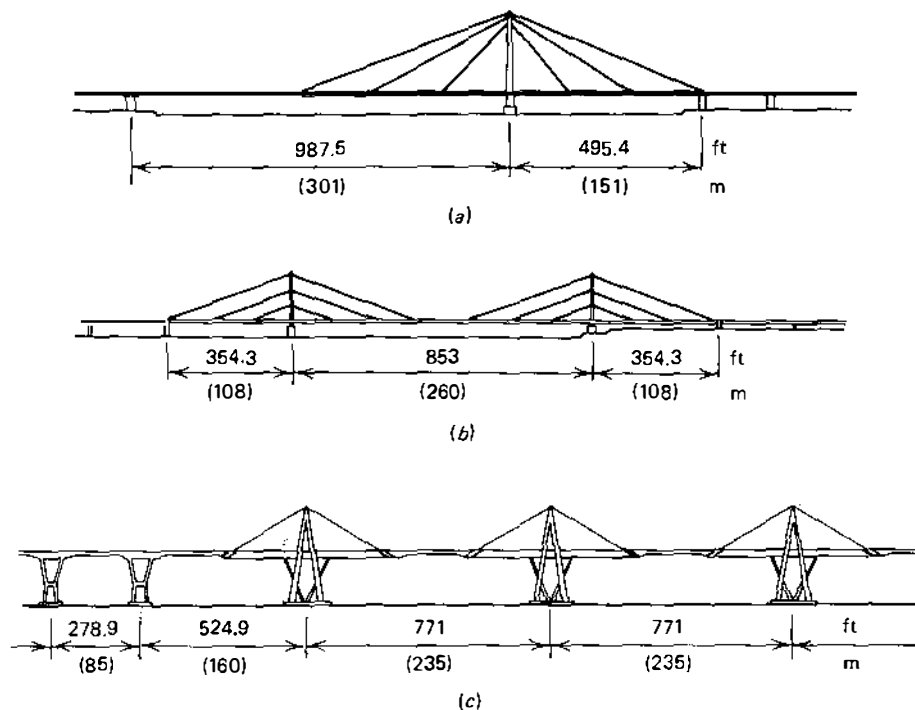


**FIGURE 2.1** Span arrangements: (a) two-span asymmetrical, Severin Bridge at Cologne, Germany; (b) three-span symmetrical, North Bridge at Dusseldorf, Germany; (c) multispan, Maracaibo, Venezuela.

double plane and may be symmetrically or asymmetrically placed, and may lie in oblique or vertical planes. These basic arrangements are illustrated in Fig. 2.4.<sup>1,2,3,4</sup> A unique arrangement having cables lying in three independent vertical planes was proposed for the Danish Great Belt Bridge competition, Fig. 2.5.

### 2.2.1 SINGLE-PLANE SYSTEM

The single-plane cable arrangement is generally used with a divided roadway deck with the cables passing

through the median strip and anchored below the roadway. This arrangement is not only economical but aesthetically pleasing as well.

With the cables lying in the plane of the median strip, the motorists enjoy an unobstructed view of the natural scenery as they drive across the bridge. For conventional roadways very little additional width is required in the deck to accommodate the cables. However, for narrow median strips additional deck width may be required in order to allow sufficient space for the towers. A single-planar cable system requires sin-

**TABLE 2.1. Ratio of Larger Span to Total Length of Two-Span Structures**

| Structure                     | Larger Span |       | Total Length |       | Ratio |
|-------------------------------|-------------|-------|--------------|-------|-------|
|                               | ft          | m     | ft           | m     |       |
| Severin (West Germany)        | 987.5       | 301   | 1482.9       | 452   | 0.67  |
| Karlsruhe (West Germany)      | 574.1       | 175   | 958.7        | 292   | 0.60  |
| Kniebrücke (West Germany)     | 1049.9      | 320   | 1689.6       | 515   | 0.62  |
| Mannheim (West Germany)       | 941.6       | 287   | 1351.7       | 412   | 0.70  |
| Maya (Japan)                  | 457.3       | 139.4 | 685          | 208.8 | 0.67  |
| East Huntington (U.S.A.)      | 900         | 274.3 | 1508         | 460   | 0.60  |
| Batman (Australia)            | 689         | 210   | 853          | 260   | 0.81  |
| Bratislava (Czechoslovakia)   | 994.1       | 303   | 1240.2       | 378   | 0.80  |
| Weirton-Steubenville (U.S.A.) | 820         | 250   | 1508         | 460   | 0.54  |

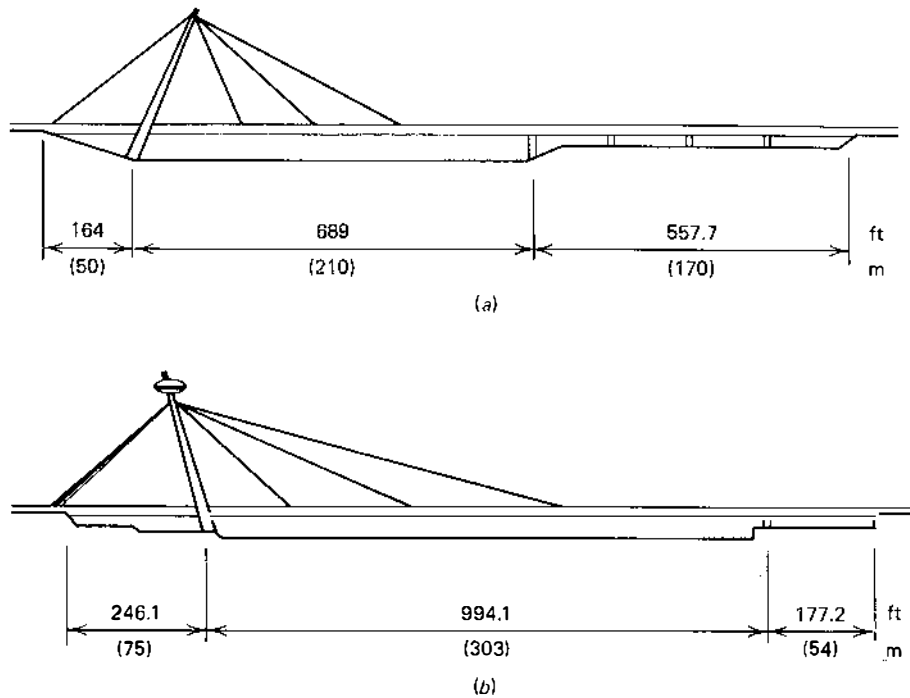


**FIGURE 2.2** Two-span cable-stayed bridge structures: (a) Batman, Australia; (b) Bratislava, Czechoslovakia.

gle towers or pylons at pier supports that are placed in the median strip, thus maintaining a minimum width of the roadway superstructure.

A possible disadvantage of the single-plane cable system is the fact that a relatively large concentrated cable force is transferred to the main superstructure

girder, thereby requiring a larger connection and girder to support the cable force. Additional reinforcement and stiffening of the deck, web plates, and bottom flange will normally be required in order to distribute the concentrated load uniformly throughout the cross section of the superstructure members.

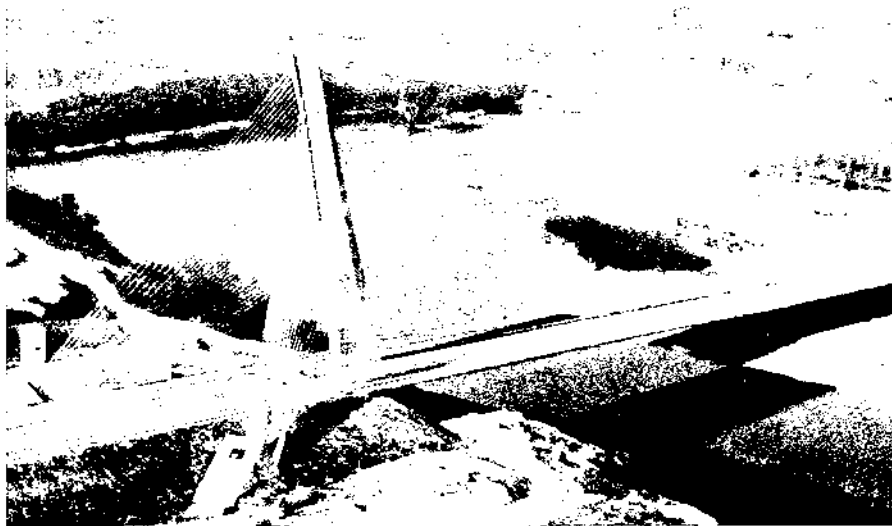


**FIGURE 2.3** Ebro River Bridge, Navarra, Spain. (Courtesy of Stronghold International, Ltd.)

TABLE 2.2. Ratio of Center Span to Total Length of Three-Span Structures

| Structure                       | Center Span |       | Total length |       | Ratio |
|---------------------------------|-------------|-------|--------------|-------|-------|
|                                 | ft          | m     | ft           | m     |       |
| Papineau (Canada)               | 787.4       | 240   | 1377.9       | 420   | 0.57  |
| Duisburg (West Germany)         | 1148.3      | 350   | 2148.9       | 655   | 0.53  |
| Rees (West Germany)             | 836.6       | 255   | 1519         | 463   | 0.55  |
| Bonn (West Germany)             | 918.6       | 280   | 1706         | 520   | 0.54  |
| Düsseldorf-North (West Germany) | 853         | 260   | 1561.7       | 476   | 0.55  |
| Leverkusen (West Germany)       | 918.6       | 280   | 1614.2       | 492   | 0.57  |
| Nordrhein (West Germany)        | 564.3       | 172   | 984.2        | 300   | 0.57  |
| Arakawa River (Japan)           | 524.9       | 160   | 920.6        | 280.6 | 0.57  |
| Suchiro (Japan)                 | 820.2       | 250   | 1542         | 470   | 0.53  |
| Onomichi (Japan)                | 705.4       | 215   | 1263.1       | 385   | 0.56  |
| Toyosato (Japan)                | 708.7       | 216   | 1236.9       | 377   | 0.57  |
| Strömsund (Sweden)              | 600.4       | 183   | 1086         | 331   | 0.55  |
| Sitka (U.S.A.)                  | 450         | 137.2 | 750          | 228.6 | 0.60  |
| Luling (U.S.A.)                 | 1235        | 376.4 | 2225         | 678.2 | 0.56  |
| Pasco-Kennewick (U.S.A.)        | 981         | 299   | 1794         | 546.8 | 0.55  |
| Menomonee Falls (U.S.A.)        | 217         | 66.1  | 361          | 110   | 0.60  |
| Sunshine Skyway (U.S.A.)        | 1200        | 366   | 2280         | 695   | 0.53  |
| Quincy (U.S.A.)                 | 900         | 274   | 1780         | 542.5 | 0.51  |
| Neches River (U.S.A.)           | 640         | 195   | 1480         | 451.1 | 0.43  |
| Dame Point (U.S.A.)             | 1300        | 396   | 2600         | 792   | 0.50  |

In a single-plane cable arrangement, the cables support vertical or gravity loads only. The torsional forces that develop because of the asymmetrical vehicular loading and/or wind forces must be resisted by a torsionally stiff box girder in order to transmit the unbalanced forces to the piers. These additional stiffness requirements for the superstructure may increase the costs, but these costs may be counterbalanced by the

advantages of simplified fabrication, erection, and added aesthetics.

Although the single-plane cable system has been used symmetrically, with respect to the longitudinal centerline, on vehicular bridges, it has been constructed off-center or asymmetrically for pedestrian bridges. In the asymmetrical applications, the plane of the cables is at the edge of the walkway. Because the

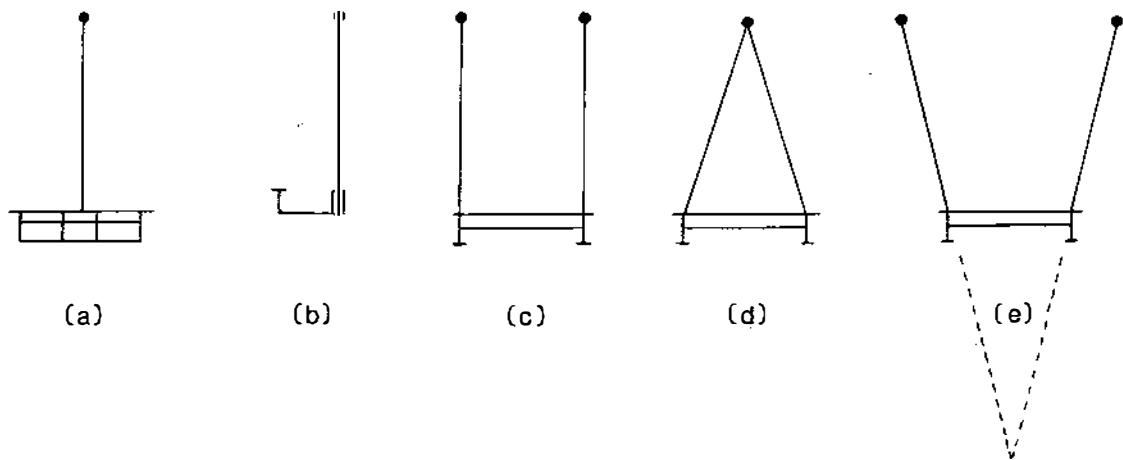


FIGURE 2.4 Transverse cable arrangement. (a) single-plane vertical, (b) single-plane vertical/lateral, (c) double-plane vertical, (d) double-plane sloping, (e) double-plane V-shaped.

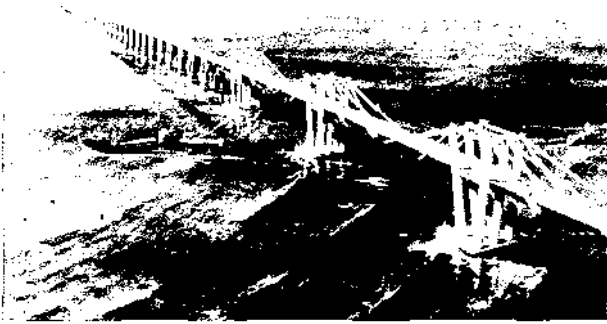


FIGURE 2.5 Danish Great Belt competition. (Courtesy of White Young & Partners.)

walkway loadings are small, the unbalanced system produces only small torsional forces that are easily resisted by the walkway structure.

### 2.2.2 DOUBLE-PLANE SYSTEM

The two principle double-planar cable systems are: one system consisting of a vertical plane located at each edge of the superstructure and another system in which the cable planes are oblique, sloping toward each other from the edges of the roadway and intersecting at the towers along the longitudinal centerline of the deck. In the double-plane oblique system the term "plane" is to be interpreted loosely. If the stays are connected at more than one level at the tower or if the roadway has any vertical or horizontal curvature each "plane" geometrically forms a warped surface in space. The tower in the oblique double-plane arrangement is generally of the A-frame type in order to receive the sloping cables that intersect along the centerline of the roadway.

Using the double-plane cable system, the anchorages may be located either on the outside of the deck structure or within the limits of the deck roadway. With the cable anchorages on the outside of the deck an advantage is gained, since no portion of the deck roadway is required for the connection fittings. A disadvantage is the fact that additional reinforcement may be required to transmit the eccentric cable loadings of shear and moment into the main girders of the superstructure.

For those applications in which the cable anchorage lies within the limits of the bridge deck, the overall width of the deck must be increased for the full length of the bridge in order to provide room for the anchorage fittings. This additional width of roadway deck

usually results in an increased cost for the superstructure.

The V-shaped double-plane system has been suggested by Ramiro Sofronie<sup>3,4</sup> as a means to reduce the tower height without changing the height ratios, avoiding the stay concentration on the tower tops and excluding any lateral sway of the girder deck. To the author's knowledge the only application of a similar system has been in pipeline cablestayed bridges.

### 2.2.3 TRIPLE-PLANE SYSTEM

A design for a three-plane cable system was submitted in competition for the Danish Great Belt Bridge by the English consulting firm of White, Young and Partners. The design requirements were for three lanes of vehicular traffic and a single rail line in each direction. The solution, illustrated in Fig. 2.5, employed three vertical planes of cables, one in the median strip and the other two on the exterior edges of the bridge deck. The concept is appropriate for use in urban areas, where it may be necessary to include mass transit center lanes or special bus lanes as well as three or four vehicular lanes in each direction.

## 2.3 Longitudinal Cable Arrangements

The arrangement of the cables in the longitudinal direction of the bridge may vary according to the designer's sense of proportion of clear spans and tower heights. For shorter span lengths a single fore stay and back stay may be sufficient to satisfy the loading requirements. For longer center and anchor spans a variety of cable arrangements satisfy not only the engineering requirements but result in a pleasing aesthetic geometrical configuration as well.

Basically, there are four cable configurations in general use throughout the world for cable-stayed bridges. The idealized arrangements are indicated in Fig. 2.6, and it may also be assumed that all the configurations or types are applicable to either the single- or double-planar cable systems. These basic systems are referred to as radiating, harp, fan, and star systems.

The radiating type, or a converging system, is an arrangement wherein the cables intersect or meet at a common point at the top of the tower, Fig. 1.30.

The harp type, as the name implies, resembles harp strings—the cables are parallel and equidistant from each other. The required number of cables are spaced uniformly along the tower height and, as a result, also

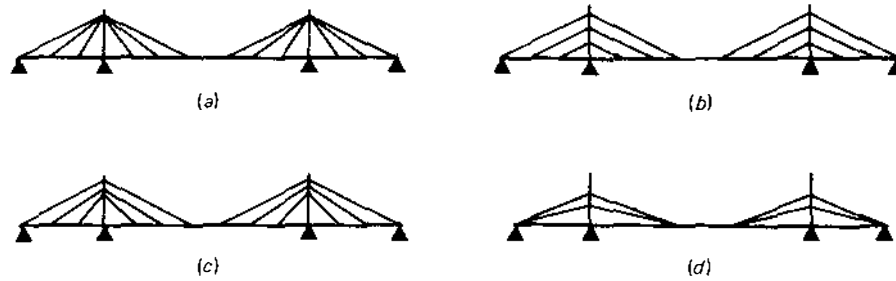


**FIGURE 2.6** Longitudinal cable arrangements: (a) radiating, (b) harp, (c) fan, (d) star.

connect to the roadway superstructure with equal spacings, Fig. 1.40.

The fan type is a combination of the radiating and the harp types. The cables emanate from the top of the tower with equal spacings and connect with equal spacings along the superstructure. Because of the small spacings concentrated near the top of the tower, the cables are not parallel, Fig. 1.34.

In the star arrangement, the cables intersect the tower or pylon at different heights and then converge on each side of the tower to intersect the roadway structure at a common point. The common intersection in the anchor span is usually located over the abutment or end pier of the bridge, Fig. 2.7.

The selection of cable configuration and number of cables is dependent on the length of span, type of loadings, numbers or roadway lanes, height of towers, economy, and the designer's individual sense of pro-

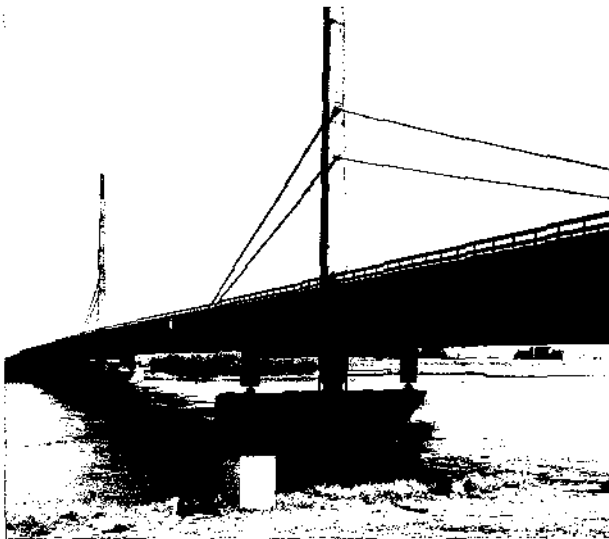


**FIGURE 2.7** Nordcrelbe. (Courtesy of Beratungsstelle für Stahlverwendung, H. Odenhausen.)

portion and aesthetics. As a result, some bridges have relatively few cable stays while others may have many stays intersecting the deck such that the cables provide a continuous elastic supporting system. Figure 2.8 illustrates the evolution of the number of cable stays.<sup>5,6</sup>

Cost factors have a great influence on the selection of the cable arrangements. Using only a few cable stays results in large cable forces, which require massive and complicated anchorage systems connecting to the tower and superstructure. These connections become sources of heavy concentrated loads requiring additional reinforcement of webs, flanges, and stiffeners to transfer the loads to the bridge girders and distribute them uniformly throughout the structural system.

When only a few cables support the deck structure, deep girders are required to span the long distance between the cable intersection points. A large number of stays simplifies the cable anchorages to the bridge girders and distributes the forces more uniformly throughout the deck structure without major reinforcements to the existing girders and floor beams. Therefore, a large number of cables can provide continuous support, thus permitting the use of a shallow depth girder that also tends to increase the stability of the bridge against dynamic wind forces.<sup>7</sup>

With numerous stays the erection of the superstructure deck can be simplified by balanced cantilever construction with each segment being supported by a stay (single plane) or a pair of stays (two planes) without auxiliary means. Thus the erection can be more economical.

Some engineers prefer the radiating cable arrangement—where all cables converge at the top of the tower—because the cable stays are at a maximum angle of inclination to the bridge girders. In this arrangement, the cables are nearly in an optimum position to support the gravity dead and live loads and simultaneously produce a minimum axial component acting on the girder system.<sup>8</sup>

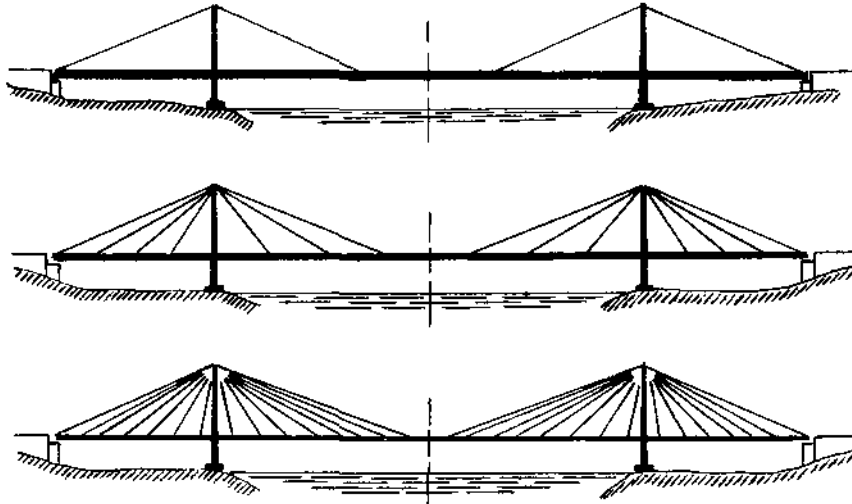


FIGURE 2.8 Evolution of number of supporting stay cables.

When using a double-plane cable system, the harp configuration may be preferred over the radiating type because it minimizes the visual intersection of cables when viewed from an oblique angle. Thus the motorist may find the harp system more attractive. The harp system, with the cable connections distributed throughout the height of the tower, results in an efficient tower design compared with the radiating system, which has all the cables at the top of the tower. The concentrated load at the top of the tower produces large shears and moments along the entire height of the tower, thus increasing its cost. In addition, the large concentrated cable force at the top of the tower usually presents difficulties in anchoring the cables to the tower or over a saddle, thus complicating the transfer of the vertical loads.

The fan arrangements represents a compromise between the extremes of the harp and radiating systems and is useful when it becomes difficult to accommodate all the cables at the top of the tower.

The star system has only been used on the Norderelbe Bridge in Hamburg, Fig. 2.7. The principal reason for its use is its unique aesthetic appearance. The additional tower height above the cable connection is purely decorative; it serves no structural purpose whatsoever. The cables are not distributed along the bridge deck, instead the cables on each side of the tower converge at the same point in the span. In this arrangement, two small cables function as a single large cable. The two cables can be more efficient to construct and the result in a more pleasing appearance than a single cable.

#### 2.4 Towers

The cable towers are often referred to as pylons, and these terms will be considered interchangeable in this text. Similar to the cable systems, the towers are of many shapes and varieties to accommodate different cable arrangements, bridge site conditions, design requirements, aesthetics, and economics.

In their simplest form, the towers may be a single cantilever to support a single-plane arrangement of cables, Fig. 1.36, or two cantilever towers to support the double-plane cable system, Fig. 1.25. The towers may be fixed or hinged at the base, depending on the magnitude of the vertical loads and distribution of cable forces along the tower height.

Other tower forms suitable for cable-stayed bridges are the portal frame, Figs. 1.22 and 1.30, and A-frame types, Fig. 1.33, either hinged or fixed at the base. The decision to use a fixed or hinged base for the tower connection either to the pier or the superstructure must be based on the magnitude and relationship of the vertical and horizontal forces acting on the tower. A fixed base induces large bending moments at the base of the tower, whereas a hinged base does not and may be preferred. However, the increased rigidity of the total structures resulting from the fixed base of the towers may offset the disadvantage of the large bending moments. Another consideration is that a fixed base may be more practical to erect and may be less costly than inserting a heavy pinned bearing, which requires the tower to be externally supported until the cables are connected. The design engineer and contractor should



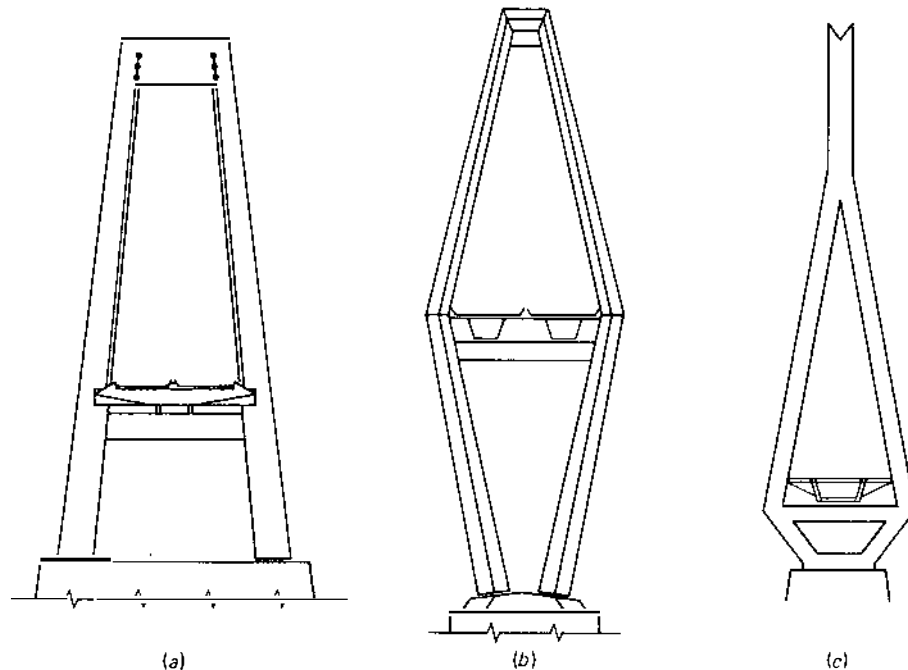


**FIGURE 2.9** Alternate tower types: (a) modified A-frame, (b) diamond, (c) modified diamond or delta.

discuss these considerations early in the design stage of the project in order to arrive at the most economical solution.

In selecting a specific type of tower, the designer must consider several factors. For example, when a large clearance is required below the superstructure, the A-frame has a decided disadvantage—a large pier width is required to accommodate the legs of the frame. In some instances a modified A-frame with a short top cross member may be the best solution considering all the factors involved, Figs. 2.9(a) and 1.33.

A variation of the A-frame is a narrow diamond-shaped tower with the roadway structure at the center of the diamond, Fig. 2.9(b). This form was selected for the proposed Southern Bay Crossing in San Francisco, Fig. 1.23.<sup>9,10</sup> A delta shape or modified diamond, Fig. 2.9(c), was used for the bridge at Köhlbrandbrücke, Hamburg, Germany. Imagination combined with engineering economics can produce many variations of tower designs, each type satisfying particular design conditions and requirements better than other conventional types. Familiarity with various construction methods and techniques can assist the design engineer and contractor to develop the best tower design.

When several long spans are required, the towers may be designed as two or more portal frames or A-frames or a combination of both. The towers of the

Maracaibo Bridge, Fig. 2.1(c), consist of two A-frames that support the cables and superstructure. The prize winning Great Belt Bridge, Fig. 2.5, has three portal frames that support the cables and deck structure. The portal frames are joined at the top by a cross member.

The towers are normally constructed of cellular sections and are fabricated of structural steel or reinforced concrete. The concrete towers are built where steel is in short supply and recourse is made to local natural materials. However, the trend recently has been toward concrete towers even with a structural steel superstructure deck because of the inherent qualities of concrete in compression. Details on fabrication and erection are discussed in Chapter 8.

The height of the tower is determined from several considerations, such as the relation of tower height to span length, the type of cable arrangement and the general aesthetic proportions of all the spans and towers visualized as an entity. The size and number of cables is determined by the geometrical configuration of the bridge and the type of loading to be imposed on the structure.

## 2.5 Cable System Summary

A tabular summary of the various cable arrangements is presented in Fig. 2.10<sup>11</sup>. This figure is a matrix of

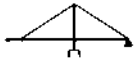












| Single  | Double  | Triple  | Multiple  | Combined   |           |
|---|---|---|---|--|-----------|
|  |  |  |  |  | Radiating |
|   |  |  |  |  | Harp      |
|   |  |  |  |  | Fan       |
|   |  |   |   |  | Star      |

FIGURE 2.10 Matrix of longitudinal configurations. (Adapted from reference 11.)

the four basic cable types and the number of cables extending from one side of the tower. It can be seen that many other variations and combinations are possible. Therefore, the cable-stayed bridge is not simply

one bridge type, but many different types based on an extremely versatile concept of bridge design.

A descriptive summary of some of the typical bridges that have been built is presented in Fig. 2.11.

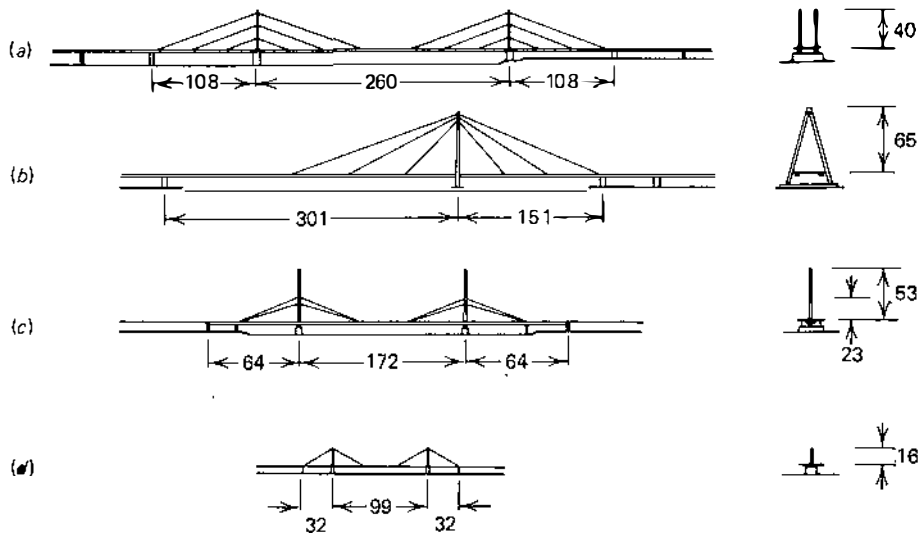


FIGURE 2.11 Cable-stayed roadbridges in Germany. (From reference 7, Leonhardt and Zellner, by permission of the Canadian Steel Industries Construction Council.) (a) Düsseldorf-North, 1958; (b) Cologne, 1960; (c) Hamburg, 1962; (d) Düsseldorf, 1963; (e) Leverkusen, 1964; (f) Karlsruhe, 1965; (g) Bonn, 1966; (h) Rees, 1967; (i) Ludwigshafen, 1968; (j) Kniebrücke-Düsseldorf, 1969; (k) Duisburg, 1970; (l) Mannheim, 1971; (m) Düsseldorf-Oberkassel, 1972. Cable-stayed roadbridges in different countries: (n) Strömsund (Sweden); (o) Maracaibo (Venezuela); (p) Saint-Florent (France); (q) Papineau (Canada); (r) Hawkshaw (Canada); (s) Batman (Australia); (t) Ganga-Bridge (India); (u) Onomichi (Japan); (v) Bratislava (Czechoslovakia). (Dimensions in meters).

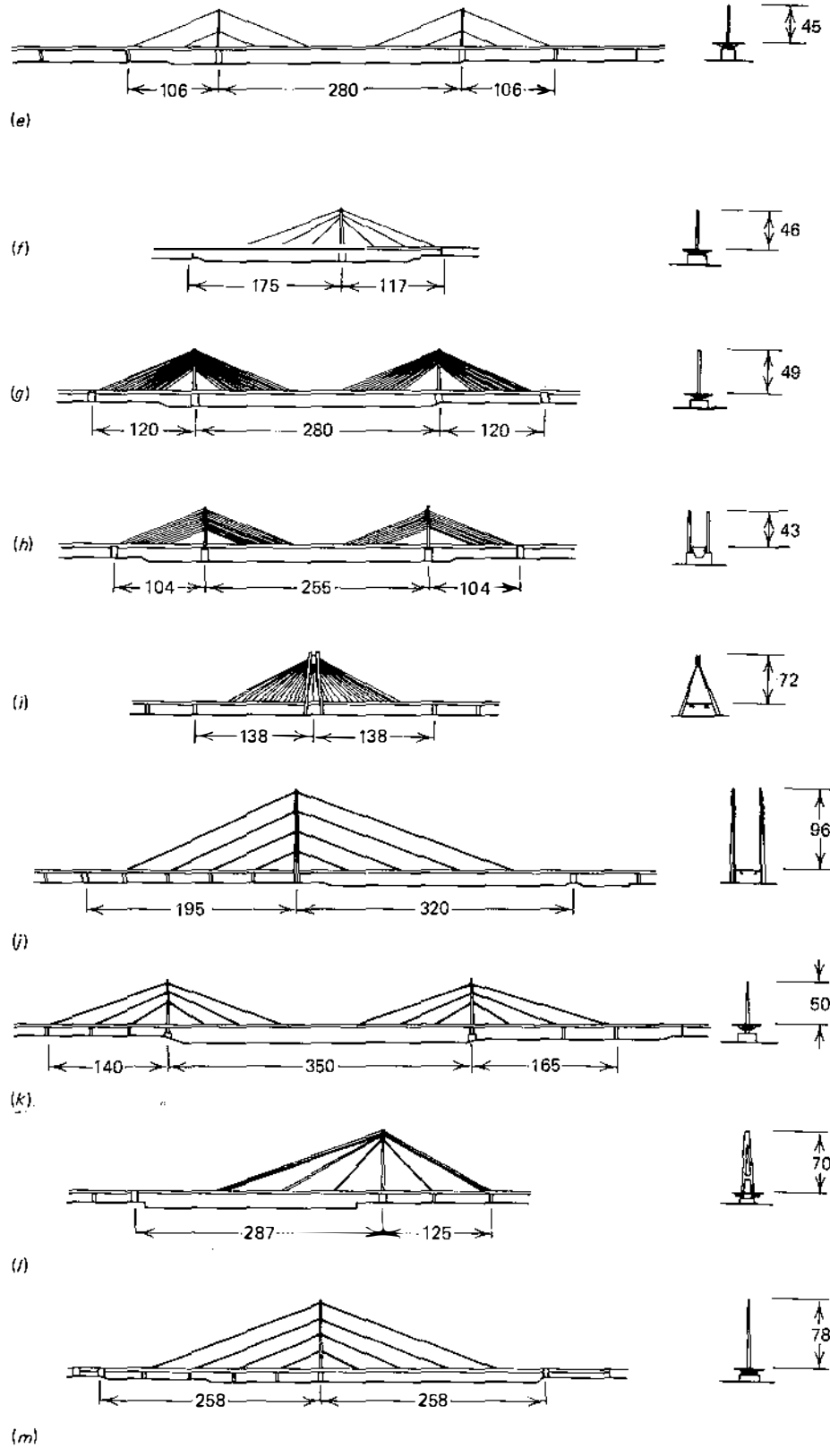


FIGURE 2.11 (Continued)

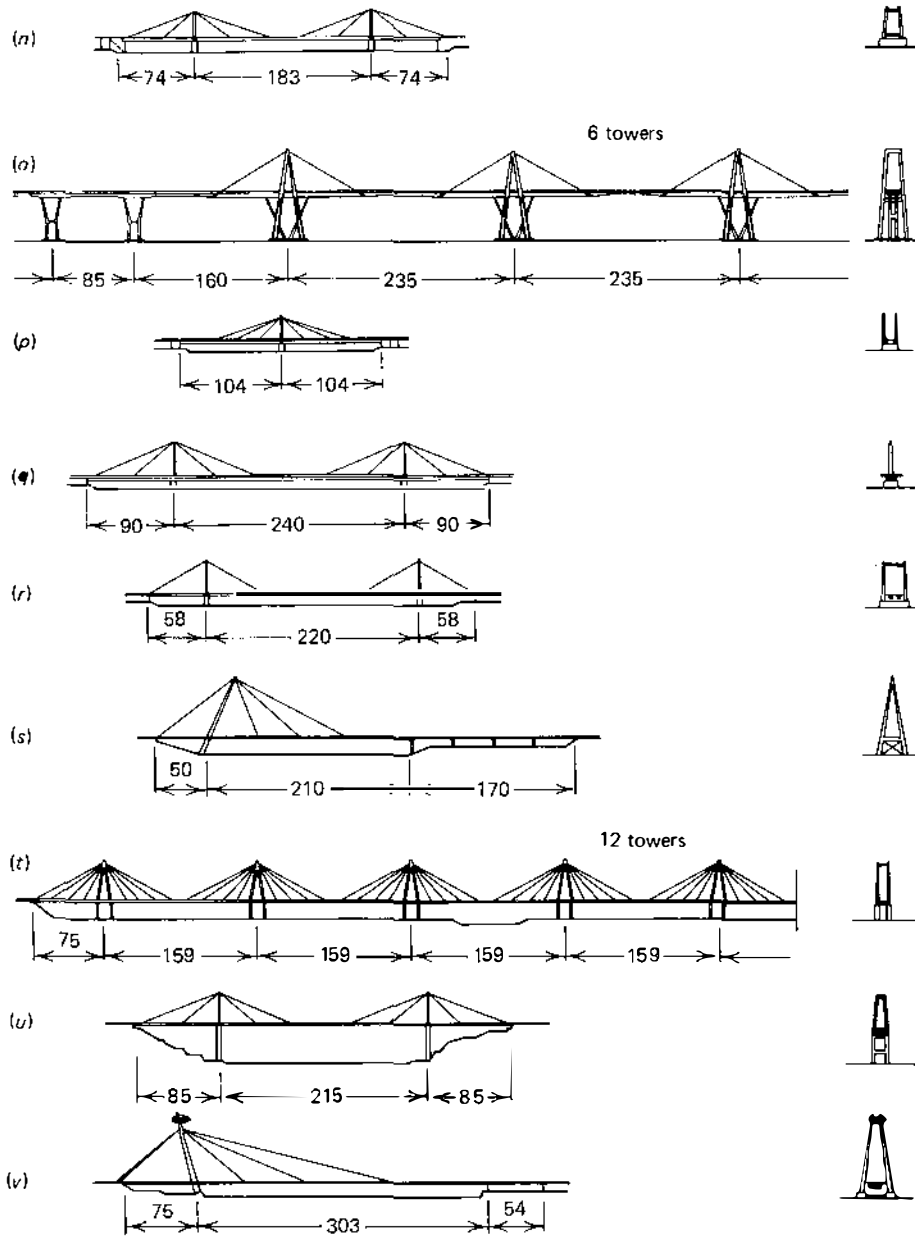


FIGURE 2.11 (Continued)

The illustrations indicate the longitudinal cable arrangements and whether the system lies in single-, double-, or oblique-plane configuration. The type of tower is also indicated by the transverse section for each bridge.

### 2.6 Superstructure Types

The superstructures for cable-stayed bridges take as many forms as there are structural systems. Basically,

however, two types of girders have been used most frequently: the stiffening truss and the solid web types. Past experience with the two systems indicates that the stiffening truss type is seldom used in current designs. The stiffening trusses require more fabrication, are relatively more difficult to maintain, are more susceptible to corrosion, and are somewhat unappealing aesthetically.

Solid web girders for various types of structural steel bridge deck cross sections are illustrated in Fig. 2.12.<sup>8, 12</sup> The range of cross sections includes the basic

## Bridge Component Configurations

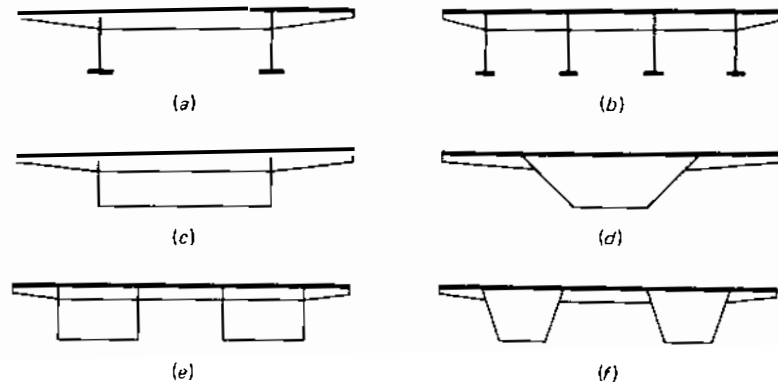


**FIGURE 2.12** Structural steel girder types: (a) twin I-girders, (b) multiple I-girders, (c) rectangular box girders, (d) trapezoidal box girder, (e) twin rectangular box girder, (f) twin trapezoidal box girder.

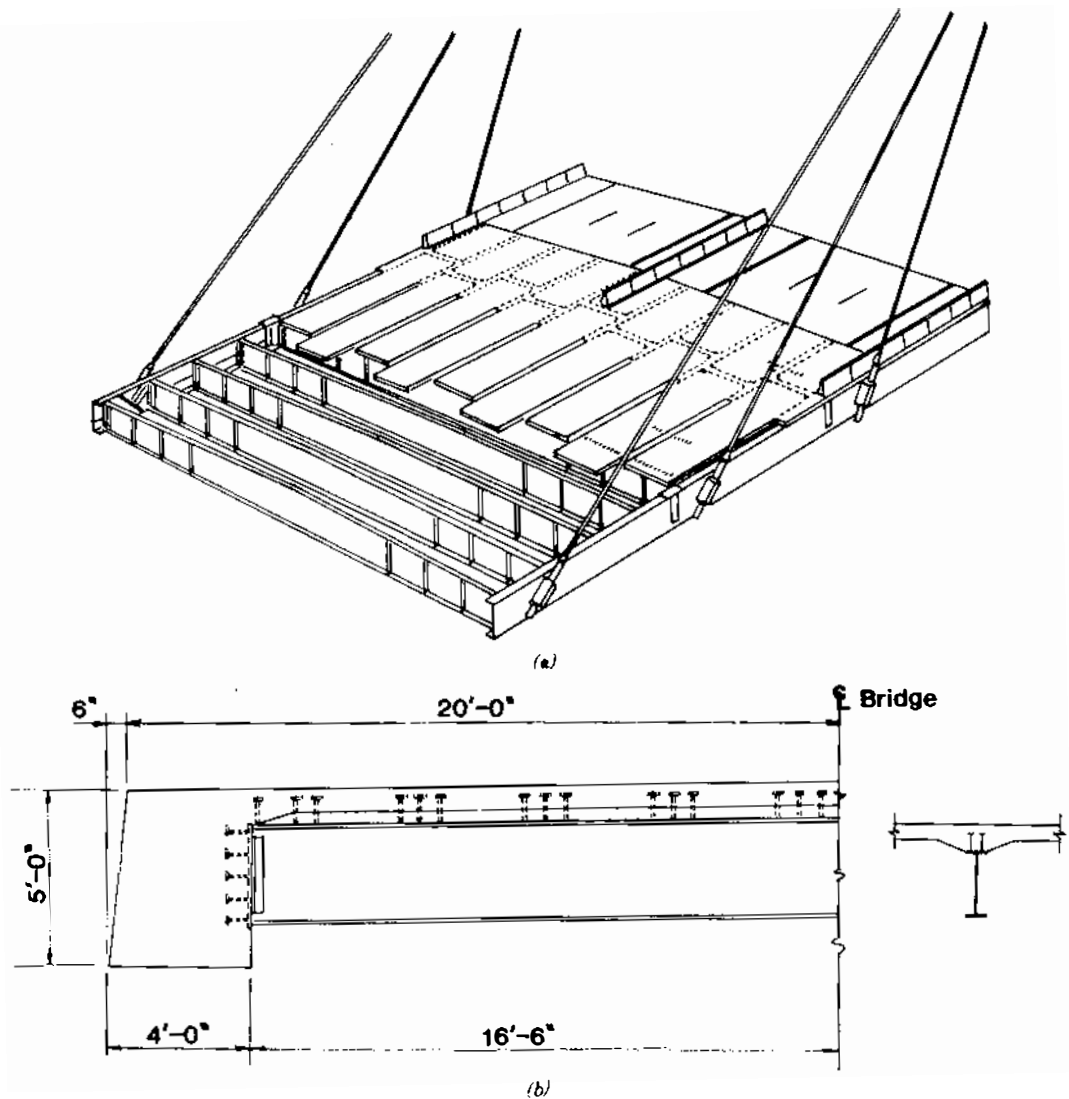


**FIGURE 2.13** Composite superstructure girders of cable-stay bridges: (a) James River isometric, (b) East Huntington cross section.

two-main-plate girders or multiple-plate girders, Fig. 2.12(a) and 2.12(b). These arrangements have the disadvantage of a low value for torsional rigidity.

An increase in torsional rigidity is achieved by using box-type cross sections, Fig. 2.12(c) and 2.12(d). They may range from the single-cell or multicell box with rectangular sides to similar trapezoidal type with sloping sides. In each of these types the roadway width extends beyond the edges of the single boxed girders.

When the roadways require a large number of traffic lanes, the transverse width requires several box-girder systems to support the deck structure, Fig. 2.12(e) and 2.12(f). Twin boxes, either of the rectangular or trapezoidal shapes, have been used to advantage when large deck widths are required.

However, in recent years structural steel box girders incorporating an orthotropic deck have not been economically successful in competition with segmental concrete box girders. As a result there has been a trend toward structural steel composite concrete deck construction as illustrated in Fig. 2.13(a) with two cable-stay planes. A similar concept was used for the unsuccessful steel alternate of the Sunshine Skyway Bridge in Florida, however, it was within approximately 2% of the successful concrete bid, indicating its competitiveness. The same or a similar concept was proposed for the steel alternate design of the I-295 James River Bridge crossing in Virginia, is proposed for the Talmadge Memorial Bridge in Savannah, Georgia, and is being used for the Weirton-Steuben-

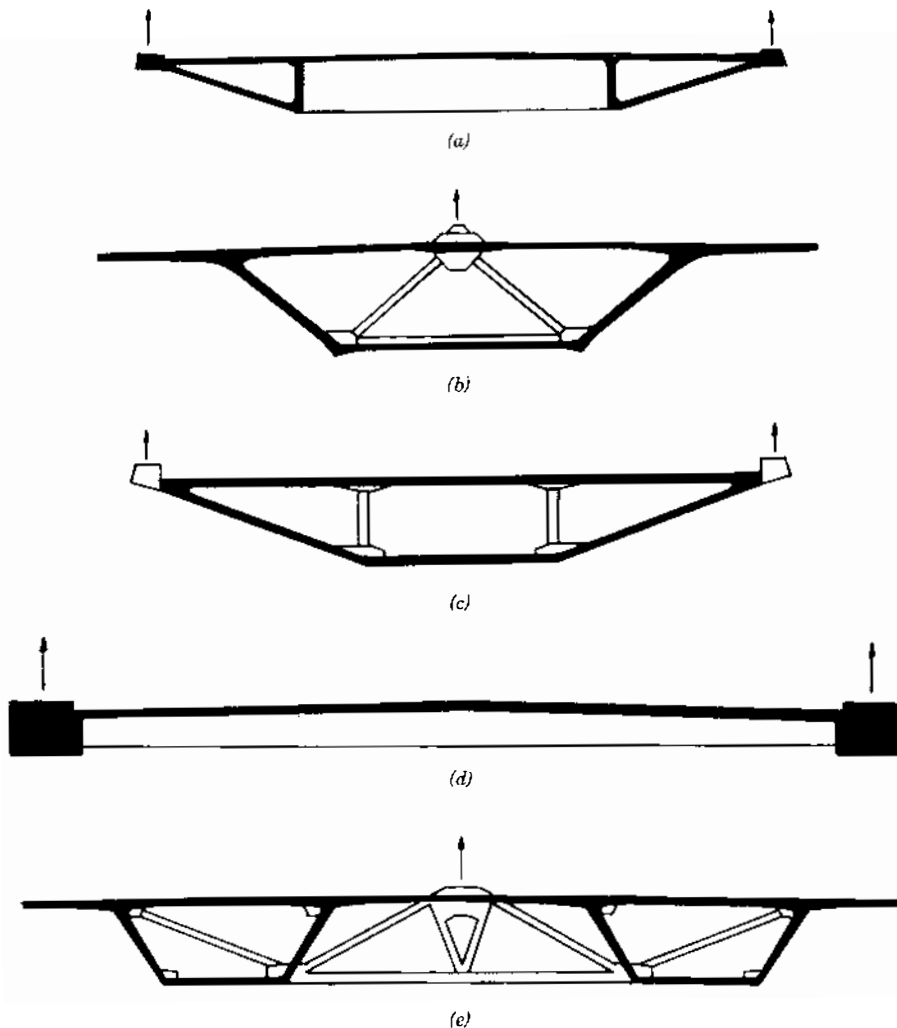


**FIGURE 2.14** Concrete superstructure girders of cable-stay girders: (a) Pasco-Kennewick Bridge, Washington, (b) Sunshine Skyway Bridge, Florida, (c) Neches River Bridge, Texas, (d) Dame Point Bridge, Florida, (e) James River Bridge, Virginia and proposed Cooper River Bridge, South Carolina.

TABLE 2.3. Girder-Depth-to-Span Ratio

| Structure                            | Transverse<br>Cable<br>Planes | Number of<br>Cable<br>Spans | Longitudinal<br>Cable<br>Configuration | Girder<br>Depth/<br>Span |
|--------------------------------------|-------------------------------|-----------------------------|--|--------------------------|
| Strömsund (Sweden, 1955)             | 2                             | 3                           | Converging                             | 1/51                     |
| Brucksal (West Germany, 1956)        | 2                             | 3                           | Converging                             | 1/53                     |
| Nordbrücke (West Germany, 1958)      | 2                             | 3                           | Harp                                   | 1/81                     |
| Severin (West Germany, 1959)         | 2                             | 2                           | Fan                                    | 1/66                     |
| Elbe (West Germany, 1962)            | 1                             | 3                           | Star                                   | 1/57                     |
| Shinno (Japan, 1963)                 | 2                             | 2                           | Converging                             | 1/40                     |
| Jülicherstrasse (West Germany, 1964) | 1                             | 3                           | Converging                             | 1/60                     |
| Leverkusen (West Germany, 1965)      | 1                             | 3                           | Harp                                   | 1/64                     |
| Maxau (West Germany, 1966)           | 1                             | 2                           | Fan                                    | 1/62                     |
| Maya (Japan, 1966)                   | 1                             | 2                           | Fan                                    | 1/50                     |
| Ludwigshafen (West Germany, 1967)    | 2                             | 2                           | Converging                             | 1/55                     |
| Rees (West Germany, 1967)            | 2                             | 3                           | Harp                                   | 1/73                     |
| Bonn (West Germany, 1967)            | 1                             | 3                           | Fan                                    | 1/61                     |
| Onomichi (Japan, 1968)               | 2                             | 3                           | Converging                             | 1/67                     |
| Knicbrücke (West Germany, 1969)      | 2                             | 2                           | Harp                                   | 1/100                    |
| Papineau-Leblanc (Canada, 1969)      | 1                             | 3                           | Converging                             | 1/67                     |
| Toyosata (Japan, 1970)               | 1                             | 3                           | Fan                                    | 1/72                     |
| Arakawa (Japan, 1970)                | 1                             | 3                           | Harp                                   | 1/67                     |
| Ishikari (Japan, 1972)               | 2                             | 3                           | Fan                                    | 1/80                     |
| Sitka harbor (U.S.A., 1973)          | 2                             | 3                           | Single-stay                            | 1/75                     |
| Brotonne (France, 1977)              | 1                             | 3                           | Fan                                    | 1/84                     |
| Pasco-Kennewick (U.S.A., 1978)       | 2                             | 3                           | Converging                             | 1/140                    |
| Luling (U.S.A., 1983)                | 2                             | 3                           | Converging                             | 1/87                     |
| East Huntington (U.S.A., 1985)       | 2                             | 2                           | Fan                                    | 1/180                    |
| Sunshine Skyway (U.S.A.)             | 1                             | 3                           | Fan                                    | 1/82                     |
| Weirton-Steubenville (U.S.A.)        | 2                             | 2                           | Fan                                    | 1/95                     |
| Neches River (U.S.A.)                | 2                             | 3                           | Harp                                   | 1/80                     |
| Quincy (U.S.A.)                      | 2                             | 3                           | Fan                                    | 1/120                    |
| Dame Point (U.S.A.)                  | 2                             | 3                           | Harp                                   | 1/260                    |

ville Bridge across the Ohio River in West Virginia. The successful concrete alternate for the East Huntington Bridge in West Virginia is composed of segments consisting of concrete edge girders and a concrete deck slab composite with structural steel floor beams, Fig. 2.13(b). When the design considers composite action between the deck and its supporting members, regardless of whether the main edge girders are concrete or steel, this text will classify such structures as composite (see Chapter 6).

Concrete superstructure girders of cable-stayed bridges completed, under construction, or proposed in the United States are illustrated in Fig. 2.14.

The proportion of the girder depth to the length of span from a survey of 29 cable-stayed bridges, Table 2.3, indicates a ratio that varies from 1/40 to 1/279. The Knicbrücke Bridge, Fig. 2.11(j), a two-span asymmetrical structure achieves its high girder-depth-to-span ratio of 1/100 by anchoring the back stays to

the girder directly over the piers. This method of anchoring the back stays produces a greater stiffness in the main span, thus permitting the shallow girder. The Pasco-Kennewick, East Huntington, Quincy, and Dame Point Bridges are all two-stay planes with multistays or relatively short spacing along the superstructure. The depth-to-span ratios for these structures range from 1/120 to 1/260, clearly indicating the influence of multistays closely spaced.

### References

1. Podolny, W., Jr. and Fleming, J. F., "Historical Development of Cable-Stayed Bridges," *Journal of the Structural Division*, ASCE, Vol. 98, No. ST 9, September 1972, Proc. Paper 9201.
2. Podolny, W., Jr., "Cable-Stayed Bridges," *Engineering Journal*, American Institute of Steel Construction, First Quarter, 1974.

3. Sofronie, Ramiro, "The V-Shaped Cable-Stayed Bridges," *Mécanique Appliquée*, Tome 26, No. 5, September-October, 1981, Académie De La République Socialiste De Roumanie, Bucarest.
4. Sofronie, Ramiro, "Equal Stay Cable Bridge System," *Mécanique Appliquée*, Tome 27, No. 3, May-June, 1982, Académie De La République Socialiste De Roumanie, Bucarest.
5. Leonhardt, F., "Latest Developments of Cable-Stayed Bridges for Long Spans," *Særtryk af Bygningsstatistiske Meddelelser*, Vol. 45, No. 4, Denmark, 1974.
6. Leonhardt, F. and Zellner, W., "Cable-Stayed Bridges," *IABSE Periodica 2/1980*, IABSE Surveys S-13/80, May 1980.
7. Leonhardt, F. and Zellner, W., "Cable-Stayed Bridges: Report on Latest Developments," *Proceedings of the Canadian Structural Engineering Conference, 1970*, Canadian Steel Industries Construction Council, Toronto, Ontario, Canada.
8. Simpson, C. V. J., "Modern Long Span Steel Bridge Construction in Western Europe," *Proceedings of the Institution of Civil Engineers*, 1970 supplement (ii).
9. Seim, C. F., Larson, S., and Dang, W., "Design of the Southern Crossing Cable-Stayed Girder," *Preprint 1352*, ASCE National Water Resources Engineering Meeting, Phoenix, Arizona, January 11-15, 1971.
10. Seim, C. F., Larson, S., and Dang, W., "Analysis of Southern Crossing Cable-Stayed Girder," *Preprint 1402*, ASCE National Structural Engineering Meeting, Baltimore, Maryland, April 19-23, 1971.
11. Feige, A., "The Evolution of German Cable-Stayed Bridges—An Overall Survey," *Acier-Stahl-Steel* (English version), No. 12, December 1966, reprinted *AISC Journal*, July 1967.
13. Feige, A., "Steel Motorway Bridge Construction in Germany," *Acier-Stahl-Steel* (English version), No. 3, March 1964.



# 3

## *Economic Evaluation*

|     |   |    |
|-----|---|----|
| 3.1 | INTRODUCTION                                      | 36 |
| 3.2 | BIDDING PROCEDURES                                | 36 |
|     | 3.2.1 Single Design                               | 37 |
|     | 3.2.2 Design and Build                            | 37 |
|     | 3.2.3 Value Engineering                           | 37 |
|     | 3.2.4 Alternate Designs                           | 38 |
|     | 3.2.5 Summary Remarks on Bidding Procedures       | 39 |
| 3.3 | ECONOMIC STUDIES                                  | 40 |
| 3.4 | ECONOMIC COMPARISONS IN THE UNITED STATES         | 44 |
|     | 3.4.1 Sitka Harbor Bridge                         | 44 |
|     | 3.4.2 Luling Bridge                               | 46 |
|     | 3.4.3 Pasco-Kennewick Bridge                      | 46 |
| 3.5 | RESULTS OF ALTERNATE BIDDING IN THE UNITED STATES | 49 |
|     | REFERENCES  | 50 |

nomics of the total structure until sufficient data is available to make general decisions quickly.

The contractor also lacks specific data on which to base cost estimates and must rely on the detailed design drawings and written specifications for this basic information. Therefore, to arrive at a realistic cost estimate, it is advisable for the designer and contractor to communicate ideas at an early stage in the design process. The method of fabrication and erection can affect both the design and the costs and may decide whether the cable-stayed bridge is the most economical one or not. Contractors must be willing to study and evaluate various methods of erection in order to arrive at a meaningful cost estimate.

### *3.1 Introduction*

The selection of a specific type of bridge to cross a river, ravine, or highway is not an automatic determination. Many factors must be considered before a final decision is made. In some instances, the factors affecting the design are similar to, if not the same as, those previously considered at another location or site, so several bridges of the same type are chosen.

The principal factors to be considered are the relationship of span lengths of various segments of the bridge, the number of piers and placement for safety, the aesthetic considerations for the site, and, finally, the relative cost of bridges of comparable acceptable proportions and type.

Many types of bridges share similar aesthetic and safety considerations, but relative costs of bridges depend on the number and length of spans and number of piers that affect the method of construction. Studies of comparative costs of cable-stayed bridges and other types of bridges are few; consequently, a design engineer must perform a detailed investigation of the eco-

### *3.2 Bidding Procedures*

A bridge design should on principle be economical and as a practical matter must fall within budgetary restrictions of a particular project. The economic "moment of truth" for a given bridge design occurs when bids are received and evaluated.

In a basically stable economy where material and labor costs are predictable within relatively small fluctuations, the selection of structure type and materials is relatively straightforward. This situation prevails when the time required for the design is relatively short and thus is not affected by economic cycles, or, if the design time is relatively long, the economic cycles are mild. In an inflationary economy there is no economic stability, and designers are hard put to make rational choices, as they have no control over economic parameters that can influence their design decisions. In short, the problem is whether economic assumptions made during the course of design are valid at the time of bidding.

Obviously, the design and the bidding (tendering) of a project are closely related. Contractual bidding procedures vary from country to country, and current economic pressures are leading to changes in these procedures. The various bidding methods used in various countries can be broadly categorized (with some possible variations) as follows: (1) single design, (2) design and build, (3) value engineering, and (4) alternate designs.

### 3.2.1 SINGLE DESIGN

Heretofore, single design was the major method used in North America and Great Britain. In this method, in general, design drawings prepared for bid are very detailed, to the extent that even the length and other dimensions of every reinforcing bar may be given. The bidding period is followed by a tight construction schedule. The contractor bids and executes the project in strict accordance with the bidding documents. No variation from the documents is allowed unless an error in design is discovered, or a specific detail proves impractical to consummate, or geological perturbations are discovered that differ from what was assumed in design and delineated in the contract documents. These changes are authorized by a change order, and if there is an increase in cost the contractor is paid an "extra."

This system worked well for many years when the economy was fairly stable and predictable when economic changes were gradual over an extended period. Its disadvantage is its lack of flexibility to accommodate an inflationary economy, sudden price changes in materials, a rapidly advancing technology, and the current emergence of specialty contractors with unique equipment or skills, proprietary designs, and patented construction methods. Its biggest advantages are ease in administering the contract and absolute control over the final design.

### 3.2.2 DESIGN AND BUILD

In some European countries, by contrast, bid documents are prepared with the intention that the contractors will prepare and submit their own detailed design for the project. Thus, bid plans will be more general and, for a bridge, may show only span lengths, profile, and typical sections. The contractors may then refine the original design or submit an alternate design of their own choice, the responsibility for producing the final design and details being theirs rather than the

engineer's. This procedure allows the contractors to use any special equipment or technique at their disposal. For example, a cast-in-place concrete box may be substituted for a steel superstructure where the contractor has special know-how in concrete construction, or the change may be less drastic and involve only a reduction in the number of webs in a box girder.

Verification of the adequacy of the contractor's final design is generally carried out by a "proof engineer" who is retained by the owner or is on the owner's engineering staff. In order to minimize disagreements between the contractor and the proof engineer, European codes have been made very specific. As a result, European contractors usually maintain large in-house engineering staffs, although they may also use outside consultants. The outcome apparently is a savings in construction cost, achieved by the investment of more design time and effort than in the single-design method.

The advantage of the design-and-build method is that in an atmosphere of engineering competition, innovative design and construction practices advance very rapidly. The state of the art of designing and constructing bridges advances in response to the need for greater productivity. The disadvantage is the lack of control over the selection of the type of structure and its design. There is some concern, too, that quality of construction may suffer as a consequence of overemphasis on productivity and initial cost. However, the contractors are usually required to produce a bond and guarantee their work over some period of time, and any defects that surface during this period have to be repaired at their expense. Whether such a system could be adopted in the United States is debatable.

### 3.2.3 VALUE ENGINEERING

Value engineering is defined by the Society of American Value Engineering as

... the systematic application of recognized techniques which identify the function of a product or service, establish a value for that function, and provide the necessary function reliability at the lowest overall cost. In all instances the required function should be achieved at the lowest possible life-cycle cost consistent with requirements for performance, maintainability, safety, and esthetics.<sup>1</sup>

In 1962 the concept of value engineering became mandatory in all U.S. Department of Defense armed services procurement regulations (ASPR). Before this time value engineering had been applied to materials, equipment, and systems. The advent of ASPR pro-

visions introduced value engineering concepts to two of the largest construction agencies in the United States: The U.S. Army Corps of Engineers and the U.S. Navy Bureau of Yards and Docks. Soon thereafter the U.S. Bureau of Reclamation and the General Services Administration (GSA) adopted and inserted the value engineering clauses in their construction contracts, and the U.S. Department of Transportation established a value engineering incentive clause to be used by its agencies.

Several value engineering clauses (or incentive clauses) are in use today by many agencies. In general, they all have the following features<sup>1</sup>.

1. A paragraph that defines the requirements of a proposal: it must require a change to the contract and it must reduce the cost of the contract without impairing essential functions.
2. A "documentation" paragraph that itemizes the information the contractor should furnish with each proposal. It should be comprehensive enough to ensure quick and accurate evaluations, detailed enough to reflect the contractor's confidence in its practicability, and refined to the point where implementation will not cause undue delay in construction operations. Careful development of this paragraph and meticulous adherence to its requirements will preclude scatter-shot proposals by the contractor and burdensome review by the agency.
3. A paragraph on "submission." This paragraph details the procedure for submittal.
4. A paragraph on "acceptance," which outlines the right of the agency to accept or reject all proposals, the notification a contractor may expect to receive, and appropriate reference to proprietary rights of accepted proposals.
5. A paragraph on "sharing," which contains the formula for determining the contract price adjustment if the proposal is accepted and sets forth the percentage of savings a contractor may expect to receive.

As generally practiced by highway agencies in the United States, a value engineering proposal must indicate a "substantial" cost savings. This is to preclude minor changes such that the cost of processing offsets the savings to be gained. Some other reasons for which a value engineering proposal may be denied are as follows:

Technical noncompliance.

Delay in construction such that the cost savings would be substantially nullified.

Proposed change would require resubmission of the project for any number of various permits, such as environmental impact statement, wetlands permit, and navigation requirements. Resubmission would in all probability delay construction and nullify any cost savings.

Savings resulting from a value engineering proposal are generally shared equally by the agency and the contractor, after an allowance for the contractor's development cost, the agency's cost in processing the proposal, or both. As practiced in the United States all contractors must bid on the design contained in the bid documents, and only a low bidder on the base bid is allowed to submit a value engineering proposal. This is, of course, value engineering's biggest disadvantage. Any number of contractors may have more-cost-effective proposals that they are not allowed to submit because they were not low bidder on the base bid. Its advantage is that to some degree it allows contractor innovation to be introduced.

#### 3.2.4 ALTERNATE DESIGNS

Alternate designs, as it is developing in the United States, basically is an attempt to produce a hybrid system consisting of the best elements of the single-design and the design-and-build methods. It attempts to accomplish the following:

Retain for the authorizing agency control over the "type selection" of the structure and its design.

Provide increased competition between materials (structural steel versus concrete or prestressing strand versus bars) or construction procedures (cast-in-place versus precast segmental or balanced cantilever versus incremental launching, and so on)

Provide contractor flexibility (construction procedures, methods and/or expertise)

This method has developed, with encouragement from the Federal Highway Administration (FHWA), as an anti-inflationary measure to combat dramatic increases in highway construction costs.

A policy statement<sup>2</sup> published by the FHWA states the following:

1. Preliminary plan developed for major bridges should be based on engineering and economic evaluation of acceptable alternate designs.

2. Alternate designs should consider the utilization of competitive materials and/or structural types.
3. Economic evaluation of preliminary estimates should take into consideration, to the maximum extent possible, the relative accuracy of estimates for state-of-the-art type methods of construction.
4. When comparative economic estimates are reasonably close to each other, two or more complete sets of contract documents should be prepared and advertised.
5. Value engineering at the design stage should be strongly encouraged.
6. Options should be considered for structure components (piling, expansion joints, bearings, prestressing systems, etc.).
7. FHWA approvals will be based on the need to ensure safe, efficient and cost effective bridge projects which meet the aesthetic and structural requirements of the site and are based on the latest, proven technology and techniques.

This document of policy further states that "This policy is written with the intent of taking advantage of the evolving state-of-the-art of bridge construction and fluctuating economic conditions in the market place while not compromising sound engineering, safety, quality control, or aesthetics."

### 3.2.5 SUMMARY REMARKS ON BIDDING PROCEDURES

All of the bidding procedures described previously have one thing in common: they all attempt to produce the lowest initial cost by competition in construction and/or design. All of the last three approaches (design-and-build, value engineering, and alternate designs) require decisions based on comparisons of basic structural materials, structure types, construction methods, and so on. This implies that the basic premise in the selection process is equivalency—comparable service, performance, and life-cycle cost of the facility.

Life-cycle costs refer not only to initial cost, but also to maintenance and any rehabilitation costs during the life of the structure. True cost of the project must be considered. What may be initially least expensive may in the long run, when future costs are accounted for, be actually most expensive. Some newer structure types and designs are at the fringe of the state of the art and have only been used in the United States within the last decade or less. Thus, an adequate background of experience is unavailable to evaluate life-cycle costs. The estimation of life-cycle costs may be difficult in

many cases, such as for new and progressive bridge designs. Functionally, alternative structures are designed to the same criteria. Only years of operational experience can provide the data base for reasonably estimating life-cycle costs and thereby true equivalency in design insofar as cost is involved. However, the problem of adequacy of data does not diminish the importance of the question and the need to attempt to answer it.

Another anti-inflationary measure used in recent years is that of stage construction. This concept may take one of two forms. Major structures, because of their size, lend themselves to stage construction—that is, separate substructure and superstructure contracts. Usually several years will elapse between bidding and awarding of the substructure contract and the superstructure contract. The economic superstructure span range for different alternative types and materials is a variable. In this form of stage construction the substructure is let first; thus the spans for the superstructure design become fixed. This may or may not impose an economic disadvantage to specific superstructure alternates. The substructure must be designed for the largest self-weight superstructure alternative, which may or may not be the successful superstructure alternative. It appears that this form of stage construction may be to some extent self-canceling or counterproductive to cost savings. With a total alternative design package, the substructure (foundation, piers, span arrangement) can also have alternatives commensurate with the superstructure alternatives.

The other form of stage construction concerns a large project, containing many bridges, that is subdivided for bidding purposes into a number of smaller projects. Its primary purpose is to encourage small contractors by providing projects of manageable size, thus increasing competition. However, certain construction techniques, by virtue of the investment in sophisticated casting or erection equipment, require a certain volume of work to amortize the equipment and be competitive. Depending on the size of the subdivided contract, this form of stage construction in some instances may also become counterproductive.

The value-engineering concept can be divided into two major areas of application: during design and during construction. Value-engineering procedures in the design stage may result in very specific recommendations based on a certain set of assumptions at a particular point in time for the design. If conditions change during the interval between the design decision and the actual construction, which can be several years, conditions on which the assumptions were based may have changed. Such changes could make the original

value-engineering decision incorrect. The alternative-design concept, on the other hand, does not make all such specific design decisions at an early stage but retains some options in order to allow a later response to changed conditions. Therefore, there is an apparent incompatibility between the application of value-engineering principles in the design stage and the concept of alternative designs for bidding purposes. However, the concept of value engineering is a powerful tool and can be made compatible with the concept of alternative designs if its principles are used to determine whether a given project should require alternative designs and, if so, what structure types should be considered as equivalent alternates.

### 3.3 Economic Studies

The open competitive design system that exists in West Germany has produced numerous feasibility studies that have resulted in actual construction of many cable-stayed bridges. The bridges have main spans ranging in length from 500 to 1200 ft. This span range was determined to be economical in the postwar period when many damaged bridges were replaced.

Often a survey and study of existing bridges can reveal meaningful data with respect to the general application of a particular type of bridge and the geometrical proportions best suited to that application. In his survey of the bridges in West Germany, Thul<sup>3</sup>

compared the center span length to the total length of the bridge for three-span continuous girder bridges, cable-stayed bridges, and suspension bridges, Fig. 3.1. This investigation may be considered a general study on the economical range of applications for the various types of bridges surveyed.

Limits of economical application appear to be 700 ft for the center span of a three-span continuous girder bridge, with ratios of center span to total length ranging from 30 to 50%. The suspension bridge begins to be economical for a center span of 1000 ft, with a ratio of center span to total length ranging from 60 to 70%. The cable-stayed bridge fills the void left by the continuous girder and suspension bridges in the range of center span from 700 to 1000 ft, with a corresponding center-to-span-total-length range of 50 to 60%.

In his comparative study, Thul has shown that the cable-stayed concept can be economical for bridges with intermediate spans. However, with greater experience in design and construction, the application of longer main spans of cable-stayed bridges has increased. Because other studies have indicated that longer center spans for cable-stayed bridges are possible, the supremacy of the conventional suspension bridge may well be challenged.

In another study of the economics of cable-stayed bridges with respect to other bridge types, a comparison was made of the weight of structural steel in pounds per square foot of roadway deck versus center span length. The study was made for girder bridges,

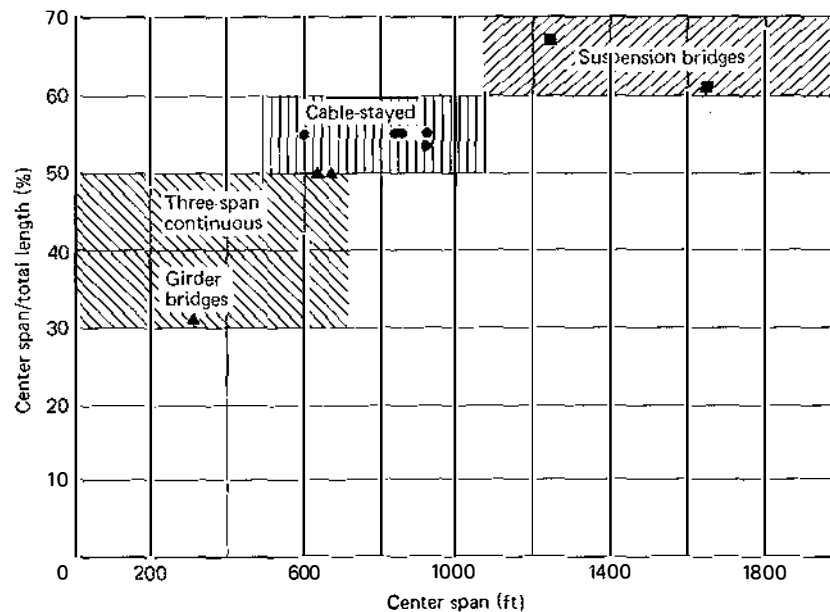
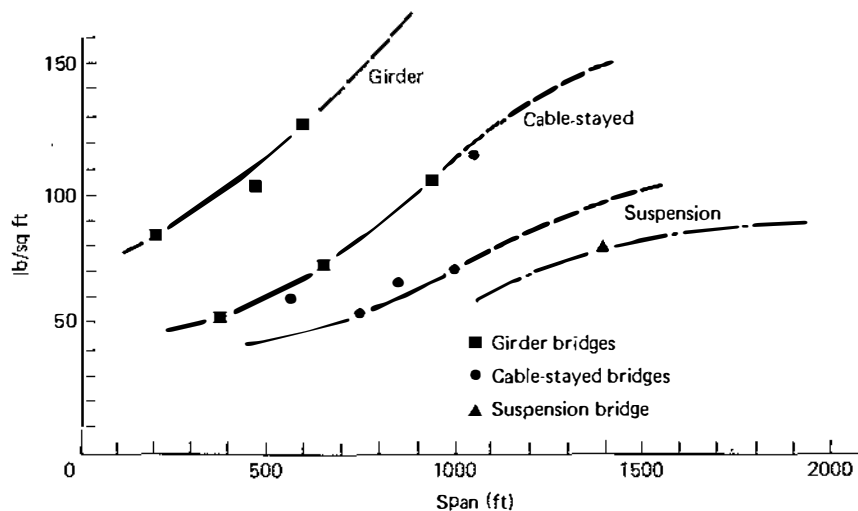


FIGURE 3.1 Bridge type span comparison (Courtesy of the British Constructional Steelwork Association, Ltd., from reference 3.)



**FIGURE 3.2** Weight of structural steel in lb/ft<sup>2</sup> of deck for orthotropic steel bridges (Courtesy of Engineering Journal (Canada), from reference 4.)

suspension bridges, and cable-stayed bridges using an orthotropic steel superstructure. The data are presented graphically in Fig. 3.2 and are the result of a study by P. R. Taylor, a Canadian engineer.<sup>4</sup>

A comparison of steel deck weights indicates that the cable-stayed bridge again fills the void between the continuous girder and suspension bridges. The data for the girder bridges fall into two distinct paths and may be the result of the different methods of design and different arrangements of the cross-sectional girders. Taylor recognized the difference in the ratio of material to labor costs in Europe and North America and concluded that for Canadian highways cable-stayed bridges with center spans ranging from 700 to 800 ft were 5 to 10% more economical than other types of comparable bridges.

Limited experience to date has indicated that cable-stayed bridges with center spans less than 500 ft are most suitable for pedestrian bridges. The total economical range of the various types of cable-stayed highway and pedestrian bridges has not been fully examined. Therefore, it is incumbent upon designers and contractors to develop the necessary data by careful study and evaluation of each new application as it presents itself. The general economy appears to be present but, for the moment, it must be evaluated separately for each individual application.

The economic survey by Taylor, Fig. 3.2, has a reference point for a cable-stayed bridge that is higher than one would expect for the magnitude of center span. It appears that this singular point is apparently based on the data taken from the Knickbrücke Bridge at Düsseldorf, Fig. 2.11(j), which is an asymmetrical

bridge with one tower. The data in Fig. 3.2 is for a center span of 1050 ft with a corresponding weight of deck structural steel of 115 pounds per square foot.

If the Knickbrücke Bridge were considered to be one-half of a symmetrical two-tower arrangement, with a center span of approximately 2000 ft, and the data replotted against previous data, Fig. 3.3, a different conclusion may be drawn.<sup>5</sup> The cable-stayed bridge is then seen to compete favorably with the suspension bridge of comparable center span. From this limited study it appears reasonable to assume optimistically that cable-stayed bridges may penetrate the complete range of spans now dominated by suspension bridges. In fact, the feasibility of a cable-stayed bridge with a center span of approximately 2000 ft is being considered in some preliminary bridge designs. Improved and imaginative methods of construction may tip the economic scale in favor of the cable-stayed bridge.

When Thul<sup>6</sup> wrote: "It is considered highly unlikely or unrealistic to build bridges with very long spans using cable-stayed construction. Such span lengths will be reserved for suspension bridges because there are considerable difficulties in construction of cable-stayed bridges," he apparently did not foresee the effects of improved technology and modern techniques of erection and construction, as perceived by Leonhardt.<sup>7,8,9</sup> Leonhardt concluded that cable-stayed bridges are particularly suited for spans in excess of 2000 ft and may even be constructed with spans of more than 5000 ft.

Dubrova<sup>10</sup> has presented some interesting data on the economies of nine types of bridge construction in the Soviet Union. Dubrova evaluated five concrete and

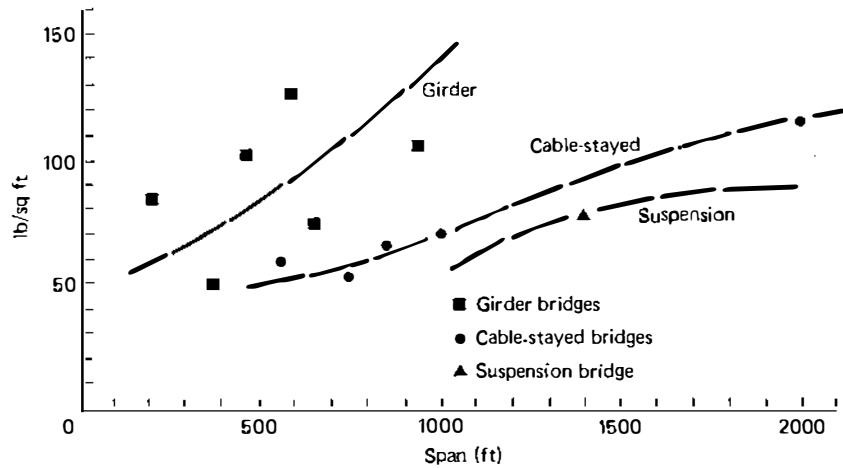


FIGURE 3.3 Weight of structural steel in lb/ft<sup>2</sup> of deck for orthotropic steel bridges, from reference 5.

four steel bridges. The concrete bridges are cable-stayed, arch-cantilever, arch, rigid frame suspension, and continuous. The continuous type consists of box-girder construction erected by the cantilever method. The arch-cantilever is constructed as a cantilever for dead load and pin-connected at midspan for live load shear transfer without moment resistance. When moment capability is built into midspan connection, the structure reacts as an arch for live loads. The rigid frame suspension bridge is constructed as a cantilever with a drop-in suspended center section. The steel bridges are cable-stayed, conventional suspension, arch, and a continuous type.

Although the relative costs of construction in the

Soviet Union differ from the costs in the United States, the economic study by Dubrova is useful in developing a comparative relationship of the relative costs of the various types of bridges.

Dubrova's economic evaluation included the costs of the piers and the erection procedures combined with the cost of the superstructure. The study of the costs of the different erection methods, illustrated in Fig. 3.4, indicates a variation of 300% between the cantilever and pontoon assemblies. The plot indicates a decided advantage for the cantilever method of construction.

Another study was concerned with the amount of concrete used in the superstructure as a function of the

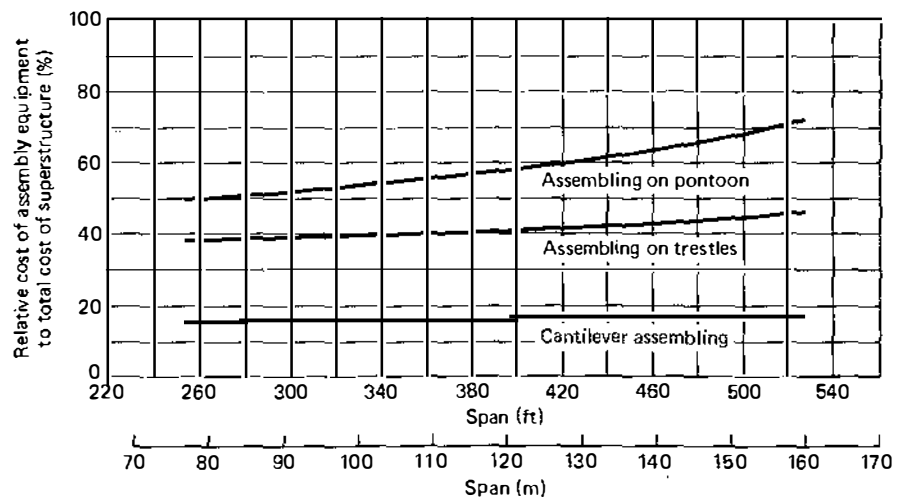


FIGURE 3.4 Relation of assembly equipment and total cost to span of bridge, from reference 10.

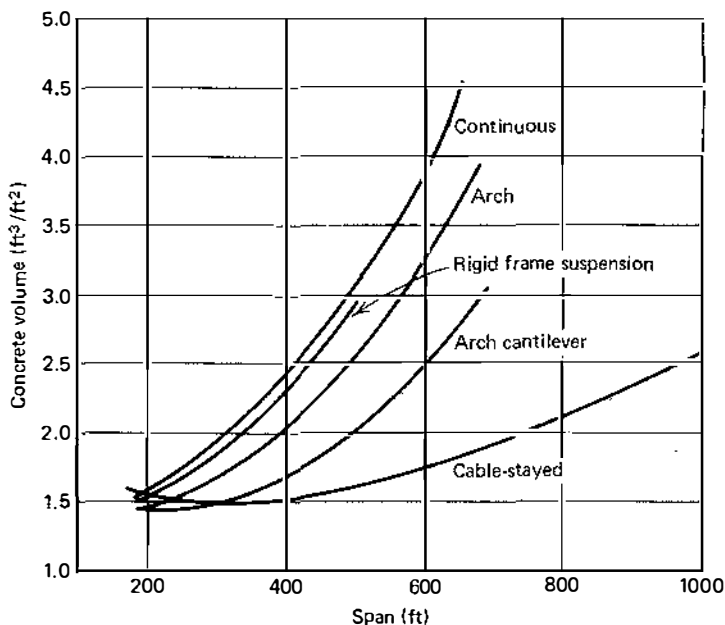


FIGURE 3.5 Concrete superstructure volume versus span of bridge, from reference 10.

span length. A graphical representation, Fig. 3.5, indicates the volume of concrete per square foot of bridge deck plotted against the span length of the bridge.

For the span length investigated, ranging from 200 to 1000 ft, the cable-stayed bridge required the least volume of concrete. The other types of bridges in order of least concrete usage are arch-cantilever, arch, rigid frame suspension, and continuous. The variation in concrete volume required for the various bridge types indicates a big difference between the lightest cable-

stayed system and the continuous system, especially as the span lengths increase beyond 800 ft.

An investigation of similar bridge types using a structural steel superstructure is illustrated in Fig. 3.6. The plot indicates the amount of steel in pounds per square foot of bridge surface versus span lengths ranging from 200 to 1800 ft. As in the previous study of concrete usage, the cable-stayed system is the most economical in the span range of 600 to 1000 ft, and the conventional system becomes the most economical

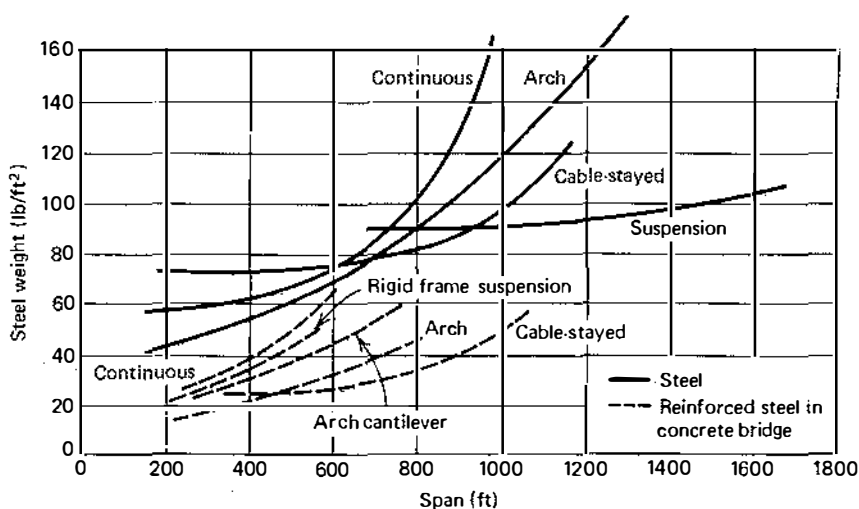


FIGURE 3.6 Steel superstructure weight versus span of bridge, from reference 10.



beyond the 1000-ft span length. The other types follow a similar ranking order with respect to concrete usage, Fig. 3.5.

The data based on the current costs of design and construction appear to reinforce the concept that suspension bridges are the most economical for the longer spans. However, Leonhardt indicated that cable-stayed bridges can be directly competitive with the classical suspension bridge when innovative methods of design and construction are considered. Figure 3.6 also indicates the amount of reinforcing steel used in the five bridges plotted in Fig. 3.5. The steel weight relationships follow very closely the concrete relationships with the exception of the interchange of the arch and arch-cantilever bridges.

A separate study of the amount of concrete required for the piers of various types of bridges is illustrated in Fig. 3.7. The plot indicates the volume of pier concrete in cubic feet per square foot of bridge deck versus span lengths ranging from 150 to 1000 ft. The figure is a composite; it includes the bridges with both steel and concrete superstructures. The solid lines are steel structures and the dashed lines represent the concrete superstructure.

As evidenced in the previous studies, the cable-stayed and suspension systems are the most economical for both types of superstructures. Furthermore, this study indicates that these systems require less pier volume for the complete range of span lengths. Evidently, this fact is the result of less total weight for the superstructures.

When Dubrova combined the cost data relationships for the individual components he determined the total cost of the bridge in terms of the unit area of

the bridge deck, Fig. 3.8. As one would expect, the cable-stayed and suspension system show up as the most economical types. The cable-stayed system falls in the range of span lengths from 400 to 1000 ft and the suspension system takes over beyond the 1000-ft span.

Dubrova's investigation in terms of current bridge construction practices in the Soviet Union indicates that continuous box girders erected by the cantilever method are most economical for the range of spans from 150 to 500 ft. The cable-stayed system with a concrete superstructure is most economical to 800 ft, while the cable-stayed system with a steel superstructure is economical to a span of 1000-ft. Beyond the 1000-ft span length the classical suspension bridge becomes the most economical type.

However, it is important to bear in mind that these are idealized studies assuming current costs and methods, which are ever-changing and influence the designs chosen. Designers and contractors should be alert to constant innovations in bridge design and construction methods. What may appear to be standard practice one day may become obsolete the next day as a result of imaginative and innovative contractors and designers.

### 3.4 Economic Comparisons in the United States

#### 3.4.1 SITKA HARBOR BRIDGE

The economic feasibility study for the Sitka Harbor Bridge considered six different types of bridges before a final decision was made to adopt the cable-stayed

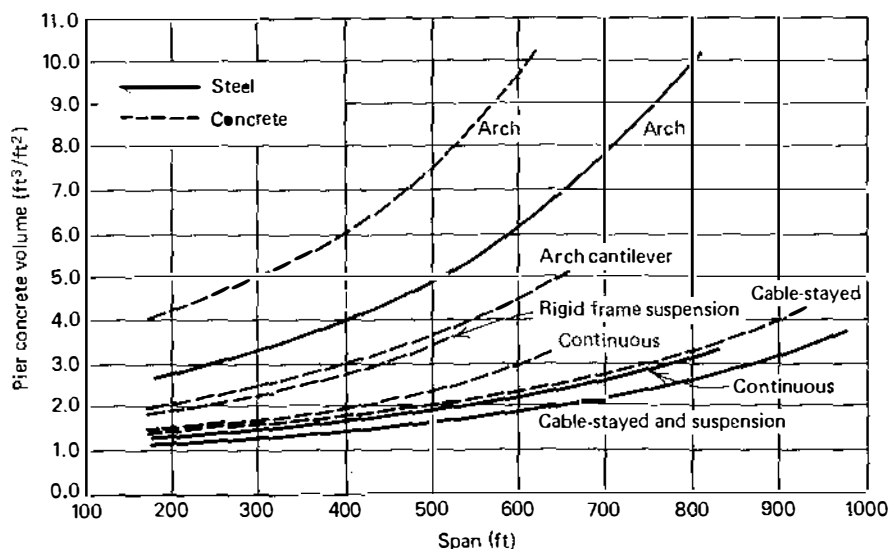
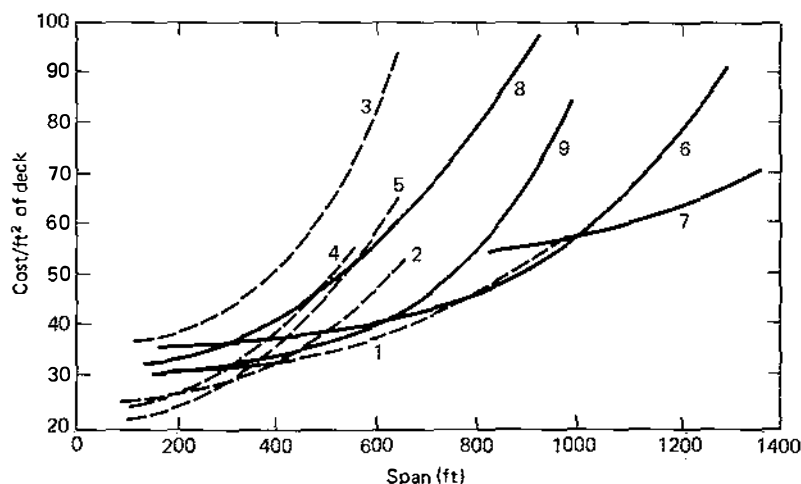


FIGURE 3.7 Pier concrete volume versus span of bridge from reference 10.



**FIGURE 3.8** Cost per ft<sup>2</sup> deck versus span, from reference 10. Concrete: (1) cable-stay, (2) arch cantilever, (3) arch, (4) rigid frame suspension, (5) continuous. Steel: (6) cable stay, (7) suspension, (8) arch, (9) continuous.

system. The various bridge types evaluated are indicated in Table 3.1, which ranks the types on a relative basis using the cable-stayed system as a base of 1.00.

Gute<sup>11</sup> discusses the advantages and disadvantages of each type studied in order to arrive at a comparable value for each type.

The plate girder system classified as Type I required a main span of 250 ft (76 m) which had to be skewed in order to accommodate the fender system along the sides of the navigation channel. Because the piers and fenders would be in 52 ft (15.8 m) of water this was the most expensive system. Other considerations that detracted from the Type I system included the expected difficulty of maintaining the fender system which would ultimately become an unsightly wall, especially at low tide. A second consideration for this bridge was the idea of increasing the main span to 450 ft (137 m), which would move the main piers out of the deep water and beyond the limits for navigation thus eliminating the fenders. However, the cost would still be high as a result of the long main span.

Bridge Types II and III had spans of 300, 450, and

300 ft (91.4, 137.0, and 91.4 m). This turned out to be too long and, therefore, too costly for the continuous plate girder. The orthotropic deck box girder, Type III, was calculated to be 4% higher than the cable-stayed system. However, its shortcoming is the large depth of girder required a midspan. Design considerations indicated a midspan depth for the superstructure to be 14 ft (4.3 m) compared to a 6-ft (1.8-m) depth required for the tied arch and cable-stayed system. The difference of 8 ft (2.4 m) would be reflected in a lower cost for the approaches because of the reduction in the grade line. This added cost must be included as a part of the cost of the total bridge structure and approaches.

The possible use of a through truss or cantilever truss was discounted on the basis of expected maintenance difficulties in a sea atmosphere and because it would be less aesthetically appealing at that particular site.

Types IV, V, and VI make use of small short piers and reduced side spans of 150 ft (46 m). The two tied arch systems would require high superstructures in the

**TABLE 3.1.** Sitka Harbor Bridge—Cost Study

| Type | Description               | Cost Ratio (Cable-Stayed Girder = 1.00) |
|------|---------------------------|---|
| I    | Plate girder with fenders | 1.15                                    |
| II   | Plate girder continuous   | 1.13                                    |
| III  | Orthotropic box girder    | 1.04                                    |
| IV   | Through tied arch         | 1.04                                    |
| V    | Half through tied arch    | 1.06                                    |
| VI   | Cable-stayed box girder   | 1.00                                    |

center of the channel, which also serves as the approach path for seaplane operations. The possible hazards eliminated these types from further consideration. In view of all the considerations and cost factors, the cable-stayed bridge system was finally selected. The actual cost of the cable-stayed bridge was \$1,900,000, which is \$52 per square foot of deck surface. Representative prices include \$145 per cubic yard for Class A concrete, 22¢ per pound for reinforcing steel, 46¢ per pound for structural steel, and \$1.63 per pound for cables and fittings.

### 3.4.2 LULING BRIDGE

The feasibility design by Modjeski and Masters<sup>12, 13</sup> for the Luling Bridge in Louisiana, Fig. 1.33, considered several bridge types: conventional suspension, steel cantilever, and cable-stayed. The study indicated that the cable-stayed bridge, with center spans of 1600 to 2100 ft, is the most favorable type for these locations. The results of the economic feasibility study is indicated in Fig. 3.9 as the total project cost in millions of dollars versus the main span length.

The plot permits a convenient comparison of the three types of bridges for a six-lane roadway and a four-lane roadway. It is to be noted that the total project cost for the six-lane suspension bridge is signifi-

cantly higher than the cantilever or cable-stayed systems. The cost differential between the cantilever and cable-stayed systems is negligible and both are acceptable. For the four-lane roadway, the cable-stayed bridge has the decided cost advantage compared with either the suspension or cantilever types.

The high cost of the conventional suspension bridge compared with the cantilever and cable-stayed types is primarily attributable to the cost of the substructure. These high costs are for the cable anchorages and foundations required and are greatly affected by the relatively poor soil conditions present in the Mississippi River delta. As a result of the study and the close economical comparison of the cantilever and cable-stayed bridges the final selection was based on the importance of other related factors in each type of bridge and the particular location.

### 3.4.3 PASCO-KENNEWICK BRIDGE

The economic evaluation of this structure considered five alternate structural designs:

1. Constant-depth steel plate girders with a precast composite deck
2. Cable-stayed girder with a deck constructed of precast concrete.

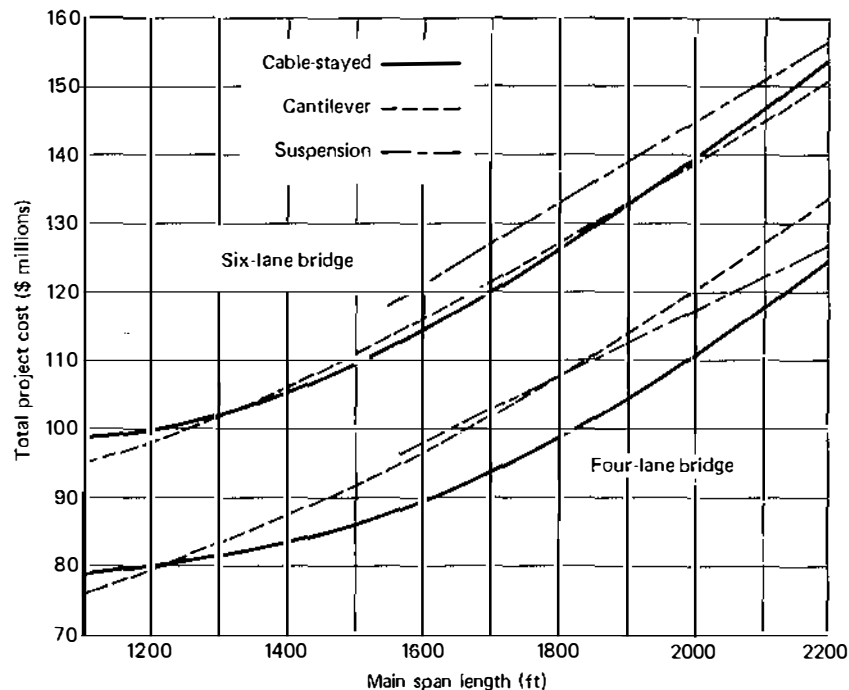


FIGURE 3.9 Comparative construction cost estimate, Luling Bridge. (Courtesy of T. Robert Kcalcy, From references 12 and 13.)

3. Continuous constant-depth posttensioned concrete box girder, constructed on shore and pushed into position.
4. Variable-depth posttensioned concrete box girder constructed segmentally by the cantilever method.
5. Asymmetrical steel box girder cable-stayed main span with concrete box-girder approach span

Studies were based on an approximate overall length of structure of 2480 ft, four traffic lanes and two side-walks, and a minimum vertical navigation clearance of 50 ft above the 50-year flood level over a horizontal channel distance of 350 ft. It is to be noted that after a final choice was made some minor changes were made in the design.

The previously mentioned alternates were considered the most feasible and were studied in detail. Other alternates were studied but were then discarded as unfeasible. These included steel orthotropic plate deck girders, cable-stayed steel orthotropic plate girders, and various span configurations of steel plate girders combined with steel or concrete girder approach spans

A brief description of the five principal alternates as presented by the consultants, Arvid Grant and As-

sociates, Inc., in professional collaboration with Leonhardt and Andra, in their preliminary design report<sup>14</sup> are summarized in the following.

The steel plate girder design, alternate 1, Fig. 3.10(a) consisted of eight continuous spans with expansion joints only at the abutments. Span arrangement starting at the Pasco abutment was 149-310-328-423-3 at 328-265 ft for a total length of 2468 ft. The superstructure consisted of four lines of girders 20 ft on centers with a constant depth of 15 ft. Fixed bearings were located at the piers adjacent to the center 432-ft span with all other bearings being expansion bearings. The deck was envisioned as precast units posttensioned longitudinally before being made composite with the deck.

The preliminary design for alternate 2, Fig. 3.10(b), contemplated an overall length of structure of 2484 ft. The 1797-ft main unit was to be supported by a cable stay configuration radiating from the pylons in two vertical planes. The deck structure was continuous from abutment to abutment, with expansion joints only at the abutments. Parallel wire strands supported the precast deck every 27 ft. The deck was only 7 ft deep and consisted of continuous triangular box beams at

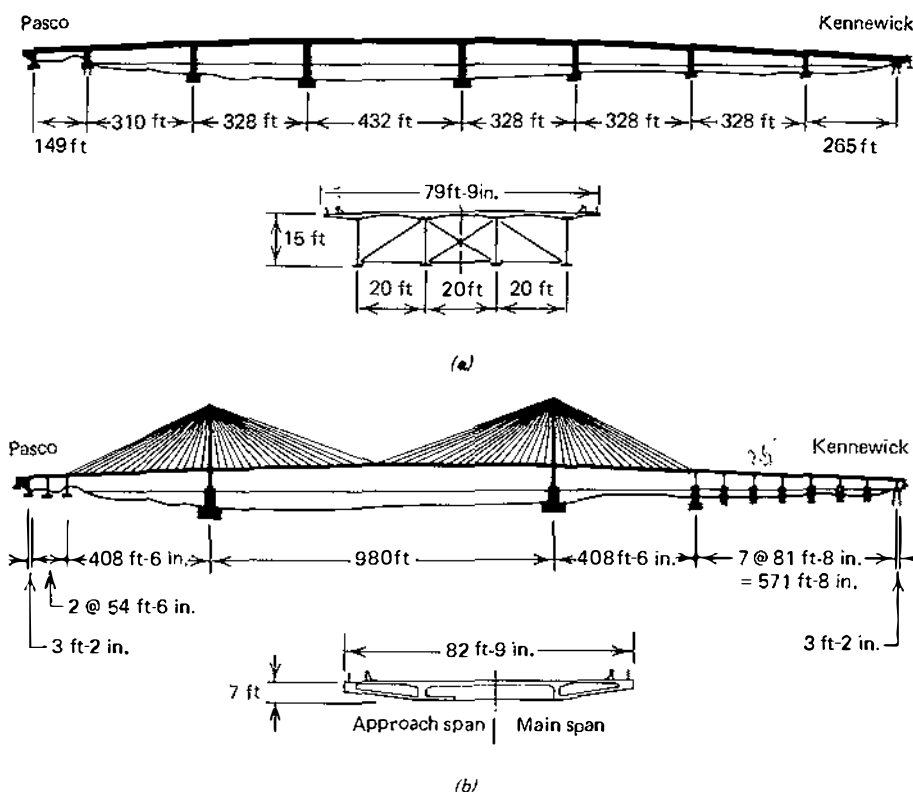


FIGURE 3.10 Pasco-Kennecock Bridge, from reference 14, (a) alternate 1, (b) alternate 2, (c) alternate 3, (d) alternate 4, (e) alternate 5.

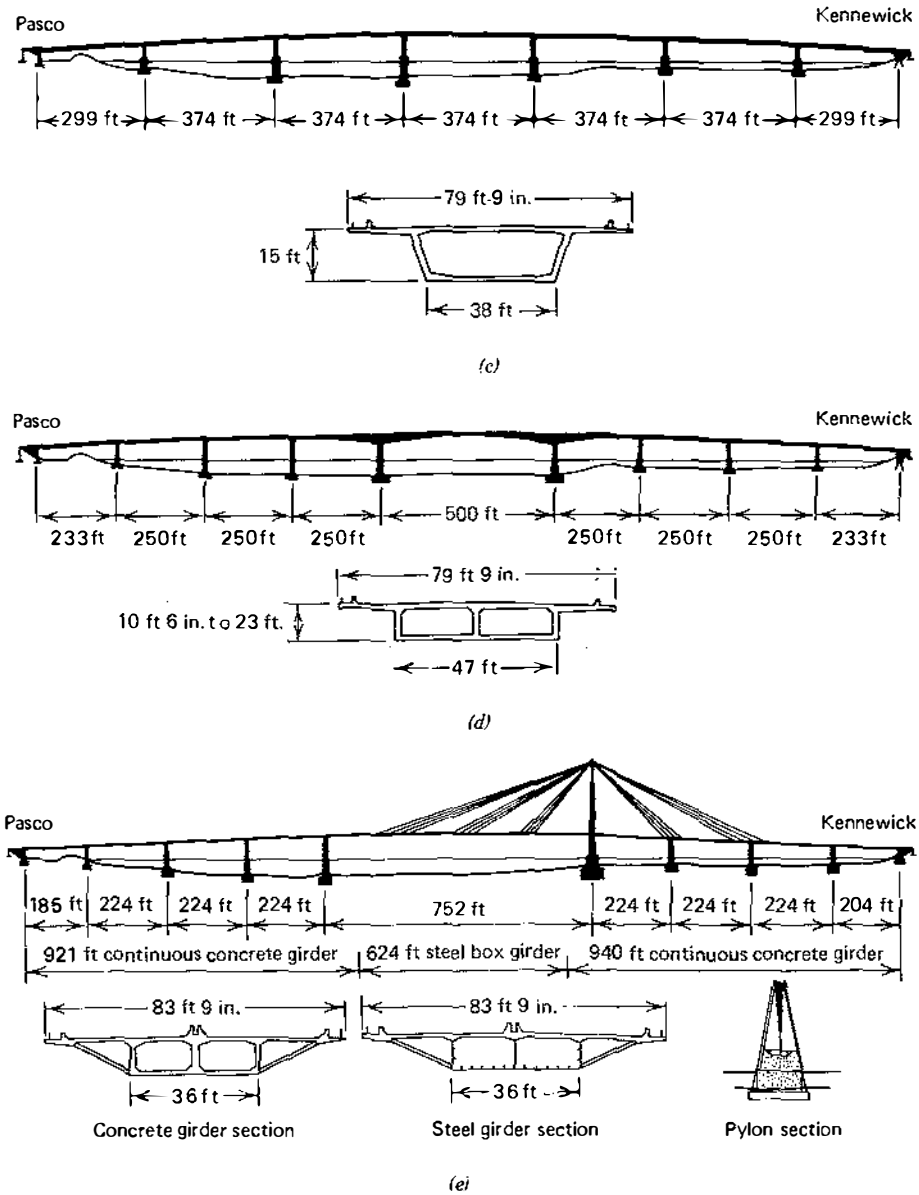


FIGURE 3.10 (Continued)

the edges connected by cross beams at 9-ft spacing. The unit was open in the cable-supported portion, (i.e., it had no enclosing bottom flange) and the approach spans were fully closed to partially closed approaching the cable-stay portion. The cross beams were prestressed except in the approach spans where only longitudinal prestressing was required. Main longitudinal webs were prestressed at the middle of the main span and at the ends of the end spans (cable-stayed) where the axial force of the cables was small. Mild steel reinforcement was utilized in both directions.

Alternate 3, Fig. 3.10(c), proposed a single-cell con-

crete box with five interior spans of 374 ft and end spans of 299 ft. The superstructure box had a constant depth of 15 ft, an overall width of 79 ft 9 in., and a bottom flange width of 38 ft, with the transverse prestressing in the top flange. Longitudinal prestressing was to be in two stages, first stage for construction and launching was a concentric force of 4400 tons positioned in the webs and flanges, second stage prestressing required 11,000 tons installed externally in the box. The superstructure would be constructed in successive 75-ft length units at one embankment and progressively pushed out until the opposite abutment was

reached. Temporary falsework bents at the center of each span and a launching nose attached to the forward end of the superstructure would be required to reduce cantilever stresses during erection.

Posttensioned balanced cantilever segmental construction, alternate 4, Fig. 3.10(d), consisted of a main span of 500 ft, three 250-ft side spans on each side, and 233-ft end spans. The main span and two flanking spans were haunched and all other spans were of constant depth. Free cantilever construction without false work was contemplated. The main span and two flanking spans had a depth varying from 10 ft 6 in. to 23 ft; all other span had a constant depth of 10 ft 6 in. Posttensioning was provided in the top of the box for cantilever erection stresses and, after closure, continuity tendons would be provided in the bottom of the box. The deck was posttensioned transversely, and diagonal and vertical tendons were required in the web for shear stress.

Design alternate 5, Fig. 3.10(e), consisted of four concrete girder approach spans on the Pasco side, one at 185 ft and three at 224 ft; a cable-stayed steel box-girder composite concrete deck main span of 752 ft; and four approach spans on the Kennewick side, three at 224 ft and one at 204 ft. This alternate was an asymmetric structure with a single A-frame pylon, a radiating stay arrangement in elevation, and a single transverse vertical plane located in the median.

The economic comparison of these five alternates using alternate 2 (the final design choice) as a base is shown in Table 3.2.

As seen from the preceding estimated construction cost comparison (including substructure) there is no conclusive economic argument for the approval of any one design. Therefore, satisfactory functional requirements, anticipating long-term performance, construction and design requirements, as well as the estimated initial costs must also be evaluated.

Functional requirements should consider channel clearance, approach grades, aesthetics, and overload capacity. Long-term performance considerations are maintenance and structure durability. Construction and design requirement considerations include famil-

ilarity of construction method, ease of construction, risk during construction, local labor and materials, overall construction time, opportunity for cost reduction in the final design process, and design complexity.

Obviously, consideration of the above items is dependent on the particular site conditions, local environmental conditions relative to natural hazards, along with the local and national economic environment at the time the estimate is made, as well as any short- and long-term economical conditions that may affect the final cost.

### 3.5 Results of Alternate Bidding in the United States

Although the economic evaluations and cost estimates were prepared for the three structures described in Section 3.4 and for the Captain William Moore Bridge in Alaska and the Meridian Bridge in California, they were bid on the basis of the single-design concept (see Section 3.2.1). Subsequent to 1979 all cable-stayed bridges have been bid on the basis of alternate designs (see Section 3.2.4), thus providing an economic evaluation in the marketplace at the time of bidding.

Bidding results on the Dame Point Bridge in Florida (1979) and the East Huntington Bridge in West Virginia (1981) indicated that steel construction was not competitive to concrete designs. However, the steel alternates for both these structures were of an orthotropic design and therefore reflected the current high fabrication costs for this type of structure. With this realization, designers turned to innovative concepts of "composite" design as opposed to a "pure" steel design. On subsequent projects, designs evolved using concrete pylons and superstructures that incorporated structural steel edge girders and structural steel floor beams composite with a concrete deck in competition with an all-concrete design.

Results of recent alternate design bidding is presented in Table 3.3. The steel alternates for the Dame Point, East Huntington, and Weirton-Steubenville bridges were of an orthotropic design and were un-

TABLE 3.2. Pasco-Kennewick Bridge—Economic Comparison

| Alternate | Description                           | Cost Ratio● |
|-----------|---------------------------------------|-------------|
| 1         | Steel plate girder                    | 1.005       |
| 2         | Cable-stayed concrete box girder      | 1.000       |
| 3         | Concrete box girder—push-out method   | 0.952       |
| 4         | Concrete box girder—cantilever method | 0.981       |
| 5         | Cable-stayed steel box girder         | 1.019       |

TABLE 3.3. Results of Alternate Design Bidding

| Project<br>(Year Bid)          | Alternate<br>Type | Estimate <sup>a</sup> | Low <sup>a</sup><br>Bid | Percentage over<br>Low<br>Bid |
|--------------------------------|-------------------|-----------------------|-------------------------|-------------------------------|
| Dame Point<br>(1979)           | Concrete          | 72                    | 64.8                    | 31                            |
|                                | Steel             |                       | 84.8                    |                               |
| East Huntington<br>(1981)      | Composite         | 26.93                 | 23.51                   | 42                            |
|                                | Steel             |                       | 24.74                   |                               |
| Sunshine Skyway<br>(1982)      | Concrete          | 111.5                 | 106.6                   | 2.5                           |
|                                | Composite         |                       | 109.3                   |                               |
| Weirton-Steubenville<br>(1983) | Concrete          | 31.43                 | no bid                  | 63                            |
|                                | Steel             |                       | 32.6                    |                               |
|                                | Composite         |                       | 19.99                   |                               |
| Annacis (Canada)<br>(1984)     | Concrete          |                       | 56.0                    | 22                            |
|                                | Composite         |                       | 45.8                    |                               |
| Quincy<br>(1984)               | Concrete          | 19.0                  | no bid                  | —                             |
|                                | Composite         |                       | 17.2                    |                               |

<sup>a</sup>Values in millions of U.S. dollars.

competitive by a considerable percentage. Although the composite design for the Sunshine Skyway was unsuccessful, it was considerably more competitive. In the case of the Annacis Bridge, the concrete design was 22% more costly than the composite design.

### References

1. "Guidelines for Value Engineering (VE)," prepared by Task Force 19, Subcommittee on New Highway Materials, AASHTO-AGC-ARTBA Joint Cooperative Committee.
2. "Alternate Designs for Bridges; Policy Statement," Federal Register, Vol. 48, No. 93, Thursday, May 12, 1983.
3. Thul, H., "Cable-Stayed Bridges in Germany," *Proceedings of the Conference on Structural Steelwork*, held at the Institution of Civil Engineers, September 26-28, 1966, The British Constructional Steelwork Association Ltd., London, England.
4. Taylor, P. R., "Cable-Stayed Bridges and Their Potential in Canada," *Engineering Journal (Canada)*, Vol. 52/11, November 1969.
5. Podolny, W., Jr., "Economic Comparisons of Stayed Girder Bridges," *Highway Focus*, Vol. 5, No. 2, August 1973, U.S. Department of Transportation, Federal Highway Administration, Washington, D.C.
6. Thul, H., "Schrägseilbrücken," Preliminary Report, Ninth IABSE Congress, Amsterdam, May 1972.
7. Leonhardt, F., "Seilkonstruktionen und seil ver-spannte Konstruktionen," Introductory Report, Ninth IABSE Congress Amsterdam, May 1972.
8. Leonhardt, F. and Zellner, W., "Cable-Stayed Bridge: Report on Latest Developments," *Proceedings of the Canadian Structural Engineering Conference, 1970*, Canadian Steel Industries Construction Council, Toronto, Ontario, Canada.
9. Leonhardt, F. and Zellner, W., "Vergleiche zwischen Hängbrücken und Schrägkabelbrücken für Spannweiten über 600 m," *International Association for Bridge and Structural Engineering*, Vol. 32, 1972.
10. Dubrova, E., "On Economic Effectiveness of Application of Precast Reinforced Concrete and Steel for Large Bridges (USSR)," *IABSE Bulletin*, 28, 1972.
11. Gute, W. L., "Design and Construction of the Sitka Harbor Bridge," Meeting Preprint 1957, ASCE National Structural Engineering Meeting, April 9-13, 1973, San Francisco, California.
12. "Feasibility Study of Mississippi River Crossings Interstate Route 410," Report to Louisiana Department of Highways in Cooperation with Federal Highway Administration, Modjeski and Masters, Consulting Engineers, Harrisburg, Pennsylvania, July 1971.
13. Kealey, T. R., "Feasibility Study of Mississippi River Crossings Interstate 410," Meeting Preprint 2003, ASCE National Structural Engineering Meeting, April 9-13, 1973, San Francisco, California.
14. "Pasco-Kennewick Intercity Bridge Preliminary Design Report," December 1972, Arvid Grant and Associates, Inc., Engineers, Olympia, Washington.

# 4

## Concrete Superstructures

|        |   |    |
|--------|---|----|
| 4.1    | INTRODUCTION  | 51 |
| 4.1.1  | Historical Review                                     | 51 |
| 4.1.2  | Advantages of Concrete Cable-Stayed Bridges           | 54 |
| 4.1.3  | Structural Style and Arrangement                      | 54 |
| 4.2    | LAKE MARACAIBO BRIDGE, VENEZUELA                      | 57 |
| 4.3    | WADI KUF BRIDGE, LIBYA                                | 59 |
| 4.4    | CHACO/CORRIENTES BRIDGE, ARGENTINA                    | 59 |
| 4.5    | MAINBRÜCKE, WEST GERMANY                              | 60 |
| 4.6    | TIEL BRIDGE, THE NETHERLANDS                          | 61 |
| 4.7    | PASCO-KENNEWICK BRIDGE, U.S.A.                        | 64 |
| 4.8    | BROTONNE BRIDGE, FRANCE                               | 66 |
| 4.9    | DANUBE CANAL BRIDGE, AUSTRIA                          | 70 |
| 4.10   | SUNSHINE SKYWAY BRIDGE, U.S.A.                        | 72 |
| 4.11   | NECHES RIVER BRIDGE, U.S.A.                           | 74 |
| 4.12   | BARRÍOS DE LUNA BRIDGE, SPAIN                         | 75 |
| 4.13   | NOTABLE EXAMPLES OF CONCEPTS                          | 77 |
| 4.13.1 | Danish Great Belt Bridge Competition                  | 77 |
| 4.13.2 | Proposed Dame Point Bridge, U.S.A.                    | 78 |
| 4.13.3 | Proposed Ruck-A-Chucky Bridge, U.S.A.                 | 79 |
| 4.13.4 | James River and Proposed Cooper River Bridges, U.S.A. | 82 |
|        | REFERENCES  | 84 |

### 4.1 Introduction

Although the modern renaissance of cable-stayed bridges is said to have begun in 1955, with steel as the favored material, a number of cable-stayed bridges in the last two decades have been constructed using a reinforced or prestressed concrete deck system. In recent years several concrete cable-stayed bridges have been built in the long-span range. Cable-stayed bridges are extending the competitive span range of concrete bridge construction to dimensions that had previously been considered impossible and were reserved for structural steel. To date (1984), approximately 29 concrete cable-stayed bridges have been constructed, and others are either in the design stage or under construction. A tabular summary of concrete cable-stayed bridges is presented in Tables 4.1 and 4.2.

### 4.1.1 HISTORICAL REVIEW

Since the beginning of the renaissance of the cable-stayed bridge in 1955, whether for technical or other reasons, structural steel has been the preferred construction material. In 1957, however, considerable excitement was generated when Riccardo Morandi's prize-winning design of a prestressed concrete 1312-ft (400 m) center span cable-stayed bridge for the Lake Maracaibo crossing was announced. Regrettably the Lake Maracaibo Bridge was not constructed as originally conceived. The modified structure, built in 1962, is generally considered to be the first modern cable-stayed bridge. However, the Lake Maracaibo Bridge was preceded by two little-known concrete cable-stayed structures noted in the following.

The first concrete structure to use cable stays was the Tempul Aqueduct crossing the Guadalete River in Spain.<sup>1</sup> Designed by the famous Spanish engineer, E. Torroja, who introduced many original concepts for prestressed concrete structures, this structure has a classical three-span symmetrical cable-stayed bridge configuration with two pylons. The stays were introduced to replace two piers that were found to be too difficult to construct in deep water. Thus, the stays were introduced to provide intermediate support in the main span.

On July 5, 1957, a stayed structure crossing the Yakima River at Benton City, Washington, was opened to traffic. Designed by Homer M. Hadley, the structure has a total length of 400 ft (122 m) with a center span of 170 ft (51.9 m) flanked on each side by two continuous spans of 57.5 ft (17.53 m) each. A 60-ft (18.3-m) central drop-in span of 33-in. (0.84-m) deep steel beams is supported by transverse concrete beams, supported in turn by structural steel wide-flange stays. Continuous longitudinal concrete beams comprise the remainder of the structure and receive support at their



TABLE 4.1. Concrete Cable-Stayed Bridges—General Data

| Bridge              | Location                    | Type           | Spans (ft) <sup>a</sup> | Year Completed     |
|---------------------|-----------------------------|----------------|-------------------------|--------------------|
| 1 Tempul            | Guadalete River, Spain      | Aqueduct       | 66-198-66               | 1925               |
| 2 Benton City       | Yakima River, Wash., U.S.A. | Highway        | 2@57.5-170-2@57.5       | 1957               |
| 3 Lake Maracaibo    | Venezuela                   | Highway        | 525-5@771-525           | 1962               |
| 4 Dnieper River     | Kiev, U.S.S.R.              | Highway        | 216.5-472-216.5         | 1963               |
| 5 Canal du Centre   | Obourg, Belgium             | Pedestrian     | 2@220                   | 1966               |
| 6 Polcevera Viaduct | Genoa, Italy                | Highway        | 282-664-689-460         | 1967               |
| 7 Magliana          | Rome, Italy                 | Highway        | 476-176                 | 1967               |
| 8 Pretoria          | Pretoria, S. Africa         | Pipe           | 2@93                    | 1968               |
| 9 Barwon River      | Gcelong, Australia          | Pedestrian     | 180-270-180             | 1969               |
| 10 Mount Street     | Perth, Australia            | Pedestrian     | 2@116.8                 | 1969               |
| 11 Wadi Kuf         | Libya                       | Highway        | 320-925-320             | 1971               |
| 12 Mainbrücke       | Hoechst, West Germany       | Highway & rail | 485.6-308               | 1972               |
| 13 Chaco/Corrientes | Parana River, Argentina     | Highway        | 537-803.8-537           | 1973               |
| 14 River Waal       | Tiel, Holland               | Highway        | 312-876-312             | 1974               |
| 15 Barranquilla     | Barranquilla, Columbia      | Highway        | 228-459-228             | 1974               |
| 16 Danube Canal     | Vienna, Austria             | Highway        | 182.7-390-182.7         | 1974               |
| 17 Kwang I'u        | Taiwan                      | Highway        | 220-440-440-220         | 1977               |
| 18 Pont de Brotonne | Normandy, France            | Highway        | 471-1050-471            | 1977               |
| 19 Carpineto        | Province Poetenza, Italy    | Highway        | 100-594-100             | 1977               |
| 20 Pasco-Kennewick  | State of Wash., U.S.A.      | Highway        | 406.5-981-406.5         | 1978               |
| 21 M-25 Overpass    | Chertsey, England           | Rail           | 2@180.5                 | 1978               |
| 22 Kaiseraugst      | Basel, Switzerland          | Pedestrian     | 153-58                  | 1978               |
| 23 Ebro River       | Navarra, Spain              | Highway        | 480                     | 1979               |
| 24 Airport Hotel    | Hong Kong                   | Pedestrian     | 157-122                 | 1982               |
| 25 Barrios De Luna  | Spain                       | Highway        | 324-1443.6-324          | —                  |
| 26 Horikoshi        | Hachioji, Japan             | Highway        | 220-122                 | 1984               |
| 27 Shunshine Skyway | Florida, U.S.A.             | Highway        | 540-1200-540            | Under construction |
| 28 Neches River     | Texas, U.S.A.               | Highway        | 280-640-280             | Under construction |
| 29 Dame Point       | Florida, U.S.A.             | Highway        | 650-1300-650            | Under construction |

<sup>a</sup>1 ft = 0.305 m.

TABLE 4.2. Concrete Cable-Stayed Bridges—Dimensional Parameters

| Bridge              | Stay<br>Planes | Number of <sup>a</sup><br>Stays | Stay<br>Arrangement | Pylon<br>Height<br>Above<br>Deck (ft) <sup>d</sup> | Pylon<br>Height-<br>to-Span<br>Ratio <sup>b</sup> | Deck<br>Width<br>(ft) <sup>d</sup> | Girder<br>Depth (ft) <sup>d</sup> | Span-to-<br>Depth<br>Ratio <sup>b</sup> | Girder<br>Construction<br>Type <sup>c</sup> |
|---------------------|----------------|---------------------------------|---------------------|--|---|------------------------------------|-----------------------------------|---|---|
| 1 Tempul            | 2              | 1                               | —                   | 14.1   | 0.07  | —                                  | 6.9                               | 28.7                                    | CIP   |
| 2 Benton City       | 2              | 1                               | —                   | —  | —   | —                                  | 3.25                              | 52.3                                    | CIP   |
| 3 Lake Maracaibo    | 2              | 1                               | —                   | 139.4  | 0.18  | 57                                 | 16.4                              | 46.7                                    | CIP/PC d-i-s                                |
| 4 Dniper River      | 2              | 3                               | Radiating           | 95   | 0.20  | —                                  | 4.8                               | 98.75                                   | PC  |
| 5 Canal du Centre   | 2              | 4                               | Radiating           | 65.6   | 0.30  | 5.87                               | 1.94                              | 113                                     | PC  |
| 6 Polcevera Viaduct | 2              | 1                               | —                   | 148  | 0.21  | 59                                 | 15                                | 46                                      | CIP/PC d-i-s                                |
| 7 Magliana          | 2              | 1                               | —                   | 111.5  | 0.23  | 79                                 | 9.8-13.2                          | 36                                      | CIP/PC d-i-s                                |
| 8 Pretoria          | 2              | 2                               | Radiating           | 41   | 0.44  | 15.8                               | 3                                 | 31                                      | CIP   |
| 9 Barwon River      | 2              | 2                               | Fan                 | 43   | 0.16  | 6                                  | 7                                 | 38.5                                    | CIP   |
| 10 Mount Street     | 1              | 2                               | —                   | 49   | 0.42  | 15.75                              | 2                                 | 58.4                                    | CIP   |
| 11 Wadi Kuf         | 2              | 1                               | —                   | 177.5  | 0.19  | 42.5                               | 11.5-23                           | 70                                      | CIP/PC d-i-s                                |
| 12 Mainbrücke       | 2              | 13                              | Harp                | 172  | 0.38  | 101.5                              | 8.5                               | 57                                      | CIP   |
| 13 Chaco/Corrientes | 2              | 2                               | Radiating           | 155  | 0.19  | 47                                 | 11.5                              | 70                                      | PC/CIP d-i-s                                |
| 14 River Waal       | 2              | 2                               | Radiating           | 151.8  | 0.17  | 101                                | 11.5                              | 76                                      | PC and CIP                                  |
| 15 Barranquilla     | 2              | 1                               | —                   | —  | —   | 37                                 | 10                                | 46                                      | CIP segments                                |
| 16 Danube Canal     | 2              | 1                               | —                   | 52.5   | 0.15  | 51.8                               | 9.2                               | 42.5                                    | PC and CIP                                  |
| 17 Kwang Fu         | 2              | 2                               | Radiating           | —  | —   | 67                                 | —                                 | —                                       | PC  |
| 18 Pont de Brotonne | 1              | 21                              | Fan                 | 231  | 0.22  | 63                                 | 12.5                              | 84                                      | PC and CIP                                  |
| 19 Carpineto        | 2              | 1                               | —                   | 94.75  | 0.16  | 41.3                               | 11.5                              | 52                                      | CIP   |
| 20 Pasco-Kennewick  | 2              | 18                              | Radiating           | 220  | 0.22  | 79.8                               | 7                                 | 140                                     | PC segments                                 |
| 21 M-25 Overpass    | 2              | 2                               | Fan                 | 71   | 0.39  | 39                                 | 9                                 | 20                                      | CIP   |
| 22 Kaiseraugst      | 1              | 5                               | Radiating           | 54.8   | 0.36  | 15.75                              | 1.67                              | 91.6                                    | CIP   |
| 23 Ebro River       | 1              | 35                              | Fan                 | 177.6  | 0.37  | —                                  | 6.56                              | 73.2                                    | PC segments                                 |
| 24 Airport Hotel    | 1              | 2                               | Radiating           | —  | —   | 17.9                               | 3.28                              | 47.9                                    | CIP   |
| 25 Barrios De Luna  | 2              | 27/28                           | Fan                 | —  | —   | 74.8                               | 7.54                              | 192                                     | CIP segments                                |
| 26 Horikoshi        | 2              | 8                               | Fan                 | 98   | 0.44  | 34.0                               | 4.6                               | 47.8                                    | CIP   |
| 27 Sunshine Skyway  | 1              | 21                              | Fan                 | 242  | 0.20  | 95.2                               | 14.7                              | 81.6                                    | PC segments                                 |
| 28 Neches River     | 2              | 14                              | Fan                 | 122  | 0.19  | 56.0                               | 8.0                               | 80.0                                    | PC segments                                 |
| 29 Dame Point       | 2              | 21                              | Harp                | 302  | 0.23  | 106                                | 5-6                               | 260                                     | CIP and PC                                  |

<sup>a</sup>Number of stays on each side of each pylon.

<sup>b</sup>See Table 4.1 for major span dimensions.

<sup>c</sup>CIP = cast-in-place, PC = precast, d-i-s = drop-in-span.

<sup>d</sup>1 ft = 0.305 m.

extremity, in the center span, from the transverse concrete beams and steel stays.<sup>2,3</sup>

In the more than half-century that has elapsed since Torroja's Tcmpul Aqueduct, 29 cable-stayed bridges have been constructed (Table 4.1). Sixteen or 55% of these structures have been constructed in the past decade. Within this decade the span of 1000 ft (300 m) has been exceeded and a current design contemplates a span of 1300 ft (400 m). It has taken almost a quarter-century to reach a span contemplated by Morandi in his original design concept for the Lake Maracaibo Bridge. Be that as it may, it is obvious from the statistics that in recent years the concrete cable-stayed bridge has been accepted as a viable structure.

#### 4.1.2 ADVANTAGES OF CONCRETE CABLE-STAYED BRIDGES

As engineers, we are aware that no particular concept or bridge type can suit all environments, considerations, problems, or site conditions. The selection of the proper type for a given site and set of circumstances must take into account many parameters. The choice of material, in addition to material properties, depends on availability and the prevailing economics at a particular time as well as the specific location of the site. The process of weighting and evaluating these parameters for various types of bridges under consideration is certainly more an art than a science.

In evaluating a concrete cable-stayed bridge, the designer should be aware of the following advantages:

1. The main girder can be very shallow with respect to the span. Span-to-girder-depth ratios vary from 45 to 260. With proper aerodynamic streamlining and multistays the deck structure can be slim, having span-to-depth ratios of 150 to 400, and not convey a massive visual impression.
2. Concrete deck structures, by virtue of their mass and because concrete has inherently favorable damping characteristics, are not as susceptible to aerodynamic vibrations.
3. The horizontal component of the cable-stay force, which causes compression with bending in the deck structure, favors a concrete deck structure. The stay forces produce a prestress force in the concrete, and concrete is at its best in compression.
4. The amount of steel required in the stays is comparatively small. A proper choice of height of pylon with respect to span can yield an optimum solution.<sup>4</sup>

5. Live-load deflections are small because of the live-load-to-dead-load ratio, and therefore concrete cable-stayed bridges are applicable to railroad or mass-transit loadings.
6. Erection of the superstructure and cable stays is relatively easy with today's technology of prestressing, prefabrication, and segmental cantilever construction.

#### 4.1.3 STRUCTURAL STYLE AND ARRANGEMENT

Many of the concrete cable-stayed bridges have been designed by Morandi or have been strongly influenced by his style. Commencing with the Lake Maracaibo Bridge, of the 21 bridges constructed, excluding pedestrian and pipe bridges (see Table 4.1), six have been designed by Morandi, Figs. 4.1 through 4.6. A third prize winner in the 1967 Danish Great Belt Bridge competition was the Morandi-style design pro-

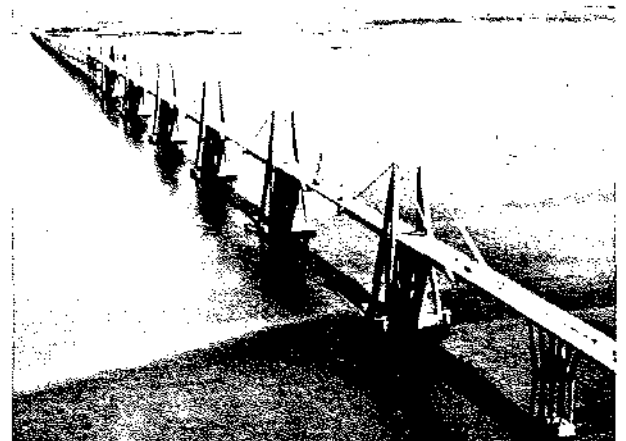


FIGURE 4.1 Lake Maracaibo Bridge, general view, from reference 7. (Courtesy of Julius Berger-Bauboag Aktiengesellschaft).

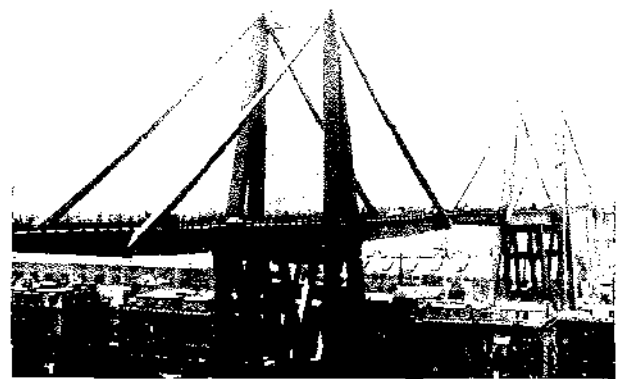


FIGURE 4.2 Polcevera Creek Bridge, general view.

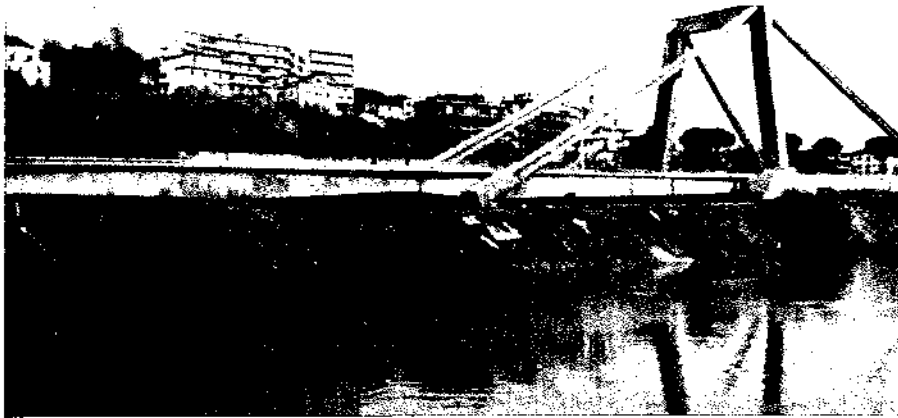


FIGURE 4.3 Magliana Viaduct. (Courtesy of L'Industria Italiana del Cemento.)



FIGURE 4.4 Wadi Kuf Bridge, general construction view. (Courtesy of R. Morandi.)

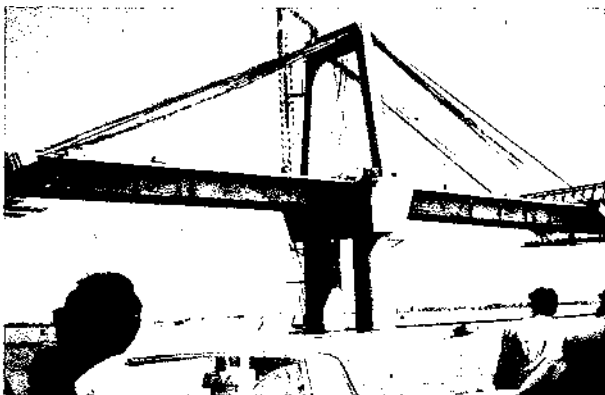


FIGURE 4.5 Barranquilla Bridge. (Courtesy of L. A. Garrido.)

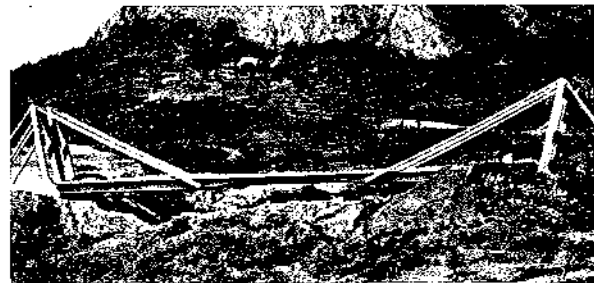


FIGURE 4.6 Carpineto Viaduct. (Courtesy of L'Industria Italiana del Cemento.)

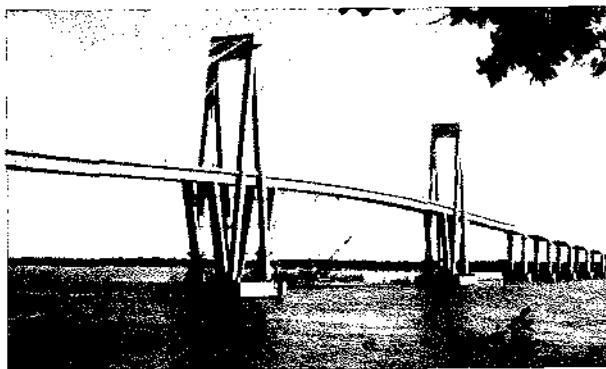


FIGURE 4.7 Chaco/Corrientes Bridge, general view, from reference 9. (Courtesy of Normer Gray.)

posed by the English consulting firm of White Young and Partners, Fig. 2.5. The Chaco/Corrientes Bridge, Figure 4.7, very much resembles the Morandi style.

These structures, with the exception of the Magliana, Barranquilla, and Carpincto bridges, are typified by the A-frame pylon positioned in the plane of the stays and an auxiliary X-frame or inclined struts to support the deck structure at the pylon. They are statically determinate systems to preclude any possible damage from differential settlements of the bridge piers and pylons or from light seismic shocks.

A simple schematic of the structural elevation is shown in Figure 4.8, which consists of a series of independent balanced systems, each carried by an individual pier and pylon. These systems are then connected by drop-in girders, which are simple span girders spanning between independent systems.<sup>5</sup> The cantilever girder is supported at two points (C and D) by a pier system and elastically supported at two points (B and E) by the cable stays, thus producing a three-span girder with cantilevers on each side. The stays are supported by a pylon portal frame that is independent of the pier system supporting the girder.

Another entry in the 1967 Danish Great Belt competition by Ulrich Finsterwalder, of the West German firm Dyckerhoff & Widmann, deviated from the Morandi style and was awarded a second prize. Finster-

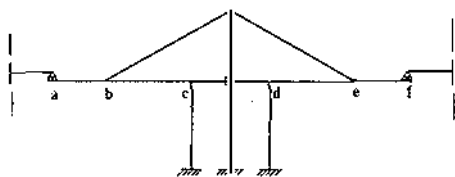


FIGURE 4.8 Schematic of Morandi-style structural scheme, from reference 5. (Courtesy of the American Concrete Institute.)



FIGURE 4.9 Danish Great Belt Bridge, artist's rendering. (Courtesy of Ulrich Finsterwalder.)

walder's design proposed a multiple-span, multistay system using Dywidag bars for the stays, Fig. 4.9. The deck was envisioned as being constructed by the cast-in-place balanced cantilever segmental method, each segment being supported by a set of stays. This concept was later to be consummated in the Main Bridge and in the design of the Dame Point Bridge.

The choice of geometrical configuration and number of stays in a cable-stayed bridge system is subject to a wide variety of considerations. If cable stays are few, they result in large stay forces, which require massive anchorage systems. A relatively deep girder is required to span the large distance between stays, producing span-to-depth ratios varying from 45 to 100 (see Table 4.2). Depending upon the location of the longitudinal main girders with respect to the cable-stay planes, large transverse cross girders may be required to transfer the stay force to the main girder.

A large number of cable stays, approaching a continuous supporting elastic media, simplifies the anchorage and distribution of forces to the girder and permits the use of a shallower girder, with span-to-depth ratios varying from 150 to 200 (see Table 4.2). The construction of the deck can be erected roadway-width by free cantilever methods from stay to stay without auxiliary methods or stays. If the depth of the roadway girder can be kept at a minimum, the deck becomes, more or less, the bottom chord of a large cantilevering truss. It needs almost no bending stiffness because the inclined stays do not allow any large deflections under concentrated loads.<sup>6</sup>

In the 55 years since Torroja's Tempul Aqueduct the concrete cable-stayed bridge has evolved from basically a statically determinate structure with one stay on each side of the pylon to a highly indeterminate system with multistays. As demonstrated by the Danish Great Belt Bridge competition, the Pasco-Kennebec Bridge, and the Pont de Brotonne, spans of approximately 1000 ft (300 m) are practical and have been accomplished. The practicality of spans of 1300 ft (400 m) is demonstrated by the Dame Point Bridge.

The Barrios De Luna Bridge has been constructed with a span of 1443 ft (440 m), and spans approaching 1600 ft (500 m) are considered technically feasible. Leonhardt<sup>6</sup> has projected that with an aerodynamically shaped composite concrete and steel deck, a span of 2300 ft (1500 m) can be achieved. With today's technology of prefabrication, prestressing, and segmental cantilever construction, it is obvious that cable-stayed bridges are extending the competitive span range of concrete bridges to dimensions that had previously been considered impossible and into a range that had previously been the domain of structural steel. The technological concepts exist; they only require implementation.

#### 4.2 Lake Maracaibo Bridge, Venezuela

This bridge, Fig. 4.1, has a total length of 5.4 miles (8.7 km). Five main navigation openings consist of prestressed concrete cable-stayed structures with suspended spans totaling 771 ft (235 m). The cantilever span is supported on four parallel X frames, while the cable stays are supported on two A-frames with a portal member at the top. There is no connection anywhere between the X- and A-frames, Fig. 4.10. The

continuous cantilever girder is a three-cell box girder 164 ft deep by 46.7 ft wide (5 m by 14.22 m). An axial prestress force is induced into the girder as a result of the horizontal component of cable force, thus, for the most part, only conventional reinforcement is required. Additional prestress tendons are required for negative moment above the X-frame support and the transverse cable-stay anchorage beams.<sup>7</sup>

The pier cap consists of the three-cell box girder with the X-frames continued up into the girder to act as transverse diaphragms, Figs. 4.10 and 4.11. After completion of the pier, service girders were raised into position to be used in the construction of the cantilever arm. Because of the additional moment, produced during this construction stage by the service girder and weight of the cantilever arm additional concentric prestressing was required in the pier cap, Fig. 4.11. To avoid overstressing the X-frames during this operation, temporary horizontal ties were installed and tensioned by hydraulic jacks.

The anchorages for the cable stays are located in a 73.8-ft (22.5 m) long prestressed inclined transverse girder. The reinforcing cages for these members were fabricated on shore in a position corresponding to the inclination of the stays. They weighed 60 tons and contained 70 prestressing tendons, Fig. 4.12. The ca-

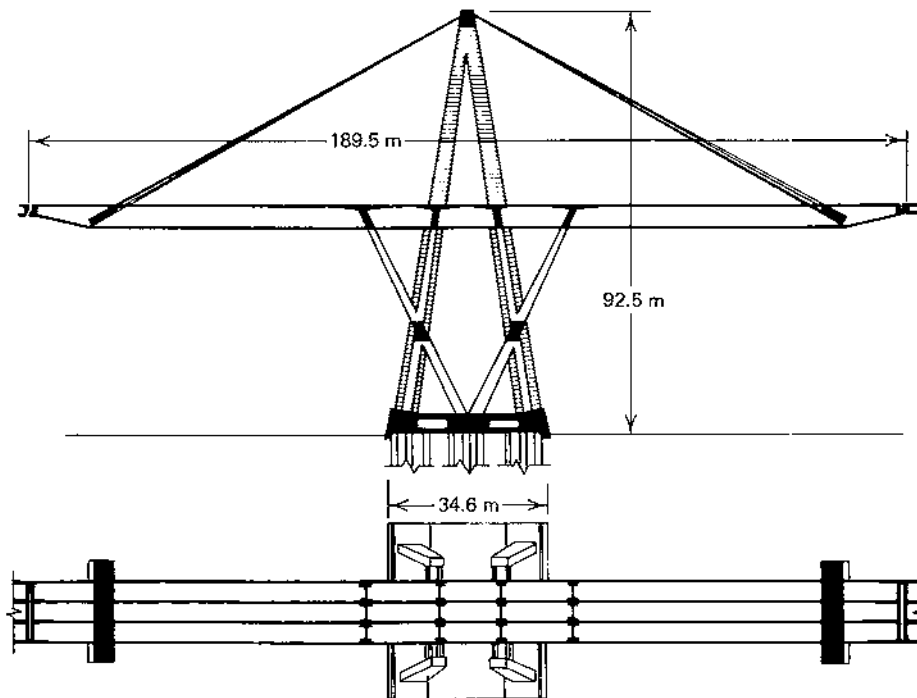


FIGURE 4.10 Lake Maracaibo Bridge, main span tower and X-frames, from reference 7. (Courtesy of Julius Berger-Bauboag Aktiengesellschaft.)

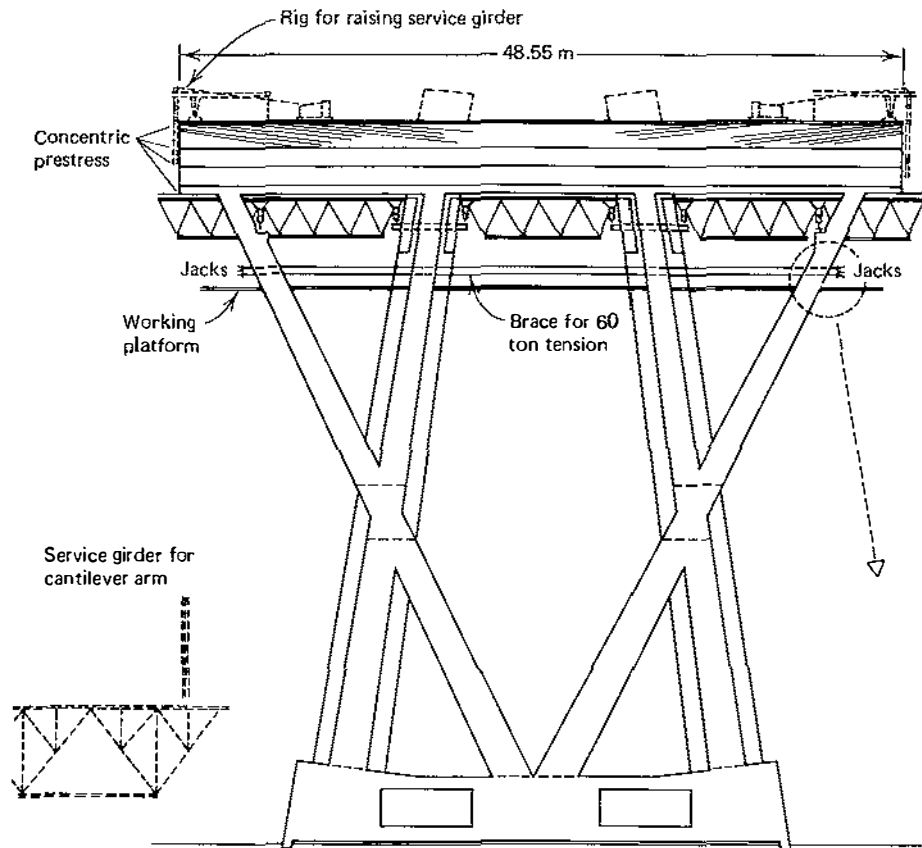


FIGURE 4.11 Lake Maracaibo Bridge, pier cap of a main span and service girder, from reference 7. (Courtesy of Julius Berger-Bauboag Aktiengesellschaft.)

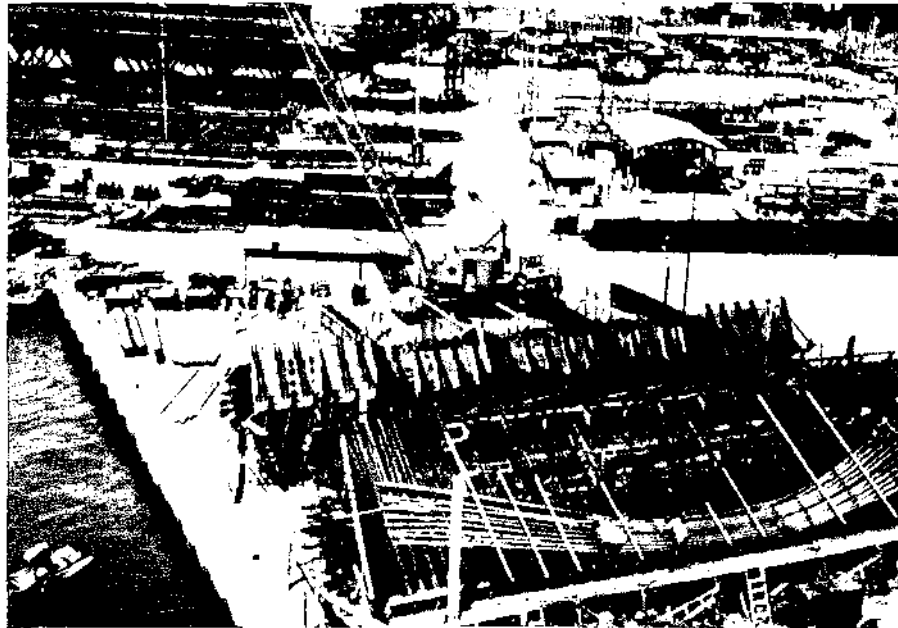


FIGURE 4.12 Lake Maracaibo Bridge, fabrication of anchorage beam, from reference 7. (Courtesy of Julius Berger-Bauboag Aktiengesellschaft.)

ble stays are housed in thick-walled steel pipes, which were welded to steel plates at their extremities and were encased in the anchorage beam. A special steel spreader beam was used to erect the fabricated cage in its proper orientation. The suspended spans are composed of four prestressed T sections.

#### 4.3 Wadi Kuf Bridge, Libya

The Wadi Kuf Bridge in Libya, designed by Morandi, consists of two independent balanced cable-stay systems having their ends anchored to the abutment by a short hinge strut. The cable-stay systems are connected by a simply supported drop-in span, Fig. 4.4

This structure consists of only three spans. The center span is 925 ft (280 m) long and the two end spans are each 320 ft (97.5 m), for a total length of 1565 ft (475 m). The simply supported drop-in center portion of the main span consists of three double-T beams 180 ft (55 m) in length; each beam weighs approximately 220 tons (200 mt).<sup>8</sup>

The A-frame towers are 459 ft and 400 ft (140 and 122 m) high and the roadway deck is 597 ft (182 m) above the lowest point of the valley beneath the structure.<sup>8</sup> The superstructure is a single-cell box girder that varies from 13 ft (4.0 m) to 23 ft (7.0 m) at the pylons. The single-cell box is 24 ft (7.4 m) wide and with cantilever flanges forms a 42.7-ft (13-m) deck.

The contractor made good use of traveling forms to construct the box girder and deck, using the balanced cantilever technique to build on both sides of the pylons at the same time. Traveling forms were used be-

cause extreme height and difficult terrain made other conventional construction methods impossible or too costly. The deck was constructed by progressive cast-in-place segments, attached to the previously completed segments by means of temporary prestress ties and subsequent permanent post-tensioning Dywidag bars. The procedure adopted required temporary cable stays to support the cantilever arms during the construction sequence as the superstructure progressed in both directions from the pylon. When the superstructure extended sufficiently, the permanent stays were installed, and the structure was completed in the same manner.

#### 4.4 Chaco/Corrientes Bridge, Argentina

The Chaco/Corrientes Bridge (also referred to as the General Manuel Belgrano Bridge) crosses the Parana River between the provinces of Chaco and Corrientes in northeast Argentina and is an important link in one of the highways between Brazil and Argentina, Fig. 4.7. It has a center navigation span of 803 ft 10 in. (245 m), side spans of 537 ft (163.7 m), and a number of 271-ft (82.6-m) approach spans on both the Chaco and Corrientes sides of the river. The vertical clearance in the main spans above flood level is 115 ft (35 m).<sup>9,10</sup>

The superstructure of this bridge consists of two cast-in-place concrete A-frame pylons, which support a deck of precast segmental posttensioned concrete. The pylons are flanked by concrete struts, which reduce the unsupported length of the deck, Fig. 4.13.

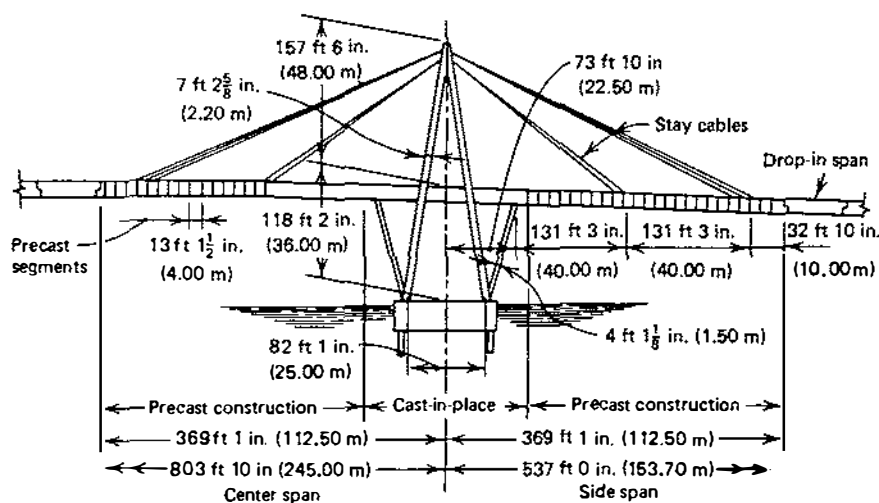


FIGURE 4.13 Chaco/Corrientes Bridge, longitudinal geometry, from reference 10. (Courtesy of Civil Engineering-ASCE.)



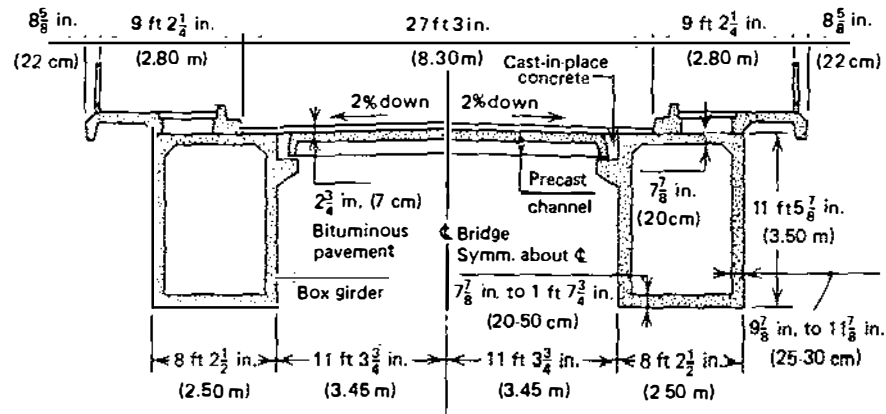


FIGURE 4.14 Chaco/Corrientes Bridge, deck cross section, from reference 10. (Courtesy of Civil Engineering-ASCE.)

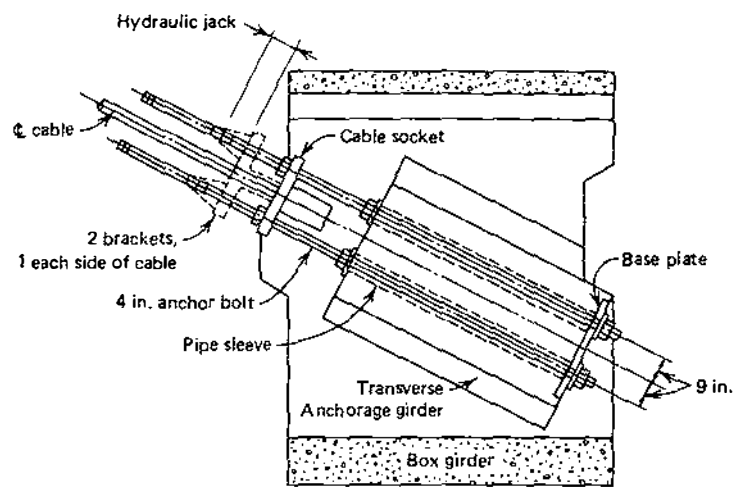


FIGURE 4.15 Chaco/Corrientes Bridge, cable anchorage at girder, from reference 10. (Courtesy of Civil Engineering-ASCE.)

Although the pier cap section of the deck (between inclined struts) is cast in place, the cantilever portion consists of precast segments. The drop-in spans are cast in place.

The deck structure consists of two longitudinal hollow boxes 8 ft 2½ in (2.5 m) wide and with a constant depth of 11 ft 6 in. (3.5 m), which support precast roadway deck elements, Fig. 4.14. The precast girder elements were match-cast on the river bank in lengths of 13 ft 1½ in. (4.0 m), with the exception of shorter units at the point of stay attachment, which contain an inclined transverse anchorage beam, Fig. 4.15

#### 4.5 Mainbrücke, West Germany

The Main Bridge near Hoechst, a suburb of Frankfurt, constructed in 1971 is a prestressed, cast-in-place,

segmental, cable-stayed structure that connects the Fabwerke Hoechst's chemical industrial complex on both sides of the River Main in West Germany, Fig. 4.16. It carries two three-lane roads separated by a railway track and pipelines. This structure, a successor to Finsterwalder's Danish Great Belt Bridge proposal, represents the first practical application of the Dywidag bar stay.<sup>11</sup>

The bridge spans the river at a skew of 70 degrees from the high northern bank to the southern bank, which is 23 ft (7 m) lower. The center navigation span is 486 ft (148.23 m) with a northern approach span of 86 ft (26.17 m) and southern approach spans of 55, 84, 95, and 129 ft (16.91, 25.65, 29, and 39.35 m), Fig. 4.17.

Railroad track and pipelines are in the median between the two cantilever pylon shafts and are supported on an 8.7-ft (2.66-m) deep torsionally stiff box

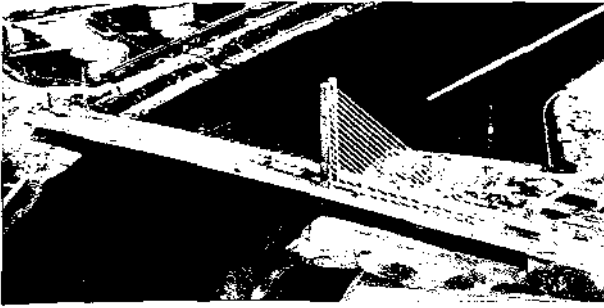


FIGURE 4.16 Mainbrücke, from reference 12.

girder, Fig. 4.18. The centerline of the longitudinal webs of the box girder coincides with the centerline of the individual cantilever pylons, and they are 26.25 ft (8 m) apart. Transverse cross beams at 9.8-ft (3-m) centers form diaphragms for the box and cantilevers, which extend 39 ft (11.95 m) on one side and 36 ft (11 m) on the other side of the central box to support the two roadways, Fig. 4.19.

The cross section of the towers consists of an anchoring web in the center, sandwiched by two flat-plate flange elements, Fig. 4.20. In a transverse elevation of the pylons, the width of the pylon increases from the top to just below the transverse strut, where it decreases to accommodate clearance requirements for both modes of traffic, Fig. 4.20. The stay cables (Dywidag bars) are in pairs, horizontal to each other in the main span and vertical in the side span, thus simplifying the anchorage detail at the pylon, Fig. 4.20.<sup>12</sup>

Construction of the bridge superstructure was by the cast-in-place segmental method. Segments in the river span were 20.7 ft (6.3 m) in length, corresponding to the spacing of the stays. Segments in the anchor span were 19 ft (5.8 m) in length. Segments in the

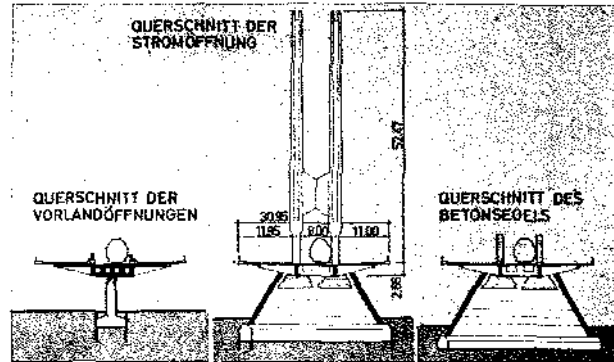


FIGURE 4.18 Mainbrücke, cross section, from reference 12.

anchor span were cast before the corresponding segment in the river span to maintain stability. The pylon segments were associated with the superstructure segments, and each pylon segment was slipformed. Each stay is composed of 25 16-mm ( $\frac{5}{8}$ -in.) diameter Dywidag bars encased in a metal duct, which is grouted for corrosion protection similar to posttensioned prestressed concrete construction.

#### 4.6 Tiel Bridge, The Netherlands

The Tiel Bridge,<sup>13</sup> Fig. 4.21, crosses the Waal River, which, together with the Maas and the Rhine, flowing east to west, divides The Netherlands into northern and southern regions. This structure provides a needed traffic link between the town of Tiel and the south of the country and is a major north-south route.

The structure has an overall length of 4656 ft (1419 m) and consists of a 2644-ft (806-m) curved viaduct

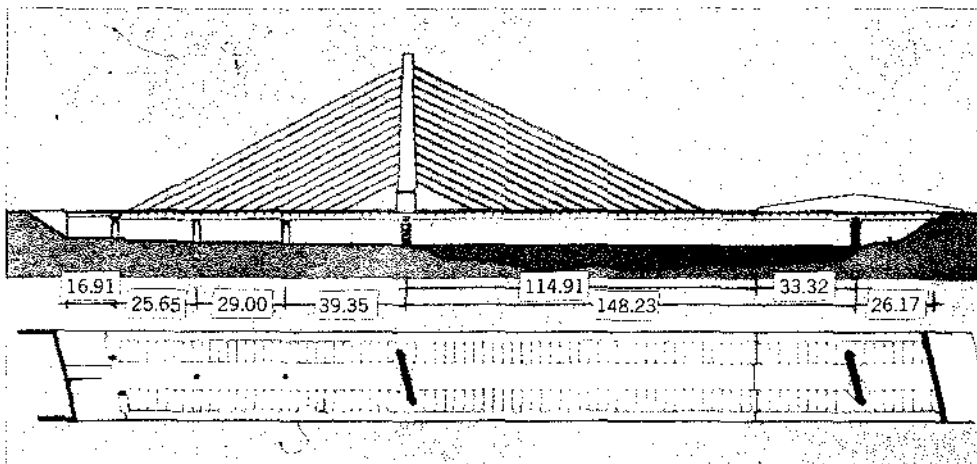


FIGURE 4.17 Mainbrücke, elevation and plan, from reference 12.



FIGURE 4.19 Mainbrücke, view of deck at pylon. (Courtesy of Richard Heinen.)

on a 19,685-ft (6000-m) radius, which includes 10 continuous 258-ft (78.5-m) long spans and a 2008-ft (612-m) straight main structure comprising three stayed spans of 312, 876, and 312 ft (95, 267, and 95 m) and two 254-ft (77.5-m) side spans.

The cross section consists of two precast concrete boxes, each supporting two vehicular and one bicycle lane. The total width of the superstructure, which is 89 ft (27.2 m) in the access viaduct, is enlarged to 103 ft (31.5 m) over the main structure to accommodate the pylon supporting the stays.

The structure crosses not only the Waal River but also a flood plain, which is underwater during the winter months. Navigation requirements dictate a horizontal clearance of 853 ft (260 m) and a vertical clearance of 30 ft (9.1 m).

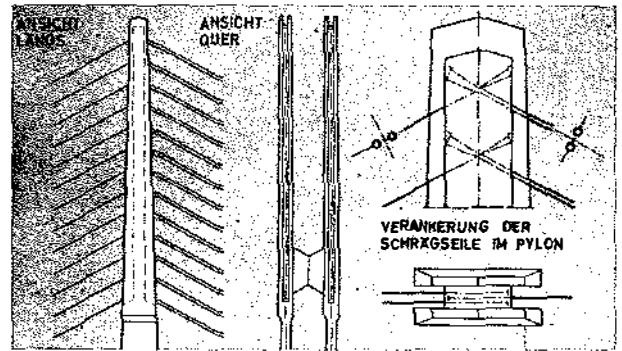


FIGURE 4.20 Mainbrücke, pylon and cable configuration, from reference 12.

The 10-span 2648-ft (806-m) long access viaduct is continuous over its entire length. The superstructure is supported on the piers by sliding teflon bearings, except at the three center piers where it is supported on neoprene bearings, having a thickness which fixes the viaduct at these piers. Expansion joints are located at piers 1 and 11. The superstructure in the access viaduct consists of two precast rectangular boxes of a constant depth of 11.5 ft (3.5 m) and width of 21 ft 8 in. (6.6 m). The top flange including cantilever overhangs has a width of 44 ft (13.44 m). The overall width of the approach viaduct deck is 89 ft 3 in. (27.2 m), including a longitudinal pour strip. The viaduct was constructed by the precast balanced cantilever method with cast-in-place closure pours at the midspans. To accommodate the cantilever compressive stresses in the bottom flange over the piers, the thickness of the bottom flange is linearly increased from a minimum of 8 in. (200 mm) to 24 in. (600 mm) over a length of 33 ft (10 m) on each side of the pier. Each pier segment contains a diaphragm.

The symmetrical box girder main structure consists of a 254-ft (77.5-m) side span, a 312-ft (95-m) side stayed span, and a 331-ft (101-m) section of stayed center span cantilevering toward the center of the bridge. The center section between the stayed canti-

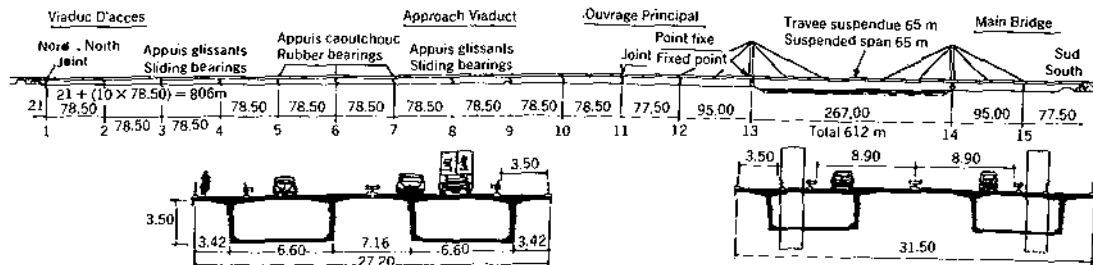


FIGURE 4.21 Tiel Bridge, general layout.

lever ends is made up of four 213-ft (65-m) suspended lightweight concrete girders.

Two alternatives were considered for the cable-stay pylons: a single pylon located on the longitudinal centerline of the bridge or a portal-type pylon. To simplify the project, the portal-type pylon was selected. The portal pylon is fixed to the pier and passes freely through the superstructure. The superstructure is fixed at the pylon piers except for rotation. It is allowed to move longitudinally at succeeding piers.

Two alternatives were also considered for the stay system: a multiple-stay system supporting the deck almost continuously and a system consisting of a few large stays. Because prestressed concrete stays had been selected, the second solution became somewhat mandatory. Construction of prestressed concrete stays is a costly operation requiring extensive high scaffolding, Fig. 4.22; thus it is advantageous to reduce the number of stays.

The short stays of the bridge have a slope of 1/1 and the long stays a slope of 1/2. Their points of anchorage to the deck are respectively at 156 ft (47.5 m) and 312 ft (95 m) on both sides of a pylon. The long stays have a cross section of 3 by 3.3 ft (0.9 by 1.0 m) and are prestressed by 36 tendons on the bank side and by 40 tendons on the river side, because of the larger load on that side. The effect of the different loads on the stays introduces a flexural moment into the pylon. The short stays have a cross section of 2.13 by 3.3 ft (0.65 by 1.0 m) and are prestressed by 16 tendons on the bank side and 20 tendons on the river side.

The concrete of the stays has a 28-day strength of approximately 8700 psi (60 MPa). Its function is not only to protect the tendons, but also to increase the rigidity of the stays, which is four times that of the tendons alone.

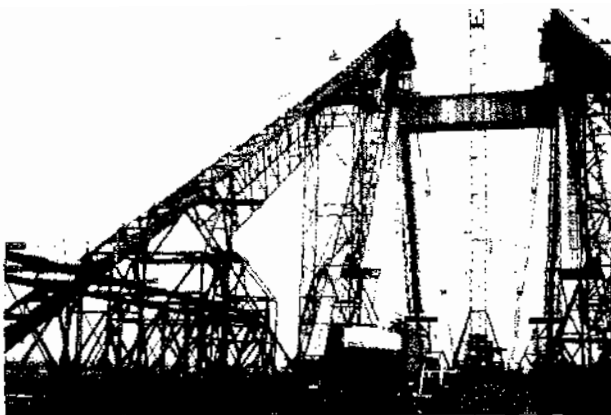


FIGURE 4.22 Falsework for stay construction.

Three loading conditions were considered for the stays from a statics point of view:

1. For the self-weight of the stays and dead load of the superstructure, the deck is considered as supported on nonyielding supports, which are the stay anchorage points, and the load in the stays results from the reactions at these points.
2. For design live load, the deck is considered as supported on yielding supports, the rigidity of which is determined by the rigidity of the prestressed stays.
3. The prestress of the stays was calculated with a safety factor against cracking of 1.1 for dead load and 1.3 for live load, without allowing any tension in the concrete. The ultimate load safety factor is 1.8. For the load condition between cracking and collapse the stay rigidity is reduced to the rigidity of the tendons alone. Their excessive elongation, in case they yielded, would lead to an excessive deflection of the box girder and a premature collapse before the proposed safety limit. Therefore, it was necessary to reduce the initial stress of the tendons to 40 to 45% of their ultimate strength in order to keep them in the elastic range up to ultimate load determined by the safety factor of the structure as a whole.

The sag of the long stay is 2.3 ft (0.70 m) in a length of 328 ft (100 m) under dead load. Under live load the sag is reduced to 1.8 ft (0.55 m). The cross section of the stays at their extremities is increased slightly to resist bending stresses. These stresses were calculated by the method of finite differences.

In the longitudinal direction the girders are prestressed primarily by the horizontal components of the stay forces. The unstayed end spans are prestressed with 54 tendons. In the other spans additional prestressing is provided by 10 tendons that overlap each other at the supports. These tendons were required until such time as the stay forces were applied and, at completion, to provide safety against cracking and collapse. The deck slab is prestressed transversely by tendons spaced at 12 to 17 in. (0.30 to 0.44 m).

The suspended 213-ft (65-m) span is composed of four precast lightweight concrete girders with a 6500 psi (45 MPa) concrete. The cast-in-place deck slab is increased from a thickness of 9.8 in. (250 mm) in the box girders to 12.6 in. (320 mm), as a result of the smaller restraint of the slab in the one-web girders.

#### 4.7 Pasco-Kennewick Bridge, U.S.A.

The first cable-stayed bridge with a segmental concrete superstructure to be constructed in the United States is the Pasco-Kennewick Intercity Bridge crossing the Columbia River in the state of Washington, Fig. 1.30. Construction began in August 1975 and was completed in May 1978. The overall length of this structure is 2503 ft (763 m). The center cable-stayed span is 981 ft (299 m), and the stayed flanking spans are 406.5 ft (124 m). The Pasco approach is a single span of 126 ft (38.4 m), while the Kennewick approach is one span at 124 ft (37.8 m) and three spans at 148 ft (45.1 m).<sup>11,14,15</sup>

The girder is continuous without expansion joints from abutment to abutment, being fixed at the Pasco (north) end and having an expansion joint at the Kennewick (south) abutment. The concrete bridge girder is of uniform cross section, of constant 7-ft (2-m) depth along its entire length and 79-ft 10-in. (24.3-m) width. The shallow girder and the long main spans are nec-

essary in order to reduce roadway grades to a minimum, to provide the greatest possible navigation clearance below, and to reduce the number of piers in the 70-ft (21.3-m) deep river.

The bridge is not symmetrical. The Pasco pylon is approximately 6 ft (1.8 m) shorter than the Kennewick pylon, and the girder has a 2000-ft (610-m) vertical curve that is not symmetrical with the main span. Therefore, the cable-stay pairs are not of equal length, the longest being 506.43 ft (154 m).<sup>15</sup>

There is no attachment of the girder at the pylons, except for vertical neoprene-*teflon* bearings to accommodate transverse loads. The girder is supported only by the stay cables. There are, of course, vertical bearings at the approach piers and abutments. It is estimated that the natural frequency of the girder, when it will respond to dynamic acceleration (i.e., earthquake), is 2 cycles per second. If the situation occurs when the longitudinal acceleration exceeds this value, the vertical restraint at the Pasco (north) abutment is designed to fail in direct shear, thus changing the

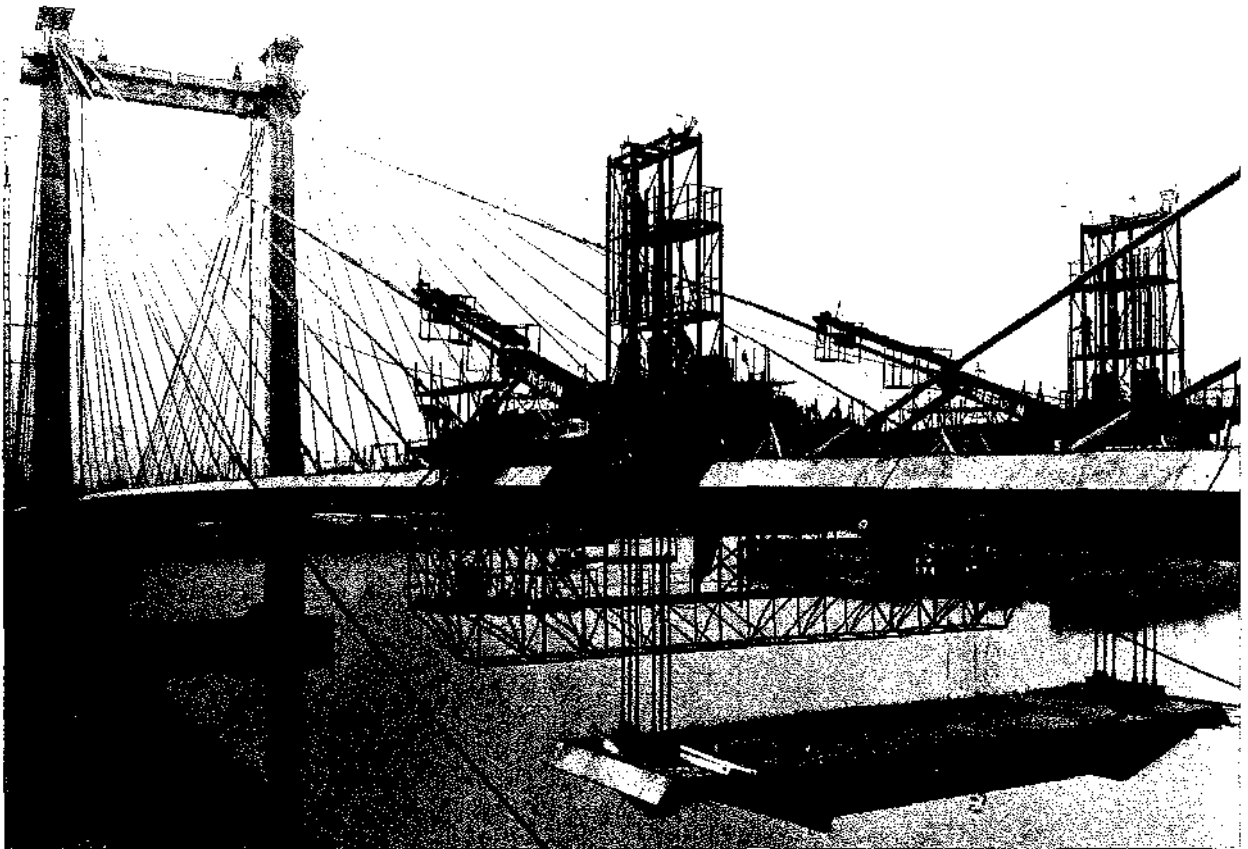


FIGURE 4.23 Pasco-Kennewick Intercity Bridge, precast segments in main spans. (Courtesy of Arvid Grant.)

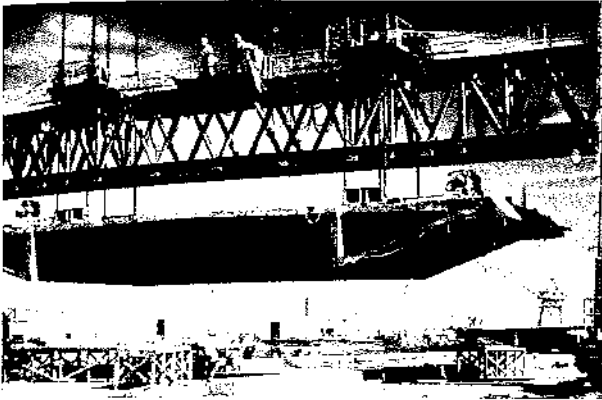


FIGURE 4.24 Pasco-Kennewick Intercity Bridge, precast segments in casting yard. (Courtesy of Arvid Grant.)

structure frequency to 0.1 cycles per second, which renders the system insensitive to dynamic excitation. The three main spans were assembled from precast, prestressed concrete segments, Fig. 4.23, while the approach spans were cast in place on falsework.

Deck segments were precast about 2 miles (3.2 km) downstream from the bridge site. Each segment weighs about 300 tons (272 mt) and is 27 ft (8.2 m) long, Fig. 4.24. The segment has an 8-in. (0.2-m) thick roadway slab, supported by 9-in. (0.22-m) thick transverse beams on 9-ft (2.7-m) centers, and is joined along the exterior girder edges by a triangular box that serves

the function of cable anchorage: stress distribution through the girder body, Fig. 4.25.<sup>6</sup> Each match-cast segment required approximately 145 yd<sup>3</sup> (111 m<sup>3</sup>) of concrete, continuously placed within six hours in a previously adopted sequence. After initial curing in the forms, the girder segments were wet cured for two weeks in the storage yard, air cured for an additional six months, prestressed transversely, cleaned, repaired, completed, loaded on a barge, and transported to the structure site for installation in their final location. For possible unpredicted developments a shimming process was held in reserve for maintaining the assembled girder geometry accuracy, but it was not used. There are no shims in the segmentally assembled, epoxy-joined prestressed concrete girder.<sup>11, 14, 15</sup> The sections were barged directly beneath their place in the bridge and hoisted into position, Fig. 4.26. Fifty-eight precast bridge girder segments were required for the project.

The stays are arranged in two parallel planes with 72 stays in each plane—that is, 18 stays on each side of a pylon in each plane. They are held at each pylon top, 180 ft (55 m) above the bridge roadway, in a steel weldment. Stay anchorages in the bridge deck are spaced at 27 ft (8.2 m) to correspond with the segment length. The stays are composed of  $\frac{1}{4}$ -in. (6-mm) diameter parallel high-strength steel wires. The prefabricated stays, manufactured by The Prescon Corporation, arrived on the job site on reels and contained

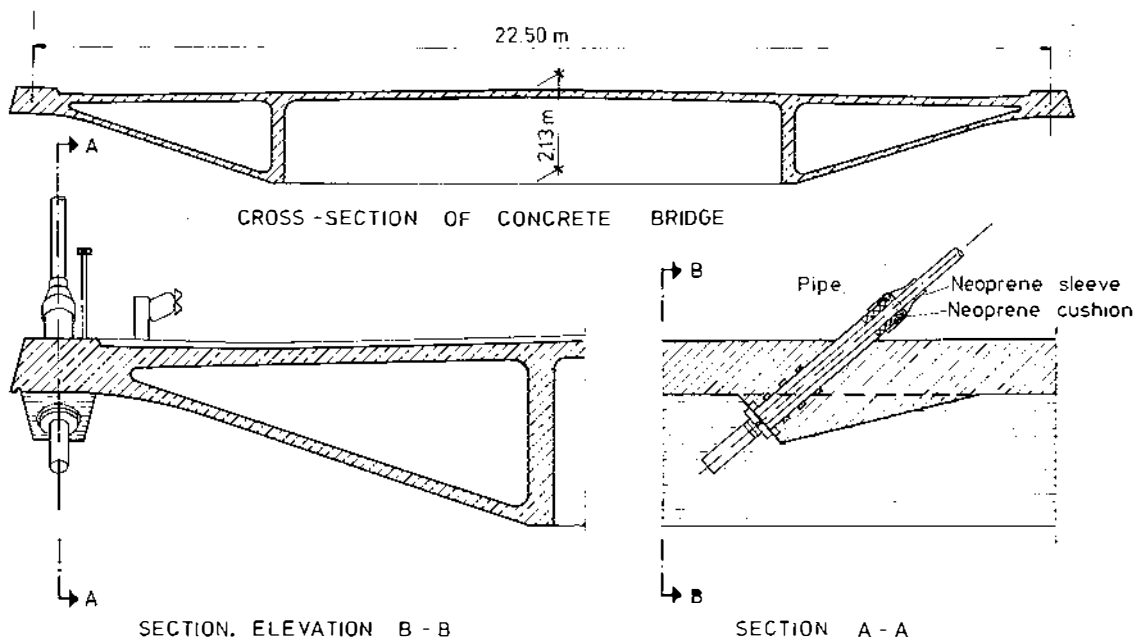


FIGURE 4.25 Pasco-Kennewick Intercity Bridge, cross section and anchorage of stay cables. (Courtesy of Fritz Leonhardt.)



**FIGURE 4.26** Pasco-Kennewick Intercity Bridge, erection of precast segments from barge. (Courtesy of Arvid Grant.)

from 73 to 283 wires, depending on their location in the structure. They were covered with a  $\frac{3}{8}$ -in. (10-mm) thick polyethylene pipe, and after installation and final adjustment were protected against corrosion by pressure-injected cement grout. The outside diameter of the pipe covering varies from 5 to 7 in. (0.12 to 0.17 m). Design stress level for the stays is 109 ksi (751.5 MPa). Stay anchorages are of the epoxy-steel ball (HiAmp) fatigue type produced by The Prescon Corporation.

This structure was designed by Arvid Grant and Associates, Inc., of Olympia, Washington, in professional collaboration with Leonhardt and Andra of Stuttgart, Germany.

#### 4.8 Brotonne Bridge, France

The Pont de Brotonne, designed and built by Campon Bernard of Paris, crosses the Seine River down-

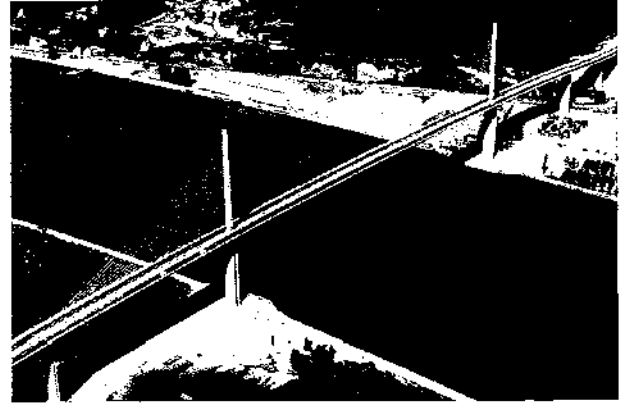


**FIGURE 4.27** Brotonne Bridge, aerial view, from reference 16.

stream from Rouen in France. Because of increased navigation traffic in the area, a second crossing over the Seine River was urgently needed between the two harbors of Le Havre and Rouen. The first one, the steel suspension bridge of Tancarville, was opened to traffic in 1959. The second, the Brotonne Bridge, was the world's largest cable-stayed prestressed concrete bridge when it was opened to traffic in June 1977,<sup>16</sup> Fig. 4.27. The box girder carries four lanes and replaces ferry service between two major highways that run north and south of the Seine. Because large ships use this section of the river to approach the inland port of Rouen 22 miles (35 km) to the east, vertical navigation clearance is 164 ft (50 m) above water level, which results in a 6.5% grade for its longer approach.<sup>11, 17</sup>

Total length of structure is 4194 ft (1,278.4 m), consisting of the main bridge and two approach viaducts. The main crossing has a span of 1050 ft (320 m). On the right bank, the transition between the main span and the ground is short because of a favorable topography where limestone strata slope upward to a relatively steep cliff. On the left bank, the terrain is flat and occupied by meadows. With an allowable maximum grade of 6.5% and a maximum height of fill of 50 ft (15 m), a nine-span viaduct was required to reach the main bridge. In a structural sense, the bridge is divided into two sections separated by an expansion joint at a point of contraflexure in the left-hand viaduct span adjacent to the cable-stayed side span, Fig. 4.28.<sup>16</sup>

The prestressed segmental concrete deck consists of a single-cell trapezoidal box girder with interior stiffening struts, Fig. 4.29. In the approach spans, web thickness is increased from 8 in. (200 mm) to 16 in. (400 mm) near the piers, and the bottom flange thick-

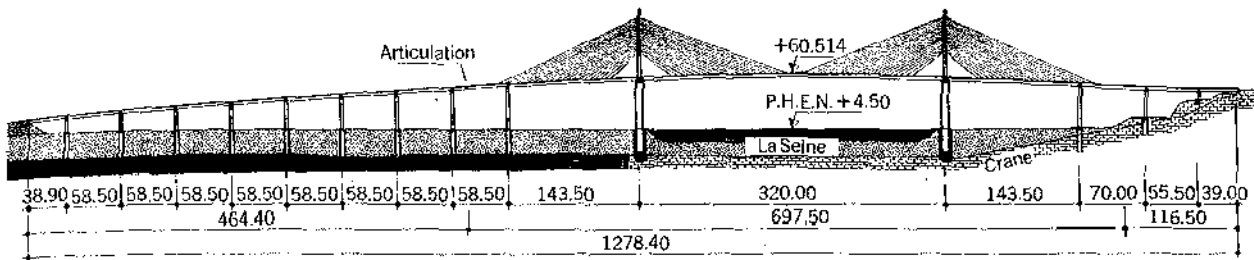


FIGURE 4.28 Brotonne Bridge, general layout.

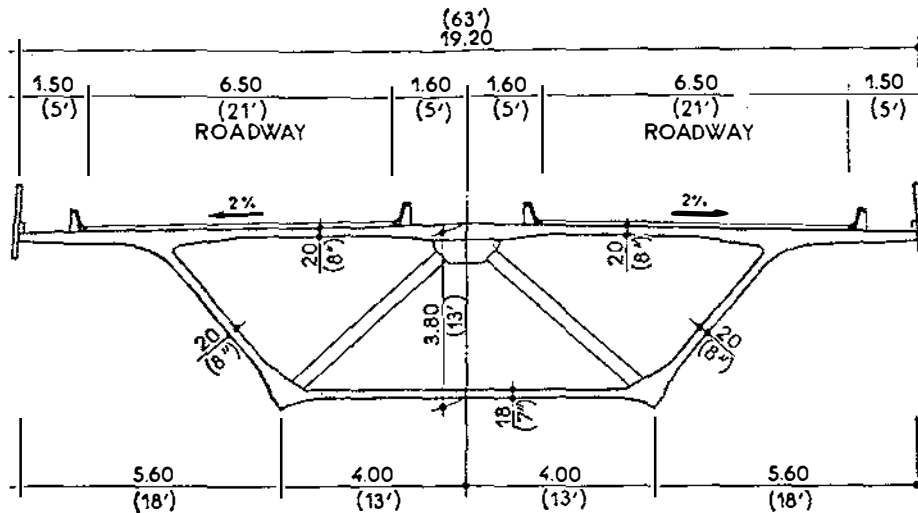


FIGURE 4.29 Brotonne Bridge, cross section.

ness is increased to a maximum thickness of 17 in. (430 mm). The only portion of the segment that was precast is its sloping webs, Fig. 4.30, which were precast at the site. The other portions of the cross section, including top and bottom flanges, interior stiffening struts, and cable-stay anchorages (in the main structure only), were cast in place. Each segment is 9.8 ft (3 m) long.

Extensive use of prestressing was made in the deck to provide adequate strength to this light structure. To resist the extreme shear stresses it was decided to place vertical prestressing in the webs. Pretensioned units were stressed on a casting bed, Fig. 4.31, and equipped with specially designed button heads, thus producing a combination of pretensioning and anchorage plates. This system has the advantage of ensuring a perfect centering of the prestressing force together with a very rapid transfer of this force at both ends. Intensive rupture tests proved that an extremely high resistance to shear was produced by this system.<sup>16</sup>

Finally, prestressing was also used as follows, Fig. 4.32.<sup>16</sup>

1. Transversely in the top flange to provide flexural strength to the thin 8-in. (200-mm) slab
2. In the inclined internal stiffeners, to accommodate tensile forces produced by the transfer of loads from the box girder to the stays
3. Transversely in the bottom flange, to counteract tensile forces created by the stiffeners
4. Longitudinally near the center of the main span, to allow for a reasonable margin of the order of 300 psi (2 MPa) of compressive stress in view of creep and secondary tensile stresses

Two single-shaft pylons support a system of 21 stays located on the longitudinal axis of the structure, Fig. 4.33. The reinforced concrete pylons required limited cross-sectional dimensions to preclude an unnecessary increase of the deck width while providing sufficient dimension to accommodate bending stresses from a transverse wind direction. Total pylon height above the deck is 231 ft (70.5 m). Construction of the pylon required leap-frog forms with 10-ft (3-m) lifts. An interesting feature is the total fixity of the pylon with the



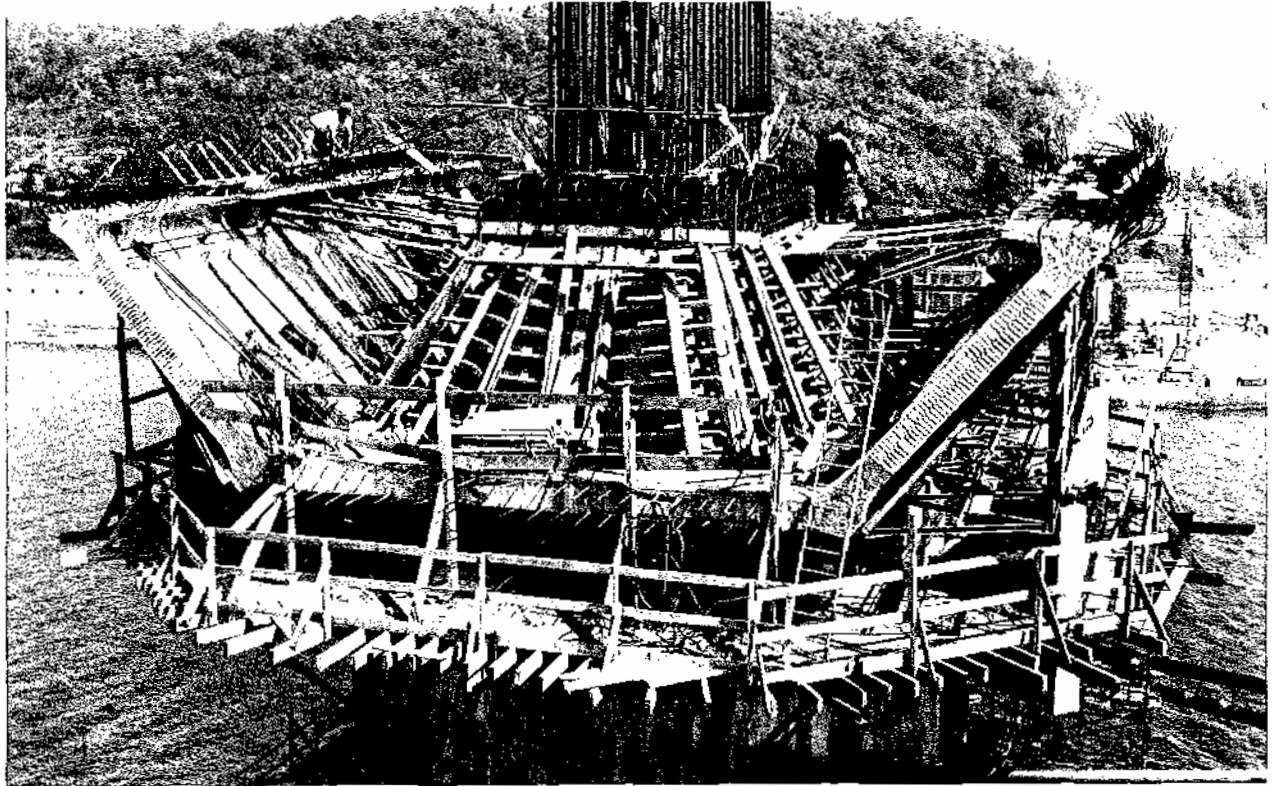


FIGURE 4.30 Brotonne Bridge, precast webs.

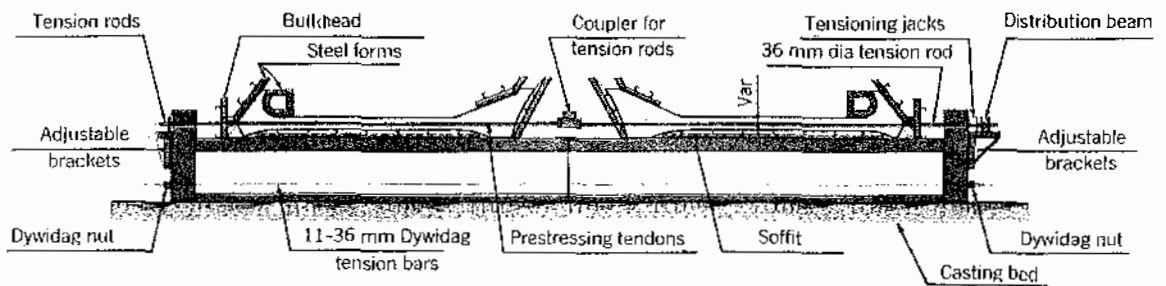


FIGURE 4.31 Casting bed for pretensioned webs.

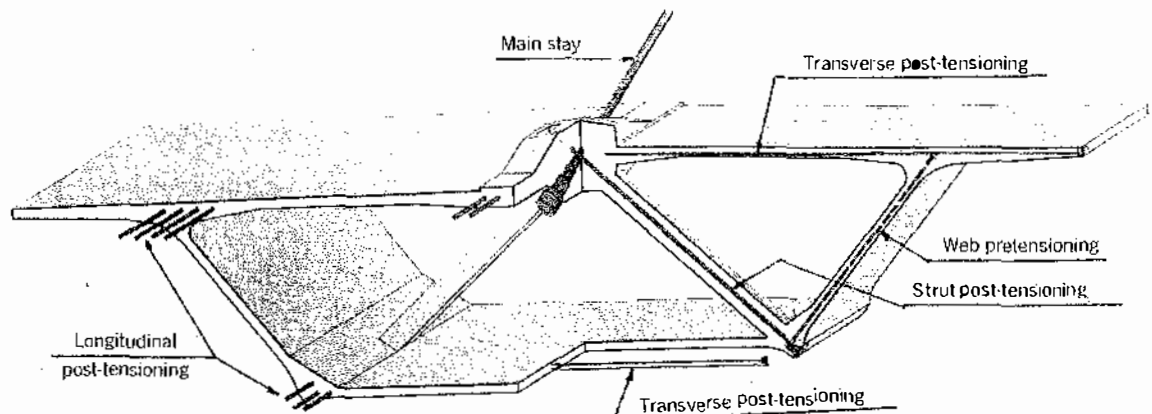
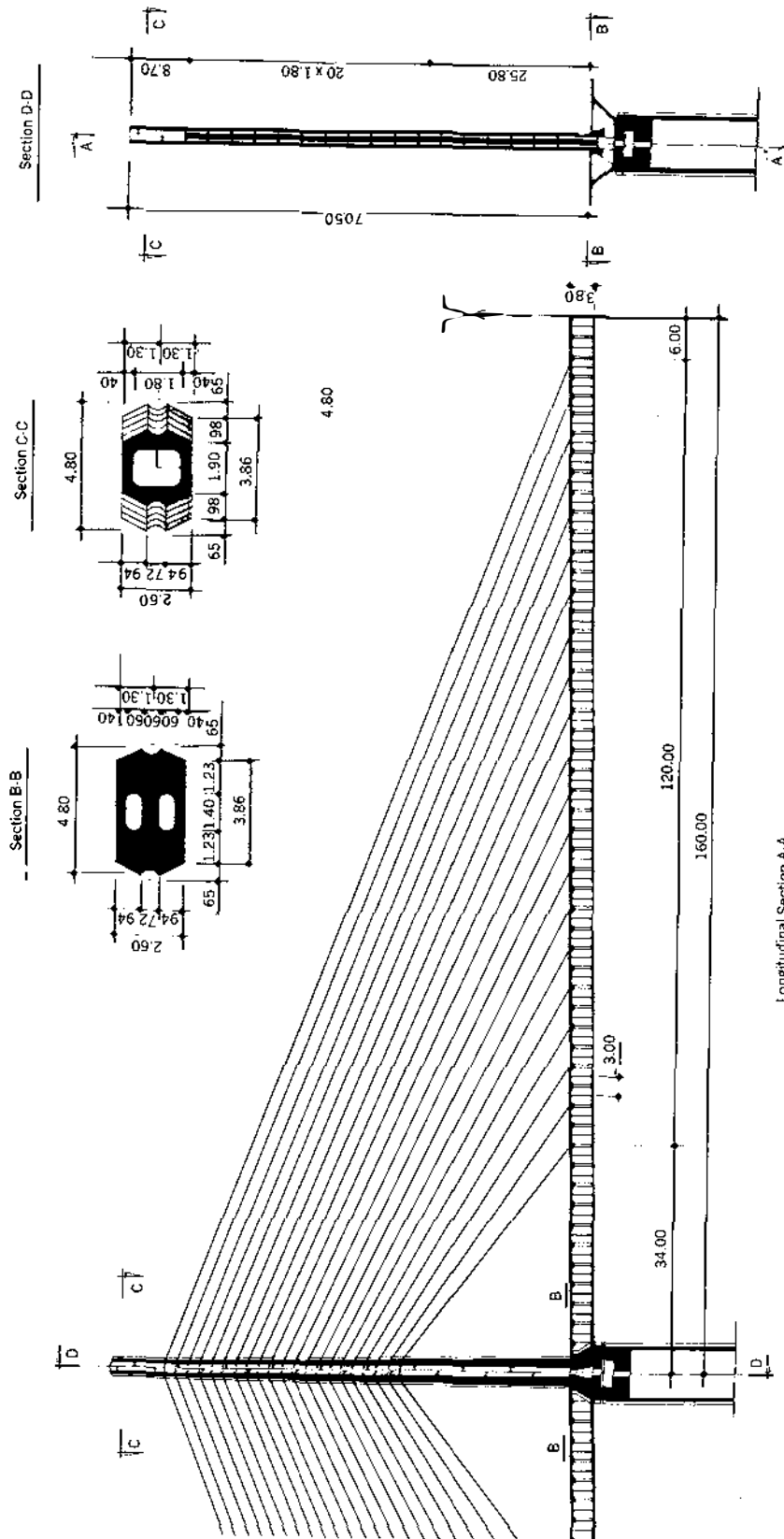


FIGURE 4.32 Various prestressing systems in the box girder.



Longitudinal Section A-A

FIGURE 4.33 Half center span and pylon.

SCHWABER ENGINEERS  
 ARCHITECTS  
 COLLEGE HAVEN CAMPUS

box girder deck. Because the bending capacity of the pylon pier and foundation had to accommodate unsymmetrical loads due to the cantilever construction, a decision was made to take advantage of this requirement in the final structure to reduce the effect of live load in the deck. Therefore, the pylon was constructed integrally with the deck at its base. Both pylon and deck were separated from the pier by a ring of neoprene bearings.

All deck loads are carried to the pylon piers by 21 stays on each pylon. Each stay consists of 39 to 60 0.6-in. (15-mm) strands encased in a steel pipe, which is grouted after final tensioning. Stay length varies from 275 to 1115 ft (84 to 340 m). Anchorage: spacing of the stays at deck level is every 19.7 ft (6 m), every other segment, where the inclined stiffeners in the deck segments converge, Fig. 4.32. A special deck-anchorage block was designed to accommodate the variable number of strands in the stay as well as to allow full adjustment of the tension in the stays by a simple anchoring nut. The anchorage of the stays is such that it is possible at any time during the life of the structure

to either readjust the tension in the stay or replace it without interrupting traffic on the bridge. Permanent jacks are incorporated into the anchorage such that by tensioning the stay the adjusting nut can be slacked off. Stays are continuous through the pylon where they transfer load to the pylon by a steel saddle. The pipe wall thickness is increased near the anchorage points and near the pylon to improve fatigue resistance of the stays with respect to bending reversals.<sup>16</sup>

#### 4.9 Danube Canal Bridge, Austria

This structure is located on the West Motorway (Vienna Airport Motorway) and crosses the Danube Canal at a skew of 45 degrees. It has a 390-ft (119-m) center span and 182.7-ft (55.7-m) side spans, Fig. 4.34. It is unique because of its construction technique. Because construction was not allowed to interfere with navigation on the canal, the structure was built in two 360.8-ft (110-m) halves on each bank and parallel to the canal, Fig. 4.35. On completion the two halves

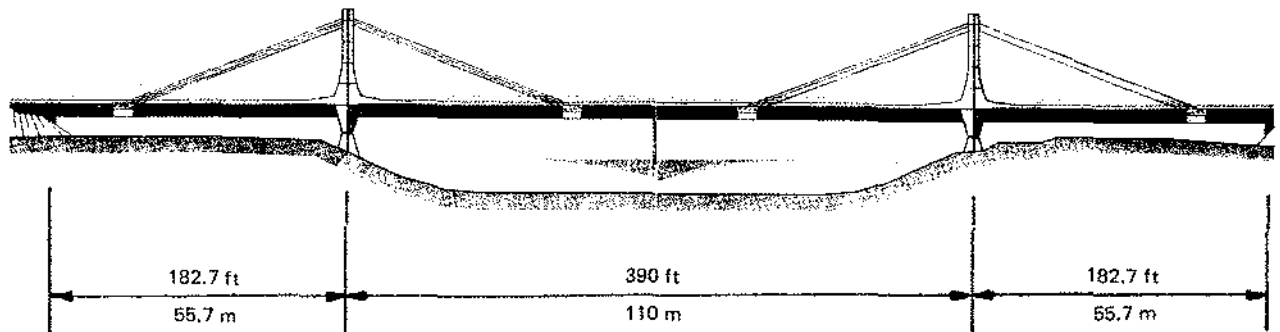


FIGURE 4.34 Danube Canal Bridge, elevation.

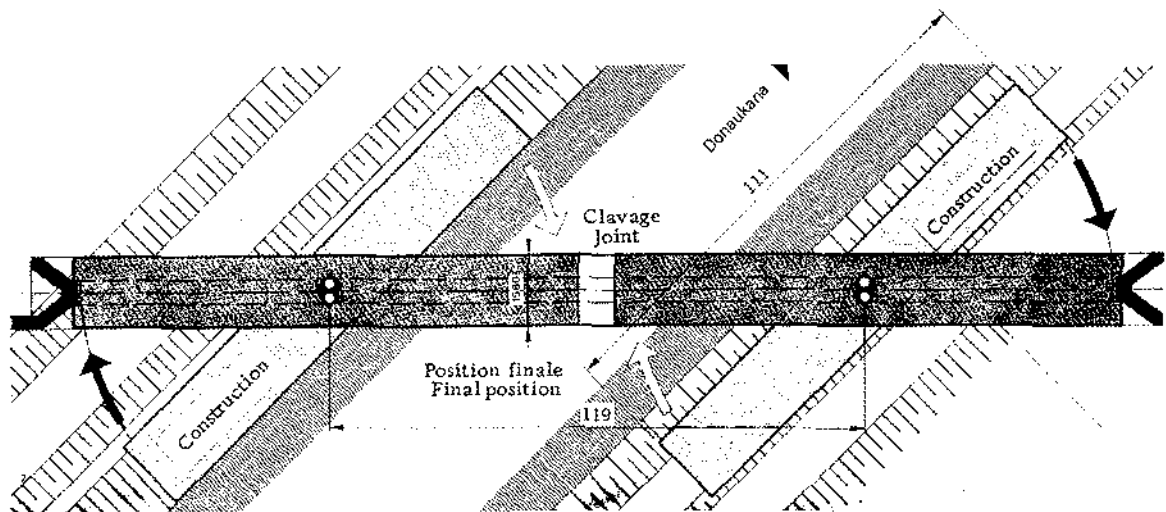


FIGURE 4.35 Danube Canal Bridge, plan during construction and final state.

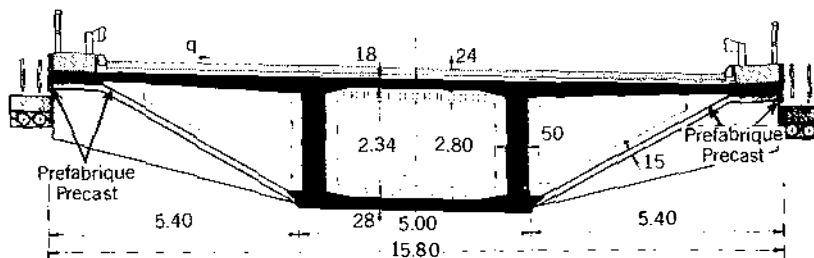


FIGURE 4.36 Danube Canal Bridge, cross section.

were rotated into final position and a cast-in-place closure joint was made. In other words, each half was constructed as a one-time swing span.

The bridge superstructure is a 51.8-ft (15.8-m) wide trapezoidal three-cell box girder, Fig. 4.36. The central box was cast in 25-ft (7.6-m) long segments on falsework. After the precast inclined web segments were placed, Fig. 4.37, the top slab was cast.

Each half-structure has two cantilever pylons fixed in a heavily prestressed trapezoidal crosshead protruding under the deck with a two-point bearing on the pier, Fig. 4.38. At the deck level the stays attach to steel brackets connected to prestressed crossbeams.

Each stay consists of eight cables, two horizontal by four vertical. At the top of the pylons each cable is seated in a cast-iron saddle. The cable saddles are stacked four high, Fig. 4.39, and are fixed to each other as well as to those in the adjacent plane. The cables were first laid out on the deck, fixed to a saddle, and then lifted by a crane for placement at the top of the pylon. The cables were then pulled at each extremity by a winch rope to their attachment point at the deck level.

During rotation of the two half-bridges, the deck and pylon sat on a bearing consisting of five epoxy-glued circular steel plates. The top plate was coated with teflon, sitting in turn on a reinforced concrete

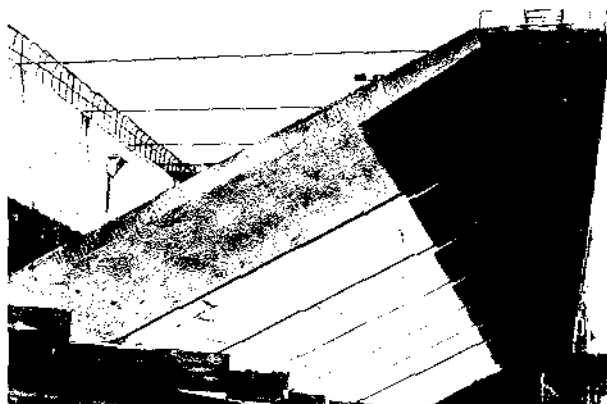


FIGURE 4.37 Danube Canal Bridge, precast webs.



FIGURE 4.38 Danube Canal Bridge, trapezoidal crosshead.

block that sat on a sand box. After rotation, the structure was lowered to permanent bearings by emptying the sand box.

At the canal-bank end the deck had a concrete wall on its underside, bearing on a circular concrete sliding track, Fig. 4.40. The bearing between the wall and the track was effected by two concrete blocks clad with steel plates, under which teflon-coated neoprene pads were introduced during the rotation movement (similar to the incremental launching method). The pivoting was accomplished by means of a jack pulling on a

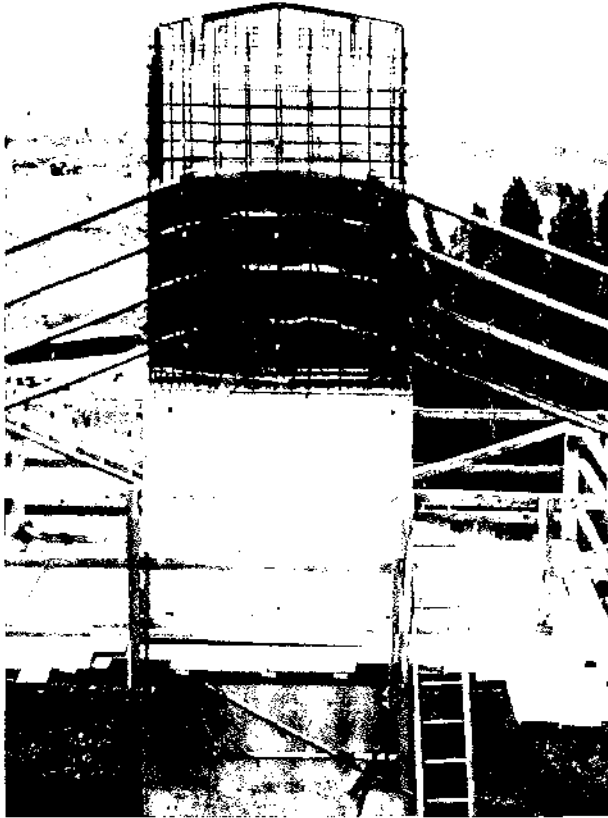


FIGURE 4.39 Danube Canal Bridge, stay saddles at pylon.



FIGURE 4.40 Danube Canal Bridge, circular concrete sliding track.

cable anchored in a block located near the sliding-track end.

After rotation the two halves of the structure were connected by a cast-in-place closure joint, and continuity tendons were placed and stressed.<sup>18</sup> The final structure is shown in Fig. 4.41.

#### 4.10 Sunshine Skyway Bridge, U.S.A.

The Sunshine Skyway Bridge crosses Tampa Bay on the west coast of Florida, connecting St. Petersburg and Bradenton, Fig. 4.42. The existing Sunshine Sky-

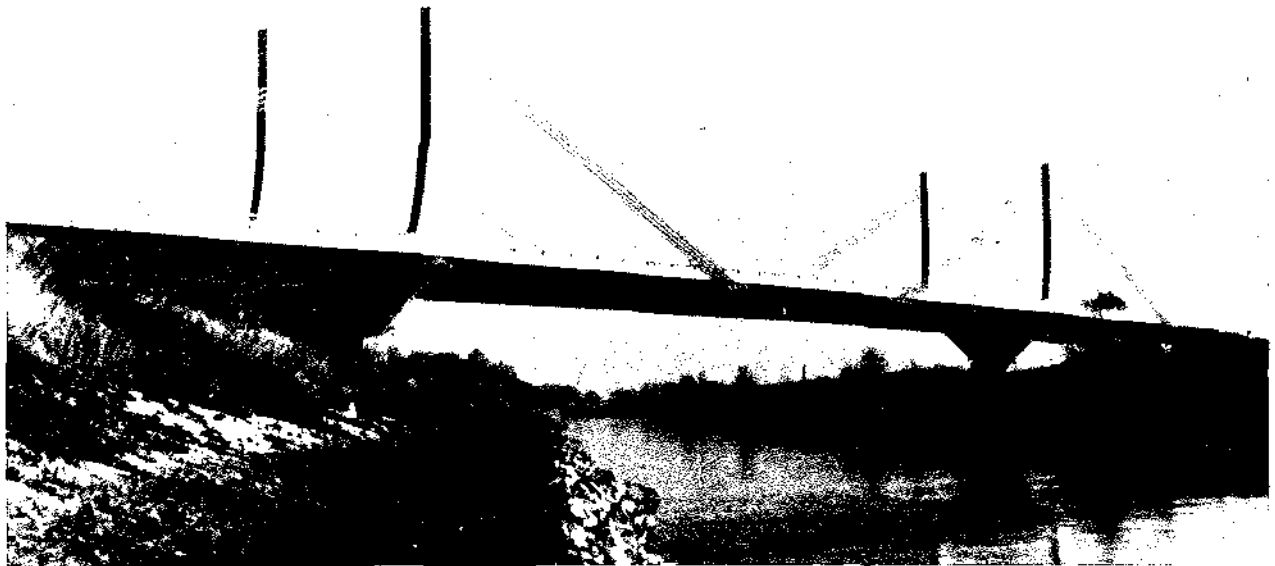


FIGURE 4.41 Danube Canal Bridge, completed.

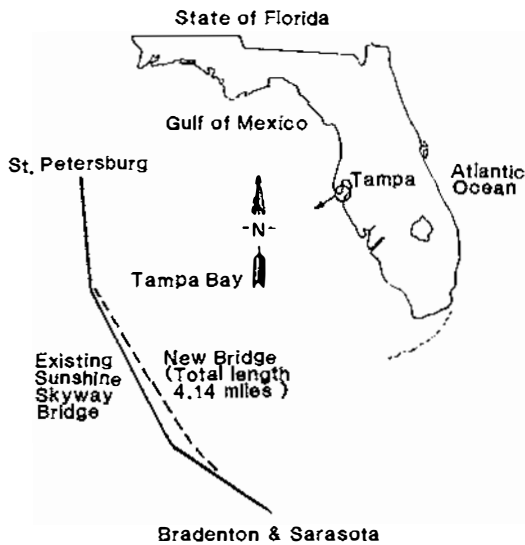


FIGURE 4.42 Sunshine Skyway Bridge, location map.

way Bridge, a structural steel cantilever truss, was completed in 1954, and a dual structure was completed in 1971. On May 9, 1980, a freighter rammied into an anchor pier of the western bridge (constructed in 1954) causing the collapse of 1300-ft (396 m) of superstructure. As a result of this event, along with the determination that the existing roadway width was inadequate for future traffic demands and the fact that the existing low-level trestle approaches were in need of repair, a decision was made to replace the existing bridge with a new one, Figs. 4.43 and 1.36.

The total length of structure for the new bridge is 4.14 miles (6.67 km), including an 8869-ft (2700-m) center portion consisting of high-level approaches and

navigation spans. The high-level approaches are: twin, single-cell, precast concrete segmental box girder units, each of which is 17 ft 10 in. (5.4 m) in length, 8 ft (2.44 m) deep, and weighs approximately 75 tons (68 mt), Fig. 4.44(a). A 4000-ft (1,219-m) continuous main span unit providing a 175-ft (53.3-m) vertical navigation clearance has spans of 140-3 at 240-540-1200-540-3 at 240, and 140 ft (42.67-3 at 73.15-164.59-365.76-164.59-3 at 73.15, and 42.67 m). In this unit, the precast concrete segmental girder unit is a 95-ft 3-in. (29-m) wide single-cell box, Fig. 4.44(b). Each will be 14 ft (4.27 m) deep, 12 ft (3.65 m) long, and will weigh approximately 175 tons (159 mt).

Main span box girder segments are conceptually similar to those of the Brotonne Bridge, Figs. 4.29 and 4.32, with the exception that at the stay anchorages, twin diagonal struts are provided. The cross section contains transverse posttensioning in the top and bottom flanges as well as in the webs. In the Brotonne Bridge the webs were precast, and the top and bottom flanges were cast-in-place, Fig. 4.30. In the Sunshine Skyway Bridge the cross section is a monolith unit. The segments are match-cast at the webs and bottom flange. The top flange is blocked back to permit a 1-ft (0.305-m) cast-in-place joint after erection.

The 21 stays on each side of the pylon are continuous through the pylon, which rests on saddles, and consist of a varying number of 0.6-in. (15-mm) 7-wire prestressing strands. Stays are connected to the box girder superstructure at 24-ft (7.3-m) centers.

In the Brotonne Bridge the single shaft pylon was rigidly connected to the box girder superstructure, Fig. 4.30, and was supported on a ring of neoprene bearings atop the pier shaft (see Section 4.8). In the Sun-

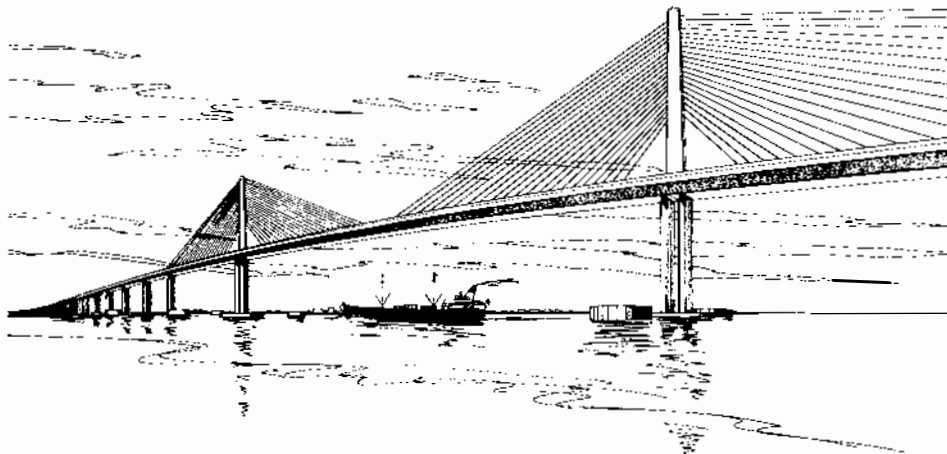
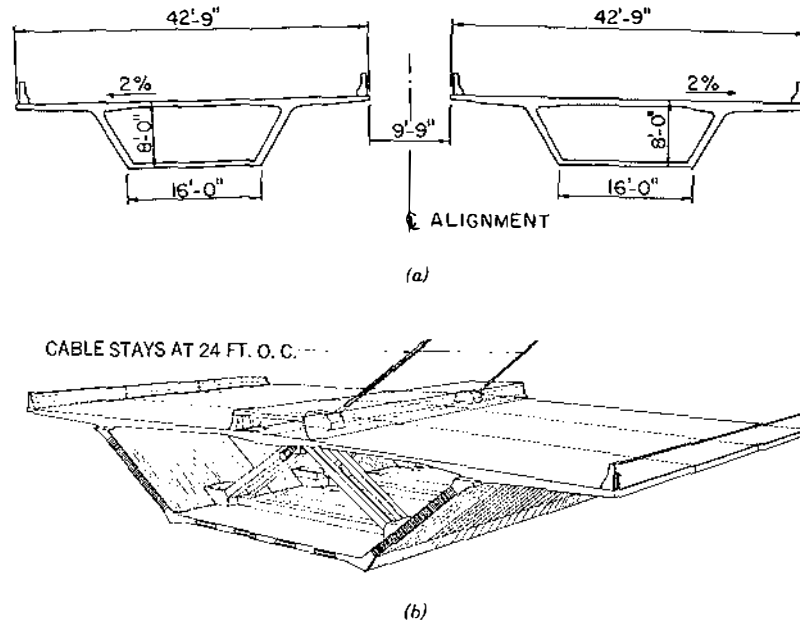


FIGURE 4.43 Artist's rendering of Sunshine Skyway Bridge. (Courtesy of figg and Muller Engineers, Inc.)



**FIGURE 4.44** Sunshine Skyway Bridge, box girder elements, main span superstructure: (a) twin single-cell box girder and (b) large single-cell box girder.

shine Skyway Bridge the single shaft pylon, the box girder superstructure, and the twin pier shafts are all rigidly connected together. Longitudinal movement is accommodated by the flexibility of the twin pier shafts.

#### 4.11 Neches River Bridge, U.S.A.

The concrete cable-stayed Neches River Bridge in Texas, Figs. 1.38 and 4.45, has a harp configuration of stays in two vertical planes. It has a center span of

640 ft (195 m) and allows a minimum vertical navigation clearance of 143 ft (43.6 m). A temporary pier adjacent to the pylon, Fig. 4.45, allows approach spans of 140 ft (42.7 m) to be constructed by the segmental span-by-span method up to the pylons. At an appropriate point during construction the temporary piers are removed producing spans of 280, 640, and 280 ft (85, 195, and 85 m). The center span is erected by the cantilever method from the pylons.

The superstructure consists of precast segmental trapezoidal box units (without flange cantilevers), Fig.

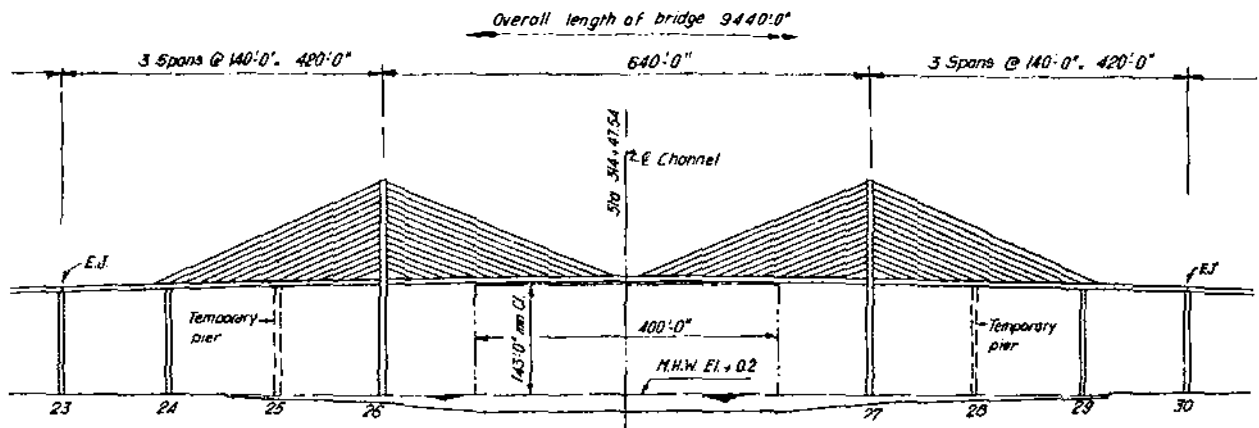


**FIGURE 4.45** Neches River Bridge, elevation of the main spans.

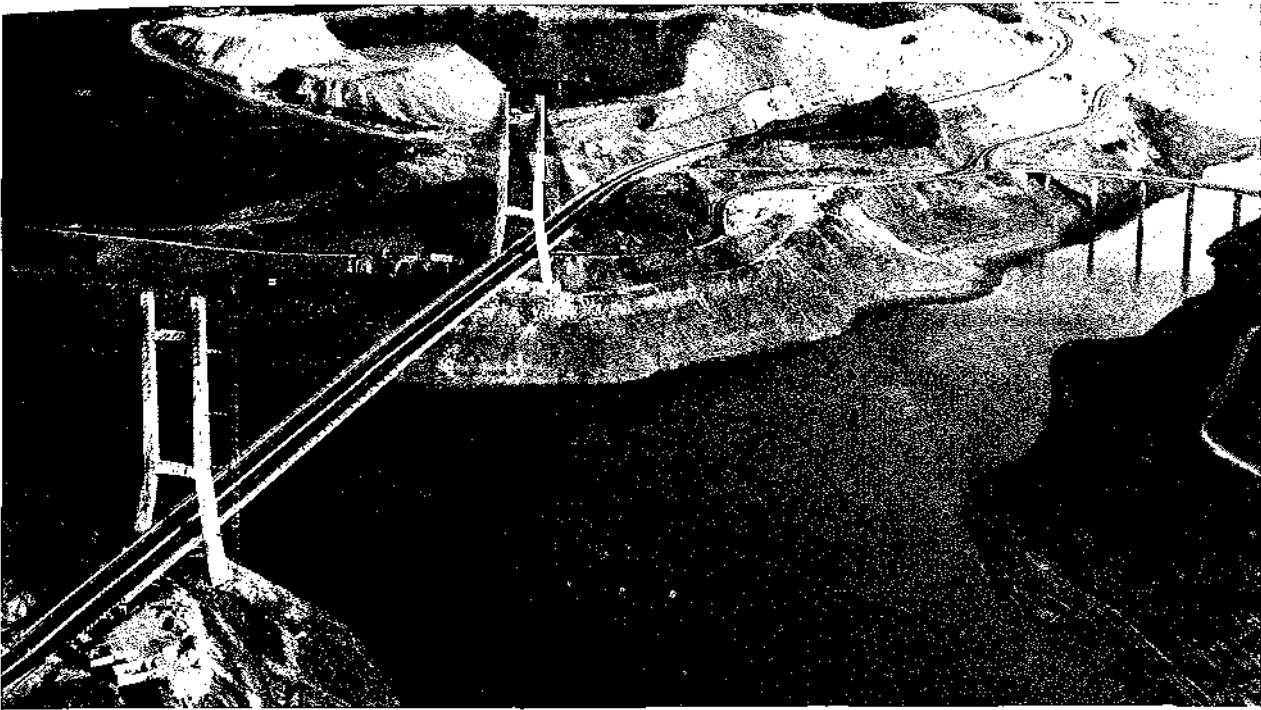


FIGURE 4.46 Barrios de Luna Bridge, aerial view. (Courtesy of W. C. Sherwood, Stronghold International, Ltd.)

2.14(c). Width of the cross section between stay anchorage blocks is 56 ft (17 m), and depth of the box is 8 ft (2.4 m). Segment length is 10 ft (3.05 m), with cable stay spacing along the girder at 20 ft (6.1 m). Stays are parallel 0.6-in. (15-mm) diameter strands continuous over saddles at the pylons.

#### 4.12 Barrios de Luna Bridge, Spain

The Barrios de Luna Bridge in northern Spain crosses a deep reservoir near the city of Leon, Fig. 4.46. The shortest crossing of the reservoir required a center span of 1443 ft 6 in. (440 m), and this structure, therefore, holds the record for the longest concrete cable-stayed span (1985). Constraints at the site that dictated this extraordinary span were:

1. Water depth of 164 ft (50 m), seasonal rainfall produces large fluctuating variations in the reservoir's depth
2. Seriously weakened strata of the flooded valley
3. Strata containing boulders up to 56 ft (17 m) thick

The structural design that evolved from all the economical alternatives studied was that indicated in Fig.

4.47, with a central span of 1443 ft 6 in. (440 m) and side spans of 219 ft (66.74 m) which are balanced by concrete counterweights. The pylon, Figs. 4.48 and 4.49, has a height above deck level of 295 ft (90 m), producing a pylon height-to-span ratio of 0.2.<sup>19,20</sup>

The shape of the pylon was determined by two conditions. In the top portion, its axis had to be in the vertical plane that contained the stay connections at the deck level, Fig. 4.49. This minimizes the lateral force imparted to the pylon and produces reasonable dimensions for the pylon size. The bottom portion of the pylon is splayed outward to produce an increase of stiffness in the pylon to accommodate transverse wind loads without complicating construction.<sup>19</sup>

Cable stays are constructed of 0.6-in. (15-mm) high-tensile strength prestressing strand. The number of strands in a stay varies from 24 to 76 depending on the position of the stay in the structure.

The superstructure has a depth of 7 ft 6 in. (2.3 m) at its edges and a depth of 8 ft 2 in. (2.5 m) at the longitudinal centerline of the bridge, Fig. 4.47. Slab thickness is  $7\frac{7}{8}$  in. (200 mm), except for the inclined webs which have a thickness of  $9\frac{1}{2}$  in. (240 mm).

In the center portion of the bridge, where axial forces produced by the stays is small, part of the lower flange was eliminated, Fig. 4.50. Thus, the weight of



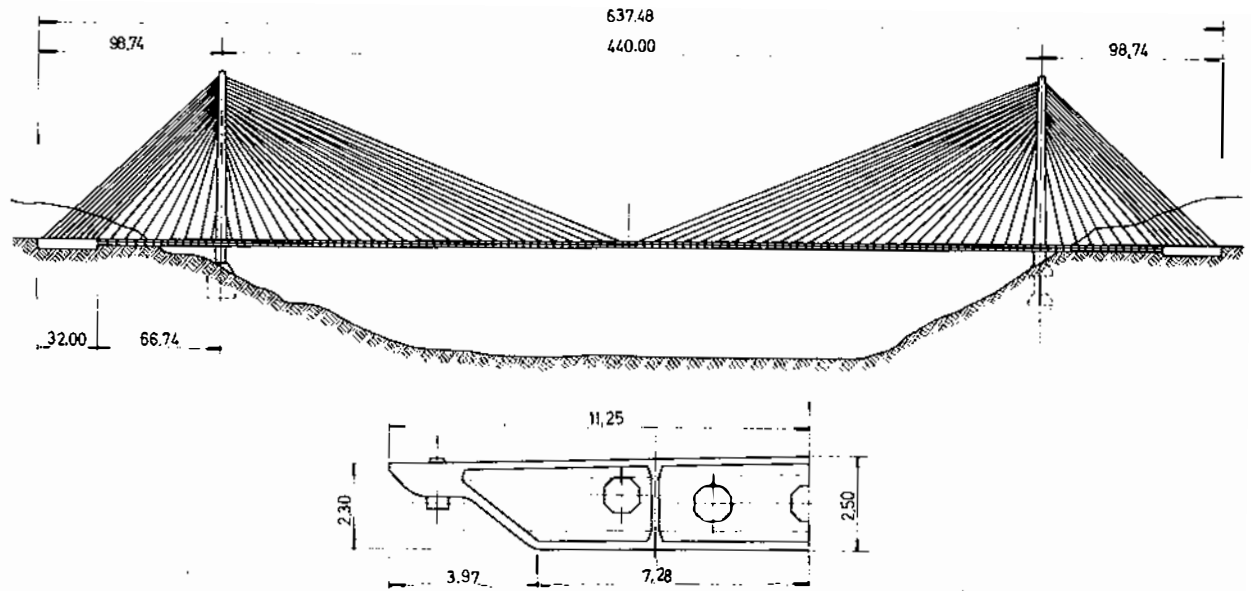


FIGURE 4.47 Barrios de Luna Bridge, elevation and cross section. (Courtesy of W. C. Sherwood, Stronghold International, Ltd.)

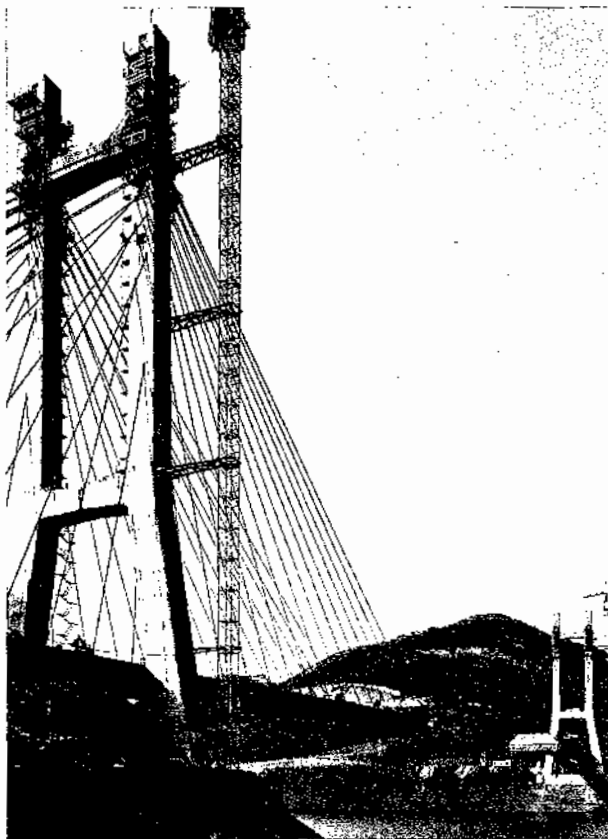


FIGURE 4.48 Barrios de Luna Bridge, pylon. (Courtesy of W. C. Sherwood, Stronghold International, Ltd.)

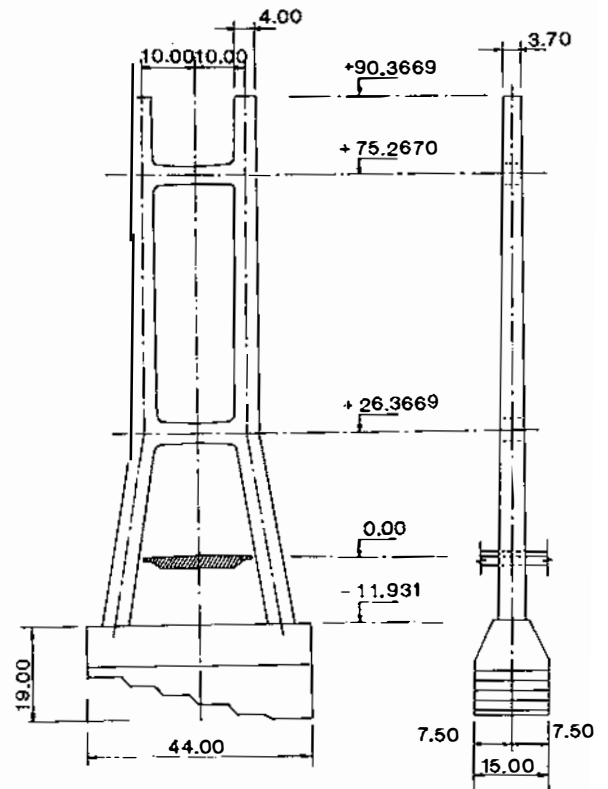
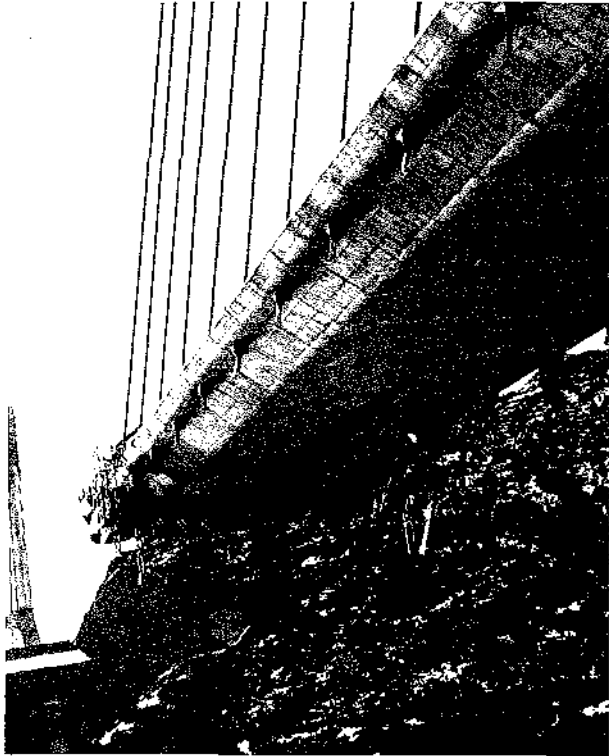


FIGURE 4.49 Barrios de Luna Bridge, pylon layout. (Courtesy of W. C. Sherwood, Stronghold International, Ltd.)



**FIGURE 4.50** Barrios de Luna Bridge, superstructure during construction. (Courtesy of W. C. Sherwood, Stronghold International, Ltd.)

the deck is reduced in that portion of the structure where stay inclination is the least. A  $7\frac{7}{8}$ -in. (200-mm) thick transverse diaphragm is located every 13 ft 4 in. (4.08 m), that is, one in every segment. The diaphragm is located at the rear of the segment, with respect to the direction of construction, to facilitate removal of the interior mandrel formwork. Transverse prestressing is provided in the diaphragm.

The deck is monolithic with the counterweight and has a sliding hinge joint at the center of the main span. The principal advantage of the center hinge is the reduction of bending moments in the center of the bridge. There are, however, disadvantages of a center hinge: (1) the joint must transmit shear and torsional forces, and (2) there is a discontinuity in the riding surface—for the loads specified by the Spanish Standards an angular discontinuity of 0.6 degree and 0.3 degree resulted for the usual loads on the bridge.<sup>19</sup>

### 4.13 Notable Examples of Concepts

#### 4.13.1 DANISH GREAT BELT BRIDGE COMPETITION

The competition for a suitable bridge design in Denmark produced many new concepts and architectural

styles. The design requirements specified three lanes for vehicular traffic in each direction and a single railway line in each direction. The rail traffic was based on speeds of 100 mph (161 km/hr).<sup>21</sup> Navigational requirements stipulated that the bridge deck be 220 ft (67 m) above water level, and the clear width of the channel was to be 1130 ft (345 m).

A third-prize winner in this competition was the Morandi-style design proposed by the English consulting firm of White Young and Partners, Fig. 2.5. This design embodied the principles of a cable-stayed bridge combined with conventional approaches of girders and piers with normal spans.

The principal feature of this bridge design is the three-plane alignment of cable stays. This feature may become more important in urban areas, where future trends may dictate multimodal transportation requirements and an increase in the number of automobile traffic lanes. The deck consists of two parallel single-cell prestressed concrete box girder segments, Fig. 4.51. The rail traffic is supported within the box on the bottom flange, and the road traffic is carried on the surface of the top flange.

The box girder contemplated a depth of 23.5 ft (7.2 m) and width of 27.75 ft (8.45 m) with the top flange cantilevering 12 ft (3.7 m) on each side. The piers and towers were to be cast-in-place construction to support the deck segments, which were to be precast at various locations on shore and floated to the bridge site for erection. The maximum weight of a single box segment was estimated at 2200 tons (2000 mt). All segments of the superstructure were to be of reinforced and prestressed concrete.

Up to the time when the competition for this structure was conducted, all the concrete cable-stayed bridges had been either designed by Morandi (Lake Maracaibo, Wadi Kuf, and so on) or strongly influenced by his style (Chaco/Corrientes). They were typified, for the most part, by the transverse A-frame pylon with auxiliary X-frame support for the girder. However, another entry in this competition by Ulrich Finsterwalder of the West German firm of Dyckerhoff & Widmann deviated from this style and was awarded a second prize.

Finsterwalder proposed a multiple span, multistay system using Dywidag bars for the stays, Fig. 4.9. This proposal contemplated a spacing between pylons of 1148 ft (350 m) and a spacing of the stays at deck level of 32.8 ft (10 m). Pylon height above water level was 520 ft (158.5 m). In a transverse cross section the deck was 146 ft (44.5 m) wide with two centrally located vertical stay planes 39 ft 4 in. (12 m) apart to accommodate the two rail traffic lanes, and three auto-

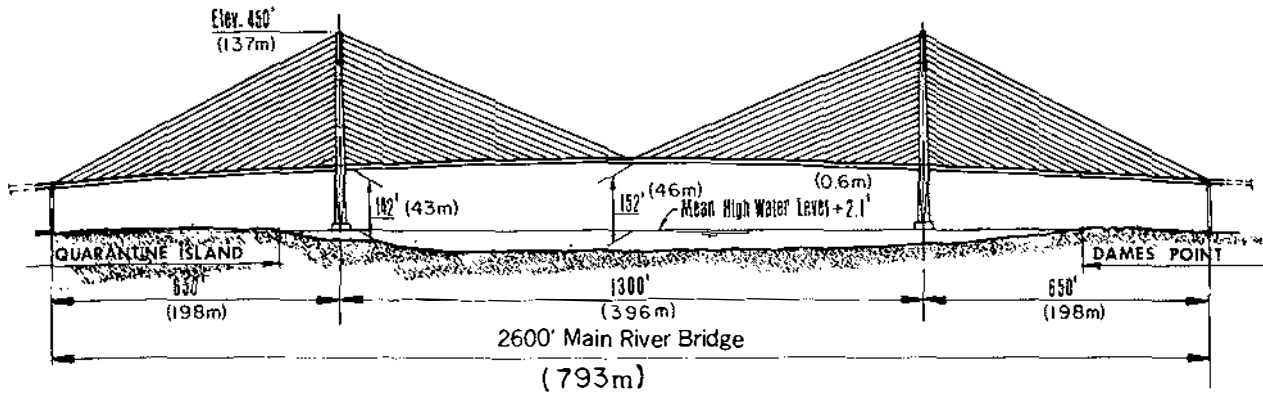


**FIGURE 4.53** Dame Point Bridge, concrete cable-stayed alternative, from reference 22. (Courtesy of Howard Needles Tammen & Bergendoff.)

requirements dictate a 1250-ft (381-m) minimum horizontal opening and a vertical clearance of 152 ft (46.3 m) above mean high water at the centerline of the clear opening. The proposed concrete cable-stayed main structure will have a 1300-ft (396-m) central span with 650-ft (198-m) flanking spans. The layout of the main structure is shown in Fig. 4.53.<sup>22</sup>

Structural arrangement of the bridge deck is shown in Fig. 4.54. The bridge deck, which will support three lanes of traffic in each direction, will span between longitudinal edge girders on each side. The longitudinal edge girder is in turn supported by a vertical plane of stays arranged in a harp configuration. The concrete deck and edge girders resist local and overall bending from dead and live load in addition to the horizontal thrust from the stays.<sup>23</sup> The stay cables are anchored in massive vertical concrete pylons, two at each main pier, which carry all loads to the foundations, Fig. 4.55.

In the center span, at each edge of the deck, the stays are in a single plane spaced 30 in. (0.76 m) vertically, Figs. 4.55 and 4.56. Stays in the side spans, along each edge, are in two planes spaced 30 in. (0.76 m) transversely. Spacing of pairs of stays along the edge beam is approximately 30 ft (9.1 m). Preliminary design contemplates 7 to 9 Dywidag bars per stay, 1 1/4

in. (31.75 mm) in diameter, the number of bars per stay being a function of stress in the stay. The Dywidag bars are to be encased in a metal duct. During erection the fabricated length of duct is left uncoupled. After final adjustment the lengths of duct are coupled and pressure-grouted, thus, the steel encasing tube will then be composite for live load and secondary dead load.<sup>23</sup>

Construction proceeds by conventional methods from the top of the pier bases at elevation 15.0 ft (4.6 m) to the level of the roadway at elevation 144.6 ft (44 m). At this point, a fixed formtable is secured and the first elements of the pylon and edge girders are cast. Erection of the deck is by the balanced cantilever method. Two pairs of traveling forms are then used for sequential casting of 17.5-ft (5.3-m) lengths of edge girders on each side of the pylon. The bridge deck consists of single-T precast floor beams spanning between longitudinal edge girders and a cast-in-place topping. The precast Ts are pretensioned for erection loads. After erection the entire deck is post-tensioned to provide positive precompression between edge girders under all conditions of loading, Fig. 4.56.<sup>22,23</sup>

A hinge expansion joint is provided at the centerline of the main span to allow for changes of superstructure length due to temperature, creep, and shrinkage. Similar joints are provided at the end piers, and link connections are used to prevent vertical movement of the superstructure.

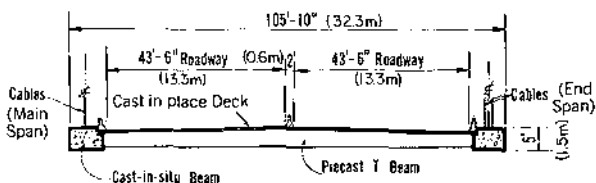


**FIGURE 4.54** Dame Point Bridge, structural arrangement of bridge deck, from reference 22. (Courtesy of Howard Needles Tammen & Bergendoff.)

#### 4.13.3 PROPOSED RUCK-ACHUCKY BRIDGE, U.S.A.

The site for the proposed Ruck-A-Chucky Bridge, designed by T. Y. Lin International, Fig. 1.32, is approximately 10 miles (16 km) north of the proposed

#### 4.7 Pasco-Kennewick Bridge, U.S.A.

The first cable-stayed bridge with a segmental concrete superstructure to be constructed in the United States is the Pasco-Kennewick Intercity Bridge crossing the Columbia River in the state of Washington, Fig. 1.30. Construction began in August 1975 and was completed in May 1978. The overall length of this structure is 2503 ft (763 m). The center cable-stayed span is 981 ft (299 m), and the stayed flanking spans are 406.5 ft (124 m). The Pasco approach is a single span of 126 ft (38.4 m), while the Kennewick approach is one span at 124 ft (37.8 m) and three spans at 148 ft (45.1 m).<sup>11,14,15</sup>

The girder is continuous without expansion joints from abutment to abutment, being fixed at the Pasco (north) end and having an expansion joint at the Kennewick (south) abutment. The concrete bridge girder is of uniform cross section, of constant 7-ft (2-m) depth along its entire length and 79-ft 10-in. (24.3-m) width. The shallow girder and the long main spans are nec-

essary in order to reduce roadway grades to a minimum, to provide the greatest possible navigation clearance below, and to reduce the number of piers in the 70-ft (21.3-m) deep river.

The bridge is not symmetrical. The Pasco pylon is approximately 6 ft (1.8 m) shorter than the Kennewick pylon, and the girder has a 2000-ft (610-m) vertical curve that is not symmetrical with the main span. Therefore, the cable-stay pairs are not of equal length, the longest being 506.43 ft (154 m).<sup>15</sup>

There is no attachment of the girder at the pylons, except for vertical neoprene-*teflon* bearings to accommodate transverse loads. The girder is supported only by the stay cables. There are, of course, vertical bearings at the approach piers and abutments. It is estimated that the natural frequency of the girder, when it will respond to dynamic acceleration (i.e., earthquake), is 2 cycles per second. If the situation occurs when the longitudinal acceleration exceeds this value, the vertical restraint at the Pasco (north) abutment is designed to fail in direct shear, thus changing the

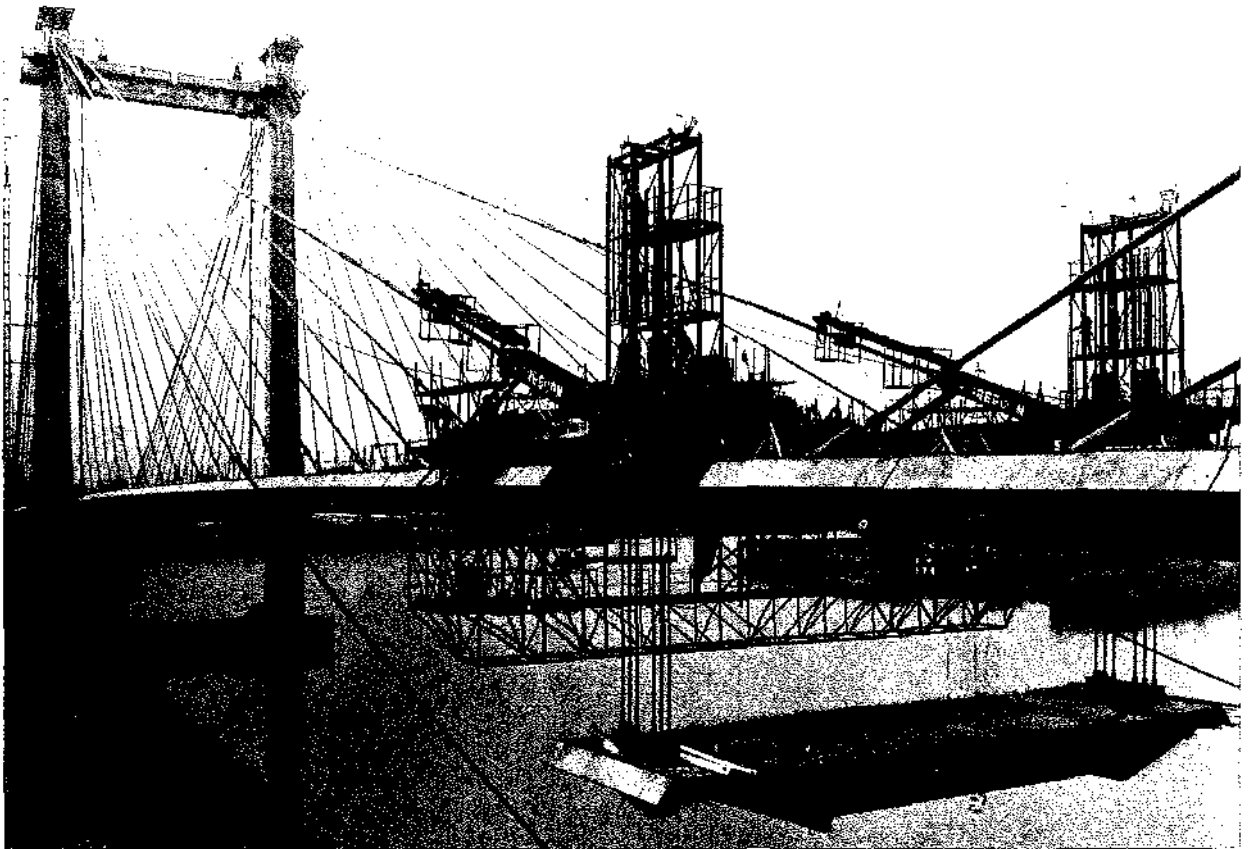


FIGURE 4.23 Pasco-Kennewick Intercity Bridge, precast segments in main spans. (Courtesy of Arvid Grant.)

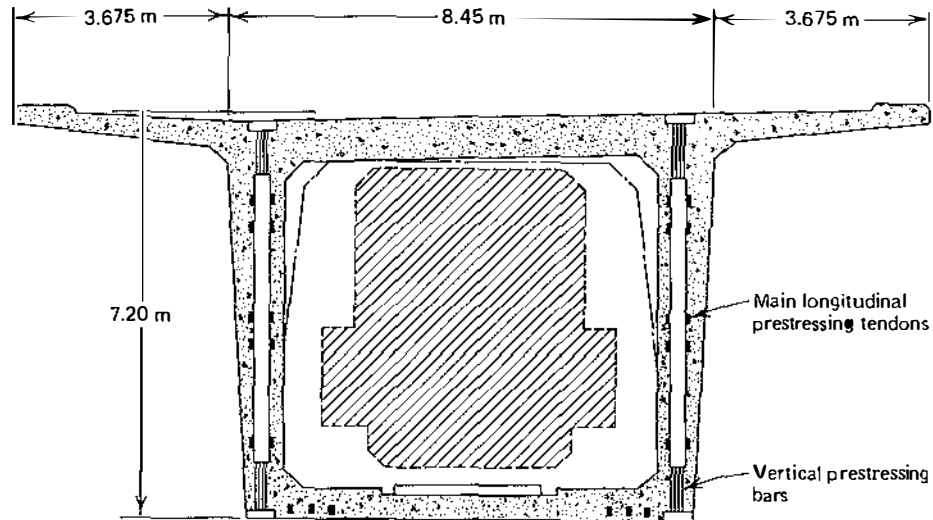


FIGURE 4.51 Danish Great Belt Bridge, section through deck beam at expansion and construction joint, from reference 21.

mobile traffic lanes in each direction outboard of the stay planes, Fig. 4.52.

The solid concrete deck had a thickness of 3 ft (0.9 m) in the transverse center portion, under the rail traffic, and tapered to a 1.3 ft (0.4 m) thickness at the edges. The deck was to be constructed by the cast-in-place balanced cantilever segmental method, each segment being supported by a set of stays.

#### 4.13.2 PROPOSED DAME POINT BRIDGE, U.S.A.

The proposed Dame Point Bridge over the St. Johns River in Jacksonville, Florida, as designed by the firm of Howard Needles Tammen & Bergendoff, is a cable-stayed structure with a concrete and a steel alternative. An artist's rendering of the concrete cable-stayed bridge alternative is shown in Fig. 1.39. Navigation

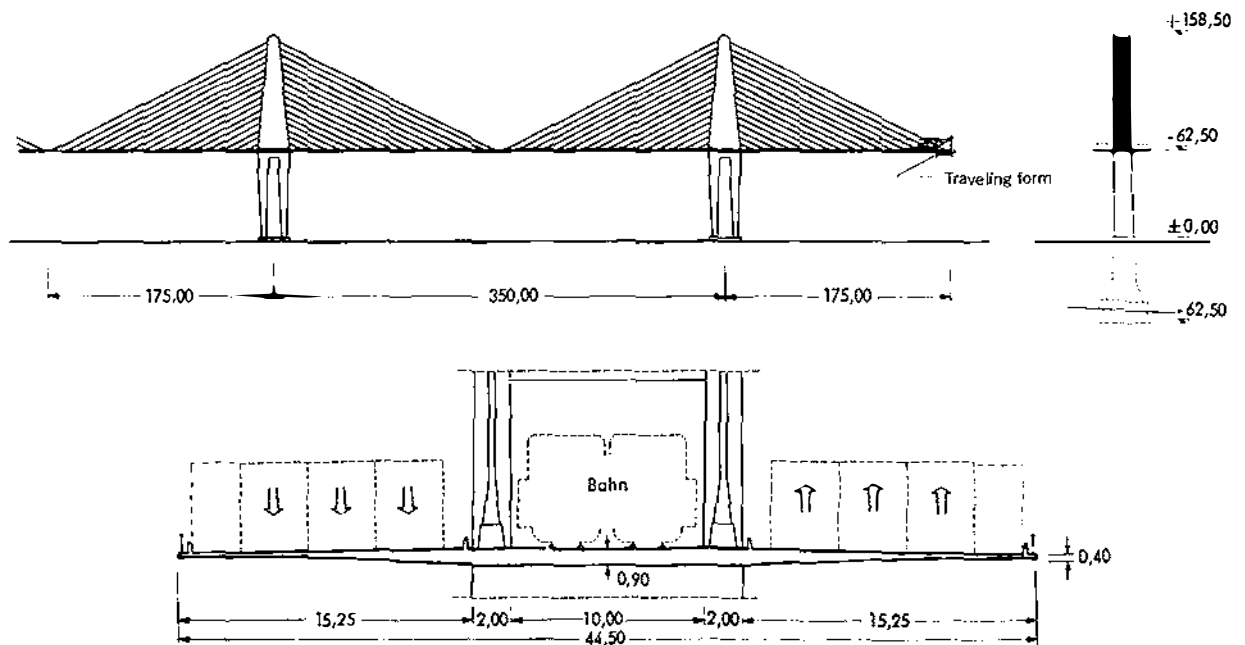


FIGURE 4.52 Danish Great Belt Bridge, elevation and cross section. (Courtesy of Dyckerhoff & Widmann.)

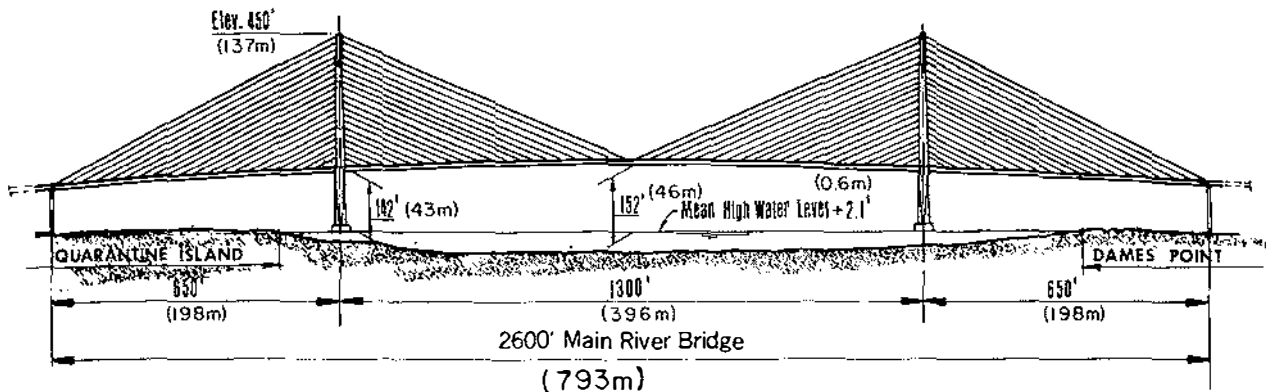


FIGURE 4.53 Dame Point Bridge, concrete cable-stayed alternative, from reference 22. (Courtesy of Howard Needles Tammen & Bergendoff.)

requirements dictate a 1250-ft (381-m) minimum horizontal opening and a vertical clearance of 152 ft (46.3 m) above mean high water at the centerline of the clear opening. The proposed concrete cable-stayed main structure will have a 1300-ft (396-m) central span with 650-ft (198-m) flanking spans. The layout of the main structure is shown in Fig. 4.53.<sup>22</sup>

Structural arrangement of the bridge deck is shown in Fig. 4.54. The bridge deck, which will support three lanes of traffic in each direction, will span between longitudinal edge girders on each side. The longitudinal edge girder is in turn supported by a vertical plane of stays arranged in a harp configuration. The concrete deck and edge girders resist local and overall bending from dead and live load in addition to the horizontal thrust from the stays.<sup>23</sup> The stay cables are anchored in massive vertical concrete pylons, two at each main pier, which carry all loads to the foundations, Fig. 4.55.

In the center span, at each edge of the deck, the stays are in a single plane spaced 30 in. (0.76 m) vertically, Figs. 4.55 and 4.56. Stays in the side spans, along each edge, are in two planes spaced 30 in. (0.76 m) transversely. Spacing of pairs of stays along the edge beam is approximately 30 ft (9.1 m). Preliminary design contemplates 7 to 9 Dywidag bars per stay, 1 1/4

in. (31.75 mm) in diameter, the number of bars per stay being a function of stress in the stay. The Dywidag bars are to be encased in a metal duct. During erection the fabricated length of duct is left uncoupled. After final adjustment the lengths of duct are coupled and pressure-grouted, thus, the steel encasing tube will then be composite for live load and secondary dead load.<sup>23</sup>

Construction proceeds by conventional methods from the top of the pier bases at elevation 15.0 ft (4.6 m) to the level of the roadway at elevation 144.6 ft (44 m). At this point, a fixed formtable is secured and the first elements of the pylon and edge girders are cast. Erection of the deck is by the balanced cantilever method. Two pairs of traveling forms are then used for sequential casting of 17.5-ft (5.3-m) lengths of edge girders on each side of the pylon. The bridge deck consists of single-T precast floor beams spanning between longitudinal edge girders and a cast-in-place topping. The precast Ts are pretensioned for erection loads. After erection the entire deck is posttensioned to provide positive precompression between edge girders under all conditions of loading, Fig. 4.56.<sup>22,23</sup>

A hinge expansion joint is provided at the centerline of the main span to allow for changes of superstructure length due to temperature, creep, and shrinkage. Similar joints are provided at the end piers, and link connections are used to prevent vertical movement of the superstructure.

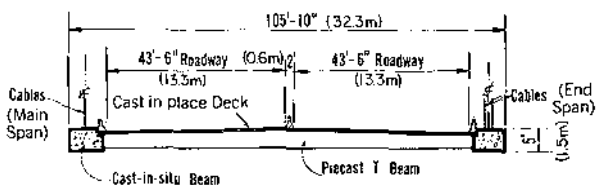
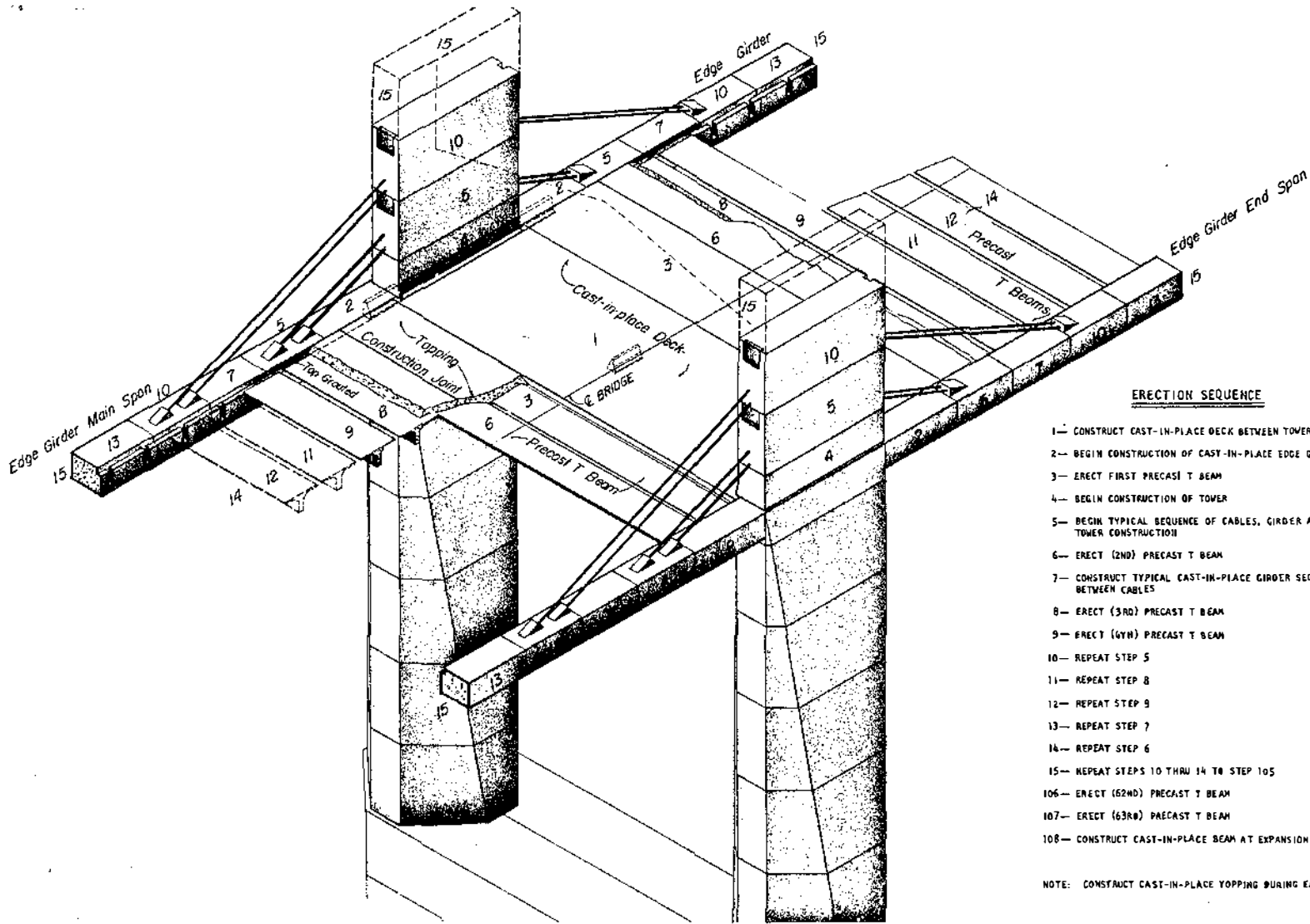


FIGURE 4.54 Dame Point Bridge, structural arrangement of bridge deck, from reference 22. (Courtesy of Howard Needles Tammen & Bergendoff.)

#### 4.13.3 PROPOSED RUCK-A-CHUCKY BRIDGE, U.S.A.

The site for the proposed Ruck-A-Chucky Bridge, designed by T. Y. Lin International, Fig. 1.32, is approximately 10 miles (16 km) north of the proposed



**ERECTION SEQUENCE**

- 1— CONSTRUCT CAST-IN-PLACE DECK BETWEEN TOWERS
- 2— BEGIN CONSTRUCTION OF CAST-IN-PLACE EDGE GIRDER
- 3— ERECT FIRST PRECAST T BEAM
- 4— BEGIN CONSTRUCTION OF TOWER
- 5— BEGIN TYPICAL SEQUENCE OF CABLES, GIRDER AND TOWER CONSTRUCTION
- 6— ERECT (2ND) PRECAST T BEAM
- 7— CONSTRUCT TYPICAL CAST-IN-PLACE GIRDER SEGMENT BETWEEN CABLES
- 8— ERECT (3RD) PRECAST T BEAM
- 9— ERECT (4TH) PRECAST T BEAM
- 10— REPEAT STEP 5
- 11— REPEAT STEP 8
- 12— REPEAT STEP 9
- 13— REPEAT STEP 7
- 14— REPEAT STEP 6
- 15— REPEAT STEPS 10 THRU 14 TO STEP 105
- 106— ERECT (52ND) PRECAST T BEAM
- 107— ERECT (63RD) PRECAST T BEAM
- 108— CONSTRUCT CAST-IN-PLACE BEAM AT EXPANSION JOINTS

NOTE: CONSTRUCT CAST-IN-PLACE TOPPING DURING EACH CYCLE.

**FIGURE 4.56** Dame Point Bridge, superstructure configuration, from reference 23. (Courtesy of Howard Needles Tammen & Bergendoff.)

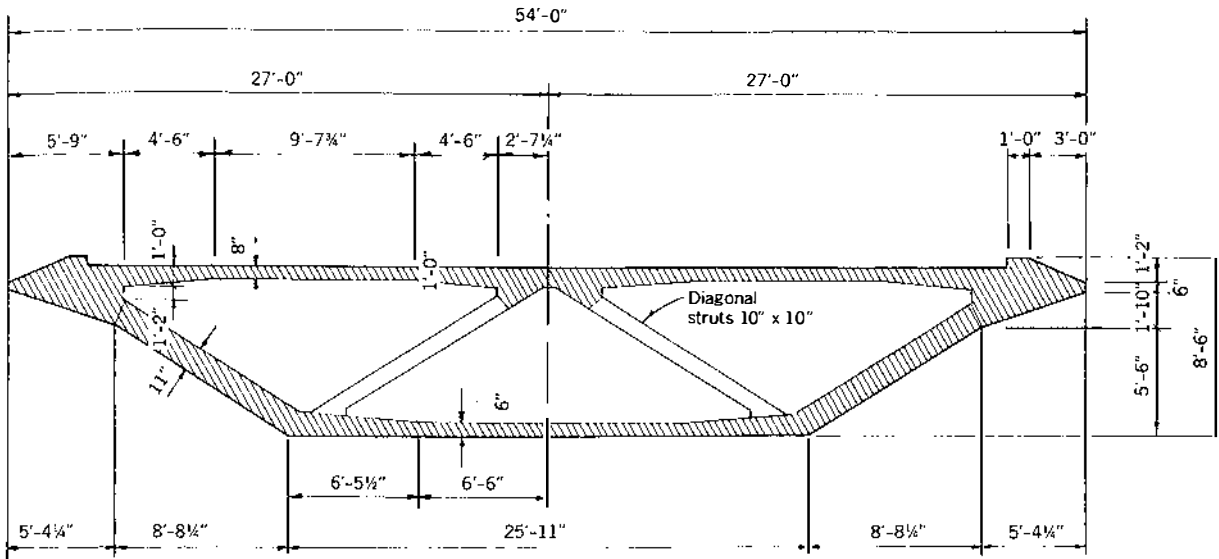


**FIGURE 4.59** Ruck-A-Chucky Bridge, cross section of concrete box girder alternate, from reference 24.

will have a 630-ft (192-m) main span with a vertical navigation clearance of 145 ft (44 m). The Cooper River Bridge, Figs. 1.42 and 4.60(b), is a segment of the I-526 Mark Clark Expressway project near Charleston, South Carolina. The main span of this structure is 800 ft (244 m) with approach spans of 150 and 300 ft (46 and 91 m). For both structures it is envisioned that the approach spans will be con-

structed by the precast concrete segmental span-by-span method up to the pylons of the main span. The main spans will be constructed by cantilever from the pylons. The purpose of this construction technique is to build the main span using most of the equipment necessary to construct the approaches, thus minimizing the special equipment involved in the fabrication and erection of the main span.

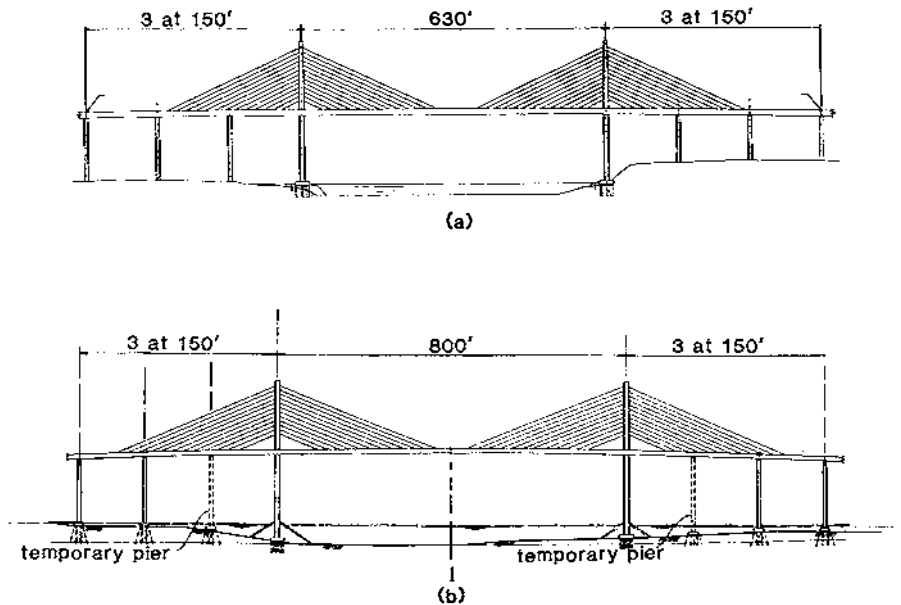


**FIGURE 4.60** Cable-stay span arrangement: (a) James River Bridge, and (b) Cooper River Bridge.



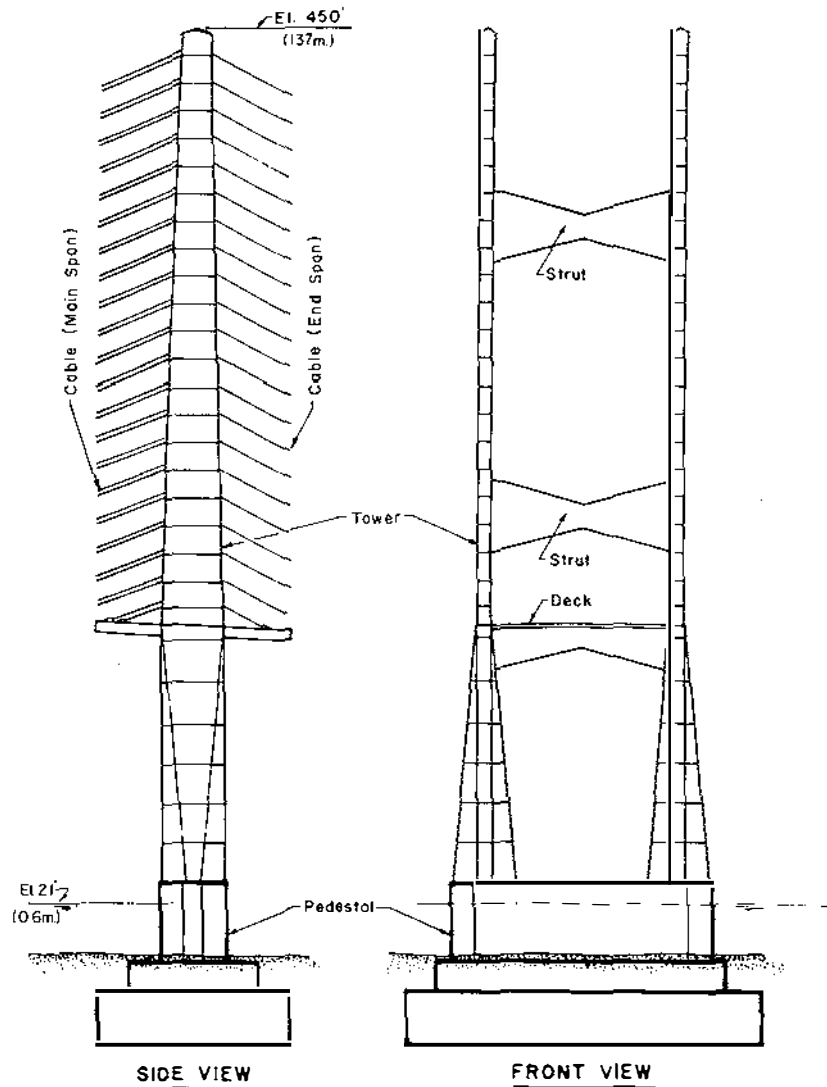


FIGURE 4.55 Dame Point Bridge, Pylon arrangement, from reference 22. (Courtesy of Howard Needles Tammen & Bergendoff.)

Auburn Dam and about 35 miles (56 km) northeast of Sacramento, California, crossing the middle fork of the American River. The river at this location is about 30 ft (9 m) deep and 100 ft (30.5 m) wide; however, upon impounding of the water behind the proposed dam, the rivers will become 450 ft (137 m) deep and 1100 ft (335 m) wide.<sup>24</sup>

In order to provide a 50-ft (15-m) vertical clearance above high reservoir water level, a bridge length of 1300 ft (396 m) will be required between the hillsides, which rise at a 40-degree angle from the horizontal. Two existing roads parallel the canyon faces; a straight bridge across the river would require extensive cuts into the rock faces of the canyon to provide the nec-

essary turning radius at the bridge approaches. This would be not only expensive but also damaging to the environment. Conventional piers in the river provide prohibitive design constraints, not only because of the 450-ft (137-m) water depth, but also because of the seismicity of the area. The hydroseismic (seiche effect) forces provide a formidable design load.

After extensive studies, the proposed final solution was that of a hanging arc, Figs. 4.57 and 4.58. The geometric configuration of this structure is such that the stays are tensioned to control the stresses and strains, in order to balance all the dead load with zero deflection; the curved girder supports the traffic and absorbs the horizontal component of the stays as axial

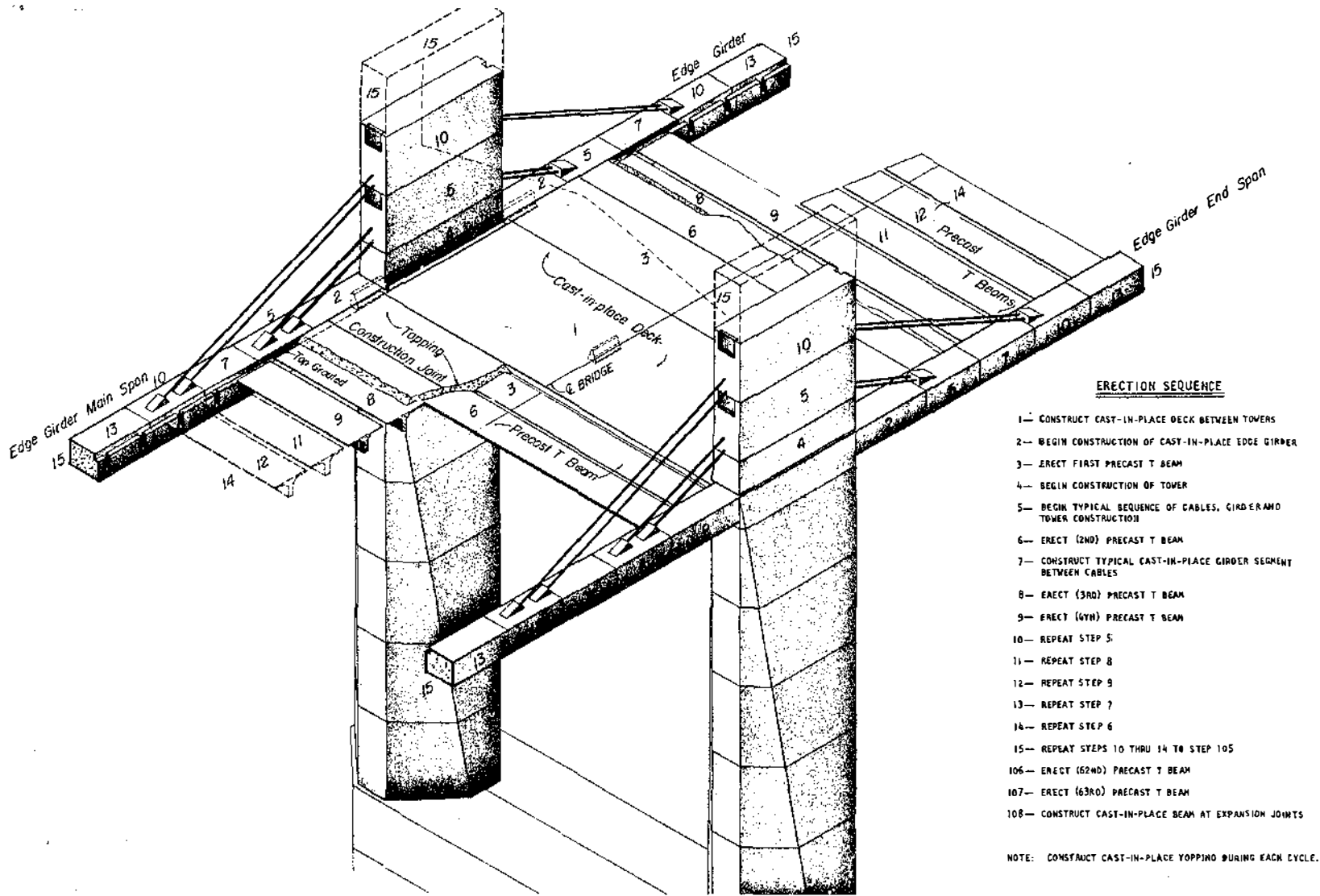


**FIGURE 4.56** Dame Point Bridge, superstructure configuration, from reference 23. (Courtesy of Howard Needles Tammen & Bergendoff.)

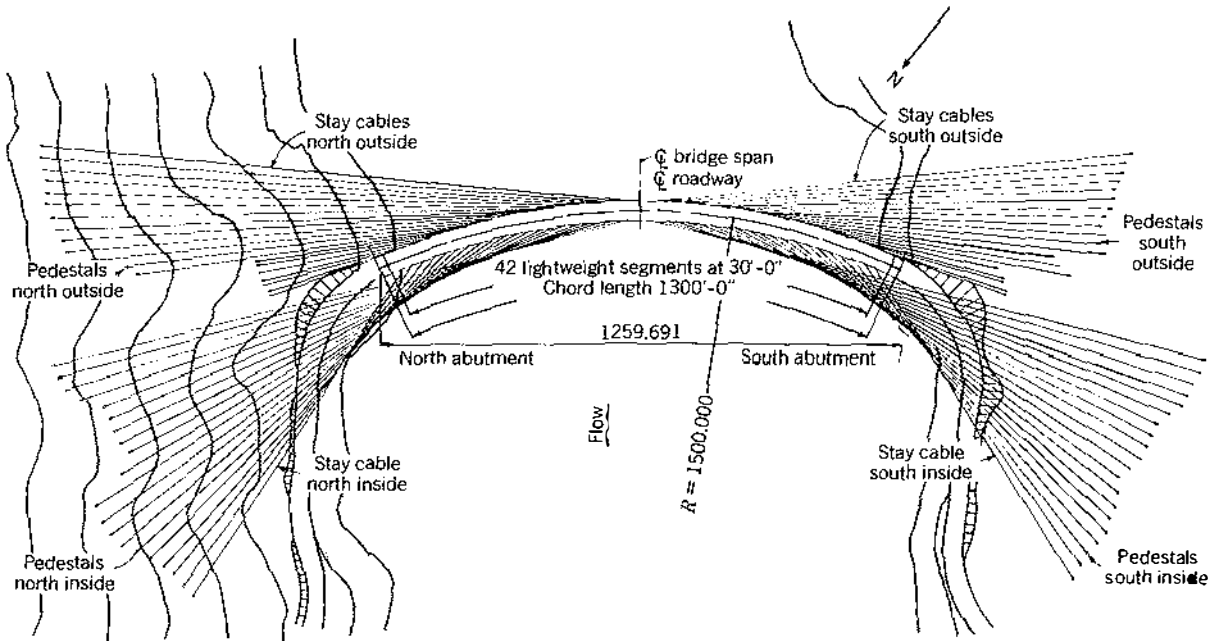


FIGURE 4.57 Ruck-A-Chucky Bridge, plan of bridge with concrete alternate, from reference 24

compression. The stays are anchored on the slope according to the design formation to control the line of pressure in the girder. Thus, an ideal stress condition is achieved with almost no bending or torsional moments. After numerous studies and trade-offs, a final radius of curvature was selected at 1500 ft (457 m).<sup>24</sup>

Two alternative designs have been prepared for this structure, one with a steel box girder and one with a lightweight concrete box girder. The concrete box girder, Fig. 4.59, is fixed at the abutments and has no hinges or expansion joints in the 1300-ft (396-m) span. Depth of this box girder is 8.5 ft (2.6 m), so as to

provide vertical stiffness and to distribute live load and construction loads on the deck to a sufficient number of adjoining cables. Stay anchorage at the girder is at 30-ft (9-m) intervals, based on construction and aesthetic considerations.<sup>24</sup>

#### 4.13.4 JAMES RIVER AND PROPOSED COOPER RIVER BRIDGES, U.S.A.

A new structure is being constructed (1985) for I-295 over the James River between Chesterfield and Henrico Counties in Virginia, Figs. 1.40 and 4.60(a). It

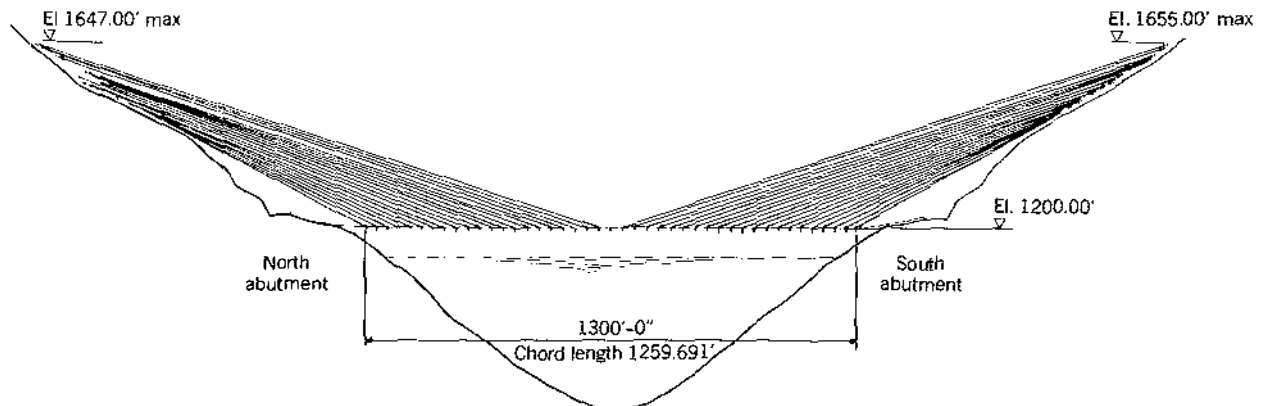


FIGURE 4.58 Ruck-A-Chucky Bridge, elevation of bridge with concrete alternate, from reference 24.

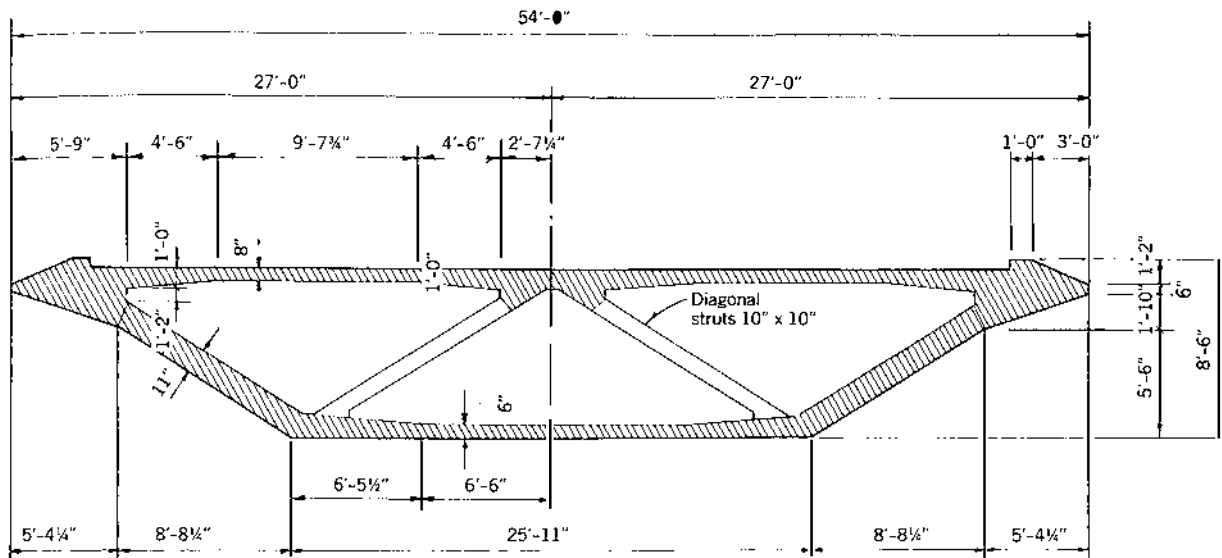


FIGURE 4.59 Ruck-A-Chucky Bridge, cross section of concrete box girder alternate, from reference 24.

will have a 630-ft (192-m) main span with a vertical navigation clearance of 145 ft (44 m). The Cooper River Bridge, Figs. 1.42 and 4.60(b), is a segment of the I-526 Mark Clark Expressway project near Charleston, South Carolina. The main span of this structure is 800 ft (244 m) with approach spans of 150 and 300 ft (46 and 91 m). For both structures it is envisioned that the approach spans will be con-

structed by the precast concrete segmental span-by-span method up to the pylons of the main span. The main spans will be constructed by cantilever from the pylons. The purpose of this construction technique is to build the main span using most of the equipment necessary to construct the approaches, thus minimizing the special equipment involved in the fabrication and erection of the main span.

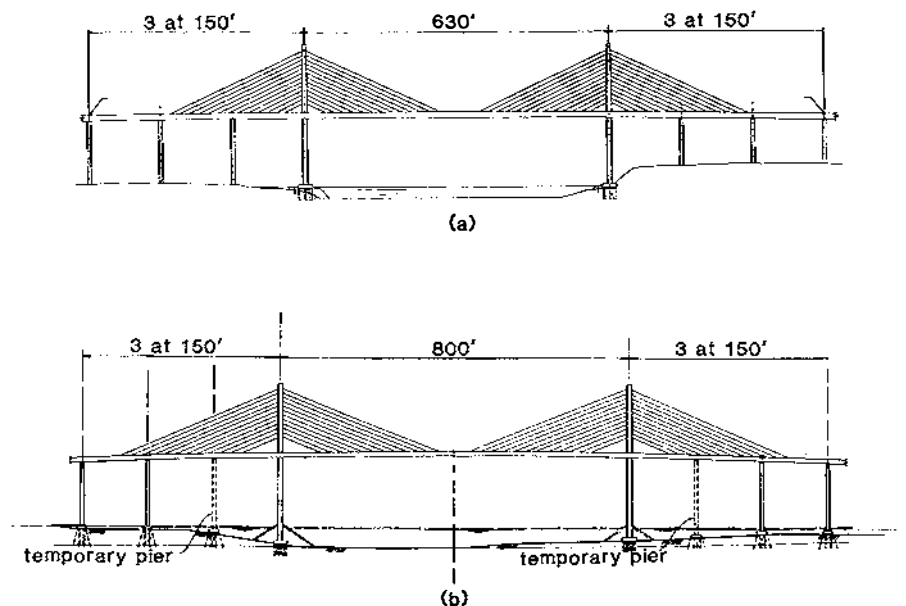


FIGURE 4.60 Cable-stay span arrangement: (a) James River Bridge, and (b) Cooper River Bridge.

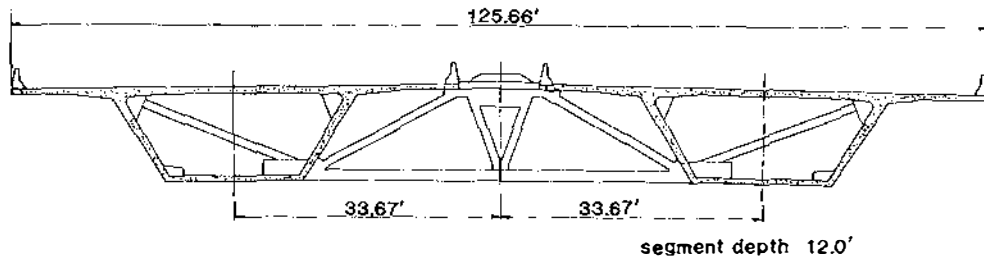


FIGURE 4.61 James River Bridge, cross section at stay anchorage, Cooper River Bridge similar.

A new concept is employed in both these structures consisting of twin parallel precast segmental box girders joined together by a closure strip and intermediate frames, Fig. 4.61. The span is suspended by a single plane of stays extending from the pylon through the closure strip and anchoring into the diaphragm frames. Stay spacing along the girder for the James River Bridge is 20 ft (6.1 m) with a segment length of 10 ft (3.05 m); for the Cooper River Bridge the stay spacing is 25 ft (7.6 m) with a segment length of 12 ft 6 in. (3.8 m).

### References

1. Torroja, E., *Philosophy of Structures*, English version by J. J. Polivka and Milos Polivka, University of California Press, Berkeley and Los Angeles, 1958.
2. Hadley, H. M., "Tied-Cantilever Bridge—Pioneer Structure in U.S.," *Civil Engineering*, ASCE, January 1958.
3. Podolny, W., Jr. and Muller, J. M. *Construction and Design of Prestressed Concrete Segmental Bridges*, Wiley, New York, 1982.
4. Leonhardt F., and Zellner, W., "Vergleiche zwischen Hängbrücken und Schrägkabelbrücken für Spannweiten über 600 m," *International Association for Bridge and Structural Engineering*, Vol. 32, 1972.
5. Morandi, R., "Some Types of Tied Bridges in Prestressed Concrete," *First International Symposium, Concrete Bridge Design*, ACI Publication SP23, Paper 23-25, American Concrete Institute, Detroit, 1969.
6. Leonhardt, F., "Latest Developments of Cable-Stayed Bridges for Long Spans," *Saetryk af Bygningstatistiske Meddelelser*, Vol. 45, No. 4, 1974 Denmark.
7. Anon., *The Bridge Spanning Lake Maracaibo in Venezuela*, Wiesbaden, Berlin, Bauverlag GmbH., 1963.
8. Anon., "Longest Concrete Cable-Stayed Span Cantilevered over Tough Terrain," *Engineering News-Record*, July 15, 1971.
9. Gray, N., "Chaco/Corrientes Bridge in Argentina," *Municipal Engineers Journal*, Paper No. 380, Vol. 59, Fourth Quarter, 1973.
10. Rothman, H. B., and Chang, F. K., "Longest Precast-Concrete Box-Girder Bridge in Western Hemisphere," *Civil Engineering*, ASCE, March 1974.
11. Podolny, W. Jr., "Concrete Cable-Stayed Bridges," *Transportation Research Record* 665, *Bridge Engineering*, Vol. 2, *Proceedings, Transportation Research Board Conference, September 25-27, 1978, St. Louis, Mo.*, National Academy of Sciences, Washington, D.C.
12. Schambeck, H. "The Construction of the Main Bridge-Hochst to the Design of the 365 m Span Rhein Bridge Dusseldorf-Flöhe," *Cable-Stayed Bridges*, Structural Engineering Series No. 4, June 1978, Bridge Division, Federal Highway Administration, Washington, D.C.
13. Anon., "Tiel Bridge," *Freysinet International, STUP Bulletin*, March-April 1973.
14. Grant, Arvid "Pasco-Kennewick Bridge—The Longest Cable-Stayed Bridge in North America," *Civil Engineering*, ASCE, Vol. 47, No. 8, August 1977.
15. Grant, Arvid, "Intercity Bridge: A Concrete Ribbon over the Columbia River, Washington," *Cable-Stayed Bridges*, Structural Engineering Series No. 4, June 1978, Bridge Division, Federal Highway Administration, Washington, D.C.
16. Leoglet, C., "Brotonne Bridge: Longest Prestressed Concrete Cable Stayed Bridge," *Cable-Stayed Bridges*, Structural Engineering Series No. 4, June 1978, Bridge Division, Federal Highway Administration, Washington, D.C.
17. Anon., "Cable-Stayed Bridge Goes to a Record with Hybrid Girder Design," *Engineering News-Record*, October 28, 1976
18. Anon., "The Danube Canal Bridge (Austria)," *Freysinet International, STUP Bulletin*, May-June, 1975.
19. Anon., "Barrios de Luna Bridge," Unpublished report provided by Stronghold International Ltd., England.
20. Anon., "Stronghold Anchorages for Cable Stayed Bridges—The Barrios de Luna Bridge (Spain)," Unpublished report provided by Stronghold International Ltd., England, November 1983.
21. Anon., "Morandi-Style Design Allows Constant Suspended Spans," *Consulting Engineer* (London), March 1967.
22. Graham, H. J., "Dame Point Bridge," *Cable-Stayed Bridges*, Structural Engineering Series No. 4, June 1978, Bridge Division, Federal Highway Administration, Washington, D.C.
23. Anon., "Dame Point Bridge," Design Report, Howard Needles Tammen & Bergendoff, November 1976.
24. Lin, T. Y., Yang, Y. C., Lu, H. K., and Redfield, C. M., "Design of Ruck-A-Chucky Bridge," *Cable-Stayed Bridges*, Structural Engineering Series No. 4, June 1978, Bridge Division, Federal Highway Administration, Washington, D.C.

# 5

## *Steel Superstructures*

|      |   |     |
|------|---|-----|
| 5.1  | INTRODUCTION  | 85  |
| 5.2  | STRÖMSUND BRIDGE, SWEDEN                              | 85  |
| 5.3  | THEODOR HEUSS BRIDGE, WEST GERMANY                    | 86  |
| 5.4  | SEVERIN BRIDGE, WEST GERMANY                          | 88  |
| 5.5  | NORDERELBE BRIDGE, WEST GERMANY                       | 89  |
| 5.6  | RHINE RIVER BRIDGE AT MAXAU, WEST GERMANY             | 89  |
| 5.7  | WYE RIVER BRIDGE, GREAT BRITAIN                       | 90  |
| 5.8  | RHINE RIVER BRIDGE AT REES, WEST GERMANY              | 92  |
| 5.9  | FRIEDRICH-EBERT BRIDGE, WEST GERMANY                  | 93  |
| 5.10 | ELEVATED HIGHWAY BRIDGE AT LUDWIGSHAFEN, WEST GERMANY | 93  |
| 5.11 | ONOMICHI BRIDGE, JAPAN                                | 94  |
| 5.12 | DUISBURG-NEUENKAMP BRIDGE, WEST GERMANY               | 94  |
| 5.13 | KNIEBRÜCKE BRIDGE, WEST GERMANY                       | 96  |
| 5.14 | PAPINEAU-LEBLANC BRIDGE, CANADA                       | 98  |
| 5.15 | TOYOSATO-OHHASHI BRIDGE, JAPAN                        | 99  |
| 5.16 | ARAKAWA RIVER BRIDGE, JAPAN                           | 100 |
| 5.17 | ERSKINE BRIDGE, SCOTLAND                              | 100 |
| 5.18 | BATMAN BRIDGE, AUSTRALIA                              | 101 |
| 5.19 | BRIDGE OVER THE DANUBE AT BRATISLAVA, CZECHOSLOVAKIA  | 102 |
| 5.20 | NORDBRÜCKE MANNHEIN-LUDWIGSHAFEN BRIDGE, WEST GERMANY | 103 |
| 5.21 | KÖHLBRAND HIGH-LEVEL BRIDGE, WEST GERMANY             | 105 |
| 5.22 | OBERKASSEL BRIDGE, WEST GERMANY                       | 105 |
| 5.23 | ZARATE-BRAZO LARGO BRIDGES, ARGENTINA                 | 107 |
| 5.24 | SACRAMENTO RIVER BRIDGE, U.S.A.                       | 108 |
| 5.25 | LULING BRIDGE, U.S.A.                                 | 113 |
| 5.26 | WEST GATE BRIDGE, AUSTRALIA                           | 116 |
| 5.27 | SAINT NAZAIRE BRIDGE, FRANCE                          | 117 |
|      | REFERENCES  | 117 |

### *5.1 Introduction*

The previous chapter discussed cable-stayed bridges constructed of cast-in-place or precast concrete, with prestressed elements in some cases. For the most part, however, cable-stayed bridges have been of steel construction.

The first modern cable-stayed bridge of steel construction was the Strömsund Bridge in Sweden, constructed in 1955. This structure had two principal plate girders in the longitudinal direction, a double-plane vertical cable arrangement transversely, and a radiating configuration in elevation. The pylon was of the portal-frame-type. From this beginning a multitude of concepts have evolved that have utilized orthotropic decks; twin box girders; single, torsionally rigid spine box girders; and single-plane cable arrangements transversely with various configurations in elevation. The single cantilever and A-frame pylon also evolved.

The following sections contain a selection of steel cable-stayed bridges presented in chronological order to indicate the constant evolution of geometric concepts.

### *5.2 Strömsund Bridge, Sweden*

As mentioned in Chapter 1, the Strömsund Bridge, Fig. 1.15, is the first modern implementation of the concept of supporting a bridge deck with inclined cable stays. For its time (1955), this structure is a monumental achievement in the ingenuity of its design. Transversely the cable stays are in two vertical planes while in elevation the stays are of the radiating or converging configuration. Each stay consists of four locked coil strands (see Chapter 9) that anchor into the pylon head and into transverse anchorage box beams between the main girders, Figs. 5.1 and 5.2 (see Chapter 10). Jacking of the stays and adjustment is accomplished at the deck level.

The pylons are portal frames with inclined legs, Fig. 5.3. The portal frame is independent of the two main longitudinal plate girders and is supported at its base by rocker bearings. These bearings are oriented to provide a rotation or hinge action in the longitudinal di-

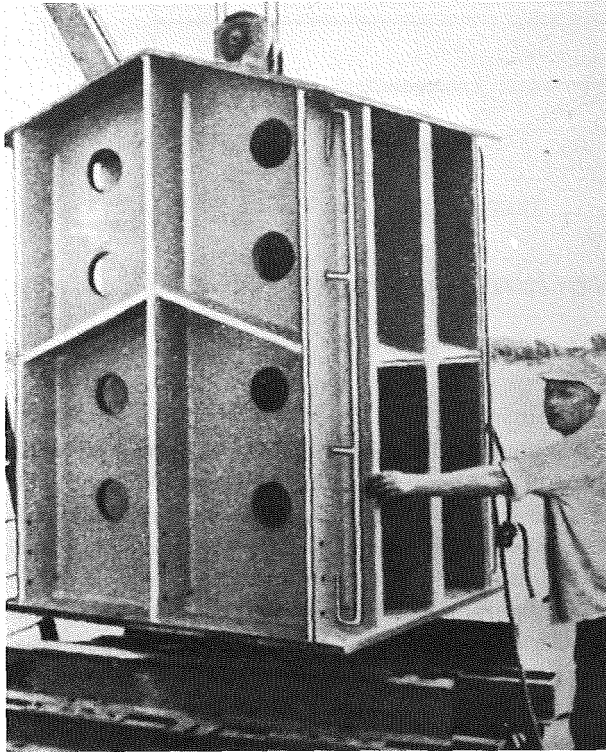


**FIGURE 5.1** Strömsund Bridge, pylon head. (Courtesy of Der Stahlbau, reference 2.)

rection of the structure but a rigidity or fixity in a transverse direction to the bridge. The cable stays provide a restraint, in the longitudinal direction, at the top of the pylon. In this manner a pendulum movement of the pylon is permitted in the longitudinal direction.<sup>1,2</sup>

### 5.3 Theodor Heuss Bridge, West Germany

Theodor Heuss Bridge, also known as the North Bridge over the Rhine at Düsseldorf, was completed in 1958 and was the first long-span, cable-stayed bridge built in Germany, Fig. 5.4. It has a main span of 853 ft (260 m) side spans of 354.3 ft (108 m), Fig. 5.5. The stays are arranged in two vertical planes transversely and are of the harp configuration in elevation. The three parallel harp stays attach at the third points of the four vertical pylons. Stays are supported on saddles and thus continuous through the pylons. Saddles for the center stays are fixed, while the upper and lower saddles are supported on movable bearings.

Pylons are of the single cantilever type and rise about 131 ft (40 m) above the roadway. These towers

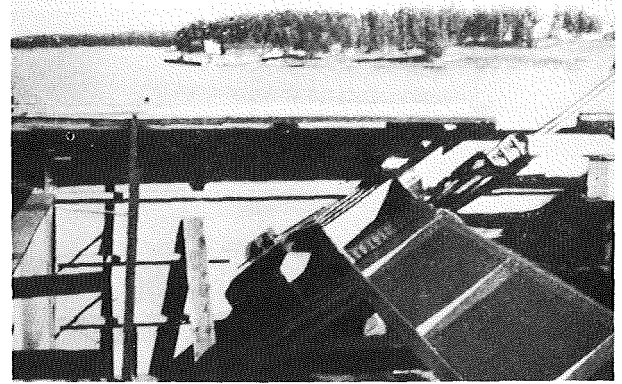


**FIGURE 5.2** Strömsund Bridge, anchorage box beam. (Courtesy of Der Stahlbau, reference 2.)

are fixed to the stiffening girder at the base, forming an inverted portal frame.

In cross section, the width of the deck is 88.9 ft (27.1 m) and consists of two box girders with an orthotropic deck spanning them, Fig. 5.5. Dimensions of the box girder are approximately 10.5 ft (3.2 m) in depth and 5.25 ft (1.6 m) in width, which produces a ratio of depth to center span of 1/81. The walkways

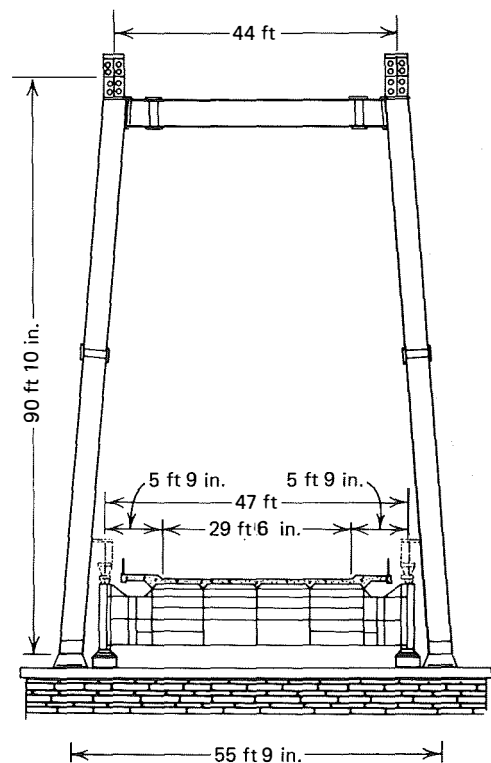


**FIGURE 5.3** Strömsund Bridge, portal frame tower. (Courtesy of Der Stahlbau, reference 2.)

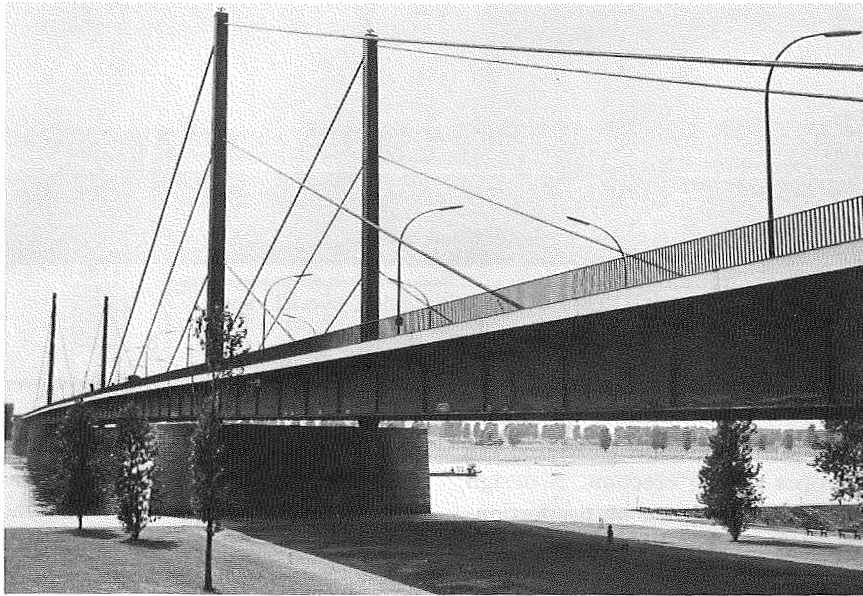


**FIGURE 5.4** Theodore Heuss-Brücke, Düsseldorf, Germany (Courtesy of Beratungstelle für Stahlverwendung, H. Odenhausen.)

are of reinforced concrete and cantilever out from the main box girders.

The top plate of the orthotropic deck has a minimum thickness of 0.55 in. (14 mm). Welded to the top surface of the plate are 1.1-in.-by-0.24-in. (28-mm-by-6-mm) flat bars set on edge and spaced 6 in. (150 mm)

on center in a herringbone pattern. The purpose of these bars is to hold the 2-in. (50-mm) asphalt wearing surface in position. Tests using alternating loads indicated that there was no hazard from fatigue, since the bars were welded to the deck plate.

One of the considerations in the planning of this

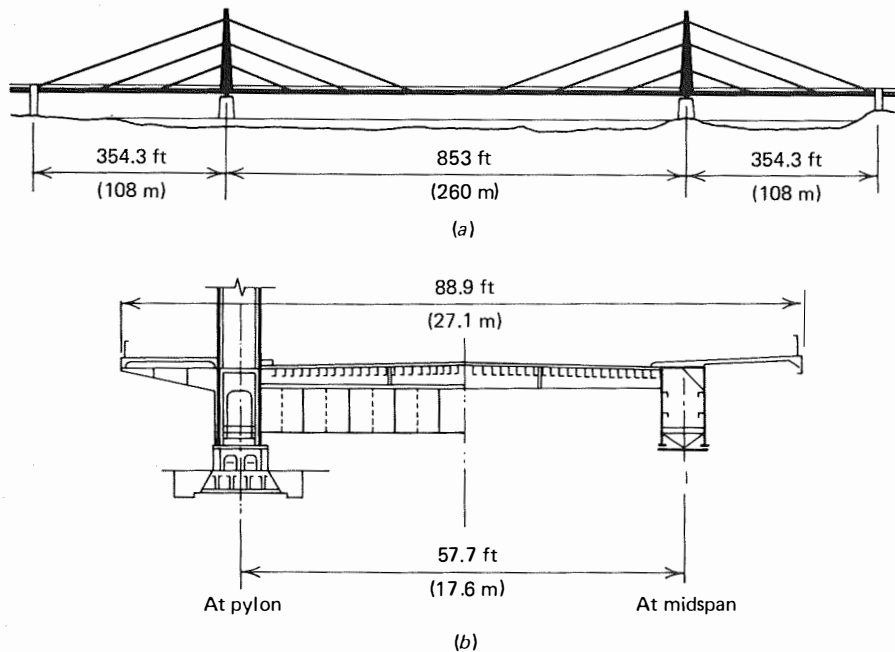


**FIGURE 5.5** Theodore Heuss-Brücke, Düsseldorf, Germany: (a) elevation and (b) cross section.



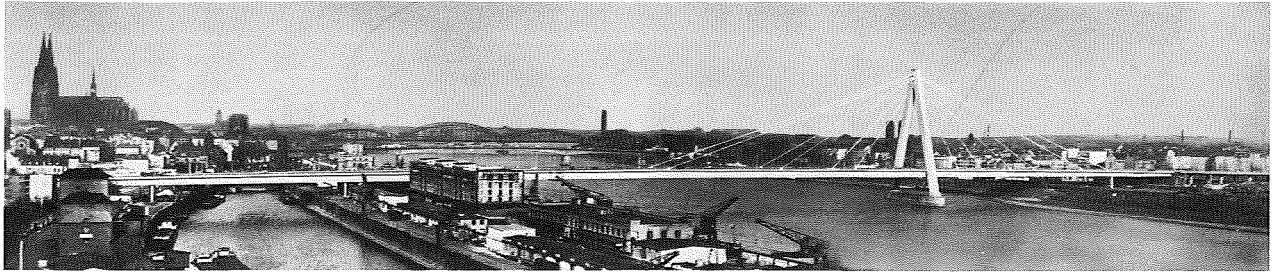


FIGURE 5.6 Severin Bridge, overall view.

structure was a requirement that the center span be erected by the cantilever method without falsework. The harp-type cable-stay configuration permitted the cables to act as guy-ropes during erection. A design requirement was that the cable thrust be proportionately distributed over the entire cross section. If the box girders had been cantilevered out and attached to the stays first, and the deck plates added later, the girders would have had to absorb individually part of the axial load, and the stress distribution over the entire cross section would not have been proportional. The deck units, box girders, and deck plate were preassembled in 118-ft (36-m) long sections, floated into position, and attached to the stays. Thus the requirement for proportional distribution of stress across the cross section was realized.<sup>3</sup>

#### 5.4 Severin Bridge, West Germany

The Severin Bridge in Cologne, Figs. 2.1 and 5.6, represents the first of the asymmetric cable-stayed structures; it has spans of 987.5 (301 m) and 495.4 ft (151 m). This structure was a second-prize winner in a design competition. This particular structural design was adopted over the first-prize girder bridge because it did not require a river pier in the vicinity of the left bank as did the girder concept. Navigation requirements in the Rhine River dictated the elimination of such a pier. The two most striking features of the structure are its asymmetry and the unusual (for its time) triangular pylon.

The choice of a triangular A-shaped pylon was based on aesthetic as well as structural considerations. From the structural point of view, the A-frame is more stable than the portal frame or individual cantilever-type of pylons. Stiffness in the face of horizontal forces such as wind is considerably improved by the inclination of the legs. With the A-frame, the horizontal portal member can be eliminated, and a weight savings in the pylons can be effected. The cable stays converge to a

single point on the apex of the tower, Fig. 5.7, which is advantageous to the three-dimensional frame structural concept. Further, there are no visual intersections of the stays, which might be distracting. The legs of the tower are splayed such that they clear the deck structure. Finally the A-frame pylon harmonizes with the tall spires of the adjacent cathedral. Aesthetic considerations precluded a tall tower in the vicinity of the spires, thus, the adoption of the asymmetric concept of one pylon on the right bank acting as a counterpoint to the cathedral and the old city on the left bank. The

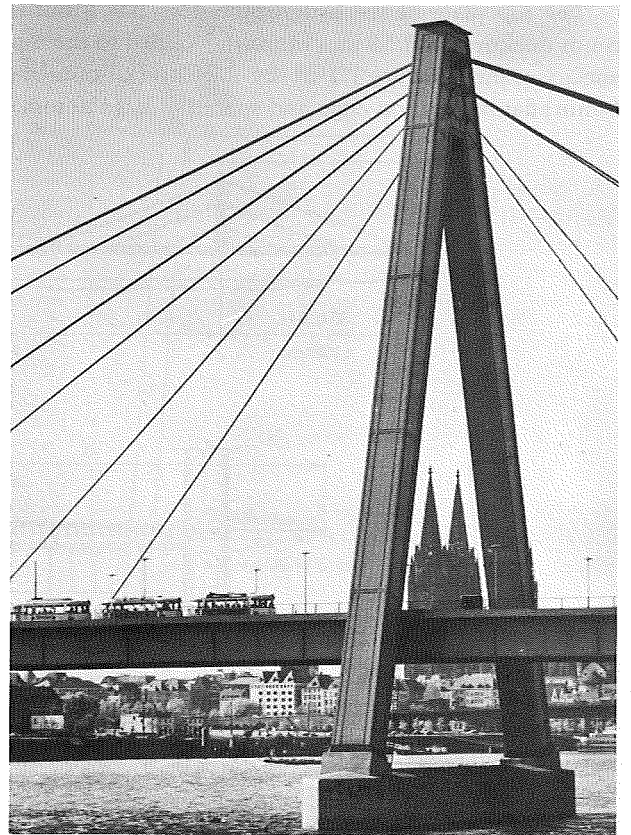


FIGURE 5.7 Severin Bridge, A-frame pylon.

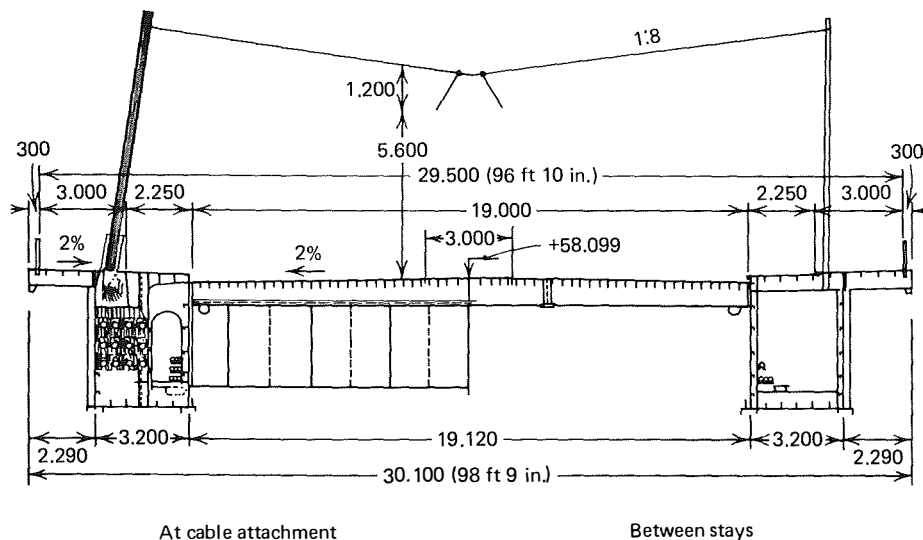


FIGURE 5.8 Severin Bridge, cross section. (Courtesy of Acier-Stahl Steel, reference 4.)

giant A-frame pylon rises to 253.3 ft (77.2 m) above its fixed base on the pier and 206 ft (62.8 m) above the deck, and serves as a monument to the medieval bishop after whom this structure is named. The geometrical concept of this structure fulfills its utilitarian purpose and at the same time achieves a harmony with its surroundings.<sup>4</sup>

The deck consists of twin box girders with an orthotropic deck and carries four lanes of traffic, a tramway, bicycle paths, and walkways. The cable stays attach to the box girders almost at the dividing line between the bicycle path and the walkway, which cantilevers out from the box girder, Fig. 5.8. In cross section all components of the deck are structurally active with the exception that an effective width for analysis had to be determined for the orthotropic deck with respect to the box girder. The box girders are 10.5 ft (3.2 m) wide and vary in depth from 9 ft 10½ in. (3 m) at the ends of the bridge to 15 ft (4.57 m) in the largest span, producing a depth-to-span ratio of 1/66. The maximum design deflection under maximum live load conditions is approximately 4 ft 5 in. (1.35 m) in the river span, which is a ratio of deflection-to-span-length of 1/225.

### 5.5 Norderelbe Bridge, West Germany

The development of the torsionally rigid box girder led to the concept of a cable-stayed bridge using a single central box girder, a single vertical cable plane located in the median, and individual cantilever py-

lons. The first such structure was the Norderelbe highway bridge over the Elbe at Hamburg, Fig. 2.7. It has spans of 210, 564, and 210 ft (64, 172 and 64 m), as shown in Fig. 5.9.

The cross section of the deck consists of four main longitudinal girders spaced 25 ft 7 in (7.8 m) on center and stiffened by transverse diaphragms. An orthotropic deck acts as a top flange and connects all four girders. In the center span the two inside girders are connected by a bottom plate which produces a torsionally rigid box section. In the side spans the bottom plate is replaced by a horizontal diagonal bracing system. The girder depth is approximately 9 ft 10 in. (3 m), producing a depth-to-span ratio of 1/57.

The pylons rise about 174 ft (53 m) above the deck and about 98 ft (30 m) above the top cable-stay support. As a result of the poor soil conditions and the size of the piers, the pylons were rigidly connected to the box girder in the longitudinal direction and to cross girders in the transverse direction.

Stays are attached to the pylons at about 56 and 76 ft (17 and 23 m) and converge downward to the deck. The upper saddles are fixed, while the lower ones are on pendulum-type rocker bearings. Structure weight is about 66 pounds per square ft (3.2 kg/m<sup>2</sup>).<sup>5,6,7,8,9</sup>

### 5.6 Rhine River Bridge at Maxau, West Germany

The first asymmetrical, single vertical plane, central torsional box girder cable-stayed structure is the Rhine Bridge at Maxau, Figs. 5.10 and 5.11. There are two

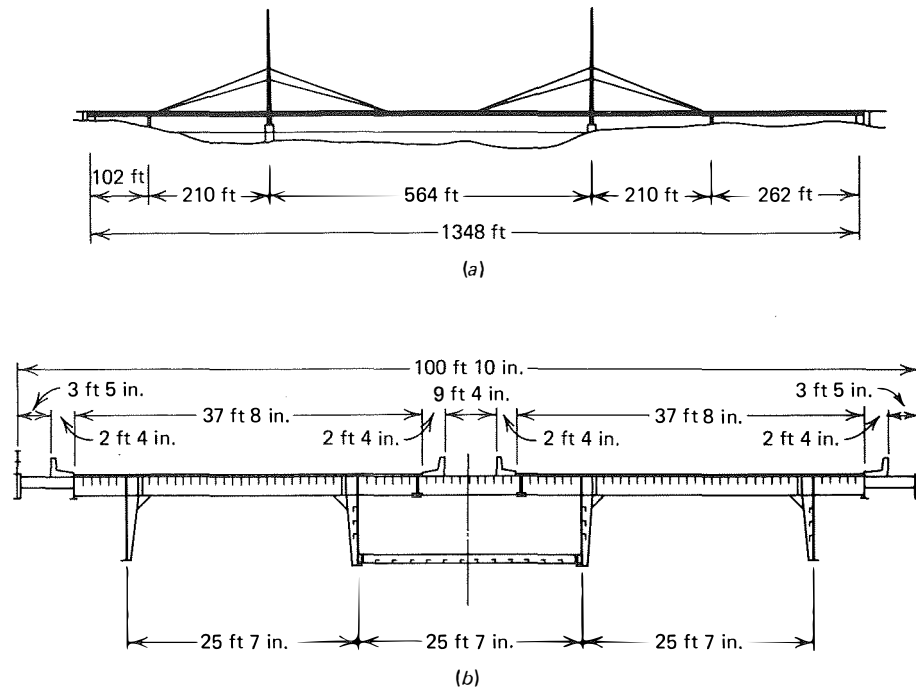


FIGURE 5.9 Norderelbe, Hamburg, Germany: (a) elevation and (b) cross section.

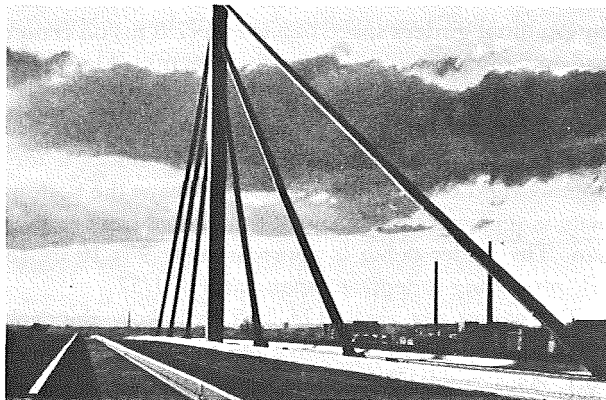


FIGURE 5.10 Rhine River Bridge at Maxau, overall view. (Courtesy of der Stahlbau, reference 10.)

spans of 575 and 383 ft (175 and 117 m), with the single pylon rising 141 ft (43 m) above roadway elevation. The three stays are arranged in the fan configuration.

Stays are continuous through the pylon and are clamped to saddles within the pylon. The upper saddle is allowed to move in the longitudinal direction, while the middle and lower saddles are fixed. The pylon is restrained within the girder and has a rocker bearing on the pier.

In cross section the total deck width is 114.8 ft (35

m) with the torsionally rigid spine box girder having a width of 39 ft 4 in. (12 m) and an average depth of about 9 ft 9 in. (3 m) resulting from superelevation. The orthotropic deck cantilevers out from the central box 38 ft 3 in. (11.65 m) on each side. Because of the long cantilever, longitudinal edge girders are utilized for load distribution.

Erection of the superstructure was from the right bank by the cantilever method (see chapter 8) and utilized temporary piers. The pylon was erected next with the stays following, starting from the top stay. Temporary catwalks were used in the stay erection. The stays were tensioned by lowering the superstructure at the temporary piers and abutments and by jacking the saddle supports.<sup>10,11</sup>

### 5.7 Wye River Bridge, Great Britain

The cable-stayed structure crossing the Wye River at Chepstow, Fig. 5.12, has received little attention in the literature, perhaps because it is dominated by the nearby Severn Suspension Bridge. The structure has a main span of 770 ft (234.7 m), side spans of 285 ft (86.8 m), and approach or viaduct spans on either side ranging from 182 to 210 ft (55.5 to 64 m), Fig. 5.13. In a transverse direction it utilizes a single vertical plane in the median and consists of a single stay em-

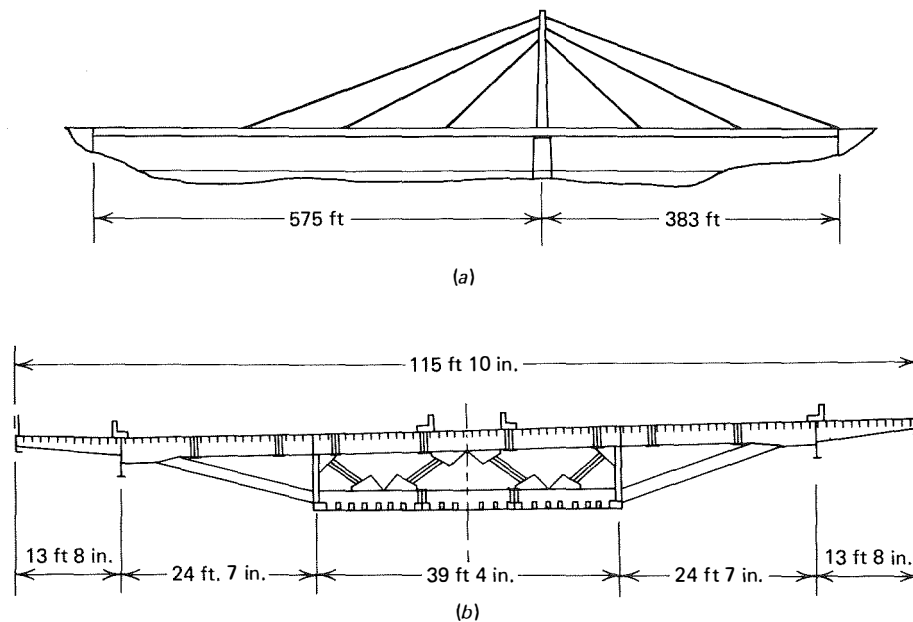


**FIGURE 5.11** Rhine River Bridge at Maxau: (a) elevation and (b) cross section. (Courtesy of The British Constructional Steelwork Association, Ltd., reference 11.)

anating from each side of the pylon. Each stay consists of 20 spiral strands built up into a triangular form.

Pylons are steel box columns that rise 96 ft (29 m) above the roadway and are located in the median. The pylon weight and vertical component of stay force is taken by a hinged bearing below the deck. The load is then transmitted to a heavy steel diaphragm which

in turn transmits it to the portal pier below. The pylons are hinged at their base in the longitudinal direction of the bridge. Cable stays are rigidly attached to the pylon top.

The design utilizes a single trapezoidal box girder with projecting cantilevers on each side for an overall width of 100 ft 6 in. (30.6 m), Fig. 5.13. The box is



**FIGURE 5.12** Wye Bridge, Severn Bridge in background. (Courtesy of The British Constructional Steelwork Association, Ltd.)

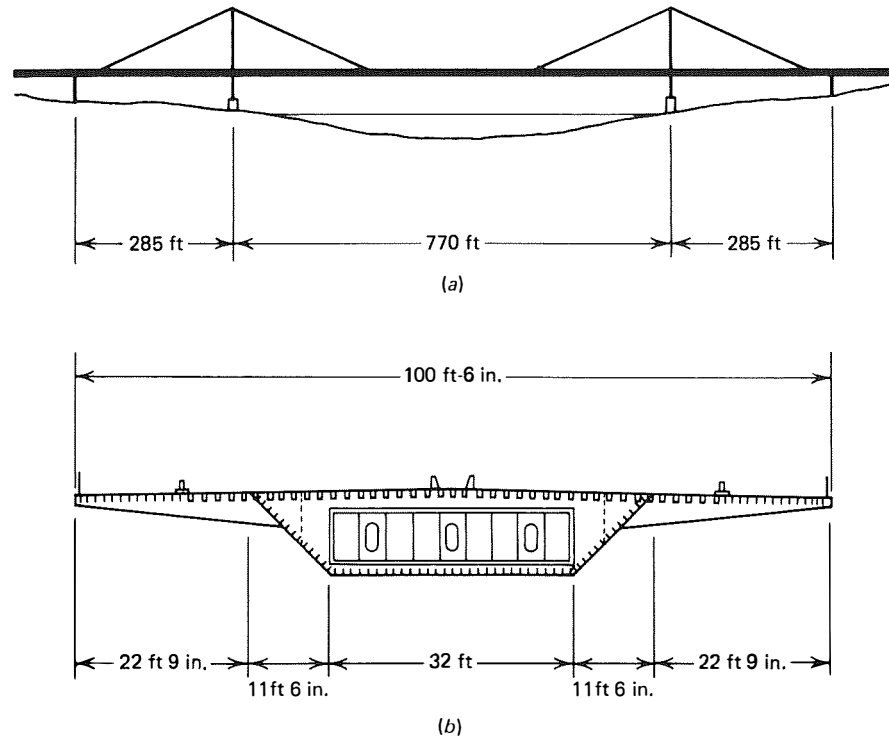


**FIGURE 5.13** Wye Bridge: (a) elevation and (b) cross section. (Courtesy of the British Constructional Steelwork Association, Ltd.)

55 ft (16.8 m) wide and 10 ft 6 in. (3.2 m) deep. The bottom flange width of the box is 32 ft (9.8 m) and the flange is supported on portal frame piers. Erection was by the cantilever method. The deck section, consisting of the steel box and two side cantilevers, was assembled at the site from fabricated plate and was then transported over the completed portion of the deck to the cantilever end. Erection was from both sides to the middle. In general, the assembled units were 56 ft (17 m) in length and weighed 120 tons (109 mt).

The average weight of the structure is 2 tons (1.8 mt) per ft, or about 40 pounds per square ft ( $195 \text{ kg/m}^2$ ). With respect to the center span the depth-to-span ratio is  $1/73$ .

### 5.8 Rhine River Bridge at Rees, West Germany

The cable-stayed structures illustrated thus far have included relatively few cable-stays, and the girder might be considered as continuous, since it is elastically supported at the distinct points of cable anchorages, which are spaced relatively far apart. The Rees Bridge, Fig. 5.14 (and the following two examples) are what might be termed multistay systems. In contrast

to the previous structures, these systems have numerous closely spaced cables, thus providing a continuous elastic support to the girder which approximates a girder supported on a continuous elastic foundation. This system evolved from a desire for a simpler transmission of forces from the cables to the girder. The structural advantage is that the relatively smaller cable force component at the attachment is distributed over a greater length of bridge girder.

The Rees Bridge employs two vertical cable planes in a harp configuration with four individual cantilever pylons. The center span is 837 ft (255 m) with equal side spans of 341 ft (104 m). The pylons rise 141 ft (43 m) above the roadway deck and are rigidly fixed to the deck structure.

The deck superstructure consists of two main plate girders 11 ft 6 in. (3.5 m) in depth, producing a depth-to-span ratio of  $1/73$  of the main span.

The main girders support I-section transverse ribs at 10 ft 6 in. (3.2 m) spacing and the orthotropic deck plate.

Each vertical plane has 10 cable stays on each side of the pylon.

The stays are spaced 8.2 ft (2.5 m) apart at the pylon and 21 ft (6.4 m) apart at the girder. The cable

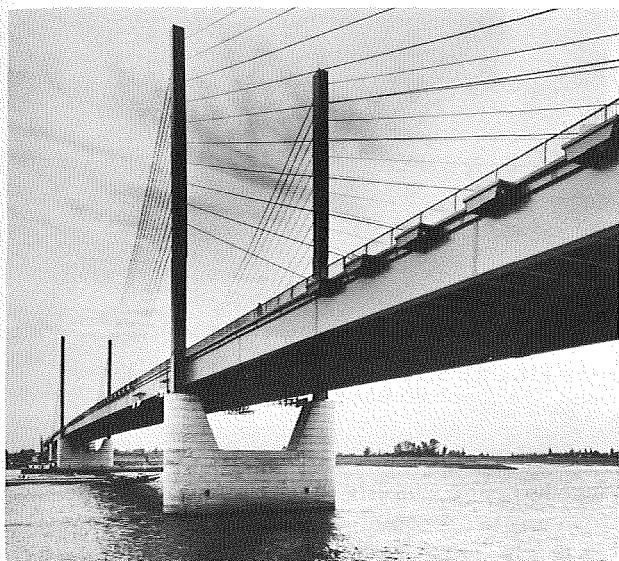


**FIGURE 5.14** Rees Bridge, general view. (Courtesy of Beratungsstelle für Stahlverwendung, H. Odenhausen.)

plane is approximately 2 ft 6 in. (0.75 m) outside the web of the main girder and the stays are attached to cross girders.<sup>12</sup>

### 5.9 Friedrich-Ebert Bridge, West Germany

This structure, Fig. 2.11(g) crosses the Rhine River at Bonn, and is sometimes referred to as the Bonn-Nord Bridge. As mentioned in the previous example, the concept of suspending the girder at a large number of points has been extended in this structure. A single central vertical stay plane is used in this structure with 20 cables on each side of the pylon. The cables are spaced at 3 ft 3½ in. (1 m) apart along the pylon and 14 ft 9 in. (4.5 m) apart along the girder, Fig. 5.15. The stays form a fan configuration in elevation. Because of the small size of the stays, varying in diameter from approximately 3 to 4¾ in. (75 to 120 mm), their appearance is not obtrusive and an overall appearance of lightness is achieved.

The structure has a center span of 918.6 ft (280 m) and side spans of 393.7 ft (120 m). Pylons are 161 ft (49 m) high above the bridge deck; they penetrate the girder and are independent of the girder. Fixity in both directions at the pier top is achieved with prestressed anchor rods.

The girder is a single cell box girder similar to that of the Maxau Bridge. The cross-sectional dimensions of the torsionally stiff box girder are 41 ft 4 in. (12.6

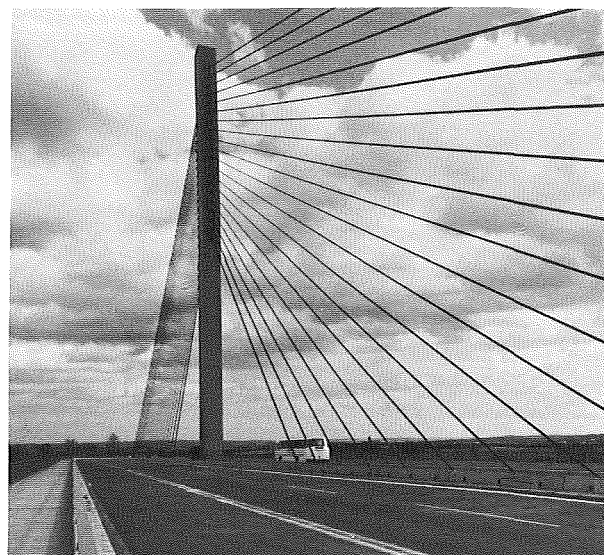


**FIGURE 5.15** Friedrich-Ebert Bridge, view of cable-stay plane. (Courtesy of Beratungsstelle für Stahlverwendung, H. Odenhausen.)

m) wide by 13 ft 10 in. (4.2 m) deep. Depth-of-girder-to-main-span ratio is, therefore, 1/67. The orthotropic deck has transverse ribs spaced at approximately 7 ft 6 in. (2.3 m) on center. Total width of the deck is 118 ft (35.8 m), with the 38 ft (11.85 m) cantilever overhangs supported by inclined struts from the bottom of the box.

Side spans of the structure were erected on temporary piers and the center span was erected by the free cantilever method. Cable stays were attached and tensioned as the erection proceeded.<sup>12</sup>

### 5.10 Elevated Highway Bridge at Ludwigshafen, West Germany

In 1968 at Ludwigshafen, West Germany an old dead-end railway station was converted into a modern through-station. Road and rail are now routed at five different levels, the highest of which is formed by a cable-stayed girder bridge with a converging cable arrangement, Fig. 5.16. This structure extends the multistay concept to two inclined planes.

The single pylon is unusual in that it is composed of four legs that form an A-frame on all four sides. The pylon rises 246 ft (75 m) above the railway lines crossed by the bridge and supports two equal spans of approximately 453 ft (138 m). The stays converge to the apex of the pylon and are attached to a rhomboid box anchorage.

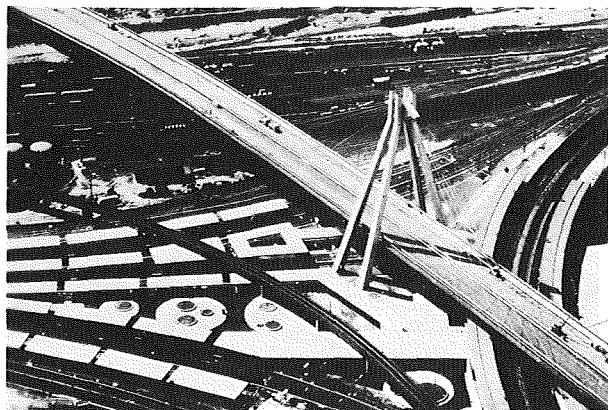


**FIGURE 5.16** Ludwigshafen Bridge, aerial view. (Courtesy of Der Stahlbau, from reference 13.)

The orthotropic deck is 80 ft (24.5 m) wide and is supported on two longitudinal web girders spaced 54 ft 9 in. (16.7 m) apart, Fig. 5.17. Longitudinal plate girders are 8 ft 2 in. (2.5 m) in depth corresponding to a depth-to-span ratio of 1/55.<sup>11,12,13</sup>

### 5.11 Onomichi Bridge, Japan

Although the Onomichi Bridge is not the first cable-stayed bridge in Japan, it is the first long-span, cable-stayed bridge and also the first in the world to be constructed almost entirely (82%) of corrosion-resistant weathering steel. This structure, Fig. 5.18, has an overall length of 1263 ft (385 m) and connects the island of Mukai-Jima to the island of Honshu. The center span is 705.4 ft (215 m) and side spans are 278.8 ft (85 m).

Geometrically it consists of two transverse vertical planes, which are of the radiating configuration in el-

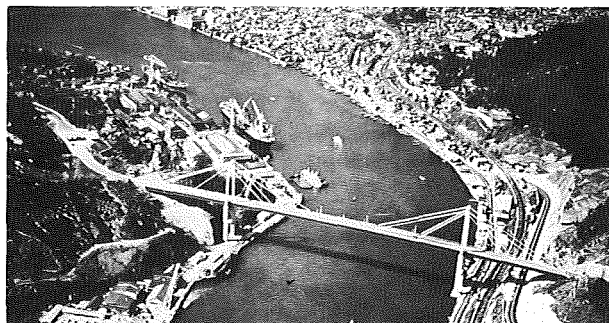


**FIGURE 5.18** Onomichi Bridge, aerial view.

evation. The pylons are of the portal-frame-type. The superstructure consists of an orthotropic plate deck spanning two longitudinal plate girders that are spaced 33 ft 6 in. (10.2 m) on center. The plate girders are 10 ft 6 in. (3.2 m) deep producing a depth-to-span ratio of 1/67.

Pylons are mounted on high piers to provide adequate navigation clearance. The top stays are fixed to the pylons, while the lower stays allow movement in the longitudinal direction of the structure. Stay anchorage cross girders span the two longitudinal plate girders. Erection of the center span was by the free cantilever method.<sup>14</sup>

### 5.12 Duisburg-Neuenkamp Bridge, West Germany

Duisburg-Neuenkamp is the first major bridge in Europe to use all-welded construction with various combinations of U.S.-developed high-strength steels in the pylons, Fig. 5.19. The bridge has a center span of 1148 ft (350 m) and an overall length of 2550 ft (777 m). Intermediate piers are used in the side spans between the pylon and the abutment to anchor all but one of

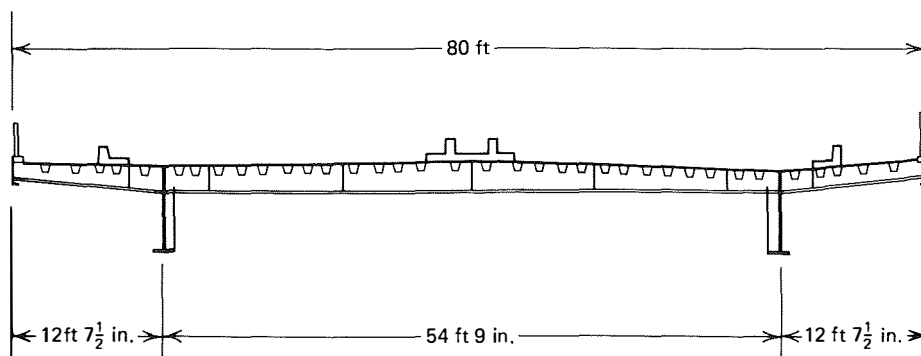


**FIGURE 5.17** Ludwigshafen Bridge, cross section. (Courtesy of The British Constructional Steelwork Association, Ltd.)

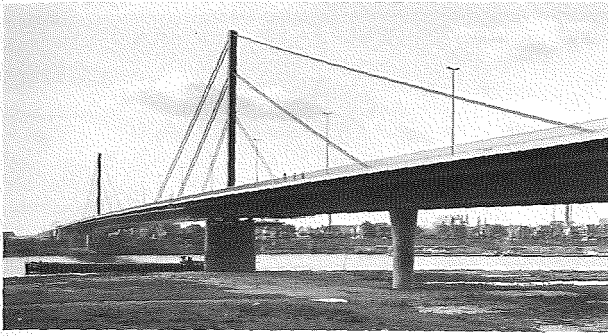


**FIGURE 5.19** Duisburg-Neuenkamp Bridge, general view. (Courtesy of Gutehoffnungshütte Sterkrade AG, Friedrich Weisskopf.)

the side span back stays, Fig. 5.20. In this manner increased stiffness is provided to the structure.

The cable stays are arranged in a fan configuration and are positioned in a single vertical plane in the median. Each stay is composed of nine locked coil strands in a cross-section grid of 3 by 3. The individual locked coil strands vary in diameter (depending on the force in a particular stay) from  $2\frac{1}{4}$  to  $3\frac{1}{4}$  in. At intervals of about 56 ft (17 m), the stays are fastened by square clamps fabricated from approximately  $\frac{3}{8}$ -in. plate. The stays may be adjusted at the girder anchorage and are continuous through the pylon, where they are supported on saddles. At each pylon the locked coil strands forming a stay are supported in layers of three in cast steel saddles that have a lead-lined bottom and sides. A lead-lined cover was clamped down on the strand by high-strength bolts. All saddles are rigidly fixed to the pylons.

Individual full-length strands arrived at the construction site fitted with their end sockets and coiled on a drum. They were then fitted to their respective saddles and erected on the pylon. With the use of electric winches, the socketed ends were pulled into the box girders and installed in the cable anchorages. One strand in each stay was tensioned to the correct tension and then served as an indicator for the tensioning of the remaining eight strands in the stay. Final tensioning was accomplished by raising or lowering the saddles in the pylons by hydraulic jacks.

The two pylons are 164 ft (50 m) high and are fixed to the girder. They are a constant dimension of 6 ft 3 in. (1.9 m) in the transverse direction of the bridge. In a longitudinal direction they are of a variable dimension. At the top they have a dimension of 10 ft (3 m) and then taper down to 6 ft 5 in. (1.95 m) at 33 ft (10 m) above the deck and then increase to an 8-ft (2.4 m) dimension at the base. The slender pylons have an aesthetically pleasing appearance. The slenderness was achieved by the use of U.S. licensed high-strength, water-quenched and tempered, fine-grained structural steel. Plate thicknesses are less than  $1\frac{3}{4}$  in. The slenderness of the pylons allows a narrow median, which in turn reduces the dead weight of the structure. The tower design in this example allows a degree of flexibility such that the bending moment in the towers is reduced considerably.

Dual three-lane roadways, a footpath, and a bicycle path are carried by a 119 ft (36.3 m) wide deck, Fig. 5.20. The center two cell box girder is 41 ft 8 in. (12.7 m) wide with constant depth webs of 12 ft 4 in. (3.7 m), producing a depth to span ratio of 1/93. The deck cantilevers from the sides of the box a distance of 38

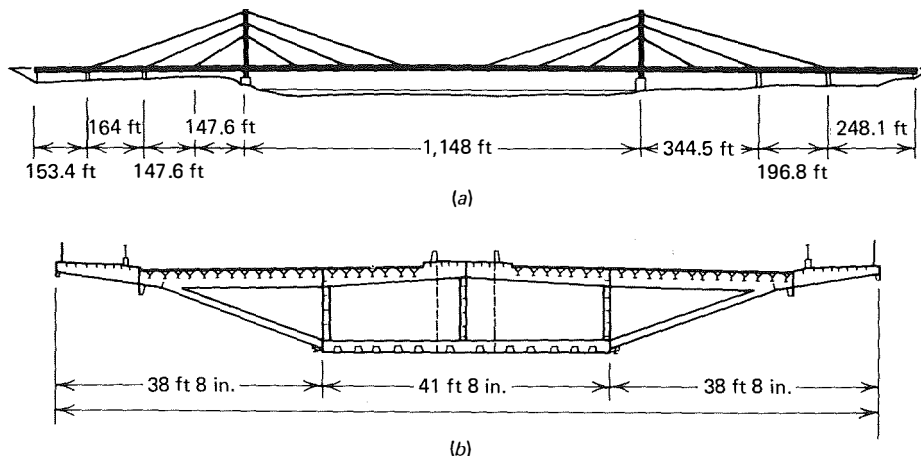


**FIGURE 5.20** Duisburg-Neuenkamp Bridge: (a) elevation and (b) cross section. (Courtesy of Gutehoffnungshütte Sterkrade AG, Friedrich Weisskopf.)



ft 8 in. (11.8 m) and is supported by box struts spaced at 16 ft 5 in. (5 m). Cross girder spacing at the top of the box is 8 ft 2½ in. (2.5 m). In the bottom, the cross girders are spaced at 16 ft 5 in. (5 m), except in those regions subject to high compressive forces where additional intermediate cross girders are added.

The orthotropic deck is stiffened by “wine glass” or Y-shaped stringers spaced 1 ft 11½ in. (0.6 m) on center. The top of the Y is 11¾ in. (300 mm) wide and the space between stringers is 11¾ in. (300 mm). The rolled T-section, which forms the stem of the “Y,” penetrates the cross girder, and the plates forming the “V” at the top are terminated at the cross girder where they are fillet welded. The bottom flange of the box is stiffened by cold-formed trapezoidal stiffeners.

The torsional rigidity of the two-cell box girder is enhanced by solid diaphragms (with the exception of two inspection walkway openings) spaced at intervals varying from 82 to 98 ft (25 to 30 m). At the two ends of the bridge the diaphragms include the triangular area formed by the inclined struts.

Erection was from both abutments toward the center and employed the cantilever erection method. Auxiliary supports were used in the side spans.<sup>15</sup>

### 5.13 Kniebrücke Bridge, West Germany

The Kniebrücke at Düsseldorf has an asymmetric harp-type cable-stay configuration with a major span of 1050 ft (320 m) and four anchor spans of 160 ft (48.75 m), Figs. 2.11(j) and 5.21. The four-stay harp configuration is in two vertical planes that, along with the pylons, are outside the width of the deck.

The stays consist of 13 locked coil strands that in cross section are arranged in three layers of 4-5-4

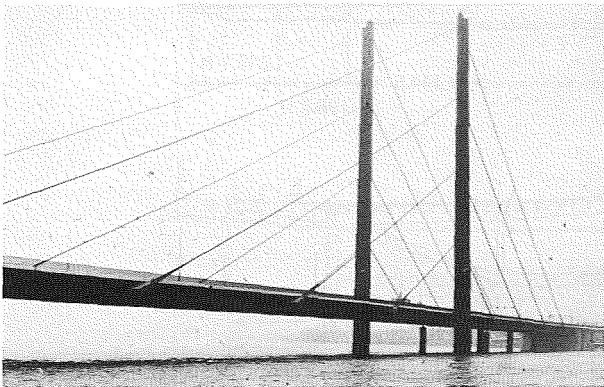


FIGURE 5.21 Kniebrücke, general view. (Courtesy of Beratungsstelle für Stahlverwendung, H. Odenhausen.)

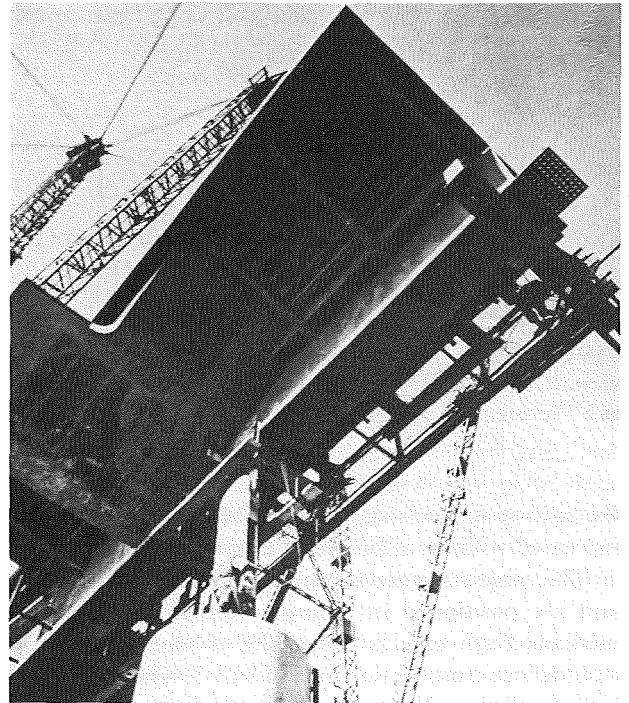


FIGURE 5.22 Kniebrücke, tension-pendulum pier, Düsseldorf, Germany. (Courtesy of Beton-Verlag, GmbH, Düsseldorf, from reference 17.)

strands which form a horizontally elongated hexagon. The stays are anchored to cantilever diaphragms at the girder. In the short span at the points of attachment of the stays, the girder is attached by a linkage to the piers such that the vertical component of stay force is taken by the pier in tension while the horizontal component is transferred to the girder, Fig. 5.22. In this manner the stiffness of the structure is not affected by the flexural stiffness of the side span and the stiffness of the longer span is enhanced. The stays pass through the pylon and are supported on saddles which are allowed a limited movement during erection, but are fixed in the final system.

The pylons are of the individual cantilever type fixed to the pier, that is, there is no portal at the top. The pylon height above the pier is 374 ft 4 in. (114.1 m) and is 313 ft (95.5 m) above the roadway. In cross section the pylon is formed of box sections in a T-shaped arrangement, see Fig. 5.23.<sup>16</sup>

An orthotropic deck plate spans the two longitudinal plate girders and provides three lanes of traffic in each direction (with no median). Overall deck width is 96 ft 2 in. (29.3 m) with the webs of the plate girders spaced 70 ft 5 in. (21.5 m) apart, Fig. 5.24. The depth of the plate girders is 9 ft 11 in. (3 m) and transverse

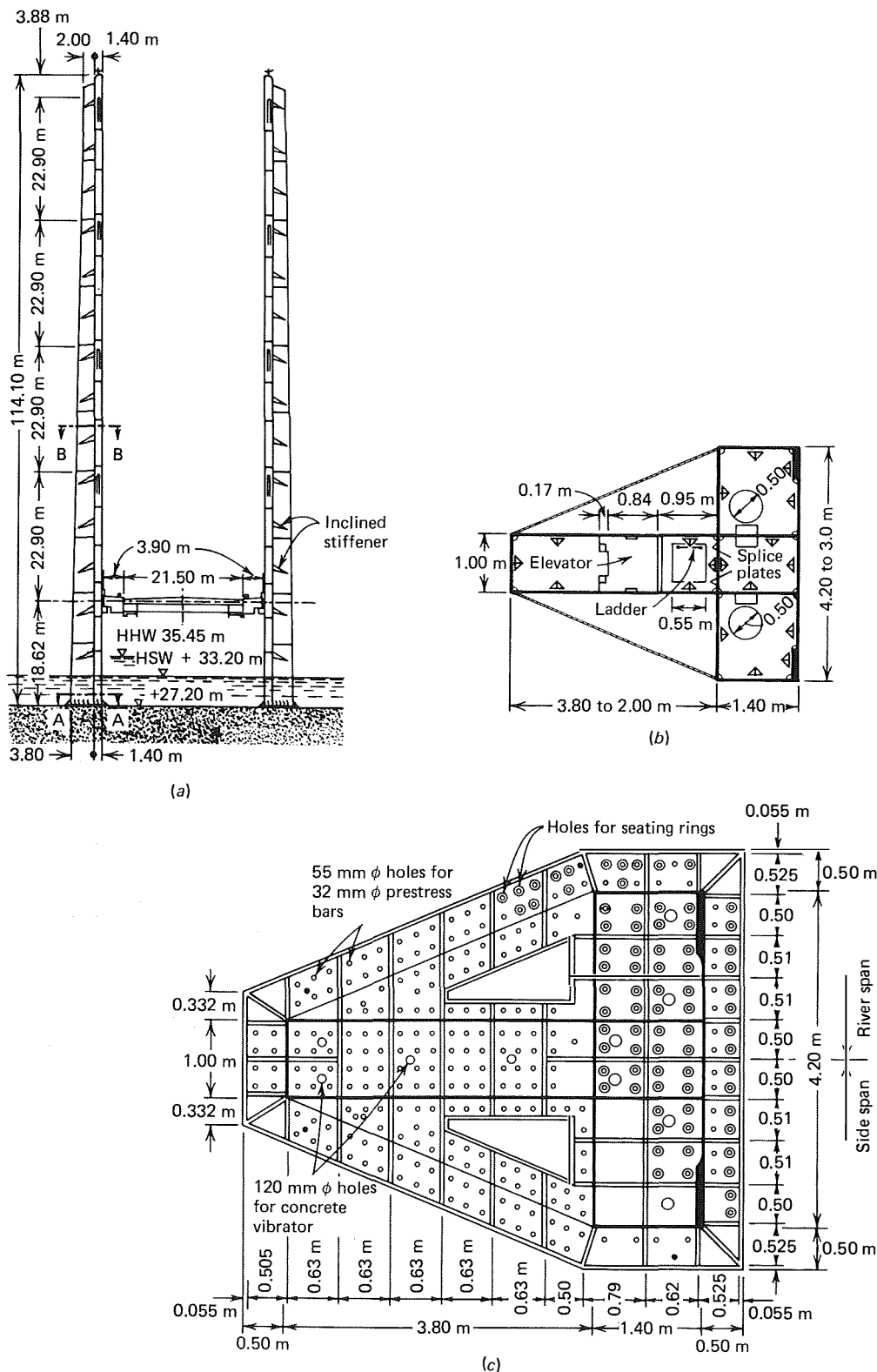
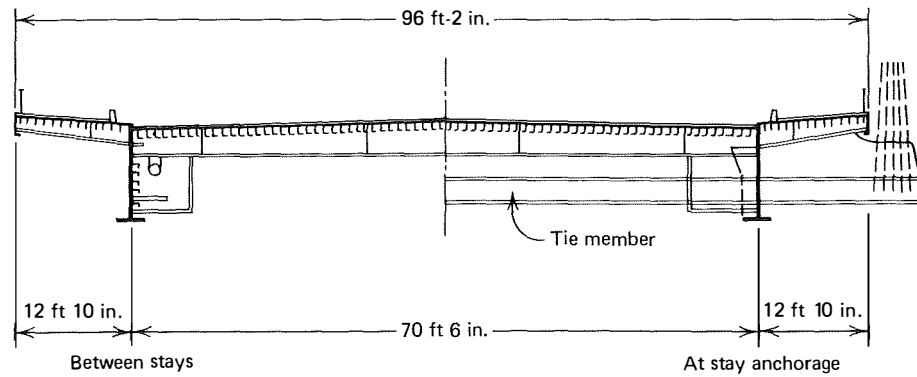


FIGURE 5.23 Kniebrücke, elevation and sections of pylon, Düsseldorf, Germany: (a) elevation, (b) Section B-B, and (c) Section A-A. (Courtesy of Acier-Stahl-Steel, from reference 16.)



**FIGURE 5.24** Kniebrücke, cross section. (Courtesy of Beton-Verlag GmbH, Düsseldorf, from reference 17.)

girders are spaced at 7 ft 7 in. (2.3 m). Footpaths cantilever out from the web of the plate girder a distance of 12 ft 10 in. (3.9 m).<sup>17</sup>

#### 5.14 Papineau-Leblanc Bridge, Canada

Papineau-Leblanc Bridge spans the Riviere des Prairies north of Montreal. It is the first to use a single vertical plane with a torsionally stiff center box girder, Figs. 5.25 and 5.26. It has a center span of 790 ft (240.8 m) and equal side spans of 295 ft (90 m). In

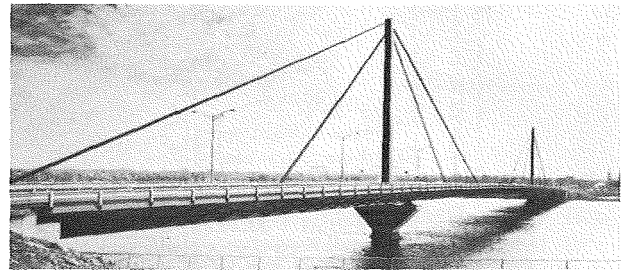


**FIGURE 5.25** Papineau-Leblanc Bridge, general view. (Courtesy of Civil Engineering-ASCE, from reference 18.)

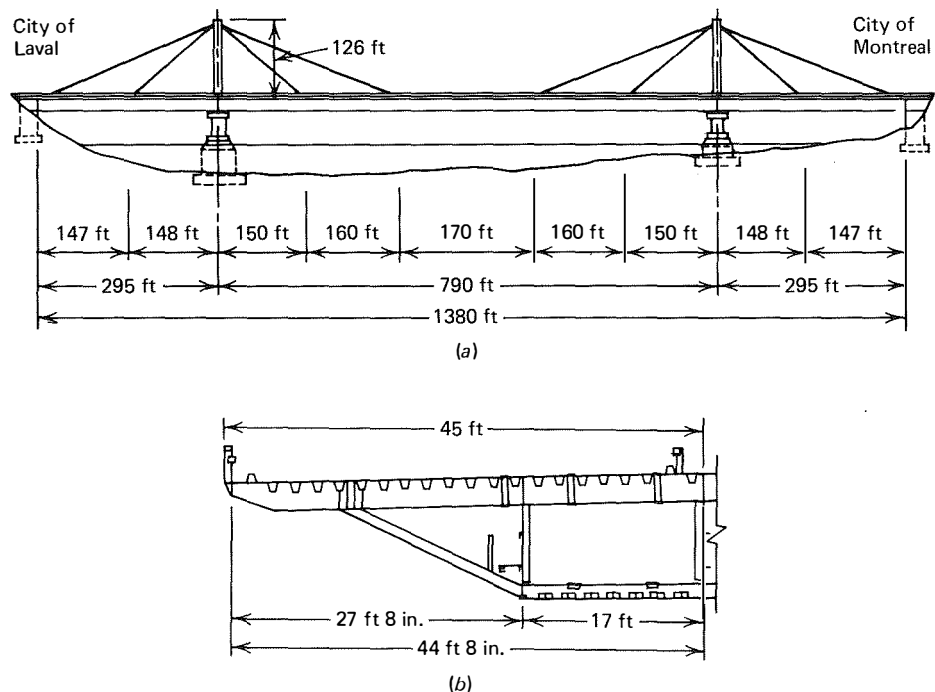


**FIGURE 5.26** Papineau-Leblanc Bridge: (a) elevation, (b) cross section. (Courtesy of Civil Engineering-ASCE, from reference 18.)

elevation the two stays emanate from each side of the pylon in a radiating configuration.

Economic comparisons were made for the following five bridge types: (1) prestressed box girders of 275-ft (83.8-m) span, (2) three steel arches of 446-ft (136-m) span with an orthotropic deck, (3) steel plate girders with 335-ft (102-m) main spans, (4) steel box girders with 260-ft (79-m) main spans, and (5) the three-span cable-stayed box girder bridge selected. Cost estimates varied from the low of \$5.5 million for cable-stayed to a high of \$6.4 million for the arch. Cost for the completed structure was \$5.4 million, \$4.6 million for the superstructure and \$0.8 million for the substructure.<sup>18</sup>

Upper stays consist of 24  $2\frac{5}{8}$ -in. (67-mm) diameter bridge strands arranged in two bundles of 12 each. Lower stays are 24  $1\frac{3}{8}$ -in. (41 mm) diameter strands also arranged in two bundles of 12 each. All stays are continuous through the tower, since they are clamped to saddles. The lower saddles are fixed to the tower, and the upper saddles are allowed to slide in the longitudinal direction to minimize the longitudinal displacement of the top of the tower. Each wire in an individual strand is galvanized and, in addition, each strand has a 0.20-in. (5-mm) thick polyethylene covering extruded directly onto the strand. Connection of the stays to the box girder superstructure is discussed in Chapter 10.

Towers rise 126 ft (38.4 m) above the deck and are of a single box section that tapers from 6 by 6 ft (1.8 by 1.8 m) at the base to 5 by 5 ft (1.5 by 1.5 m) at the top. The towers are fabricated from 2-in. (500-mm) thick ASTM A441 high-strength steel plate. The box section is formed from four unstiffened plates, butt welded at the edges. Each tower is rigidly fixed to the girder, which in turn is supported by sliding rotaflon bearings. Each tower weighs 140 tons (127 mt) and supports a load of 4500 tons (4082 mt).

The deck structure consists of a two-cell rectangular box girder 34 ft (10.4 m) wide and 11 ft 8 in. (3.6 m) deep, producing a depth-to-span ratio of 1/68. Transverse floor beams at 15-ft (4.57-m) spacing are 2 ft 6 in. (0.76 m) deep and cantilever out approximately 28 ft (8.5 m) on each side of the box. The orthotropic deck and transverse floor beams are supported by diagonal struts. At 45-ft (13.7-m) intervals the box girder is stiffened by transverse diaphragms. The main span was erected by the free cantilever method, see Chapter 8.<sup>18,19</sup>

### 5.15 Toyosato-Ohhashi Bridge, Japan

The Toyosato-Ohhashi Bridge was built at the intersection of the Shinjo Yamatogawa Highway with the

Yodo River as part of the public works for Expo 70. It is a single vertical plane fan configuration with A-frame pylons and a trapezoidal box girder, Fig. 5.27.

The stays in this structure represent the first use of prefabricated parallel wire strands in Japan. Upper stays consist of 16 strands of 154 wires each. Lower stays consist of 12 strands of 127 wires each. Wire diameter is approximately 0.2 in. (5 mm) Each strand is fabricated of parallel wires bunched in a hexagonal shape. The strands in the stays are compacted into a circular shape such that the upper and lower stays have diameters of approximately 11 in. and  $8\frac{5}{8}$  in. (280 and 220 mm), respectively. In addition to zinc coating, the stays are covered by a synthetic resin wrapping. Stays are continuous over saddles in the pylon. At the girder anchorage, the stress condition was evaluated by a three-dimensional finite element analysis and checked by model testing. Upper saddles in the pylon are fixed, while the lower ones are allowed to move.

A-frame pylons, Fig. 5.27, rise 114 ft 6 in. (34.87 m) above the pier. They are hinged in the longitudinal direction and fixed in the transverse direction of the bridge and are designed to withstand earthquake forces.

The three-span continuous girder has spans of 264 ft, 708 ft 8 in., and 264 ft. (80.5, 216, and 80.5 m). The spans are trapezoidal box sections, 34 ft 5 in. (10.5 m) wide at the top flange and 23 ft (7 m) wide at the bottom flange. Depth is 9 ft 10 in. (3.0 m), about 1/72 of the span. The orthotropic deck is supported by transverse cross beams at 5.9 ft (1.8 m) on centers which cantilever out from the box 15 ft 6 in. (4.7 m) to produce a total deck width of 65 ft 5 in. (28 m).<sup>20</sup>

Erection of the bridge and stressing of the stays are discussed in Chapter 8.



FIGURE 5.27 Toyosato-Ohhashi Bridge, Osaka, Japan.

### 5.16 Arakawa River Bridge, Japan

This three-span symmetrical structure, Fig. 5.28, carries metropolitan Highway Route 7 over the Arakawa River linking downtown Tokyo with the Narita International Airport and the eastern suburban districts of Tokyo. Transversely the stay geometry is a single plane of stays in the median. In elevation, two stays emanating from each side of the pylon have a harp configuration. It has a center span of 525 ft (160 m) with flanking spans of 198 ft (60.3 m).

In cross section the superstructure consists of a 13-ft (4-m) wide central box girder and two outside plate girders spaced 14 ft 9 in. (4.5 m) from the web of the box. Overall width of the orthotropic deck is 58 ft 9 in. (17.9 m). Depth of the cross section is 7 ft 10 in. (2.4 m) for a depth-to-span ratio of 1/67.<sup>21</sup>

Aerodynamic studies indicated restricted vibration occurred at a wind velocity of 62 ft/sec (19 m/s). To improve wind stability,  $\frac{3}{32}$ -in. (2.3-mm) thick plates were installed from the bottom flange of the outside plate girders to the central box girder, producing the appearance of a large single closed box.

A one-side automatic welding method was applied to the field splices of the orthotropic steel deck. Total steel weight was 2438 tons (2212 mt), including the prefabricated parallel wire stays which weighed 113.5 tons (103 mt). Unit weight is 90 lbs/ft<sup>2</sup> (440 kg/m<sup>2</sup>).

### 5.17 Erskine Bridge, Scotland

The total length of this multispan, all-welded steel box girder bridge is 4334 ft (1321 m). The main cable-stayed span of Erskine Bridge is 1000 ft (305 m), with two anchor spans of 360 ft (109.7 m). Approach spans on the south side starting at the abutment are 168 ft (51 m) and three at 224 ft (68.3 m). On the north side from the abutment, approach spans consist of one span at 206 ft (62.8 m), and seven at 224 ft (68.3 m), Fig. 5.29.

In cross section, the steel deck is aerodynamically similar to the Severn Suspension Bridge and the Wye Bridge discussed previously, Fig. 5.30. The depth of the cross section is 10 ft  $7\frac{1}{2}$  in. (3.2 m), producing a depth to span ratio of 1/94. The overall width of the deck for the cable-stayed portion is 102 ft 6 in. (31.24 m) because of the narrower median requirements. The deck cantilevers approximately 20 ft 9 in. (6.32 m) from each side of the trapezoidal box. The box is of all-welded construction and consists of a  $\frac{1}{2}$ -in. (12.7-mm) deck plate throughout. The  $\frac{3}{8}$ -in. (9.5-mm) in-

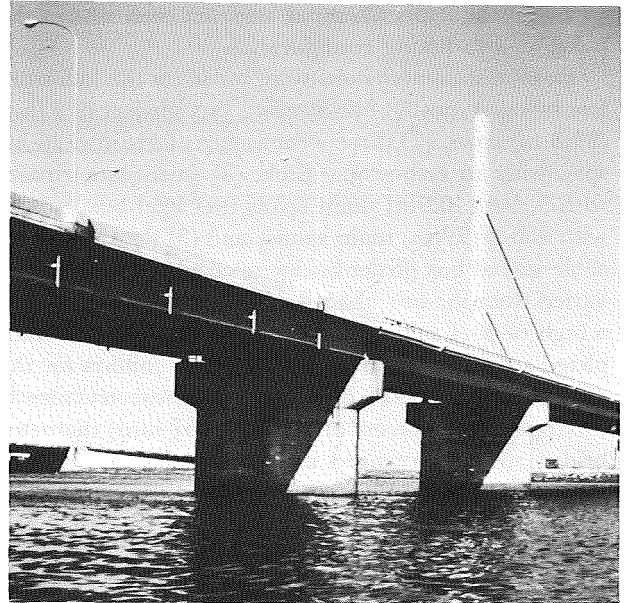


FIGURE 5.28 Arakawa River Bridge.

clined web plates are increased to  $\frac{7}{16}$  in. and  $\frac{1}{2}$  in. (11 and 12.7 mm) in portions of the main and anchorage spans, and a  $\frac{3}{8}$ -in. (9.5-mm) bottom plate increases to  $\frac{1}{2}$ -in. (12.7 mm) thickness at the piers and  $\frac{3}{4}$  in. (19 mm) at the pylons. V-shaped longitudinal stiffeners for the deck are spaced 2 ft (0.6 m) on centers, 8-in. (203-mm) bulb flats on 1-ft 4-in. (0.4-m) centers stiffen the bottom flange and the lower web sections, and 5-in. (127-mm) bulb flats on 2-ft (0.6-m) centers are used for the upper and central web sections. Transverse diaphragms on 14-ft (4.27-m) centers are of  $\frac{1}{4}$  in. (6.3 mm) plate (except at the piers, where they are increased to 1 in (25 mm)).

The stay system comprises a single vertical plane in the median with one stay on each side of the pylons. Stays are anchored at the girder, 330 ft (100 m) on each side of the pylon and are continuous through the pylons being supported on saddles. The stay consists of 24 3-in. (76-mm) diameter strands laid up in four layers of six strands each. Each spiral strand consists of 178 wires with diameters of 0.198 in. (5 mm).

The pylons are single-cell boxes that taper from 5 ft 6 in. by 4 ft 6 in. (1.67 by 1.37 m) at the base to 4 ft by 3 ft 6 in. (1.3 by 1.1 m) at the top. The pylon cell is made up of  $1\frac{1}{2}$ -in. (38-mm) high-strength plate that is internally stiffened and filled with high-strength concrete (7500 psi). Longitudinal movement is provided at deck level by a rocker bearing. Pylon load is carried through a massive diaphragm in the box girder to bearings on the piers.<sup>22, 23</sup>

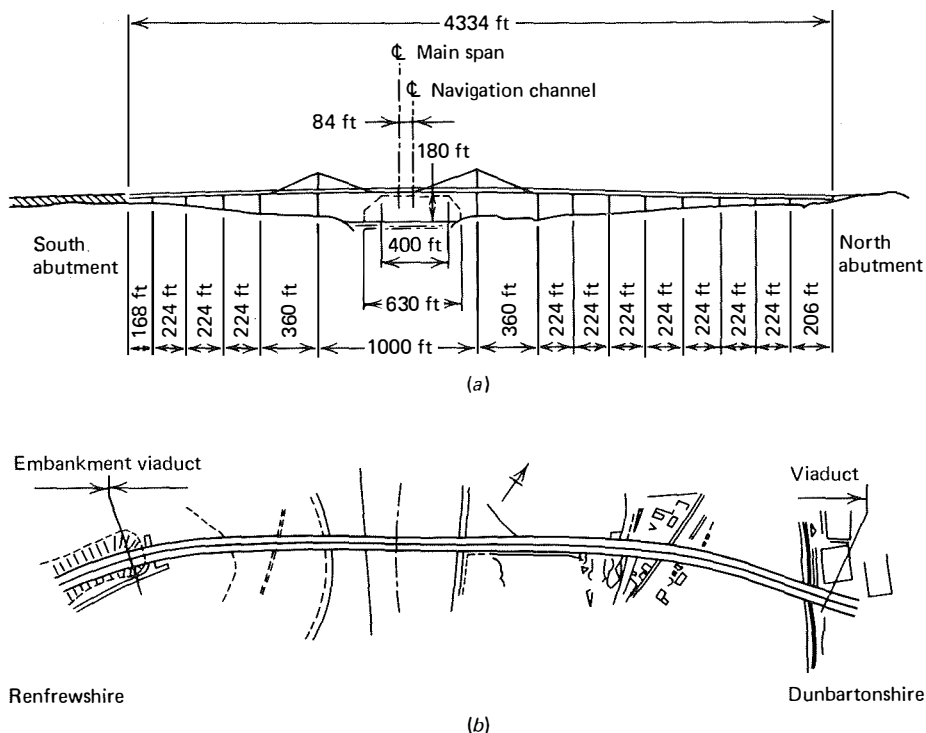


FIGURE 5.29 Erskine Bridge: (a) elevation and (b) plan. (Courtesy of The British Constructional Steelwork Association, Ltd., from reference 22.)

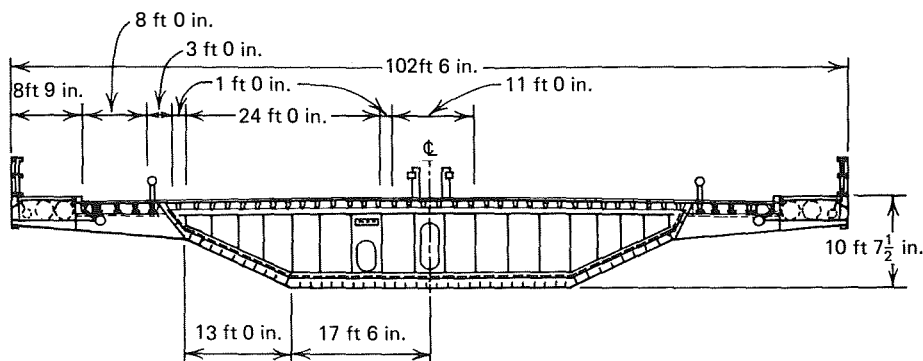


FIGURE 5.30 Erskine Bridge, typical cross section. (Courtesy of The British Constructional Steelwork Association, Ltd., from reference 22.)

### 5.18 Batman Bridge, Australia

Another asymmetric structure with an inclined A-frame tower is the Batman Bridge in Tasmania, Australia, Figs. 5.31 and 5.32. Cable stays are in two sloping planes in a radiating configuration.

The deck structure is of the conventional stiffening truss type used in suspension bridge structures, Fig. 5.33. The trusses are 12 ft 9 in. (3.88 m) deep, that is, a ratio of depth to span of 1/53, and are 29 ft 9 in.

(9 m) on centers. The chords of the trusses and principal bracing members are box sections with the gussets fabricated integrally with the chord members. Truss diagonals are fabricated H-sections and the verticals are made up of two T-sections that are battened between the stems. Main members are of welded construction. The deck is all steel, fully welded and orthotropic. It consists of  $\frac{1}{2}$  in. (12.7 mm) thick plate stiffened by longitudinal V stiffeners formed from  $\frac{5}{16}$  in. (8 mm) plates that span between cross beams at 11

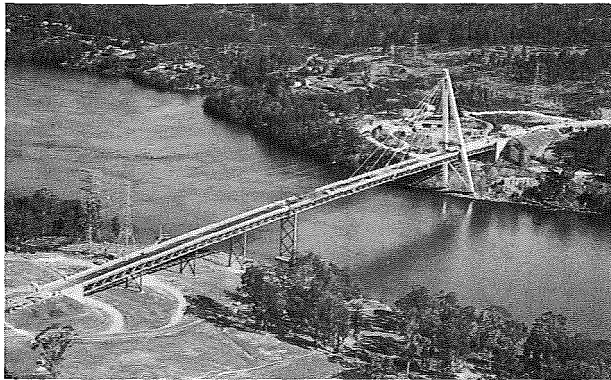


**FIGURE 5.31** Batman Bridge, view looking west. (Courtesy of Department of Public Works, Tasmania, from reference 24.)

ft 3 in. (3.4 m) on centers. These cross beams bear on rubber pads placed on top of the top chord of the trusses.

The A-frame is of box construction with the plates varying from  $\frac{1}{2}$  in. (12.7 mm) to 2 in. (50 mm) in

thickness. Legs of the A-frame taper from 13 ft by 7 ft 6 in. (4 × 2.3 m) to 6 by 7 ft. (1.8 × 2.1 m) Plates of the box are stiffened on the inside both vertically and horizontally. The pylon is inclined 20 degrees toward the center, Fig. 5.32.

Stays are made up of  $2\frac{3}{8}$  in. (60 mm) diameter locked coil strand. Each strand is cut to length and socketed in the shop. The back-stay in each plane is made up of 16 strands in four layers of four each, the inside fore-stay is 2 strands in one layer, and the center and outside fore-stays consist of 4 strands in two layers of two each.<sup>24,25</sup>

### 5.19 Bridge over the Danube at Bratislava, Czechoslovakia

This highway bridge crossing the Danube River was opened to traffic in August 1972. It is an asymmetric structure with a major span of 994 ft (303 m) and an anchor span of 246 ft (75 m), Fig. 2.2(b). The single

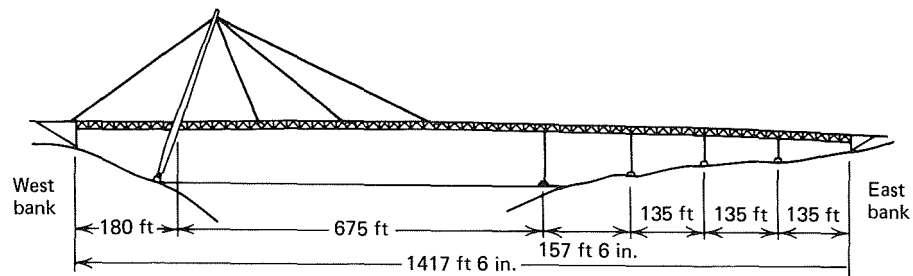


**FIGURE 5.32** Batman Bridge. (Courtesy of Department of Public Works, Tasmania, from reference 24.)

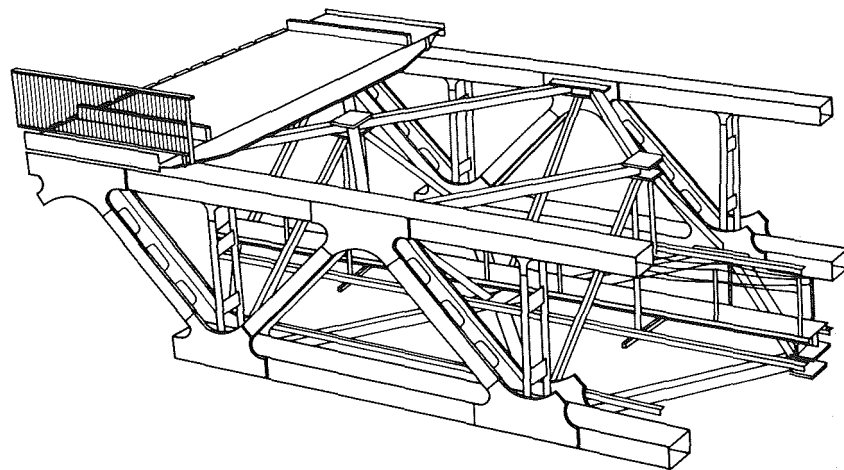


**FIGURE 5.33** Batman Bridge, truss arrangement. (Courtesy of Department of Public Works, Tasmania, from reference 24.)



**FIGURE 5.34** Bratislava Bridge, tower showing stay arrangement. (Courtesy of John H. Garren, FHWA Region 10.)

A-frame pylon is unusual in that it is inclined backward and supports a coffeehouse on top, Fig. 5.34. This concept of a restaurant at the top of the pylon may be an additional means of financing bridge structures.

The supporting stay system consists of six pairs of stays, three pairs of fore stays, and three pairs of back stays. In elevation, the fore stays are of a radiating configuration while the back stays are all in the same position anchoring to the abutment, Fig. 2.2(b). However, in plan the stays are distributed along the portal member at the top of the A-frame and then converge to the median or abutment anchorages, Figs. 5.34 and 5.35. Stays are continuous from abutment anchorage to girder anchorage and are supported on rocker-type saddles at the pylon portal member. The stays are composed of locked coil strands, each strand approximately  $2\frac{3}{4}$  in. (70 mm) in diameter. The number of

strands and configuration of each strand is indicated in Fig. 5.35. The excess strands indicated in stays D are individually anchored at the pylon by bearing sockets.

The A-frame tower is approximately 278 ft (85 m) high with tapered rectangular box section legs. One leg contains a high-speed elevator, the other contains a stairwell. The tower legs are fixed at their base.

The deck structure consists of a two-cell box girder 41 ft 4 in. (12.6 m) wide by 15 ft (4.6 m) in depth. Depth-to-span ratio is 1/66. The orthotropic deck cantilevers 13 ft 9 in. (4.2 m) out from the box on each side. Total width of the deck is 68 ft 10 in. (21 m). The footpaths are below the roadway and cantilever out from the box 11 ft 6 in. (3.2 m) on each side, Fig. 5.36.

This structure indicates the versatility of the cable-stay concept for bridge design.<sup>26,27</sup>

### 5.20 Nordbrücke Mannheim-Ludwigshafen Bridge, West Germany

The Nordbrücke Rhine River Bridge, also known as the Kurt-Schumacher-Brücke, connects the cities of Mannheim and Ludwigshafen, Figs. 5.37 and 5.38. In elevation it is an asymmetric structure with a major span of 941.4 ft (286.9 m) and a minor span of 480.3 ft (146.4 m). The stays are in the radiating configuration, Fig. 5.38. Transversely the stays are in two sloping planes.

The major span superstructure consists of a 121-ft (36.9-m) wide orthotropic deck supported on two rectangular box girders. The center portion of the deck between box girders and through the A-frame pylon is for trams. Two lanes for auto traffic are supported over the box girders on each side of the pylon, and bicycle paths are at the extreme edges of the deck. At the Ludwigshafen side the superstructure widens to 170.3 ft (51.9 m) to accommodate ramps on both sides and the center tramway portion depresses below the roadway elevation, Fig. 5.38. The minor span, including the portion over the pylon pier, is a box girder of prestressed concrete construction. A rigid connection is provided between the steel and concrete superstructure construction. The superstructure has a constant depth of 14 ft 9 in. (4.5 m) producing a depth-to-main-span ratio of 1/64.

The pylon rises 234 ft 6 in. (71.5 m) above the roadway elevation and is of steel construction. Legs of the pylon pierce the prestressed concrete box girder superstructure to be supported by the pylon pier.



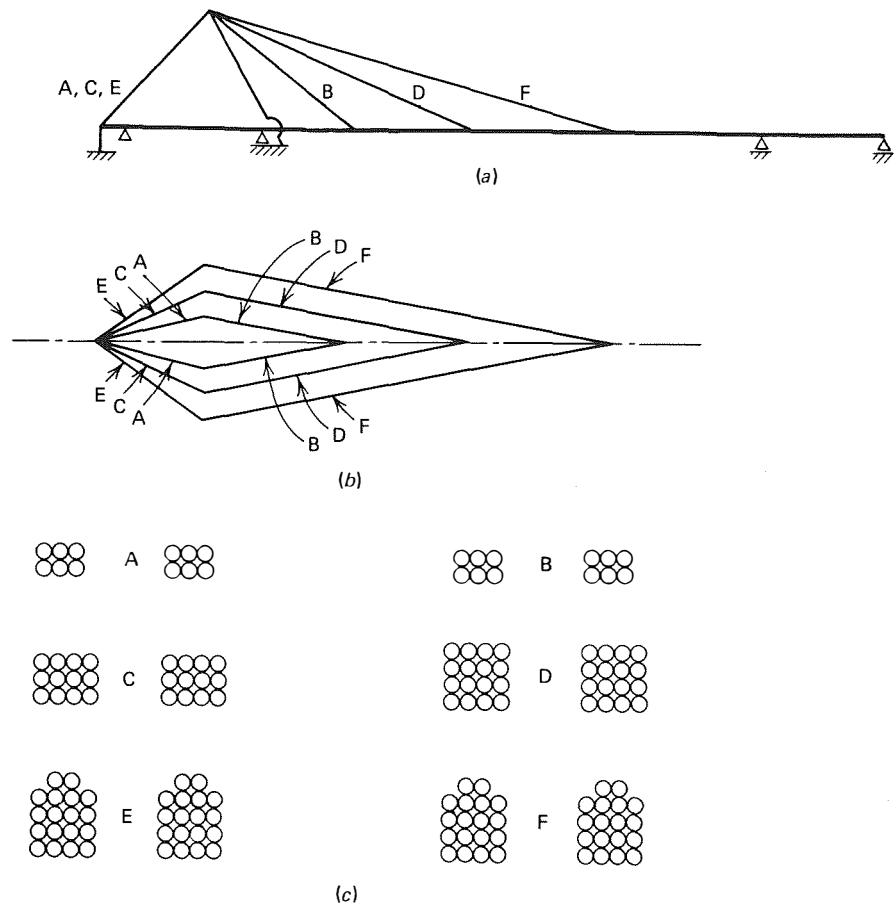


**FIGURE 5.35** Bratislava Bridge: (a) elevation, (b) plan, and (c) stay arrangement. (Courtesy of Der Bauingenieur, from reference 26.)

Each parallel wire strand in the stays consists of 295 wires approximately  $\frac{9}{32}$  in. (7 mm) in diameter compacted to a strand of approximately 5 in. (127 mm) in diameter. In each sloping plane the stays take the fol-

lowing strand pattern: top fore stay, six strands in three layers of two strands each; center fore stay, four strands in two layers of two strands each; lower fore stay and back stay, two strands in one layer of two; top back

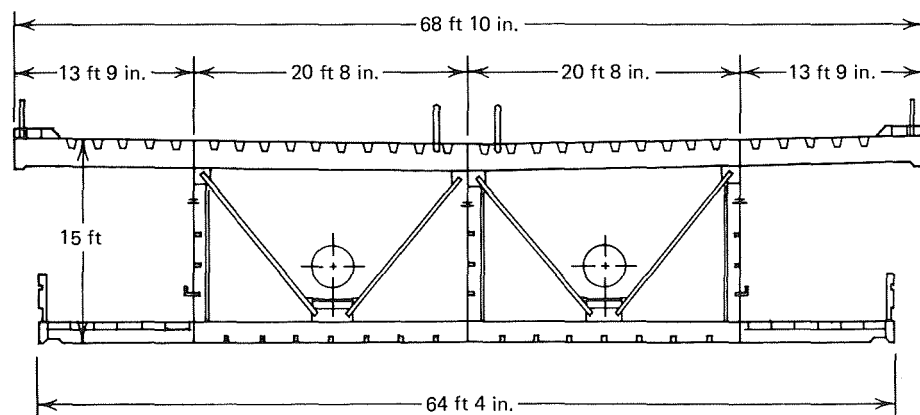


**FIGURE 5.36** Bratislava Bridge, cross section. (Courtesy of Acier-Stahl-Steel, from reference 27.)

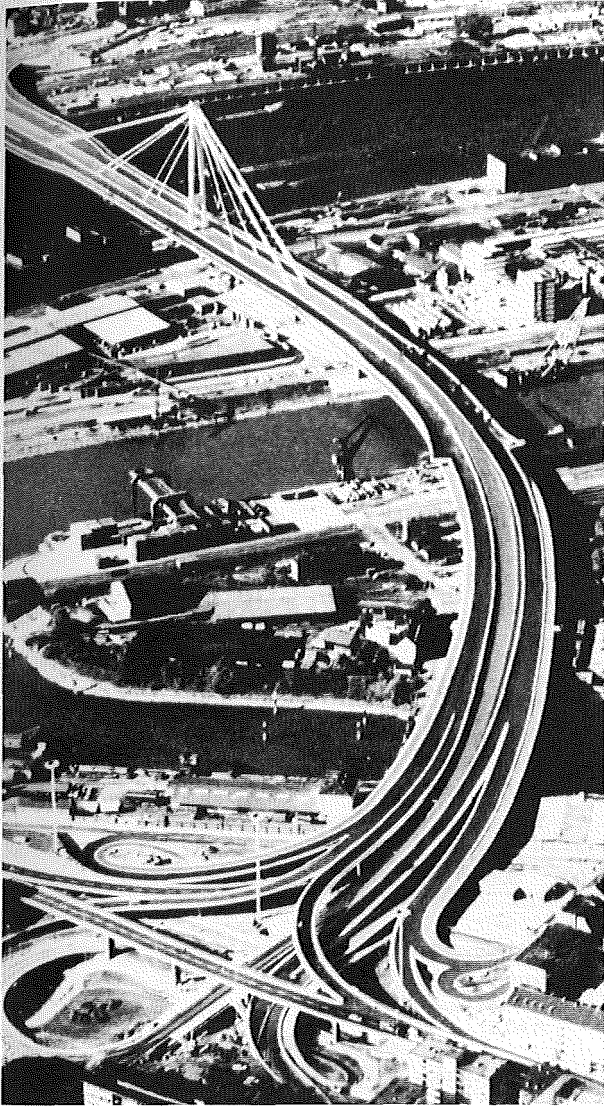


**FIGURE 5.37** Nordbrücke Mannheim-Ludwigshafen, aerial view. (Courtesy of Wolfgang Borelly.)

stay, 10 strands in five layers of two strands each. Each strand is individually anchored at the pylon.<sup>28, 29, 30</sup>

### 5.21 Köhlbrand High-Level Bridge, West Germany

Construction of this six-lane, high-level bridge over the Köhlbrand, an arm of the River Elbe at Hamburg, Fig. 5.39, began in autumn 1970. This structure connects the Hamburg Free Port area with a western motorway bypass. Its main span of 1066 ft (325 m) makes it one of the largest cable-stayed bridges in Germany, Fig. 5.40. The distinctive delta-shaped towers provide

for narrow pylon piers, Fig. 5.39. It is anticipated that at a future date a twin structure will be built along side of the completed structure.

Geometrically the stays are in two sloping planes and are of the radiating configuration. The 1706-ft (520-m) long cable-stay portion of this structure is of steel construction and has a center span of 1066 ft (325 m) and equal anchor spans of 320 ft (97.5 m). The cable-stayed superstructure is a trapezoidal box with side cantilevers and accommodates six lanes of traffic. Eighty-eight locked coil strands, ranging in diameter from  $2\frac{1}{8}$  in. to  $4\frac{3}{32}$  in. (55 to 104 mm) support the superstructure. Other than for lateral support the 1706-ft (520-m) length of steel box girder is supported by the stays and is independent of the pylons.

The west approach spans total 3438 ft (1048 m) in length, with spans varying from 111 ft 6 in. to 229 ft 8 in (34 to 70 m) of a single trapezoidal concrete box-girder construction, Fig. 5.40. The east approach spans total 6222 ft (1896.5 m) in length, with spans varying from 114 ft 10 in. to 213 ft 3 in. (35 to 65 m) of a two-cell concrete box-girder construction, Fig. 5.40.

The steel pylon rises 321 ft 6 in. (98 m) above the pier, Fig. 5.41. The distinctive shape of the pylon results from the height of the superstructure above the water and an especially narrow pylon pier. A much wider pier would have resulted if the legs were extended as in the conventional A-frame. Figure 5.42 is a view of the completed structure, which is, in our opinion, an excellent example of form following function.

### 5.22 Oberkassel Bridge, West Germany

This structure, completed in 1975, replaces a narrow truss bridge which was constructed after World War II. The new structure, Fig. 5.43, has a single plane with a harp configuration in elevation. Overall length of the bridge is 1937.2 ft (590.5 m) with a major span over the Rhine River of 845.6 ft (257.75 m) and five anchor spans of 169.1 ft (51.55 m), Fig. 5.44. Back stays are attached to the piers by a linkage, and the stays are continuous through the pylon on saddles. The structural system is similar to that of the Kniebrücke Bridge (see Section 5.13).

Overall width of the orthotropic box girder is 114 ft 10 in. (35 m) and carries a tramway, two lanes of vehicular traffic, a bicycle path, and a sidewalk in each direction, Fig. 5.44. Girder depth is 10 ft 4 in. (3.15 m) resulting in a depth-to-span ratio of 1/82. Pylon height is 328 ft (100 m) above the deck.

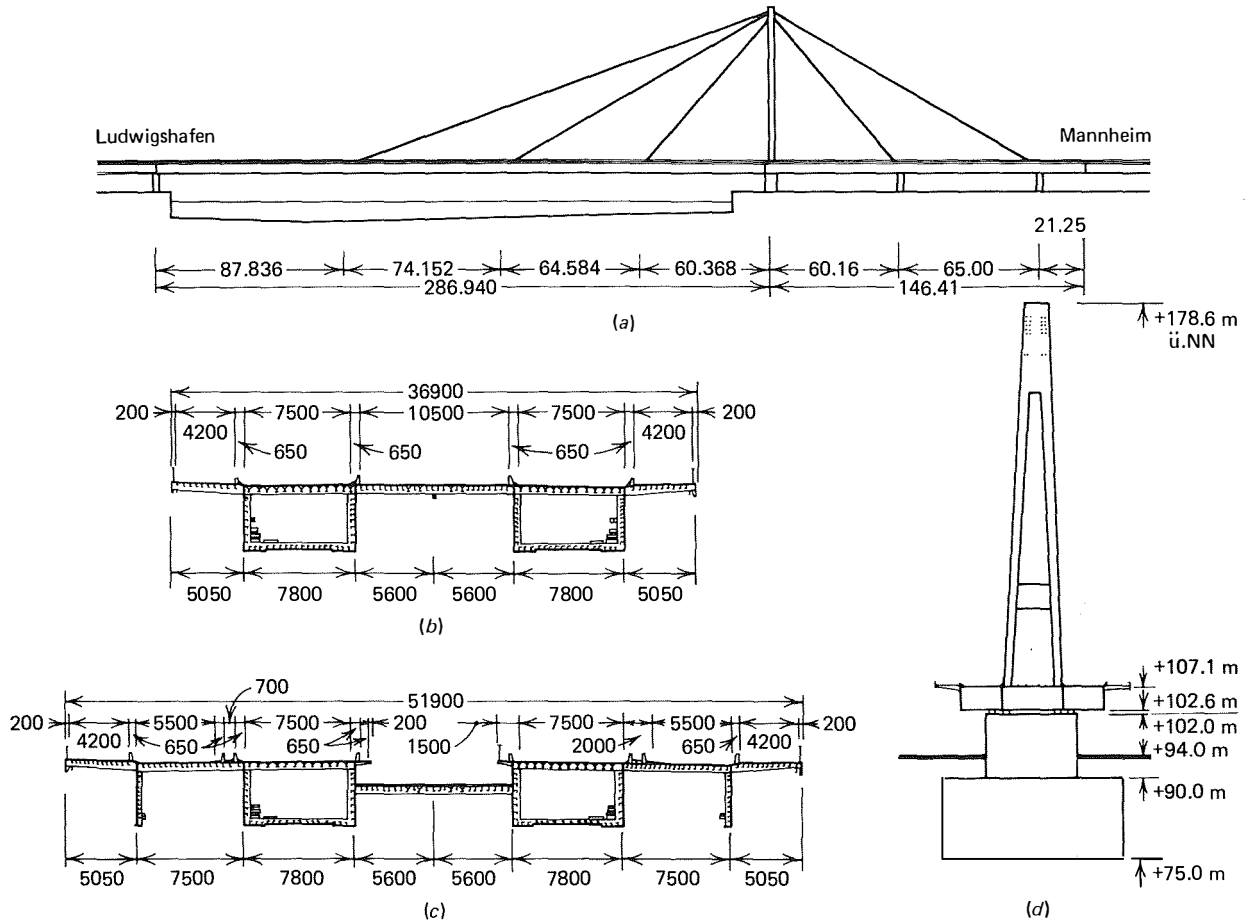


**FIGURE 5.38** Nordbrücke Mannheim-Ludwigshafen: (a) elevation, (b) typical cross section, (c) cross section in the area of the sloping streetcar ramp, and (d) cross section at pylon (dimensions are given in meters.)

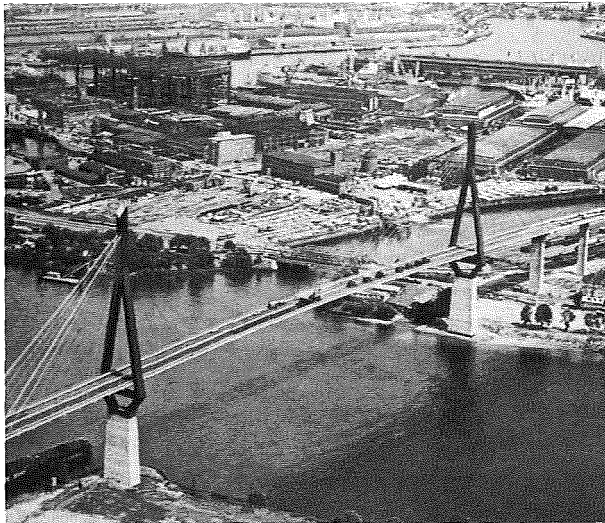


**FIGURE 5.39** Köhlbrand High-Level Bridge, aerial view. (Courtesy of Wolfgang Borelly.)

The unique problem facing the west German engineers was that the alignment of the new bridge was required to be on the same alignment as the old truss bridge. Because the approach streets of both the Oberkassel and Düsseldorf sides of the river pass through developed areas it would have been extremely costly and disruptive to build the bridge on a new alignment. At the same time, the heavy traffic demands made it impossible to demolish the old bridge and wait several years for construction of the new bridge. The new bridge was constructed on a parallel alignment 156 ft (47.5 m) upstream from the old alignment. When the new bridge was completed, traffic was temporarily rerouted to the new bridge by sharply curved approach spans. The old bridge was then demolished. The new bridge was then jacked downstream to the old alignment.<sup>31</sup> This unique procedure will be described in detail in Chapter 8.

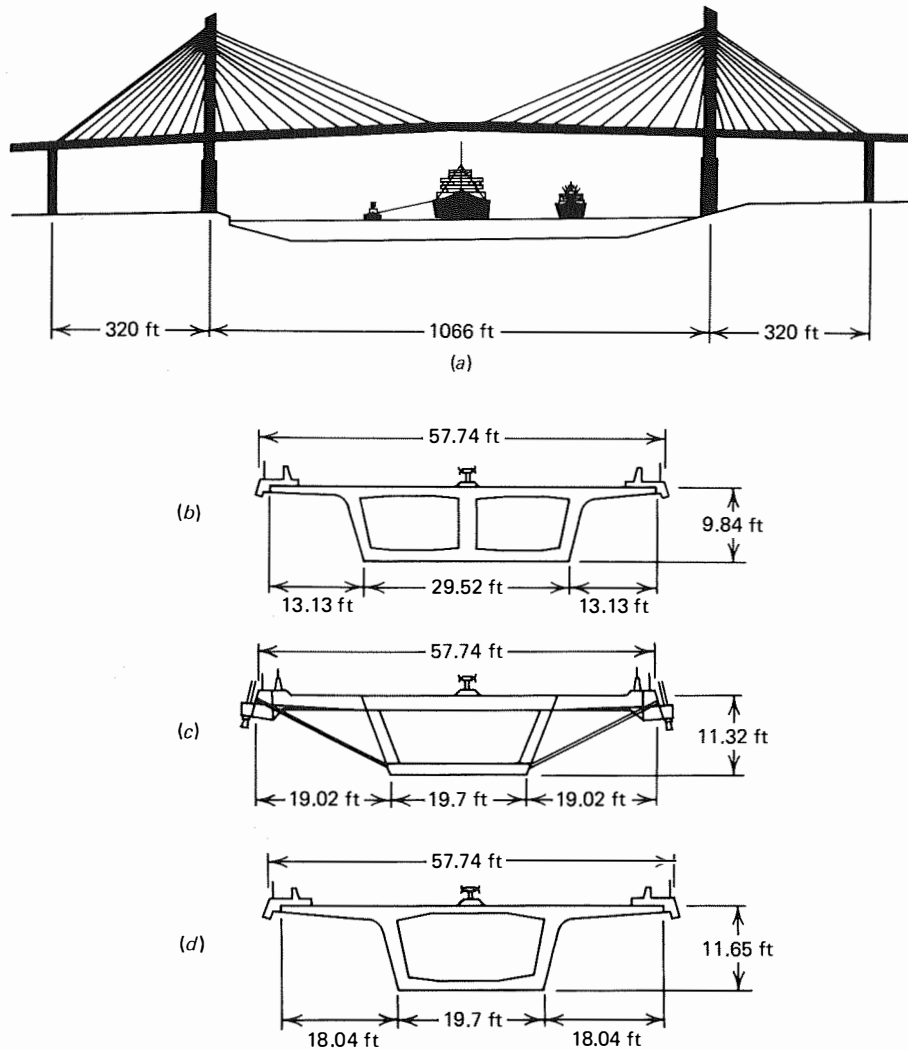


**FIGURE 5.40** Köhlbrand High-Level Bridge: (a) elevation, (b) concrete cross section, east approach spans, (c) steel cross section, cable-stay spans, and (d) concrete cross section, west approach spans. (Courtesy of Wolfgang Borelly.)

### 5.23 Zarate-Brazo Largo Bridges, Argentina

The Zarate-Brazo Largo system of bridges provides both highway and railroad links across the Parana River. Two major bridges cross the two arms of the Parana River—one crosses the Parana de las Palmas and the other crosses the Parana Guazu, Fig. 5.45. The two identical bridges are 18.6 miles (30 km) apart, each supporting a four-lane highway and a railway line. Each bridge has a center span of 1083 ft (330 m) with flanking spans of 360 ft (110 m) and a navigation clearance of 164 ft (50 m).

Concrete pylons are of a variable rectangular hollow

cross section constructed by sliding forms and rise to a height of 394 ft (120 m) above the water. There is a concrete portal cross-tie between pylon shafts below the superstructure and a structural steel cross-frame at the top, Fig. 5.46.

Superstructure components are illustrated in Fig. 5.47 and consist principally of the trapezoidal box edge girders, transverse plate girder floor beams at the stay anchorage locations, secondary transverse trusses, the orthotropic deck, and bracing of the lower flange of the transverse members.

This structure is unique not only because it supports both highway and railroad traffic, but also be-

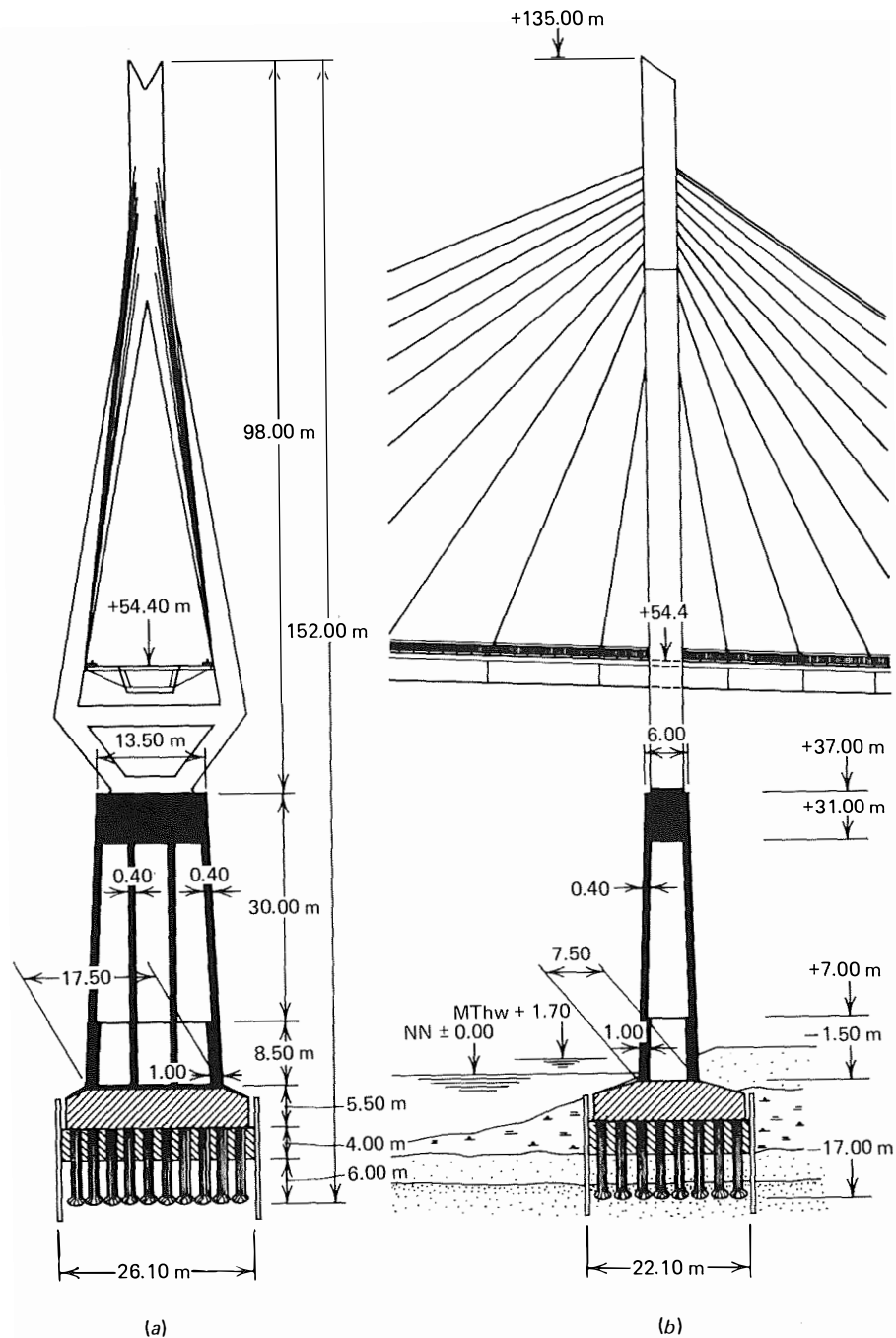


**FIGURE 5.41** Köhlbrand High-Level Bridge: (a) pylon cross section, and (b) pylon elevation. (Courtesy of Wolfgang Borelly.)

cause the rail line is on one side of the structure. Consequently, this required that the stays on the railroad side be larger than those on the highway side.

Designers were Leonhardt and Andra of Stuttgart, Germany.

#### 5.24 Sacramento River Bridge, U.S.A.

This structure designed by the California Department of Transportation is an unusual cable-stay swing span bridge that replaced a conventional steel truss swing

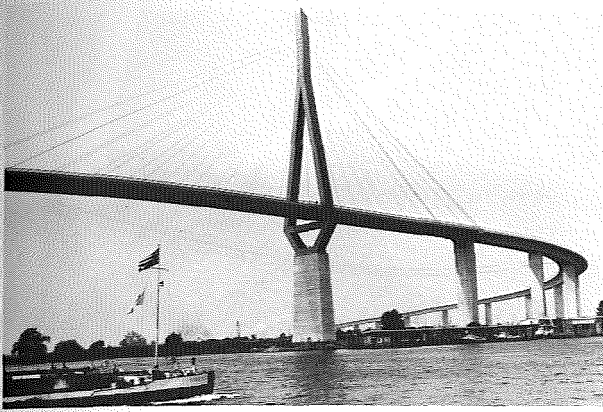


FIGURE 5.42 Köhlbrand High-Level Bridge. (Courtesy of Wolfgang Borelly.)

span, Fig. 1.29. Existing piers and turning mechanism of the old structure were incorporated into the new bridge. Use of the existing piers and a profile within 5 ft (1.5 m) of the old bridge resulted in the bridge structure having two symmetrical swing spans of 180 ft (55 m), Fig. 5.48.

The swing spans are stayed at their extremities by



FIGURE 5.43 Oberkassel Bridge in final position, from reference 31.

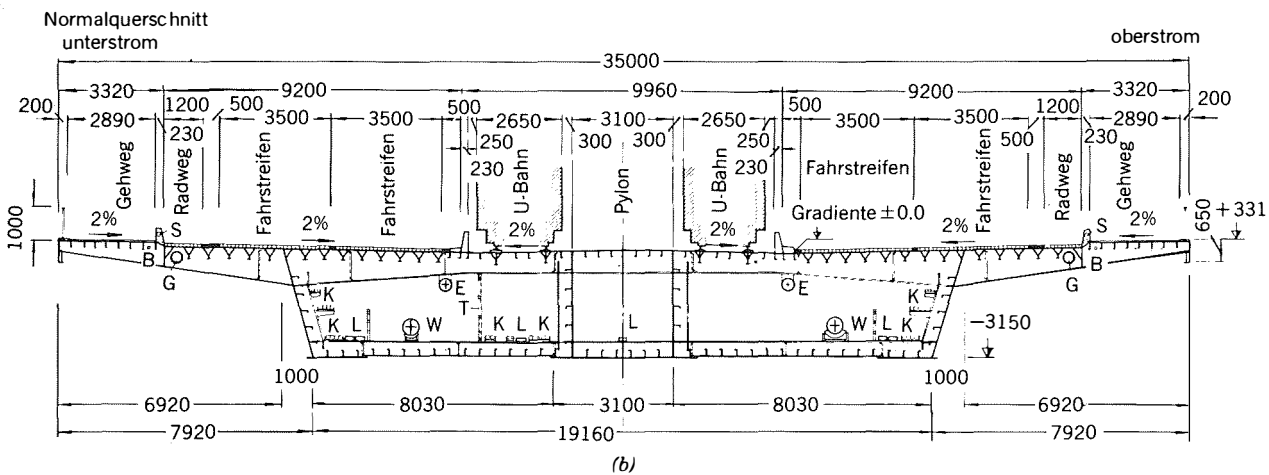
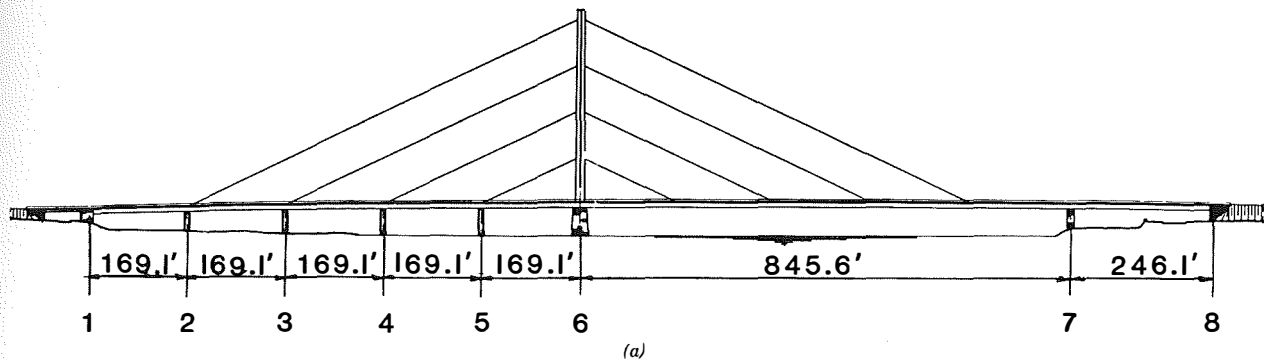
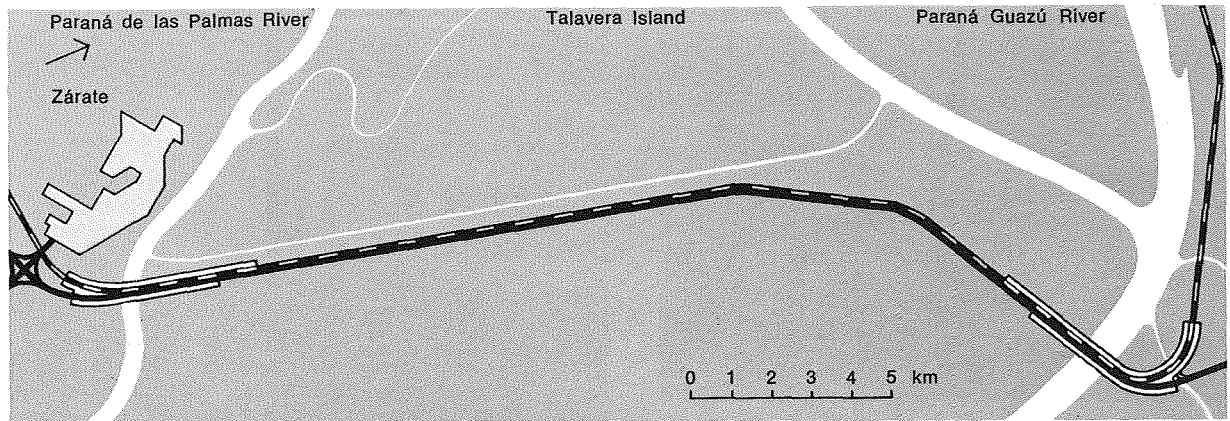
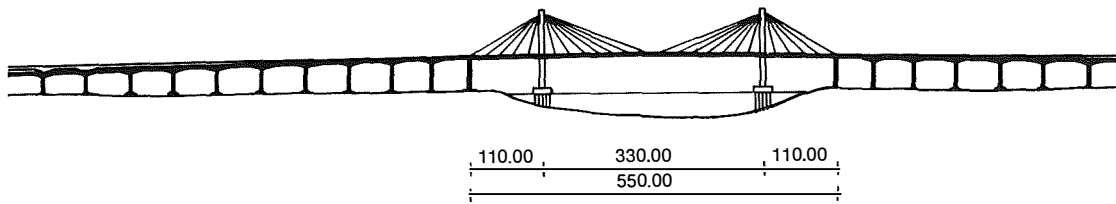


FIGURE 5.44 Oberkassel Bridge: (a) span arrangement and (b) cross section.



Bridge over the Paraná de las Palmas River



Bridge over the Paraná Guazú River

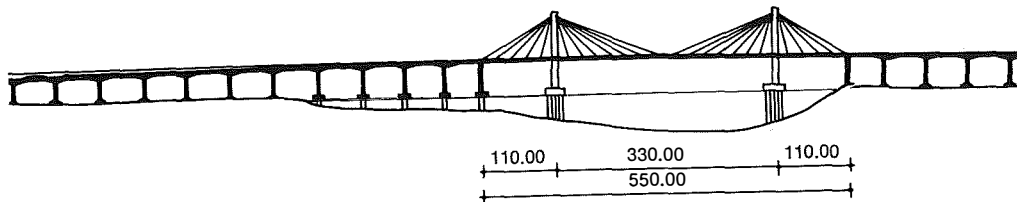


FIGURE 5.45 Zarate-Brazo Largo Bridges, orientation and location.

three  $3\frac{1}{4}$ -in. (82.5-mm) ASTM A586 structural strands, and at the 0.4 points by three  $3\frac{1}{2}$  in. (89-mm) strands. Stays are continuous through the pylon. Primary use of the stays is to control deflection, particularly when the bridge is in the open position. In the open position, Fig. 5.48(a), all stays participate in resisting dead load. In the closed position only the lower stays participate in carrying live load, Fig. 5.48(b). Use of the inter-

mediate stays enabled the structure to swing easily with a dead load deflection of not more than 2 in. (51 mm).

Deck superstructure consists of five welded steel girders that are continuous over two large caps at the center pier, which also support the A-frame tower legs. The cap beams in turn are supported on massive loading girders and a ring girder, Fig. 5.49. The entire load of the superstructure is subsequently transferred

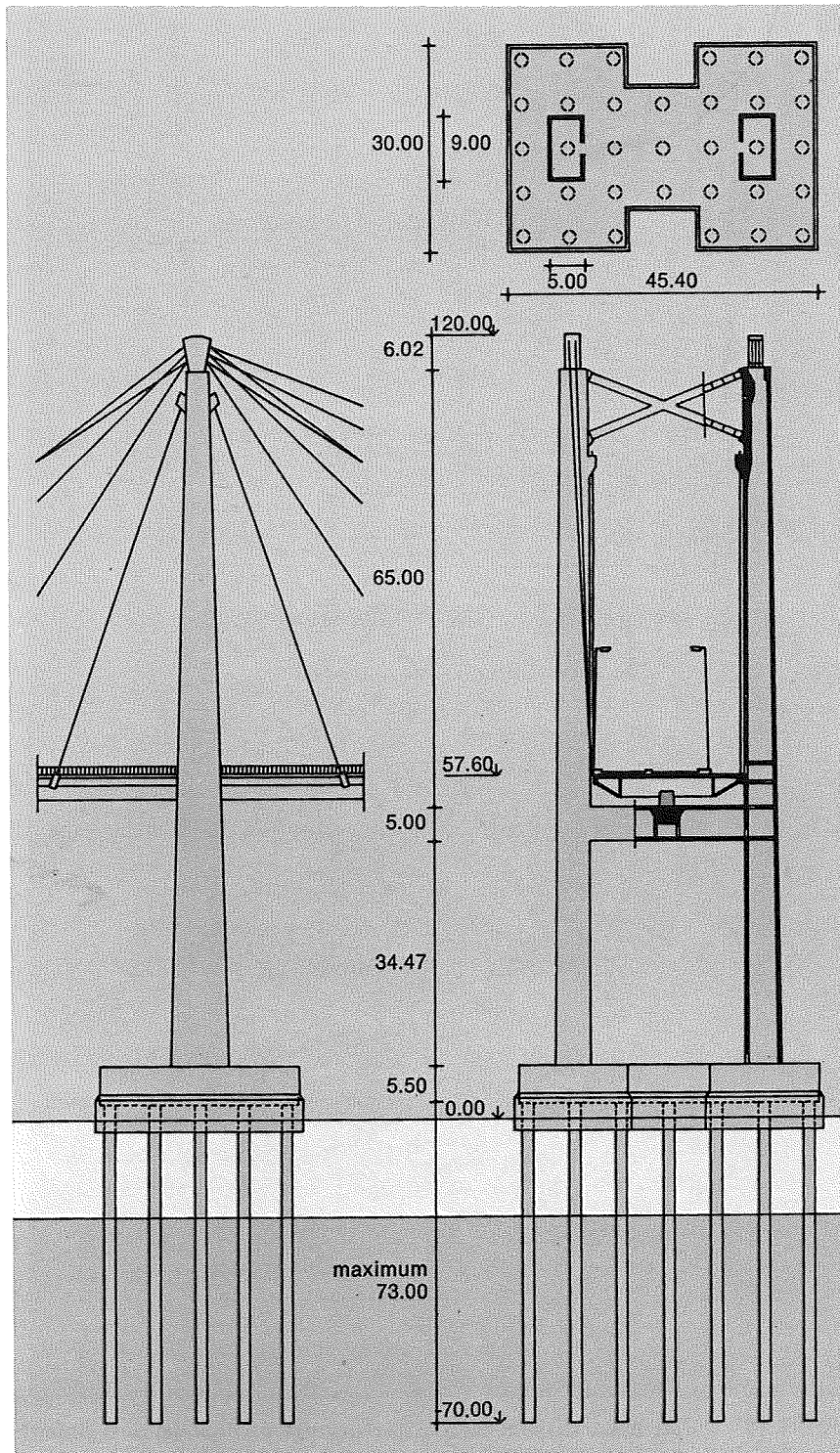
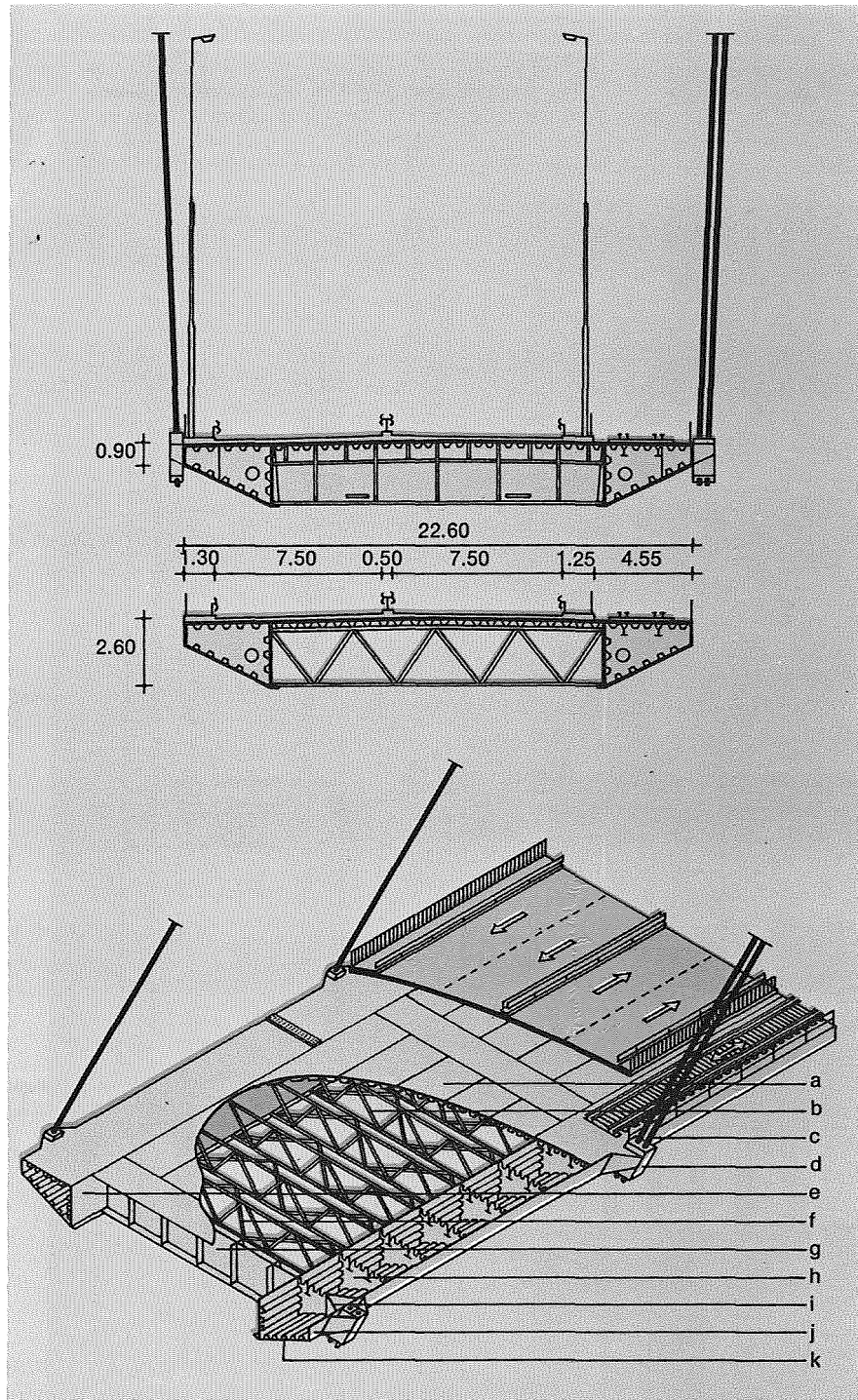
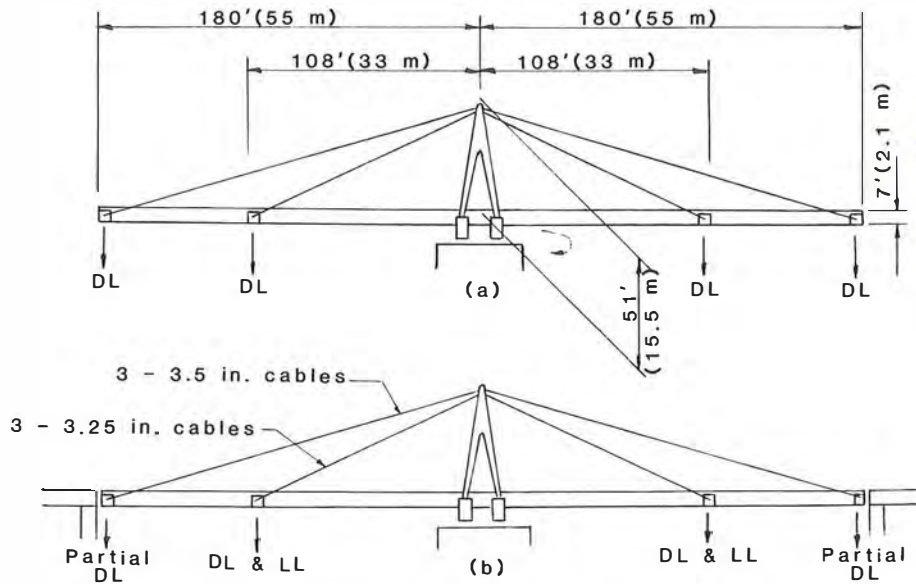


FIGURE 5.46 Zarate-Brazo Largo Bridges, pylon.





**FIGURE 5.47** Zarate-Brazo Largo Bridges, superstructure: (a) deck, (b) truss girder, (c) stays, (d) anchorage box, (e) roadway box girder, (f) torsion bracing, (g) plate girder, (h) typical diaphragm, (i) bifurcated diaphragm, (j) railway box girder, and (k) stiffeners (ribs).



**FIGURE 5.48** Sacramento River Bridge at Meridian, California: (a) load condition in open position, and (b) load condition in closed position from reference 32.

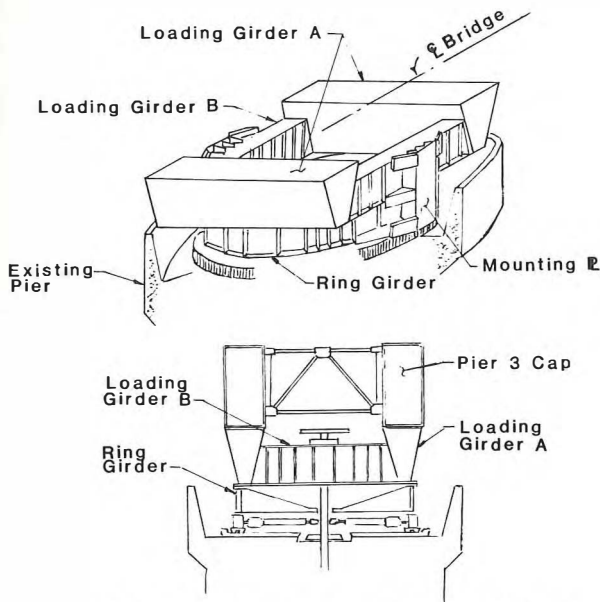


**FIGURE 5.49** Sacramento River Bridge at Meridian, California, support at center pier, from reference 32.

to the existing pier through 48 14-in. (356-mm) diameter rollers salvaged from the old structure.<sup>32</sup>

### 5.25 Luling Bridge, U.S.A.

The Luling Bridge is a high-level crossing over the Mississippi River located in St. Charles Parish, Lou-

isiana at a point approximately 12 miles (19 km) upstream from New Orleans, Fig. 1.33. At the bridge site, the Mississippi River is approximately 0.7 miles (1.1 km) wide between levees. Main channel navigation requirements were a clear horizontal clearance of 1200 ft (364 m) and a required vertical clearance of 133 ft (40.5 m).

The American Association of State Highway and Transportation Officials (AASHTO) Standard Specifications for the Design of Highway Bridges was the basic governing design code. Live load deflection requirements were relaxed to be more in line with common practice for cable-stayed bridges. However, because of hurricane winds at the site, wind loads on the bridge were increased to pressures of 110, 65, and 50 lbs/ft<sup>2</sup> of the exposed area of cable stays, main span girders, and main bridge piers respectively.

Geometric layout of the five-span continuous central portion of the bridge is illustrated in Fig. 5.50. All five spans are of a constant depth of 14 ft (4.3 m) which produces a depth-to-span ratio of 1/87. Depth was derived from the center span and, therefore, the end spans do not require the assistance of stays or intermediate supports. Contiguous end spans tend to increase the positive reaction of the deck over the first continuous pier (Piers 1 and 4) where it is most needed to help resist the tension in the back stays. In addition, with the annexing of the end spans, bulky roadway expansion joints needed at the ends of the continuous structure were relocated away from the complex anchorage



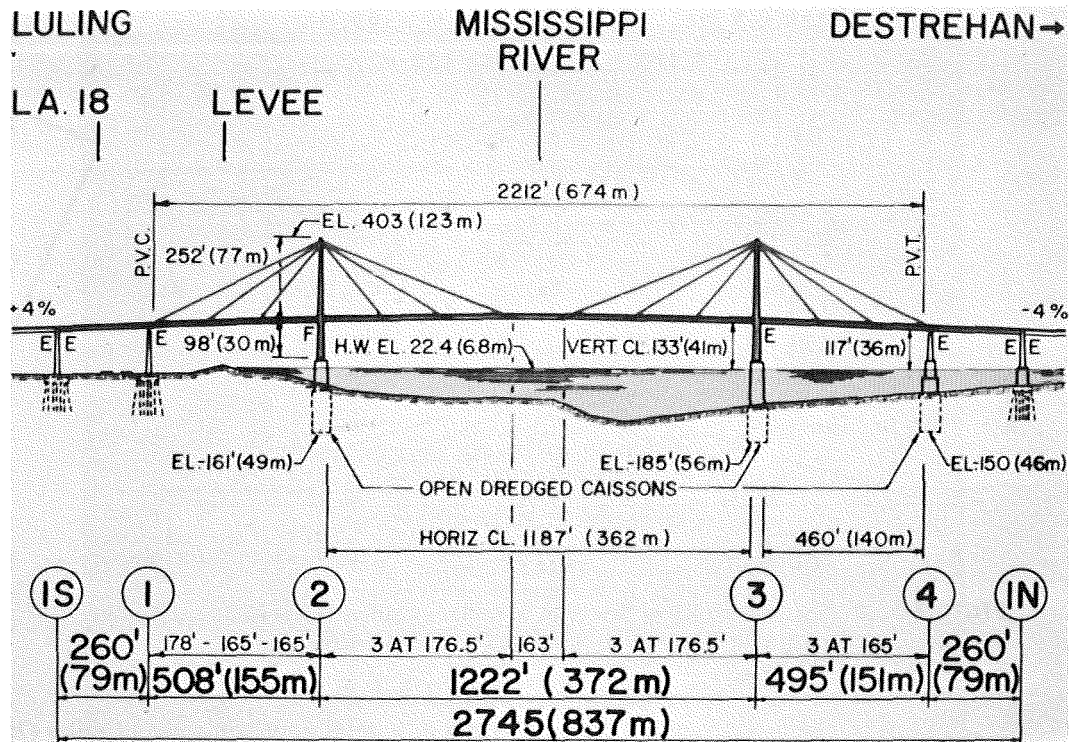


FIGURE 5.50 Luling Bridge, span layout, from reference 33.

detail at the lower ends of the backstays, simplifying detailing and fabrication at this location.<sup>33</sup>

Transverse configuration of the deck girder is shown in Fig. 5.51. Overall width of the cross section is 82 ft (25 m). The top flange is of an orthotropic design utilizing 9-in. (228-mm) deep trapezoidal closed ribs spaced about 2 ft 2 in. (0.66 m) on center. Deck plate thickness is  $\frac{7}{16}$  in. (11 mm) except at points of stress concentration where thicker plates of appropriate size are used. Deck ribs are continuous and penetrate the transverse floor beams which are spaced at about 15 ft (4.6 m). All material is ASTM A588 weathering steel.

The orthotropic deck serves as the top flange of the two parallel longitudinal box girders. Bottom flange and webs of the box girders are stiffened longitudinally and transversely. In the center span, fairing plates are added to the basic cross section which by virtue of their inclination decrease the amplitude of vortex excited vibrations of the deck. These plates are not considered in the load-carrying capacity of the girder. To increase torsional stiffness of the cross section, the longitudinal box girders are connected by full depth plate diaphragms at about 45-ft (13.7-m) spacing. Torsional

rigidity is further enhanced by transverse rectangular box girders at stay anchorage locations. Floor beams of the deck system are 3-ft (0.9-m) deep welded plate girders which cantilever out to support a 2-ft (0.6-m) deep edge beam which secures the edge of the orthotropic deck against buckling.<sup>33</sup>

A-frame pylons are 350 ft (106.7 m) in height above their base, Fig. 5.52. In elevation, each box leg of the A-frame tapers from 25 ft (7.6 m) at the base to 12 ft (3.6 m) at the top. Transversely each leg has a constant width of 20 ft (6.1 m). The bridge deck is supported by an 8-ft wide and 20 ft (2.4 m wide 6.1 m) deep box girder strut located at a height of 98 ft (29.9 m) from the base of the pylon. A 31-ft (9.4-m) deep strut at the top accommodates three tiers of stay anchorages. All components of the pylons are welded steel boxes composed of plate material stiffened longitudinally and transversely. Interior column space is subdivided into compartments by means of horizontal and longitudinal plate diaphragms.

Stays are composed of parallel  $\frac{1}{4}$ -in. (6-mm) diameter wire encased in mortar grouted polyethylene ducts. Anchorages are of the Hi-Amp type (see Chapters 9 and 10).

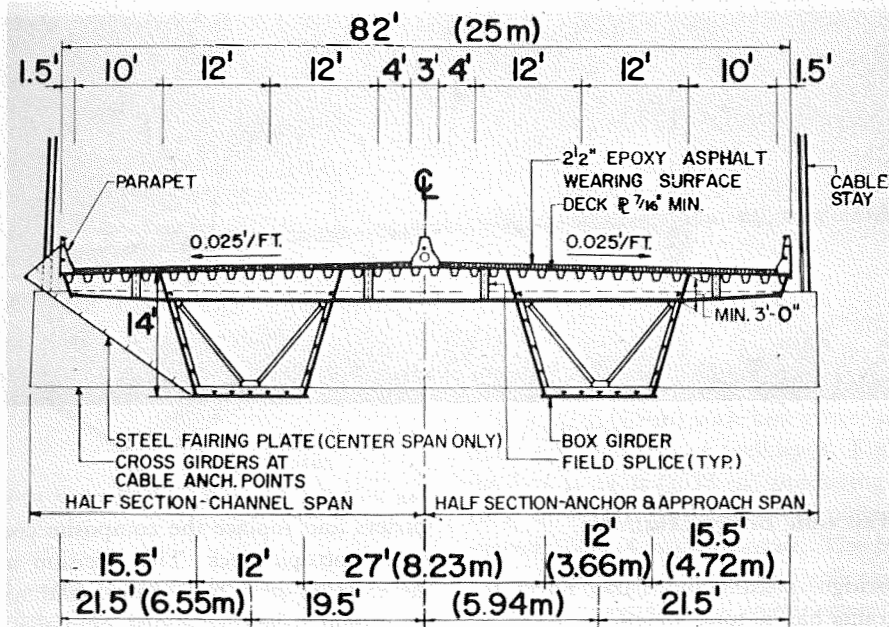


FIGURE 5.51 Luling Bridge, typical cross section, from reference 33.

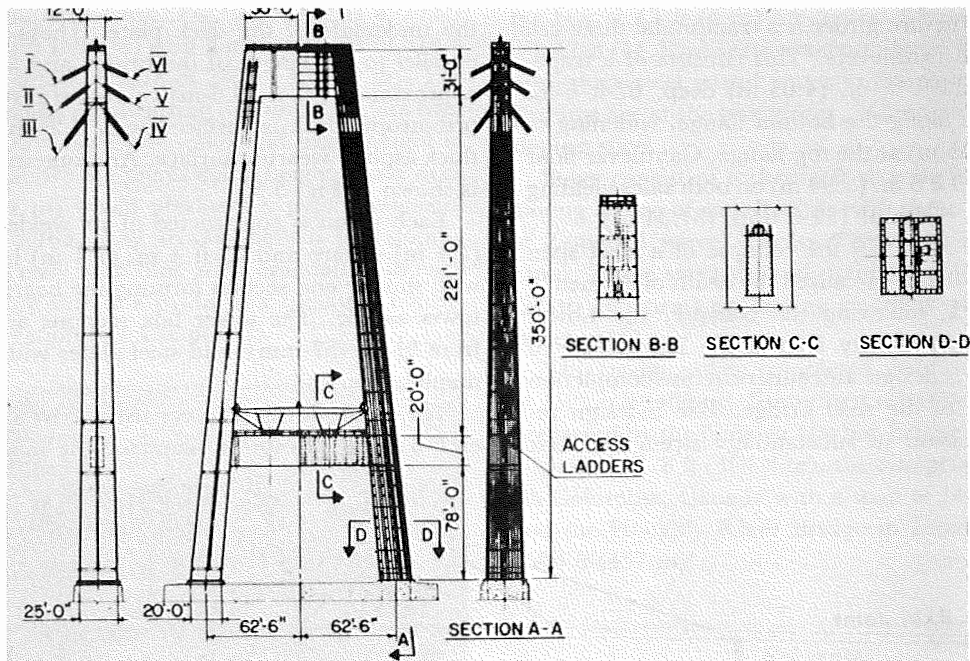


FIGURE 5.52 Luling Bridge, pylons, from reference 33.

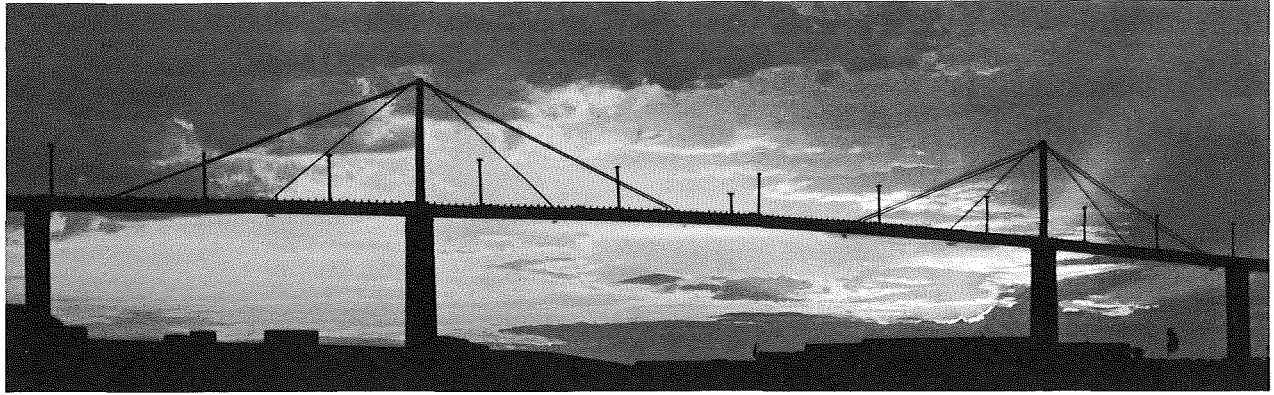


FIGURE 5.53 West Gate Bridge.

### 5.26 West Gate Bridge, Australia

The West Gate Bridge crossing the Yarra River in Melbourne, Australia has a total length of 8473 ft (2582.6 m). Overall length of the main steel bridge is 2782 ft 6 in. (848.1 m). The five-span river-crossing unit has spans of 367.5, 472.5, 1102.5, 472.5, and 387.5 ft (112.01, 144.02, 336.04, 144.02, and 112.01 m) with the center three spans supported by cable stays, Figs. 5.53 and 5.54. Minimum navigation clearance to low water is 176 ft (53.65 m), and the height of the pylon above low water is 336 ft (102.4 m). Pylon height above the deck is 150 ft (45.7 m).

The superstructure girder is a trapezoidal three-cell box girder with cantilevers. This consists of a trapezoidal section 13-ft 3½-in. (4.05-m) deep, 62-ft 6-in. (19.05 m) wide along the bottom flange, widening to 83 ft 6 in. (25.45 m) at the top flange. Cantilever floor beams extend 19 ft 6 in. (5.94 m) on both sides yielding an overall deck width of 122 ft 6 in. (37.34 m).

On October 15, 1970 the collapse of a steel span between Piers 10 and 11 caused the death of 35 men.<sup>34</sup> In August 1971, following the collapse, the Lower Yarra Crossing Authority formed the Directorate of Engineering to redesign and supervise the completion of construction of the steel bridge. The redesign resulted in a decision to substantially strengthen box

girders and replace the composite concrete deck with an orthotropic deck. This decision meant that all of the existing steel box girders had to be dismantled, additional stiffening added, and the new orthotropic deck placed in position prior to erecting the boxes into position.

In the revised design the steel orthotropic deck was placed over the whole superstructure to form the top flange of the box girder. The deck consists of a high-yield deck plate varying in thickness from ½ in. to ¾ in. (12.7 to 19 mm) depending on its location in the bridge, and trapezoidal stiffeners or “troughs” of ¼-in. or ⅝-in. (6.3- or 8-mm) thickness were welded to the underside of the deck plate. These troughs run parallel to the length of the bridge and are spaced at approximately 2-ft (0.6-m) centers transversely. The orthotropic deck is surfaced with a 2½-in. (63.5-mm) thick asphalt wearing surface. An isometric of the deck is shown in Fig. 5.55.

Each pylon is constructed of six welded boxes 8 ft (2.4 m) square and 23 ft 4 in. (7.1 m) long together with shorter end section forming the bearing base and tower saddle. The tower box sections are fabricated from 2¼-in. (57-mm) mild steel plates with connecting diaphragms.

The single inner stay consists of 16 spiral strands each 3 in. (76.2 mm) in diameter and made up of 178

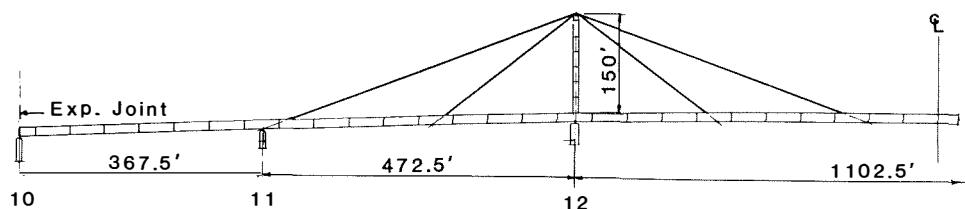


FIGURE 5.54 West Gate Bridge, span layout.

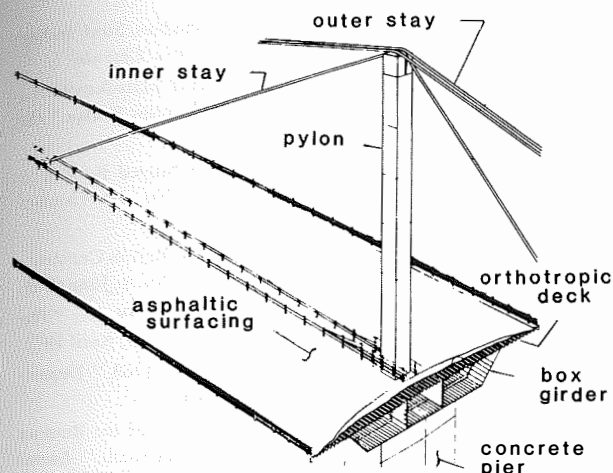


FIGURE 5.55 West Gate Bridge, isometric of deck assembly.

galvanized round wires in seven layers over a core strand of three wires. The two outer stays consist of 16 spiral strands,  $2\frac{7}{8}$  in. (73 mm) in diameter and made up of 162 galvanized round wires in seven layers over a central wire. Wire size is 0.196 in. (5 mm).

### 5.27 Saint Nazaire Bridge, France

This structure crossing the Loire River was constructed in 1975 and connects the port of Saint-Nazaire to the rural southern bank, Fig. 5.56. It has a center span of 1325.5 ft (404 m) with flanking spans of 518.4 ft (158 m) for a total length of 2362.3 ft (720 m). The inverted-V-shaped pylon sitting on concrete piers rises 429.8 ft (131 m) above low water and has a height of 223 ft (68 m) above the piers. Pylon height above deck is 220 ft (67.1 m) which produces a pylon-height-to-span ratio of 0.166. Stay arrangement is two sloping planes transversely with nine stays emanating in each plane from each side of a pylon in a radiating configuration in elevation (see Chapter 2).

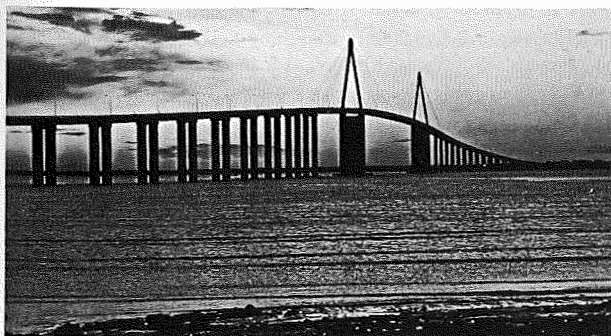


FIGURE 5.56 Saint Nazaire Bridge, France.

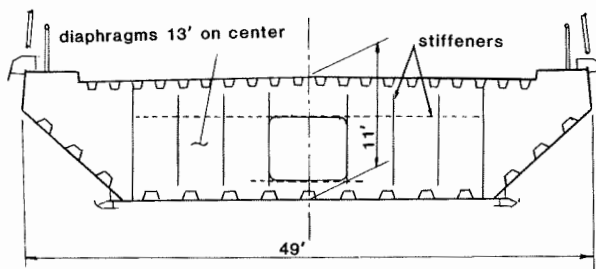


FIGURE 5.57 Saint Nazaire Bridge, cross section, from reference 35.

The 49-ft (15-m) wide box girder carries four traffic lanes and two service walkways, Fig. 5.57. Depth of the box is 11 ft (3.38 m) producing a depth-to-span ratio of 1/120. Stiffened steel plate diaphragms are spaced 13 ft (4 m) on center. The box is completely welded except for bolted field splices of the 52-ft 6-in. (16-m) segments in the center span. Side spans were fabricated as one unit, barged out to the site, and lifted up the piers by jacks. Aerodynamic studies indicated that despite the streamlined shape, at certain moderate wind velocities vortex vibrations could be induced. To minimize user discomfort, deflector plates were installed over partial lengths of the structure.<sup>35</sup>

Pylon legs are 170 ft (51.8 m) in length composed of a stiffened plate box section with dimensions of 8.2 by 6.6 ft (2.5 by 2.0 m). Diaphragms are located inside the box at 13 ft (4 m) on center. Above the two legs is a 47-ft (14.3-m) vertical section fitted with 3-in.- (80-mm) thick steel gusset plates to attach the stays. Similar lugs are at the box girder, inclined in line with the sloping stays.

Stays consist of locked-coil strands (see chapter 9) having a core of round wires with three or four layers of Z-shaped wires. The two outer layers are galvanized. These stays vary in diameter from  $2\frac{7}{8}$  to  $4\frac{1}{8}$  in. (72 to 105 mm) depending on their position in the structure.<sup>35</sup>

This bridge, when completed, held the record span of 1325.5 ft (404 m). Since then it has been or is being surpassed by the Nagoya Harbor Bridge in Japan with a span of 1328 ft (404.8 m); the Annacis Bridge, British Columbia, Canada with a span of 1444 ft (440 m); and the Hooghly River Bridge in India at a span of 1500 ft (457 m).

### References

1. Wenk, H., "Die Strömsundbrücke," *Der Stahlbau*, No. 4, April 1954.

2. Ernst, H. J., "Montage eines seilverspannten Balkens im Gross-Brückenbau," *Der Stahlbau*, No. 5, May 1956.
3. Wintergerst, L., "Nordbrücke Düsseldorf. III. Teil: Statik und Konstruktion der Strombrücke," *Der Stahlbau*, No. 6, June 1958.
4. Fischer, G., "The Severin Bridge at Cologne (Germany)," *Acier-Stahl-Steel* (English version), No. 3, March 1960.
5. Anon., "Norderelbe Bridge K6: A Welded Steel Motorway Bridge," *Acier-Stahl-Steel* (English version), No. 11, November 1963.
6. Havermann, H. K., "Die Brücke über die Norderelbe im Zuge der Bundesautobahn Südliche Umgehung Hamburg, Teil I: Ideen-und Bauwettbewerb," *Der Stahlbau*, No. 7, July 1963.
7. Aschenberg, H. and Freudenberg, G., "Die Brücke über die Norderelbe im Zuge der Bundesautobahn Südliche Umgehung Hamburg, Teil II: Konstruktion des Brückenüberbaus," *Der Stahlbau*, No. 8, August 1963.
8. Aschenberg, H. and Freudenberg, G., "Die Brücke über die Norderelbe im Zuge der Bundesautobahn Südliche Umgehung Hamburg, Teil III: Statische Berechnung des Brückenüberbaus," *Der Stahlbau*, No. 9, September 1963.
9. Havermann, H. K. and Freudenberg, G., "Die Brücke über die Norderelbe im Zuge der Bundesautobahn Südliche Umgehung Hamburg, Teil IV: Bauausführung der stähleren Überbauten," *Der Stahlbau*, No. 10, October 1963.
10. Schöttgen, J. and Wintergerst, L., "Die Strassenbrücke über den Rhein bei Maxau," *Der Stahlbau*, No. 1, January 1968.
11. Thul, H., "Cable-Stayed Bridges in Germany," *Proceedings of the Conference on Structural Steelwork held at the Institution of Civil Engineers*, September 26-28, 1966, The British Constructional Steelwork Association, Ltd., London.
12. Thul, H., "Stählerne Strassenbrücken in der Bundesrepublik," *Der Bauingenieur*, No. 5, May 1966.
13. Freudenberg, G., "Die Stahlhochstrasse über den neuen Hauptbahnhof in Ludwigshafen/ Rhein," *Der Stahlbau*, No. 9, September 1970.
14. Naruoka, M. and Sakamoto, T., "Cable-Stayed bridges in Japan," *Acier-Stahl-Steel* (English version), No. 10, October 1973.
15. Weisskopf, F., "World's Longest-Span Cable-Stayed Girder Bridge over the Rhine near Duisburg (Germany)," *Acier-Stahl-Steel* (English version), July-August 1972.
16. Schreier, G., "Bridge over the Rhine at Düsseldorf: Design, Calculation, Fabrication and Erection," *Acier-Stahl-Steel* (English version), May 1972.
17. Tamms and Beyer, "Kniebrücke Düsseldorf," Beton-Verlag GmbH, Düsseldorf, 1969.
18. Demers, J. G. and Simonsen, O. F., "Montreal Boasts Cable-Stayed Bridge," *Civil Engineering*, ASCE, August 1971.
19. Taylor, P. R. and Demers, J. G., "Design, Fabrication and Erection of the Papineau-Leblanc Bridge," Canadian Structural Engineering Conference, 1972, Canadian Steel Industries Construction Council, Toronto, Ontario, Canada.
20. Kondo, K., Komatsu, S., Inoue, H., and Matsukawa, A., "Design and Construction of Toyosato-Ohhashi Bridge," *Der Stahlbau*, No. 6, June 1972.
21. Naruoka, M. and Sakamoto, T., "Cable-Stayed Bridges in Japan," *Acier-Stahl-Steel* (English version), No. 10, October 1973.
22. Anon., "Erskine Bridge," *Building with Steel*, British Constructional Steelwork Association Limited, Vol. 5, No. 4, June 1969.
23. Kerensky, O. A., Henderson, W., and Brown, W. C., "The Erskine Bridge," *Structural Engineer*, Vol. 50, No. 4, April 1972.
24. Anon., "Opening Batman Bridge 18th May, 1968," Department of Public Works, Tasmania, Australia.
25. Payne, R. J., "The Structural Requirements of the Batman Bridge as They Affect Fabrication of the Steelwork," *Journal of the Institution of Engineers*, Australia, Vol. 39, No. 12, December 1967.
26. Tesár, A., "Das Projekt der neuen Strassen brücke über die Donau in Bratislava/CSSR," *Der Bauingenieur*, No. 6, June 1968.
27. Mohsen, H., "Trends in the Construction of Steel Highway Bridges," *Acier-Stahl-Steel* (English version), June 1974.
28. Borelly, W., "Nordbrücke Mannheim-Ludwigshafen," *der Bauingenieur*, No. 8, August 1972; No. 9, September 1972.
29. Volke, E., "Die Strombrücke im Zuge der Nordbrücke Mannheim-Ludwigshafen (Kurt-Schumacher-Brücke), Teil I: Konstruktion und Statik," *Der Stahlbau*, No. 4, April 1973; No. 5, May 1973.
30. Rademacher, C. H., "Die Strombrücke im Zuge der Nordbrücke Mannheim-Ludwigshafen (Kurt-Schumacher-Brücke), teil II: Werkstattfertigung und Montage," *Der Stahlbau*, No. 6, June 1973.
31. Firmage, D. A., "The Final Positioning of the Oberkassel Cable-Stayed Bridge," *Cable-Stayed Bridges*, Structural Engineering Series No. 4, June 1978, Bridge Division, Federal Highway Administration, Washington, D.C.
32. Bacher, A. E., Kirkland, D. E. and Klein, E. G., Jr., "The Sacramento River Bridge at Meridian—A Cable-Stayed Swing Bridge," *Cable-Stayed Bridges*, Structural Engineering Series No. 4, June 1978, Bridge Division, Federal Highway Administration, Washington, D.C.
33. Jarosz, E. S., "Luling Bridge," *Cable-Stayed Bridges*, Structural Engineering Series No. 4, Bridge Division, Federal Highway Administration, Washington, D.C.
34. "Report of Royal Commission into the Failure of West Gate Bridge," Government Printer, Melbourne, Australia, 1971.
35. Sanson, R., "Saint-Nazaire-Saint-Brevin Bridge over the Loire Estuary (France)," *Acier-Stahl-Steel*, (English version), May 1976.

# 6

## Composite Superstructures

|     |                                      |     |
|-----|--------------------------------------|-----|
| 6.1 | INTRODUCTION                         | 119 |
| 6.2 | SITKA HARBOR BRIDGE, U.S.A.          | 119 |
| 6.3 | EAST HUNTINGTON BRIDGE, U.S.A.       | 122 |
| 6.4 | SUNSHINE SKYWAY ALTERNATE, U.S.A.    | 122 |
| 6.5 | WEIRTON-STEUBENVILLE BRIDGE, U.S.A.  | 124 |
| 6.6 | QUINCY BRIDGE, U.S.A.                | 125 |
| 6.7 | JAMES RIVER BRIDGE ALTERNATE, U.S.A. | 128 |
|     | REFERENCES                           | 128 |

### 6.1 Introduction

When steel superstructures (see Section 2.6) are bid against concrete segmental construction they are usually not competitive, at least not in the United States. This noncompetitiveness results from the high fabrication costs of orthotropic deck designs. As a result, designers in the United States have turned to a "composite" design as opposed to a "pure" steel design to increase its competition with concrete designs.

In recent designs the composite concept has generally taken the form of concrete pylons with the superstructure deck composed of structural steel edge girders and transverse floor beams with either a cast-in-place or precast concrete deck. The precast deck concept is illustrated in Fig. 2.13(a). A variation of this design concept was proposed for the unsuccessful steel alternate of the Sunshine Skyway Bridge in Florida. This concept is also proposed for the steel alternate of the James River Bridge in Virginia. A similar design, except that the deck is cast-in-place as opposed to precast, is proposed for the Talmadge Memorial Bridge in Savannah, Georgia. A cast-in-place deck is being used for the Weirton-Steubenville Bridge in West Virginia. Another variation is that of the East Huntington Bridge in West Virginia, which has concrete edge girders with transverse structural steel floor beams, Fig. 2.13(b).

Economic results of recent bidding with the steel

alternate as a composite design are indicated in Table 3.3, of Chapter 3.

### 6.2 Sitka Harbor Bridge, U.S.A.

Sitka Harbor Bridge, Fig. 1.25, is the first vehicular cable-stayed bridge built in the United States. It is located in Sitka, Alaska and connects Baranof Island to Japonski Island. (Bridge-type selection was discussed in Section 3.4.1.) The bridge is a symmetric three-span structure and has a 450-ft (137-m) center span and 150-ft (45.7-m) side spans. There are three 125-ft (38-m) approach spans on the Sitka side and one approach span on the Japonski side of 125-ft (38-m). The total length of the structure is 1250-ft (381-m). Stay geometry in a direction transverse to the longitudinal axis of the bridge is two vertical planes. In elevation, only one stay emanates from each side of the pylon, Fig. 6.1. Fore stays are attached to the girder at the third points of the center span. Back stays anchor over approach piers. Each stay consists of three 3-in. (76-mm) in diameter galvanized bridge strands oriented in a vertical plane. The stays are anchored at the girder to 47-ft (14.3-m) long, 5-ft (1.5 m) diameter tubes that cantilever out from the longitudinal girders, Fig. 6.2. Connection of the cables to the girder and pylon is discussed in Chapter 10.

The cross section of the superstructure, Fig. 6.3, consists of two longitudinal box girders spaced 32-ft 6-in. (9.9-m) center to center. Box girders are 2-ft 6-in. (0.76-m) in width by 6-ft (1.8-m) in depth, providing a depth-to-main-span ratio of 1/75. The girders are constant depth throughout the 1250-ft (381-m) length. Box girders are framed by 3-ft (0.9-m) deep plate girder floor beams at 25-ft (7.6-m) on centers. Stringers spanning between floor beams are 18-in (457-mm) deep, wide flange sections, Fig. 6.4. Girders, floor



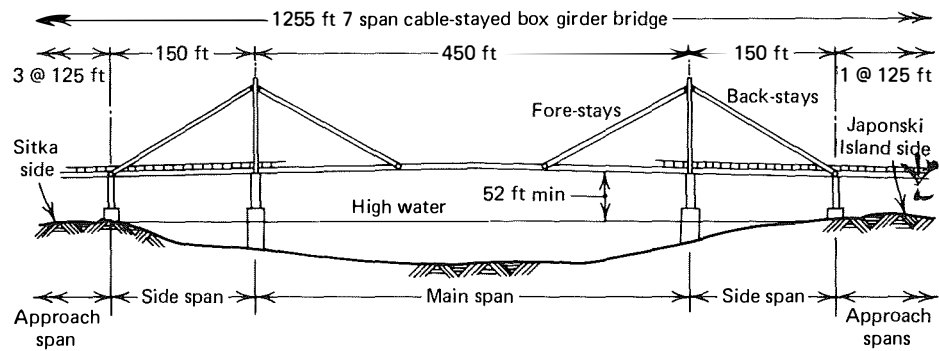


FIGURE 6.1 Sitka Harbor Bridge, elevation. (Courtesy of Civil Engineering-ASCE, from reference 1.)

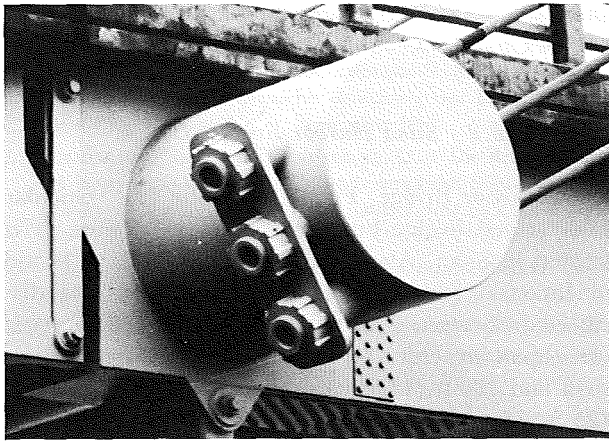


FIGURE 6.2 Sitka Harbor Bridge, cable anchorage at girder. (Courtesy of John H. Garren, FHWA Region 10.)

beams, and stringers are all composite with the  $6\frac{1}{2}$  in. (165-mm) deck slab.

Pylons are of the free standing cantilever type that rise 100-ft (30.5-m) above the pier, Figs. 1.25 and 6.3, and are fixed to the pier. They are single-cell rectangular boxes 3 by 4-ft (0.9 by 1.2-m) with the minor dimension parallel to the longitudinal axis of the bridge. Plate stiffeners, 6 by  $\frac{3}{8}$ -in. (152 by 9.5 mm) reinforce the plates of the box in the vertical and horizontal directions of the pylon.

Deck superstructure steel was erected by conventional methods, without falsework, from both sides until it reached the pylon piers. Pylons were then erected. Temporary guys or stays were utilized to support the deck as it cantilevered out into the main span. After the transverse anchorage beam was installed 150-ft. (45.7-m) from the pylons, and the permanent stays installed, the center girders were erected.<sup>1</sup>

Design plans and specifications indicated the tension and camber required at the completion of steel

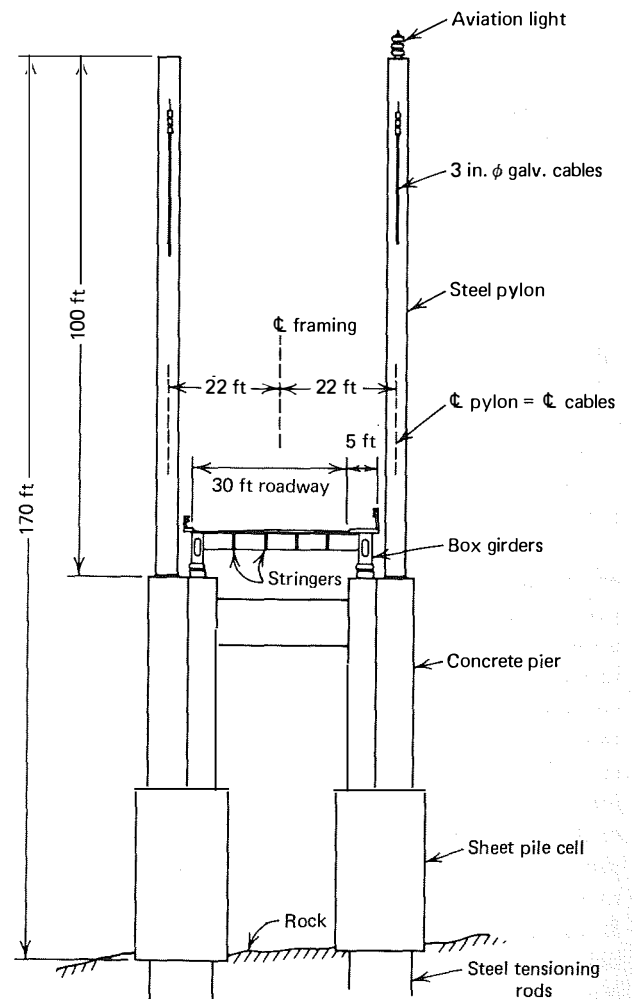
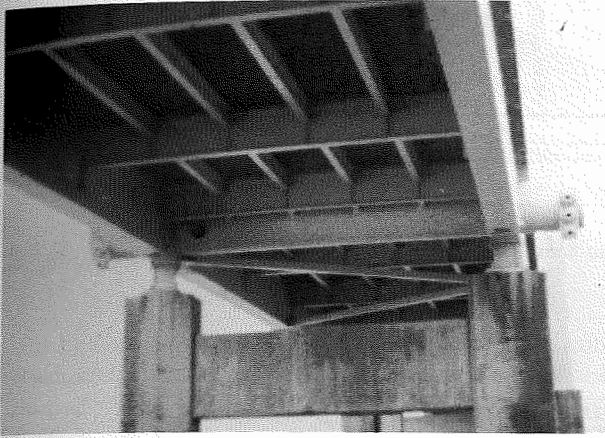


FIGURE 6.3 Sitka Harbor Bridge, cross section of bridge deck and supporting piers. (Courtesy of Civil Engineering ASCE, from reference 1.)



**FIGURE 6.4** Sitka Harbor Bridge, underside of deck showing framing. (Courtesy of John H. Garren, FHWA Region 10.)

superstructure erection and prior to the installation of concrete roadway, handrail, and other final attachments. Tensioning of each strand was accomplished with center-hole jacks using calibrated pressure gauges for determination of the force applied by the jacks. Upon completion of jacking, the steel box girders at midspan were approximately 27-in. (686-mm) above final design grade. After installation of the roadway deck and other miscellaneous items, the final roadway grade was within 0.03-ft (9-mm) of design grade.

The special provisions required balancing and adjustment of the design tension in the strands after application of full dead load by use of a calibrated jack. An allowable variation of 5% of mean stress in the strands was called for, with strand stress to be adjusted if necessary. The anticipated method of tension check would have required a reattachment of the center-hole tensioning jacks at 24 locations. This method was complicated by the fact that should it become necessary to adjust the tension in one strand the tension in the remaining strands would be affected.

A method of checking the tension by vibrating the strand and measuring the frequency of vibration was proposed by Albert W. O'Shea, Project Engineer for Associated Engineers and Contractors, Inc. This methodology had been previously used in Germany.<sup>2</sup>

Before measuring cable stresses by harmonics, a correlation test with a calibrated jack was required in order to confidently use the harmonic method. The strands can actually resist some bending and they are virtually fixed at the socketed ends. This results in a shortening in the effective length of the strands for use in the harmonics formula.

Upon assembly of the jacking apparatus to the

strand selected by the Alaska Department of Highways for the correlation test, pressure was applied until the spanner nut came free from the cable anchor assembly and the entire load of the cable was being carried by the jack. At this point the gauge pressure was read and the load on the cable computed. While pressure was maintained, frequency of vibration was determined by physically inducing an oscillation within the cable and visually counting these oscillations for 1 minute. Timing was done with a stop watch.

After the vibration frequency was determined the load was computed from the following formula:

$$P = \frac{4WL^2F^2}{g} \quad (6.1)$$

where  $P$  = Cable tension

$L$  = Cable length

$g$  = 32.2-ft/sec<sup>2</sup>

$F$  = Vibration frequency

$W$  = Unit weight of the cable

Frequency of vibration was determined at seven different gauge pressures. The load determination by the seven readings averaged 7.14 tons (6.48-mt) higher than the load determined by hydraulic jacking. This corresponds to an effective cable shortening of about 6-ft (1.8-m). On this basis, loading of the other bridge strands was determined by obtaining a frequency of vibration, calculating the loading from the formula, and reducing this figure by 7 tons (6.35-mt). All the strands on this structure were checked for actual tension in this manner and found to be balanced within the 5% tolerance. The total check was accomplished in less than a day.

The harmonic method of determining cable stress can be employed at any time with no more equipment than a stop watch. It therefore becomes an advantageous method that can be easily implemented; for example,

1. If for some reason a strand or strands have to be replaced, tensions can be easily checked.
2. Changes in strand tension can be easily determined if the bridge deck is resurfaced or other modifications are made.
3. It is easily implemented by bridge inspectors on routine inspection.
4. In the event of damage to a strand or strands, the stresses in the remaining strands can be readily determined.

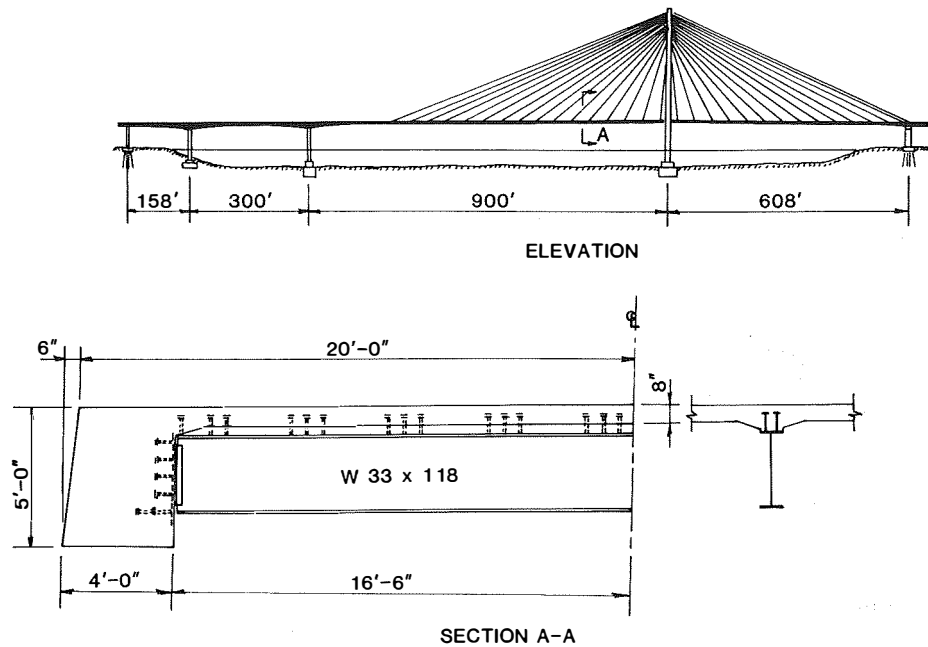


FIGURE 6.5 East Huntington Bridge, elevation and section.

### 6.3 East Huntington Bridge, U.S.A.

This bridge crosses the Ohio River at East Huntington, West Virginia, Fig. 1.34. It is a single-pylon asymmetrical structure with spans of 158, 300, 900, and 608-ft (48.16, 91.44, 274.32, and 185.32-m), Fig. 6.5. The structure was initially intended to be a toll facility and was designed with a structural steel pylon and a structural steel orthotropic box girder. The first stage of construction, consisting of the two river piers, was completed when Federal funds became available. However, Federal Highway Administration policy required that a concrete alternative be designed and offered for competitive bidding. This placed a constraint on the concrete design because the existing river piers, designed for the lighter structural steel alternate, had to be retained. Thus, the design of the concrete alternative had to transmit forces to the existing piers without overstressing them or the foundations.

In order to comply with this restraint, the consultants for the concrete alternate, Arvid Grant and Associates, Inc. and Leonhardt and Andra, utilized high-strength concrete, 8000 psi (55 MPa), in the girder to reduce its size and thus its weight. Further, 33-in. (838-mm) deep transverse floor beams composite with the deck were used to reduce the dead weight, Fig. 6.5.

Cable stays are in two sloping planes transversely and in a harp configuration when viewed in elevation. There are 15 stays in each plane in the anchor span

and 16 stays in each plane in the fore span. Height of the pylon above the deck is 179.4-ft (54.7-m), producing a ratio of height of pylon to major span of 0.2. Depth of the girder cross section is 5-ft (1.52-m) resulting in a span-to-depth ratio of 180.

Typical length of precast segments in the stayed portion of the structure is 44-ft 10-in. (13.7-m), with floor beams spaced at 9-ft (2.74-m) on center. The edge girders, steel floor beams, and deck slab are constructed monolithically, therefore, the steel floor beams do not have to support the weight of deck forms and fresh concrete as in conventional construction.

Cable stays are anchored at both the pylon and deck. They consist of parallel  $\frac{1}{4}$ -in. (6.35-mm) diameter wires varying in number from 85 to 307 depending on their position in the structure. Anchorages are of the HiAm type (see Chapter 10).

This alternate was designed in eight months. The low bid, in May 1981, was \$9.76 million lower than the competing steel alternate and was \$3.42 million lower than that estimated by the designers, (see Table 3.3, Chapter 3).

### 6.4 Sunshine Skyway Alternate, U.S.A.

The successful concrete alternate for this structure was previously discussed in Section 4.10. The composite steel alternate was bid 2.5% higher than the concrete alternative, which indicates its competitiveness. Design

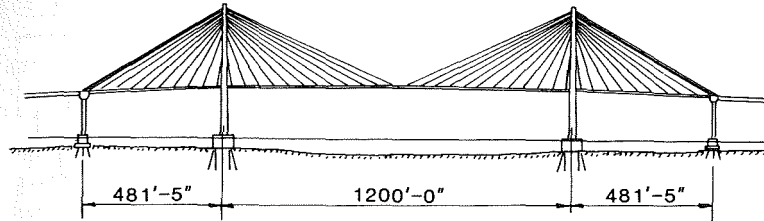


FIGURE 6.6 Sunshine Skyway Steel Alternate, layout.

was by Greiner Engineering Sciences, Inc. and Leonhardt and Andra. Span layout for the cable-stayed portion of the composite steel alternate is 481-ft 5-in., 1200-ft, and 481-ft 5-in. (146.74, 365.76, and 146.74-m), Fig. 6.6. The pylon is of a diamond configuration, Fig. 6.7. Transversely the cable configuration consists of two inclined planes; in elevation the harp stay configuration was selected. The pylon height above the deck is 275-ft. 9-in. (84-m), producing a height-to-span ratio of 0.23. Depth of the superstructure is 7-ft 8-in. (2.3-m) resulting in a span-to-depth ratio of 156.

Composition of the deck superstructure is similar

to that illustrated in Fig. 2.13(a) except that stay anchorages are located on the inside web face of the edge girders. Edge girders are spaced 90-ft 4-in. (27.53-m) on center and are of an unsymmetrical cross section, Fig. 6.8. Floor beams are spaced at 12-ft 6-in. (3.8-m) centers and cable stay anchorages are spaced at the edge girder from a minimum of 48-ft 1-in. (14.7-m) at the pylon to a maximum of approximately 50-ft 9-in. (15.5-m) near mid-span and at back stays. To minimize secondary stresses produced by the eccentricity of stay forces with respect to the centerline of the edge girder, the anchorages were located as closely as possible to a floor beam,<sup>3</sup> Fig. 6.8.

Plate girder floor beams have a horizontal bottom flange with a sloping top flange corresponding to the cross slope of the deck, Fig. 6.8. Depth at the center is 5-ft 9-in. (1.75-m). To simplify fabrication a  $\frac{9}{16}$ -in. (14-mm) thick web is used to eliminate the necessity of transverse stiffeners.

Edge girders and floor beams are shop welded with all field splices and connections bolted. Composite action with precast deck slabs is achieved with  $\frac{7}{8}$ -in. (22-mm) diameter shear studs.

Precast deck slab units are 48-ft 6-in. (14.78-m) long by 11-ft 4-in. (3.45-m) wide and 9-in. (229-mm) thick. They rest on a thin layer of grout with shear studs protruding into the blockouts, Fig. 6.9. The weight of each precast deck slab unit is approximately 33 tons (29.9-mt). Longitudinal and transverse joints, Fig. 2.13a, have sufficient width to lap the deck reinforcement, and the slab faces have half-sphere keys to provide a shear transfer. Longitudinal joints are continuous for the structure length. Transverse joints are staggered across the bridge width and located at points of contraflexure between the supporting floor beams. All deck slab reinforcement is epoxy coated.

Stay cables were detailed as  $\frac{1}{4}$ -in. (6-mm) diameter parallel wires encased in polyethylene pipe and grouted. Anchorages were of the HiAm type. The contractor was given the option of parallel seven-wire strand and other anchorage and corrosion protection methods.

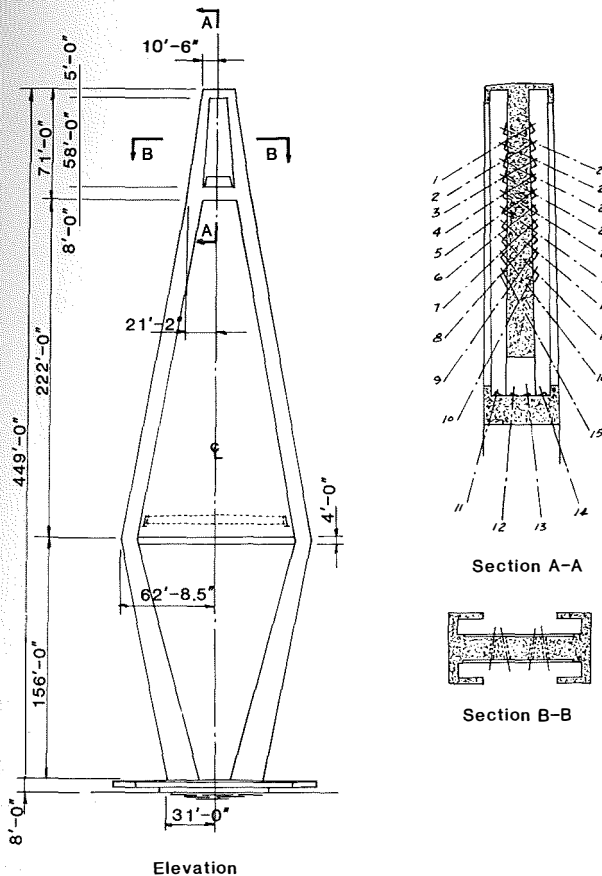


FIGURE 6.7 Sunshine Skyway Steel Alternate, pylon.

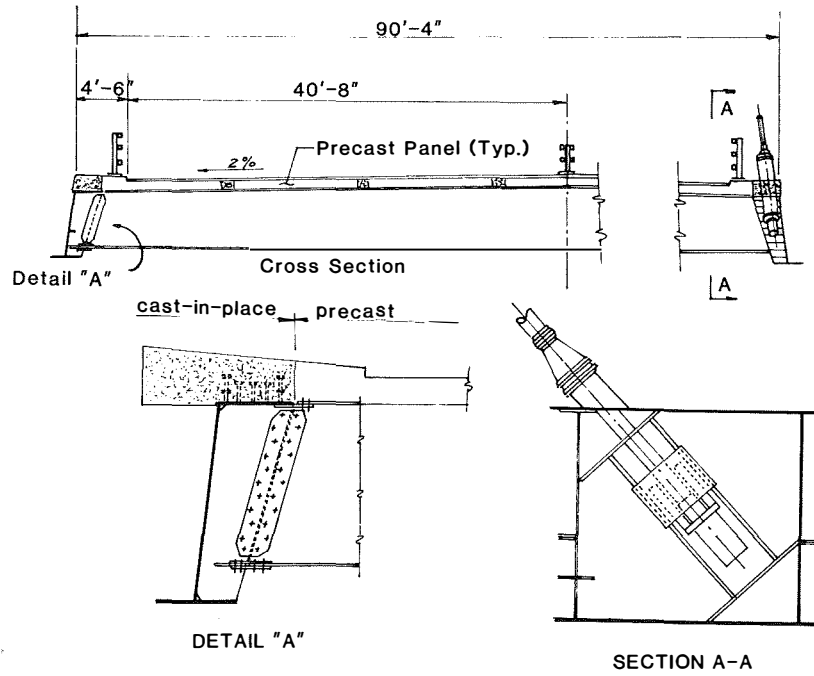


FIGURE 6.8 Sunshine Skyway Steel Alternate, superstructure cross section and details.

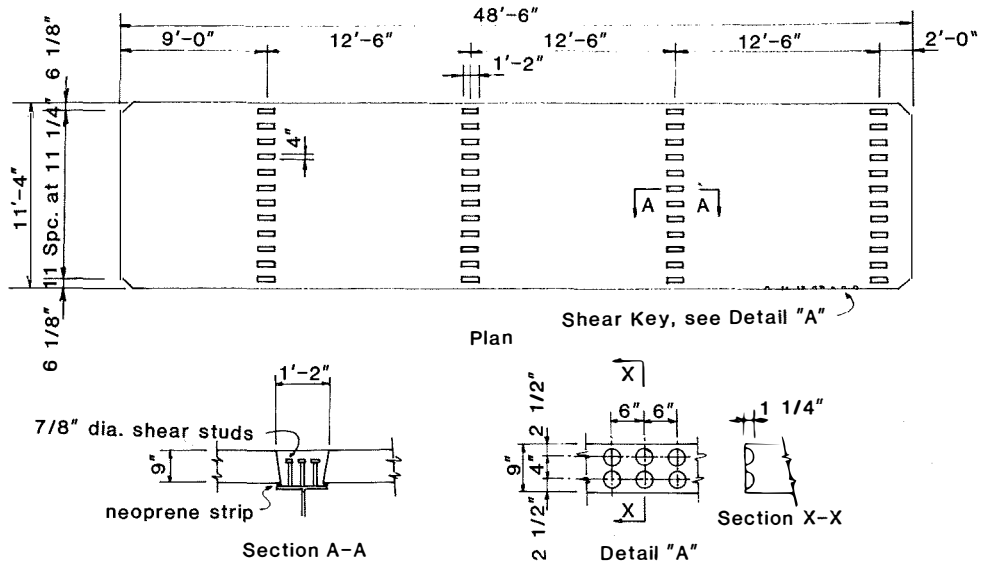


FIGURE 6.9 Sunshine Skyway Steel Alternate, details of precast roadway plank.

6.5 Weirton-Steubenville Bridge, U.S.A.

The Weirton-Steubenville Bridge in West Virginia, Fig. 1.35, currently (1985) under construction is another composite structure. It differs in concept from the Sunshine Skyway Bridge steel alternate because the roadway deck is of cast-in-place conventionally rein-

forced concrete as opposed to a prestressed, precast deck.

It is an asymmetric structure with a major span of 820-ft (250-m) and an anchor span of 687-ft 11-in. (210-m), Fig. 6.10. Girder depth is approximately 8-ft 8-in. (2.64-m) and pylon height above the roadway is approximately 349-ft (106.4-m), resulting in a ma-

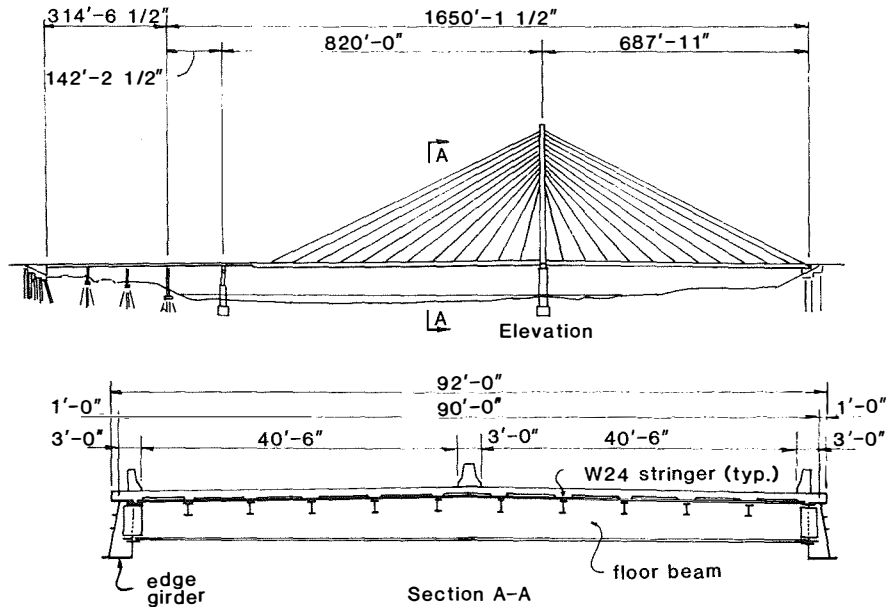


FIGURE 6.10 Weirton-Stuebenville Bridge, elevation and section.

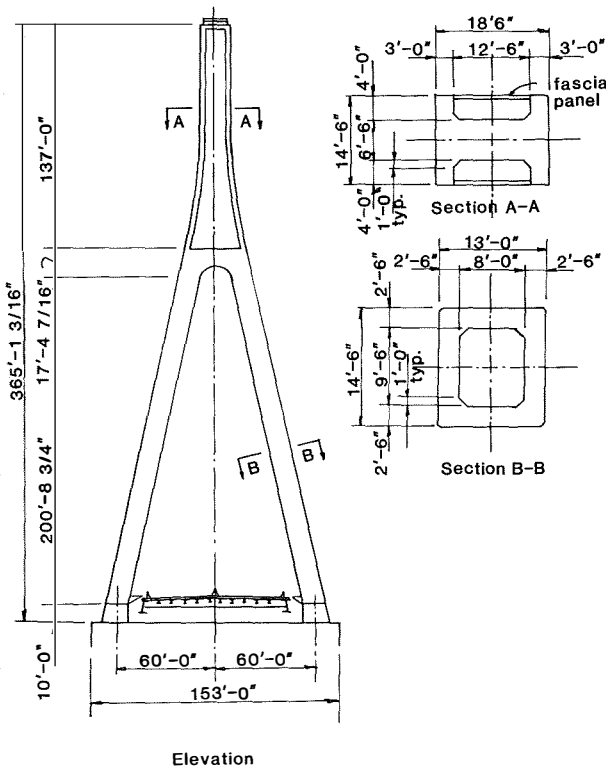


FIGURE 6.11 Weirton-Stuebenville Bridge, pylon.

gor-span-to-depth ratio of 95 and a pylon-height-to-span ratio of 0.43. Transverse stay arrangement is two sloping planes, and a fan arrangement is used in elevation. The pylon is an inverted-Y, Fig. 6.11.

The transverse superstructure girder dimension is 92-ft (28-m) out to out of the concrete deck. The deck has a thickness of 8 1/2-in. (216 mm). Floor beams are spaced at 20-ft (6.1-m) and are 24-in. (610-mm) deep; stringers are spaced at 8-ft (2.4-m), Fig. 6.10. Stay connection at the edge girder, Fig. 6.12, is similar to that of the Sunshine Skyway, Fig. 6.8, except that the anchorage is located on the outside face of the girder as opposed to the inside face. Anchorage spacing along the edge girder is 60-ft (18.3-m). The designer of this structure is Michael Baker, Jr., Inc.

### 6.6 Quincy Bridge, U.S.A.

This structure carries U.S. Route 24 over the Mississippi River at Quincy, Illinois at the boundary between the states of Illinois and Missouri. The symmetrical three-span structure has a channel span of 900-ft (274-m) and side spans of 440-ft (134-m), Fig. 6.13, and was designed by Modjeski and Masters.

Pylon configuration is indicated in Figs. 1.37 and 6.14. Height of pylon above the roadway is 181-ft 10-in. (55.4-m), producing a pylon-height-to-span ratio of 0.2. Transversely, the stay cables are in two vertical planes; in elevation, a fan configuration of stays is used. There are seven stays on each side of the pylon for total of 28 stays.

Superstructure edge girders have a constant web depth of 72-in. (1829-mm) and are 43-ft 6-in. (13.25-

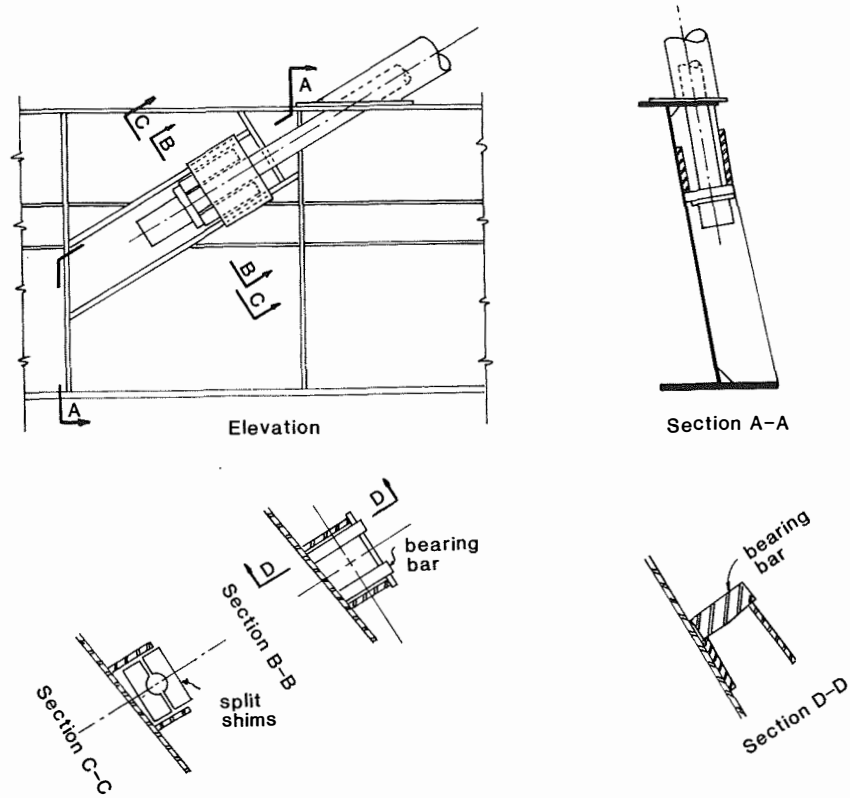


FIGURE 6.12 Weirton-Steubenville Bridge, stay anchorage detail at deck.

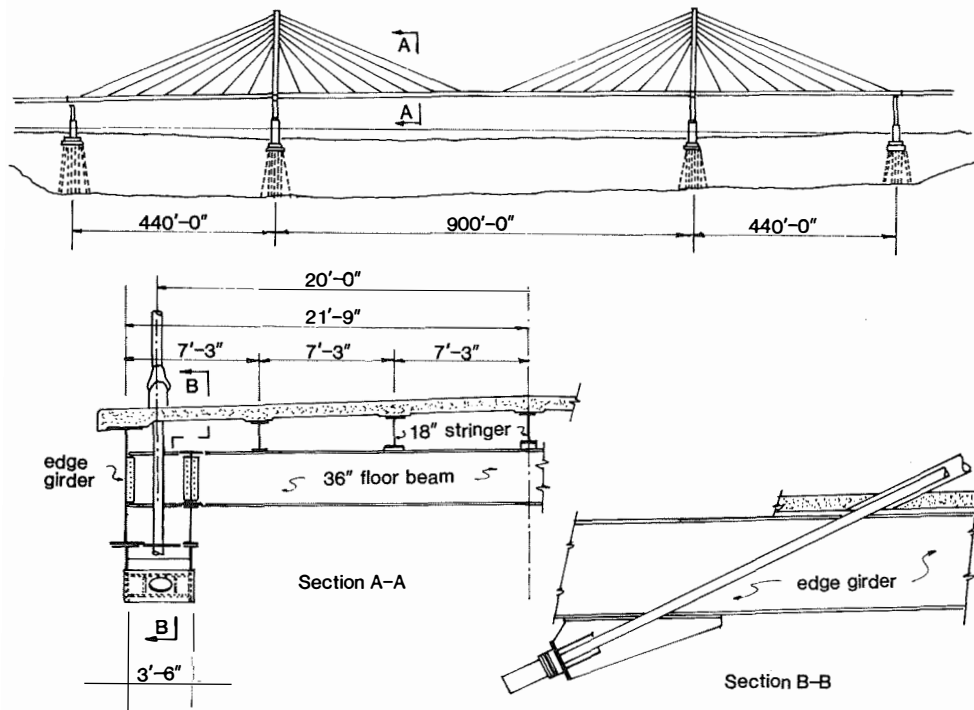


FIGURE 6.13 Quincy Bridge, elevation and section.

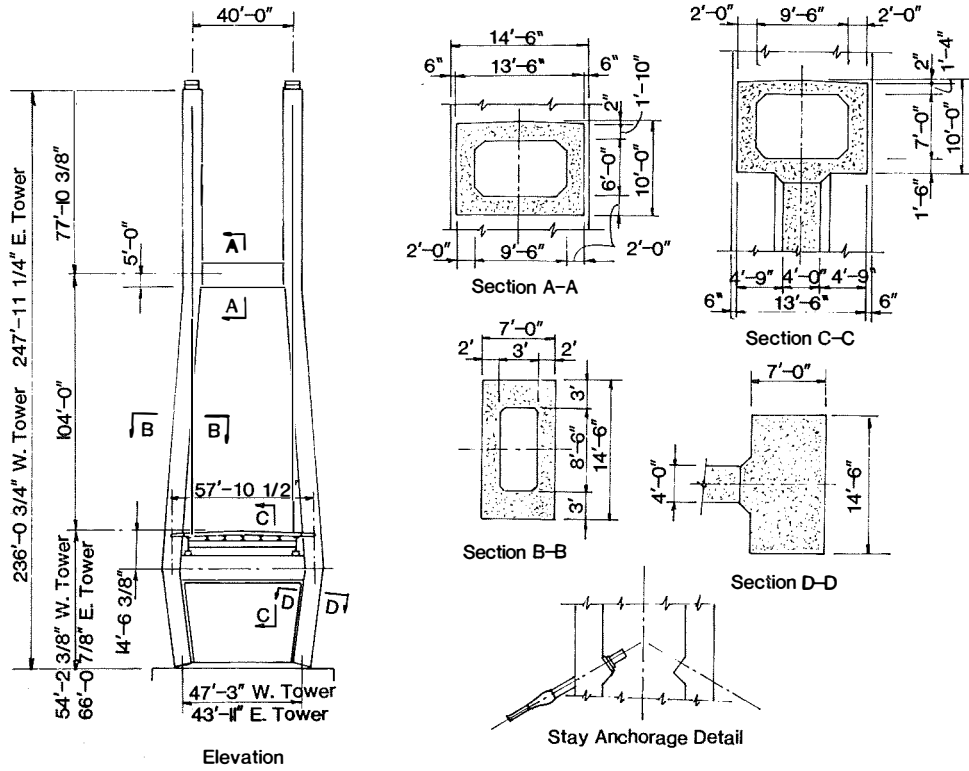


FIGURE 6.14 Quincy Bridge, pylon elevation and sections.

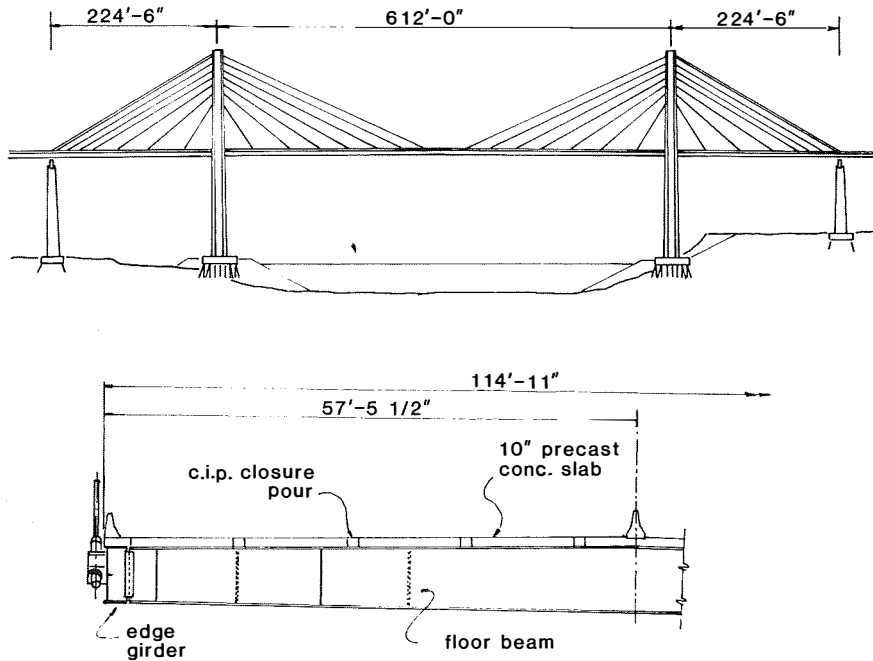


FIGURE 6.15 James River Bridge, elevation and section.



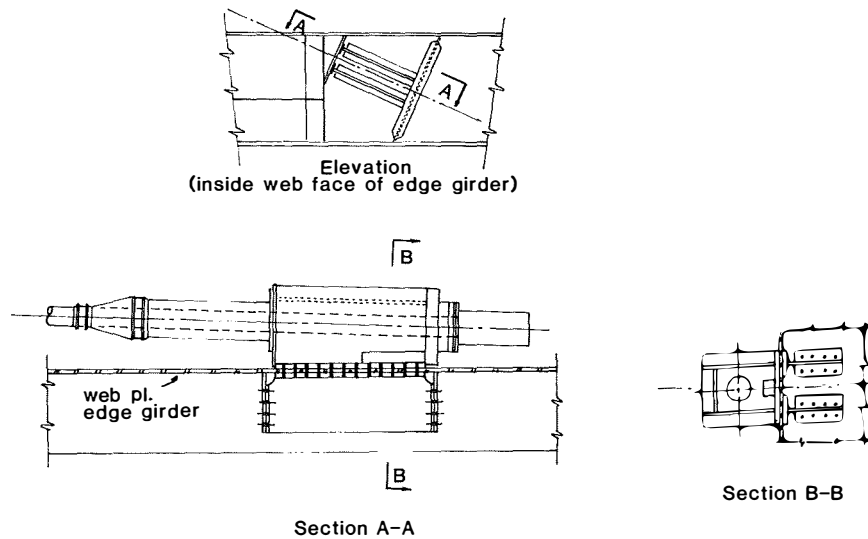


FIGURE 6.16 James River Bridge, cable-stay attachment to edge girder.

m) on center, Fig. 6.13. Total depth of superstructure at the edge girder is about 7-ft 4-in. (2.2-m), which is a span-to-depth ratio of 123. Spacing of 36-in. (914-mm) deep floor beams varies from 17 to 24-ft (5.2 to 7.3-m) depending on the location in the structure. Stringers are 18-in. (457-mm) deep and are spaced 7-ft 3-in. (2.2-m) on centers. Connections of the cable stays at the edge girder and pylon are shown in Figs. 6.13 and 6.14, respectively.

The deck consists of full roadway width, 9-in. (228-mm) thick precast planks that are made composite with the edge girder and the stringers. They are conventionally reinforced in the transverse direction of the bridge and posttensioned together in the longitudinal direction of the bridge. Portions of the deck at the anchor piers and at the pylons are cast-in-place.

### 6.7 James River Bridge Alternate, U.S.A.

The unsuccessful steel alternate for the I-295 James River Bridge near Richmond, Virginia contemplated a 1061-ft (323-m) three-span cable-stayed unit with a center span of 612-ft (186.5-m) and flanking spans of 224-ft 6-in. (68.4-m), Fig. 6.15. Cable-stay geometry consists of two vertical planes transversely and of the fan configuration in elevation. A simple H-shaped por-

tal frame is used for the pylons, with the cross strut located below the roadway superstructure.

Edge girders of the superstructure are a built-up C-shape with a constant web depth of 68-in. (1727-mm). Floor beams are spaced 12-ft. (3.66-m) on centers and are of variable depth, 68-in. (1727-mm) at the edge girder to 80 $\frac{3}{4}$ -in. (2050-mm) at the centerline, Fig. 6.15 and 2.13(a). Cable-stay anchorages are bracketed on the outside web of the edge girder, Fig. 6.16 and 2.13(a). Precast deck slab units are 10-in. (254-mm) thick and are made composite with the edge girder and floor beams by shear studs placed in preformed pockets.

The designer for this project was Greiner Engineering Sciences, Inc.

### References

1. Gute, W. L., "First Vehicular Cable-Stayed Bridge in the U.S.," *Civil Engineering*, ASCE, November 1973.
2. Ernst, H. J., "Montage eines seilverspannten Balkens im Grossbrückenbau," *Der Stahlbau*, No. 5, May 1956.
3. Saul, R., Svensson, H., Andra, H. P., and Selchow, H. J., "Die Sunshine-Skyway Brücke in Florida, U.S.A.—Entwurf einer Schrägkabelbrücke mit Verbundüberbau," *Bautechnik*, Heft 7, July 1984 and Heft 9, September 1984.

# 7

## *Pedestrian Bridges*

- 7.1 INTRODUCTION 129
- 7.2 FOOTBRIDGE AT THE WEST GERMAN PAVILION, BRUSSELS EXHIBITION, 1958 129
- 7.3 VOLTA-STEG BRIDGE AT STUTTGART-MÜNSTER 130
- 7.4 BRIDGE OVER THE SCHILLERSTRASSE, STUTTGART 131
- 7.5 THE GLACISCHAUSSEE BRIDGE, HAMBURG 131
- 7.6 LODEMANN BRIDGE, HANOVER, WEST GERMANY 132
- 7.7 RAXSTRASSE FOOTBRIDGE, AUSTRIA 132
- 7.8 PONT DE LA BOURSE, LE HAVRE, FRANCE 133
- 7.9 CANAL DU CENTRE, OBOURG, BELGIUM 134
- 7.10 RIVER BARWON FOOTBRIDGE, AUSTRALIA 135
- 7.11 MOUNT STREET FOOTBRIDGE, AUSTRALIA 136
- 7.12 MENOMONEE FALLS PEDESTRIAN BRIDGE, U.S.A. 136
- 7.13 PRINCE'S ISLAND PEDESTRIAN BRIDGE, CANADA 139
- 7.14 FOOTBRIDGE LIEBRÜTI, KAISERAUGST, SWITZERLAND 139
- 7.15 HORIKOSHI BRIDGE, HACHIOJI CITY, JAPAN 140
- 7.16 FOOTBRIDGE OVER MOTORWAY M-30, MADRID, SPAIN 141
- REFERENCES 142

### *7.1 Introduction*

Previous chapters have emphasized vehicular cable-stayed bridges. In this chapter we present a few examples of cable-stayed pedestrian bridges. Some of these structures provide architecturally attractive and exciting designs. As one might suspect, a number of pedestrian bridges have been built in Germany and in the natural course of evolution have extended to a number of other countries.

There are advantages in reduced superstructure depth, simplicity of erection, and aesthetics. The lightness of appearance that is obtainable will become ap-

parent. When conditions are suitable, and they generally are, most pedestrian bridges have been built as asymmetric structures with only one pylon. Superstructures can be quite conventional and, if cable-stayed, can be designed as continuous beams on elastic supports.

### *7.2 Footbridge at the West German Pavilion, Brussels Exhibition, 1958*

This bridge, Figs. 7.1 and 7.2, was the main feature of the West German Pavilion at the Brussels Exhibition in 1958. After the exhibition closed it was dismantled and re-erected over a roadway near Duisburg, Fig. 7.3

The West German Pavilion Bridge is unusual in that it represents a laterally displaced, single vertical plane, transverse stay geometry (see Fig. 2.4). The offset torsionally resistant box girder consists of four  $\frac{13}{16}$ -in. (20-mm) thick plates, has a constant depth of 4 ft 4 in. (1.3 m), and a width that varies from 13 to 28 in. (330 to 711 mm). It has a short span of 60 ft (18 m), which is anchored to the abutment and cantilevers out from the pylon 120 ft (36 m). A 10-ft (3-m) wide timber deck is supported on 11-ft (3.3-m) centers by 10-in. (255-mm) deep transverse wide flange beams which cantilever out 13 ft (4 m) from the box girder. A streamlined multicell steel pylon, approximately 165 ft (50 m) in height (Fig. 7.4), supports the superstructure. The torsion box girder is supported from the pylon by six stays, approximately 2 in. (50 mm) in diameter, in a harp configuration, Fig. 7.2.

The girder and pylon were originally painted white. When the structure was re-erected at Duisburg, the girder and pylon were repainted yellow to contrast with the green foliage.<sup>1,2,3</sup>

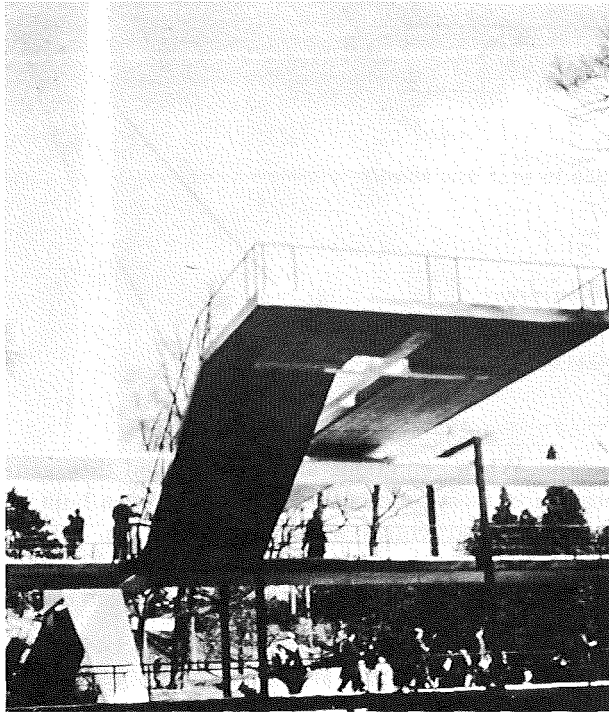


**FIGURE 7.1** German Pavilion, Brussels, 1958. (Courtesy of the British Constructional Steelwork Association, Ltd.)

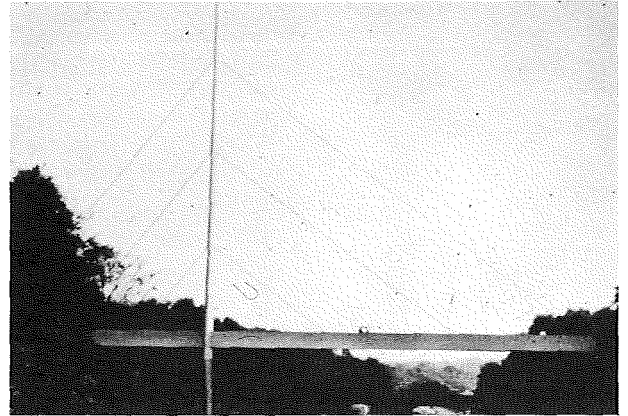


**FIGURE 7.3** Duisburg Pedestrian Bridge. (Courtesy of the British Constructional Steelwork Association, Ltd., from reference 1.)

### 7.3 Volta-Steg Bridge at Stuttgart-Münster

The asymmetric Volta-Steg Bridge, Fig. 7.5, spans the Neckar River at Stuttgart with a major span of 246 ft (75 m), and a minor span of 69 ft (21 m). The pylon height is approximately 40 ft (12 m) above the pier. Superstructure width is  $11\frac{1}{2}$  ft (3.5 m). The two prin-

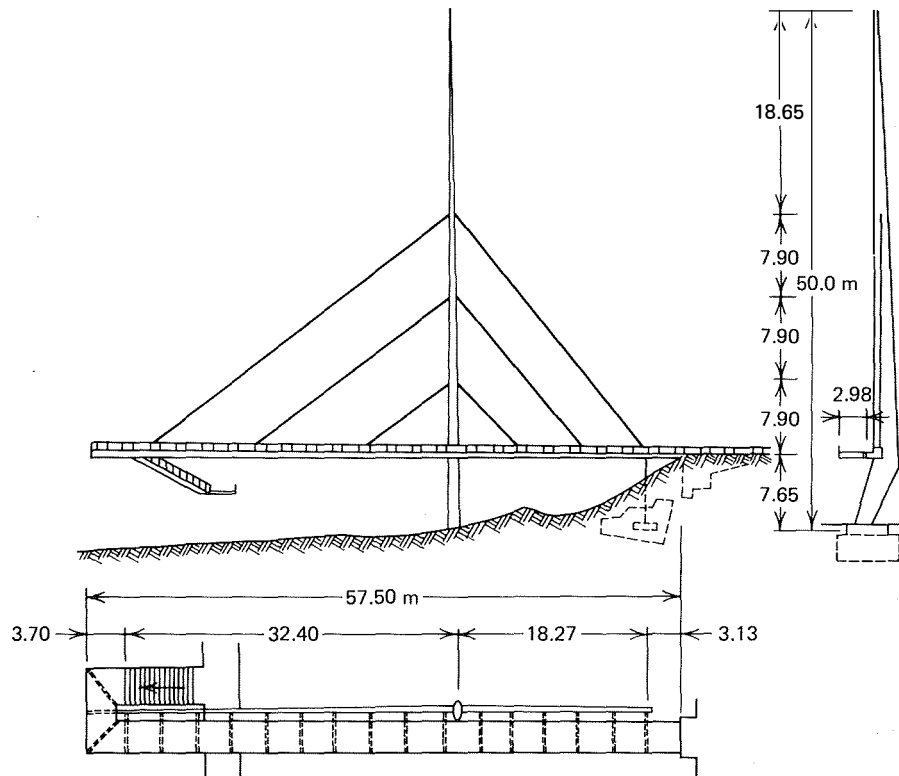


**FIGURE 7.2** Footbridge, German Pavilion, Brussels, 1958. (Courtesy of The British Constructional Steelwork Association, Ltd.)

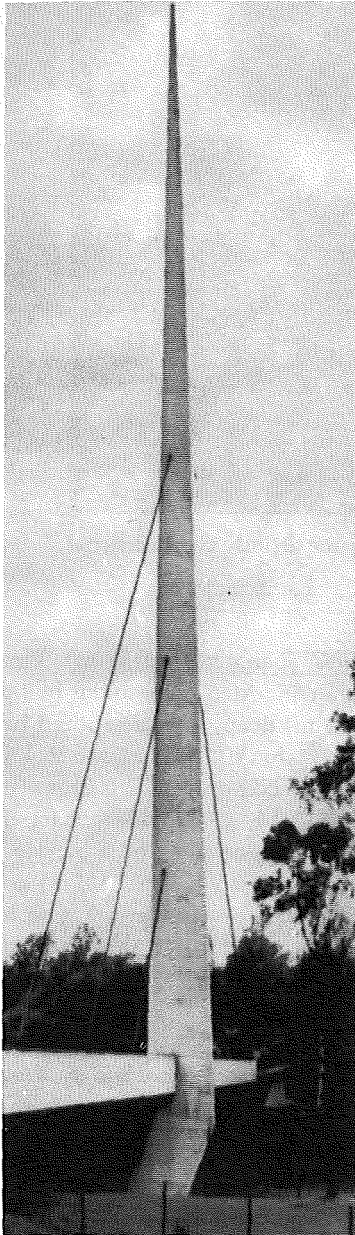


**FIGURE 7.4** Duisburg pedestrian bridge, view of pylon. (Courtesy of Beratungsstelle für Stahlverwendung, from reference 3.)

cipal girders have a depth of 3 ft 9 in. (1.14 m), and the deck is of orthotropic construction with an approximately  $\frac{3}{4}$ -in. (20-mm) asphalt surface. Total steel weight is 146.6 tons (133 mt).<sup>1,3</sup>

#### 7.4 Bridge over the Schillerstrasse, Stuttgart

A rather spectacular structure, also located in Stuttgart, is the Schillerstrasse pedestrian bridge, Fig. 7.6.

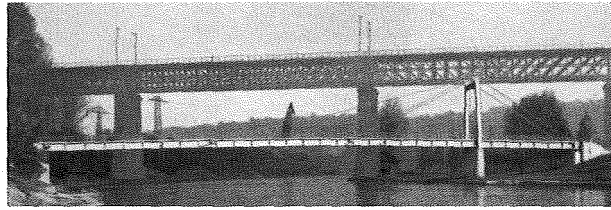


**FIGURE 7.5** Volta-Steg Footbridge. (Courtesy of Beratungsstelle für Stahlverwendung, from reference 3.)

This structure was sited in an ancient royal park and aesthetic considerations were very important. A slender superstructure was dictated with gently sloping approaches rather than staircases. As can be seen in Fig. 7.7, the structure forks at the pylon, providing two approaches on that side; the other side has a single straight approach. As seen in elevation, the total length of the structure from abutment to abutment is 304 ft (92.6 m). The major span is 225 ft (68.6 m) and the minor span is 79 ft (24 m), measured from the pylon. Cable geometry is a double sloping plane with three fore stays and two back stays in each plane. The stays all converge at the top of the tower.

The superstructure in the long, straight portion is a very flat box girder, 18 ft (5.5 m) in width and 20 in. (500 mm) in depth, Fig. 7.8. Top and bottom flange plates are longitudinally stiffened by trapezoidal stiffeners. The thickness of the top and bottom flange plates are  $\frac{5}{16}$  in. (8 mm) and  $\frac{1}{4}$  in. (6 mm), respectively. Web plates are  $\frac{5}{16}$  in. (8 mm) in thickness. Transverse diaphragms are provided at 7-ft 10 $\frac{1}{2}$ -in. (2400 mm) intervals, and consist of trusses made of approximately 1-in. (25-mm) diameter bars forming the diagonals. The transverse diaphragm is very similar in appearance to the conventional bar joist used in floor construction of buildings, Fig. 7.8.

The slender pylon has a height of 78 ft 9 in. (24 m). In cross section it is a hollow octagonal steel section tapering from 4 ft (1.2 m) wide at the base to 1 ft 10 in. (0.56 m) wide at the top, Fig. 7.7. Plate thickness varies from 1 in. (25 mm) at the top to  $\frac{13}{16}$  in. (20 mm) at the bottom. The stays and their connection details are discussed in Section 10.14.<sup>1,3,4</sup>

#### 7.5 The Glacischaussee Bridge, Hamburg

The Glacischaussee Bridge is a single vertical plane structure, Fig. 7.9, with the fore stays in a fan configuration and the back stays in a star configuration. The 178-ft (54-m) long steel superstructure is a trapezoidal box with side cantilevers, Fig. 7.10. The 93-ft 10-in.

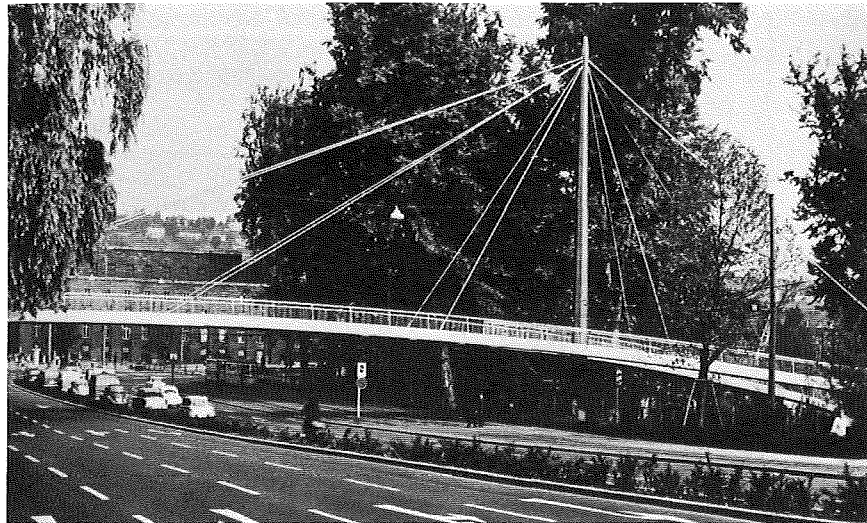


**FIGURE 7.6** Schillerstrasse Footbridge. (Courtesy of the British Constructional Steelwork Association, Ltd.)

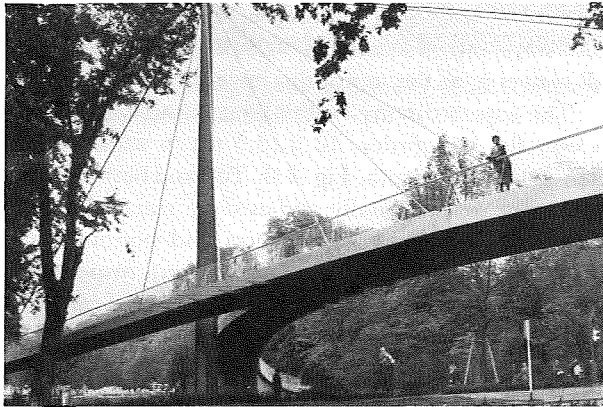


**FIGURE 7.7** Schillerstrasse Footbridge. (Courtesy of Beratungsstelle für Stahlverwendung, from reference 3.)

(28.6-m) high triangular cross section pylon pierces the deck as indicated in Fig. 7.10. The girder was fabricated in five longitudinal sections and field bolted. It took only two hours to erect the girder using mobile cranes. Views of the stay anchorage are shown in Figs. 7.11 and 7.12<sup>1,3,5,6</sup>

#### 7.6 Lodemann Bridge, Hanover, West Germany

The Lodemann Bridge has an inverted-Y pylon, Fig. 7.13, with a single vertical cable plane that radiates from the peak of the A-frame. It is a single-pylon asymmetric structure with a major span of 223 ft (68

m) and a minor span of 187 ft (57 m). The superstructure is a center inverted trapezoidal box girder about 4 ft 8 in. (1.4 m) deep, with a top and bottom flange width of 2 ft 7½ in. (0.8 m) and 4 ft 4 in. (1.3 m), respectively. The box projects 2 ft 7½ in. (0.8 m) above the deck, Fig. 7.14, to provide a barrier between a pedestrian walk on one side and a bicycle track on the other, each of which is 9 ft 4 in. (2.8 m) in width. Steel members cantilever out from each side of the center girder to support a 4¼-in. (120-mm) thick reinforced concrete deck slab.<sup>3,6</sup>

#### 7.7 Raxstrasse Footbridge, Austria

This asymmetric structure has a 111-ft 6-in. (34-m) high inclined A-frame pylon, Fig. 7.15. The superstructure has a clear span of 177 ft (54 m) between abutments and is free of the pylon. It has a clearance above the roadway of approximately 16 ft 4 in. (5 m). Walkway width is 13 ft (4 m).

The superstructure is an orthotropic deck with two longitudinal inverted-T plate girders spaced at 9 ft 10 in. (3 m), Fig. 7.16. The deck plate is about ⅝-in. (8-mm) thick. Longitudinal stiffeners are 4¼-in. by ⅝-in. (120 by 8 mm) flat plates at 19¾ in. (500 mm). Transverse stiffeners are 9⅝ in. by ⅝ in. (250 by 8 mm) plates at 8 ft 10⅝ in. (2.7 m). Longitudinal edge stiffeners are 11⅓ in. by ⅝ in. (300 by 8 mm). Every fourth transverse stiffener is cantilevered out to pick up a cable-stay anchorage, Fig. 7.17. These stiffeners

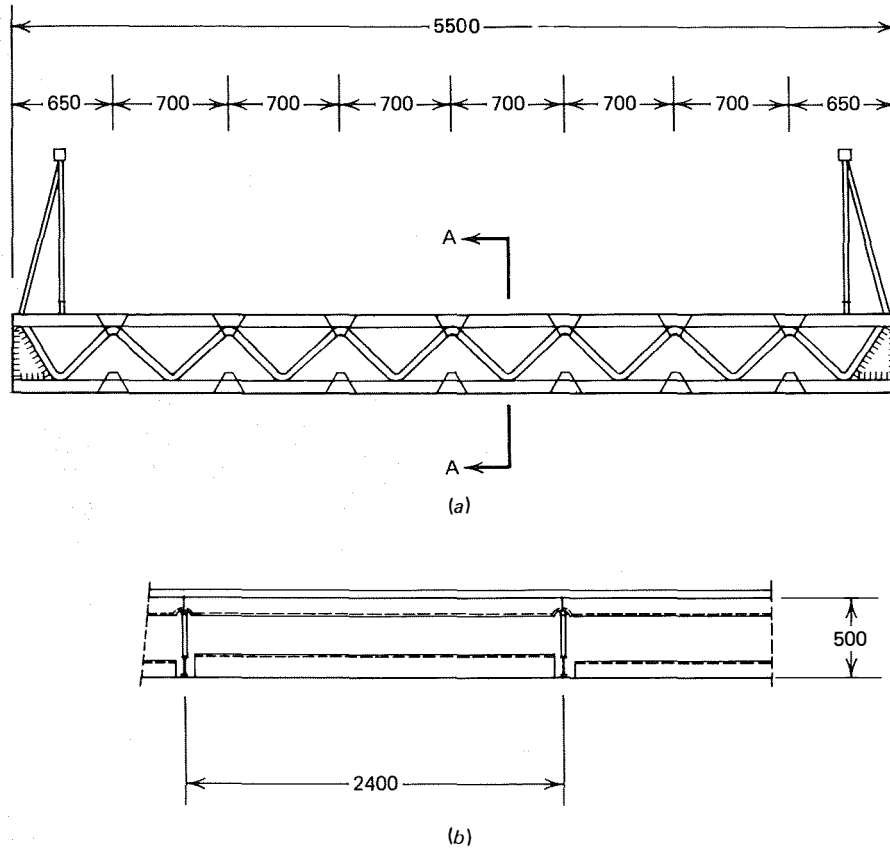


**FIGURE 7.8** Schillerstrasse Footbridge: (a) deck cross section and (b) section A-A. (Courtesy of the British Constructional Steelwork Association, Ltd., from reference 1), all dimensions in millimeters.

are  $17\frac{23}{32}$  in. by  $\frac{5}{16}$  in. (450 by 8 mm) and are inclined to match the inclination of the stays.

Cable stays support the superstructure at the fifth points and are  $\frac{29}{32}$  and  $1\frac{1}{16}$  in. (23 and 27 mm) in diameter, fixed at the pylon anchorage, and adjustable at the

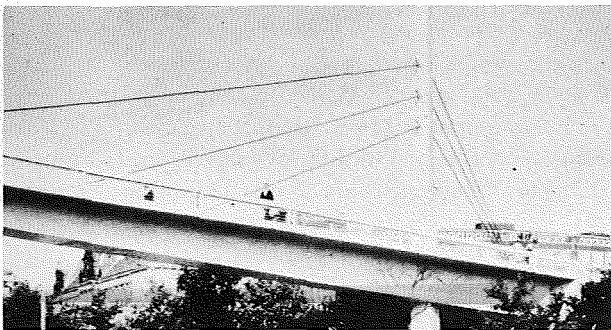


**FIGURE 7.9** Glacischaussee Footbridge. (Courtesy of the British Constructional Steelwork Association, Ltd., from reference 1.)

deck anchorage. Back stays are  $1\frac{11}{32}$  in. (35 mm) in diameter and anchored to gravity foundations independent of the northern abutment.

The all-welded, A-frame pylon straddles the deck and is  $39\text{ ft }4\frac{7}{16}$  in. (12 m) wide at its base. Pylon legs are tapered and triangular in cross section with a maximum measurement on a side of  $4\text{ ft }7\frac{1}{8}$  in. (1.4 m). Plate thickness is about  $\frac{3}{8}$  in. (10 mm). The pylon is pin connected at its base. Structural steel weight was approximately 77 tons (70 mt). Cable weight was 1.65 tons (1.5 mt).

### 7.8 Pont de la Bourse, Le Havre, France

This graceful asymmetric structure is located in Le Havre, France. It is a double inclined plane cable arrangement transversely and a radiating configuration in elevation, Figs. 7.18 and 7.19. Total length of superstructure is  $344\text{ ft }6$  in. (105 m) with a major span

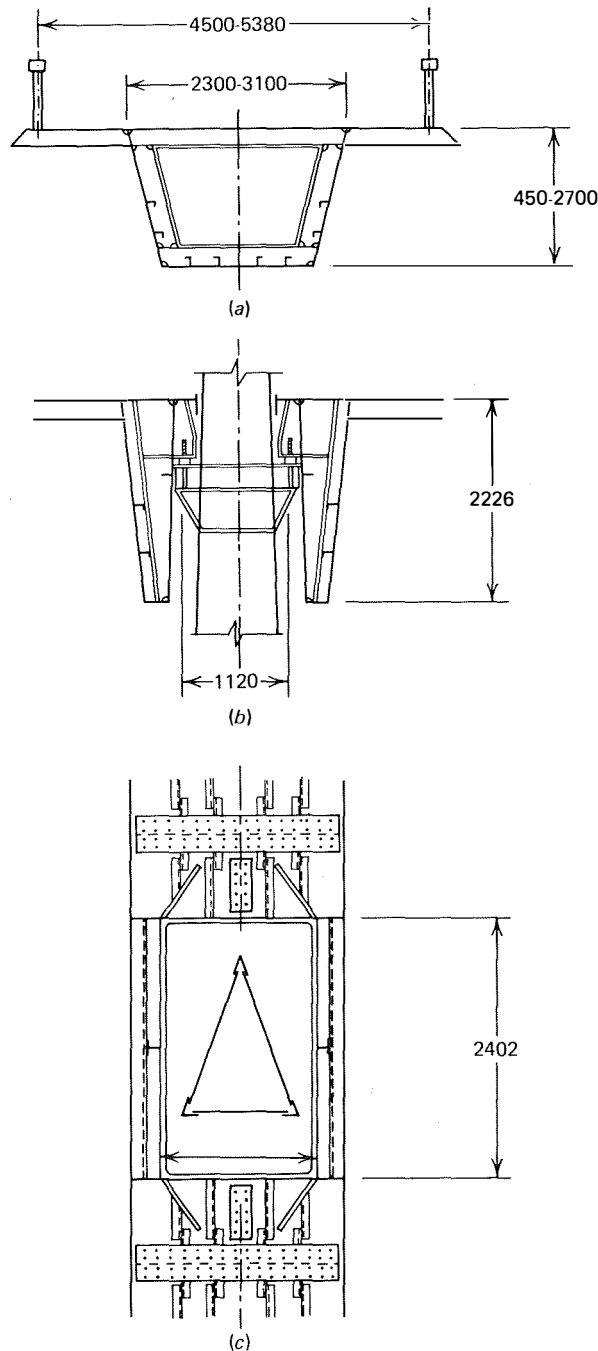


**FIGURE 7.10** Glacischaussee Bridge: (a) girder cross section, (b) girder cross section at pylon, and (c) plan cross section of pylon. (Courtesy of The British Constructional Steelwork Association, Ltd., from reference 1.)

of 240 ft 10 in. (73.4 m) and a minor span of 103 ft 8 in. (31.6 m).

The superstructure has a depth of 3 ft. 6 in. (1.06 m) with a marked camber of 19 ft 8 in. (6 m) in the

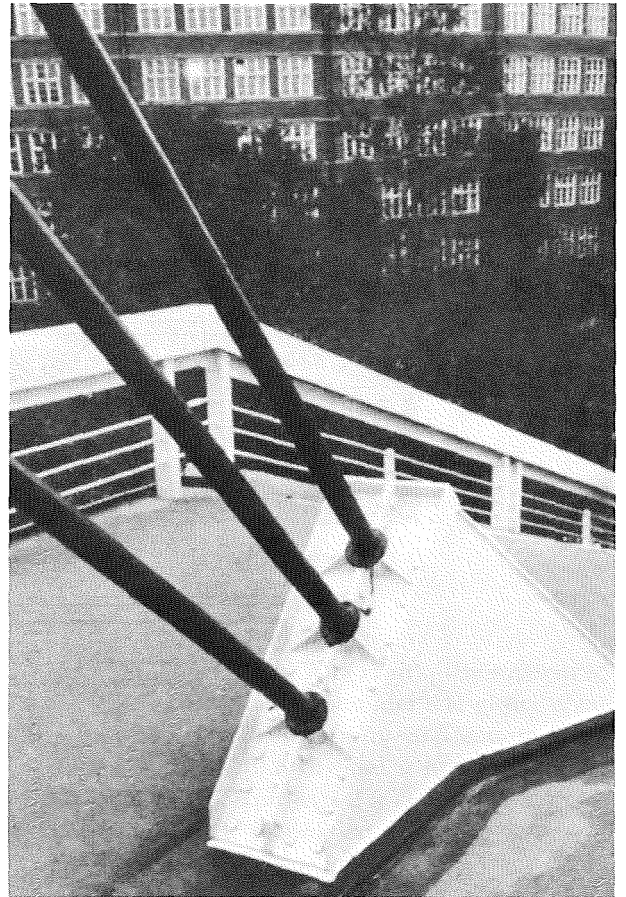


**FIGURE 7.11** Glacischaussee Footbridge, view of girder anchorage. (Courtesy of The British Constructional Steelwork Association, Ltd., from reference 6.)

344-ft 6-in. (105-m) length to provide a clearance of 23 ft (7 m) at high water and 30 ft 6 in. (9.3 m) at mean water level.

In cross section, the superstructure consists of two longitudinal edge girders 19 ft (5.8 m) on centers. Cross beams frame-in at the lower flange so that the longitudinal girder forms part of the parapets. The deck is a  $3\frac{7}{8}$ -in. (100-mm) reinforced concrete slab.

Pylon height is 114 ft 10 in. (35 m) with triangular cross-section legs. Outside stays are  $3\frac{3}{8}$  in. (85 mm) in diameter, inside stays are  $2\frac{1}{4}$  in. (57 mm) in diameter.<sup>7</sup>

### 7.9 Canal du Centre, Obourg, Belgium

Located in Obourg, Belgium, this concrete pedestrian bridge, Fig. 7.20 consists of eight precast double-T deck sections approximately 55 ft (16.7 m) in length. It is a single-pylon symmetric structure with an in-

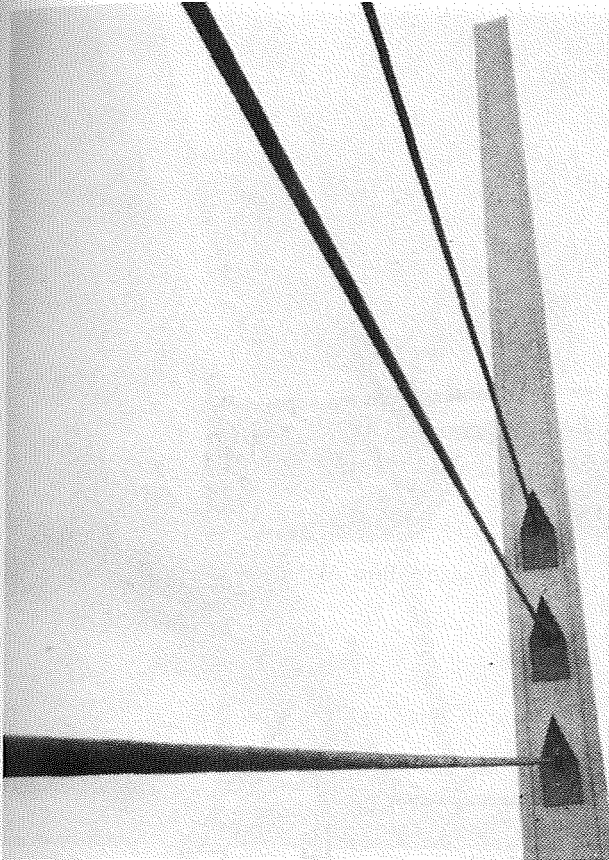


**FIGURE 7.12** Glacischaussee Footbridge, view of pylon anchorage. (Courtesy of the British Constructional Steelwork Association, Ltd., from reference 6.)

clined double-plane stay arrangement transversely and a radiating stay configuration in elevation. The only function of the outer stay is to position the hinged pylon. Erection of the foundation took 24 days: 8 days

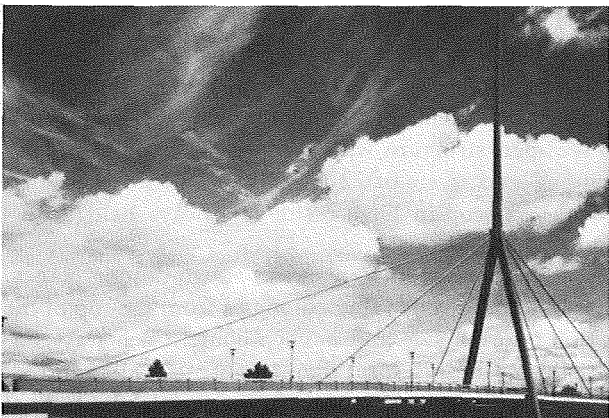


**FIGURE 7.13** Lodemann Footbridge. (Courtesy of Beratungsstelle für Stahlverwendung, from reference 3.)

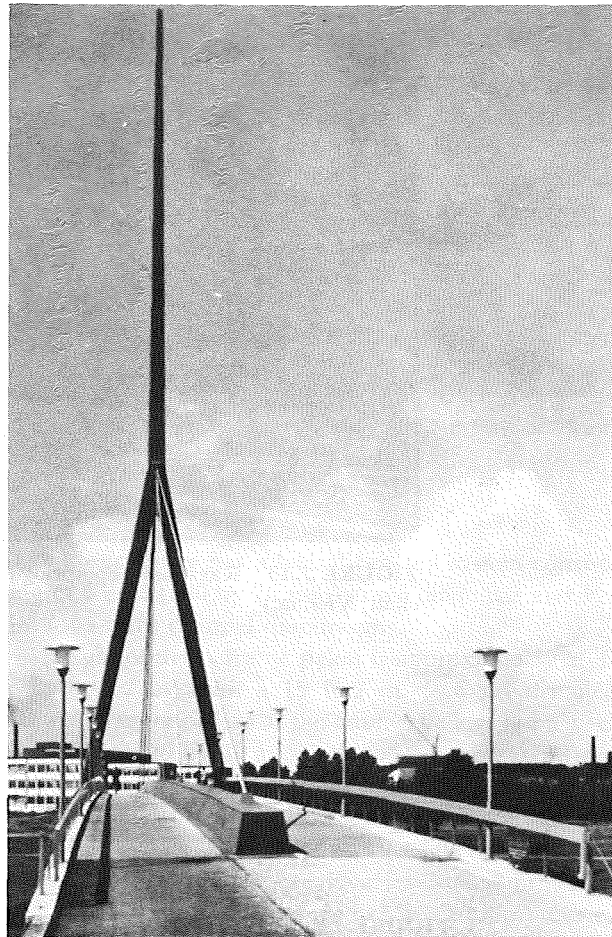


**FIGURE 7.14** Lodemann Footbridge. (Courtesy of Beratungsstelle für Stahlverwendung, from reference 3.)

to erect the deck sections; 2 days for the pylon; 10 days to place and anchor the stays and stress the outer stays; 3 days to stress and adjust the remaining stays to obtain the proper profile; and 1 day to complete the joints between deck units.<sup>8</sup>

### 7.10 River Barwon Footbridge, Australia

The solid trapezoidal deck of this structure located in Geelong, Australia, is unusual in that it encases an approximately 3-ft 7-in. (1.1-m) diameter PVC (Polyvinyl chloride) sewer pipe, Fig. 7.21. The end spans and lower section of the pylon were of cast-in-place construction on falsework, while the center span was cast-in-place cantilever construction in segments of approximately 9 ft 10 in. (3 m) in length. Legs of the upper portion of the pylon were precast and bolted



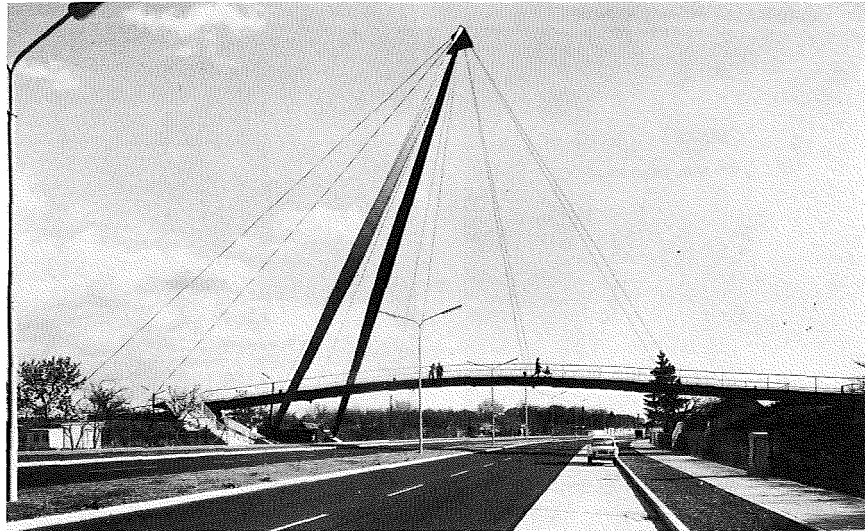


**FIGURE 7.15** Raxstrasse Footbridge. (Courtesy of Waagner-Biro Aktiengesellschaft, Vienna.)

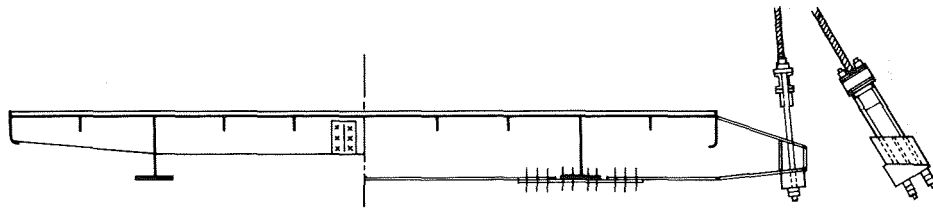


**FIGURE 7.16** Raxstrasse Footbridge, deck cross section. (Courtesy of Waagner-Biro Aktiengesellschaft, Vienna.)

at the cross beam. The pylon is hinged at the base and has Freyssinet flat jacks in the joint for adjustment that may be required to compensate for distortions arising from creep and shrinkage.<sup>8</sup>

### 7.11 Mount Street Footbridge, Australia

A single vertical plane pedestrian bridge located in Perth, Australia has an unusual cable configuration in elevation which must have been selected for aesthetic reasons, Fig. 7.22. The cast-in-place superstructure is trapezoidal in cross section and has a varying depth, haunching at the pier. The pylon consists of precast units that are prestressed vertically to the deck. Stays are of parallel wire construction with proprietary prestressing anchorages. A dead-end anchorage is used at the deck and a jacking anchorage at the pylon.<sup>8</sup>

### 7.12 Menomonee Falls Pedestrian Bridge, U.S.A.

The Menomonee Falls Pedestrian Bridge, Figs. 1.24, 7.23, and 7.24, received an Award of Merit 1971/Special Type in the Prize Bridge Contest sponsored by the American Institute of Steel Construction. It is the first modern cable-stayed bridge, either vehicular or pedestrian, built in the U.S.A. It is a 361-ft (110-m), three-span structure with a center span of 217 ft (66 m) and end spans of 72 ft (22 m), and was designed by the Wisconsin Division of Highways Bridge Section.<sup>9</sup>

Transverse stay arrangement is two sloping planes. In elevation a single stay emanates from the top of the pylon on each side and in each plane. Each stay consists of a 3-in. (75-mm) diameter structural strand.

The superstructure has two principal longitudinal girders (W 33 by 130) spaced at 8 ft 3 in. (2.5 m) and supporting a 5½-in. (140-mm) reinforced concrete slab.



**FIGURE 7.17** Raxstrasse Footbridge. (Courtesy of Waagner-Biro Aktiengesellschaft, Vienna.)

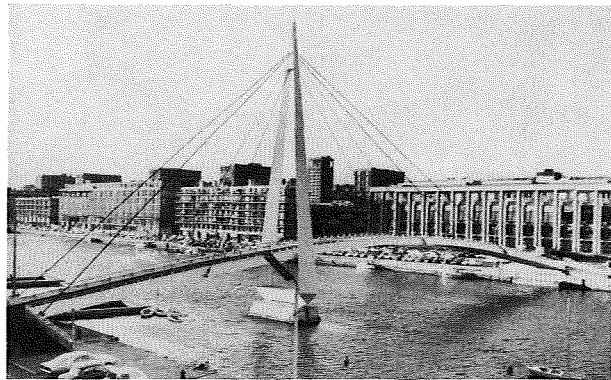


**FIGURE 7.18** Pont de la Bourse. (Courtesy of Acier-Stahl-Steel, from reference 7.)

The lower flange has a lateral bracing system consisting of 4 by 3 (100 by 76 mm) angle diagonals and 12-in. (305-mm) channel diaphragms.

Height of the A-frame pylon is approximately 56 ft 6 in. (17.2 m) with a 15 ft 2 in. (4.6 m) distance between center of legs at the base. The legs are a steel box section 20 by 10 in. (508 by 254 mm), with the larger dimension parallel to the longitudinal axis of the bridge. Plates on the 20-in. (508-mm) side are a constant thickness of  $\frac{1}{2}$  in. (12.7 mm), while on the 10-in. (254-mm) side the thickness varies from  $\frac{1}{2}$  in. (12.7 mm) below the superstructure to  $\frac{3}{8}$  in. (10 mm) above.

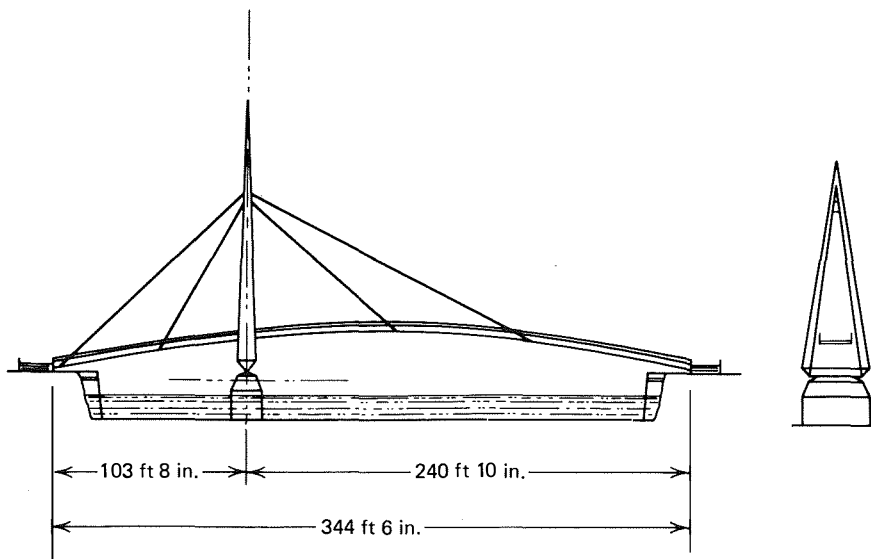


**FIGURE 7.19** Pont de la Bourse. (Courtesy of Acier-Stahl-Steel, from reference 7.)

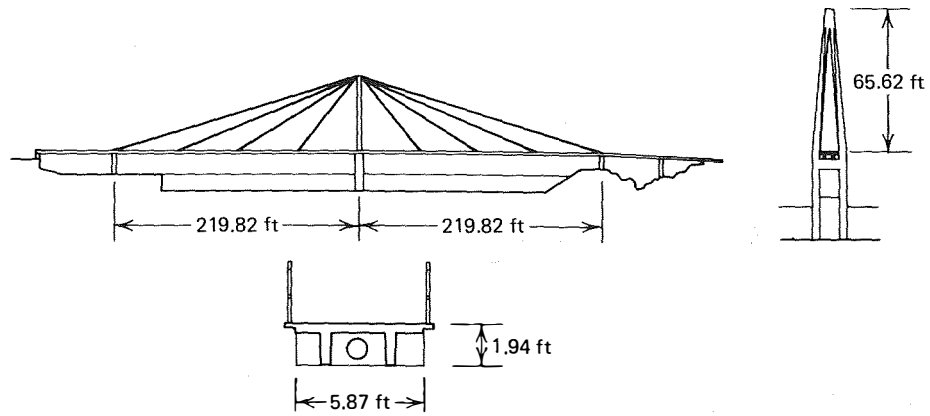


**FIGURE 7.20** Canal du Centre Footbridge. (Courtesy of Crosby Lockwood & Sons, Ltd., from reference 8.)

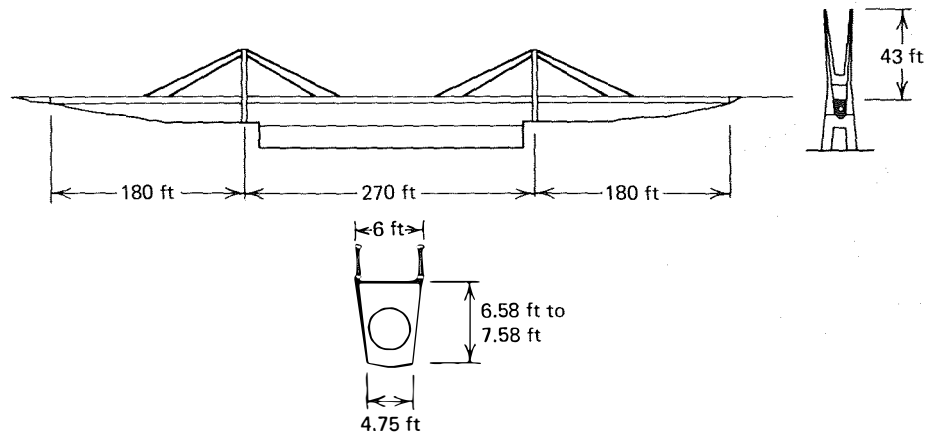


**FIGURE 7.21** River Barwon Footbridge. (Courtesy of Crosby Lockwood & Sons, Ltd., from reference 8.)

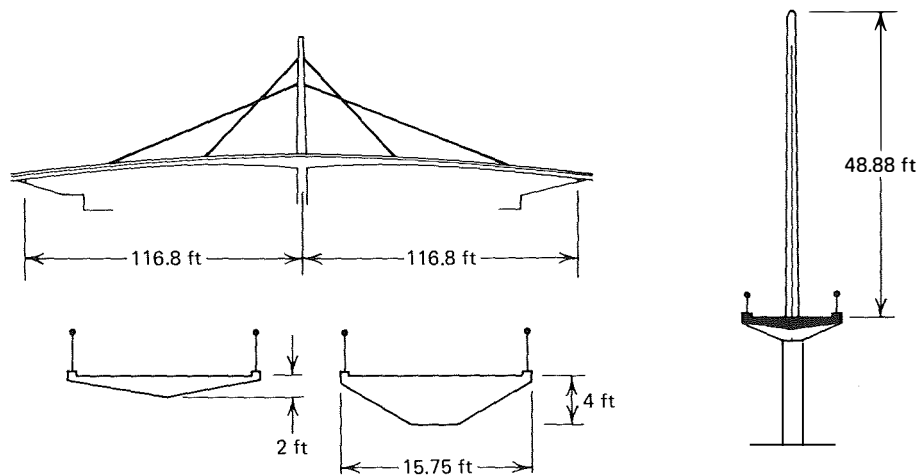


**FIGURE 7.22** Mount Street Footbridge. (Courtesy of Crosby Lockwood & Sons, Ltd., from reference 8.)

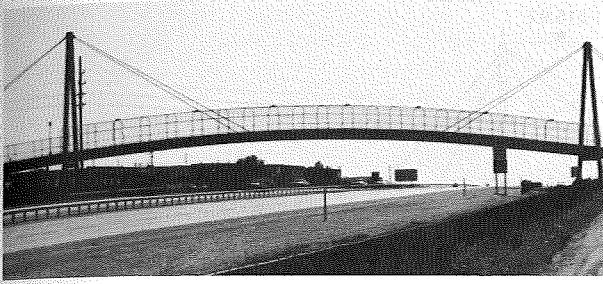


**FIGURE 7.23** Menomonee Falls Pedestrian Bridge. (Courtesy of the Wisconsin Division of Highways.)

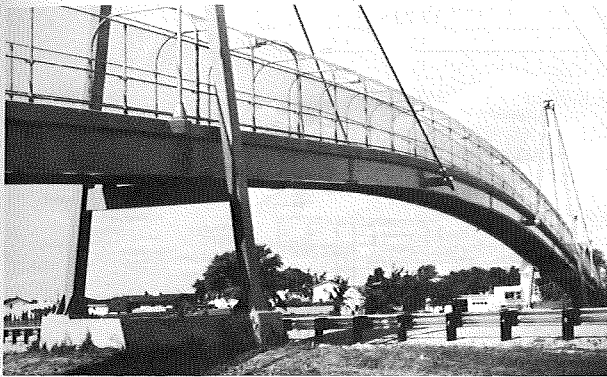


**FIGURE 7.24** Menomonee Falls Pedestrian Bridge. (Courtesy of the Wisconsin Division of Highways.)

### 7.13 Prince's Island Pedestrian Bridge, Canada

This structure, located in Calgary, Alberta, Canada, is an asymmetrical, cable-stayed pedestrian and cycle bridge with a total length of 600 ft (183 m) and a 220 ft (67 m) suspended river span, Fig. 7.25. The box girder has a depth of 3 ft 2 in. (96.5 mm), a top flange width of 12 ft (3.66 m), and a bottom flange width of 5 ft (1.5 m). An epoxy and silica sand wearing surface is bonded to the orthotropic deck, Fig. 7.26. The A-frame pylon, Figs. 7.25 and 7.26, attains a height of

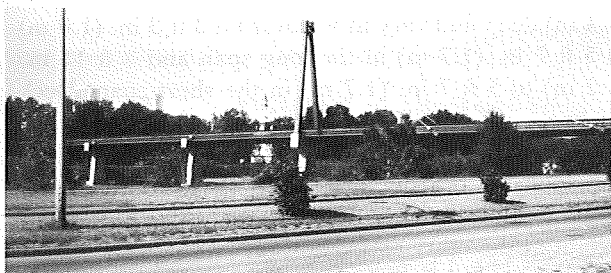


**FIGURE 7.25** Prince's Island Pedestrian Bridge, general view. (Courtesy of Joseph A. Chilstrom, FHWA, Washington Division.)



**FIGURE 7.26** Prince's Island Pedestrian Bridge, longitudinal view of deck. (Courtesy of Joseph A. Chilstrom, FHWA, Washington Division.)

55 ft (16.7 m) above the deck surface and supports four  $1\frac{3}{4}$ -in. (45-mm) diameter galvanized structural strands. The piers are supported on steel pipe piles driven to bedrock. The foundations also include rock anchors for stability under ice pressures and anchor pier uplift. The structure was designed by Carswell Engineering Ltd. of Calgary.

### 7.14 Footbridge Liebrüti, Kaiseraugst, Switzerland

This structure, constructed in 1977–1978, is part of a commercial development consisting of apartments, underground parking garages, a shopping center, and other ancillary facilities, Fig. 7.27. Total length of the bridge is 211 ft 6 in. (64.45 m), with a major span of 153 ft 4 in. (46.73 m) and an anchor span of 58 ft 2 in. (17.72 m), Fig. 7.28. A fixed bearing is located at

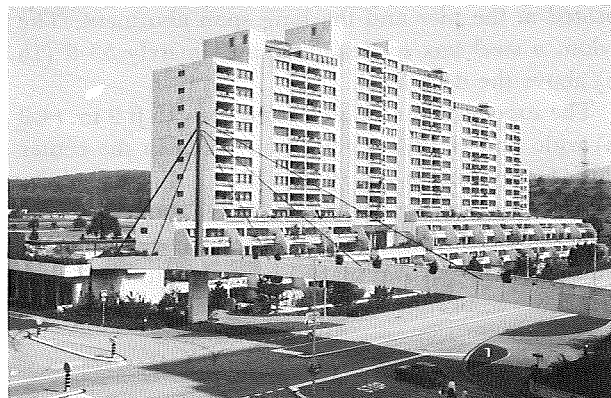


**FIGURE 7.27** View of the Footbridge Liebrüti. (Courtesy of H. U. Aeberhard, VSL International.)

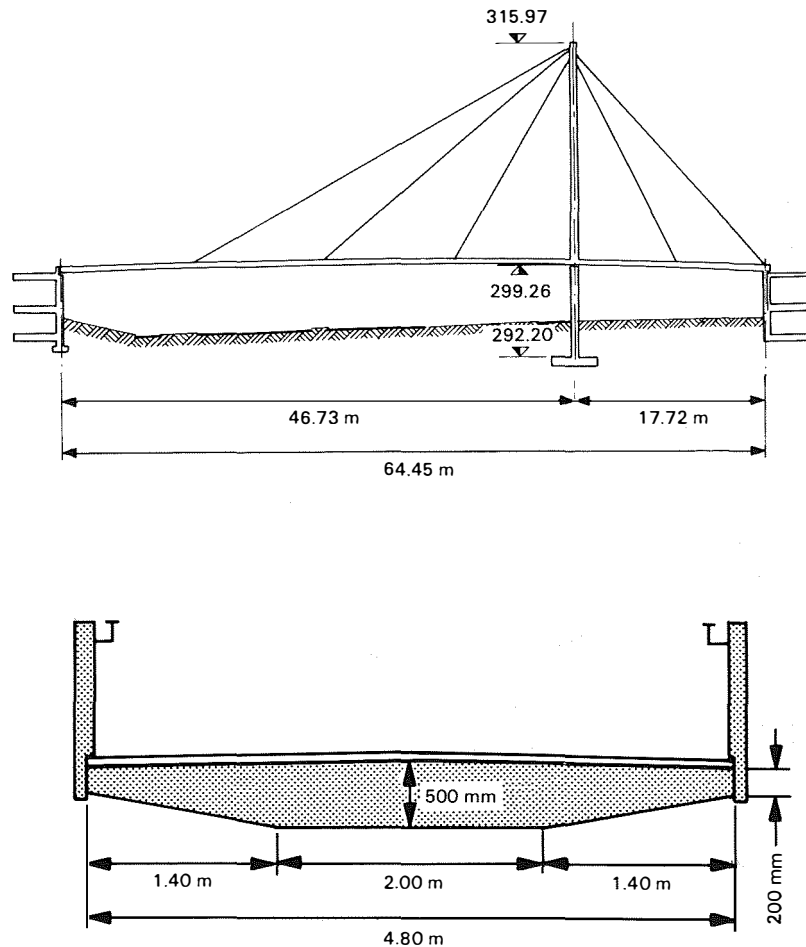


FIGURE 7.28 Footbridge Liebrüti, elevation and section. (Courtesy of H. U. Aeberhard, VSL International.)

the short span abutment and expansion bearings are located at the pier and the long span abutment. The pylon, a steel box section, is approximately 53 ft (16 m) above the deck level.

The superstructure is a concrete slab 15 ft 9 in. (4.8 m) wide and is 19½ in. (500 mm) deep in the center portion, tapering to 7 ft 10 in. (200 mm) at the edges. Lightweight concrete was used in the long span and conventional weight concrete in the anchor span. Stays are in a single vertical plane on the longitudinal centerline of the bridge.<sup>10</sup>

#### 7.15 Horikoshi Bridge, Hachioji City, Japan

This structure, constructed in 1984, provides access to a new high school. It has a total length of 383 ft 2 in.

(116.8 m), with a major span of 219 ft 10 in. (67 m) and a minor span of 122 ft (37.2 m), Fig. 7.29. The superstructure is 34 ft (10.35 m) wide with longitudinal posttensioned edge girders. Edge girders are 4 ft 7 in. (1.4 m) deep and vary in width from 3 ft 3 in. (1.0 m) to 5 ft 7 in. (1.7 m) in the long span and 3 ft 11 in. (1.2 m) to 5 ft 7 in. (1.7 m) in the short span. Deck thickness is 9⅞ in. (250 mm). Transverse floor beams are spaced at 10 ft 10 in. (3.3 m). The superstructure has an expansion bearing at the long span abutment and is monolithically fixed to a concrete block counterweight at the other end, Fig. 7.29.

Stays are in a fan configuration in elevation and in two vertical planes transversely. The pylon is of the portal-frame-type with a strut 36 ft 5 in. (11.1 m) below the top of the pylon, Fig. 7.30.<sup>10</sup>

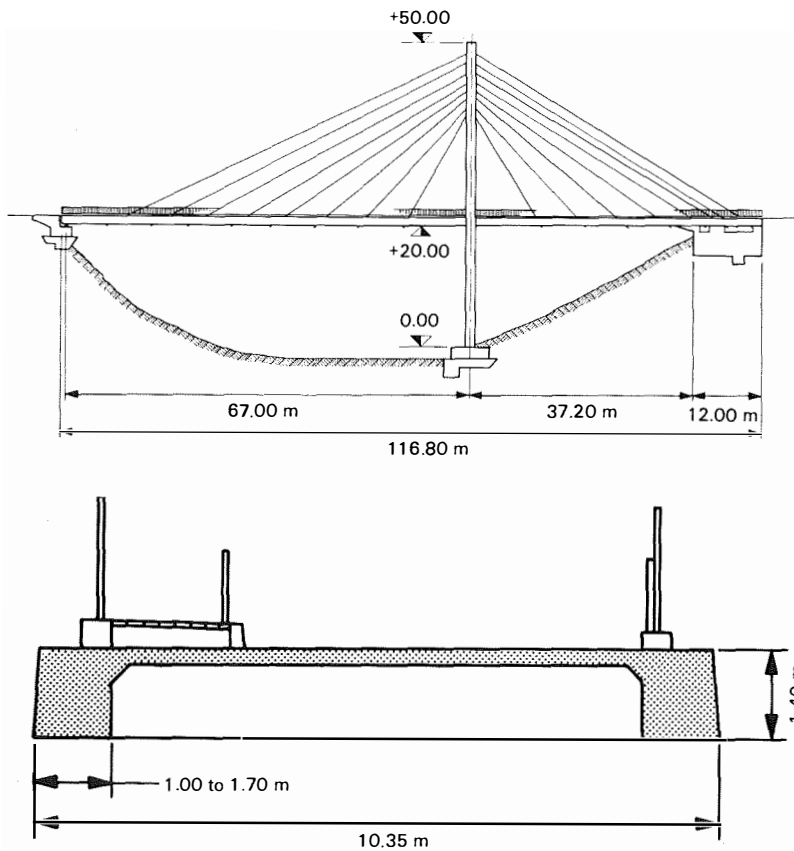


**FIGURE 7.29** Horikoshi Bridge, elevation and section. (Courtesy of H. U. Aeberhard, VLS International.)

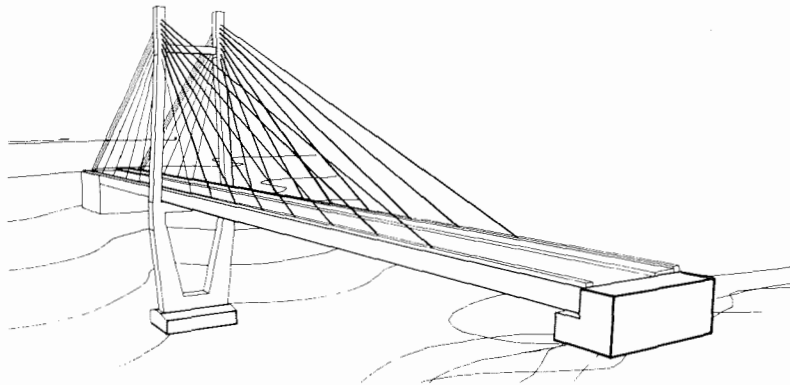


**FIGURE 7.30** Horikoshi Bridge, perspective. (Courtesy of H. U. Aeberhard, VSL International.)

### 7.16 Footbridge over Motorway M-30, Madrid, Spain

This precast concrete structure has a main span of 281 ft 6 in. (85.8 m) and anchor spans of 68 ft 10 in. (21 m), Fig. 7.31. Transversely the stays are in two in-

clined planes. The pylons were cast in a horizontal position and then rotated into a vertical position and placed on their foundations by a crane. The main span was precast in three segments which were placed on falsework above traffic. Cast-in-place joints were cast, followed by placement and stressing of longitudinal



**FIGURE 7.31** Footbridge over Motorway M-30. (Courtesy of W. C. Sherwood, Stronghold International, Ltd.)

tendons. Finally, the stays were installed and stressed causing the superstructure to lift clear of the falsework, thus allowing its removal.

### References

1. Anon., "Steel Footbridges," British Constructional Steelwork Association, Ltd., 16M/623/1266.
2. Fuchs, D., "Der Fussgängersteg auf der Brüsseler Weltausstellung 1958," *Der Stahlbau*, No. 4, April 1958.
3. Feige, A., "Fussgängerbrücken aus Stahl," Merkblatt 251, Beratungsstelle für Stahlverwendung, Düsseldorf.
4. Leonhardt, F. and André, W., "Fussgängersteg über di Schillerstrasse in Stuttgart," *Die Bautechnik*, No. 4, April 1962.
5. Reimers, K., "Fussgängerbrücke über die Glacischaussee in Hamburg für die Internationale Gartenbau-Ausstellung 1963," Schweissen and Scheiden, June 1963.
6. Anon., "Suspended Structures," British Constructional Steelwork Association, Ltd., 16M/842/68.
7. Bachelart, H., "Pont De La Bourse Footbridge over the Bassin du Commerce Le Havre (France)," *Acier-Stahl-Steel* (English version), No. 4, April 1970.
8. Gee, A. F., "Cable-Stayed Concrete Bridges," in *Developments in Bridge Design and Construction*, edited by Rockey, Bannister, and Evans, Crosby Lockwood & Son, Ltd., London, 1971.
9. Woods, S. W., Discussion to "Historical Development of Cable-Stay Bridges," by Podolny and Fleming, *Journal of the Structural Division*, ASCE, Vol. 99, No. ST 4, April 1973, Proc. Paper 9640.
10. Anon., "VSL Stay Cables for Cable-Stayed Bridges," *VSL International*, Losinger Ltd., Berne, Switzerland, January 1984.

# 8

## *Erection and Fabrication*

|     |  |     |
|-----|--|-----|
| 8.1 | INTRODUCTION   | 143 |
| 8.2 | METHODS OF ERECTION                                    | 143 |
| 8.3 | STAGING METHOD   | 144 |
|     | 8.3.1 Rhine River Bridge at Maxau, West Germany        | 144 |
|     | 8.3.2 Toyosato-Ohhashi Bridge, Japan                   | 145 |
| 8.4 | PUSH-OUT METHOD  | 146 |
|     | 8.4.1 Jülicher Strasse Bridge, West Germany            | 146 |
|     | 8.4.2 Paris-Masséna Bridge, France                     | 149 |
|     | 8.4.3 Oberkassel Bridge, West Germany                  | 153 |
| 8.5 | CANTILEVER METHOD                                      | 156 |
|     | 8.5.1 Strömsund Bridge, Sweden                         | 156 |
|     | 8.5.2 Papineau-Leblanc Bridge, Canada                  | 158 |
|     | 8.5.3 Severin Bridge, West Germany                     | 159 |
|     | 8.5.4 Batman Bridge, Australia                         | 163 |
|     | 8.5.5 Kniebrücke Bridge, West Germany                  | 165 |
|     | 8.5.6 Lake Maracaibo Bridge, Venezuela                 | 169 |
|     | 8.5.7 Chaco/Corrientes Bridge, Argentina               | 174 |
|     | 8.5.8 Pasco-Kennewick Intercity Bridge, U.S.A.         | 176 |
|     | 8.5.9 East Huntington Bridge, U.S.A.                   | 180 |
| 8.6 | FABRICATION  | 184 |
|     | 8.6.1 General Structural Steel Fabrication and Welding | 185 |
|     | 8.6.2 Structural Steel Superstructures                 | 186 |
|     | 8.6.3 Structural Steel Pylons                          | 188 |
|     | 8.6.4 Concrete Fabrication                             | 189 |
|     | REFERENCES   | 189 |

### *8.1 Introduction*

Fabrication and erection costs add significantly to project cost estimates, and, as a result, present trends are to fabricate components as large as possible for simplified erection. In this manner larger components of the project are assembled in the shop in contrast to assembling many smaller units in dangerously elevated, exposed positions on the project site. The vagaries of inclement weather are avoided to a certain extent because fewer components must be erected.

The techniques and methods of erecting cable-stayed bridges are as varied and numerous as the in-

genuity and number of erector contractors. It is common practice for the design engineers to suggest methods of erection in the bid document, because of their knowledge of the specific design details. The contractor has the option of accepting the suggested construction method or submitting an alternate method of choice. Alternate methods are normally subject to the approval of the design engineer. The required approval is considered necessary because the erection method not only affects the stresses in the structure during erection but may also have an effect on the final stresses of the completed structure. The design engineers must satisfy themselves that the final stress distribution and geometry of the completed structure is in accord with their concepts and calculations.

The methods of erection for cable-stayed bridges are broadly described by three general methods: the staging method, the push-out method, and the cantilever method. In this chapter, these methods are generally described and then discussed on a case-study basis of completed bridges.

### *8.2 Methods of Erection*

A general description of the three erection methods is provided in this section; more specific details are provided in the following sections.

The staging method of erection is most often used where there is a low clearance requirement to the underside of the structure and temporary bents will not interfere with any traffic below the bridge. Its advantage is its accuracy in maintaining required geometry and grade and its relatively low cost for low clearance.

The push-out technique has been used successfully on a number of occasions in Europe but is relatively new to American construction. This method is commonly used in Europe where care must be taken not to interfere with traffic below the bridge and where



cantilever construction is impractical. In this method, large sections of bridge deck are pushed out over the piers on rollers or sliding teflon bearings. The deck is pushed out from both abutments toward the center, or, in some instances, from one abutment all the way to the other abutment. Assembling the components in an erection bay at one or both ends of the structure and progressively pushing the components out into the span as they are completed can simplify construction and reduce costs. With this method as much as 1500 tons of steel, spanning a number of supports, have been pushed out and, in some instances, it has been used where a horizontal curvature is required.

A variation of the push-out technique was used for the final positioning of the Oberkassel Bridge in West Germany (see Sections 5.22 and 8.4.3) whereby the completed bridge was moved laterally 156 ft (47.5 m). Aside from the obvious change in movement direction, that is, laterally as opposed to longitudinally, the bridge was pulled into position rather than pushed into position.

The cantilever erection method is very often employed in cable-stayed bridge construction where temporary supports are necessary. It may increase the steel requirements over that required for final positioning to accommodate the increased moments and shears during the erection process. The principal advantage is that it does not interfere with traffic below the bridge.

### 8.3 Staging Method

#### 8.3.1 RHINE RIVER BRIDGE AT MAXAU, WEST GERMANY

The superstructure erection for the Rhine Bridge at Maxau (see Section 5.6) began at an abutment on two temporary land piers and then proceeded by short cantilevers to rest on a temporary river pier and the permanent tower pier, Fig. 8.1. Generally, the units were approximately 65 ft (20 m) in length and each weighed up to 27.5 tons (25 mt). They were placed by a derrick

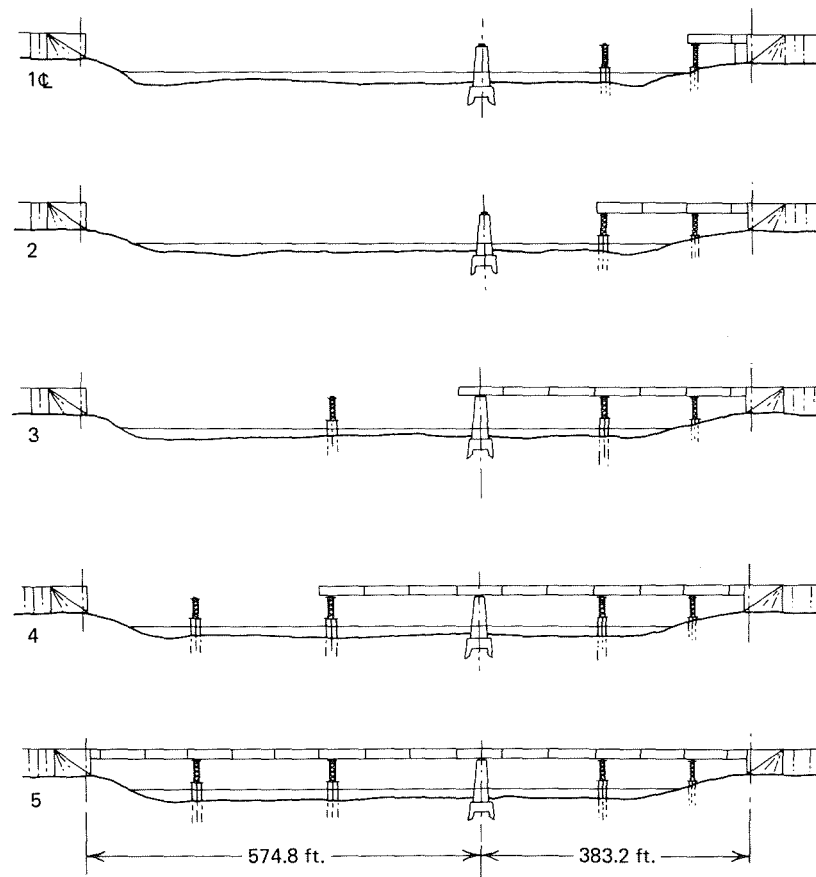


**FIGURE 8.1** Rhine River Bridge at Maxau. (Courtesy of Der Stahlbau, from reference 1.)

mounted on rails on the bridge deck. In the navigation channel, two temporary piers located at the third points of the navigation channel were utilized, Fig. 8.1. Upon completion of the suspended structure the tower erection was begun. The tower was erected in nine units, each weighing up to 4.4 tons (4 mt) with cross-sectional dimensions of 6.5 by 9.8 ft (2 by 3 m).

The erection method for this bridge consisted simply of erecting the entire suspended structure on temporary piers, followed by the tower erection, and cable connections. Finally, the tower saddles were jacked to stress the cables to the desired tensile load to obtain profile and the temporary piers were removed.<sup>1</sup>

### 8.3.2 TOYOSATO-OHHASHI BRIDGE, JAPAN

The Toyosato Bridge structure is a three-span, continuous orthotropic box girder with a single-plane fan

configuration of stays and A-frame towers (see Section 5.15). The box girder was erected by the staging method, Fig. 8.2. Field welding was used for the longitudinal joints of the deck plates, and high-strength bolts were used for the transverse joints.<sup>2</sup> The legs of the A-frame towers were erected independently and then joined by the lower saddle support portal member, Fig. 8.3. The main girder was jacked into position to enable all the cables to be installed and then the jacks were released and the temporary bents were removed, Fig. 8.2.

The stays on this project were prefabricated parallel wire strands. To facilitate their erection, temporary bents were erected on the deck at approximately 65-ft (20-m) intervals, and a catwalk was installed from the bridge deck to the towers, Fig. 8.4. Rollers were installed on the catwalk to temporarily support the strands of the cable, while a carrier that pulls the

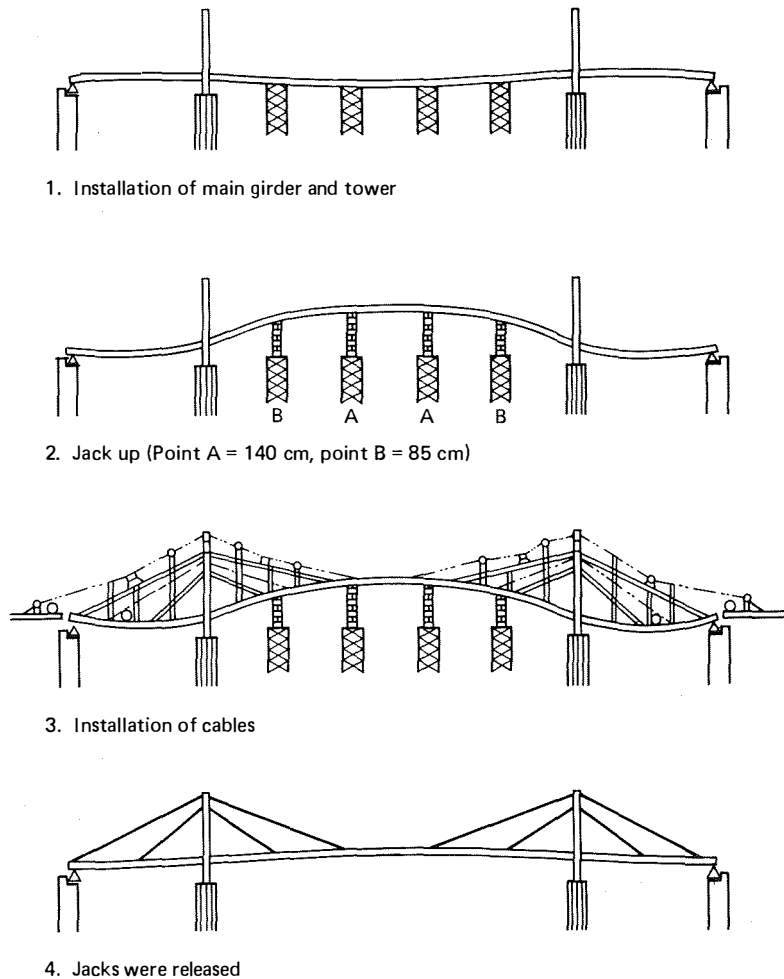


**FIGURE 8.2** Erection procedure. (Courtesy of Der Stahlbau, from reference 2.)

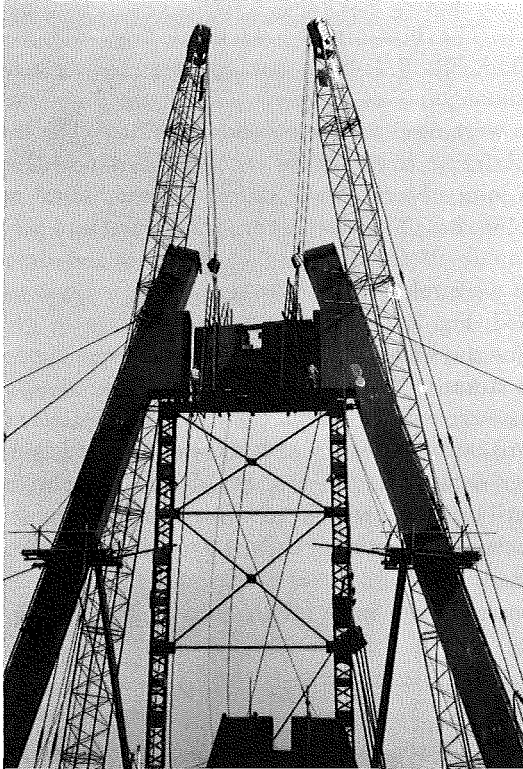


**FIGURE 8.3** Toyosato-Ohhashi Bridge, tower erection. (Courtesy of A. Matsukawa.)

strands was also installed. The carrier grips the socket of the strand, draws it out of its reel, and pulls the strand over the rollers on the catwalk.

Each shop-fabricated hexagonal strand is composed of bundled parallel wires. The top stay consists of 16 strands of 154 wires each, and the bottom stay is composed of 12 strands of 127 wires each. To avoid bend-

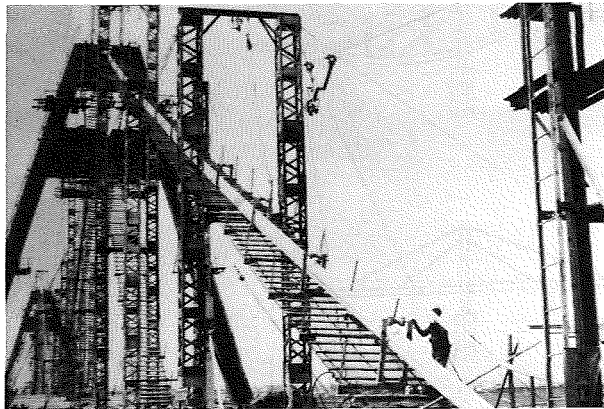


**FIGURE 8.4** Toyosato-Ohhashi Bridge, cable erection. (Courtesy of A. Matsukawa.)

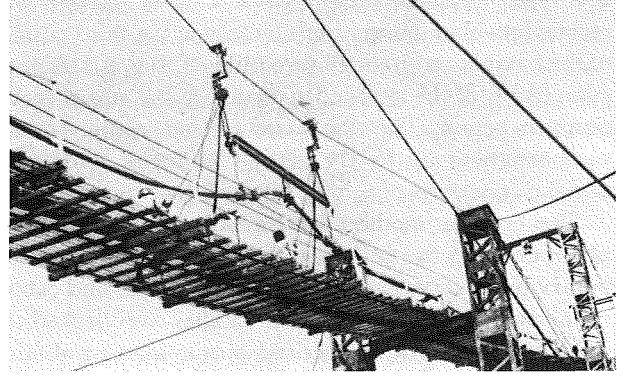


**FIGURE 8.5** Toyosato-Ohhashi Bridge, erection of curved strand. (Courtesy of Der Stahlbau, from reference 2.)

ing stresses in the strands as they pass over the saddle, the strands are prefabricated with a curvature to fit that of the saddle (referred to as “curved strands”). To preclude stretching or deforming during installation, that part of the strand called “curved strand” required an additional strong-back support rigging as it was pulled up the catwalk, Fig. 8.5. After adjustment for sag, the cable made up of strands is squeezed into a circular shape using a technique similar to that employed with conventional suspension bridges.

#### 8.4 Push-Out Method

##### 8.4.1 JÜLICHER STRASSE BRIDGE, WEST GERMANY

The Jülicher Strasse Bridge is a highway overpass crossing a railroad installation in an urban area of Düsseldorf, Fig. 8.6. It is a three-span structure with a center span of 324 ft (98.7 m) and equal side spans of 104 ft (31.8 m). In cross section it consists of a 6-ft 6-in. (2-m) median, two roadways of 24 ft 7 in. (7.5 m), two walkways of 10 ft 2 in. (3.1 m), and two safety strips of 5 ft 3 in. (1.6 m); the overall width is 86 ft 6 in. (26.4 m). These features are combined in an orthotropic deck, three-cell center box girder with overhangs. The torsionally stiff center box girder is divided into three cells of 13 ft 1½ in., 6 ft 1 in., and 13 ft 1½ in. (4, 1.85, and 4 m) wide and a constant depth of 4 ft 7 in. (1.4 m), 1/70 of the span. The transverse girders cantilever out from the box girder and are spaced at intervals varying from 6 ft 10½ in. to 7 ft 6½ in. (2.1 to 2.3 m). The tower is 54 ft (16.5 m) high

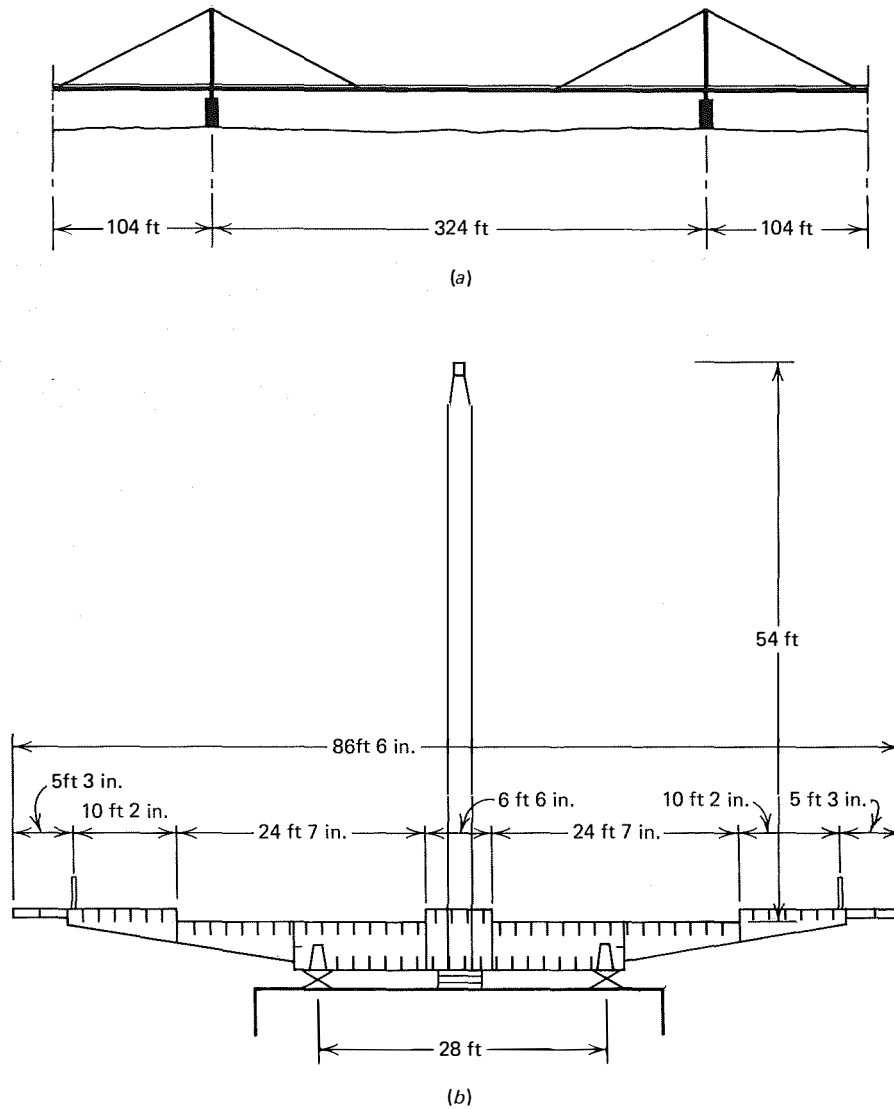


**FIGURE 8.6** Jülicher Strasse Bridge: (a) elevation, and (b) cross section, (Courtesy of Acier-Stahl-Steel, from reference 3.)

and is an externally smooth box. Structural steel weight was  $62\frac{1}{2}$  lb/ft<sup>2</sup> (307 kg/m<sup>2</sup>).<sup>3</sup>

The erection problem was that the federal railway operation, which consisted of six electrified tracks under the eastern side span and the marshalling yard under the center span, could not be interrupted. The pushout concept was selected as the most feasible for the site conditions. The concept was not entirely new, but had never before been used on a cable-stayed bridge. In addition, flat teflon bearings were used for the first time.<sup>4</sup>

An area behind the west abutment of approximately 200 by 130 ft (60 by 40 m) was utilized as the assembly shop. It was possible to assemble the entire bridge cross

section to an approximate length of 165 ft (50 m) in this area. A portal crane with a 100-ton (90 mt) capacity was able to handle the largest components of the deck. Erection units were approximately 53 ft (16 m) in length and were assembled from six subunits and, as much as possible, were automatically welded at the assembly site. As a result of the length of the assembly work area and the performance range of the crane, it was possible to have three units in various stages of assembly at one time. In this manner, relatively large assembly units were fabricated and welded in a concentrated area under "workshop" conditions, thus providing the greatest possible accuracy in transverse and longitudinal alignments. The cable stays

could be laid out on the deck next to the pylon and erected along with the saddles to the top of the tower by the portal crane.

The erection procedure is shown in Fig. 8.7. It should be noted that in the final position the reaction load of the towers is borne by the permanent piers VIII and XI. However, during the push-out operation the tower reaction must be resisted by a lateral-beam diaphragm which in turn transmits the load to the longitudinal box girders. For this reason the cable stays are only partially tensioned. The jacking mechanism at the saddle is used to compensate for the cantilever

deflection of the leading edge of the pushed-out section.

When the leading edge of the bridge reaches pier VIII, Fig. 8.7, the bearing is elevated approximately 4 in. (100 mm) by jacks. As a result of this action the bearing pressure at pier VII is relieved. As the structure is pushed out farther, the bearing pressure at pier VIII will increase. It was determined that the allowable bearing pressure was reached when the leading edge extended approximately  $24\frac{1}{2}$  ft (7.5 m) past pier IX. At this point the bearing at pier VIII is lowered to its original position. This procedure is then repeated

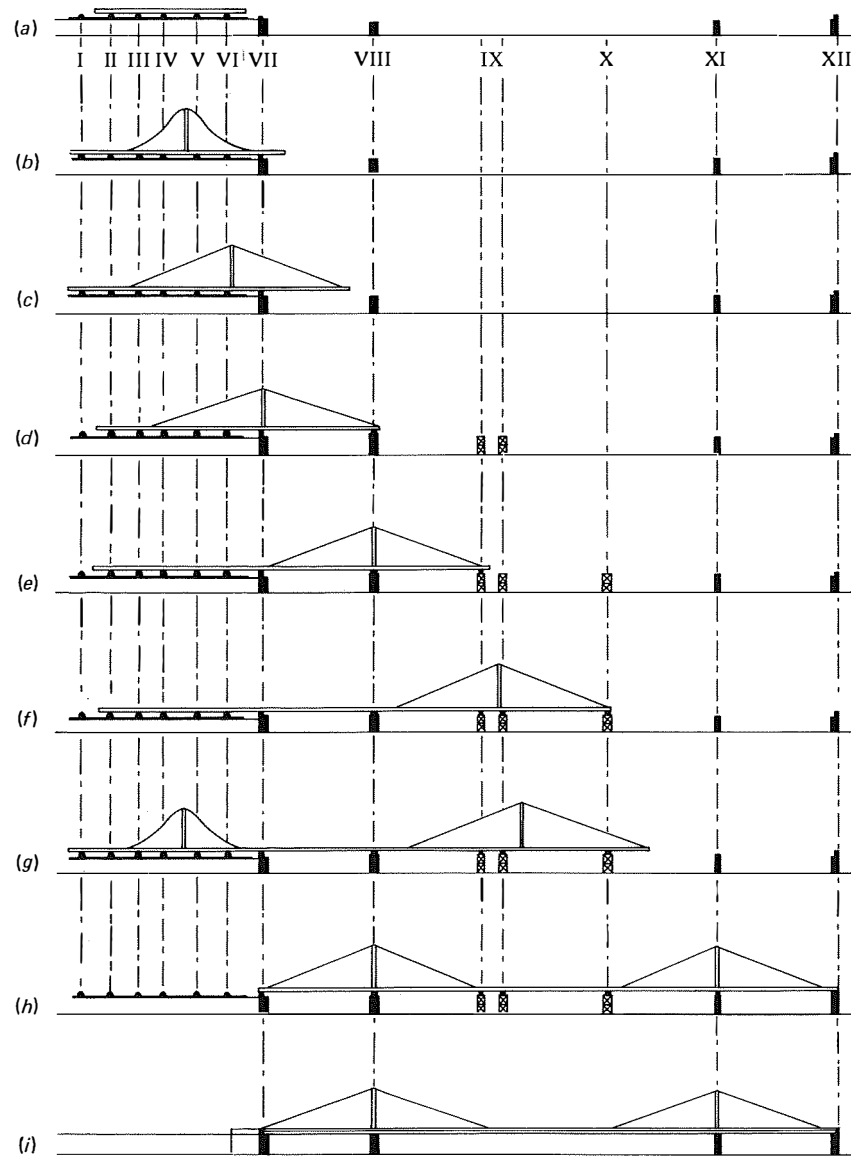


**FIGURE 8.7** Jülicher Strasse Bridge, erection procedure (Courtesy of Der Bauingenieur, from reference 4.)

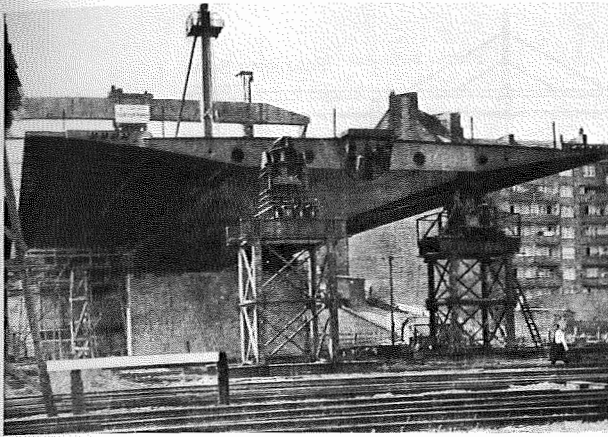


**FIGURE 8.8** Jülicher Strasse Bridge, erection at pier IX. (Courtesy of Der Bauingenieur, from reference 4.)

until the structure is in its final position. The erection condition at pier IX is illustrated in Fig. 8.8. Pier IX is at a skew to the longitudinal axis of the bridge as a result of the railway trackage. The final bridge profile is obtained by simultaneously jacking the bearings at piers IX and X at the saddle bearings until the proper

elevation is reached and the required tensile force is developed in the cable stays.

No special reinforcement of the box girder was required other than the accommodation of the bearing pressure from the sliding bearing at the outside cells of the box girders.<sup>4</sup>

8.4.2 PARIS-MASSÉNA BRIDGE, FRANCE

The Masséna Bridge spans 73 tracks from the Austerlitz station. Included in the crossing are the four main lines from Paris to Orleans, shunting yards, sidings for marshalling main and suburban passenger train lines, and the Paris-Masséna Shop. A site plan is shown in Fig. 8.9.<sup>5,6</sup> The bridge has an overall length of 1615 ft 9 in. (528.48 m) divided into six spans of 137 ft 6 in., 182 ft 3 in., 265 ft 7 in., 529 ft 7 in., 264 ft 7 in., and 236 ft 3 in. (41.9, 55.54, 80.95, 161.43, 80.66, and 72.0 m), Fig. 8.10. The deck has an overall width of 118 ft (36 m), consisting of a 13-ft (4-m) median, two roadways of 46 ft (14 m) and two sidewalks of 6 ft 6 in. (2.0 m). The cable stays are in a single vertical plane and transmit the cable thrust to two main longitudinal box girders, Fig. 8.11.

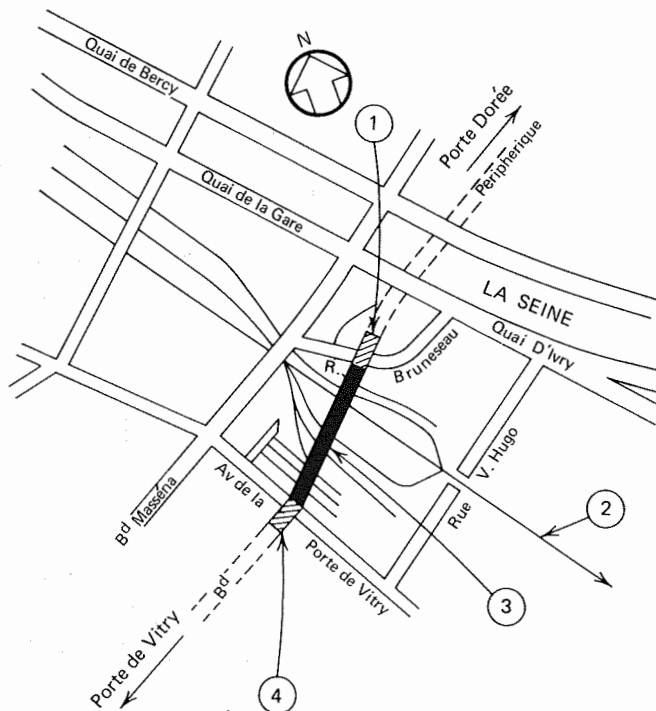


**FIGURE 8.9** Paris-Messéna Bridge: (1) access structure over Rue Bruneseau, (2) main railway line to Bordeaux, (3) cable-stayed bridge, and (4) access structure over Avenue de la Porte de Vitry. (Courtesy of Acier-Stahl-Steel, from references 5 and 6.)

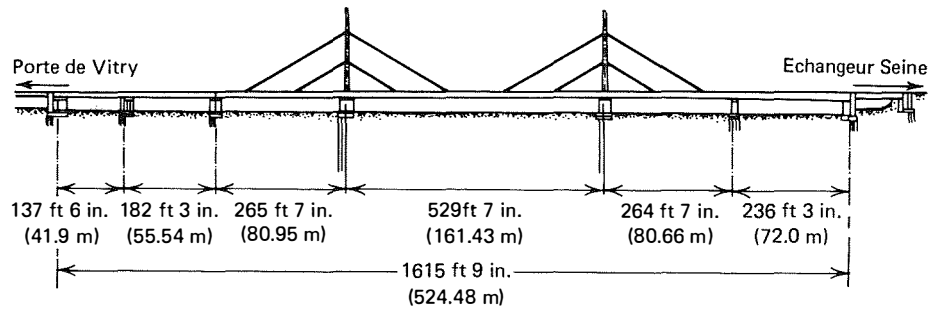


**FIGURE 8.10** Paris-Masséna Bridge, elevation. (Courtesy of Acier-Stahl-Steel, from references 5 and 6.)

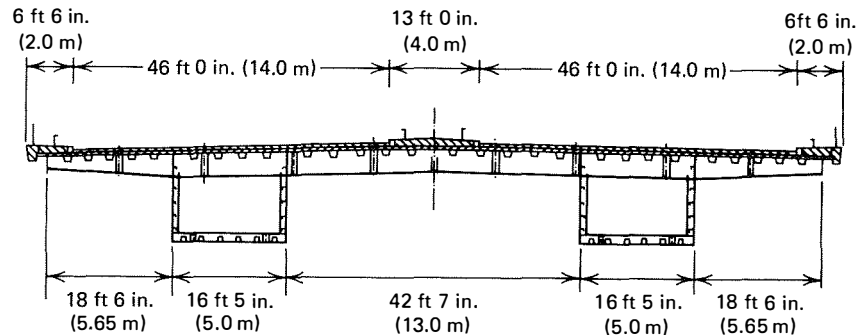


**FIGURE 8.11** Paris-Messéna Bridge, deck cross section. (Courtesy of Acier-Stahl-Steel, from references 5 and 6.)

The box girders are 13 ft 1½ in. (4 m) deep and 16 ft 5 in. (5 m) wide, spaced 59 ft (18 m) center to center. Clearance from top of rail is 28 ft (8.5 m). In the suspended spans, the deck is composed of an orthotropic plate composite with a 4-in. (100-mm) reinforced concrete deck slab. In the approach spans, which do not take a cable longitudinal force, the girders are connected by lateral beams with an 8⅜-in. (220-mm)

thick concrete slab, which takes the place of the orthotropic deck.

The towers are tapered steel boxes 108 ft 3 in. (33 m) above the deck with cable saddles at 59 and 82 ft (18.5 and 25 m) Fig. 8.12. The top saddles are articulated and the lower ones fixed to obtain a balance between shear forces and buckling strength of the towers. The towers are rigidly connected to transverse

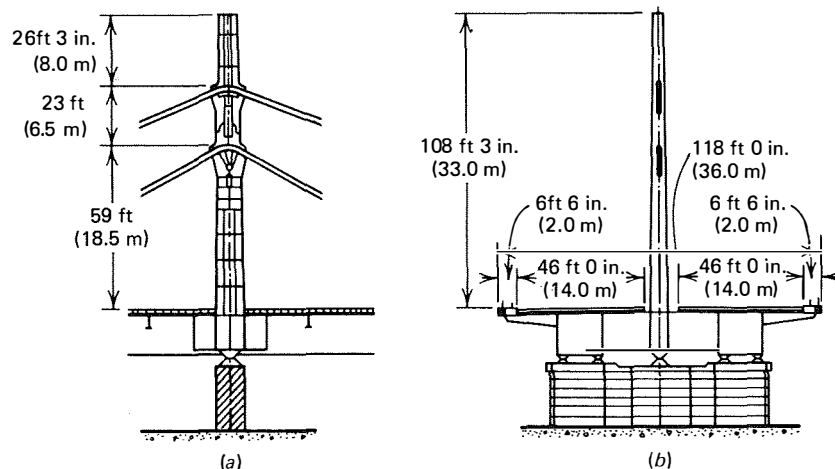


**FIGURE 8.12** Paris-Messéna Bridge, Tower. (a) elevation, and (b) cross section. (Courtesy of Acier-Stahl-Steel, from references 5 and 6.)

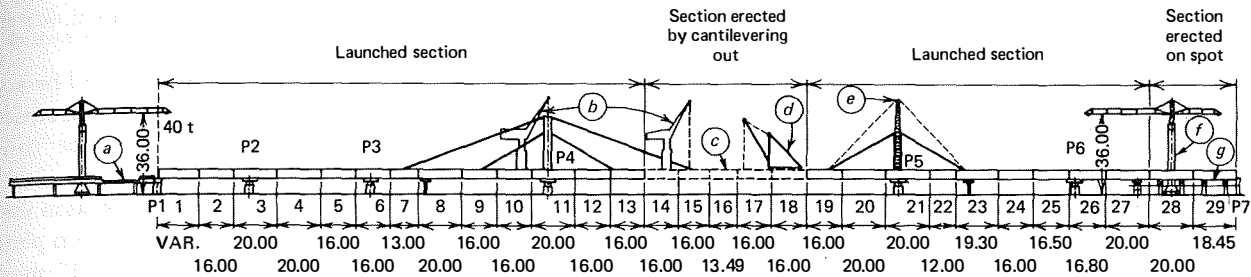


**FIGURE 8.13** Paris-Messéna Bridge: Erection procedure (dimensions in meters), (a) working platform at Porte de Vitry approach, (b) 15-ton tower crane traveling on box-girders, (c) center of main span, (d) double-jib crane, each jib of 1065 ft ton capacity, (e) gantry for erection of towers and cable stays, maximum capacity, 69 tons, (f) tower crane of 30-ton capacity, for handling units into position, and (g) section numbers 28 and 29 assembled in position. (Courtesy of Acier-Stahl-Steel, from reference 5.)

girders between the main box girders and are supported on the pier by spherical bearings. The cables are anchored to the deck 105 and 210 ft (32 and 64 m) from the tower.

This structure was essentially erected by the push-out technique. The sections were pushed out from both ends of the bridge until they cantilevered into the center span approximately 148 ft (45 m) past the towers. The center portion was then erected by the cantilever method. Fig. 8.13.<sup>5</sup> The box girders were assembled on working platforms at either end of the structure by tower cranes. Each segment of a box girder consisted of five shop-fabricated components, Fig. 8.14. Most of the girder segments were either 52 ft 6 in. or 65 ft 7½ in. (16 or 20 m) in length and had an average weight of 16.8 tons (15.2 mt). Twenty segments exceeded 33 tons (30 mt), and the lower section of the tower weighed 68 tons (62 mt).

After three girder segments were assembled on the working platform, they were launched by means of cradles fitted with rollers hung from steel wire stands, Fig. 8.15. The two box girders were launched separately. When the launching operation was completed, the girders were transferred to permanent bearings. Two cranes on the Vitry end traveling on girders lifted and erected the deck plates, box section stay anchorage units, box section units under the tower, the lateral cantilevers, and steel tower. From the Seine end, a double-jib derrick crane was mounted on the two box girders and traveled from the end to the center of the bridge. These cranes were used to erect the center portion of the structure, by the cantilever method, after the lower stays were in place.<sup>5,6</sup>

The stays were erected strand by strand. When the upper stay was anchored to the deck, the tension was adjusted to allow the closure segment to be erected. The stays that were continuous over the saddles were

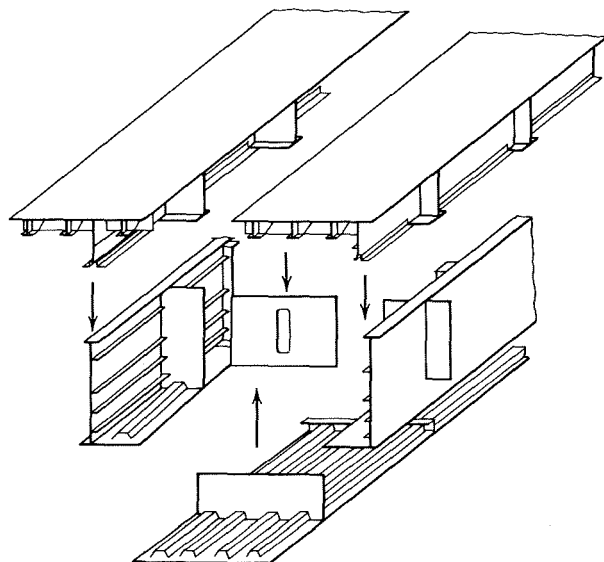


**FIGURE 8.14** Paris-Messéna Bridge, isometric diagram of the five components of the box girder section. (Courtesy of Acier-Stahl-Steel, from references 5 and 6.)

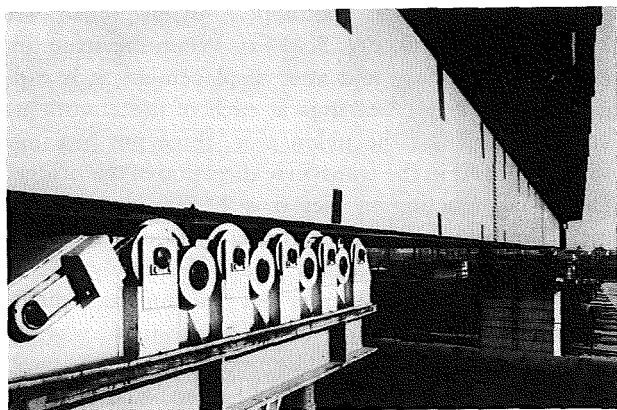


**FIGURE 8.15** Paris-Messéna Bridge, launching a box girder. (Courtesy of Acier-Stahl-Steel, from references 5 and 6.)



anchored to the deck with an initial tension of 11 tons (10 mt). The saddles, which were on telescoping supports sliding in the tower, were jacked until the stays were under full load. The lifting force in the lower stays was obtained by six 330-ton (300-mt) jacks with a travel of 1 ft  $7\frac{3}{4}$  in. (0.5 m) upper stays were lifted by four 550-ton (500 mt) jacks with a possible 3-ft  $3\frac{1}{2}$ -in. (1.0-m) travel.

#### 8.4.3 OBERKASSEL BRIDGE, WEST GERMANY

This structure was described in Section 5.22 along with the unique problem that necessitated the lateral translation of the finished bridge from its as-constructed position to its final position. The sequence of events that led to the final positioning of the bridge on April 7-8, 1976 is depicted in Fig. 8.16.<sup>7,8,9,10</sup>

The span configuration of the structure is indicated in Fig. 5.44 (a). Cable stays, four on each side of the pylon, are twin cables spaced laterally at 4 ft 9 in. (1.44 m) and are anchored to the superstructure in the central cell of the box girder, Fig. 5.44 (b). Spacing of the stays in the river span is five equal spaces of 169.1 ft (51.55 m) such that the structure in elevation, between abutment 1 and pier 7, is symmetrical about the pylon, pier 6. In the anchor span, each back stay is attached to the piers by a linkage arrangement similar to that used for the Kniebrücke Bridge, Fig. 5.22. The main purpose of these linkages is to serve as a stiffening mechanism for the structural system under live load. Under dead load the bridge superstructure is balanced, due to symmetry of the stay arrangement, such that the linkages are virtually free of stress. For this reason the linkages could be disengaged for the subsequent transverse displacement operation without a shift of forces resulting in the system.<sup>7</sup>

With the linkages released, the structure is supported at four points; abutment 1, pylon pier 6, pier 7, and abutment 8, Fig. 5.44 (a). When the structure is in service, before and after displacement, it is supported by two pot bearings at each of the abutments and at pier 7. At the pylon pier, three pot bearings were arranged in the transverse direction of the bridge. Dead load reaction at pier 6 is 22,700 kips (10,300 mt). The center pot bearing directly under the pylon supports a vertical reaction of approximately 18,200 kips (8240 mt).<sup>10</sup> The center pot bearing has a diameter of 9 ft 10 in. (3 m) which, at the time, was the largest ever constructed. The outer bearings allowed movement in all directions including rotation and, therefore, was able to accommodate the transverse ex-

pansion and, most importantly, any torsional forces caused by moving loads and wind.<sup>8</sup>

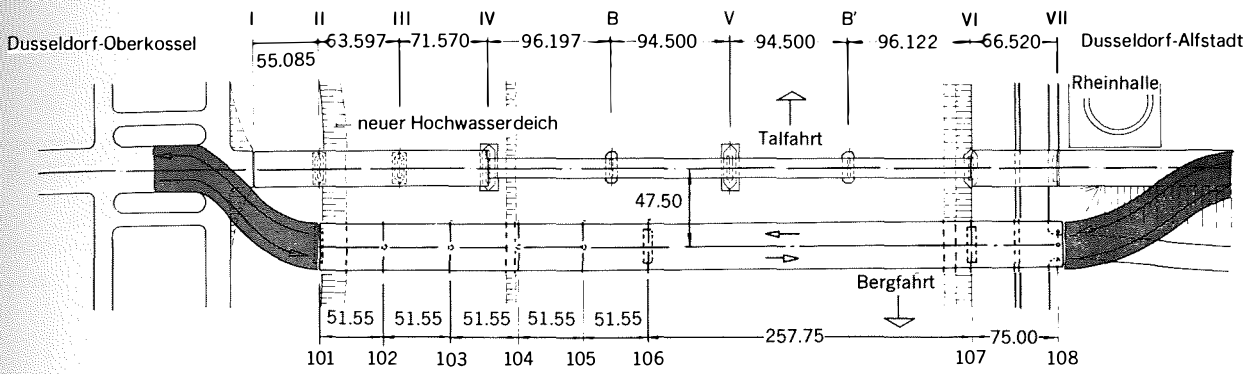
Before lateral translation of the bridge could be accomplished the new piers and a transverse infill structure between the piers, Fig. 8.17, had to be constructed to support the structure during its movement. As indicated previously, support during translation was provided at four points: the abutments, the pylon pier, and pier 7. Under the pot bearings, a  $\frac{1}{2}$ -in. (12-mm) stainless steel plate rested on a steel plate 230 ft (70 m) long, 10 ft (3 m) wide, and 0.7 in. (18 mm) thick. After all bridge construction was completed, the bridge was jacked up about  $1\frac{1}{2}$  in. (40 mm). The in-service bearings were replaced by sliding bearings consisting of heavy steel plates surfaced with teflon. The teflon contained channels and indented pockets for silicone as a further measure to decrease the friction coefficient.<sup>9</sup>

Vertical reactions and tractive forces for the structure during movement is indicated in Fig. 8.18. Coefficients of friction assumed were 0.06 from a standing start and 0.03 throughout the movement.<sup>8</sup> The calculated frictional and inertial forces were about 827 kips (375 mt) at the pylon and 132 kips (60 mt) at pier 7. At the abutments the structure "rides along" on the sliding bearings.

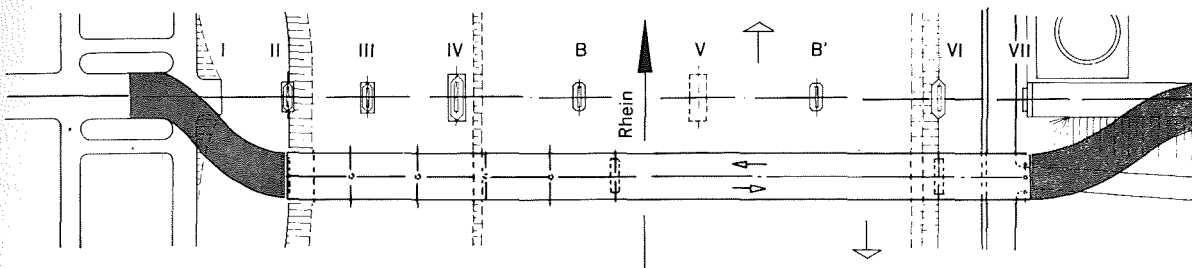
Lateral movement of the superstructure was accomplished by means of two  $7\frac{7}{8}$ -in. (200-mm) diameter rods at each jacking station which were connected to the bridge and were pulled by two jacks, Fig. 8.17. The rod was burned off as movement progressed. The jacks pushed against large concrete pedestals that were part of a temporary concrete bracket on the downstream side of the permanent piers.<sup>9</sup> Rate of movement was about  $2\frac{3}{8}$  in./min. (3.6 m/hr). Total time to accomplish the required displacement of 156 ft (47.5 m) was approximately 13 hours.<sup>10</sup>

As a precaution against wind load or unanticipated pier settlement, which would produce a downhill path for the moving structure, a braking device was installed at both piers on the upstream side, Fig. 8.17. Connected to the bridge were 140  $\frac{1}{4}$ -in. (7-mm) diameter wires which passed through a gripping device and were then wound on a rotating drum that let out the wires (cable) as the bridge moved. The gripping device would be activated in the event the bridge moved due to its own weight.<sup>9,10</sup> Fortunately, it never had to be activated.

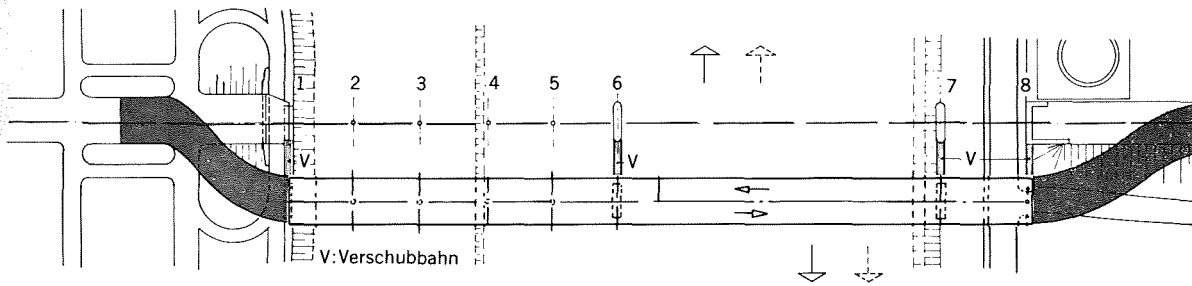
Edwin Beyer, director of Bridge and Tunnel Construction for the City of Düsseldorf, was in charge of the project. The firm of Leonhardt, Andra and Partner



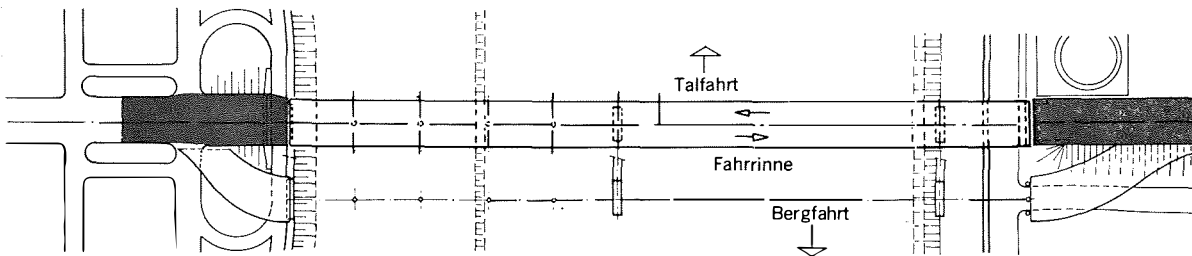
(a)



(b)



(c)



(d)

**FIGURE 8.16** Oberkassel Bridge, sequence of operations of final positioning: (a) new bridge with temporary ramps and under traffic alongside old parallel bridge, (b) old bridge demolished, (c) extension of abutments 1 and 8, and piers 6 and 7 to accommodate lateral translation, and (d) lateral translation completed and new bridge in service.

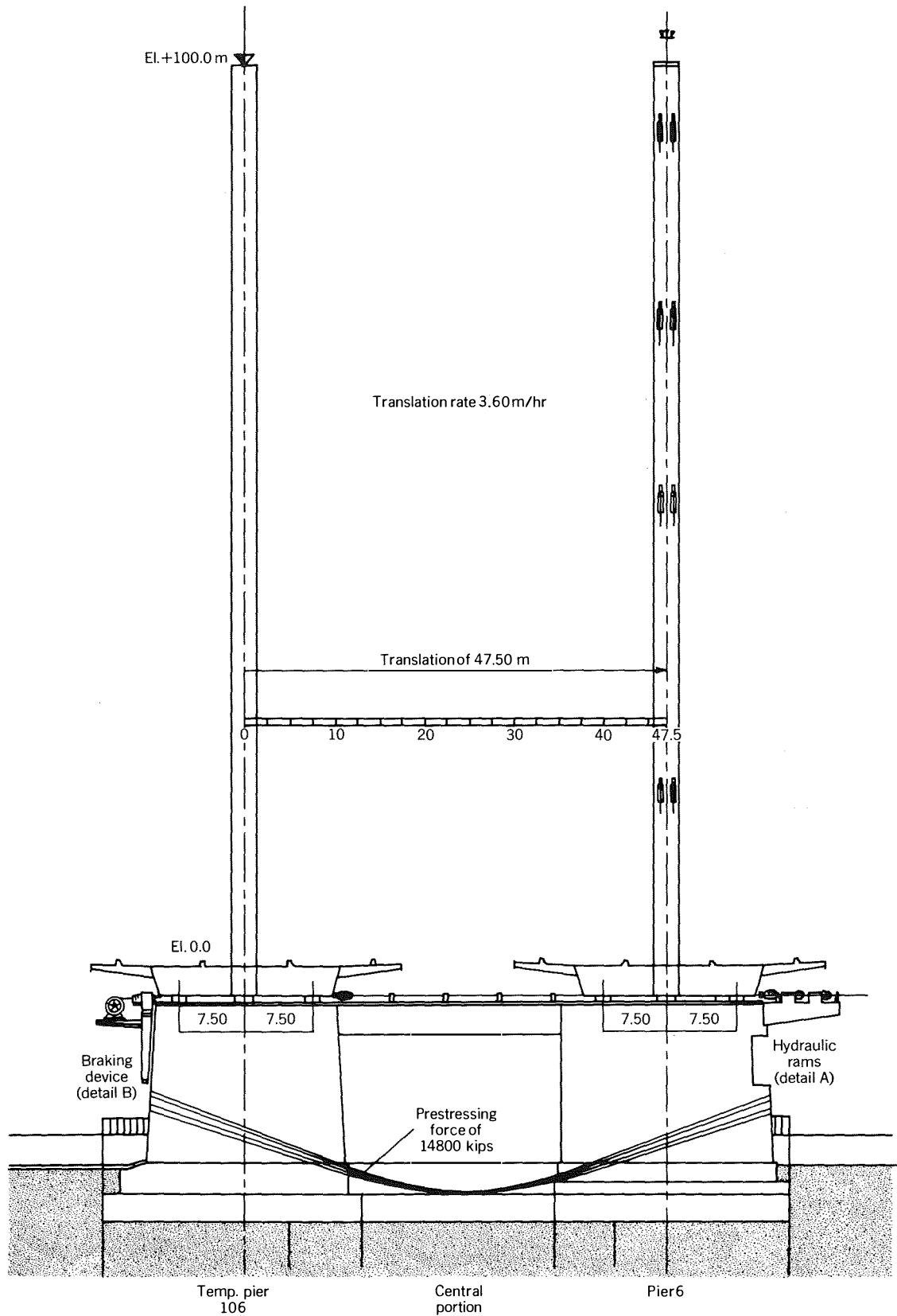


**FIGURE 8.17** Oberkassel Bridge, pylon pier cross section and details, from reference 10, dimensions in meters and millimeters.

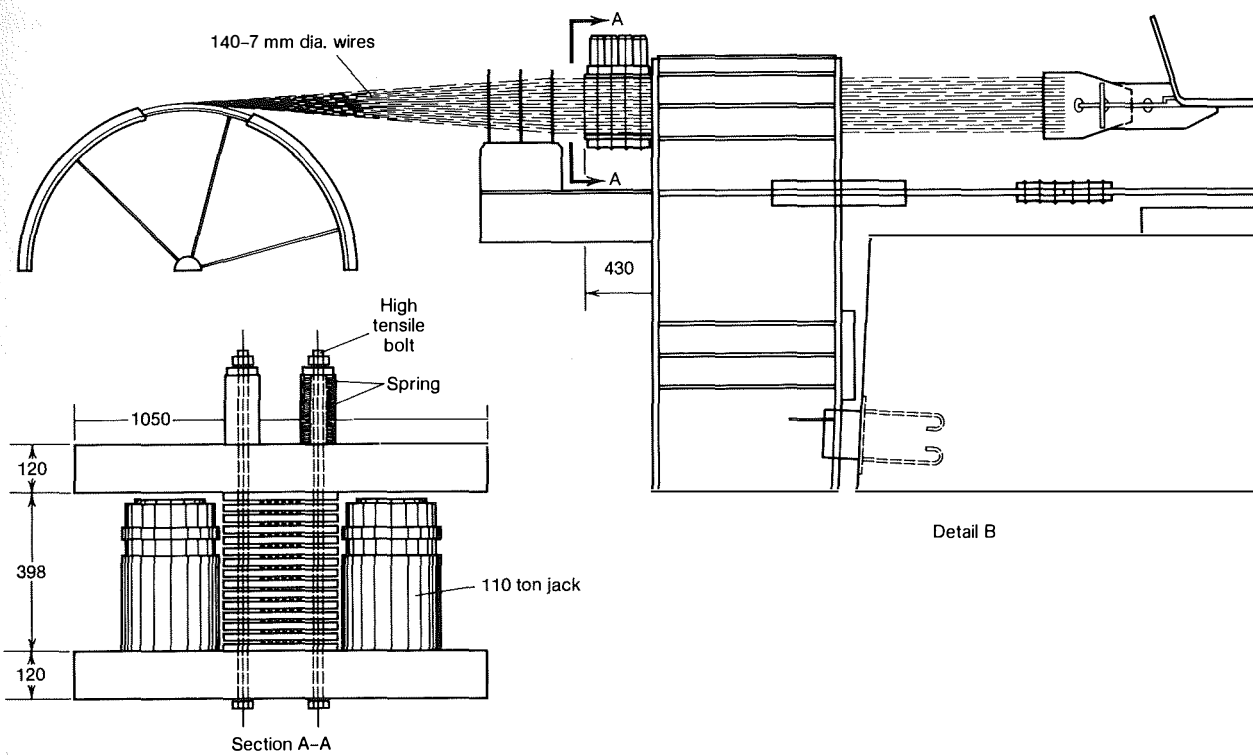
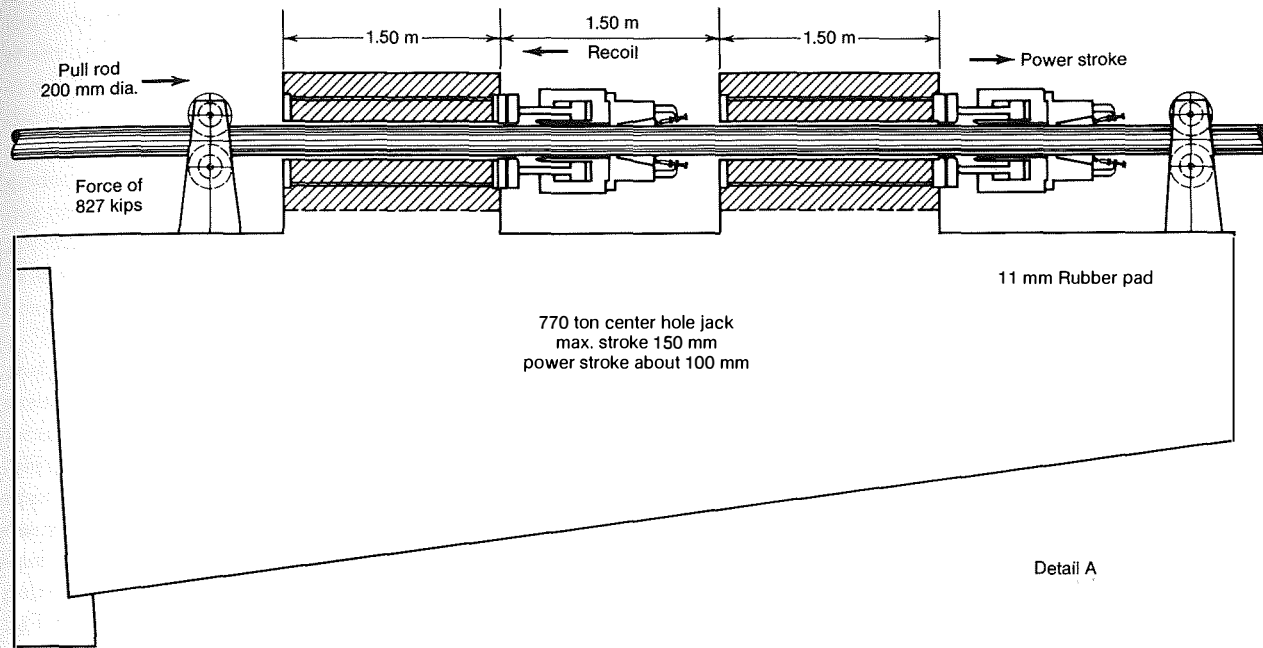
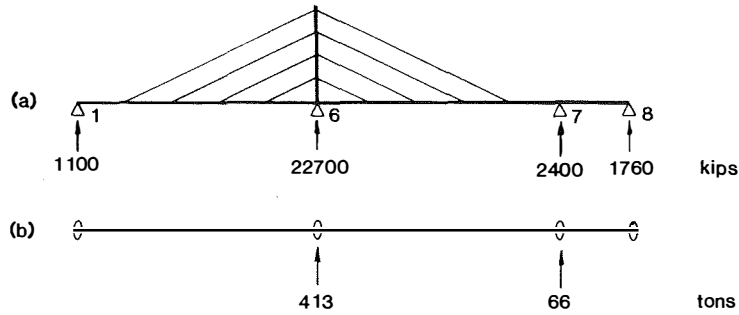


FIGURE 8.17 (Continued)



**FIGURE 8.18** Oberkassel Bridge, schematic of forces: (a) dead load vertical reactions, and (b) lateral tractive forces. (Adapted from reference 10.)

GmbH were consultants for the moving of the bridge, and Hein, Lehmann AG was the contractor.

**8.5 Cantilever Method**

**8.5.1 STRÖMSUND BRIDGE, SWEDEN**

The Strömsund Bridge described in Chapter 5 is notable because it was the first modern cable-stayed bridge. It is a three-span structure with end spans of 242.8 ft

(74 m) each and a center span of 600 ft (183 m), Fig. 1.15. The cable geometry is of the converging type with two vertical planes, one at each side of the roadway deck structure. The portal frame towers are supported at the pier independently of the deck structure, Fig. 5.3. The erection procedure is illustrated in Fig. 8.19.<sup>11</sup> Erection proceeded from both abutments independently of each other with final closure at midspan producing a completed structure.

The end spans were erected to the tower pier with

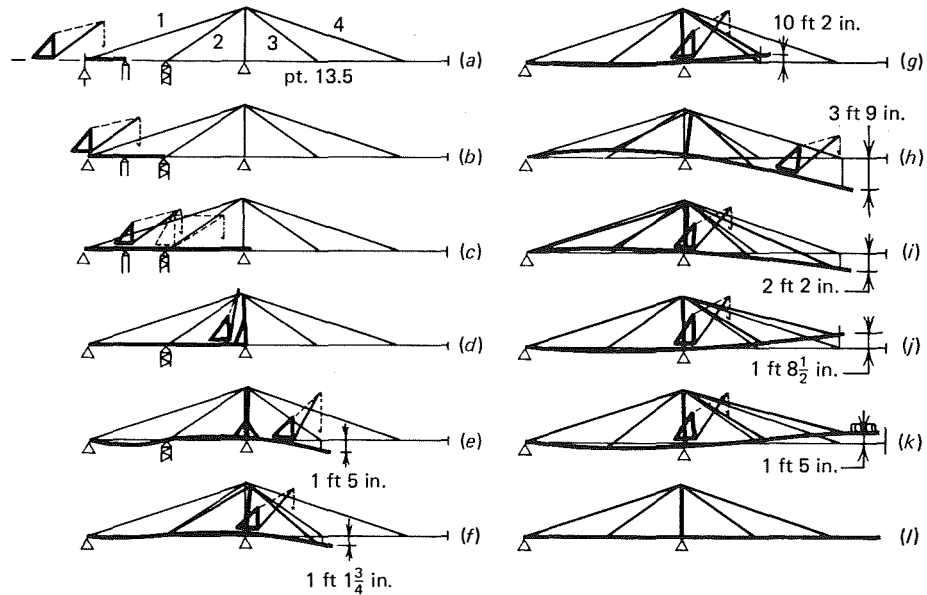


**FIGURE 8.19** Strömsund Bridge, erection sequence: (a) erection up to the first temporary support, (b) erection up to the second temporary support, (c) erection up to the tower pier, (d) erection of the tower and brace against the stiffening girder, (e) erection past point 13.5, the connection of the inside stay 3, (f) derrick moved back to the tower pier. Girder jacked at tower. Erection of the inside stays 2 and 3, (g) inside stays 2 and 3 tensioned, (h) erection past point 18.5, the connection of the outside stay 4, (i) derrick moved back to the tower pier. Stay 4 installation, (j) stay 4 initially tensioned, (k) closure and final tensioning of stay 4, (l) completion of superstructure, concrete slab, and so forth, and final position of the bridge geometry. (Courtesy of Der Stahlbau, from reference 11.)

the help of two false-work bents. After erection of the tower, which was braced against the girder, cantilever erection proceeded to a point just beyond position 13.5, the anchorage point of stay 3. Because of the negative moments developed in the girder at the main pier, the girder is braced against an erection bracket and bearing mounted to the tower leg, Fig. 5.3. Lateral forces are transmitted from the floor beam through the girder bearings which are in lateral contact with the tower bearings.

To decrease the bending in the girder at the tower and also the deflections of the cantilevered girder, the crane is moved back to the tower pier. While at this location, the crane is used to erect the cables of stays 2 and 3 to the top of the tower. The cables are about  $4\frac{3}{4}$  in. (120 mm) shorter than the required lengths under total load to compensate for the tensile elongation under total load. In order to facilitate the installation of the stays, the girder at the tower pier is jacked about 21 in. (550 mm). After installation of the second and third stays, the girder is lowered to its previous posi-

tion. During this phase, with stays 2 and 3 in position, the top of the tower moves approximately 7 in. (180 mm) toward shore. This change in geometry is used to advantage to install stay 1, which had been pre-shortened by  $8\frac{1}{2}$  in. (220 mm). At this stage the erected portion of the suspended structure is relatively stiff because stay 1 is rigidly anchored and supports the force transmitted by stay 3. The derrick is then moved to its previous position at the end of the cantilever and the girder is erected to a point just beyond station 18.5, which is the connection of stay 4 to the girder. The derrick crane is returned to the tower until stay 4 is installed and initially tensioned. Cantilever erection of the girder is then continued until closure is accomplished at midspan. After closure, final tensioning of stay 4 is accomplished. At this time the steel erection is completed. After the concrete deck is poured, final adjustments are made to obtain the desired profile, Fig. 8.20. The deflected positions of the girder and tower at various stages of erection<sup>12</sup> are illustrated in Fig. 8.20.

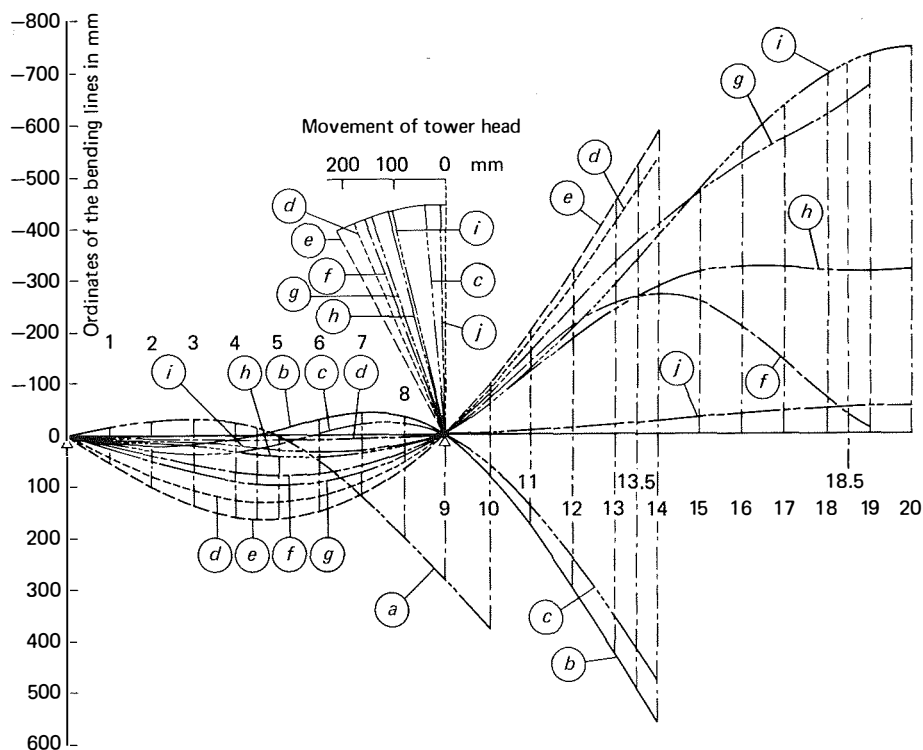


**FIGURE 8.20** Strömsund Bridges, erection displacements: (a) erection to station point 9, (b) erection to station point 13.5, (c) installation of stays 2 and 3, (d) tensioning of stays 2 and 3, (e) tensioning of stay 1, (f) erection to station point 18.5, (g) preliminary tensioning of stay 4, (h) erection to station point 20, (i) final tensioning of stay 4, and (j) final erection condition. (Courtesy of Der Stahlbau, from reference 12.)

## 8.5.2 PAPINEAU-LEBLANC BRIDGE, CANADA

The Papineau-Leblanc Bridge, described in Section 5.14, has an orthotropic deck structure with a single-plane converging cable geometry and consists of a 790-ft (240.8-m) center span and 295-ft (90-m) end spans. Because a greater portion of the bridge is approximately 35 ft (10.7 m) above water, an erection method was developed that utilized a 110-ton (100 mt) stiff-leg derrick mounted on two 60-by-120-ft (18-by-36-m) barges. Limited temporary supports were required. The supports were in the form of a single pile supported bent, driven through fill, and located 87 ft (26.5 m) from each abutment. After erection of the temporary bents on the pile caps, the first two sections of the girder, from abutment to pile cap, were erected in one piece by two crawler cranes on the river banks. The barge-mounted derrick then erected two more sections that cantilevered out approximately 90 ft (27 m) past the pile bent. In this position, the stresses in the deck would not allow any further cantilevering, therefore, the capacity of the barge-mounted derrick was utilized to erect the next three units as a single closure unit to the tower pier, Fig. 8.21. The three units comprising the closure lift were spliced together on the barge before being erected. A "pin" connection was made by inserting a few bolts at the bottom of the web splice at the previously erected deck sections. After alignment of all three webs of the two-cell box girder, the side span was jacked down at the temporary pile bent and

flange splice bolts were inserted as the holes became aligned. All field splices were bolted using ASTM A325 hex head bolts. The remaining bolted splice connections in the bottom flange were accomplished by the use of a traveling platform that was suspended from the deck and traveled beneath the deck,<sup>13,14</sup> Fig. 8.22.

When the side spans were completed, the temporary bents were removed and cantilever erection proceeded to the first main span cable-stay attachment. The sections were placed at the front end of the progressive erection by truck and lifted into position by the barge-mounted derrick. The barge alternated between the north- and south-side erection every two days. In the intervening time the sections already erected were bolted.

The towers are 126 ft (38.4 m) in height and taper from 6 ft sq to 5 ft sq (1.8 and 1.5 m sq) and were erected in two major lifts by a pair of 110-ton (100-mt) mobile cranes resting on the deck, Fig. 8.22. The individual cables of the stays were erected one at a time using the mobile cranes. Tensioning of the stays was performed simultaneously from both ends at the deck anchorage.<sup>15</sup>

Erection of the deck continued by the cantilever method, to the outside stay connection. After erection of the outside stay, cantilever erection continued to closure at midspan.

The sequence of erection of the deck structure was performed in several steps. The center web section weighing 30 tons (27 mt), except at the cable stay an-

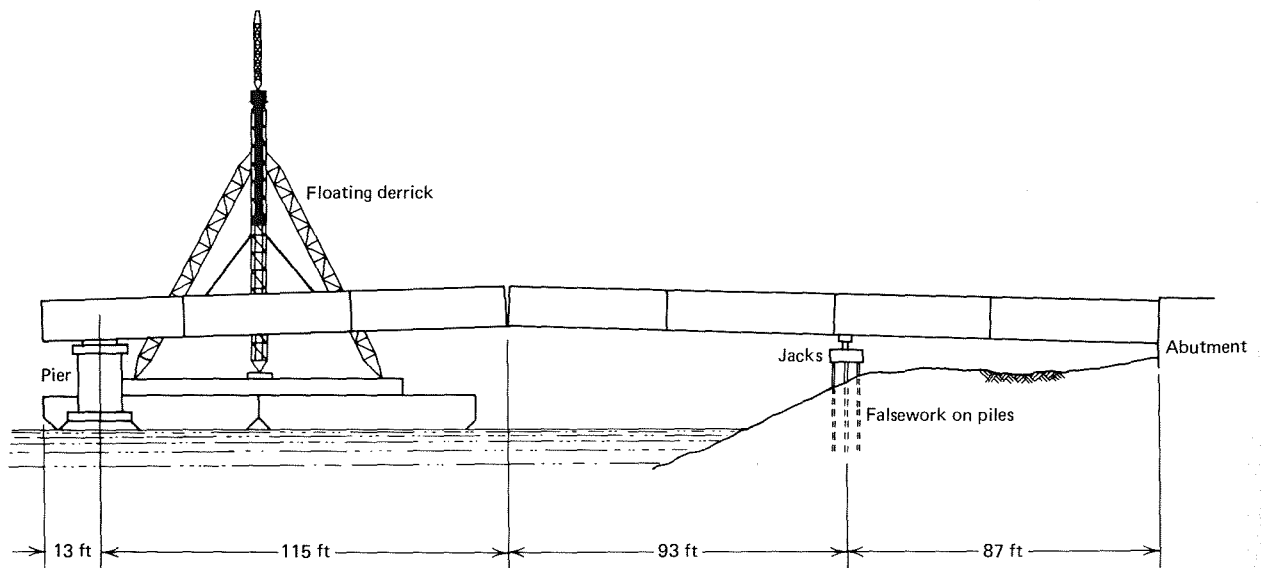


FIGURE 8.21 Papineau-Leblanc Bridge, erection of sidespan closure segment. (Courtesy of Canadian Steel Industries Council, from reference 13.)



**FIGURE 8.22** Papineau-Leblanc Bridge, tower and inside stay erection. (Courtesy of Paul Marquis, Gendron Lefebvre and Associates.)

chorage location where they weighed 45 tons (41 mt), was erected first. The two outside webs, weighing 20 and 25 tons (18 to 23 mt), followed. The bottom panels were placed linking the three webs, and the top orthotropic deck panels were installed completing the box. Finally, the 11- to 14-ton (10- to 13-mt) cantilever overhang of the deck was installed which required careful slope adjustment before final bolting was completed. A computer analysis was performed at various stages of erection to verify tower and girder deflections as well as cable tension values. In this manner the proper distribution of dead load was proportioned to all elements: tower, girder, and stays.<sup>13</sup>

### 8.5.3 SEVERIN BRIDGE, WEST GERMANY

Erection of the Severin Bridge was divided into three principal suberection sequences:<sup>16</sup>

1. Erection of the right-hand Rhine side from abutment to point 18, Fig. 8.23(a)-(h)
2. Erection of the left-hand Rhine side from abutment to point 17, Fig. 8.24(a)-(e)
3. Closure, Fig. 8.25

Erection was essentially by the cantilever construction method with the principal box girders erected in

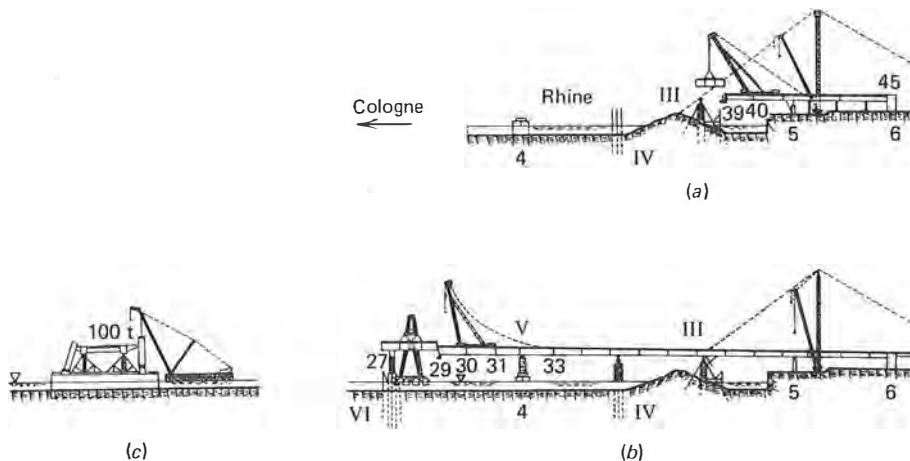


**FIGURE 8.23** Severin Bridge, erection sequence: (a) erection on temporary piers, sections 41-42, 42-43, 43-44, and 44-45. Cantilever erection toward river from panel 40-41, (b) cantilever erection over temporary piers III, IV, and V. Floating crane erection of preassembled sections 27-28-29, (c) erection of the first pylon lift with a floating crane (cross section), (d) cantilever erection over temporary pier VI and pylon erection to 130 ft height, (e) pylon erection to 230 ft height, (f) installation of cables III, IV, and II, V, (g) cantilever erection to temporary pier VII, and (h) installation of cables I and VI. (Courtesy of Der Stahlbau, from reference 16.)





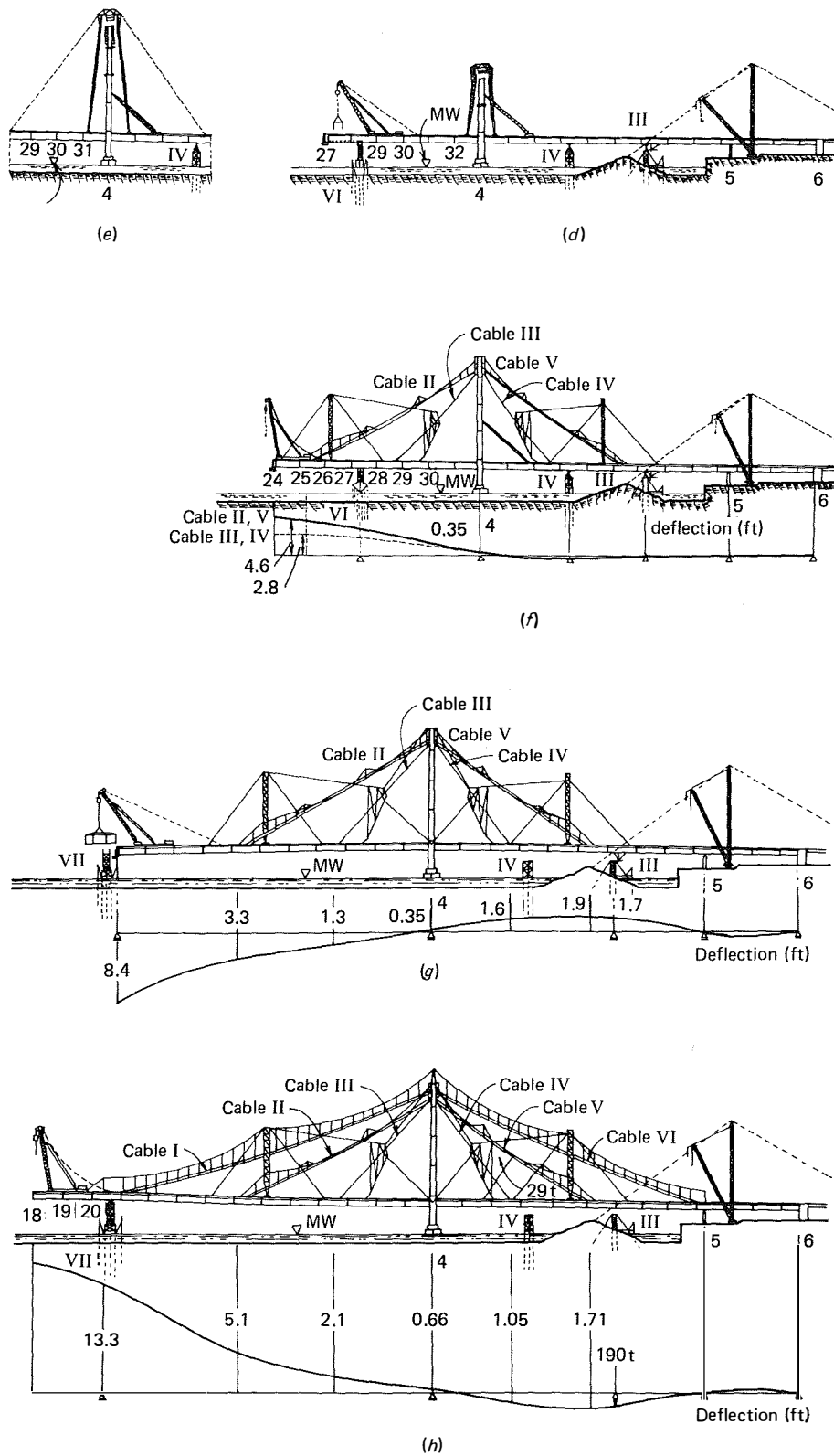
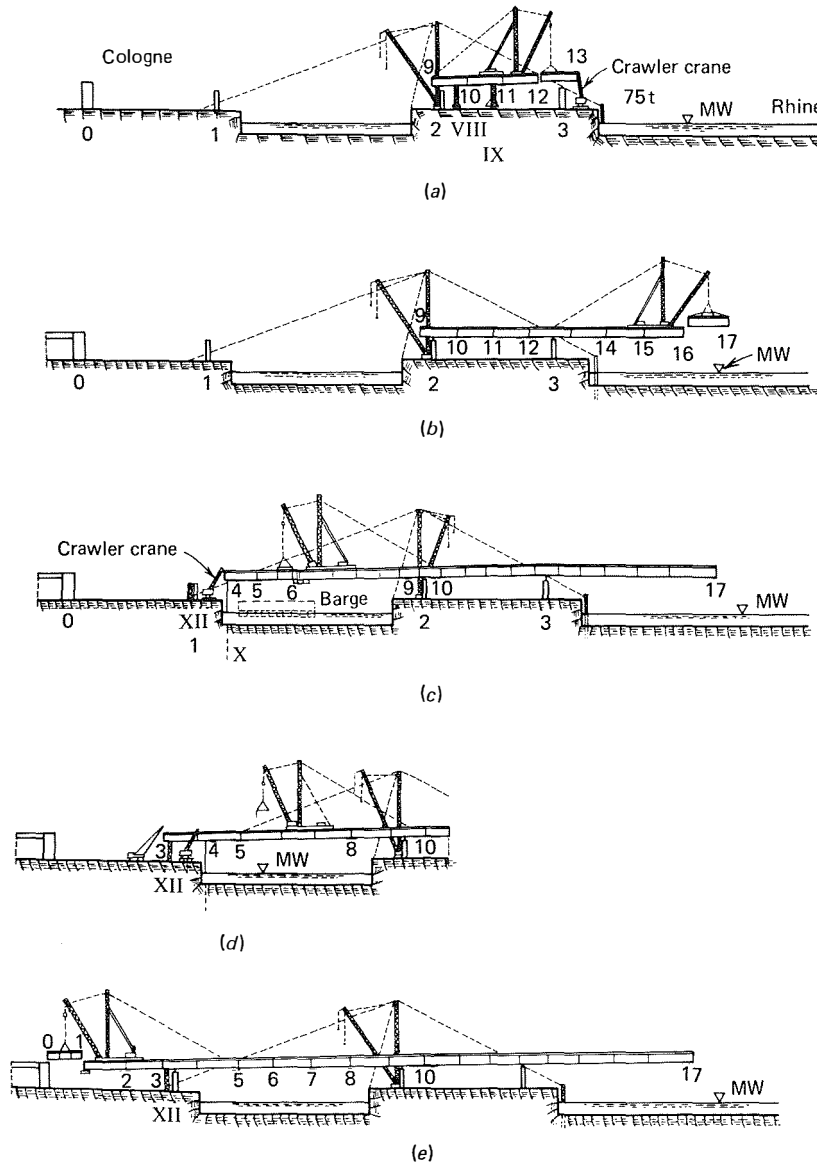


FIGURE 8.23 (Continued)



**FIGURE 8.24** Severin Bridge, erection sequence: (a) erection of section 9-10-11 with derrick, cantilever erection toward river, erection of section 12-13 with aid of crawler crane, (b) cantilever erection to point 17, (c) cantilever erection from point 9 to point 6, section 4-5-6 erected with aid of crawler crane, (d) erection section 3-4 with crawler crane and truck crane, and (e) cantilever erection to abutment 0. (Courtesy of Der Stahlbau, from reference 16.)

successive lengths of 52 ft 6 in. (16 m) and connected by field riveting. The joints between girder segments were prepared during fabrication so that when segments of the girders were joined in the field the proper camber would result. Erection of the center roadway deck between girders and sidewalk sections, which

cantilevered out from the main girders, followed closely behind the erection of the principal girder. The deck sections were shop fabricated in units 52 ft 6 in. (16 m) in length and approximately 21 ft (6.5 m) in width. Three of these units were then field assembled at a preassembly area on a portion of the bridge that had

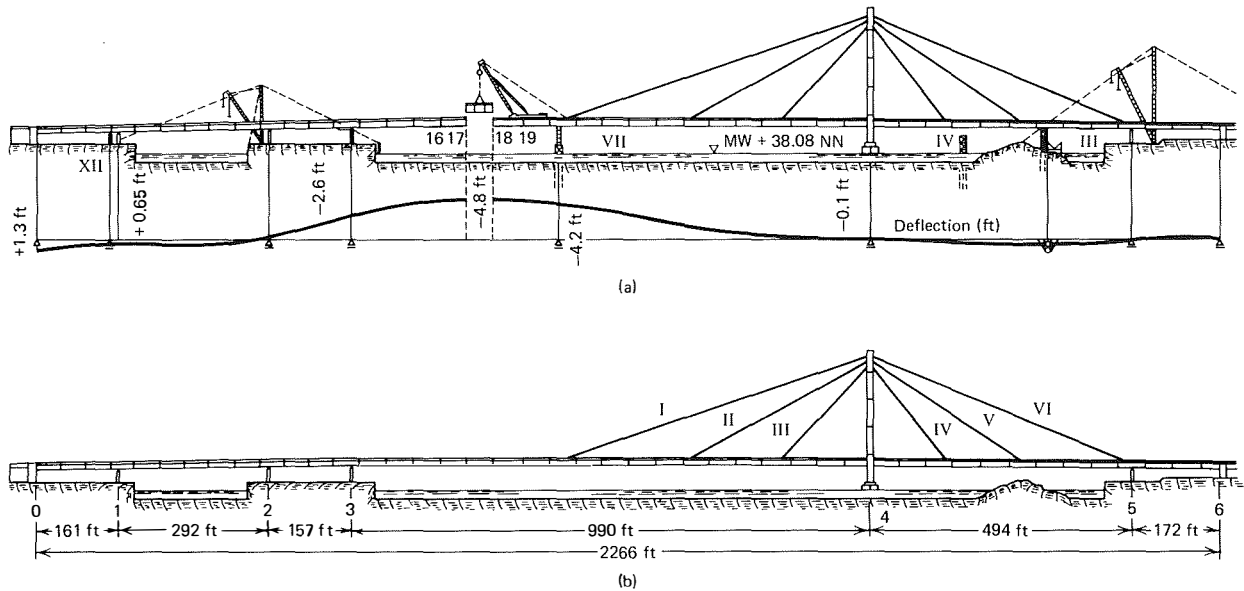


**FIGURE 8.25** Severin Bridge: (a) closure, and (b) completed structure. (Courtesy of *Der Stahlbau*, from reference 16.)

been completed to form a work space of 52 ft 6 in. (16 m) by 62 ft 6 in. (19 m). The two longitudinal joints were field welded and the transverse joints at the cross girders were field riveted. The entire deck unit was then erected between the previously erected principal longitudinal girders. The transverse joint between successively erected deck units were field welded and the longitudinal connection to the girders was field riveted. The longitudinal orthotropic ribs of the deck plate had been fabricated 10 in. (250 mm) short of both ends of the deck plate, leaving a 20-in. (500-mm) gap in the ribs after the transverse joints in the successive deck plates had been welded. These gaps were filled by field welding short portions of ribs that were accurately cut to the required length into position. Ten working days were required to install each 52-ft 6-in. (16-m) length of deck.<sup>17</sup>

Erection of the bridge structure began in April 1958, when pier 5 and three falsework bents were constructed on the right bank of the Rhine River. With the aid of a cable-supported derrick, the suspended structure from point 41 to abutment 6 was then erected, Fig. 8.23(a). At this point, transverse bracing was installed between the two shafts of pier 5 to resist lateral wind forces. The K bracing between the pier 5 shafts had its node point connected to a concrete beam that joined the foundations of the two shafts. A diagonal bracing was also installed from the footing of the shafts to the lower flange of the principal girders to stiffen the structure in the longitudinal direction. Cantilever

construction, with the assistance of temporary piers, was employed from this position to erect the deck structure to point 18. Temporary pier III consists of four vertical piles cross braced for wind forces and eight battered piles to resist other horizontal forces.<sup>16</sup>

Cantilever erection of the suspended structure proceeded from the right bank of the Rhine. Upon reaching permanent pier 4, the pylon pier, temporary support piers held the two principal box girders while cantilever erection of the roadway structure continued and erection of the pylon commenced, Fig. 8.23(b). A floating crane was used to erect the preassembled girder sections 27-28, 28-29 in order not to overstress the previously erected long cantilever superstructure, Fig. 8.23(b). The crane was also used to erect the first two sections of the pylon. Each section weighed 90 tons (81.6 mt), Fig. 8.23(c). The balance of the pylon lifts, which weighed somewhat less, were erected by means of a deck-mounted derrick, Fig. 8.23(d) and (e). The struts between the pylon legs and the deck that stiffen and support the pylon during erection are illustrated in Fig. 8.26. The struts were adjustable such that at the time of erection of the pylon head the legs could be adjusted to compensate for any inaccuracies during fabrication and erection. Provision was also made for a torsional moment to be introduced into the pylon legs to correct for fabrication and erection errors that might occur.<sup>16,17</sup> The cable-stay erection sequence was III-IV, II-V, and I-VI. The cable stays are considerably shorter in an unstressed condition than they are

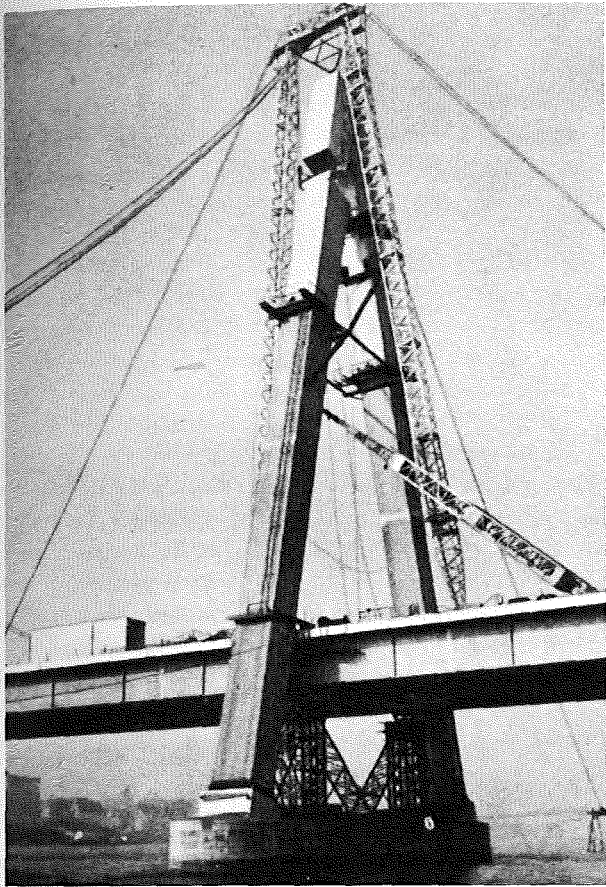


**FIGURE 8.26** Severin Bridge, A-frame pylon erection. (Courtesy of Der Stahlbau, from reference 16.)

in the final stressed condition. To minimize the reduction in cable chord length caused by the cable sag under its own weight, it became necessary to install them as straight as possible into their final alignment. The individual strands of each cable were pulled up along a suspended walkway, Fig. 8.27, and hung in pulley blocks such that they were as straight as possible and approximately in their final geometrical position. A force of approximately 10 tons (9 mt) was required to draw the strands over the deflection bearing (see Chapter 10) to the cross members to which they were anchored. To compensate for the shortened cable length, the structure had to be elevated at the points of cable attachment. For example, the installation of cables I and VI required that the suspended structure be jacked approximately 16 in. (40 cm) and, concurrently, the top of the pylon be displaced toward the abutment by tensioning cable V which had been installed previously.

When erection of the cables was completed and prior

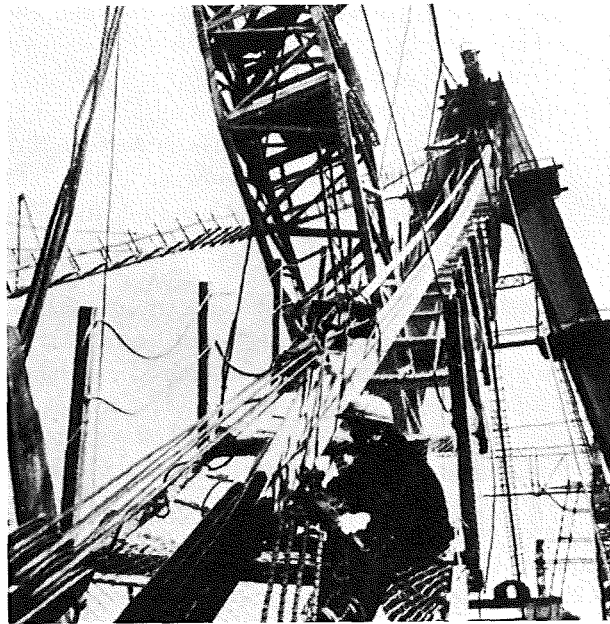


**FIGURE 8.27** Severin Bridge, strand being pulled over the saddle and down the catwalk. (Courtesy of Der Stahlbau, from reference 16.)

to closure, the right-hand portion of the structure had all temporary supports freed. At this time, a check was made to verify that the position of the superstructure was as required by design. This freeing of temporary supports required some minor corrections only at the cable anchorages.<sup>16,17</sup>

Erection on the left-hand side commenced with the erection of that segment of the superstructure between piers 2 and 3, Fig. 8.24. The shafts of pier 2 were cross braced similar to that of pier 5. The superstructure was then cantilevered out over the Rhine approximately 200 ft (60 m). Erection then proceeded in the opposite direction until abutment 0 was reached. Erection of the structure was completed in September 1959 with the installation of the closure girders 17-18, Fig. 8.25(a).

#### 8.5.4 BATMAN BRIDGE, AUSTRALIA

The intended sequence for the Batman Bridge (see Section 5.18) was as follows,<sup>18</sup> Fig. 5.32:

1. Erect the truss superstructure from the west abutment to the intersection of the superstructure with the pylon.
2. From the east abutment, erect the truss superstructure westward to an expansion joint 56 ft 3 in. (17 m) west of the first pier on the east shore.

3. While the trusses are being erected on the east shore, erect the pylon to its full height and install the permanent back stays.
4. Upon completion of the erection of the east shore and the pylon, extend the trusses eastward from the pylon to the expansion joint.
5. Erect and weld the deck and handrails following the truss erection from each side of the river.

Completed sections of the stiffening truss, which are 45 ft (13.7 m) in length including all lateral bracing and secondary members, were assembled and bolted with friction grip bolts prior to erection. Each section weighed approximately 55 tons. The first section was erected in place spanning from the west abutment to a temporary steel pier. A special erection frame was mounted on the top of the truss section to erect subsequent 45-ft (13.7-m) preassembled sections, Fig. 8.28. The next truss section was cantilevered from the first temporary pier. The subsequent section was erected to extend from the cantilever end to a second temporary pier. The first temporary pier was then removed, producing a 135-ft (41-m) span from the abutment to the second temporary pier. The second temporary pier was such that its legs straddled the width of the pier. In the same manner subsequent truss sections were transported down the bank on a rail-mounted carriage, passed through the second temporary pier, and were lifted by the erection frame and

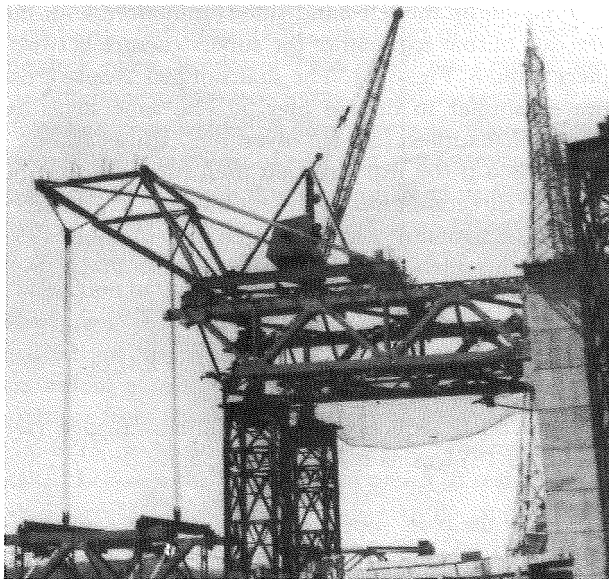


**FIGURE 8.28** Batman Bridge, erection frame on bridge section 1. (Courtesy of Department of Public Works, Tasmania, from reference 18.)

cantilevered outwardly. An additional 45-ft (13.7-m) section was cantilevered from temporary pier 2 to produce a section 180 ft (55 m) in length from the abutment to the pylon intersection.<sup>19</sup>

The pylon consists of 40 segments, each approximately 15 ft (4.5 m) in length. For the first nine sections of each pylon leg the cross beam and cross bracing were erected from a crane mounted on the trusses. When the pylon reached truss elevation, the trusses were raised from the temporary piers by jacks placed on the pylon cross beam. When the temporary pier was removed, the truss was anchored to the abutment and the other end was lowered onto bearings on the pylon cross beam. As the pylon construction rose above the main trusses, the crane used for pylon erection was mounted on a platform on rails attached to the west face of the pylon. The crane in this position proceeded to climb up the pylon erecting two sections on each leg ahead as it climbed, Fig. 8.29. Each pylon unit was lowered down the west bank on temporary rail tracks, taken through the pylon legs, and raised into position. Temporary back stays, connected to anchorages that were held down by prestressed rock-anchored cables grouted into the bed rock, were installed at various positions to stabilize the leaning pylon until the permanent back stays were installed at the completion of the pylon erection.

While the pylon was under construction, the bridge truss erection proceeded westward from the east abutment in a similar manner to that of the west side. After assembling an erection frame on the first truss section spanning from the east abutment to a temporary pier, complete bridge sections were alternately cantilevered forward. Additional sections were added to span onto temporary piers, Fig. 8.30. At this time erection of deck units proceeded from the east abutment, and each unit was fully site welded to the preceding unit.<sup>18,19</sup>

Because some pylon units arrived late at the job site, the truss on the west side was erected 90 ft (27 m) past the pylon. After the back stays were installed, the erection of the trusses proceeded across the river from the west side. Assembled bridge sections were lowered down the west bank, passed through the pylon legs, lifted to the underside of the truss and suspended from a monorail system attached to the underside of the trusses. The assembly was moved out to the erection face and positioned by the erection frame, Fig. 8.31.<sup>18,19</sup> The bridge sections were cantilevered 90 ft (27 m). A temporary fore stay from the pylon top was installed and the elevation of the leading end of the truss raised to a predetermined level. Two additional truss sections were cantilevered from the temporary



**FIGURE 8.29** Batman Bridge, climbing crane on pylon. (Courtesy of Department of Public Works, Tasmania, from reference 18.)

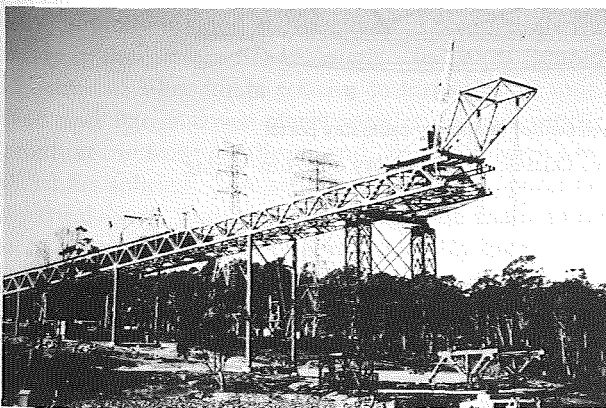


**FIGURE 8.30** Batman Bridge, truss erection, east side. (Courtesy of Department of Public Works, Tasmania, from reference 18.)

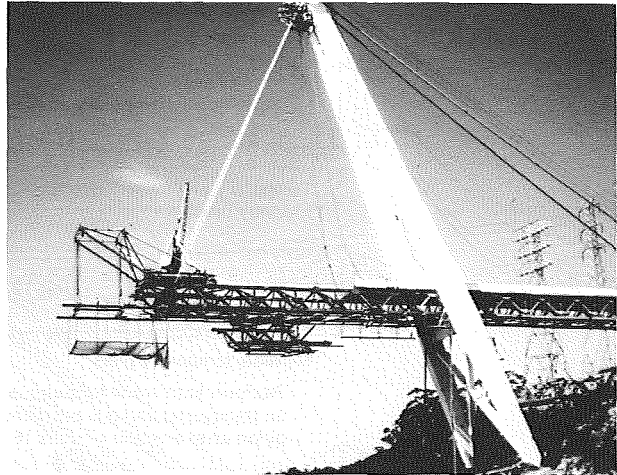


**FIGURE 8.31** Batman Bridge, cantilever erection of truss from pylon. (Courtesy of Department of Public Works, Tasmania, from reference 18.)

fore stay, and a permanent fore stay was attached. This procedure was repeated with temporary fore stays attached at three points between the permanent fore stays.

Throughout erection a careful check of the stresses in the forestays and principal truss members was maintained. Deck erection followed the truss erection in a prescribed pattern to avoid overstressing the structure.

Subsequent to the installation of handrails and road surfacing, the tension in all fore stays and reactions of the truss at the expansion joint and pylon were adjusted to obtain the required load distribution.

#### 8.5.5 KNEIBRÜCKE BRIDGE, WEST GERMANY

The Kniebrücke Bridge was erected by the cantilever method starting at the left bank of the Rhine River, Fig. 8.32. Unlike the Severin Bridge, the 1050 ft (320 m) river span was erected without resorting to the use of temporary supports, which would have impeded navigation in the channel. The erection procedure is summarized in Fig. 8.32.<sup>20</sup>

The roadway superstructure is divided into 34 longitudinal sections varying in length from 46 ft 6 in. to 63 ft 6 in. (14.18 to 19.36 m). The pylon was divided into 15 units for the inside cell adjacent to the deck and 10 units for the outside cell. The inside cells varied in length from 20 ft 4 in. to 30 ft 10 in. (6.2 to 9.38 m). The joints of the inside and outside cells are staggered in relation to each other as a result of the overlap of 3 ft 3½ in. (1.0 m) Fig. 5.23.<sup>21</sup>

The superstructure was delivered to the site in seven

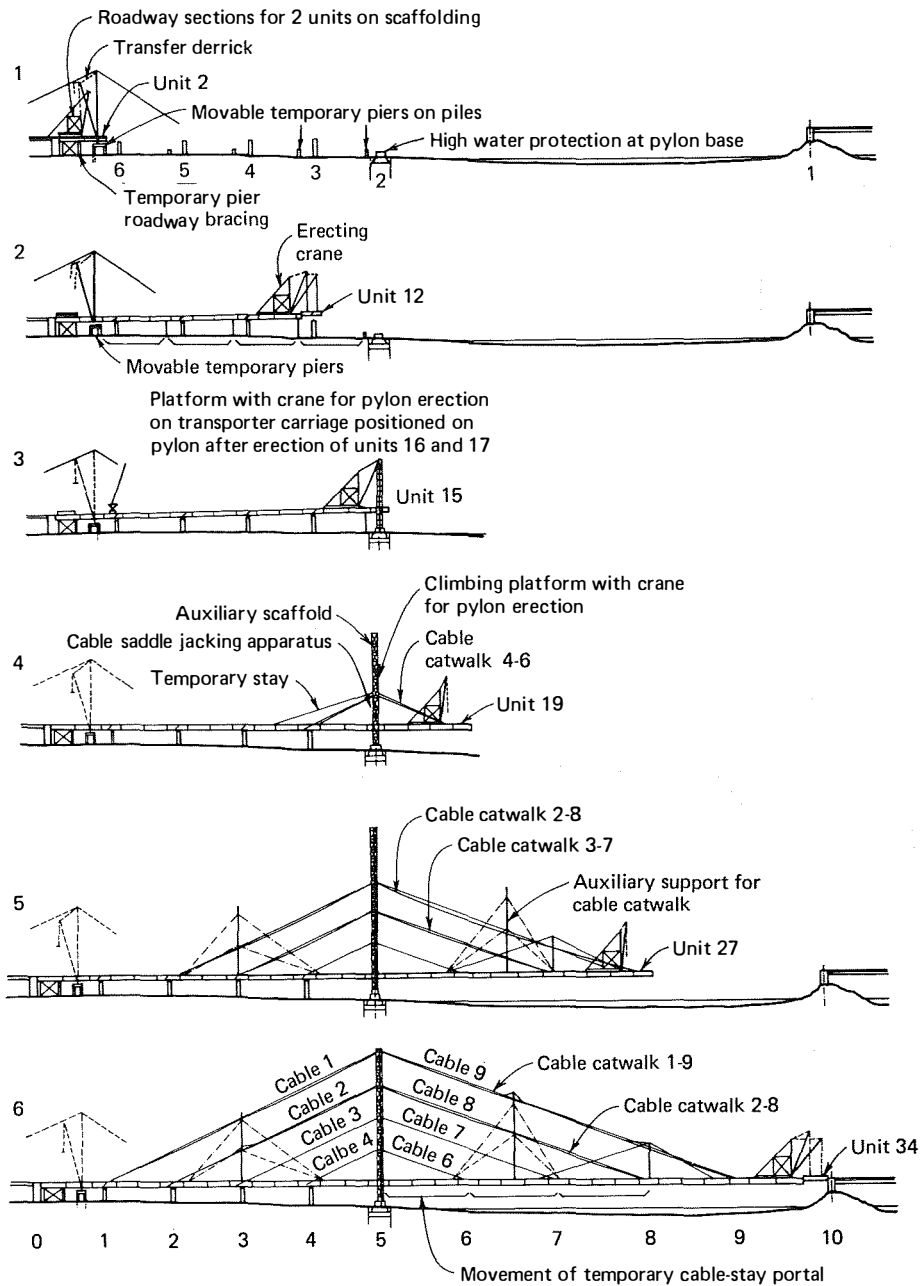


**FIGURE 8.32** Kniebrücke, erection sequence, Düsseldorf. (Courtesy of Beton-Verlag GmbH, Düsseldorf, from reference 20.)

subassemblies: two main girder elements consisting of the bottom flange, web, roadway strip adjacent to the girder, and walkway strip; the three center roadway sections; and the two walkway assemblies. Additional secondary units consisted of the diaphragms and cantilever diaphragm sections, Fig. 8.33.

A preassembly and storage area was located on the left bank of the river. A transfer derrick was used to

move the materials from the preassembly area to the bridge deck. The same derrick was used to erect the first two deck units, which were supported on falsework, and install on this portion of the superstructure an erecting crane for the cantilever erection procedure. This portion of the deck also served, throughout the entire erection procedure, as a work area to assemble the three center roadway units.

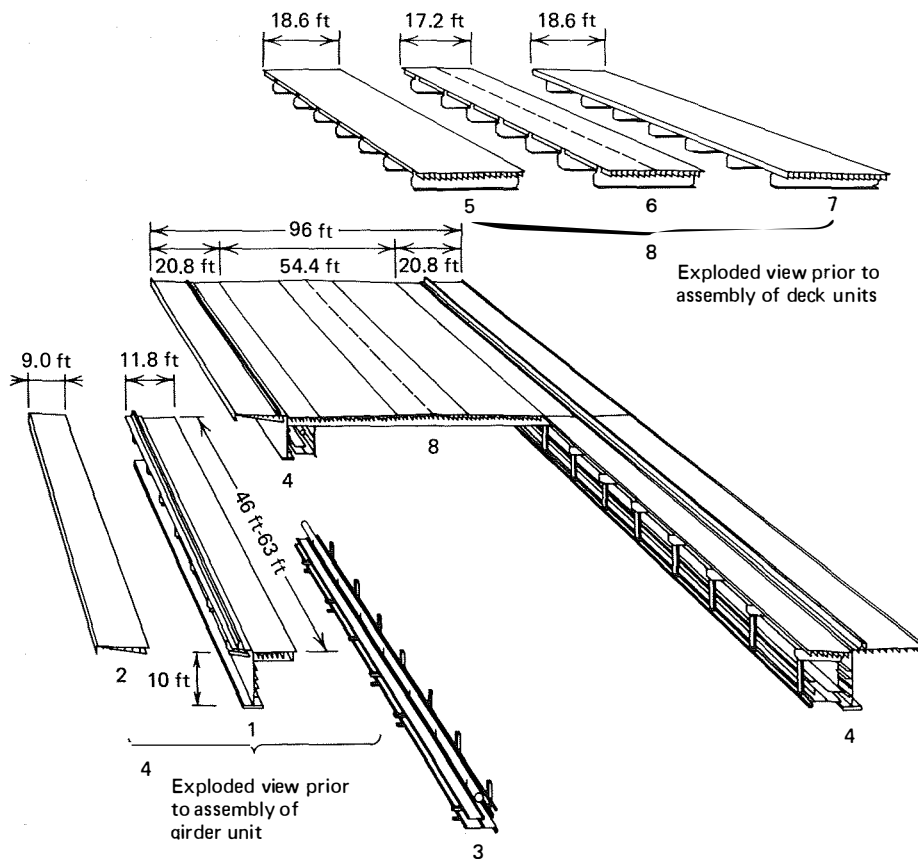


**FIGURE 8.33** Kniebrücke, isometric view of erection components of the superstructure Düsseldorf. (Courtesy of Beton-Verlag GmbH, Düsseldorf, from reference 20.)

In the preassembly area, the main girder units were assembled to the walkway units and necessary field adjustments were made at the main splices for the cantilever erection. The main splices, referred to as universal splices, extended across the full cross-sectional width of the decks. During this operation, rivet holes were carefully reamed at the splices to compensate for errors in the bottom flange length. Necessary camber adjustments were made relative to the adjacent unit. Web and flange cover plates were cut to the proper length at the front cantilever end, and units were prepared for splicing. The service walkway, supports for electrical lines, and stormwater and gas main pipes were installed in the units at the assembly area.

On the left bank the superstructure was supported on tension-pendulum piers, which stiffened the river span by supporting the component from the cable stays, Fig. 5.22. Cantilever erection of the principal girder units in this area of the structure was assisted by a pair of movable auxiliary supports, Fig. 8.34. These units, successively placed approximately 40 ft (12 m) in front of the piers and the pylon, shortened

the cantilever and provided the clearance whereby the sections could be adjusted for level. A similar procedure was used in erecting the river span with a movable auxiliary cable-stay system supported by a pair of

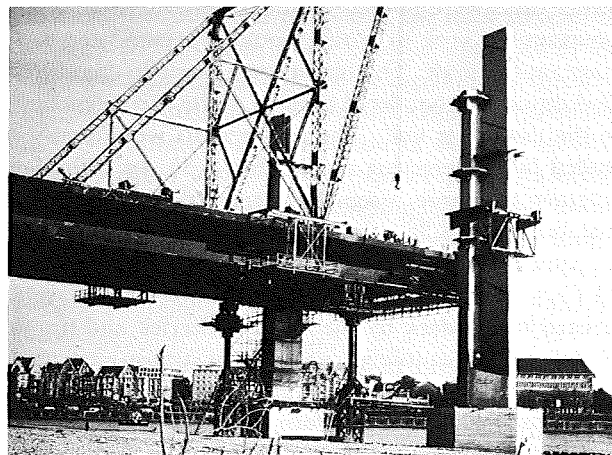


**FIGURE 8.34** Kniebrücke, erection to pylon, Düsseldorf. (Courtesy of Beton-Verlag GmbH, Düsseldorf, from reference 20.)



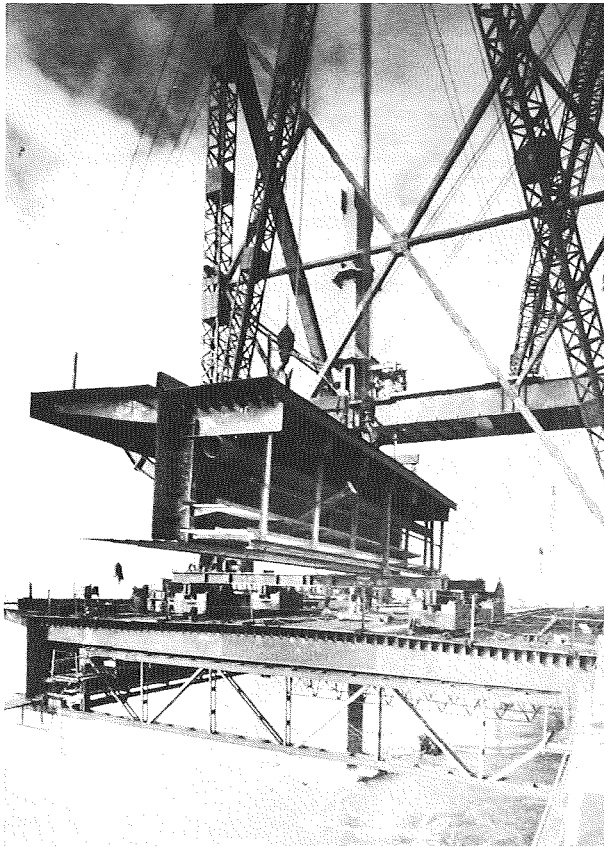


**FIGURE 8.35** Kniebrücke, cantilever erection of girder units. (Courtesy of Beton-Verlag GmbH, Düsseldorf, from reference 20.)

masts, Fig. 8.32. The masts were successively located at the cable attachment points to the deck.<sup>20,21</sup>

In the cantilever erection procedure, the two main girder units were hoisted by the transfer derrick at the preassembly area to a rail-mounted transporter carriage on the deck. The transporter carriage then traveled down the completed portion of the superstructure to the cantilever end. The girder units were then installed by the erecting crane, Fig. 8.35. In a similar manner the three assembled center deck units were installed, Fig. 8.36.

After the superstructure had been erected to point 14 (just behind the pylon) the pylon cell units were hoisted to the deck by the transfer derrick and transported to the cantilever end by the transporter carriage. When the pylon base units were installed, they were posttensioned to the foundation. The bases were adjusted by jacks, previously installed beneath them; when the bases were at the proper elevation, they were filled with concrete and all the tendons were tensioned. The derrick erected the pylon to a height of 150 ft (46

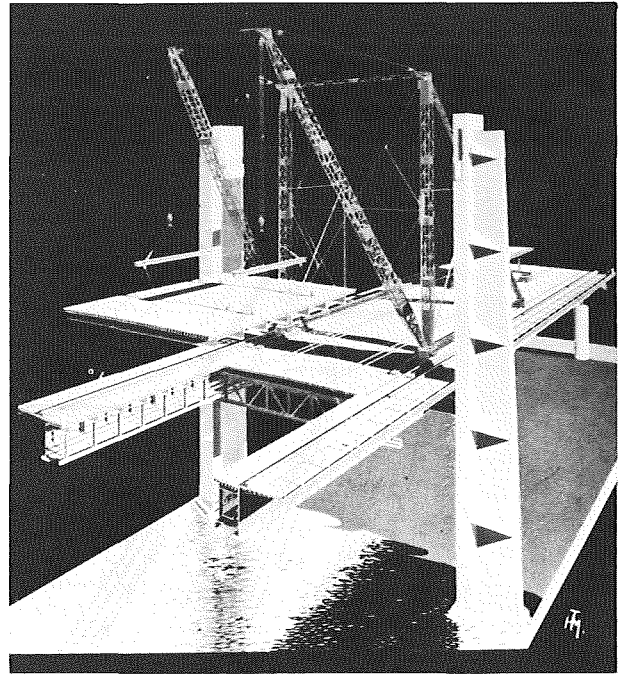


**FIGURE 8.36** Kniebrücke, isometric model of erection, Düsseldorf. (Courtesy of Beton-Verlag GmbH, Düsseldorf, from reference 20.)

m). After the deck structure unit was cantilevered beyond the pylon, the erecting crane traveled out upon it and proceeded with the remaining superstructure erection. At this point erection of the pylon proceeded by a crane mounted on a climbing platform that traveled up the pylon as it increased in height. The pylon erection to full height was completed prior to the installation of the cable stay from the bottom.<sup>20,21</sup>

To facilitate the installation of the cable stays, the saddles were initially positioned lower than their final position and were also displaced in a longitudinal direction. Portable jacks located under the end beam of the bearing girder, which cantilevered on each side beyond the pylon, allowed the saddles to be jacked to their specified elevation after the stays were installed, Fig. 8.37. Jacks placed between saddles and bearing girder controlled the sliding or longitudinal movement of the saddle. Cables were erected using suspended catwalks. With the exception of the bottom pair of catwalks and the second one in the side-span, all catwalks received additional support from a stayed portal frame resting on rocker supports. The top cable in the river span received additional support from auxiliary cable stays. The first strand of the 13 strands comprising each stay was carefully positioned to serve as a guide for the following 12 strands.

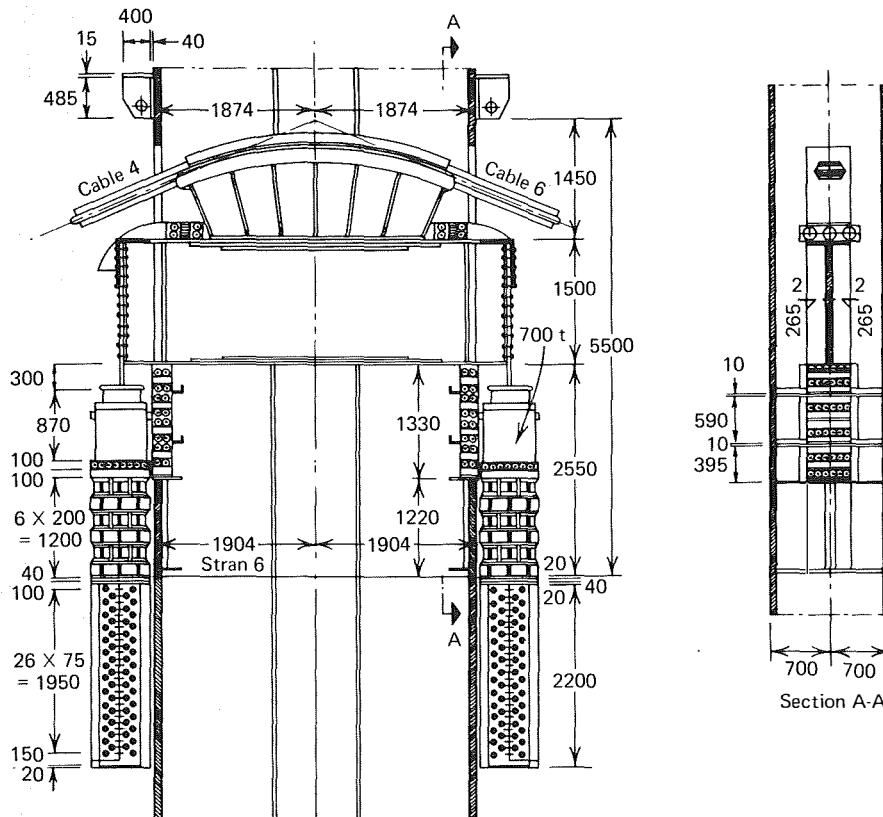


**FIGURE 8.37** Kniebrücke, jacking mechanism at the cable saddle bearing, Düsseldorf. (Courtesy of Beton-Verlag GmbH, Düsseldorf, from reference 20.)

### 8.5.6 LAKE MARACAIBO BRIDGE, VENEZUELA

The general structural configuration of the Lake Maracaibo Bridge (also called the General Rafeal Urdaneta Bridge) was presented in Chapter 4. This section discusses the construction features of the 771-ft (235-m) main span units, Fig. 4.1. The material and illustrations presented have been extracted from reference 22 through the courtesy of Julius Berger-Bauboag Aktiengesellschaft, Wiesbaden. During construction, structural analyses were performed for the various stages of the erection process. It is interesting to note that the erection analysis involved five times more effort than was required for the design of the structure.

Approximately 13,080 yd<sup>3</sup> (10,000 m<sup>3</sup>) of the concrete and 882 tons (800 mt) of reinforcing steel were required to construct a pier, tower, and a continuous cantilever girder. The materials had to be transported 303.5 ft (92.5 m) vertically for the tower and 308 ft (94 m) horizontally at the end of the 131-ft (40-m) jib with a 226-ft (69-m) hook height. For construction of the upper half of the pylon, the main tower crane was extended to a hook height of 321 ft (98 m). The second

tower crane was located on the opposite side of the pile cap and was used for placing and removing formwork as well as placing reinforcement and concrete for the X-frames and the lower half of the A-frame pylon. Additional tower cranes were positioned on the service trusses of the cantilever portion of the deck structure. In Fig. 8.38, the main tower crane is extended to its full height. The crane and the next pylon has the service girder in position with a tower crane mounted on it. Also illustrated is the erection of the rear service girder, a pylon with the pier cap completed, a small tower crane ready for dismantling, and two tower cranes pouring concrete for the X-frames and the lower half of the next A-frame pylon. All tower cranes were assembled on shore and positioned as a unit by floating cranes.

Temporary bracing was required during the various erection stages to maintain deformations and stresses within allowable limits. Concrete for the X-frame and the lower half of the A-frame pylon (see Section 4.2) was poured simultaneously. The concrete pouring sequence for the X-frame is indicated in Fig. 8.39. Before concreting section 4, inclined braces were installed

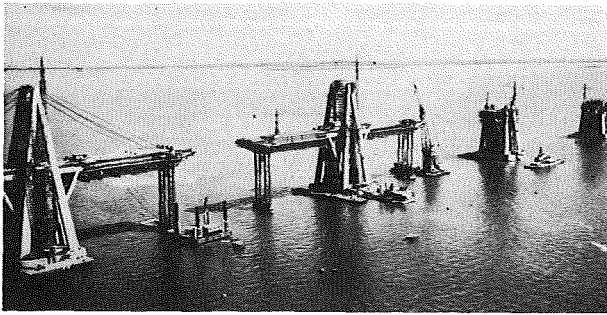


**FIGURE 8.38** Lake Maracaibo Bridge, various stages of erection. (Courtesy of Julius Berger-Bauboag Aktiengesellschaft, from reference 22.)

for each leg until section 8 was completed. After completion of section 13 and prior to pouring section 15, the X-frame outer legs were tied together by six prestressed 1-in-diameter (26-mm) high-tensile steel bars, which were tensioned to the required load. Stresses in the rods were continuously monitored and adjusted by jacks as required. For each X-frame interior leg, two braces were required; each brace had 18 tons of jack pressure before placement of the transverse cross beam and 35 tons after placement.

The legs of the A-frame tower are of varying dimensions in cross section, decreasing from bottom to top. Because of this shape the formwork and reinforcement required a close check of alignment. Therefore, the formwork for the A-frame pylon also required bracing similar to the legs of the X-frames. The legs of the X-frames were erected before the legs of the A-

frame and could be used to brace the A-frame. Erection sequence of the A-frame is illustrated in Fig. 8.40. After erection of section 5, a longitudinal brace and transverse braces were installed between the A- and X-frames. Upon completion of section 9, transverse braces were installed at the section. After section 15 was completed and permanent longitudinal and transverse beams were in place, transverse bracing was installed at section 15. After completion of section 18, additional transverse bracing was installed at this elevation.

The pier cap is a three-cell box section 16.4 ft (5 m) in depth, 46.7 ft (14.22 m) in width, and 159.3 ft (48.55 m) in length, Figs. 4.10 and 4.11. The X-frame legs were continued into the pier cap to act as a transverse diaphragm. Upon completion of the pier cap, the service girders for the cantilever portion of the deck structure were hoisted into position. As a result of the additional moment produced during this stage of erection additional concentric prestressing was required in the pier cap, Fig. 4.11. Additionally, because the wet weight of the cantilever and dead load could overstress the X-frames during construction before the cable stay was installed, temporary horizontal ties, tensioned by hydraulic jacks, were required, Fig. 4.11.

To form the 236-ft (72-m) long cantilever girders, special steel trusses were used to support the formwork and wet weight of concrete. These service girders were supported on one end by the completed pier cap and on the other end by temporary rocking piers supported on auxiliary foundations, Fig. 8.38. The cantilever girder is a four-cell box, 16.4 ft (5 m) deep with 9.8-

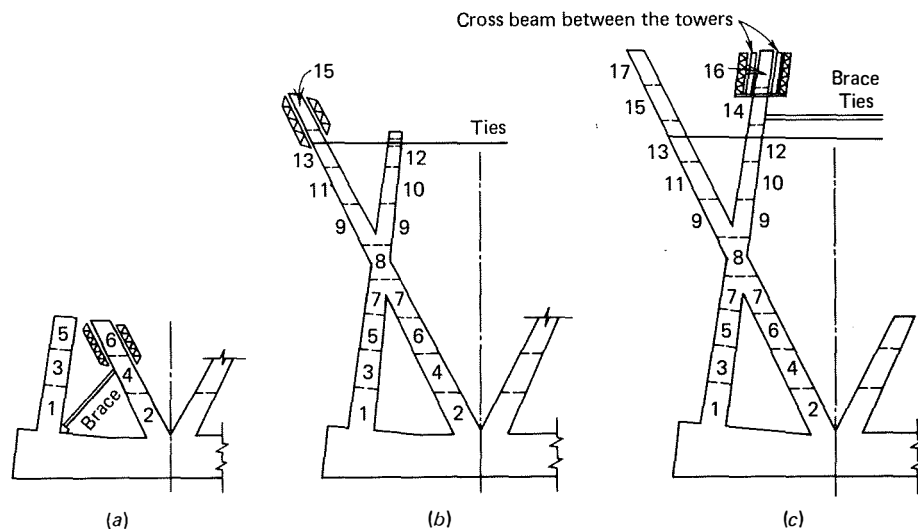


**FIGURE 8.39** (a)-(c) Lake Maracaibo Bridge, erection sequence at X-frames. (Courtesy of Julius Berger-Bauboag Aktiengesellschaft, from reference 22.)

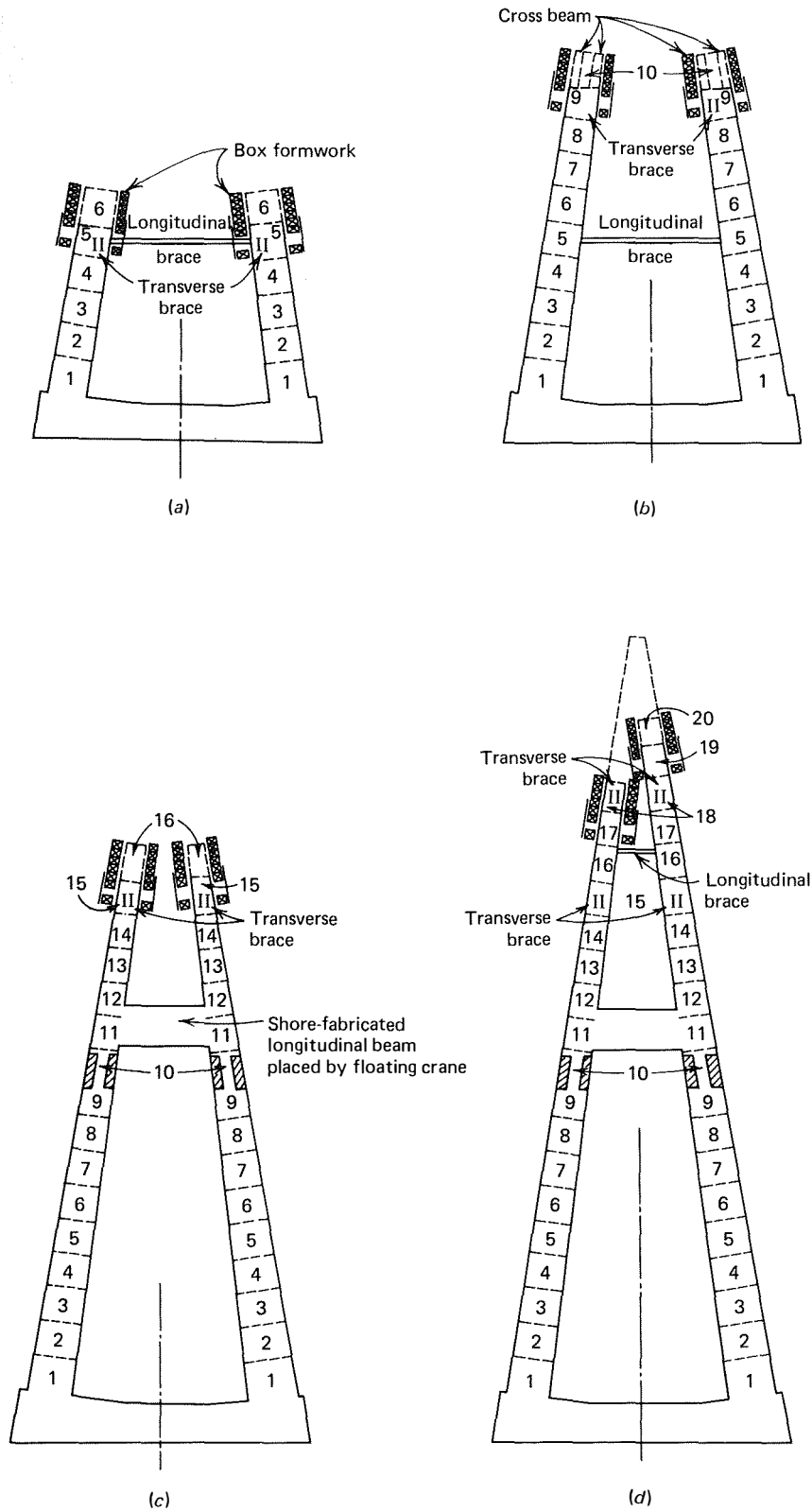


**FIGURE 8.40** (a)-(d) Lake Maracaibo Bridge, erection sequence of A-frames. (Courtesy of Julius Berger-Bauboag Aktiengesellschaft, from reference 22.)

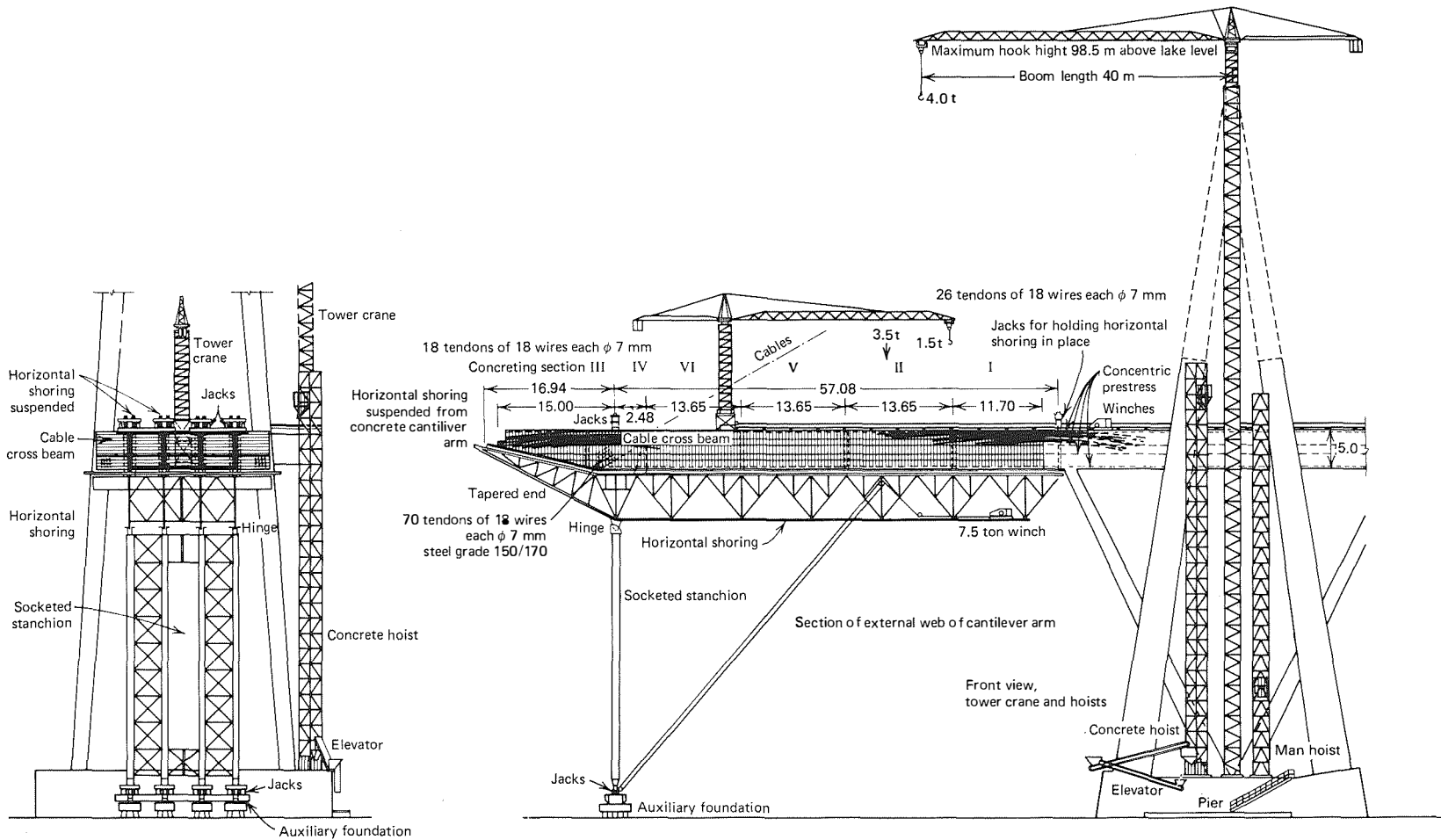


**FIGURE 8.41** Lake Maracaibo Bridge, cantilever girder construction. (Courtesy of Julius Berger-Bauboag Aktiengesellschaft, from reference 22.)

in (25-cm) thick webs. It was poured in six sections in the numerical sequence indicated in Fig. 8.41 to equalize deformations during the concreting operations. The sequence of pouring was established to avoid overstressing the pier and cap. Joints of 2 ft 6 in. (75 cm) were left open between the sections. On completion of the last section, the service girder was raised or lowered to its proper elevation by hydraulic jacks located under the rocking piers, and the joints between the cantilever girder sections were poured. A floating concrete mixing plant was anchored alongside the pier where concrete was raised by a hoist and conveyed by power buggies to the tower crane and poured into place, Fig. 8.41.

The transverse cable-stay anchorage girder is 73.8 ft (22.5 m) in length and has its cross section oriented to the inclination of the stays. The 60-ton (54 mt) reinforcing cage was fabricated on shore in its proper orientation, Fig. 4.12, and contained the 70 prestress tendons, mild reinforcement, and thick-walled steel pipes for housing the strands of the cable stay. A steel spreader bar was used to erect the prefabricated cage into its position in the structure to be ready for concrete placement.

Catwalks, which were used to facilitate the installation of the strands of the cable-stay, were prefabricated on shore, barged to piers, and placed on the pier caps by a floating crane. One end of the catwalk was raised by winches to the top of the pylon and anchored; the other end was pulled to the anchorage girder and fixed at that location, Fig. 8.42. The strands were delivered to the erection site in 13-ft (4-m) to 16-ft (5-m) coils, unreel on the surface of the roadway girder, checked for length, cleaned, and given a prime coat. The strands were threaded into pipes in an anchorage girder, pulled up the catwalk to a roller saddle support provided for mounting purposes on the top of the pylon, pulled down the catwalk on the other side, and threaded into the pipes of the opposite anchor girder.

The strands at the anchorage girder are arranged in a grid of 4 by 4 while at the pylon saddle they are arranged in two layers of eight each. Two to three strands were erected during the day and stretched at night to minimize the effect of thermal expansion of the strands. Each strand was initially tensioned by a hand winch and jacked to an amount that caused the strand socket to project out of the anchorage girder approximately 6 in. (150 mm). The sockets have internal threads to accept the jacking screws. Two 250-ton jacks, Fig. 8.43, pull the strand out enough that a  $3\frac{1}{8}$ -in. (80-mm) thick washer can be inserted between the anchorage girder and the strand socket. The strand

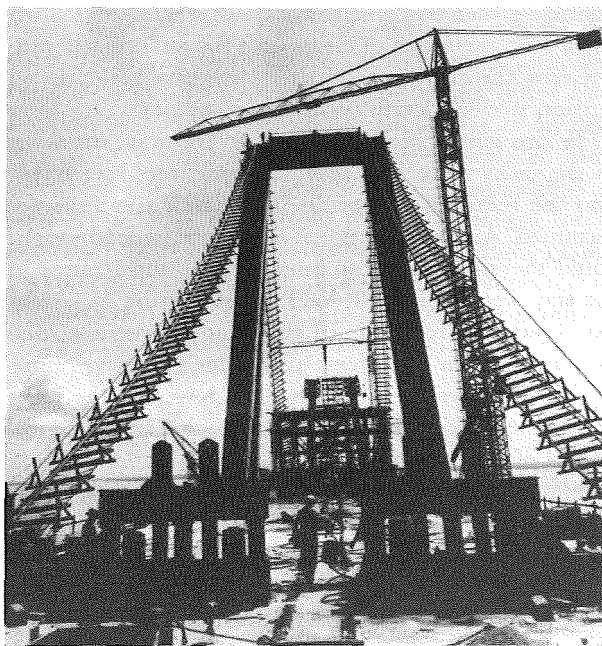


**FIGURE 8.42** Lake Maracaibo Bridge, catwalk for cable-stayed installation. (Courtesy of Julius Berger-Bauboag Aktiengesellschaft, from reference 22.)

was tensioned to 106 tons. A second jacking operation tensioned the strands to the theoretically required tension of 161 to 172 tons, then additional washers were inserted and the jacking screws removed. Finally, the cables were fixed in the saddles by high-strength bolts and clamping plates.

While the strands were being tensioned, the an-

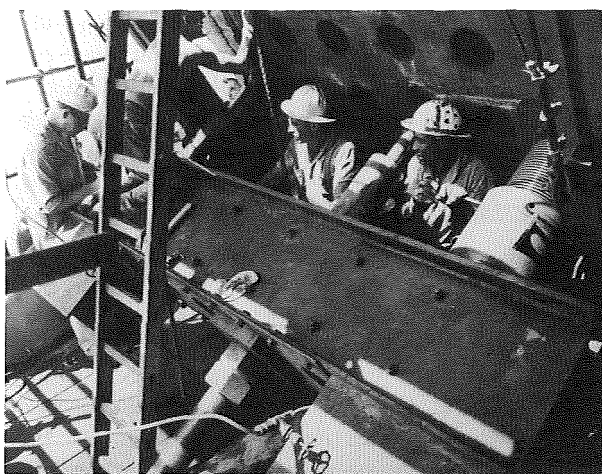


**FIGURE 8.43** Lake Maracaibo Bridge, two 250-ton jacks used for tensioning. (Courtesy of Julius Berger-Bauboag Aktiengesellschaft, from reference 22.)

chorage girder was posttensioned in stages. By following a strict sequence of tensioning the strands and prestressing the anchorage girder it was possible to avoid tension stresses detrimental to the concrete.

Before tensioning the strands in the stay, the force in the jacks under the rocking piers were measured, and the required tension in the strands was thus determined. Any unintentional difference in dead weight could therefore be accommodated. As the strands in the stay were tensioned, load in the rocking pier jacks was gradually relieved. In this manner, vertical displacement of the transverse anchorage girder was eliminated. This was accomplished by lowering the jacks under the rocking piers in stages such that elastic rebound of the rocking piers and their foundation were simultaneously equalized.

When the stays were finally tensioned to their full value, the rocking piers were relieved of load and the jacks under the rocking piers removed. This prevented the rocking piers from accepting any load resulting from deflection of the cantilever girder as a result of thermal elongation of the stays. After a few hours, the service girders were removed along with the rocking pier and its foundation.

After the service girder was removed, the tension in each strand was reduced approximately 30 tons (27 mt). To avoid redistribution of the forces, concrete weights totaling 550 (499 mt) tons were stacked on the end of the cantilever girders. The weights were distributed symmetrically to avoid any warping of the cantilever arm resulting from creep. Before the drop-in suspended girders between the ends of the cantilever girders were erected, all but 150 tons (136 mt) of the weight was removed from each cantilever end. The remaining weight represented the roadway surface and sidewalk, and was subsequently removed at a rate corresponding to the rate of progress of the installation of the finishing work. The suspended drop-in spans were made up of four precast T sections.

#### 8.5.7 CHACO/CORRIENTES BRIDGE, ARGENTINA

The superstructure of the Chaco/Corrientes Bridge (also referred to as the General Manuel Belgrano Bridge) consists of two concrete A-frame pylons connected by transverse beams at the apex of the A-frame and at deck level, Figs. 4.7 and 4.13. The deck system is comprised of two lines of posttensioned concrete box girders supported by two stays radiating from each side of the pylon in two vertical planes, Fig. 4.14. The deck is also supported by inclined struts flanking the pylon legs.

To eliminate the need for falsework, the inclined struts and pylon legs were supported by horizontal ties at successive levels as construction proceeded, Fig. 8.44. The legs were poured in segments by cantilevering the formwork from previously constructed segments. On reaching deck level, the girder section between the extremities of the inclined ties was cast on formwork. To further stiffen the pylon structure, a slab was cast between box girders at the level of the girder bottom flanges. This slab is within the limits of the cast-in-place box girders and inclined struts and serves as an additional element to accept the horizontal thrust from the cable stays. The upper portion of the pylon was then completed using horizontal struts to brace the legs until they were connected at the apex, Fig. 8.44.<sup>23,24</sup>

The precast box girder units, with the exception of those at the cable-stay anchorage were cast 13 ft 1½ in. (4 m) in length by the long-line, match-cast procedure. The soffit bed of the casting form had the required camber built in. Alignment keys were cast into both webs and the top flange. Match casting and alignment keys were required to ensure a precise fit during erection. Each 44-ton (40 mt) unit was transported by barge to the construction site and erected by a traveling crane operating on the erected portion of the deck. Since each box was lifted by a balance beam, four heavy

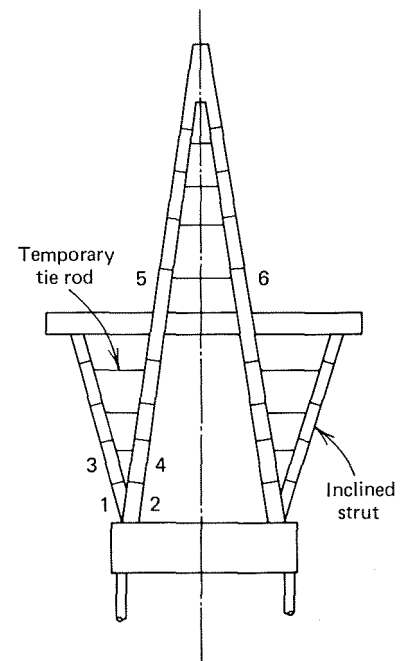


**FIGURE 8.44** Chaco/Corrientes Bridge, erection sequence of pylon. (Courtesy of Civil Engineering-ASCE, reference 24.)

vertical bolts had to be cast into the top flange of each box.

The lifting crane at deck level allowed longitudinal movement of the suspended box. On erection to the proper elevation, the unit was held to within 6 in. (150 mm) of the mating unit while epoxy joint material was applied. Bearing surfaces of the unit were sand blasted and water soaked prior to erection. The water film was removed before erection and application of the epoxy joint material. The traveling deck crane held the unit in position against its mating unit until it could be posttensioned into position. The crane was slacked off without waiting for the joint material to cure.<sup>23, 24</sup>

To minimize overturning forces and stresses in the pylon, it was necessary to erect the precast box units in a balanced cantilever method on both sides of the

center line of the pylon. The erection schedule demanded simultaneous erection at each pylon, although the pylons are independent of each other. When four precast box units were erected in the cantilever on each side of the pylon, temporary stays were installed from the top of the pylon to their respective connections at deck level. After installation of the temporary stays, cantilever erection proceeded to the positions of the permanent stays and the procedure was repeated to completion of the installation of the precast box units.<sup>23</sup>

The cable stays are composed of locked-coil strands (Chapter 9)  $3\frac{5}{8}$  in. (92 mm) in diameter. Because of the cable length and weight, and the acute angle of inclination of the pylon, saddles were impractical. Each strand was anchored at the top of the pylon and the deck using individual pipe sleeves, Figs. 8.45 and 8.46.

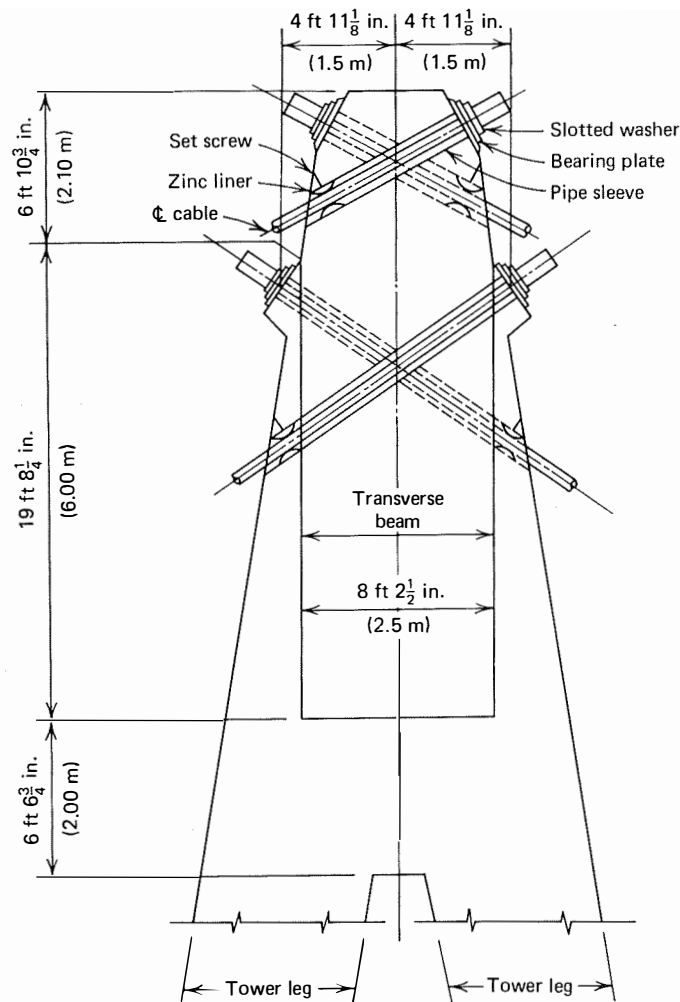


**FIGURE 8.45** Chaco/Corrientes Bridge, cable anchorage at top of pylon. (Courtesy of Civil Engineering-ASCE, reference 24.)



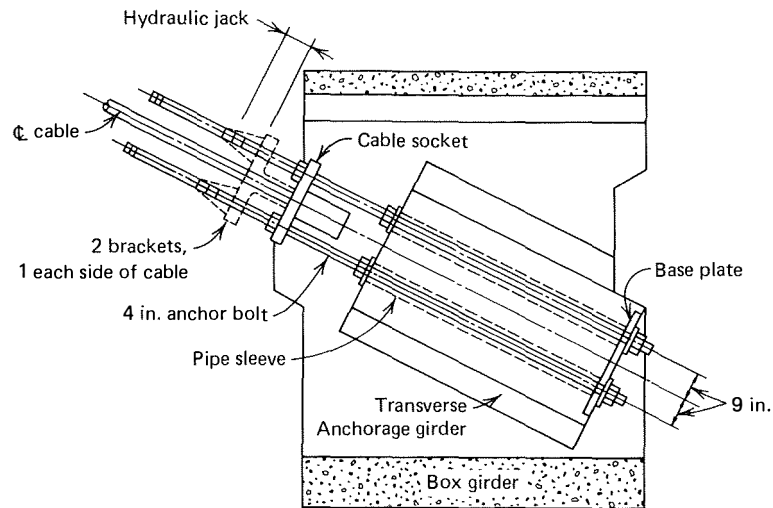


**FIGURE 8.46** Chaco/Corrientes Bridge, cable anchorage at girder. (Courtesy of Civil Engineering-ASCE, reference 24.)

To prolong strand life, zinc liners were used at the end of the pipe sleeve opposite the strand bearing socket. The zinc holds the strand rigid and at deck level separates the point of maximum vibration from the point of potentially maximum corrosion. The strand sockets were first attached at the pylon, then at the deck, and subsequently tensioning of the cable was performed from the deck level. To minimize the effect of aeolian vibration of strands, separators were installed to ensure nodes at selected locations<sup>24</sup>

A summary of the erection sequences used is outlined as follows:

1. Erect precast boxes and posttension successively
2. Erect diaphragms between lines of boxes and post-tension
3. Place temporary and permanent stays as erection proceeds
4. Remove temporary stays
5. Remove temporary posttensioning in the cantilevered sections.
6. Place precast deck slabs between box girders
7. Concrete the three 65-ft 8-in. (20-m) drop-in spans
8. Place asphalt pavement, curbs, and railings

#### 8.5.8 PASCO-KENNEWICK INTERCITY BRIDGE, U.S.A.

A suggested methodology for the erection of the Pasco-Kennewick Intercity Bridge, by the consultants Arvid Grant and Associates, Inc. and Leonhardt and Andrä,

is illustrated in Fig. 8.47, as extracted from the design drawings.

*Phase I:* Abutment 1 and pier 2 are completed and the cofferdam is erected for pylon 3.

*Phase 2:* Foundation of pylon 3 is completed, and the cofferdam is erected for pier 5.

*Phase 3:* Piers 5 through 8 and abutment 9 are completed. Formwork for span 1 and the cantilever section is erected. The caisson is erected for pylon 4. The casting of pylon 3 begins and contemplates 15 lifts of approximately 15 ft (4.6 m) each.

*Phase 4:* Span I and cantilever are cast and ready for prestressing. Formwork for spans V through VIII are erected (this operation can be accomplished after the prestressing of span I). Foundation for pylon 4 is completed.

*Phase 5:* Span I is prestressed. The auxiliary pier at the end of the cantilever is left in place to be utilized for adjustment of structure elevation and forces. Spans V through VIII and the cantilever section are cast and ready for prestressing. Pylon 3, including the portal strut, is completed. Derricks are erected on the strut. Casting of pylon 4 is begun using the same formwork as for pylon 3, which consists of 16 lifts, 14 ft (4.3 m) each. The cast-in-place portion of the deck structure at pylon 3 is completed. Auxiliary cables on reels arrive at the construction site. The top socket is hoisted in the top of the pylon and anchored at the position for permanent stay 1. The reels are unrolled and the

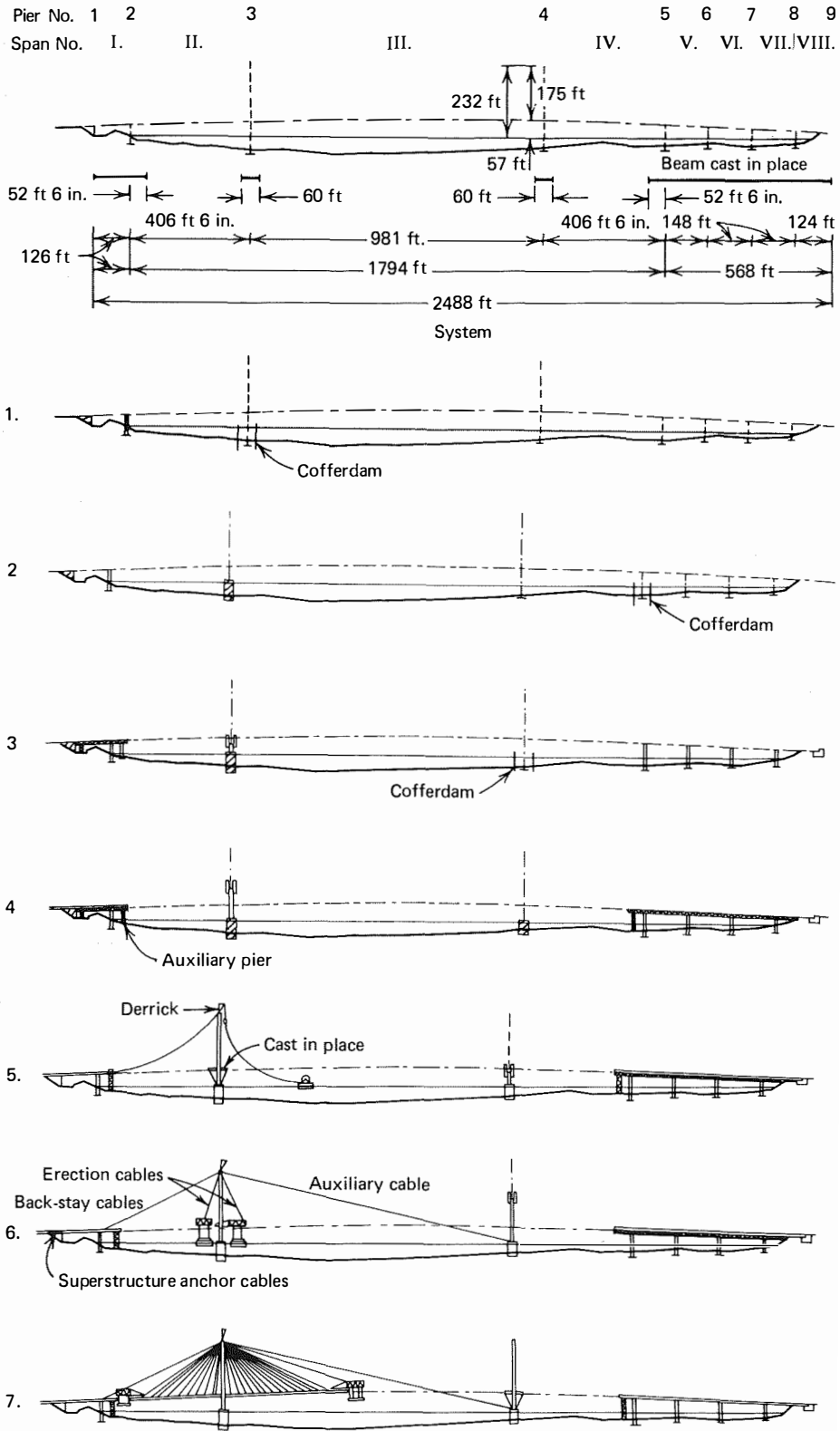


FIGURE 8.47 Pasco-Kennewick Intercity Bridge, erection sequence. (Courtesy of Arvid Grant, Arvid Grant and Associates, Inc.).

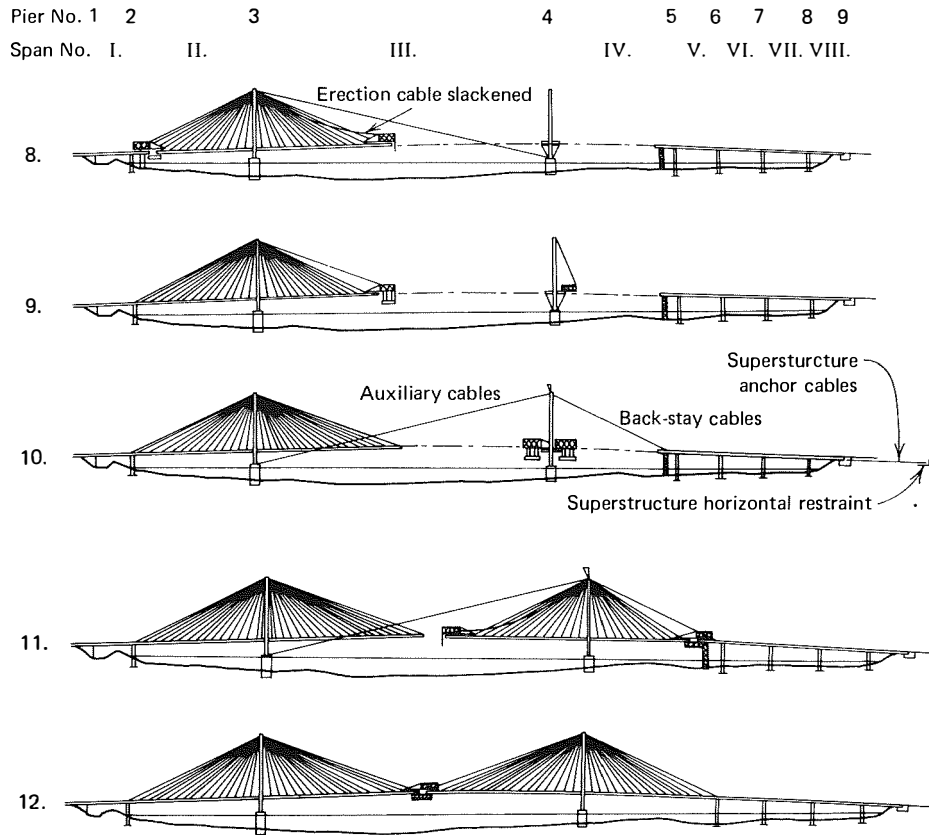


FIGURE 8.47 (Continued)

bottom socket is pulled to the anchorage point by grip hoists.

*Phase 6:* The back stay and auxiliary cables are connected at the anchorage for the permanent stay 1. The fore-stay auxiliary cables are anchored at the bottom of pylon 4. Superstructure anchor cables between the end girder of span I and abutment 1 are installed. Back-stay, auxiliary, and superstructure anchor cables are stressed simultaneously by means of pull-rods and center hole jacks. The vertical position of the pylon is checked during stressing and adjusted if required. Floating cranes lift the erection trusses in sections onto the cast-in-place girder and the trusses are then assembled. The erection truss is supported on one end by the completed deck and at the other end by erection cables from the pylon portal strut. Two corresponding precast elements are shipped to the site by barges, connected with lift-slab pull rods, and lifted simultaneously. They are then connected to the erected portion of the deck and the permanent stay is installed (see precast element erection sequence). The trusses are then moved forward and the sequence repeated.

*Phase 7:* Spans V through VIII and cantilever are prestressed. The auxiliary pier is left in place for future adjustments. Pylon 4 erection is completed along with the cast-in-place portion of the deck superstructure. The last precast element in the side span, along with its corresponding element in the center span, is erected.

*Phase 8:* Pylon 3 moments are adjusted with the back-stay and auxiliary cables. The cast-in-place joint in the outer span between approaches and main span is formed. Fore- and back-stay erection cables are slackened. Erection trusses are resting on the girder. The back-stay erection cable is removed and the back-stay erection truss is positioned over the joint and rigidly attached to preclude any movement in the joint resulting from thermal elongation of cables and over-stressing the green concrete. After the closure joint has attained sufficient age the erection truss is dismantled and relocated to the cast-in-place girder at pylon 4. During this stage, the auxiliary pier is used to adjust the elevation of the cantilever, if required. The longitudinal restraint of the deck at the pylon as well as the transverse erection wind bracing are removed.

*Phase 9:* To erect the last five precast elements in the Pasco half of the center span, the fore-stay erection cable and the corresponding permanent back-stay cable are stressed simultaneously. For the last element the fore-stay auxiliary cable is removed to allow for the anchorage of the permanent fore-stay cable 1. Superstructure anchor cables at abutment 1 are released.

*Phase 10:* Auxiliary cables are relocated to pylon 4 and anchored along with the back-stay cables at the anchorage for permanent cables no. 1. Superstructure anchor cable between the end of girder VIII and the superstructure horizontal restraint is installed. Back-stay, auxiliary, and superstructure anchor cables are stressed simultaneously. Erection trusses are anchored to the cast-in-place portion of the girder at pylon 4, and the first two elements are erected.

*Phase 11:* Pylon 4 measurements are adjusted with the auxiliary and back-stay cables. The cast-in-place joint in the side span is formed and cast. The back-stay erection truss is rigidly positioned over the joint. An auxiliary pier is used for any necessary adjustment. The back-stay erection cable is removed. Auxiliary cable is removed prior to erection of last element. Longitudinal girder restraint at pylon 4 and transverse erection and wind bracing is removed.

*Phase 12:* The last precast element is erected. The fore-stay erection cable has been removed. The superstructure anchor cables at abutment 9 are released. An erection truss is rigidly located over the gap in the center of span III. The cast-in-place joint is formed and cast.

*Phase 13:* The membrane and asphalt wearing surface are placed. Railings and lighting fixtures are installed. Final adjustments in all stays are made. Cables are grouted and remaining work completed.

The precast erection sequence is as follows:

1. Connect lift-slab pull rods and lift precast element to deck elevation
2. Couple the longitudinal stress bars and shift the element against the erected superstructure to check the matching of the joints
3. Pull back the element, trowel on the epoxy, and shift the element back to its final position
4. Stress bars for initial joint pressure. Jack load increment on last installed cables for control of erection bending moments in the structure
5. Pull in permanent cables and stress simultaneously with the releasing of the erection cables

6. Complete the stressing of the longitudinal bars. Grout all stressed bars
7. Weld the top layer of reinforcement and grout the remaining joint
8. Shift the erection truss to a new position and prepare to lift the next element. This is accomplished by adding additional length to the erection cables, anchoring the erection truss, and stressing the erection cables until the erection truss is resting on its back support

Installation of the permanent cables is illustrated in Fig. 8.48. The sequence of operations for the cable erection is briefly outlined in the following. After fabrication, each cable is rolled on a reel and transported to the site. When the cable is due to be erected, it is shipped to the bridge site on a barge. The cable is lifted onto an auxiliary platform at deck level outside the plane of the permanent cables. It is taken up by a trolley, shifted onto the beam, and moved forward to the erection truss. In the meantime, the sky line (guide rope) has been installed at its new position. Its upper end is hinge connected to a trestle on top of the tower head, which permits the rope to follow the different positions of the erection truss. On the trestle the rope can slide in a transverse direction so that it is always on top of the saddle to be installed. The top anchorage remains unchanged during the entire erection process. The lower end of the sky line is anchored at the erection truss by a clamp whose position is adjusted for each new cable.

From the working platform the permanent cable is inspected and hung into sliding hangers that run on the guide rope and are interconnected by the pull rope. The first two hangers are adjustable in length to facilitate threading the cable at the tower head after it has been pulled up by the pull cable. It is finally drawn into the tower head from the inside by an auxiliary tackle. There the head is supported by cross bars and horseshoe washers. While the permanent cable is unwound, brakes (installed at the trolley to control the unwinding operation) are applied to the reel.

After the upper end is installed, the bottom anchor head is pulled with grip hoists to the end of the steel pipe at the permanent anchorage. There the pull rod of a center-hole jack is screwed into the inside thread of the anchor head and the cable is pulled into its final position where it is anchored with horseshoe washers.

The clamps at the lower end of the hangers by which the permanent cable is supported are bigger than the outside diameter of the polyethylene pipe (the pull force is working at the anchor head only), so that after the

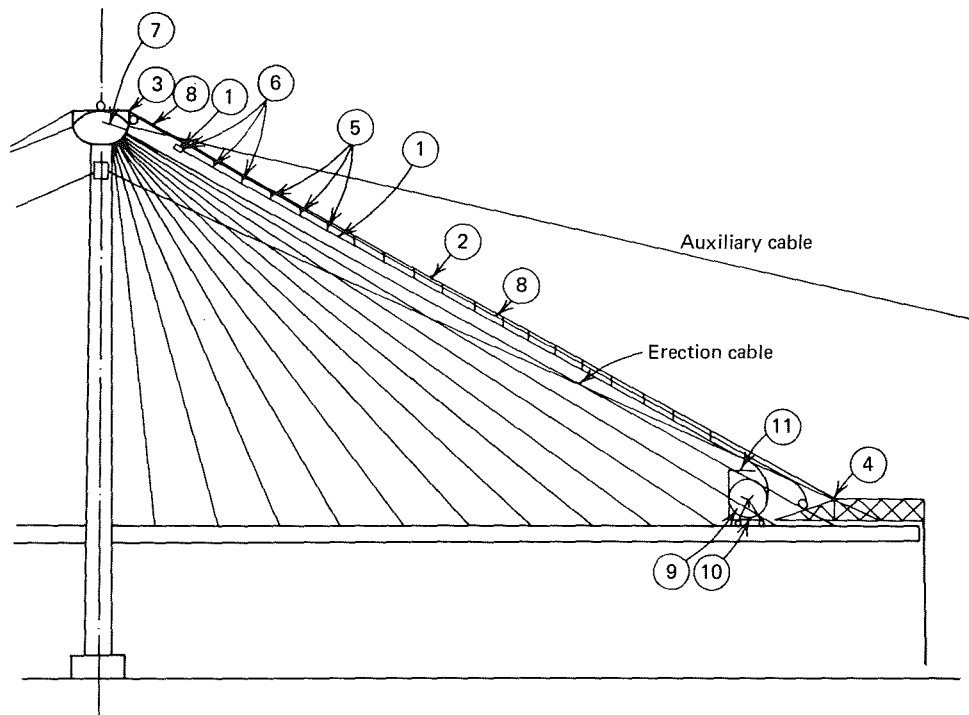


**FIGURE 8.48** Pasco-Kennewick Intercity Bridge, installation of permanent cables. List of components: (1) permanent cable to be erected, (2) guide rope, (3) top anchorage of the guide cable at towerhead, (4) bottom anchorage of the guide cable at erection truss, (5) sliding hangers with fixed length, (6) sliding hangers with adjustable length, (7) auxiliary tackle, (8) pull rope, (9) reel for transport of permanent cable, (10) trolley for supporting the reel, (11) working platform. (Courtesy of Arvid Grant, Arvid Grant and Associates, Inc.)

permanent cable has been installed and partly stressed, they come free of the polyethylene pipe and can be pulled back with the pull cable.

#### 8.5.9 EAST HUNTINGTON BRIDGE, U.S.A.

Erection of the superstructure of this bridge was predominantly from a barge-mounted crane. The operations, as extracted from the erection manual, are depicted in Fig. 8.49 and described as follows:

*Phase 1:* Piles for Pier S3 are driven. Cofferdam for Pier S2 is constructed. Top of Piers S1 and N1 are constructed. Brackets are installed at Pier S1 for construction of a pier table.

*Phase 2:* Formwork is installed at Pier N1 for pylon legs. Cable 32 (auxiliary fore-stay erection cable) loop anchors are positioned in Pier S2 footing. Ducts from these anchorages are sealed prior to removal of Pier S2 cofferdam. Pier table at Pier S1 is cast and post-tensioned to Pier S1. Pier S1 form traveler is erected and superstructure segments are constructed by bal-

anced cantilever. Pier table at Pier S2 is cast and post-tensioned to Pier S2. Pier at S3 and N3 are under construction.

*Phase 3:* Pylon legs are being constructed in lifts of 18 ft (5.5 m). Form travelers are relocated to Pier S2 and construction is continued at Pier S2. Falsework for north cast-in-place ballast section is installed at Pier N3. Ballast section at Pier N3 is cast on falsework.

*Phase 4:* Remainder of north cast-in-place portion is cast on falsework and posttensioned. Closure pour between cantilevers in span 2 is cast. Temporary bearings at Pier S2 are removed and permanent bearings are installed. Form travelers are removed. Precasting beds are constructed offsite, and precast segments are match-cast in a long bed from starter segments at the cantilever ends.

*Phase 5:* Pylon is completed and formwork is dismantled. North approach structure is completed. Falsework is installed for cast-in-place portion at pylon. Superstructure at pylon is cast. Translation restraints between superstructure and pylon are installed. Both

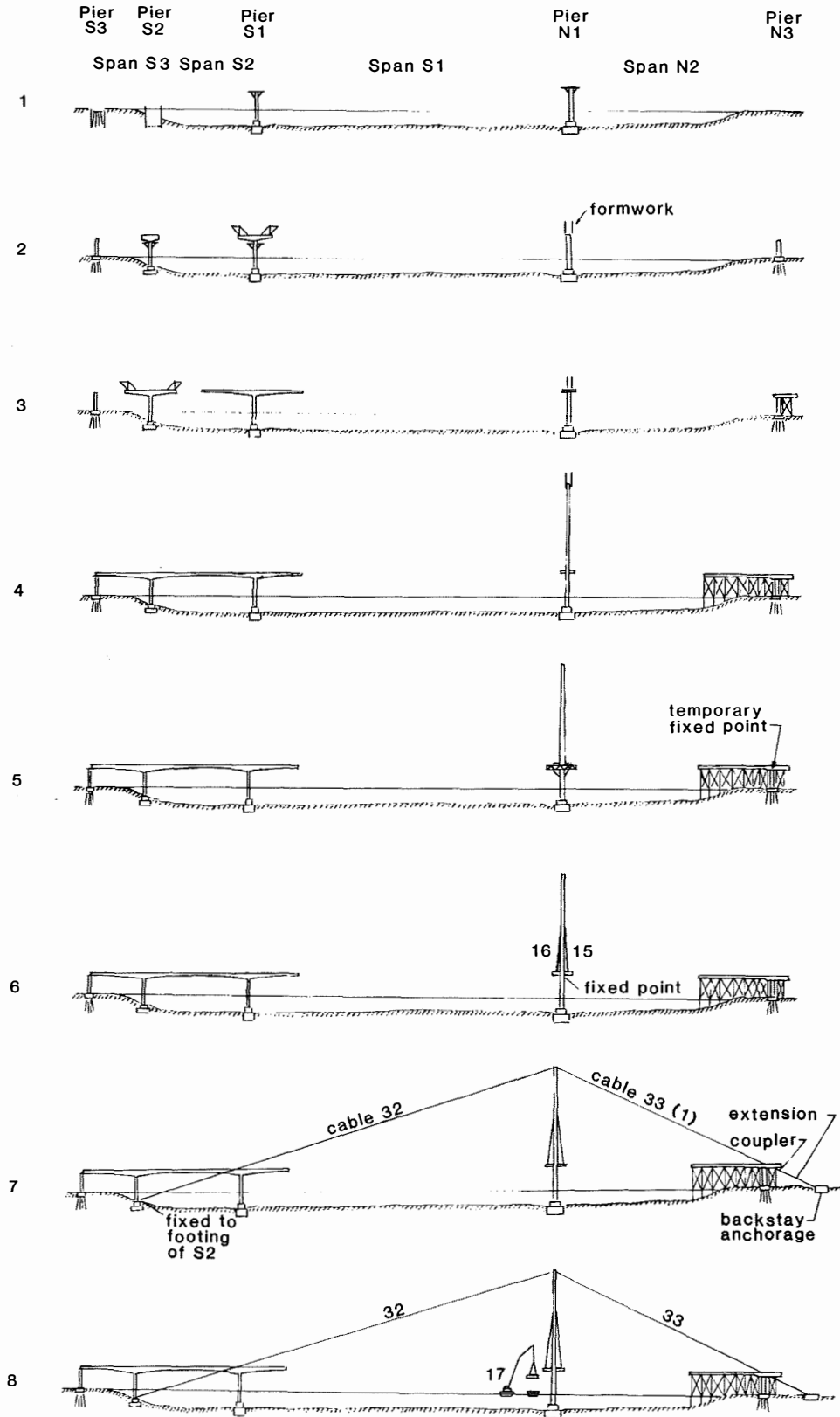


FIGURE 8.49 East Huntington Bridge, erection sequence.

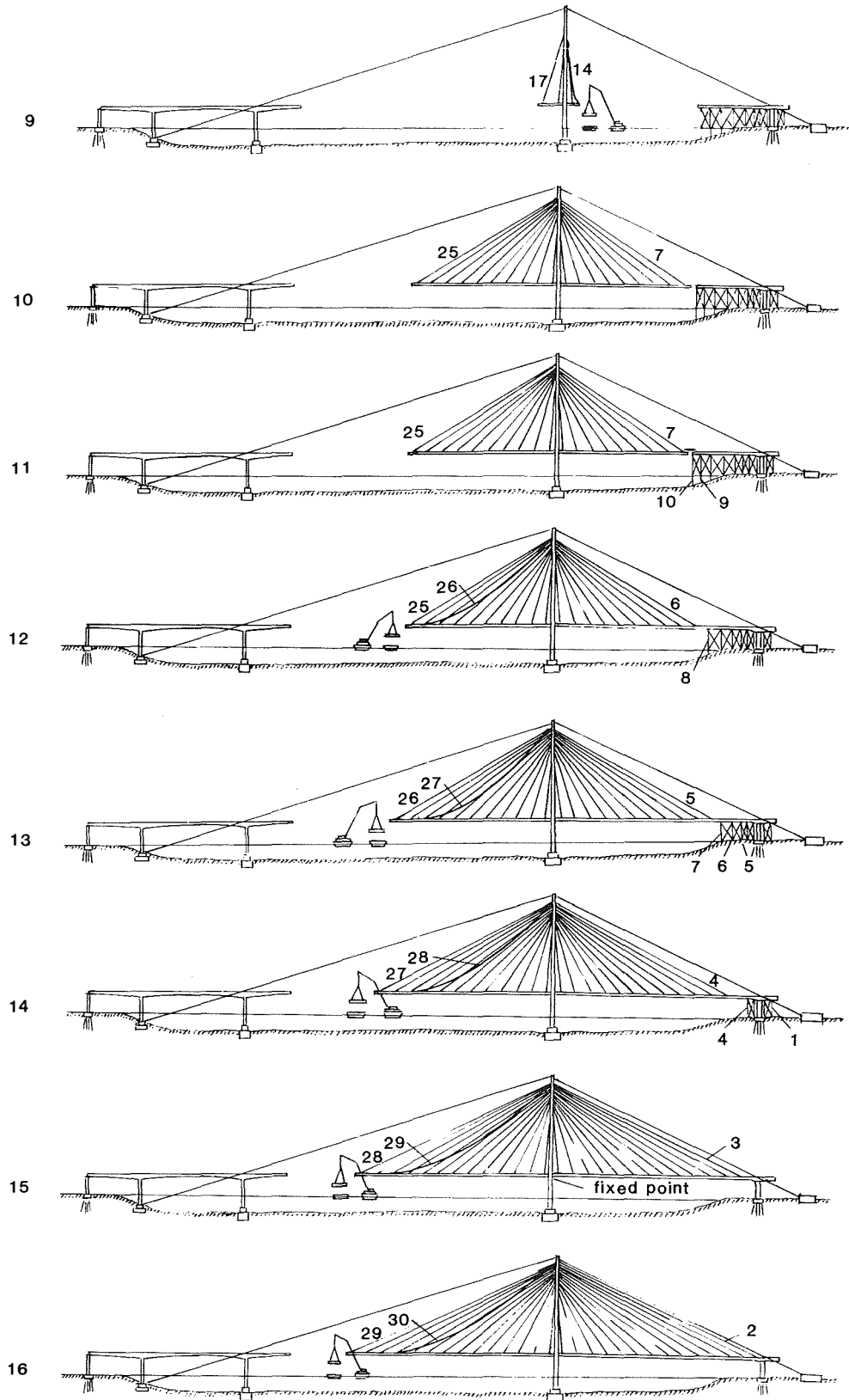


FIGURE 8.49 (Continued)

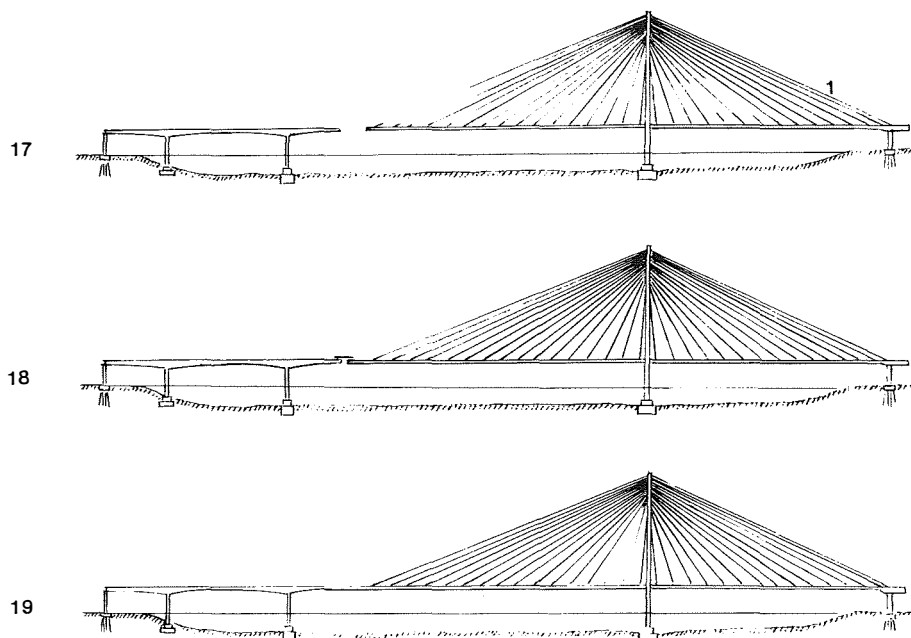


FIGURE 8.49 (Continued)

starter segments are positioned, aligned, and temporarily post tensioned to the cast-in-place superstructure. Closure pours are made between the starter segments and the cast-in-place superstructure.

*Phase 6:* Stays 15 and 16 are installed to support the superstructure. Falsework at pylon is removed. Work platform and equipment support structure is installed at top of pylon.

*Phase 7:* Permanent stay 1 with its extension (auxiliary erection back-stay cable 33) and auxiliary fore-stay cable 32 are installed simultaneously. Auxiliary cables are anchored to the foundation of Pier S2 and a temporary anchorage behind Pier N3.

*Phase 8:* Stay cable 17 is temporarily on superstructure near pylon. Components of erection equipment installed at erected superstructure and segment 17. Segment 17 is lifted from barge and readied for installation.

*Phase 9:* Segment 17 is installed. Stay cable 14 is erected and stored temporarily at erected superstructure. Components of erection equipment installed at erected superstructure and segment 14. Segment 14 is lifted from barge and readied for installation.

*Phase 10:* Erection continues with maximum unbalance of one segment toward main-span side until segment 25 is installed.

*Phase 11:* Entire north cast-in-place girder unit is jacked northward to provide for future shortening of side span. Stays are adjusted as necessary to align girder vertically. A clamping device is installed and stressed to the girders across the side-span closure gap.

*Phase 12:* Side-span closure joint has been cast and stressed. Stay cable 6 is installed and stressed. Bents 9 and 10 are removed. Stay cable 26 is erected and stored temporarily on the girder. All necessary equipment is installed and ready for erection of segment 26.

*Phase 13:* Segment 26 is installed. Stay 5 is installed and stressed. Bent 8 is removed. Stay cable 27 is erected and stored on the girder. All necessary equipment is installed and ready for erecting segment 27.

*Phase 14:* Segment 27 is installed. Stay 4 is installed and stressed. Bents 5, 6, and 7 are removed. Stay 28 is erected and stored temporarily on the girder. All necessary equipment is installed and ready for erecting segment 28.

*Phase 15:* Segment 28 is installed. Stay 3 is installed. Bents 1 through 4 are removed. Stay 29 is erected and stored temporarily on the girder. All necessary equipment is installed and ready for erecting segment 29.

*Phase 16:* Segment 29 is installed. Stay 2 is installed and stressed. Segments 30 and 31 are installed in succession.



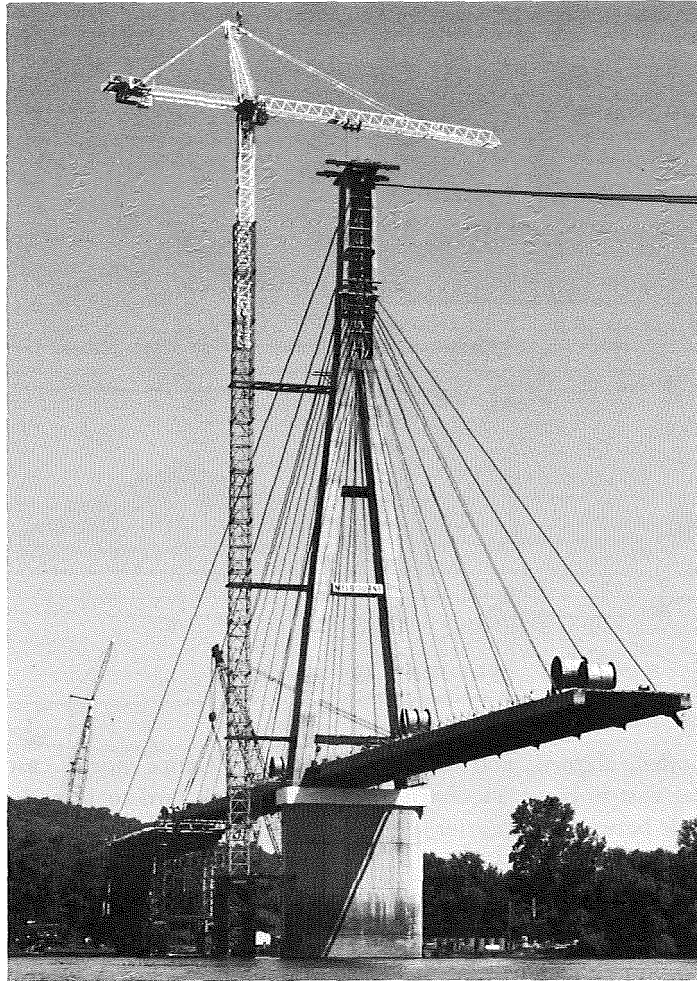


**FIGURE 8.50** East Huntington Bridge, during construction.

*Phase 17:* Segment 31 is in place. Auxiliary cable 32 is removed after stay 1 is installed. Stay 1 extension is removed. Stay 1 is anchored to girder. Horizontal restraint (4 devices) at Pier S1 are installed. Tie-down bars/temporary bearings are removed at Pier S1.

*Phase 18:* Precast closure portion and its steel support beams are installed. Stay adjustment before closure is made. Formwork for first closure pour is installed. First 3-ft closure pour is cast and posttensioned. Relieve 51 kips from the reaction at the south end of the steel support beams by removing shim plates between steel beam and superstructure. Stress tie-down bars at south end of steel support beams, connecting them to the south cast-in-place structure. Remove horizontal restraint at Pier S1. Formwork for second closure pour is installed.

*Phase 19.* Second closure pour of 3 ft 6 in. is cast and stressed. Steel support beams are removed. Final stay

adjustments are completed. Roadway overlay is placed on superstructure. Erect traffic railing, install sign structures and lighting, and grout stays. Complete all other work.

A view of the structure during erection is presented in Fig. 8.50.

### 8.6 Fabrication

Aside from technical considerations, the factor that most affects bridge design is economics, especially the ratio of material cost to fabrication cost. Therefore, a discussion of fabrication is closely related to economics and is included here for a better understanding of the influence of fabrication on total costs. In the United States the cost of rolled steel members has been relatively low compared to fabrication costs, especially la-

bor costs. This condition has not generally been favorable to least-weight design. Generally, bridge designs in the United States stress simplicity and minimize fabrication, thus producing a heavier structure than is required from a purely analysis point of view. Conversely, until the mid-1950s the European philosophy had been diametrically opposite—relatively elaborate fabrication procedures had been used to produce a least-weight design. Understandably, the material shortages of the post-World War II era created an environment conducive to the development of such innovative concepts as orthotropic plate girders and cable-stay designs in bridges.

However, economic conditions in postwar Europe have changed gradually in some areas. The costs of rolled steel products have remained relatively stable since 1952, but the costs of labor and/or fabrication have been steadily rising. Thus the ratio of material costs to fabrication costs in Europe has been approaching that which exists in the United States. As a result, there has been a great interest in Europe in reducing fabrication costs. Simplified design, mass production, and automation have become increasingly more important than material savings alone. With respect to automation, there has been an increasing trend toward the use of machine-programmed numerically controlled fabrication plants. This has led to the development of drilling and milling machines controlled by means of computer and of automatic welding machines.

This convergence of European and American economic philosophy, at least in construction activity, will undoubtedly lead to an increased interchange of ideas and concepts of building and bridge designs. Americans will no longer be able to shrug off European concepts with a simplistic statement such as: "We cannot do that here, the economic situation is different."

It is difficult to predict future trends, but it appears that there may be a merging of the least-weight concept with the automation and simplified design concept. This will undoubtedly result from increased pressures to conserve natural resources and energy and from the necessity to reduce the labor costs.

Cable-stayed bridges are, in general, a statistically indeterminate system, but may become highly hyperstatic because of the geometrical configuration, number of stays, and built-in redundancies. The completed structural geometry must agree with the specified design geometry for dead loads. One consideration of this design condition is that the elevation of the deck structure must be consistent with the required roadway grade elevations, the cable alignments, and the girder and pylon position dimensions under dead load, such

that the pylons are vertical and the bearings are in a no-load position. To satisfy these requirements, structural components must be fabricated to a length that not only meets the required grade, but is properly cambered for the live load deflection. The length must be sufficient to compensate for the elastic shortening caused by axial load and long-term creep effects. The same considerations are true for the pylons and the cable stays. If these requirements are carefully considered, the desired results will be obtained, irrespective of the method or sequence of erection.

The successful completion of a cable-stayed bridge requires, if not demands, the transfer of design concepts into acceptable fabrication techniques. Thus, a high degree of cooperation is required of the designer, fabricator, and erector. The design engineer must be willing to modify the concept, if necessary, for ease of fabrication and erection. The fabricator and erector must be able to adapt their procedures to the design concept wherever possible.

It is not the intent of this section to describe fabrication procedures in detail. These procedures are the responsibility of the fabricator and may vary from one fabricator to another, depending on equipment and experience. This section will present only those reasons for fabrication decisions as presented by several projects that were reviewed. Bear in mind that what may be a valid decision for one fabricator may not be for another. Furthermore, as a result of the rapidly changing fabrication technology, what may have been economically and technically valid in 1955 is not necessarily applicable in 1985. However, on the premise that one can always learn from previous experiences, a few specific comments appear to be justified.

#### 8.6.1 GENERAL STRUCTURAL STEEL FABRICATION AND WELDING

Bridge structures are subject to fatigue stresses, and this is particularly true of cable-stayed bridges because of their inherent flexibility. Therefore, the possibility of brittle fracture and fatigue requires special attention to ensure that stress concentrations will not develop from notches, poor edge preparation, welding defects, poor weld shapes, poor welding methods, and, in general, low-quality fabrication techniques.

To avoid fatigue and fracture failures, the fabrication requirements of the Batman Bridge specified that shearing or flame cutting of plates have an allowance that would permit the removal of at least  $\frac{1}{8}$  in. (3 mm) of metal by machining for plates up to  $\frac{1}{2}$  in. (12 mm) in thickness and at least  $\frac{1}{4}$  in. (6 mm) of metal for plates in excess of  $\frac{1}{2}$  in. (12 mm) in thickness. Machine flame

cut edges were accepted, at the discretion of the engineer, if the edge thus produced was essentially as straight, smooth, and regular as that produced by the finishing cut of a planing machine. Where some doubt existed, a light grinding of the edge was required. Shearing in a direction perpendicular to the direction of main stresses was permitted for minor gusset plates and splice plates. However, shearing was not permitted on plates in main structural members.<sup>19</sup>

With respect to possible stress raisers in welds, the fabricator of the Batman Bridge was not permitted to finish welds with a bad profile. Welds had to be produced with a minimum amount of smooth over fill (i.e., no over-roll), and, if required, fillet welds were to be ground to a smooth finish. Wherever possible, intersection of weld lines were to be avoided. Where this was impossible, the first weld laid down was ground smooth and flush in the region of the intersection, in a direction parallel to the direction of stress. Weld spatter and arc strikes outside of the welds were avoided. Tack welds were required to be kept to a minimum and where possible to be kept in the weld area so that the subsequent automatic welding procedure would tend to "float" them out. Automatic or semiautomatic welding procedures were required for all main longitudinal welds and transverse butt welds in the truss chords. In general, for good fabrication practice, automatic or semiautomatic procedures are encouraged. A general requirement for the Batman Bridge specifications was the use of properly prepared run-on and run-off plates so that butt welds could be carried beyond the edges of the plate. In addition, electrodes were required to be stored in heated boxes or ovens.<sup>9</sup>

#### 8.6.2 STRUCTURAL STEEL SUPERSTRUCTURES

From the standpoint of material handling during fabrication and erection, it is generally preferred to reduce the bridge cross section into several manageable com-

ponents. This technique is illustrated for the Kniebrücke Bridge, Fig. 8.33; the Paris-Masséna Bridge, Fig. 8.14; and the Papineau-Leblanc Bridge, Fig. 8.51.

In the fabrication process of the Papineau-Leblanc Bridge, considerable effort was exercised to maximize repetition of the structural components. The cross section was divided into 11 components along longitudinal splice lines indicated in Fig. 8.51. Girder webs were assembled from three panels. Thus a total of 17 stiffened panels compose the cross section. A typical cross section is indicated in Fig. 5.26. Longitudinally, the superstructure was divided into 31 sections, requiring a total of 527 stiffened panels (excluding those required for the pylons). As a result of this large amount of repetitive fabrication, cost savings were realized in material orders, jigs, welding, and drilling operations. Standardization of the center to center dimension of the orthotropic stiffeners in the top and bottom flanges further simplified fabrication. Where the bottom flange increased in thickness and fewer stiffeners were required, alternate stiffeners were omitted and a multiple of the basic spacing was maintained. Thus, the jigs remained constant and no additional fixture layout was required.<sup>13</sup>

The top flange of the box girder also acts as the orthotropic roadway deck. The thickness of the deck plate is 0.437 in. (11 mm). The longitudinal through stiffeners, Fig. 5.26, are  $\frac{1}{4}$  in. (6 mm) thick, 13 in. (330 mm) deep, and are spaced on 2-ft (0.6-m) centers. Transverse floor beams are spaced 15 ft (4.6 m) on centers. The longitudinal through stiffeners were produced in straight 45-ft (13.7-m) lengths, kink free, on a patented hydraulic machine designed and built by Dominion Bridge. Since the through stiffener to deck weld was critical, specifications demanded a minimum of 90% penetration weld at the connection. The straight edge produced by the stiffener bending machine made it possible to produce high-quality welds at these critical locations. A rolling pressure head on top of the through stiffener forced the plates into close

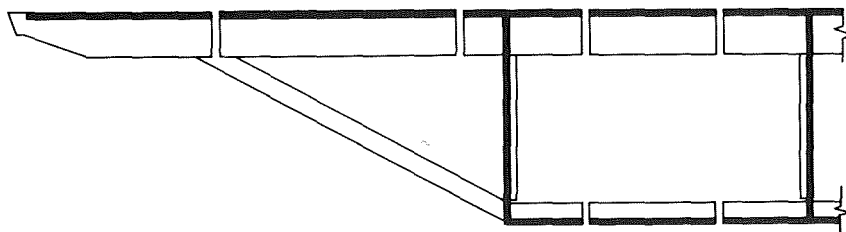


**FIGURE 8.51** Papineau-Leblanc Bridge, breakdown of cross section into stiffened panels. (Courtesy of the Canadian Steel Industries Construction Council, from reference 13.)

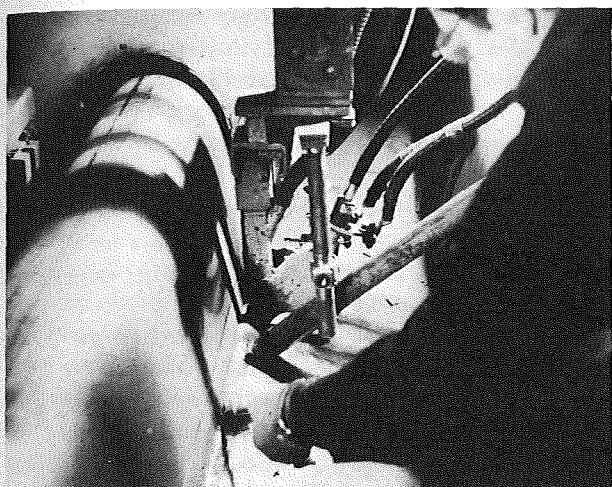


**FIGURE 8.52** Papineau-Leblanc Bridge, welding longitudinal stiffener. (Courtesy of Paul Marquis, Gendron Lefebvre and Associates.)

contact at the welding head and prevented weld blow-through. All panel welding was done by a fully automatic, twin tandem, submerged arc rig mounted on a gantry spanning the welding bed, Fig. 8.52. The subsequent operation position and the transverse floor beams, which were profile burned to fit over the through stiffeners, were jacked down flat and then tack welded. At another location the floor beams were welded by semiautomatic  $\text{CO}_2$  machines.

In the fabrication of the West Gate Bridge,<sup>25</sup> the deck plates for the orthotropic deck panels were initially passed through a set of heavy flattening rolls to ensure their flatness. They were then machine flame cut to size with a tolerance for shrinkage in both directions, and bevels for the field welds were also cut at this time. A simultaneous operation was the cold rolling of the longitudinal trapezoidal stiffeners from  $\frac{1}{4}$ -in. (6-mm) and  $\frac{5}{16}$ -in. (8-mm) coiled strip and accurately cut to length with an allowance for longitudinal shrinkage. Edges of the stiffeners were machined to proper dimensions and prepared for the partial penetration butt weld that joined them to the deck plate. Transverse stiffeners were cut and profiled to the required shape and spacing of the longitudinal stiffeners.

The trapezoidal longitudinal stiffeners were clamped and tacked to the deck plate at 1000 mm (39.37 in.). The maximum allowable gap between the contact edges of the stiffeners and the plate was 0.5 mm (0.02 in.), Fig. 8.53. A problem was encountered in the partial penetration butt weld joining the longitudinal stiffener to the deck plate. The minimum manual tack weld compatible with the required hardness level had

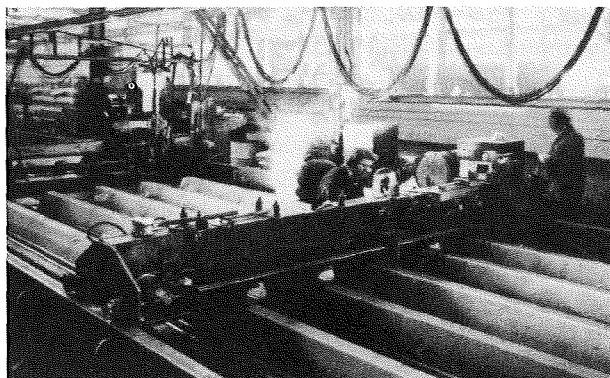


**FIGURE 8.53** West Gate Bridge, clamping and tack welding. (Courtesy of Acier-Stahl-Steel, from reference 25.)

a tendency to over-roll in the continuous automatic submerged arc weld and was rejected. Acceptable solutions were to preheat and use a smaller tack weld or to arc air gouge and grind approximately 50% of the metal from the larger tack weld. On the basis of cost economies, the fabricator chose the latter solution. The longitudinal butt welds were accomplished by a unit that completely welds two stiffeners at each pass.

To correct for the transverse camber in the panels produced by the longitudinal welding, the panels were turned right side up and the correction was made by the controlled application of heat. During this operation, the temperature of the metal was not permitted to exceed  $600^\circ\text{C}$ . The transverse stiffeners were then fitted and welded, Fig. 8.54. Upon completion of all welding, the panels were inspected and corrected for flatness. Panels were required to be flat within 3 mm (0.118 in.) in 3000 mm (approximately 10 ft) measured in any direction.

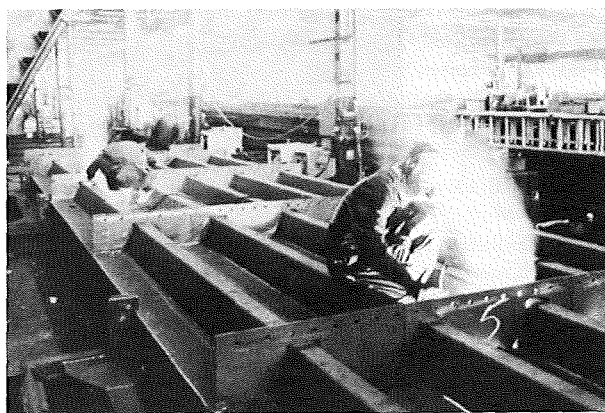


**FIGURE 8.54** West Gate Bridge, transverse stiffener attachment. (Courtesy of Acier-Stahl-Steel, from reference 25.)

### 8.6.3 STRUCTURAL STEEL PYLONS

Typically, pylons are designed as box sections with longitudinal and transverse stiffeners. The transverse stiffeners are normally notched to allow the longitudinal stiffeners to pass through. At each end of a box section of pylon, heavy internal flanges are butt welded to the four sides of the box. In this manner the box sections are bolted together without the need for external splices.

In the Batman Bridge, a submerged arc welding process was used and a fully automatic machine was used for the longitudinal butt welds in the sides of the boxes and for the partial penetration welds for the box corners. For the flange to side wall welds a semiautomatic machine was used. Square butt welds were used for the longitudinal welds with either a  $\frac{7}{32}$ -in. (5.5-mm) or  $\frac{5}{32}$ -in. (4-mm) gap, depending on the plate thickness. Corner welds were prepared for an inclusive angle of 70 degrees, with either two or four runs depending on thickness. Preparation for the flange to side plate weld consisted of a double J for thick plates and a partial penetration double V for thinner plates.<sup>19</sup>

The Papineau-Leblanc Bridge pylon was assembled from four unstiffened plates, with a partial penetration U weld at each corner that was ground flush for appearance. A welding head on a long-reach boom was used to place a fillet weld on the inside of each corner.<sup>13</sup>

The principal problem in the fabrication of the larger sections is the difficulty in achieving a good fit. If in a nominally vertical cable plane geometry, the

cable plane is not truly vertical, the pylon may be required to be cambered in the transverse direction of the bridge to accommodate the bending forces that may be induced. Therefore, the ends of the section will require milling at a very small angle.

Requirements for the Batman Bridge were that the sections butt evenly together at least 80% on any side and 90% over the entire perimeter. This meant that a three-thousandths feeler gauge could not be entered into the joint from the outside.<sup>19</sup>

Strict mating restrictions were placed on the pylon sections in order to transfer the large compressive loads carried by the pylon from one section to another by direct bearing. To minimize the potential for eccentricity of the load caused by misalignment of the pylon wall plates, specifications required the sections to be fabricated within plus or minus  $\frac{1}{16}$  in. (0.6 mm) between faces and to within plus or minus  $\frac{1}{8}$  in. (1.2 mm) across the corners. Between adjacent sections a maximum  $\frac{1}{16}$ -in. (0.6-mm) tolerance in the inside dimension was specified.<sup>19</sup>

In the Kniebrücke Bridge<sup>21</sup> the pylons were fabricated with a camber of 22 in. (560 mm) at the top, which was displaced away from the bridge deck. Individual units of the pylon were fabricated as straight units such that the transverse camber curve of the pylon was a polygonal profile with "kinks" at the joints rather than a smooth curve. It was considered impossible to estimate the relative displacement of one pylon section with respect to an adjacent one during erection. It was impossible to evaluate the temperature de-

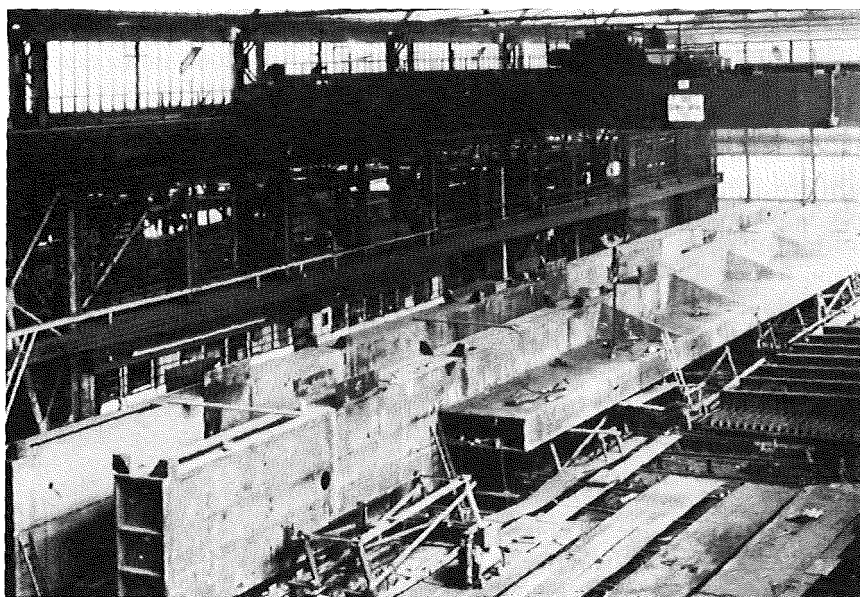


FIGURE 8.55 Kniebrücke, fabrication of pylons, Düsseldorf, from reference 20.

formation precisely even if the temperature variation across the cross section were known. Furthermore, the deformation caused by the erection loading acting upon the previously erected portion of the pylon was unknown. Therefore, it was decided to mill the butting faces in the shop and then have a trial assembly. The trial assembly was to place the inside cell, which was toward the bridge deck, Fig. 5.23, on a transverse face, Fig. 8.55. In this manner the deflection between supports was eliminated and the camber in the pylon was observed and measured as a horizontal curve. Upon being positioned and fitted, the new cell was jacked against the previously positioned cell and the contact of the mating surfaces checked. If the bearing surface had to be corrected it was done on the surface of the new section being fitted.

#### 8.6.4 CONCRETE FABRICATION

Fabrication of cast-in-place or precast segments is a topic that will not be discussed in depth in this book. Indeed, it would require a chapter of its own. The reader is referred to a companion book in this Series of Construction Guides.<sup>26</sup>

However, it should be pointed out that a concrete cable-stay bridge is subject to the same time-dependent losses as prestressed concrete structures, that is, creep, shrinkage, and so on. In fact, a simplistic analogy can be drawn that a cable-stayed girder is a continuous prestressed member with the tendon profile located outside of its cross section. The appropriate component of a cable-stay force, in fact, produces a prestressing in the girder and the pylon.

Creep of concrete is a time-dependent deformation resulting from sustained stress. Determination of creep effects is complicated by the number of dependent variables, such as the age of the concrete when loaded, the amount of deformation varies with time; the water-cement ratio; the aggregate-cement ratio; the type of cement; and the type of aggregate to name just a few. In addition, the age of each individual segment in the girder, as it is constructed, will be different. The same is true of the age of the various lifts in the pylon.

The practical aspect is that the geometry and thus the stresses in the completed structure will vary with time. During the conceptual design stage, the engineer will use a creep coefficient as an "educated estimate." To verify this assumption, the "Special Provisions" or "Specifications" will require tests, including creep tests, to be conducted of the proposed concrete mix for the purpose of deformation control during construction/erection. Young's Modulus Tests (ASTM C469) will normally require specimens to be tested at ages of

3, 7, 14, 28, 56, 90, and 180 days. Creep and shrinkage tests (ASTM C512) will normally be required at ages of 7, 14, 28, 56, 90 days, and 1 year from initial loading and for a duration of one year. Specifications or Special Provisions will state how many samples of each specimen are to be produced and will also indicate a time frame, that is, how far in advance of actual construction testing will commence. The purpose of these tests is to determine the actual properties of the concrete to be used in construction so that if the values are unacceptable appropriate modifications can be made to correct the mix proportions or ingredients. It is important for the contractor to be cognizant of these requirements in order not to delay or alter the construction schedule.

#### References

1. Schöttgen, J. and Wintergest, L., "Die Strassenbrücke über den Rhein bei Maxau," *Der Stahlbau*, Vol. 37, No. 2, February 1968.
2. Kondo, K., Komatsu, S., Inoue, H., and Matsukawa, A., "Design and Construction of Toyosato-Ohhasi Bridge," *Der Stahlbau*, No. 6, June 1972.
3. Fiege, A., "Steel Motorway Bridge Construction in Germany," *Acier-Stahl-Steel* (English version), No. 3, March 1964.
4. Beyer, E. and Ernst, H. J., "Brücke Jülicher Strasse in Düsseldorf," *Der Bauingenieur*, Vol. 39, No. 12, December 1964.
5. Anon., "The Paris-Masséna Bridge: A Cable-Stayed Structure," *Acier-Stahl-Steel* (English version), No. 6, June 1970.
6. Balbachevsky, G. N., "Study Tour of the A.F.P.C.," *Acier-Stahl-Steel* (English version), No. 2, February 1969.
7. Beyer, E., et al. *Die Oberkasseler Rheinbrücke und der geplante Querverschub*, Beton-Verlag GmbH, Düsseldorf.
8. Scheuch, G., "Moving the Oberkasseler Brücke at Düsseldorf," *Acier-Stahl-Steel* (English version), February 1976.
9. Firmage, D. A., "The Final Positioning of the Oberkassel Cable-Stayed Bridge," *Cable-Stayed Bridges*, Structural Engineering Series No. 4, June 1978, Bridge Division, Federal Highway Administration, Washington, D.C.
10. Anon., *Düsseldorf-Oberkassel-Rhinebridge, Construction and Displacement*, Hein, Lahmann AG, Düsseldorf.
11. Wenk, H., "Die Strömsundbrücke," *Der Stahlbau*, Vol. 23, No. 4, April 1954.
12. Ernst, H. J., "Montage eines seilverspannten Balkens im Gross-Brückenbau," *Der Stahlbau*, Vol. 25, No. 5, May 1956.
13. Taylor, P. R. and Demers, J. G., "Design, Fabrication and Erection of the Papineau-Leblanc Bridge," *Canadian Structural Engineering Conference*, 1972, Canadian Steel Industries Construction Council, Toronto, Ontario.
14. Demers, J. G. and Simonsen, O. F., "Montreal Boasts Cable-Stayed Bridge," *Civil Engineering*, ASCE, August 1971.
15. Rooke, W. G., "Papineau Bridge Steel Erected in Record Time," *Heavy Construction News*, September 1, 1969.
16. Vogel, G., "Die Montage des Stahlüberbaues der Severinsbrücke Köln," *Der Stahlbau*, Vol. 29, No. 9, September 1960.

17. Fischer, G., "The Severin Bridge at Cologne (Germany)," *Acier-Stahl-Steel* (English version), No. 3, March 1960.
18. Anon., "Opening Batman Bridge 18th May, 1968," Department of Public Works, Tasmania, Australia.
19. Payne, R. J., "The Structural Requirements of the Batman Bridge as They Affect Fabrication of the Steelwork," *Journal of Institution of Engineers*, Australia, Vol. 39, No. 12, December 1967.
20. Tamms and Beyer, *Kniebrücke Düsseldorf*, Beton-Verlag GmbH, Düsseldorf, 1969.
21. Schreier, G., "Bridge over the Rhine at Düsseldorf: Design, Calculation, Fabrication and Erection," *Acier-Stahl-Steel* (English version), May 1972.
22. Anon., *The Bridge Spanning Lake Maracaibo in Venezuela*, Bauverlag GmbH., Wiesbaden, Berlin, 1963.
23. Gray, N., "Chacos/Corrientes Bridge in Argentina," *Municipal Engineers Journal*, Paper No. 380, Vol. 59, Fourth Quarter, 1973.
24. Rothman, H. B. and Chang, F. K., "Longest Precast-Concrete Box-Girder Bridge in Western Hemisphere," *Civil Engineering*, ASCE, March 1974.
25. Burns, C. A. and Fotheringham, W. D., "Deck Panels for West Gate Bridge (Australia)," *Acier-Stahl-Steel* (English version), June 1974.
26. Podolny, W., Jr. and Muller, J. M., *Construction and Design of Prestressed Concrete Segmental Bridges*, Wiley, New York, 1982.

# 9

## *Cable Data*

|      |                                      |     |
|------|--------------------------------------|-----|
| 9.1  | INTRODUCTION                         | 191 |
| 9.2  | DEVELOPMENT OF CABLE APPLICATIONS    | 191 |
| 9.3  | MANUFACTURING PROCESS                | 193 |
| 9.4  | STRUCTURAL STRAND AND ROPE           | 194 |
|      | 9.4.1 Prestretching                  | 195 |
|      | 9.4.2 Modulus of Elasticity          | 195 |
|      | 9.4.3 Strand and Rope Compared       | 197 |
| 9.5  | LOCKED-COIL STRAND                   | 197 |
| 9.6  | PARALLEL BARS                        | 197 |
| 9.7  | PARALLEL WIRE                        | 197 |
| 9.8  | PARALLEL STRAND                      | 198 |
| 9.9  | COMPARISON OF VARIOUS TYPES OF STAYS | 198 |
| 9.10 | CORROSION PROTECTION                 | 198 |
| 9.11 | HANDLING                             | 199 |
|      | REFERENCES                           | 200 |

### *9.1 Introduction*

Several types of cables are available for use as stays in cable-stayed bridges. The form or configuration of the cable depends on its make-up; it can be composed of parallel wire, parallel strands or ropes, single strands or ropes, lock-coil strands, or solid bars, Fig. 9.1.<sup>1</sup>

This chapter discusses cables made from the basic single wire and describes the manufacturing process and mechanical properties that influence design and construction practices.

A definition of the terms useful in this section is given below. The reader should understand the specific meanings of the terms and their unique application.<sup>2</sup>

**Cable**—any flexible tension member, consisting of one or more groups of wires, strands, or ropes

**Wire**—a single continuous length drawn from a cold rod

**Strand**—(with the exception of parallel wire strand) an arrangement of wires helically placed about a center wire to produce a symmetrical section, Figs. 9.2 and 9.4

**Rope**—a number of strands helically wound around a core that is composed of a strand or another rope, Fig. 9.3

**Locked-coil strands**—resemble strands except the wires in some layers are shaped to lock together when in place around the core, Figs. 9.1 and 9.4

**Parallel wire strand**—individual wires arranged in a parallel configuration without the helical twist, Figs. 9.1 and 9.4

### *9.2 Development of Cable Applications<sup>3</sup>*

The structural application of a flexible tension member or cable dates back to the period before recorded history. Primitive man constructed cables of tangled grape vines to bridge large ravines and small rivers. The early Chinese built suspension bridges of hemp rope and iron chains. The Incas of Peru constructed their suspension bridges over major rivers with cables of hemp rope as the principal load-supporting member.

Records indicate that copper cables were used in the ancient city of Ninevah near Babylon about 685 B.C. A short piece of such a cable is on display in an English museum.

Another old piece of wire rope made of bronze and used in a treadmill at Pompeii was discovered in the ruins caused by the eruption of Mount Vesuvius in 79 A.D. There is evidence that the Romans manufactured cables of wire and wire rope; a specimen 1 in. in diameter and 15 in. in length, (25 mm in diameter and 375 mm in length) is displayed at the Musio Barbonico at Naples, Italy.

The wires for the early ropes were constructed by hand. In the succeeding centuries the only changes were refinements of the craftsmen's skill and the introduction of new materials and field construction



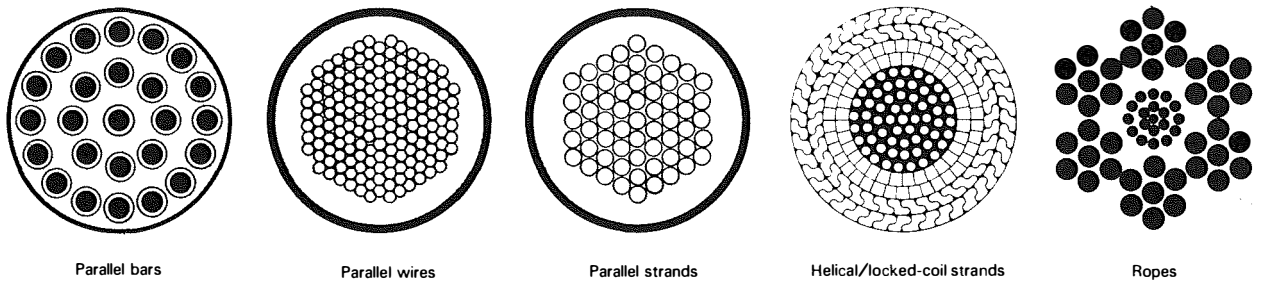


**FIGURE 9.1** Various types of stay cables. (Courtesy of VSL International, Losinger, Ltd., from reference 1.)

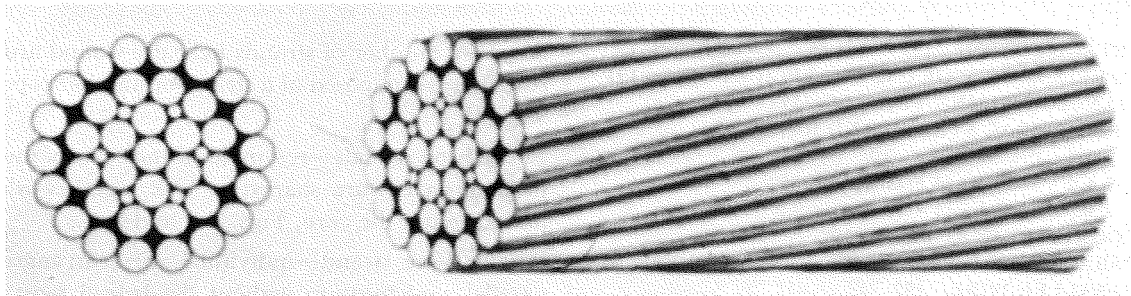


**FIGURE 9.2** Structural strand. (Courtesy of the United States Steel Corporation, from reference 3.)

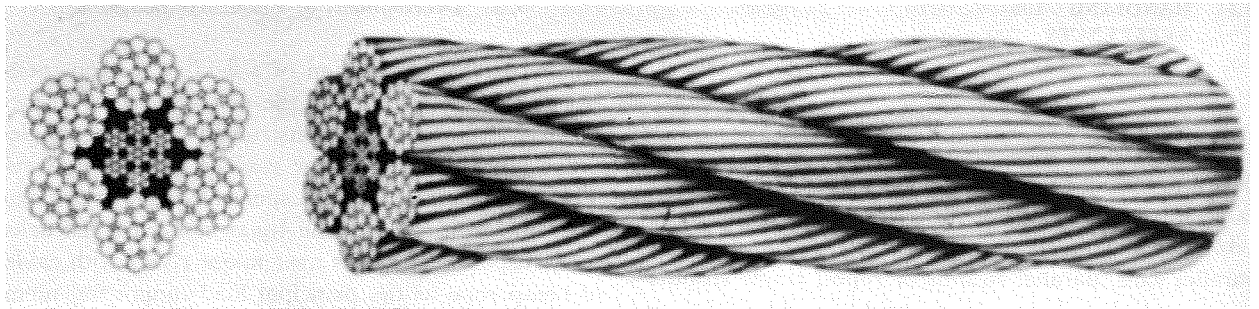


**FIGURE 9.3** Structural rope. (Courtesy of the United States Steel Corporation, from reference 3.)

techniques. The art of cable manufacture reached such a height of perfection that only a close examination could reveal that the wires were hand made. Examples of wire made by the Vikings are so uniform that some are of the opinion that they were mechanically drawn.

Machine-drawn wire first appeared in Europe during the fourteenth century, but A. Albert of Germany is credited with producing the first wire rope that closely resembles the wire rope of today in 1834. Some sources claim that a man named Wilson produced the first wire rope in England in 1832. These dates may be somewhat in error but indicate the general period of time of the development of the wire rope in Europe.

The first American machine-made rope was used in a service application in 1846. Since then many changes have taken place, such as the introduction of better quality, high-strength steels, efficient manufacturing processes and machines, and new field applications accompanied by new techniques of construction. The technology of structural strand and rope has improved consistently with time.

V. G. Shookhov, a Russian engineer, was one of the first to use cables as a structural load-carrying member in a building. He designed cable-suspended roofs for four pavilions at an exhibition at Nijny-Novgorod in 1896 and used the same design for the Bary

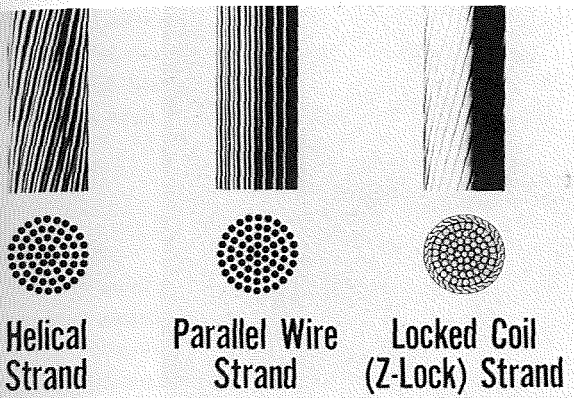


**FIGURE 9.4** Strand types. (Courtesy of the Bethlehem Steel Corporation.)

Boiler works in Moscow. In 1933, at the Chicago Worlds Fair, a pavilion to house a locomotive round-house was constructed with a cable-suspended roof structure.

Since 1933, many buildings have been constructed using cables as suspension systems for roof structures, as hangers supporting roofs, and as stays for roof structures. The application of cables to cable-stayed bridge construction is presented in Chapter 1.

### 9.3 Manufacturing Process

One of the most important features of steel cables is their inherent strength and structural integrity. This strength is a result of the excellent quality control maintained throughout the manufacturing process, from the selection of iron ore to the finished product.<sup>3</sup>

Wires are produced by cold drawing a rod through a series of successive dies, Fig. 9.5. This process reduces the cross-sectional area of the rod by 65 to 75%.

At the same time, cold drawing improves the internal structure of the steel and thus increases the tensile strength.

The rods for the wire-drawing operation are reduced from billets, heat-treated, carefully quenched at controlled temperatures, and inspected to ensure that all physical and chemical standards are met. They are then cleaned by dipping in acid to remove mill scale, rinsed in water, neutralized, coated with a lubricant which facilitates the drawing process, and, finally, coiled for shipment to the wire mill. The heat treatment improves the tensile strength, relieves the stresses caused by the hot rolling, and controls the crystalline structure.

After the wire is drawn to a finished size, it undergoes a series of quality control tests. The tests include the usual tensile test for strength, the torsion test to determine uniformity and toughness, and careful gauging to verify the diameter. The objective of all the operations of hot rolling, wire drawing, heat treating, and quality inspection is to ensure a wire of proper size, strength, and toughness before it is made into a rope or strand.

Strands and rope are produced from the individual wire that have been wound on steel spools, similar to bobbins of an ordinary sewing machine, before placed in the cradle of a stranding machine, Fig. 9.6. In the stranding operation the individual wires are led from the spools over sheaves, through bushings along the periphery of the machine, converging through a twister-head into the proper location for the strand, which is guided through a stationary die. As the strand is pulled through the stationary die, the stranding machine and twister-head rotate continuously, forming the strand.

Larger structural strands are made by adding successive layers of wires. As the strand is pulled off the stranding machine it is wound on a reel or spool, depending on its subsequent use, as a finished structural

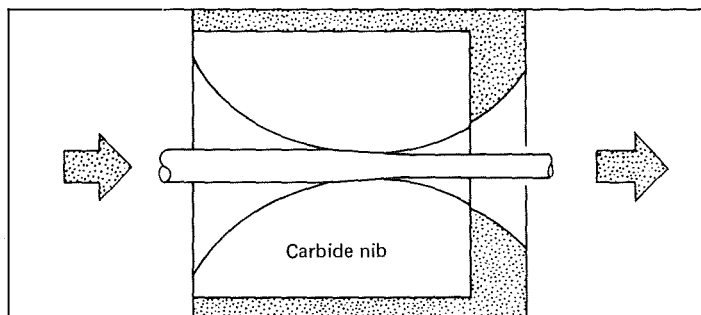


**FIGURE 9.5** Cross section of die. (Courtesy of the United States Steel Corporation, from reference 3.)

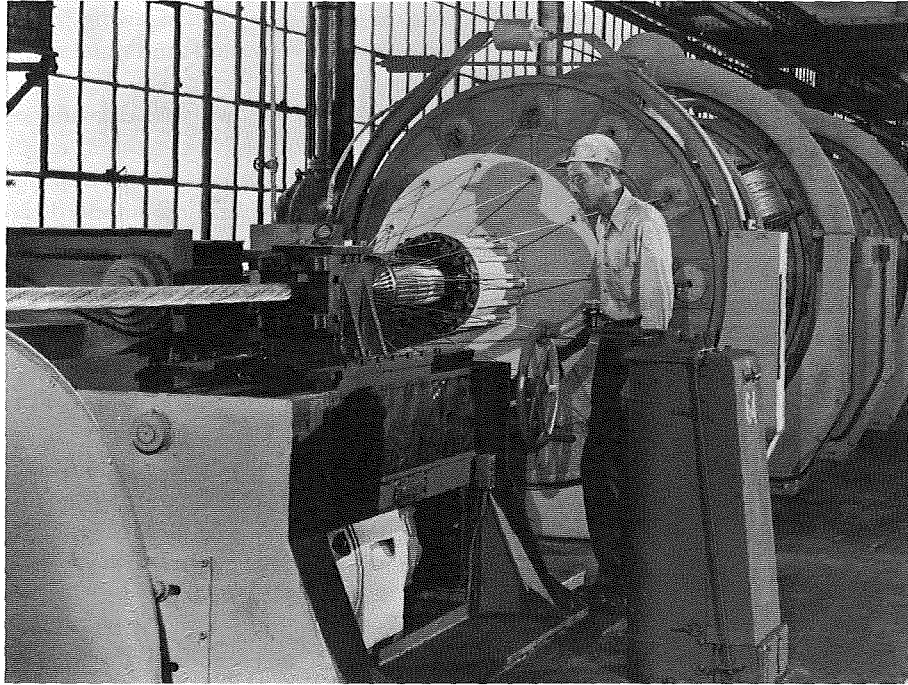


**FIGURE 9.6** Stranding machine. (Courtesy of the Bethlehem Steel Corporation.)

strand or a strand to be used to produce a structural rope.

A structural rope is made in much the same manner as a strand except that strands replace wires in a larger machine.

#### 9.4 Structural Strand and Rope

The static mechanical properties of structural strand and rope are stated in two standard specifications of the American Society for Testing and Materials (ASTM) designated as:

1. Standard Specification for Zinc-Coated Steel Structural Strand, ASTM A586-68
2. Standard Specification for Zinc-Coated Steel Structural Wire Rope, ASTM A603-70

These specifications contain information on the physical requirements, tests for zinc coating weight, data on the wires used to make the strands, strength tables, sampling, testing, inspecting, and packaging. Those planning to use the strands in construction should familiarize themselves with the two ASTM Standards in order to know how to design for its properties or handle the material knowledgeably during the construction stages.

The wire basic to the strand and rope has an ultimate tensile strength ranging from a high value of 220,000 psi (1520 MPa) for wires with class A zinc coating to a low value of 200,000 psi (1380 MPa) for wires with class C zinc coating.

The breaking strength for strand and rope with class A zinc coated (Section 9.10) wires throughout, range as shown in Table 9.1.

Other combinations of zinc coatings and number of

**TABLE 9.1. Breaking Strength—Strand, Rope**

| Item                      | Strand                 |                         | Rope                  |                       |
|---------------------------|------------------------|-------------------------|-----------------------|-----------------------|
| Minimum size, diameter    | $\frac{1}{2}$ in.      | 12.7 mm                 | $\frac{3}{8}$ in.     | 9.53 mm               |
| Minimum breaking strength | 15.0 tons <sup>a</sup> | 13.6 tons <sup>b</sup>  | 6.5 tons <sup>a</sup> | 5.9 tons <sup>b</sup> |
| Maximum size, diameter    | 4 in.                  | 101.6 mm                | 4 in.                 | 101.60 mm             |
| Maximum breaking strength | 925 tons <sup>a</sup>  | 839.2 tons <sup>b</sup> | 730 tons <sup>a</sup> | 662 tons <sup>b</sup> |

<sup>a</sup>These are in tons of 2000 pounds.

<sup>b</sup>Metric tons.

wires will affect the minimum breaking strength to the extent that designers and contractors should refer to the ASTM Standards for the specific strength associated with each manufactured rope or strand size.

#### 9.4.1 PRESTRETCHING

Although steel ropes and strands are considered to have safe and satisfactory elastic properties for most conventional service requirements, for certain end uses, such as structural applications, additional stretching of the manufactured product is necessary. True elasticity is required for applications such as main cables for suspension and stayed bridges, hangers or suspenders for arch and suspension bridges, guy ropes for high towers, cable-supported roof structures, and hangers for buildings.

Prestretching may be defined as the application of a predetermined tension force to a finished strand or rope in order to remove the cable looseness (constructional stretch) inherent in the manufacturing process. The prestretched cable becomes an elastic material within the limits of the prestretching operation, which enables a designer or contractor to predict the elongation under load with the high degree of accuracy necessary for structural applications. Another reason for prestretching the cables is that it permits measuring and marking of the proper spacing for the location of suspenders or the center of the towers. Although this marking is not required for cables to be installed in cable-stayed bridges there may be an occasion to locate spacers or vibration tie downs for certain configurations.

The prestretching operation consists of stretching a certain specified length of cable (sometimes as long as 5000 ft), in long successive "bites," on a stretching machine with tension jacks or screws.<sup>4</sup>

Removal of the constructional stretch is effected by repeated applications of a tension load to the cable, which forces the component wires to seat themselves in closer contact. On removal from the prestretching bed, the cable is left with well-defined and uniform elastic properties that are similar to the steel itself. The prestretching load applied to the cable does not usually exceed 55% of the rated minimum breaking strength of strand or 50% for rope, which essentially eliminates the constructional stretch of the cable or rope.

The prestretching equipment used by the cable manufacturers enables the designer to better predict the elastic behavior of the strand or rope after erection in the structure, because it eliminates the construc-

tional stretch of the cable. Loading curves can be furnished as proof of the results of the operation.

#### 9.4.2 MODULUS OF ELASTICITY

The magnitude of the elastic elongation of a cable under tension is dependent upon the value of the Young's modulus of elasticity ( $E$ ), which is defined as "the ratio of unit stress in the cable to a corresponding unit strain within a defined stress range."<sup>2</sup> Unlike the usual conventional tension test, the value for the modulus of elasticity for cables is determined from a gauge length of not less than 100 in. (254 cm) and is computed on the basis of the gross metallic area, which includes the zinc coating. Experience in prestretching has indicated that stress-strain data taken from 1600-ft (487.7-m) lengths are much more accurate than those taken from a 100-in. (254-cm) gauge length.

The elongation data used to compute the modulus of elasticity are taken when the cable is stressed not less than 10% of the minimum breaking strength and not more than 90% of the prestretching load. The data is presented in the form of a load deflection diagram, Fig. 9.7.

The value for the modulus of elasticity is determined by calculation using the conventional expression for elastic elongation of a specified length of the material such that:

$$E = \frac{Pl}{Ae}$$

where  $E$  = Young's Modulus of Elasticity, psi

$P$  = increment of load, lb

$l$  = gauge length, in.

$A$  = gross metallic area, in.<sup>2</sup>

$e$  = elongation caused by load increment, in.

As an example, a  $2\frac{1}{8}$  in. in diameter galvanized structural strand has the following data:

At 10% breaking strength (58,400 lb) the elongation is 0.102 in. At 90% prestretching load (259,200 lb) the total elongation is 0.395 in. The difference in load and elongation is:

$$P = 200,800 \text{ lb}$$

$$e = 0.293 \text{ in.}$$

$$A = 2.715 \text{ sq in.}$$

$$l = 100 \text{ in.}$$

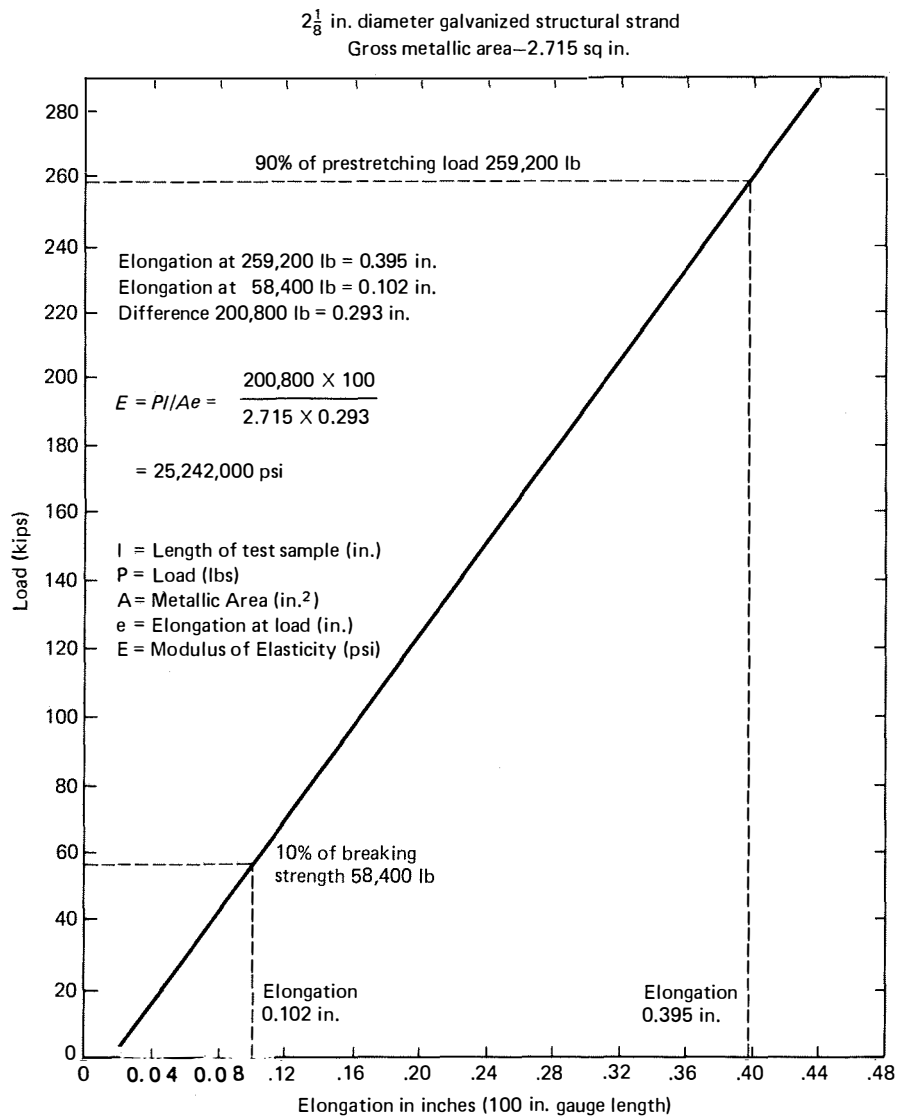


**FIGURE 9.7** Typical modulus of elasticity chart, based on data recorded during prestretching. (Courtesy of the United States Steel Corporation, from reference 3.)

Therefore,

$$E = \frac{(200,800)(100)}{(2.715)(0.293)} = 25,242,000 \text{ psi}$$

It is to be noted that the value for *E* is somewhat less than the usual 29,000,000 psi for structural steel.

In fact, the value of *E* varies with the type of cable, such as strand, rope, or parallel wires, and is also dependent on the amount of zinc coating applied to the wires. The ASTM Specifications state minimum values to be used for the various sizes and coatings. The minimum modulus of elasticity of prestretched strand and rope for class A coating of zinc on the wires is given in Table 9.2.

The ASTM Specifications also state that for heavier zinc coatings, classes B and C, on outside wires, the value of *E* is to be reduced by 1,000,000 psi; for other combinations of zinc coatings on all wires, the manufacturer should be consulted.

**TABLE 9.2. Minimum Modulus of Elasticity Class A Coating of Zinc**

| Type   | Diameter             | Modulus of Elasticity |
|--------|----------------------|-----------------------|
| Strand | 1/2 to 2 9/16 in.    | 24,000,000 psi        |
|        | 2 5/8 in. and larger | 23,000,000 psi        |
| Rope   | 3/8 to 4 in.         | 20,000,000 psi        |

### 9.4.3 STRAND AND ROPE COMPARED

The difference in the ASTM Specifications for the breaking strengths of strand and rope for a given diameter is not the only consideration involved in choosing the cable for a specific application. Because of the difference in the manufacturing process that uses strands instead of wires to make a rope, other characteristics of strand and rope may influence the choice.

The significant differences between strand and rope, which should be considered in making a selection, are summarized in the following:

1. Strand is stronger than rope of the same diameter.
2. Strand has a higher modulus of elasticity than rope.
3. Strand is less flexible than rope, and is not used with small bend radius curvatures.
4. Strand has larger diameter wires than rope of the same size, consequently, strand of a given class of zinc coating is more resistant to corrosion because of the thicker coating on the larger wires.
5. Strand is specified when flexibility or bending is not a major requirement.
6. Rope is specified when bending of the cable is an important consideration in the application of the cable.
7. The outside surface of strand is smoother than rope, therefore it may be protected more easily with a paint covering.
8. Strand uses smaller accessory fittings, because the strand diameter required for a given load is smaller than rope.
9. Rope is easier to handle in the field because it is more flexible.
10. Saddles for ropes are generally smaller than those for strands because rope can be bent to a shorter radius.
11. Angles changes at bands and clamps may be larger for rope than strand because of the flexibility of the rope.

### 9.5 Locked-Coil Strand

The locked-coil strand, which had been used extensively in Europe (primarily West Germany) in many of the early cable-stayed bridges, is also a helical-type strand. The locked-coil strand has a center portion composed of a number of round wires, several inner

layers of wedge- or keystone-shaped wires and, finally, several outer layers of Z- or S-shaped wires, Fig. 9.1.<sup>5</sup>

The advantages of this type of strand compared with the ASTM A586 structural strand previously discussed is as follows:

1. Increased corrosion protection by virtue of the exterior tightly locked, shaped wires
2. Density of the strand is approximately 90% for the locked-coil strand compared to approximately 70% for the structural strand with all round wires
3. A higher modulus of elasticity of approximately 25,400,000 psi
4. Because of the special profiled Z or S wires a locked-coil strand is relatively insensitive to bearing pressures when compared with structural strands

A type of locked-coil strand is manufactured in the United States primarily for cable and tramway applications. However, as yet, it has not been utilized for bridges.

### 9.6 Parallel Bars

Parallel bar stays, to the authors' knowledge, have only been used in two cable-stayed bridges: the Main River Bridge constructed in 1971 (see Section 4.5) and the Penang Bridge in Malaysia completed in 1985.

Bars of this type are specified as ASTM A722-75, Type II. They have a minimum ultimate tensile strength of 150,000 psi (1035 MPa) and range in size from  $\frac{5}{8}$  to  $1\frac{3}{8}$  in. (15 to 36 mm) in diameter. In the fabrication of a stay the bars must be coupled together. Because of the coupler the fatigue resistance is lower than that of a wire strand.

### 9.7 Parallel Wire

Current state-of-the-art parallel wire stays consist of ASTM A421-80, Type BA,  $\frac{1}{4}$ -in. (6.35-mm) diameter wire with a minimum tensile strength of 240,000 psi (1655 MPa). The button-headed wires are individually anchored in the anchor socket (see Section 10.3.2), consequently requiring prefabrication of the stay.

The fabrication process for parallel wire stays uses the same diameter wire in various numbers to form a hexagonal configuration, Fig. 9.1. Experience has indicated that the perfect hexagon is the most compact grouping of wires and provides a geometry in which

equal length of individual wires can most easily be maintained, thus achieving uniform stressing in all wires.

Preassembled parallel wire stays, in contrast to structural strands, do not require prestretching because there is no constructional stretch to be eliminated. All wires are in a straight alignment and the elastic behavior of the stay approaches that of the wire.

The minimum modulus of elasticity of a parallel wire strand is in the range of 27,500,000 to 28,500,000 psi (189,655 to 196,552 MPa) compared to the lower value of 24,000,000 psi (165,517 MPa) for strand of  $2\frac{9}{16}$  in. (64 mm) in diameter and smaller. The higher modulus is the result of the wires being placed in a parallel position and, therefore, approaching the elastic characteristics of the individual wire.<sup>6</sup>

Some laboratory tests for the modulus of elasticity for parallel wire strands have indicated a value of 27,500,000 psi, which is slightly lower than the value for the individual wire.<sup>7</sup> As a result, some engineers prefer to use an effective value of 27,500,000 psi (189,655 MPa) for the parallel wire strand to account for the fact that the modulus of elasticity of the individual wires tends to fall over time.

### 9.8 Parallel Strand

A rather recent innovation for cable stays is the current use of parallel 0.6-in. (15.24-mm) diameter ASTM A416-80, 7-wire prestressing strand, Fig. 9.1. This material has a minimum ultimate tensile strength of 270,000 psi (1860 MPa). These strands have a relatively high breaking strength which results in less volume of steel and thus less weight of the stays.

The individual strands are anchored in the end anchorages of the stays by wedges or swaged fittings and, therefore allow prefabrication or fabrication on the bridge site for the stays (see Chapter 10).

### 9.9 Comparison of Various Types of Stays

Table 9.3 presents a comparison of minimum breaking strengths and allowable working stress for the various types of stays discussed in the previous section. It is obvious from Table 9.3 that the most structurally efficient cable stays are those composed of A421 parallel wire or A416 parallel strand.

### 9.10 Corrosion Protection

Protection of structural cables against corrosion is essential because the pitting and/or nicking of the surface of the steel wires creates points of weakness, so they cannot resist stress concentrations at these points. Corrosion affects all steel products in varying degrees, and structural cables are no more or less susceptible to rusting than other steel products. Therefore, protection of the wires is provided by various thickness of zinc coatings, depending on the location of the wire in the cable and the degree of atmospheric exposure expected.

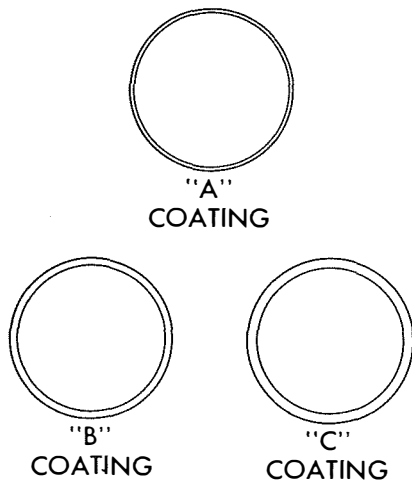
The ASTM Specifications (A586 and A603) require that zinc conform to ASTM Specification B6, for zinc metal (slab zinc), high grade or better. The various thicknesses of zinc coatings are classified as class A, B, and C. The class A coating is the basic thickness that varies from 0.40 to 1.00 ounce per square foot of uncoated wire surface, (122.0 to 305.0 g/m<sup>2</sup>), Class B coatings are twice as heavy, and Class C coatings are three times as heavy, Fig. 9.8.<sup>3</sup> The ASTM Specifications indicate values for breaking strength for three types of cables, depending on the zinc coatings and location of wires in the cable, such as:

1. Class A coating throughout all wires
2. Class A coating for the inner wires and class B coating for the outer wires

**TABLE 9.3. Comparison of Breaking and Allowable Stress for Various Types of Cable Stays**

| Type                              | Minimum Breaking Stress |        | Allowable Stress        |       |
|-----------------------------------|-------------------------|--------|-------------------------|-------|
|                                   | psi                     | (MPa)  | psi                     | (MPa) |
| A603 Rope <sup>a</sup>            | 220,000                 | (1520) | 0.33 $f_{pu} = 73,300$  | (507) |
| A586 Strand <sup>a</sup>          | 220,000                 | (1520) | 0.33 $f_{pu} = 73,300$  | (507) |
| A722 Bars                         | 150,000                 | (1035) | 0.45 $f_{pu} = 67,500$  | (466) |
| A421 Parallel Wire                | 240,000                 | (1655) | 0.45 $f_{pu} = 108,000$ | (745) |
| A416 Parallel Strand <sup>a</sup> | 270,000                 | (1860) | 0.45 $f_{pu} = 121,500$ | (837) |

<sup>a</sup>Class A Zinc coating



616  
617

the zinc coating to the wire can reduce the tensile strength of the wire by approximately 8%.

Current state-of-the-art corrosion protection for cable stays consists of encapsulating the stay in a sheathing and injecting cement grout. The sheathing may be a steel tube or a polyethylene tube.

Requirements for the polyethylene tube are that it be black polyethylene plastic pipe conforming to ASTM D3035, Grade P33, and in addition meet the following mechanical properties:

|                                 |                   |
|---------------------------------|-------------------|
| Elongation at yield point       | 16%               |
| Tensile strength at yield point | 3000 psi          |
| Elongation at breaking          | Greater than 100% |

FIGURE 9.8 Zinc coatings. (Courtesy of the Bethlehem Steel Corporation.)

- Class A coating for the inner wires and class C coating for the outer wires

Other coatings and arrangements are possible if the atmospheric conditions warrant more or less protection. The contractor and designer should consult a manufacturer for any special weight of zinc coating desired on the wires.

As a general guideline the *Manual for Structural Applications of Steel Cables for Buildings*,<sup>2</sup> states that a class A coating is adequate for indoor use and most outdoor exposures. For more severe exposures, classes B and C are available as noted in the ASTM Specifications. If the exposure is extreme, such as conditions of heavy condensation, salt or chemical atmosphere, added protection should be supplied.

Acceptable methods of added cable protection are painting, plastic jacketing, and the use of rust-preventive compounds, which are noted in the recommendations of the Steel Structures Painting Council publication. The federal specification TT-P-641 suggests that zinc dust-zinc oxide paints can be used to restore the original zinc-coating protection, especially where there is little bending action in the cables.

It is to be noted, however, that as the zinc coating is increased in thickness it displaces a larger portion of steel area, and as a result, the breaking strength of the same size cable is reduced when using the heavier coatings. Therefore, the contractor and designer must consider the advisability of a reduced strength when requiring more zinc protection for a given diameter of cable.

It should also be noted that the process of applying

Radial expansion at injection points of the grout should be limited within 2% of the original diameter of the tube. Carbon black is incorporated into the polyethylene pipe resin in sufficient amounts to provide resistance to ultraviolet degradation in accordance with ASTM D1248. The ratio of external diameter to wall thickness of the tube is approximately 18/1 in order to withstand handling and erection stresses in addition to the grouting pressure.

The sheathing around the stay bundle is filled with Portland cement grout and provides the same objective as the for posttensioning tendons. The alkaline properties of the grout make it an active corrosion protection.

A more recent proposal is to coat the individual wire or strands with an epoxy material in the same manner as epoxy coating reinforcing bars, except that a heavier thickness is used. In this manner the temporary corrosion-protection methods required during construction, before grouting the stay, is avoided.

### 9.11 Handling

The handling of cable stays to prevent damage is an important consideration which may save lives and money during the erection and life of the structure.

The strands or wire should not be dragged over obstacles that can cause cuts, nicks, or abrasions on the wires before they are encased in the sheathing. These defects can cause premature failure of the cables because of the local stress concentrations.

Storing unprotected strands of wires in locations subject to corrosive elements can cause pitting and rusting, which are detrimental to the wires, thus re-



ducing the tension load capacity and increasing the likelihood of early failure.

The reel should be permitted to rotate as the wire or strand is unwound to avoid kinks or twisting which will damage the wires.

During erection, when lifting a stay into position, the crane or sling attachment should be connected in such a manner as to avoid sharp bends in the cable, and the cable should be kept clear of obstructions in order to avoid abrasion.

Strands are packaged at the manufacturer's plant in accordance with approved practices. The strands are packaged in coils or on reels at the discretion of the manufacturer and in such a manner that no permanent deformation of the wires will occur.

For the case of prefabricated stays sheathed in polyethylene tubes, careful coordination is required with the fabricator to avoid having the reeled stays in storage for a long time before installation. The polyethylene tube may take a permanent set with subsequent damage upon unreeling. In the event that the polyethylene tube has taken a permanent set, it should be placed in an enclosure and the temperature raised to soften the polyethylene tube prior to unreeling. The

manufacturer should be consulted with respect to the proper procedure and temperature to be used.

### References

1. Annon., *VSL Stay Cables for Cable-Stayed Bridges*, VSL International, Lossinger Ltd., Berne, Switzerland, January 1984.
2. *Manual For Structural Applications of Steel Cables for Buildings*, American Iron and Steel Institute, Washington, D.C., 1973.
3. Scalzi, J. B., Podolny, W., Jr. and Teng, W. C., "Design Fundamentals of Cable Roof Structure," ADUSS 55-3580-01, United States Steel Corporation, Pittsburgh, Pennsylvania, October 1969.
4. "Bethlehem Wire Rope for Bridges, Towers, Aerial Tramways, and Structures," Catalog 2277-A, Bethlehem Steel Corporation, Bethlehem, Pennsylvania.
5. Podolny, W., Jr. and Fleming, J. F., "Historical Development of Cable-Stayed Bridges," *Journal of the Structural Division*, ASCE, Vol. 98, No. ST9, September 1972.
6. Scalzi, J. B. and McGrath, W. K., "Mechanical Properties of Structural Cables," *Journal of the Structural Division*, ASCE, Vol. 97, No. ST 12, December 1971, Proc. Paper 8604.
7. Birdsall, B., Discussion to "Mechanical Properties of Structural Cables," by Scalzi and McGrath, *Journal of the Structural Division*, ASCE, August 1972.

# 10

## *Cable-Stay Anchorages and Connections*

|        |   |     |
|--------|---|-----|
| 10.1   | INTRODUCTION  | 201 |
| 10.2   | GENERAL CONSIDERATIONS                                    | 201 |
| 10.3   | END ANCHORAGES  | 202 |
| 10.3.1 | Swaged and Zinc-Poured Anchorages                         | 203 |
| 10.3.2 | HiAm Anchorages   | 205 |
| 10.3.3 | VSL Anchorages  | 206 |
| 10.3.4 | Stronghold Anchorages                                     | 209 |
| 10.3.5 | Freyssinet Anchorages                                     | 213 |
| 10.3.6 | Considerations in the Selection of Stay Anchorage Systems | 214 |
| 10.4   | SADDLES   | 214 |
| 10.5   | CONNECTION OF CABLE STAYS TO PYLON                        | 215 |
| 10.6   | CONNECTION OF CABLE STAYS TO GIRDER                       | 222 |
|        | REFERENCES  | 226 |

### *10.1 Introduction*

The structural design and construction details of the individual component members of cable-stayed bridges are similar to those of suspension bridges and/or other conventional bridge types. The one principal difference is the attachment of the special end fittings to the cable itself.

Many types of fittings are available, depending on the size of the cable, the manufacturer producing the fitting, and the unique desires of the designer. Cables may be connected to the towers and the superstructure by pins joining the end fittings of the cables to the attaching fittings on the supporting member or by terminal fittings that transmit their force in bearing. As in suspension bridges, saddles may be used on the towers to permit the use of a continuous cable and allow movement to take place.

This chapter first discusses the general considerations of these connections, which are applicable to all geometrical types of cable-stayed bridges, and then discuss typical terminal fittings and saddles.

Specific cable anchorage details for selected existing bridge structures are illustrated and discussed as case studies. Other unique construction and erection details

that are of interest to the designer and the contractor are also included. It is assumed that all conventional details are familiar to the professionals and contractors and, therefore, they are not included.

American designers and contractors have expertise and experience with cable assemblies in bridge structures and in cable-supported roofs of many varieties. However, because experience with the type of cables and methods of construction of cable-stayed bridges is quite limited, a review of the details of construction by others will be helpful. The experience gained in other countries may not be directly applicable to practice in the United States, but concepts may be adapted and improved by our techniques and ingenuity. As in any new concept and innovation we must evaluate the experience of others carefully. This chapter illustrates the type of connections used in existing bridges in Europe without attempting to evaluate or compare them in any way, either with each other or with an equivalent American practice.

In general cable connections should:

1. Provide full transfer of loads
2. Provide access for inspection
3. Provide protection against weather
4. Provide protection against accidental damage to the cable
5. Provide sufficient space for initial tensioning and later adjustments
6. Use standard fittings as much as possible
7. Consider erection procedures when selecting types of connections

### *10.2 General Considerations*

When choosing the particular geometrical configuration of the cable stays and the number of cables to be

used in a specific system, several considerations must be taken into account. Foremost among these considerations is the comparative cost of additional material required in the superstructure to resist the horizontal thrust versus the increased cost of the tower, cables, and their connections to the supporting members of the bridge. In other words, the number of cables used may depend on the economic balance between the distribution of the cables along the span and the number of cables to be connected at the tower and superstructure.

The use of a few cables results in large tensile forces, which require massive and sometimes complicated anchorage systems to transfer the loads to the tower and the bridge deck. The deck structure will have to be heavily reinforced at a few points of attachment as a result of the concentration of loads. When only a few cables are used, the deck structural system must be composed of a relatively deep girder or box in order to span the large distances between the cable connections. In addition to a deeper deck structure, the transverse girders at the cable attachments may also require reinforcement in order to distribute the horizontal thrust of the cable as uniformly as possible throughout the structural system. With only a few cables connected to the tower, large connection details are required, and these become exceptionally bulky, heavy, and cumbersome if all the cables are to converge at one point near the top.

When a large number of cables are used, the connections along the bridge deck are generally uniformly spaced and provide a nearly continuous elastic supporting media for the deck structure. With closely spaced connection points, the principal longitudinal girders or box members can be shallow in depth, thus requiring less material and simplifying the fabrication and erection procedures. The use of a large number of cables implies smaller diameter cables requiring smaller terminal fittings and connection details to the tower and bridge girders. Although the handling of the cables may be increased slightly, the reduced weight and easier fabrication and erection may more than offset this disadvantage by reducing the total time and cost of the project. With a larger number of connection points along the bridge deck, the designer can distribute the cable horizontal thrust more efficiently along the deck, use smaller anchorage details, and, usually, needs no additional reinforcement to the transverse beams. The connections to the towers will be distributed to many locations along the height of the tower, thus simplifying the fitting details and distributing the gravity load almost uniformly along the height instead of concentrating the total load at the top.

In all configurations the designer has the choice of terminating the cables at the tower connections or permitting them to pass through the tower as a continuous member. In the latter case the cable must be supported on a special fitting, referred to as a saddle, designed to fit the number and size of cables passing through the tower at that location. When only a few cables are to be connected to the tower, it may be more advisable to pass them over a saddle, rather than attempt a costly or impractical terminating connection to the tower. When a large number of smaller cables are distributed throughout the height of the tower, it becomes more practical and sometimes more economical to terminate the cables at the tower.

The cable saddles may be either rigidly connected to the tower or supported on expansion bearings that permit longitudinal movements to take place. When the saddles are fixed to the tower they add stiffness to the structural system, thus increasing the rigidity of the total bridge structure.

On some structures the designer may choose to connect the base of the tower to the supporting structure, thus producing a fixed condition. In this instance the saddle is allowed to move longitudinally, thus reducing the bending moments acting on the tower. Only the gravity load is transferred to the tower. The saddle movement adjusts itself to accommodate the necessary balance of the horizontal forces on each side of the tower. When a large number of cables are used, the saddle for the top cable stay may be fixed and all or a few of the lower saddles permitted to move. As may be expected, the selection of a geometrical cable arrangement depends on many conditions particular to a specific application.<sup>1</sup>

### 10.3 End Anchorages

Cable stays have end anchorages by which they can be connected to other parts of a structure. These fittings vary in shape, size, and weight depending on the diameter of the cable to which they are attached. Experience in the shop and field has indicated that anchorages should be designed, manufactured, and attached to the cable so that they are capable of transferring the breaking strength of the cable without exceeding the yield strength of the fitting.

An important criteria for cable-stay end anchorages is that they be accessible for inspection and retensioning, if necessary, during the life of the structure. The potential of cable-stay replacement, in the event of damage, is another important reason for accessibility,

that is, so that jacks can be properly placed and the stay detensioned.

10.3.1 SWAGED AND ZINC-POURED ANCHORAGES

Two types of end fittings are used for structural strand and are generally referred to as sockets: the swaged type and the zinc-poured type. The swaged sockets are used for small diameters of strand and rope, ranging from  $\frac{1}{2}$  to  $1\frac{3}{8}$  in. for strand cables and  $\frac{3}{8}$  to 2 in. for rope

cables.<sup>2</sup> The swaging process consists of carefully pressure squeezing the fitting over the cable in a hydraulic press in order not to damage the wires. The size limitations of the swaged fittings restrict their use and they are only used for small individual strands. The poured-zinc type of fitting had been an accepted method for the large strand sizes used in cable-stayed bridge construction in the United States. The standard fittings are illustrated in Fig. 10.1,<sup>2</sup> which denotes the type of fitting and the size of the cable which it can accom-

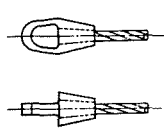
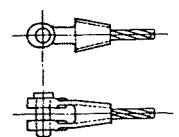
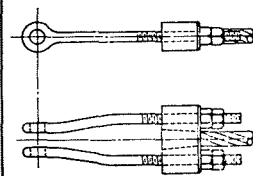
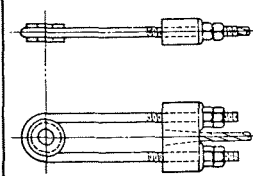
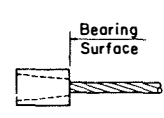
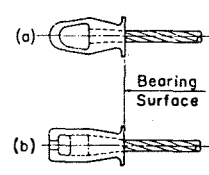
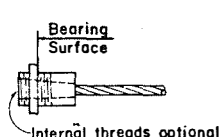
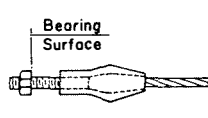
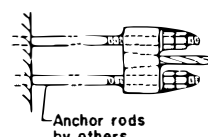
| Name                     | Description  | Attachment  | Sizes Available Diam. in. |                  |
|--------------------------|--|-------------|---------------------------|------------------|
|                          |  |             | Strand                    | Rope             |
| Closed Socket (a)        |     | Poured Zinc | $\frac{1}{2}$ -4          | $\frac{3}{8}$ -4 |
| Open Socket (b)          |    | Poured Zinc | $\frac{1}{2}$ -4          | $\frac{3}{8}$ -4 |
| Open Bridge Socket (c)   |   | Poured Zinc | $\frac{1}{2}$ -4          | $\frac{3}{8}$ -4 |
| Closed Bridge Socket (d) |   | Poured Zinc | $\frac{1}{2}$ -4          | $\frac{3}{8}$ -4 |
| Button Socket (e)        |     | Poured Zinc | $\frac{1}{2}$ -4          | $\frac{3}{8}$ -4 |
| Bearing Sockets (f)      |   | Poured Zinc | $\frac{1}{2}$ -4          | $\frac{3}{8}$ -4 |
| Threaded Socket (g)      |  | Poured Zinc | $\frac{1}{2}$ -4          | $\frac{3}{8}$ -4 |
| Threaded Stud Socket (h) |  | Poured Zinc | $\frac{1}{2}$ -4          | $\frac{3}{8}$ -4 |
| Bridge Socket Bowl (i)   |  | Poured Zinc | $\frac{1}{2}$ -4          | $\frac{3}{8}$ -4 |

FIGURE 10.1 Socketed end fittings. (Courtesy of the American Iron and Steel Institute, from reference 2.)

modate. The cable diameters range from  $\frac{1}{2}$  to 4 in. for strand and  $\frac{3}{8}$  to 4 in. for rope.

The standard fittings shown in Fig. 10.1 can have many different applications. With the open and closed sockets, a pin can be inserted through the fitting and connect it to other parts of the structure, Fig. 10.1(a) and (b). Several types of bridge sockets are available that meet the needs of the various designs, Fig. 10.1(c), (d), and (i). Sockets that transfer their loads by direct bearing on another structural component have various configurations in order to suit the specific method of application, Fig. 10.1(e), (f), (g), and (h). The type with external nuts and internal threads allow for periodic checks and adjustments of the cable tension. Jacks are used to apply tension to the cable through the threaded portions of the fittings. The use of the bearing sockets is analogous to the concept of the dead-end anchorage of a post-tensioned, prestressed concrete member.

The poured-zinc method of attaching the end fittings to the cable is a unique technique, which must be performed by experienced technicians. The method involves several operations, and each must be accomplished properly in order to guarantee the full strength of the cable.

The sequence of operations begins with the "brooming" of the individual wires of the cable for the length sufficient to be inserted in the "basket" of the socket, Fig. 10.2.<sup>3</sup> These broomed ends are care-

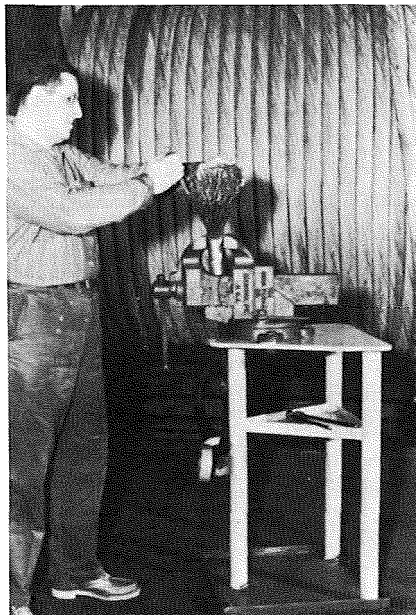


**FIGURE 10.2** Brooming out. (Courtesy of the United States Steel Corporation, from reference 3.)

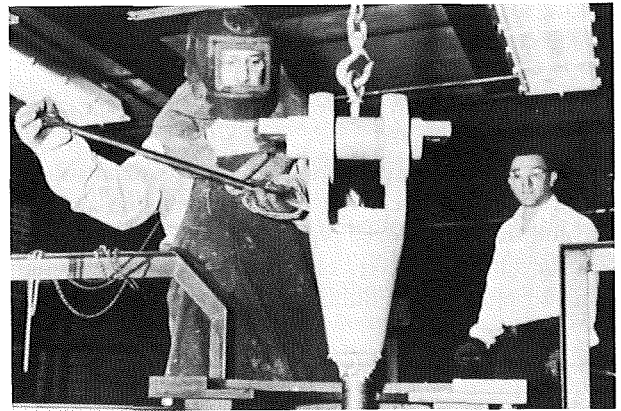


**FIGURE 10.3** Pouring zinc into socket. (Courtesy of the United States Steel Corporation, from reference 3.)

fully cleaned and immersed in a flux solution to prepare them to adhere to the zinc. The wires are then placed in the basket of the socket in a manner that will ensure that every wire will be surrounded by the poured molten zinc, Fig. 10.3. The ASTM Specifications A586 and A603 for strand and rope, respectively, specify that the slab zinc shall conform to ASTM Specification B6 for zinc metal (slab zinc), high grade or better. By careful attention to each phase of the operation, the attached fitting will develop the full breaking strength of the cable.

The Japanese have reported<sup>4</sup> that the pouring temperature of the zinc alloy when filling the socket affects the fatigue strength of the wires at the socket. The results of the study, indicated graphically in Fig. 10.4,

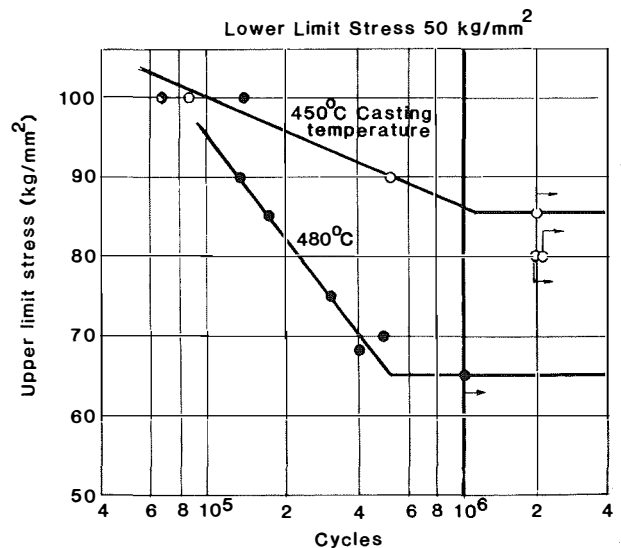


**FIGURE 10.4** Fatigue test of wire 5-mm-diameter with zinc-copper-alloy filled sockets. (Courtesy of Der Stahlbau, from reference 4.)

show that a casting temperature of 450°C increases the fatigue strength of the wires when compared to a temperature of 480°C. A West German report<sup>5</sup> has indicated that at the 450°C casting temperature there is still a decrease in fatigue resistance as compared to the original parent wire material, in or near the cable anchorage.

Another problem with the poured-zinc method is that the massive socket acts as a “heat sink” when the hot zinc is poured into the basket of the socket, Fig. 10.5.<sup>6</sup> In a recent investigation of fatigue failure of wires at a socket of this type, an autopsy of the anchorage indicated that an area of zinc adjacent to the inside surface of the basket had cooled at a faster rate than at the core of the zinc because of the “heat-sink” effect. As a result the “whetin” (bonding of wires to zinc) was not as effective as at the core of the zinc. In fact, the wires could be driven out of the zinc casting with a punch when given a slight tap with a hammer.

An additional problem is that of anchorage slippage. The molten zinc assumes more volume than cold zinc because of thermal expansion. The zinc cone shrinks as it cools off and hardens, hence a gap is formed between the zinc cone and the socket. This gap must be eliminated by a process called precompression of the socket. The displacement of the zinc cone in this process is in the range of 0.2 to 0.4 in. (5 to 10 mm). However, creep slippage continues under design and dynamic loads (see the following section).

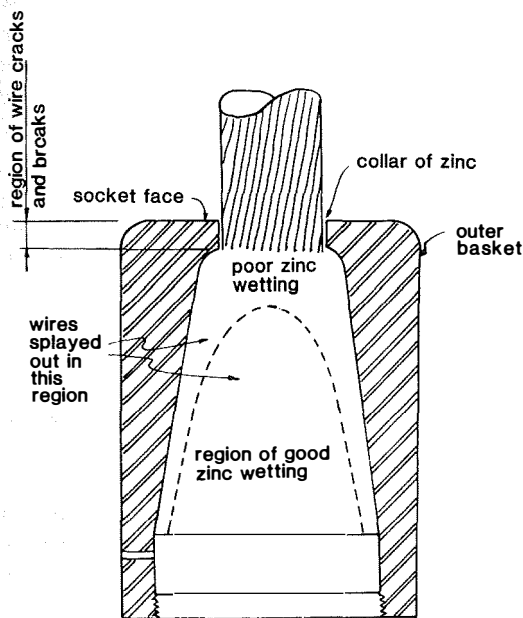


FIGURE 10.5 Heat-sink effect in poured-zinc socket, from reference 6.

For the preceding reasons the poured-zinc method of socket attachment is not recommended for cable-stayed bridges in the United States. Other than for a few early short-span bridges, current state-of-the-art fatigue-resistant anchorages are utilized on cable-stayed bridges in the United States.

### 10.3.2 HiAm ANCHORAGES

Recognizing the low fatigue strength of structural strand with zinc-poured sockets, Fritz Leonhardt, in conjunction with Bureau BBR Ltd., Zurich, in 1968 began the development of the HiAm (High Amplitude) socket for use with parallel wire stays, Fig. 10.6.

The stays are parallel  $\frac{1}{4}$ -in. (6-mm) diameter high-tensile steel wires (ASTM A421 type BA) which terminate with buttonheads in an anchor plate. The wire anchorage plate shown in Fig. 10.6 is a spherical plate to accommodate the transition flare of the individual wires from the compact bundle entering the anchorage to their termination in the anchorage plate (all wires are cut to the same length). Current technology is to use a flat plate with countersunk radial holes to accommodate the geometry of the flared wires. The anchorage socket is filled with steel balls, and an epoxy-and-zinc dust binder. This method of anchoring the stays increases the magnitude of fatigue resistance to almost twice that for zinc-poured sockets.<sup>7</sup> The bundle of parallel steel wires is encased in a polyethylene pipe, and the void between wires and pipe wall is grouted under pressure for corrosion protection after erection of the structure is completed.

The HiAm anchor filler material is poured at ambient temperature and cured at a temperature of less than 100°C. The cable is, therefore, not subjected to the high heat of zinc-poured sockets and thus can develop the full fatigue capacity of the element wires. Because of the high coefficient of friction of the HiAm filler material, HiAm anchors can be dimensioned smaller than conventional zinc-poured anchorages. The generally accepted coefficient of friction between the cone and the inner surface of the steel socket is 0.45 for HiAm and 0.2 for zinc. This makes a great difference in the hoop stress in the socket, that is, HiAm material permits a smaller taper angle of the cone and, therefore, a smaller socket diameter. The compact anchor socket allows the design of compact details at the pylon and girder.

The HiAm anchor socket is a cold-cast type of anchorage, and the socket is not influenced by the same temperatures that are developed in zinc-poured sockets. The cast material is very hard and resists the creep

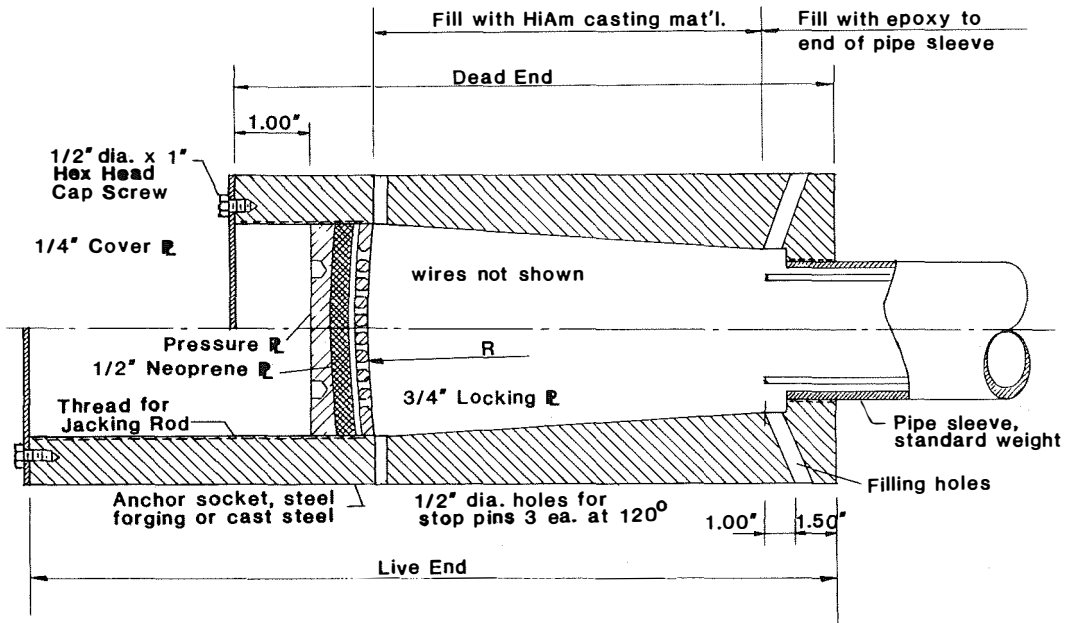


FIGURE 10.6 HiAm socket.

slippage and the cone in the socket. The slippage of the cone of HiAm sockets under design and dynamic loads is negligibly small, Fig. 10.7.

A stay cable when fully assembled is one continuous member free of splices in the primary load-carrying components. Only the protective polyethylene pipe is spliced using complete fusion techniques to provide a full-sealed encasement over the wire bundle. The dead (nonjacking) anchor end of the cable stay is not as long as the live anchor or stressing end of the cable stay. The difference in length is due to the internally-threaded section, which is part of the live end socket and provides a means for attaching a pull rod to the stay during the erection stressing operations, Fig. 10.6. Fittings are installed at each end of the cable stay adjacent to the anchorage to provide for the injection of a temporary corrosion protection and, after the cable stay has been erected and final adjustments made, the cement grout.

Each prefabricated cable stay is shipped to the erection site with a lifting plate attached onto the anchor socket at each end of the stay anchorage. The lifting plate provides a means for handling the stay during the final fabrication steps, coiling and uncoiling operations, and installation of the cable stay during erection phases on the bridge. The live end lifting plate must be removed to install the pull rod for stressing. However, up to this point, the lifting plate, in addition to providing a means for handling the cable, has sealed the end of the anchor from dirt, moisture, and so forth,

preventing corrosion. After the cable stay has been erected on the bridge and all stressing operations completed, the dead end lifting plates are removed and the end of the socket sealed with sealant and coated with corrosion protective grease. A cover plate is then bolted over the end of the socket to provide a tight seal.<sup>8</sup>

In recent years the availability of  $\frac{1}{4}$ -in. (6 mm) diameter prestress wire in the United States has diminished to a point that designers have turned to 7-wire prestressing strand for the tension stay component. As a result, there has been a proposal to use a button-headed 7-wire strand, Fig. 10.8.<sup>9</sup> Although there is very limited use of a button-headed strand in West Germany,<sup>10</sup> there is also no experience as yet in the United States. The authors are unaware of a manufacturing capability for such strands in the United States or even if this concept presents any long-term service problems.

### 10.3.3 VSL ANCHORAGES

Technical data presented in this section on the VSL anchorage system is reproduced from reference 9 by permission of VSL International, Losinger Ltd. VSL anchorages are an adaptation of the VSL posttensioning system used in prestressed concrete construction. Thus, the system is not a new one but an adaptation from an existing technology. Its main characteristic is the cable stay which is composed of parallel conventional 7-wire prestressing strands. It is a modular sys-

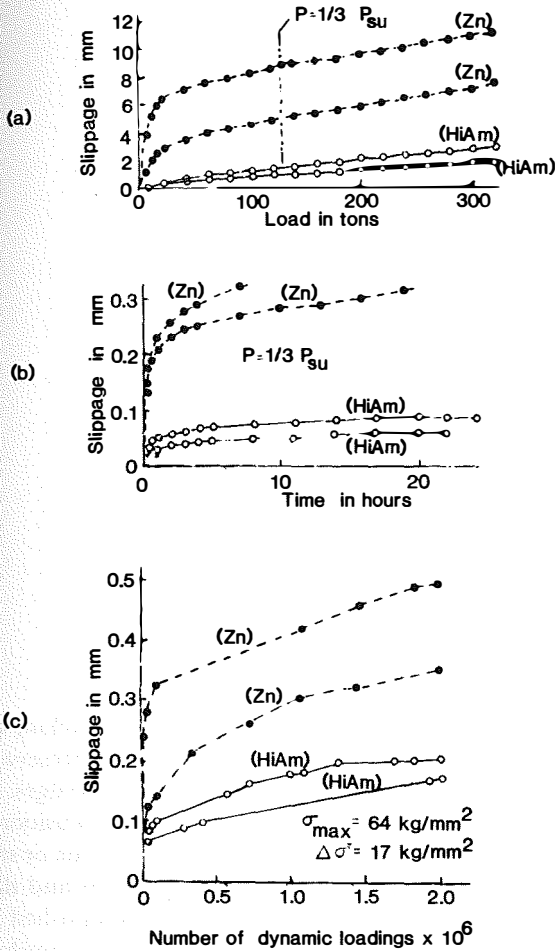


**FIGURE 10.7** Experimental results of anchor cone slippage: (a) slippage under static load, (b) creep slippage under a constant load, and (c) creep slippage under a dynamic load. (Data provided by Shinko Wire Company, Ltd.)

tem that enables any desired stay stay to be fabricated from standard units.

Parallel strand stays consist of 7-wire prestressing strands of 0.6-in. (15-mm) diameter strands of low relaxation quality. Strands of 0.5-in. (13-mm) diameter

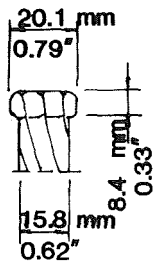


**FIGURE 10.8** Button headed 7-wire strand, from reference 10.

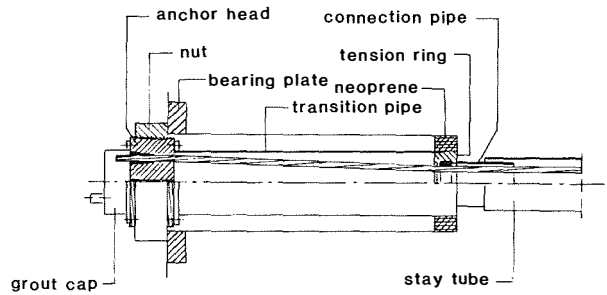


**FIGURE 10.9** VSL stressing anchorage. (Courtesy of VSL International, Losinger, Ltd., from reference 9.)

would be less economical, but 0.7-in. (18-mm) diameter strands have reduced fatigue properties. Both the stressing and the dead end anchorages consist of a bearing plate, an anchor head, wedges, a transition pipe, a tension ring, a connection pipe, and a protection cap with grout/air vents, Fig. 10.9. The stressing anchorage is generally provided with a thread of the anchor head and a ring nut, which allows an adjustment or total destressing whenever it is required. The transition ring is provided with a damping device (neoprene ring) which absorbs lateral vibrations caused by wind effects. Possible construction variants are illustrated in Fig. 10.10, and the adjustment potential is illustrated in Fig. 10.11.

The VSL stay cables are either prefabricated in a plant and shipped to the project site for installation or fabricated at the project site in their final position. Assembly of the prefabricated stay, Fig. 10.12, commences with cutting the strands to the length required for the cable. Then the stressing anchorage with anchor head, ring nut, wedges, and a temporary retainer plate are fitted to one end of the strand bundle. The resultant layout of the strands is continued along the cable by “combing” and fixed at the other end. Depending upon whether a polyethylene or a steel tube is provided for encasing the strand bundle, the cable is then completed as follows: the polyethylene tube (butt-welded by means of a plate thermowelding apparatus to provide the required length) is drawn over the strands, or for the case of a steel tube, the strand bundle is pulled through the tube.

In a following step, the cable, prefabricated at a plant or at the project site, is brought into its inclined position. For this operation, either the site crane is used, or a temporary guying system is erected for this purpose from which the cable is suspended and lifted by means of a winch or a VSL lifting unit. In the final phase of installation, the strands projecting from the upper end of the tubing are pulled through the opening



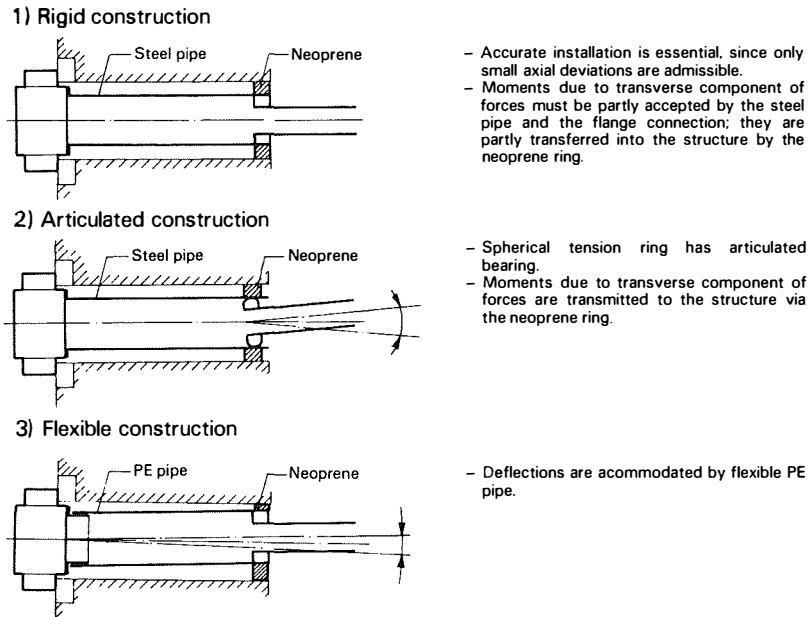


**FIGURE 10.10** Construction variants of VSL stressing anchorage. (Courtesy of VSL International, Losinger, Ltd., from reference 9.)

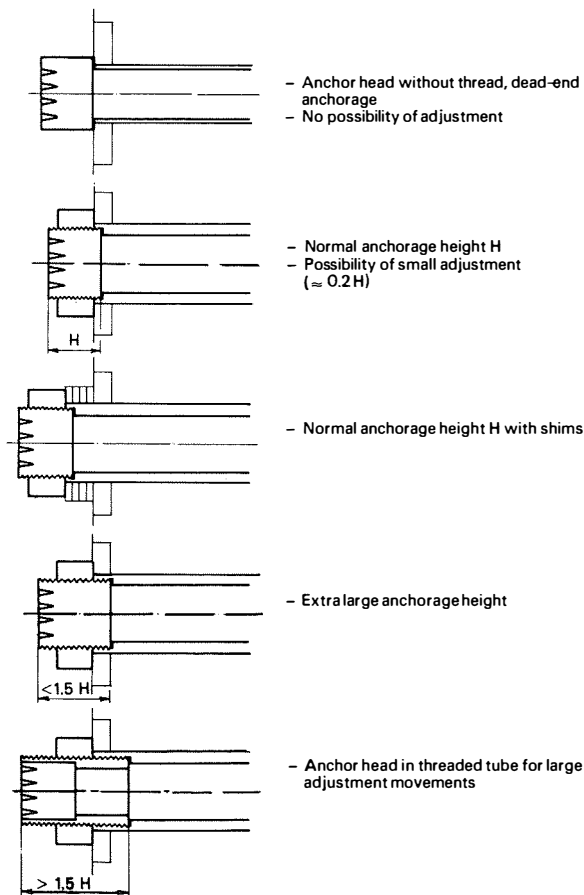


**FIGURE 10.11** Adjustment potential of VSL anchorage. (Courtesy of VSL International, Losinger, Ltd., from reference 9.)

of the anchorage fitted to the head of the pylon, the parallelism of the strands being carefully preserved, and fixed in the anchor head by means of wedges.

Where fabrication of the stay in its final position is utilized, the stay sheathing (either polyethylene or steel tube) is first erected in its inclined position and then the cable stay is installed. This is accomplished by either pulling through the entire cable or by pushing through individual strands.

The pull-through method, Fig. 10.13, is accomplished in the following operations:

1. Preparation of the cable bundle
2. Preparation of the lifting equipment for the empty polyethylene or steel tube and for the strand bundle
3. Preparation of the tubing: individual lengths of tubing are welded together
4. Raising of the tube into the inclined position
5. Pulling of the cable through the lower anchorage
6. Fitting of the upper anchor head
7. Stressing of the strands to a certain (low) force and releasing the lifting equipment

Where the stay cables are assembled in their final position strand-by-strand by the push-through method, from the top end of the cable, the sequence is as follows, Fig. 10.14:

1. Installation of the upper and lower anchorages

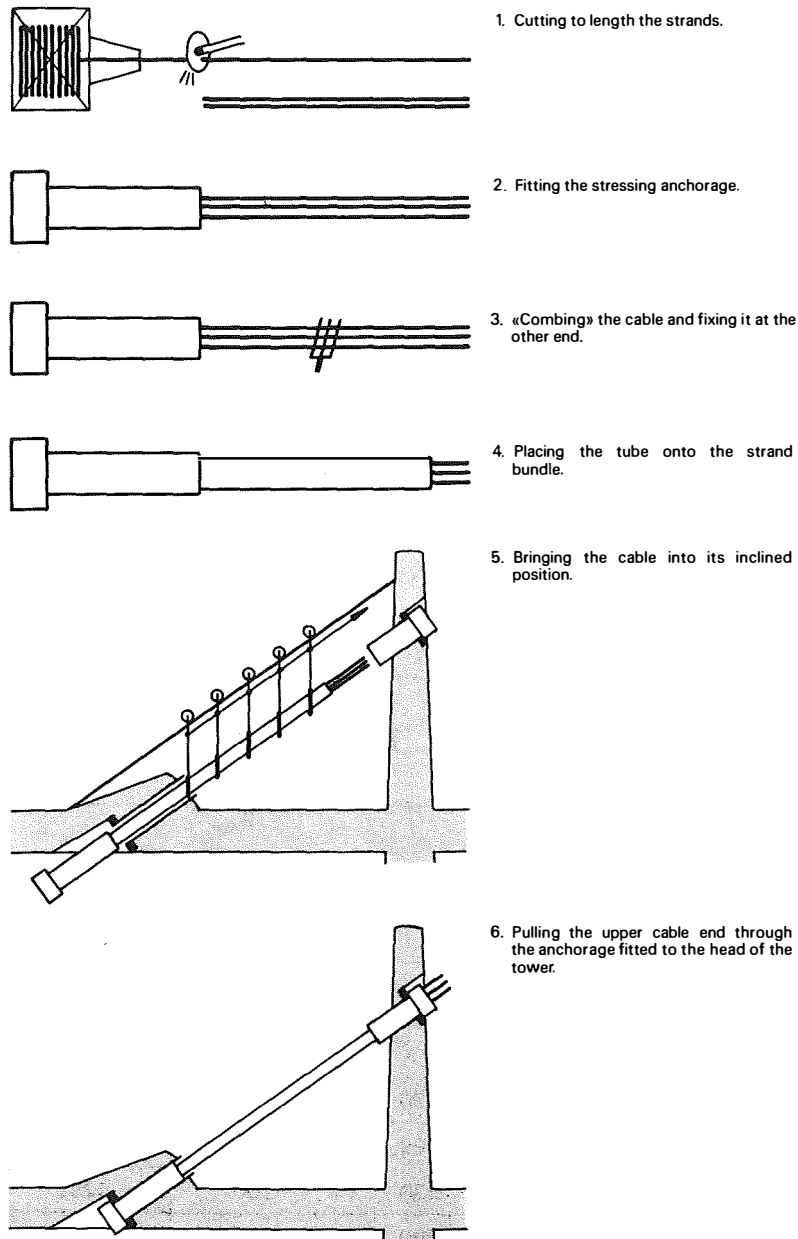


**FIGURE 10.12** Assembly of VSL prefabricated stay. (Courtesy of VSL International, Losinger, Ltd., from reference 9.)

2. Lifting of the polyethylene or steel tube into the inclined position
3. Pushing-through a first strand
4. Stressing of the first strand to a predetermined force so that the polyethylene or steel tube moves into its final position
5. Attaching the polyethylene or steel tube to the upper anchorage
6. Pushing through the second strand

7. Stressing of the second strand to the length of the first strand
8. Pushing through the third strand, and so on

#### 10.3.4 STRONGHOLD ANCHORAGES

Technical material<sup>11</sup> and data presented in this section on the development and application of the Stronghold Anchorage System has been provided through the

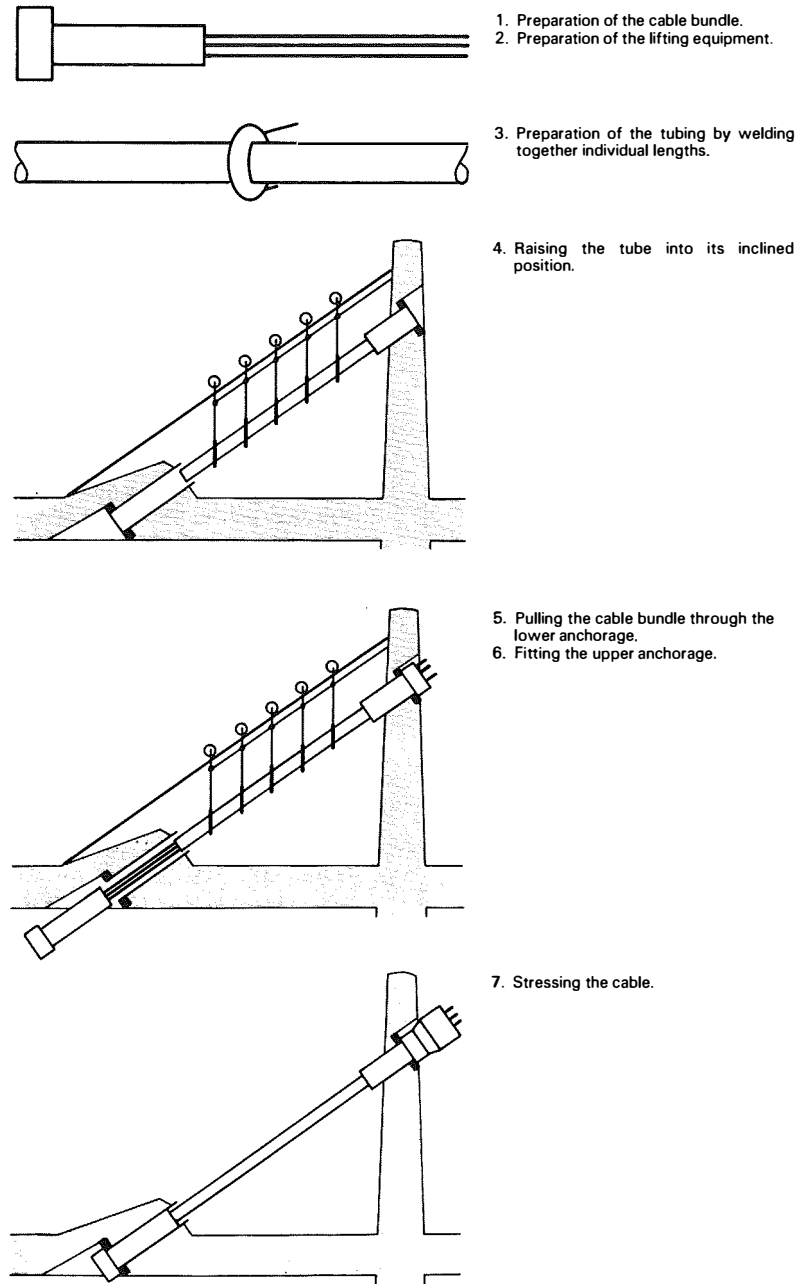
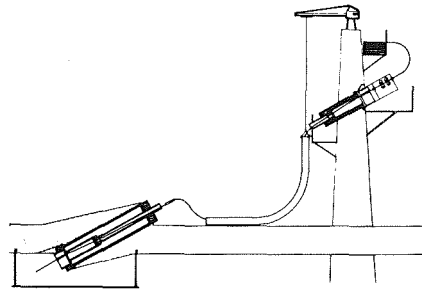


**FIGURE 10.13** Pull-through method of fabrication in the final position. (Courtesy of VSL International, Losinger, Ltd., from reference 9.)

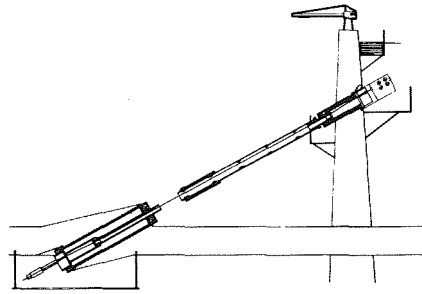
courtesy of Stronghold International Ltd., Star House, Oxford Road, Stone, Aylesbury, Buckinghamshire, England.

Anchorage used in conventional prestressed concrete construction are designed to resist cyclic loads directly related to the maximum allowable tendon forces. Such criteria are inadequate for cable-stay

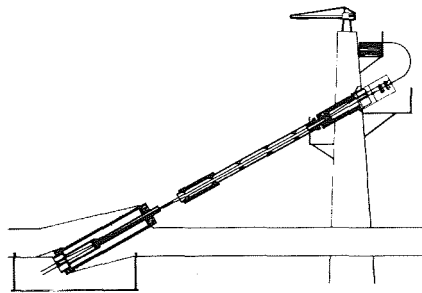
structures. Specifications governing cable-stayed bridges require a higher cyclic performance both in amplitude and frequency. The fact that mechanical anchorages are not able to meet these rigid requirements led to the development (by Stronghold International Ltd.) of an anchorage form known as the Type B Stronghold Anchorage.



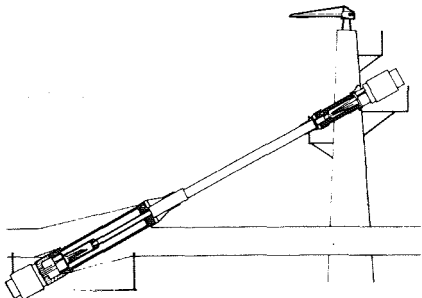
1. Installation of the upper and lower anchorages.
2. Lifting of the polyethylene or steel tube into the inclined position.
3. Pushing-through of a first strand.



4. Stressing of the first strand to a predetermined force, so that the tube comes more or less into its final position.
5. Fixing the tube to the upper anchorage.



6. Pushing-through of the second strand.
7. Stressing of the second strand to the length of the first strand.
8. Pushing-through of the remaining strands.



9. Finishing work.
10. Additional stressing or force re-adjusting, if required.

**FIGURE 10.14** Push-through method of fabrication in the final position. (Courtesy of VSL International, Losinger, Ltd., from reference 9.)

Stronghold's approach in the development of their system followed the following sequence: selection of stay, construction of stay, and selection of anchorage. It appeared that any tangible savings over existing practice would necessitate a departure from factory-produced prefabricated stays, whether of structural strand (zinc-poured anchorages) or parallel wire (HiAm) to a site-assembled stay system.

When prefabricated stays comprised of parallel wire or strands require precision in their measurement and cutting, any mistake that exceeds the available thread of the live anchorage renders the stay useless. Prefabricated anchorages also necessitate enclosing the stay in its protective duct at the factory. The degree to which the stay can then be coiled is thereby limited if deformation and damage of the duct is to be avoided.

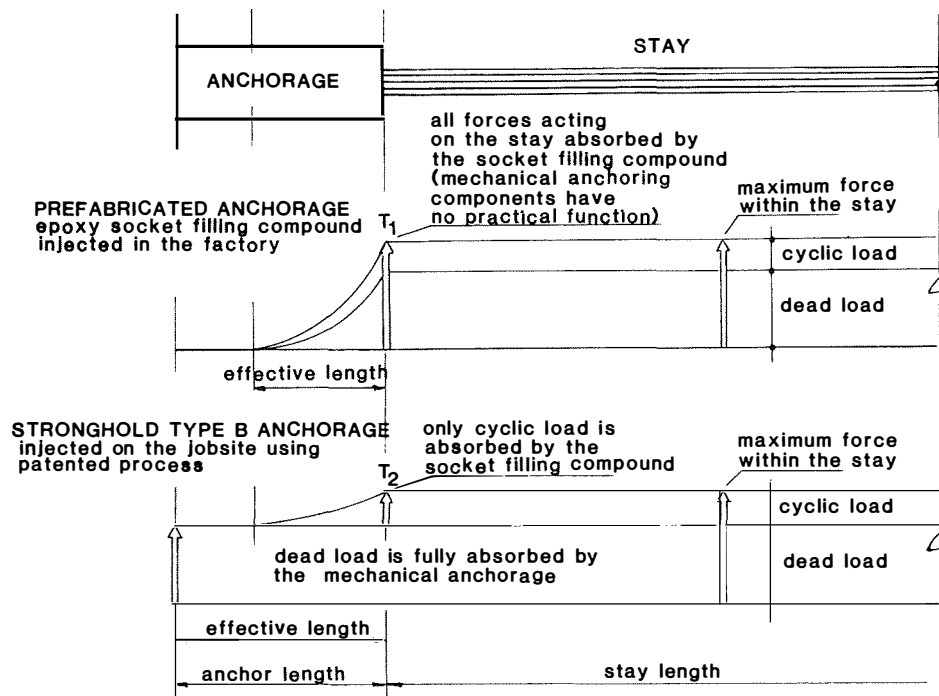


**FIGURE 10.15** Comparisons of dead and live load distribution in anchorage. (Courtesy of Stronghold International, Ltd., from reference 11.)

The cost of transporting and handling is compounded by the greater coil size.

The need for purpose-built equipment to best facilitate duct joining and erection, as well as strand cutting and threading, could create the factory condition on the site and would only require unskilled local labor. This was seen as the first objective. Material supply could be simplified down to transporting in stock lengths the polyethylene ducts and reels of strand in order to complete the bulk of the work. The addition of special machinery such as highly maneuverable stressing jacks, pumps for stay grouting and anchor socket injection, as well as epoxy curing apparatus for the anchorages completed the plant development. With the need to erect prefabricated stays removed, prestressing strand became the obvious choice of alternative steel choices that could be site assembled without the use of a large plant.

It appeared equally likely that site fabrication might offer possibilities for improving the stay anchorage. By stressing the stay prior to epoxy filling the anchor socket, the structure's dead load is supported by the wedges/compression grips (swages) restraining each component strand, leaving the socket-filler compound to support live load only when subsequently injected. This distribution of force would be much more satis-

factory for the range and amplitude of stress reversals than occurs with a prefabricated stay whose socket-filler material must absorb both dead load and live load, Fig. 10.15. This division of function allows the anchorage to be simplified and reduced in size.

Wedges used for conventional prestressed concrete are designed to support loads ranging from 92 to 100% of ultimate tendon strength. Such wedges usually have conic angles greater than the mating holes of anchor plates or barrels, and possess teeth relieved of incisive edges at their leading (narrow) ends, thereby ensuring high efficiency up to ultimate load, Fig. 10.16(a).

Numerous tests have been conducted in Germany to identify wedges capable of supporting cyclic loads, of range, amplitude, and duration known to occur in cable-stayed bridges. From the studies of Nurnberger,<sup>12</sup> Rehm,<sup>13</sup> Patzak,<sup>14</sup> and Köhler<sup>15</sup> it can be demonstrated that a reversal of these mating angles and the resulting stress concentrations occurring at points M and N, will produce a very high efficiency in cyclic terms provided a sharp tooth profile occupies the full wedge length, Fig. 10.16(b).

The sharp tooth profile which serves to prevent interface movement creates, in turn, a major disadvantage by biting the strand to a degree that drastically reduces ultimate load efficiency from 100% to approx-

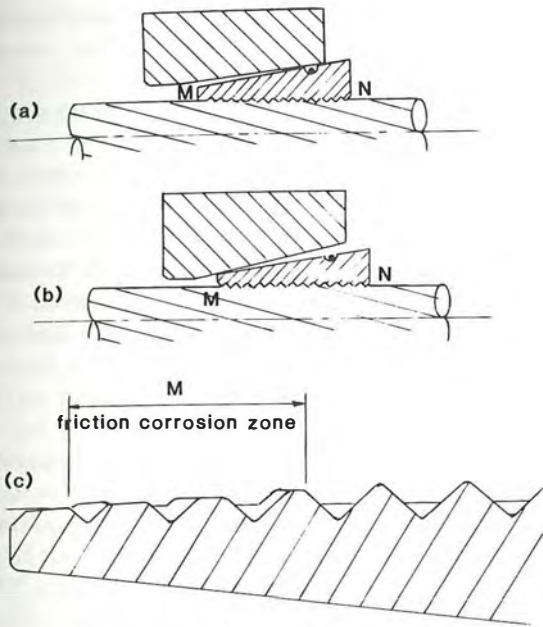


**FIGURE 10.16** Wedge mechanisms. (Courtesy of Stronghold International, Ltd., from reference 11.)

imately 70% when compared with conventional wedges. Therefore, if the stay is to work within 45% of ultimate, whereas the wedge efficiency is limited to 70%, its security is unavoidably reduced to an unacceptable safety factor of 1.5. This, in itself, is a valid reason for avoiding the use of mechanical wedges in a cable-stay anchorage.

The inability of wedges profiled for ultimate efficiency to perform as capably in cyclic terms as in static conditions is due to the interface movement at their leading ends where the teeth have been progressively relieved. Denied the restraint of sharp edges, they generate "friction corrosion" of the strand in the region M of Fig. 10.16(c), causing wire failure. A mechanical anchorage relying only on wedges is consequently unsuitable for cable stays because it fails to satisfy the conflicting criteria for fatigue and efficiency response.

It was necessary to identify a filling material of minimum shrinkage to ensure that a cyclic load is absorbed by the filler material and the static load by other anchor elements. A mix of a special epoxy compound with zinc powder and a high percentage of steel balls met this expectation most effectively. The final design of the anchorages is shown in Fig. 10.17. It was tested at Stuttgart University where it fully satisfied the specified cyclic loading.

Installation of the individual strands composing a stay is similar to that described for the VSL push-through method described in the previous section. A

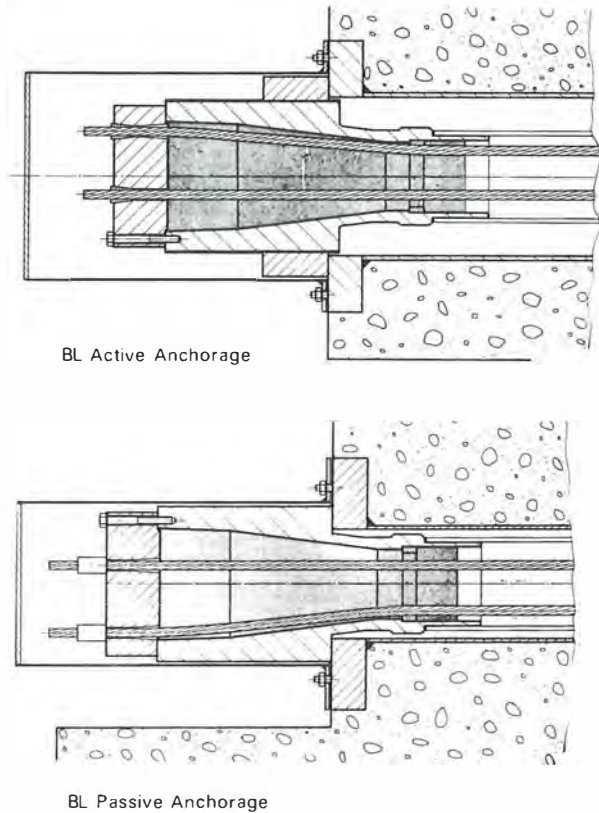


**FIGURE 10.17** Stronghold anchorages. (Courtesy of Stronghold International, Ltd.)

schematic illustration of this method is shown in Fig. 10.18.

### 10.3.5 FREYSSINET ANCHORAGES

The Freyssinet anchorage, Fig. 10.19, consists of a trumpet, which accommodates the flare of the strands within the anchorage; a heavy steel pipe trumpet extension, which is sized to reduce the range of stresses transmitted to the anchorage; a bearing plate; an anchorage block; and epoxy, cement, or other compound grout filler material. The jacking (or adjustable) anchorage also has a threaded adjusting nut. A neoprene damper is generally installed between the light steel pipe and the structure to minimize vibration due to wind-induced oscillation. The individual strands are anchored in the anchorage blocks by means of jaws or swaged sleeves, depending on stressing and installation procedures. Stays can be prefabricated with anchorages installed at the plant, or the stays can be installed in the field similar to that described for the VSL and Stronghold anchorages.

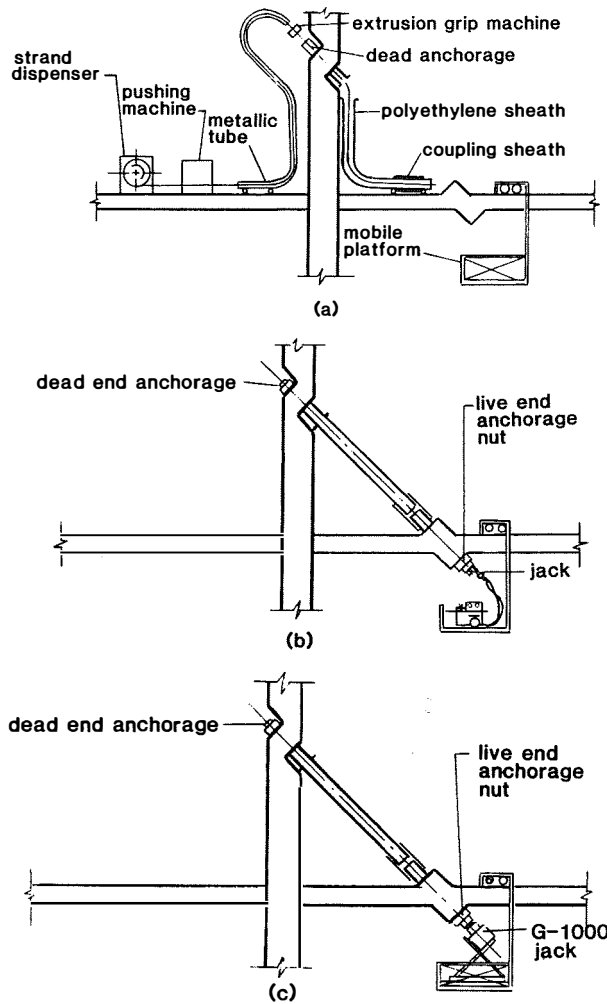


**FIGURE 10.18** Schematic erection sequence of Stronghold stays: (a) installation of the sheath, (b) single strand stressing, and (c) adjusting the anchorage with G-1000 jack. (Courtesy of Stronghold International, Ltd.)

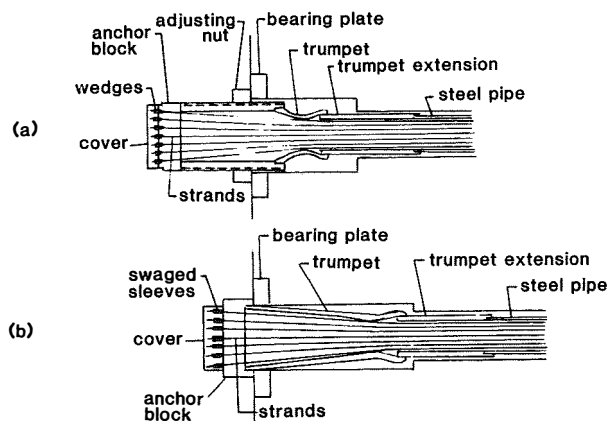


**FIGURE 10.19** Freyssinet anchorage: (a) live end and (b) dead end.

10.3.6 CONSIDERATIONS IN THE SELECTION OF STAY ANCHORAGE SYSTEMS

There are a number of considerations that need to be evaluated by the engineer in the selection of a cable-stay and anchorage system. In the United States the Federal Highway Administration requires a design criteria for the structure such that a cable stay may be removed (under live load) and replaced in the event of damage or some other unanticipated event. This then requires accessibility to the anchorage and, further, requires that the details of the system be such that the stay can be completely detensioned and be removable.

Although the design criteria requires the capability of replacing a cable stay, the engineer must evaluate the redundancy of the individual stay. In the event of an accidental dynamic load (ship impact or an errant vehicle impacting more than one stay) a shock wave may travel through the stay. If there is total reliance on a single component in the anchorage system and it fails, there could be a “domino effect,” which might lead to a catastrophic failure.

In the United States, the Federal Highway Administration requires fatigue testing of cable stays (including anchorages). In addition, the test specimens must be able to develop the guaranteed ultimate static tensile capacity after fatigue testing. These tests are considered essential not only as a proof test of the system but also as a form of quality control.

Another consideration is that of corrosion protection. A temporary system of corrosion protection is required for the stays from the time of manufacture (prefabricated stays) or assembly (field assembly) through completion of the structure when final tension adjustments are made. A final corrosion-protection system is then required for the expected life of the structure.

10.4 Saddles

Saddles are grooved cable supports designed with due consideration of the bearing pressures, bend radii, and groove diameters. All surfaces in contact with the cables should be smooth to avoid nicks in the wires. To avoid stress concentrations and minimize excessive bending at the end of the grooves, a generous contour is provided, which eliminates cable chafing.

A bridge engineer must consider both the design features of a saddle and the requirements of the cables before designing the saddle. Because design conditions vary for each bridge, the saddles must be designed and

fabricated expressly for each installation (as is current practice for conventional suspension bridges), Fig. 10.20. The saddles may be produced from fabricated plates or steel castings with grooves in the form of an arc for the individual cables to rest on. The profile of the saddle transverse to the direction of the cables is formed to suit the desired cable arrangement.

In order to ensure the proper seating of the individual cables or strands, a zinc or aluminum filler may be used in the groove. These soft materials will flow plastically and provide a smooth surface for the cables to rest upon.

The radius of the saddle grooves must provide a contact area between cable and saddle that results in permissible bearing pressures on the cables and the

saddle. The radius must also be selected to maintain the bending stresses in the outer fibers of the cable within allowable limits. When movement of the saddle is not provided in the design and construction, the unbalanced forces at the saddle must be resisted by friction and shear on the plates between layers of strands or cables. Additional clamping force may be provided by a clamp over the top of the cables that holds them in a fixed position.

In current state-of-the-art design of cable-stayed bridges the stays are composed of a bundle of parallel wires or 7-wire prestressing strands in contrast to a grouping of structural (or locked-coil) strands. As a consequence, saddles, where used, have been simply a prebent steel tube.

In view of the many special features involved in the design and fabrication of saddles, engineers and contractors should consult a manufacturer or cable specialist. There is needed expertise from experience in determining:

1. Adequate tolerances for the saddle grooves
2. Values for the coefficient of friction to prevent sliding of the cables on the grooves
3. Maximum allowable bearing pressures
4. The percentage reduction in breaking strength for various ratios of saddle radius to cable diameter
5. The suitable deflection angles for live loads
6. The best method of supporting a bundle of cables

Saddles are an important construction detail, and engineers should consult with a contractor or cable specialist on methods of erection and a manufacturer or cable specialist on the best composition and geometry to suit the load conditions of each application. The best bridge design on paper is of no value to anyone unless it can be built easily and economically to perform its function.

### 10.5 Connection of Cable Stays to Pylon

Basically, cable stays are either individually anchored at the top of the pylon or pass through the pylon on saddles. Where saddles are used there are two options: the saddle is fixed to prevent translation with respect to the pylon or it is supported on rollers to allow translation. If the structural intent is to fix the saddle, then the friction between the stays must be sufficient to overcome the net horizontal force of the stay on each side of the pylon. If friction is not sufficient to overcome this force then the stays must be clamped to the

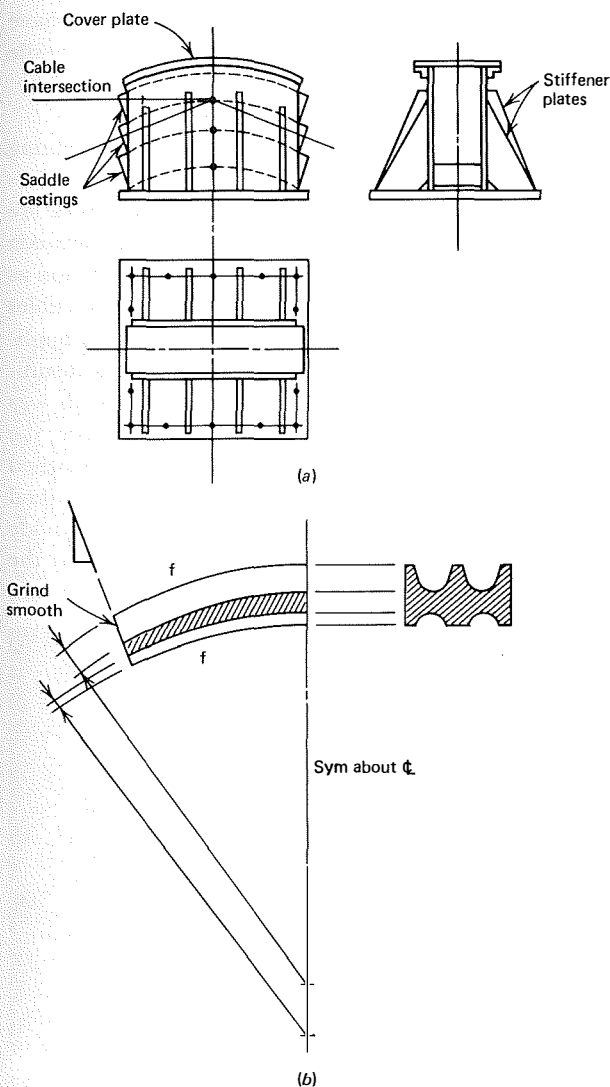


FIGURE 10.20 Typical saddle: (a) tower saddle and (b) saddle casting.



saddle to provide increased frictional capacity. Where a saddle is on rollers and allowed to translate, the translation is a self-equilibrium mechanism that equalizes the stress in the stay on either side of the pylon.

The advantage of a saddle is that it automatically reduces the number of expensive stay anchorages by one-half. However, the disadvantages are that the stay, being continuous, must be sized for the larger force coming from one side of the pylon, and there is an inefficiency in material usage in the stay on the opposite side of the pylon. Current criteria requires that a stay be replaceable, for any unforeseen event, and thus requires that the continuous stay be replaced from girder anchorage, through the pylon, and to the opposite corresponding girder anchorage.

As stated in Section 10.4 there is currently, at least for concrete pylons, a trend toward the use of prebent steel tubes as saddles, in contrast to the fabricated grooved saddles that had been used on earlier cable-stayed bridges. The fabricated grooved saddles are a transfer of technology from conventional catenary suspension bridges.

The Severin Bridge at Cologne, West Germany, has one tower and six cables that radiate in two directions from the top of the tower to the deck structure. Fig. 10.21. The size of the cables vary with the location of the intersection point along the deck span. The cables closest to the tower are the smallest in size and the ones extending further away are the largest as indicated by an increased further cross section Fig. 10.21. Each of the cables includes 4 to 16 individual strands. Most of the cables are continuous through the tower, resting on saddles and clamped rigidly to them, Fig. 10.22. All cables intersect the centerline of the tower in elevation; viewed transversely, they are slightly offset

from the centerline of each leg toward the longitudinal center line of the bridge, Fig. 10.22. However, the planes of the cables intersect at the centerline of the bridge at a theoretical connection point above the tower.

The cable sag caused by cable dead weight is vertical, which offsets the inclined plane in space. Because the cable planes are inclined, the saddles are also inclined to receive the cables more efficiently.<sup>16,17</sup> When the number of strands in a cable is different on each side of the tower at a common intersection point (see cables 1-6 and 2-5 in Fig. 10.22), the additional unbalanced strands are anchored directly to the tower, Figs. 10.22 and 10.23. Cables 3 and 4 are anchored and terminated at the tower because the angle of intersection is too acute for a saddle. A radius of curvature appropriate for the tower structure would have been too small for an effective saddle, and a saddle with proper radius would have been large, unsightly, and uneconomical.

The unbalanced forces from the two cables meeting at a common intersection point are resisted by frictional forces. Normally sufficient frictional forces are developed from the gravity pressure contact between the cables and the saddle and the additional friction as a result of the clamped bearing lid holding the cables fixed in position. Fig. 10.24. However, in this application the total frictional force developed was insufficient to provide the factor of safety of 2.5 which was required to resist the unbalanced forces. Therefore, the necessary additional frictional capacity was furnished by horizontal plates inserted between the individual layers of strands. These plates are tapered to provide a gradual transition from the pressure region to the nonpressure region, Fig. 10.24.<sup>16,17</sup> The plates are

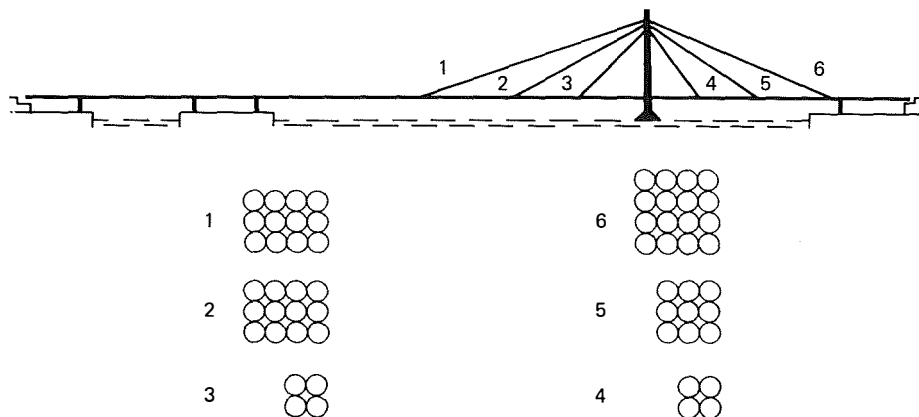


**FIGURE 10.21** Severin Bridge, cable arrangement. (Courtesy of Acier-Stahl-Steel, from reference 16.)

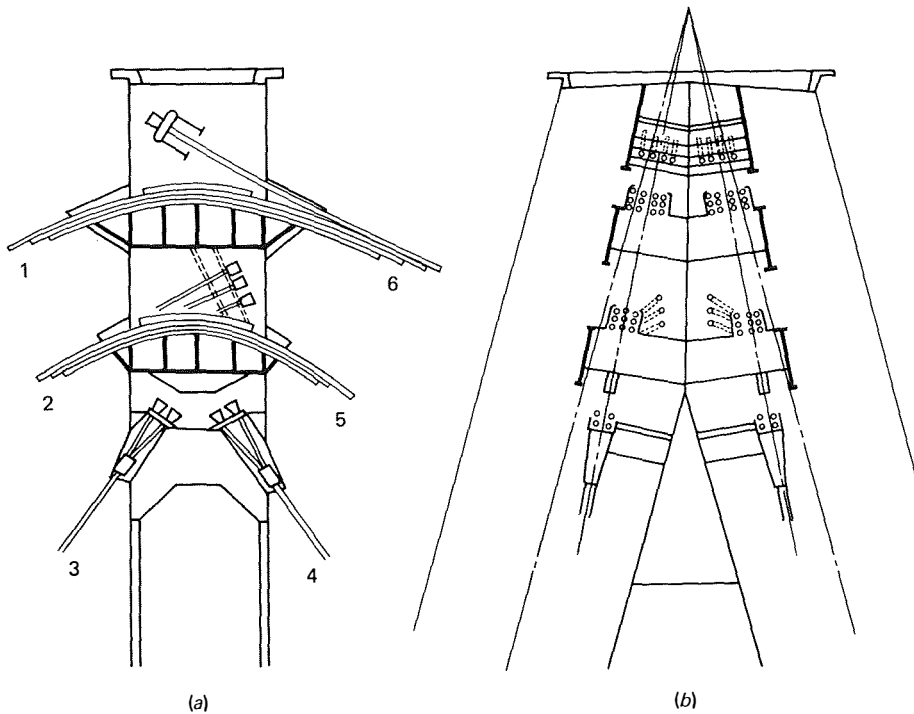
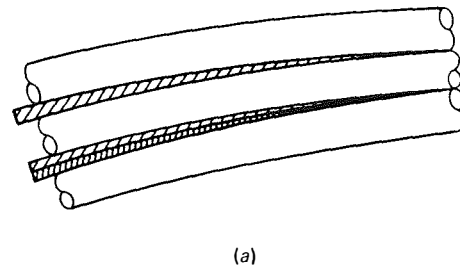


**FIGURE 10.22** Severin Bridge, anchorage of strands to tower: (a) elevation, and (b) transverse section. (Courtesy of Acier-Stahl-Steel, from reference 16.)

fixed to the seat and cover saddle. The plates increase the number of friction planes from two to six, and therefore, the frictional stress is increased three times for the same cable pressure.

The George Street Bridge crossing the Usk River at Newport, Monmouthshire, England, has main towers of rectangular hollow concrete, Fig. 10.25(a). The towers are 170 ft (51.8 m) above the caisson and have



(a)

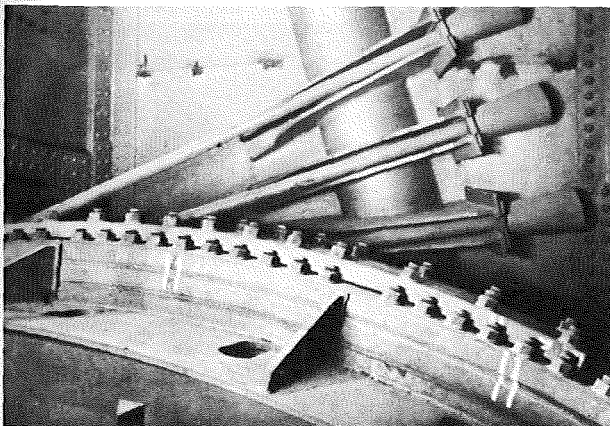
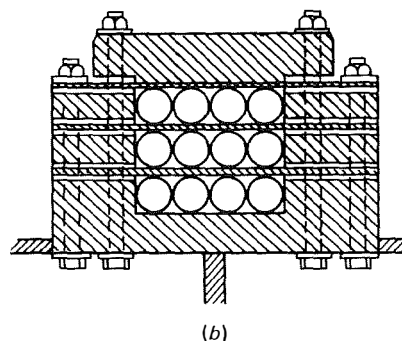


**FIGURE 10.23** Severin Bridge, unbalanced strands anchored to tower. (Courtesy of Acier-Stahl-Steel, from reference 16.)



(b)

**FIGURE 10.24** Severin Bridge, friction plates: (a) elevation and (b) cross section. (Courtesy of Der Stahlbau, from reference 17.)

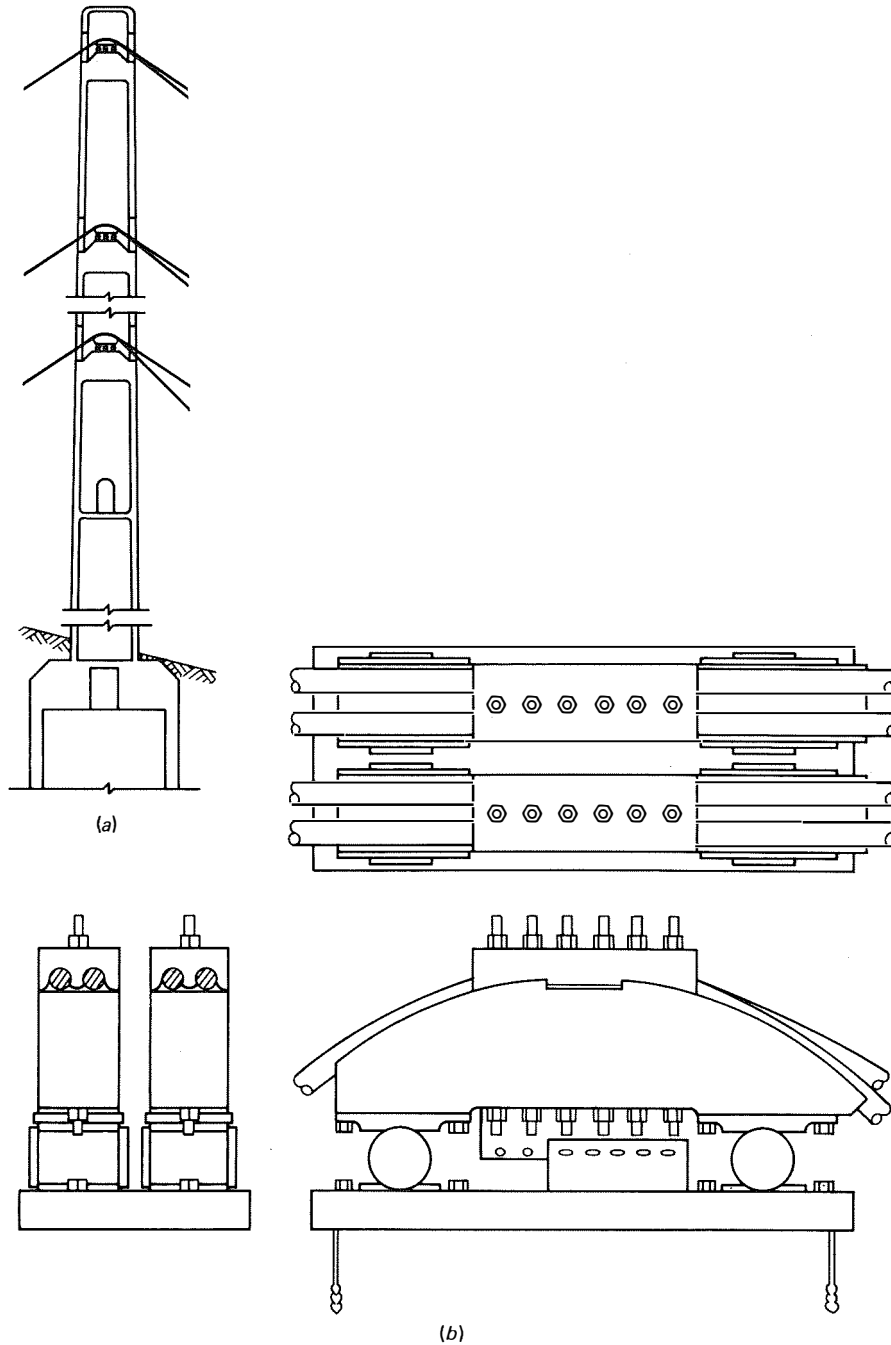


**FIGURE 10.25** George Street Bridge: (a) cross section of pylon and (b) detail of saddle. (Courtesy of the Institution of Civil Engineers, from reference 18.)

a base dimension of 13 ft 6 in. by 9 ft 10 in. (4.1 by 3 m) tapering to 9 ft 11½ in. by 7 ft (3 by 2.1 m) at the top. The wall thickness of the towers varies from 18 in. (457 mm) at the base to 12 in. (305 mm) below the uppermost saddle.

The cables are supported in pairs by cast steel sad-

dles located within the hollow sections of the tower. To achieve fixity of the cables at the towers, they are securely held to saddles by a clamp over the top, Fig. 10.25(b). In order to compensate for the longitudinal movement of the cables from traffic loadings and differential temperature effects, the saddles are placed on

high-load steel roller bearings, which permit the necessary movements to take place. The steel rollers are  $6\frac{1}{2}$  in. (165 mm) in diameter and are subjected to a maximum load of approximately 33 tons per lineal inch (1.18 mt/mm).<sup>18</sup>

In the case of the Rhine River Bridge at Maxau, West Germany (see Section 5.6), the cable lies in two horizontal planes and pass continuously through the tower over a saddle near the top of the tower, Fig. 10.26. The saddle has two friction plates held in place by a cover that is bolted securely to the flanges of the saddle, Fig. 10.27. The additional plates are installed to develop the total frictional capacity required to accommodate the differential force between the cables on each side of the tower.<sup>19</sup>

Where the cable stays terminate at the pylon, the connection detail takes various forms from being very simple, where there are only a few stays to attach, to being very complex, where there are numerous stays to attach. The cable anchorages for the Strömsund Bridge in Sweden are more conventional because of the typical standard fittings for the individual strands, as a result, the installation is simpler than that of the Severin Bridge. At the top of the tower the cables are connected with open strand sockets, thus terminating them there, Figs. 10.28. and 5.1.<sup>20</sup> For the Sitka Harbor Bridge the stay cables are 3-in. (762-mm) diameter galvanized structural strands that terminate at the pylon. The pylon connection is a standard open socket for each strand and is pinned to a gusset plate that is continuous through the center of the pylon, Fig. 10.29.

The Schillerstrasse Footbridge is a single-tower, five-cable bridge. Its slim octagonal tower has a slight taper that narrows to limiting dimensions for the cable

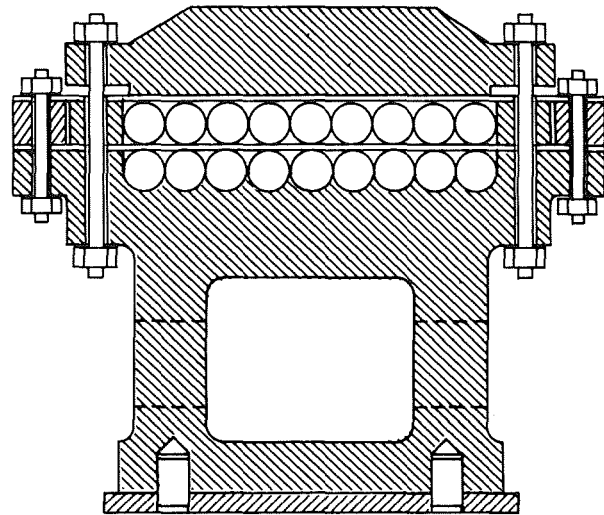


FIGURE 10.27 Rhine River Bridge at Maxau, tower saddle. (Courtesy of Der Stahlbau, from reference 19.)

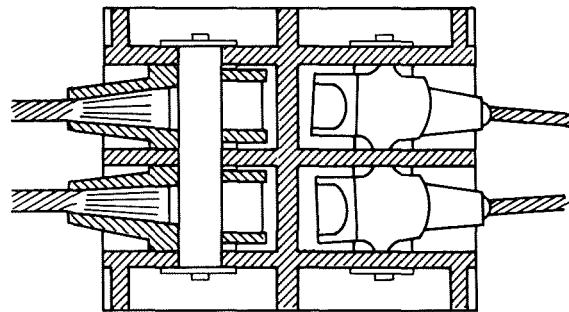


FIGURE 10.28 Strömsund Bridge, tower connection. (Courtesy of Der Stahlbau, from reference 20.)

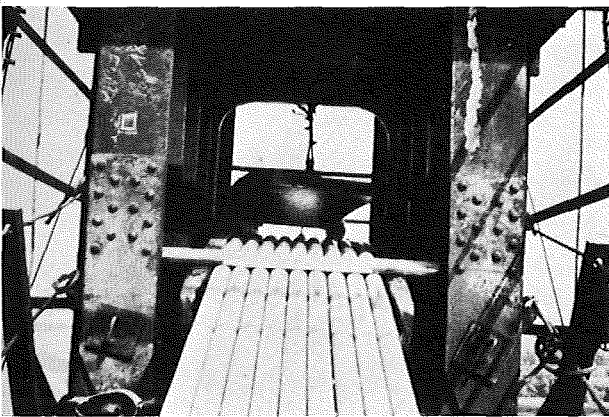
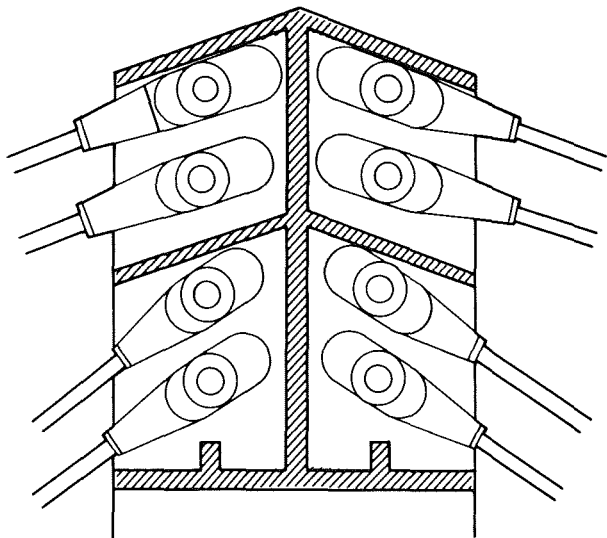


FIGURE 10.26 Rhine River Bridge at Maxau, view of cables at tower saddle. (Courtesy of Der Stahlbau, from reference 19.)



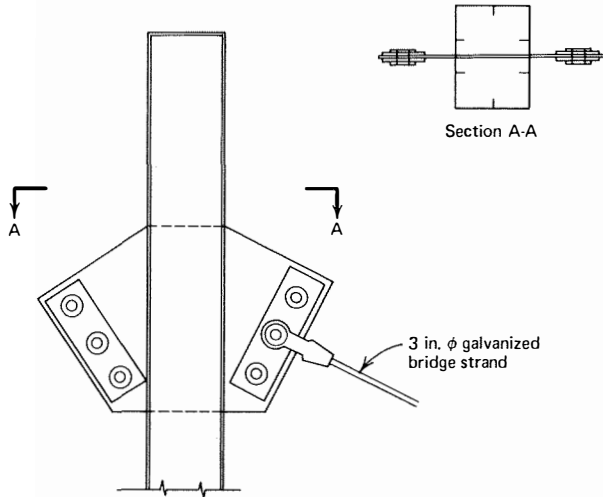


FIGURE 10.29 Sitka Harbor Bridge.

anchorages, Figs. 10.30 and 10.31. The cables are terminated at the tower in a space of only 3 ft.  $3\frac{7}{8}$  in. (1000 mm) high by 1 ft  $7\frac{5}{16}$  in. (490 mm) wide. Since this bridge is the first cable-stayed bridge to use parallel wire strands, it is quite unique. The cables consist of a varying number of  $\frac{1}{4}$ -in. (6 mm) diameter wires, Table 10.1, of the type common to posttensioned, prestressed tendons using the BBRV anchorages.

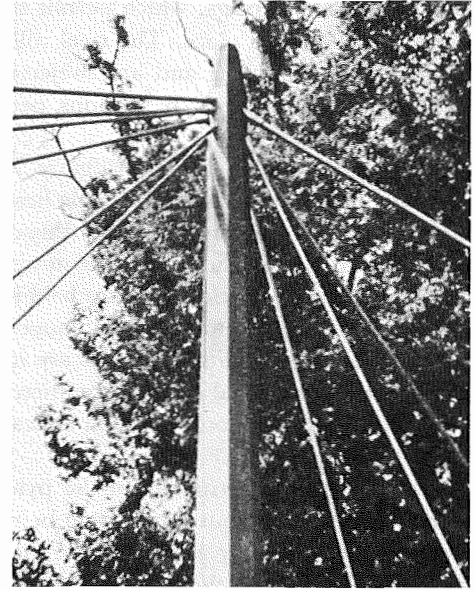


FIGURE 10.30 Schillerstrasse Footbridge, view of anchorage at tower. (Courtesy of Die Bautechnik, from reference 21.)

The use of the smaller diameter BBRV anchorages resolves the difficult problem of fitting the 10 cable anchorages in the restricted top portion of the tower. The anchorage is accomplished by installing a pipe or

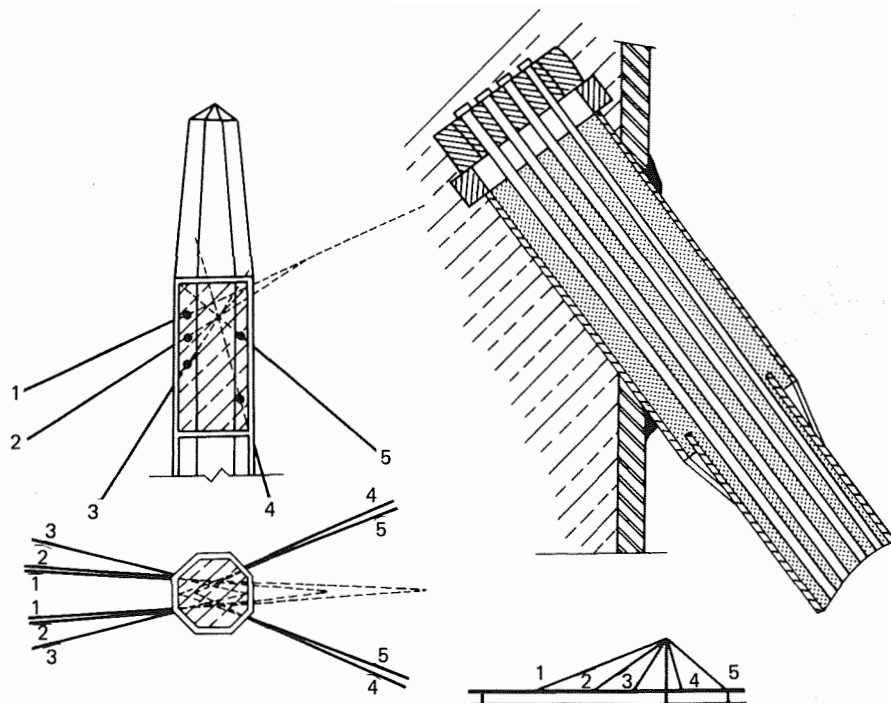


FIGURE 10.31 Schillerstrasse Footbridge, tower anchorage details. (Courtesy of Die Bautechnik, from reference 21.)

TABLE 10.1. Number of Wires Per Stay

| Stay number               | Cable Number |    |    |    |    |
|---------------------------|--------------|----|----|----|----|
|                           | 1            | 2  | 3  | 4  | 5  |
| Number of wires per cable | 44           | 28 | 20 | 22 | 90 |

trumpet into the tower and welding it so that it is aligned with the direction of the cable. After the cable and anchorages are installed, the cavity in the tower is filled with high-strength concrete. The concrete provides a bearing medium for the cable anchorages and at the same time increases the mass of the octagonal cross-sectional shape, Fig. 10.31.

A typical detail for a stay anchorage at the pylon head of the Luling Bridge is illustrated in Fig. 10.32. The anchorage connection system is a pyramid-shaped compression block consisting of a thick plate weldment. The block is attached to a grid of closely spaced steel girders by high-strength bolts. Each girder frames into a longitudinal stiffener attached to the steel plate walls of the pylon. Sockets of individual cables bear on a pair of deep ASTM A514 steel bar beams, which transfer the thrust to bearing surfaces machined into the plates of the compression block.<sup>22</sup>

In the case of the Pasco-Kennewick Bridge, the cable stays are attached to massive structural steel weld-

ments that were posttensioned to the top of the concrete pylon, Fig. 4.26. The weldment at the top of each pylon leg consists of three independent cellular units, Fig. 10.33(a), which are bolted together. Detail of the stay attachment is indicated in Figs. 10.33(b) and (c) which is a cutaway model of one of the cellular units. Fig. 10.33(d) is a schematic of the assembly of attachment components.

Termination of stays in a concrete pylon are of two basic forms. In the first case, the stays cross each other and transfer their load by bearing on the opposite face of the pylon from which they enter the pylon, Figs. 10.34(a) and (b). However, the arrangement of stays must be such that they do not produce a torsion in the pylon, Fig. 10.34(c). This arrangement basically places the concrete in compression, except for any net difference in the horizontal component of force in opposing stays.

In the second case, a box-shaped pylon is used and the stays bear on the inside face of the pylon wall, Fig. 10.35(a). In this situation the opposing horizontal components of stay forces produce tensile stresses in the walls parallel to the stay planes, Fig. 10.35(b), and posttensioning is provided to counteract this tensile stress. When two inclined planes of stays are used a tensile stress is developed in the transverse as well as the longitudinal direction and posttensioning is provided in all four walls, Fig. 10.35(c). An alternate so-

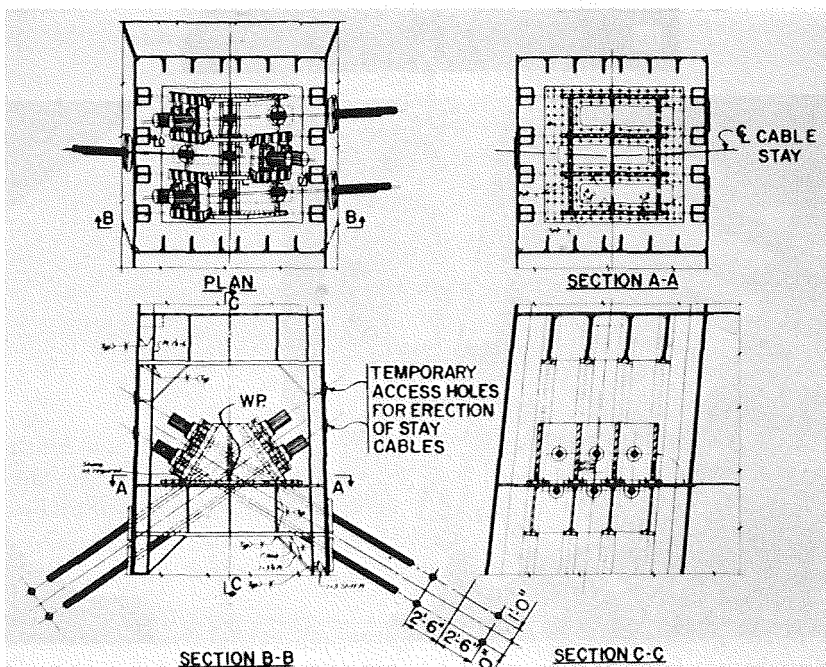


FIGURE 10.32 Luling Bridge, anchorage connection detail at pylon, from reference 22.)

lution to posttensioning is to utilize a structural steel tension member, Fig. 10.35(d).

### 10.6 Connection of Cable Stays to Girder

Cable-stay connections require careful consideration and analysis with respect to the distribution of the stay force into the superstructure girder. They can be rather straightforward and simple or become complex, depending upon the configuration of the superstructure.

There are basically three configurations: (1) for the case of a single plane of stays in the median there is usually a longitudinal spine box coinciding with the plane of stays; (2) for the case of a double plane of stays, longitudinal edge girders are provided at the plane of stays; and (3) in some instances, for the double-plane system, the longitudinal girders are not in the same plane as the cables and transverse anchorage girders must be provided to transfer the cable force to the primary longitudinal girders.

For the Strömsund Bridge in Sweden the locked-

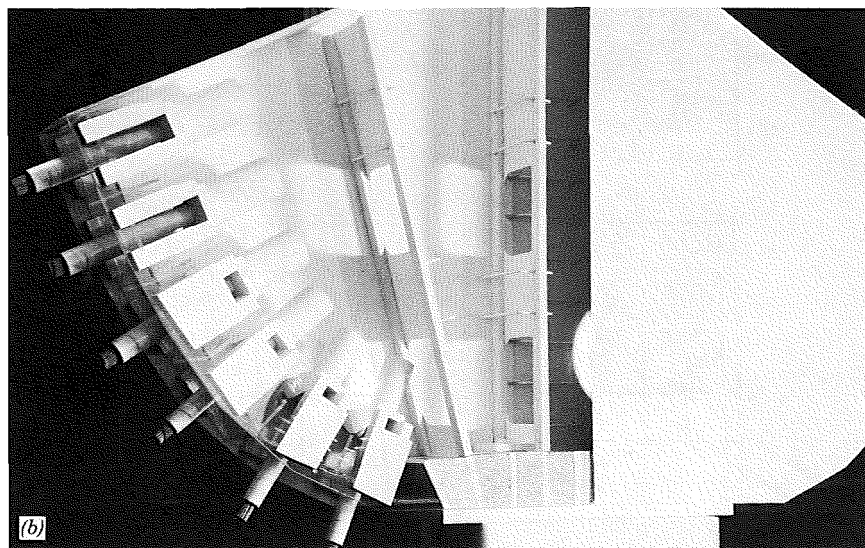
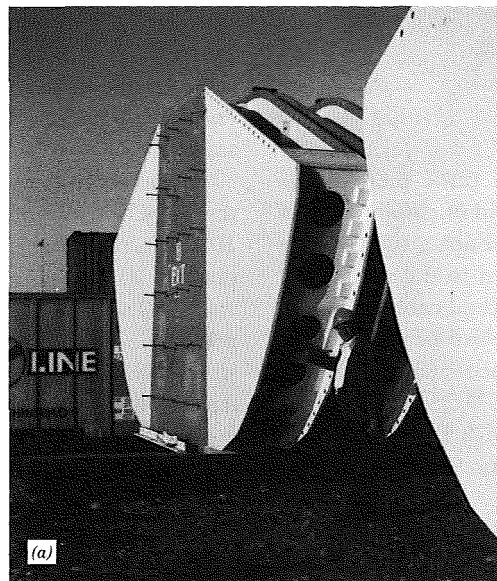
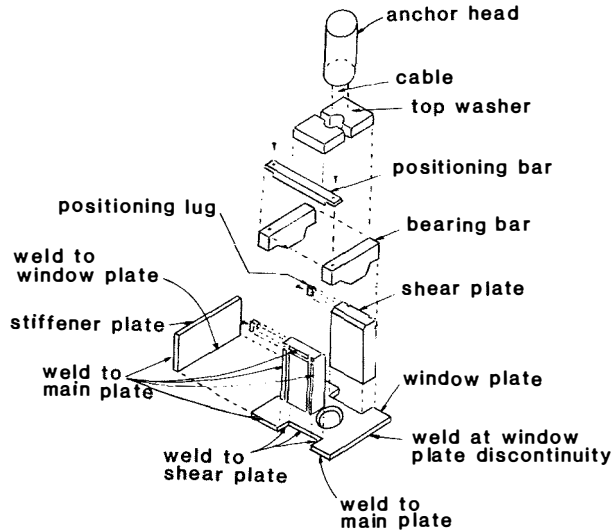
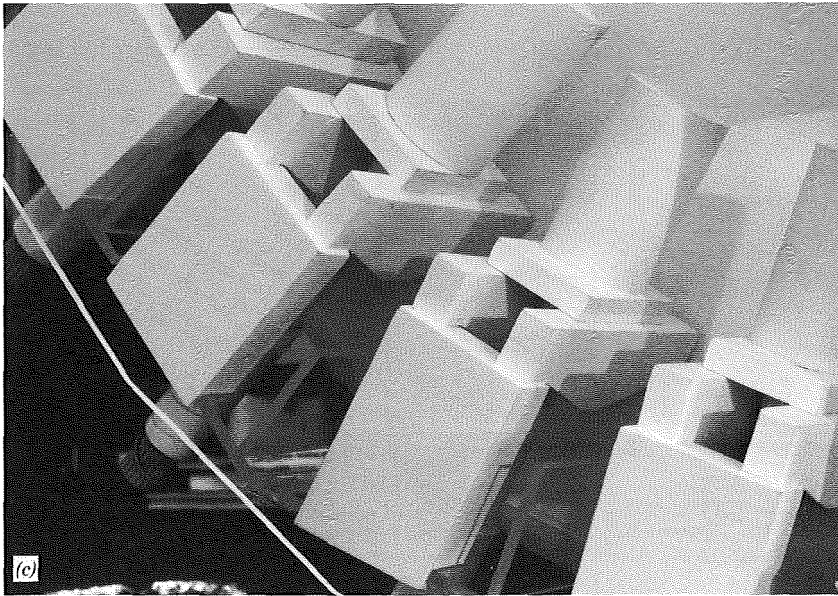


**FIGURE 10.33** Pasco-Kennewick Bridge, stay attachment at pylon: (a) cellular steel weldments, (b) and (c) model of stay attachment to cellular units, and (d) schematic of attachment components.



tower head main plate is not shown

(d)

FIGURE 10.33 (Continued)

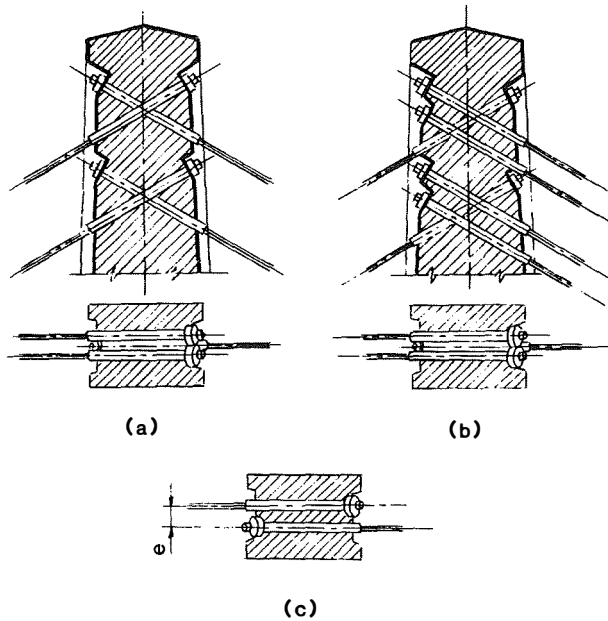
coil strand stays anchor into a transverse anchorage box beam between the main girders, Fig. 5.2, and are terminated with standard bearing sockets, Fig. 10.36. Shims are inserted under the sockets to provide for adjustment against a bearing block that rests against the inclined transverse box beam.

A single plane of stays was used for the Papineau-Leblanc Bridge in Canada and the superstructure consists of a two-cell box (three webs). Each stay is divided into two bundles of 12 strands each, which facilitates

the anchorage to the box girder. Each bundle of strands is connected to one side of the center web of the two-cell box girder, Fig. 10.37. The longer stays have  $2\frac{5}{16}$ -in. (59-mm) diameter strands, and the shorter stays have strands of  $1\frac{5}{8}$ -in. (41-mm) diameter.

The connection of the cables to the girder is accomplished by terminating the individual strands in a socket with internal threads. The threads accommodate ASTM A354 threaded rods, which pass through and are anchored to a curved bearing plate attached

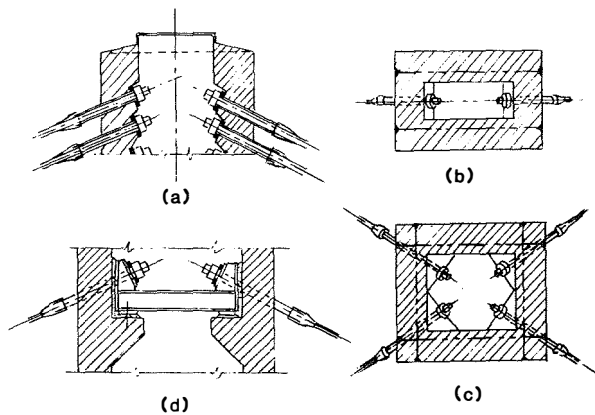




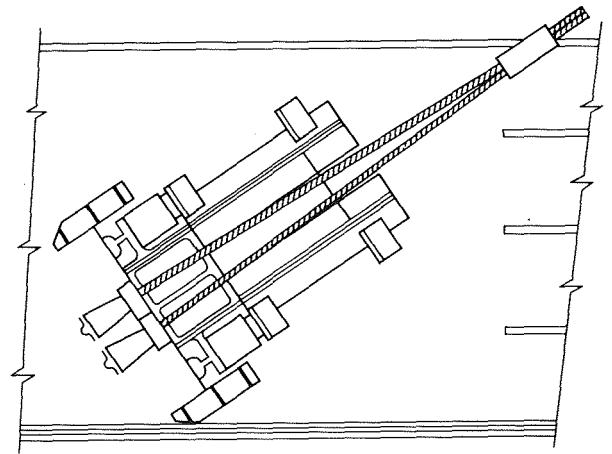
**FIGURE 10.34** Stay arrangement for concrete pylon: (a) one stay bifurcated, (b) both stays bifurcated, and (c) single eccentric stays producing torsion in pylon.

to the web of the girder. The bearing plate is finished on the back face to provide proper seating of the washers. As the strand is pulled to the correct tension, adjustments are made by the thickness of washers and positioning of the nuts on the back face of the bearing plate. The bearing plate must be designed to accept the tension loads and transfer them to the adjacent webs by stiff diaphragms.<sup>23,24</sup>

The Sitka Harbor Bridge is noteworthy because of its unusual cable connections to the deck structure,



**FIGURE 10.35** Stay arrangement for concrete pylon: (a) cross section, (b) one directional prestressing, (c) two directional prestressing, and (d) alternate structural steel tension member.



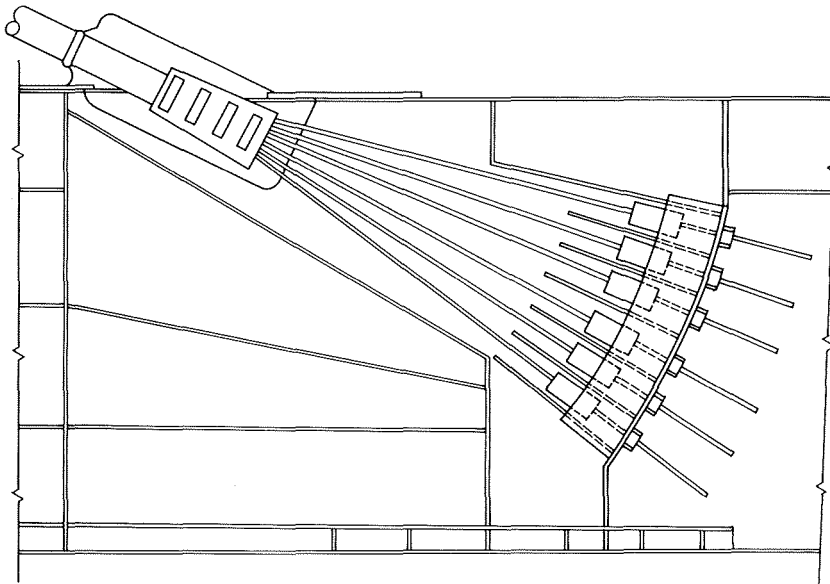
**FIGURE 10.36** Strömsund Bridge, girder connection. (Courtesy of Der Stahlbau, from reference 20.)

Fig. 10.38. The uniqueness of the design is the fact that the cables are anchored to a transverse tube, 5 ft (1.5 m) in diameter and 47 ft (14 m) long. The tube passes through the longitudinal box girders as a transverse diaphragm and cantilevers outward on each side of the deck, Fig. 6.2.

The stay cables are 3 in. (76 mm) diameter galvanized structural strands which terminate at the towers and the transverse tubes. The connection of the cables to the transverse tube makes use of a 10 $\frac{3}{4}$ -in. (273-mm) pipe sleeve which permits the cables to pass through and become anchored at a bearing plate attached to the pipes. The bearing plate is 20 in. by 5 ft (0.5 by 1.5 m).

The cable fittings are standard bearing sockets with internal threads for jacking and external threads to hold the spanner nut. The 10 $\frac{3}{4}$ -in. (273-mm) pipes transfer the cable tension load to the transverse tube by welds along the pipes on the stiffener plates attached to the tube, Fig. 10.38. The space between the cable and the pipe is fitted with a polymer sealer for protection against the severe climatic conditions.

In the Luling Bridge the longitudinal superstructure box girders do not coincide with the cable-stay planes, thus necessitating transverse anchorage box girders, Fig. 5.51. Anchorage cross girders are welded rectangular steel box girders 7 ft (2.1 m) wide and 8 to 10.5 ft (2.4 to 3.2 m) deep. Cross girders run continuously under the deck, penetrating the strengthened webs of the main girders. Stays terminate in anchorage chambers, Fig. 10.39, formed from heavy steel diaphragms built into the anchorage ends of the cross girders. Stay sockets bear through split shims bearing on finished surfaces of thick bearing plates that have



**FIGURE 10.37** Papineau-Leblanc Bridge, anchorage of web of box girder. (Courtesy of the Canadian Steel Construction Council, from reference 24.)

round holes large enough to pass the socket. Bearing plates in turn transfer the load to a diaphragm grid composed of thick plate weldments.<sup>22</sup>

Other attachments of stays to structural steel edge girders are illustrated in Figs. 6.8, 6.12, 6.13, and 6.16.

Stay attachments at the girder in concrete cable-stay superstructures generally take the form of a blister block at the edge of the deck, Fig. 4.25, for a two-plane cable-stay system. Where a single plane of stays is used, the blister block is located in the deck slab at the median, Figs. 4.32 and 4.44.

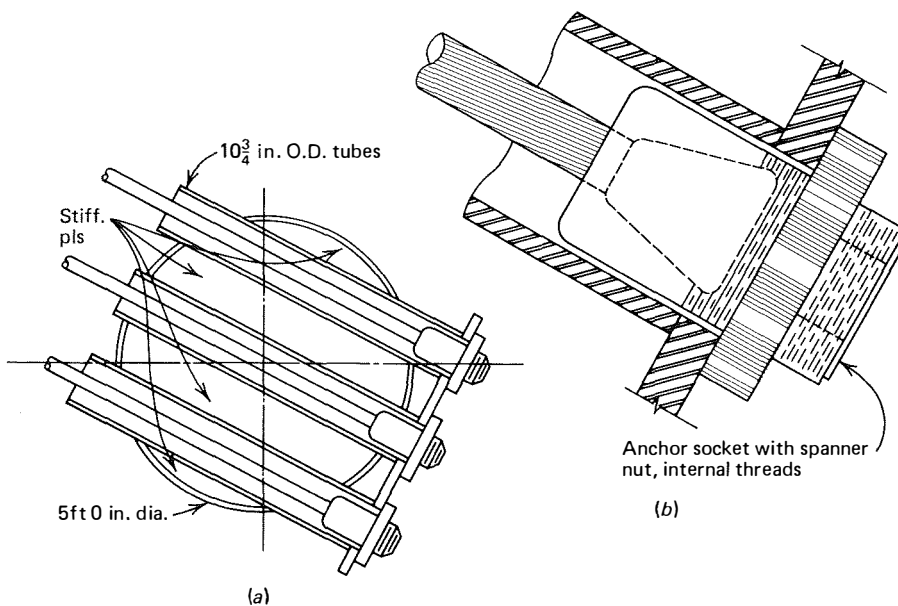


**FIGURE 10.38** Sitka Harbor Bridge: (a) cable anchor tube, and (b) cable connection at anchor.

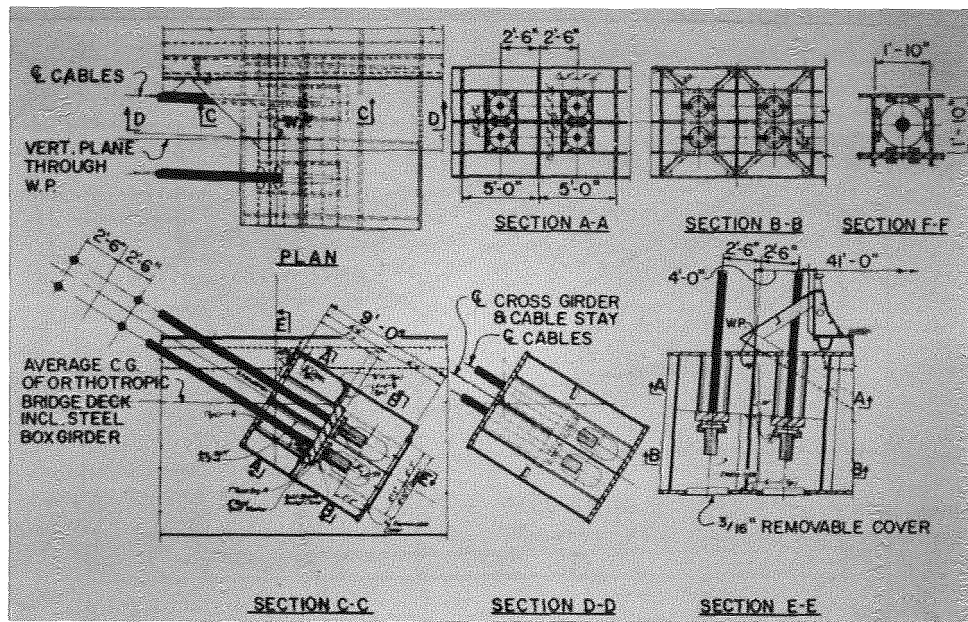


FIGURE 10.39 Luling Bridge, detail at stay attachment to girder, from reference 22.

### References

1. Simpson, C. V. J., "Modern Long Span Steel Bridge Construction in Western Europe," *Proceedings of the Institution of Civil Engineers*, 1970 Supplement (ii).
2. *Manual for Structural Applications of Steel Cables for Buildings*, American Iron and Steel Institute, Washington, D.C., 1973.
3. Scalzi, J. B., Podolny, W., Jr., and Teng, W. C., "Design Fundamentals of Cable Roof Structures," ADUSS 55-3580-01, United States Steel Corporation, Pittsburgh, Pennsylvania, October 1969.
4. Kondo, K., Komatsu, S., Inoue, H. and Matsukawa, A., "Design and Construction of Toyosata-Ohhashi Bridge," *Der Stahlbau*, No. 6, June 1972.
5. Thul, H., "Schrageilbrücken," Preliminary Report, Ninth IABSE Congress, Amsterdam, May 1972.
6. Phoenix, S. L., "An evaluation of the Condition of the Removed Backstay Cable (A12-3) from the Arecibo Radio Telescope," Unpublished Report, Cornell University, 1983.
7. Andrä, W., and Zellner, W., "Zugglieder aus Paralleldrahtbündeln und ihre Verankerung bei hoher Dauerschweißbelastung," *Die Bautechnik*, No. 8, August 1969 and No. 9, September 1969.
8. Cutler, E. and Castellaw, T., "Manufacture of Stay Cables for the Pasco-Kennewick Bridge," *Cable-Stayed Bridges*, Structural Engineering Series No. 4, June 1978, Bridge Division, Federal Highway Administration, Washington, D.C.
9. Anon., *VSL Stay Cables for Cable-Stayed Bridges*, VSL International, Losinger Ltd., Berne, Switzerland, January 1984.
10. Andra, W. and Saul, R., "Versuche mit Bündeln aus parallelen Drähten und Litzen für die Nordbrücke Mannheim-Ludwigshafen und das Zeltdach in München" *Die Bautechnik*, Heft 9, 10 und 11, 1974.
11. Gomez, Juan B. Ripoll, "Practical Experience in the Design of Anchorages for Cable-Stay Bridges" Unpublished Report.
12. Nurnberger, U., "Verhalten von Spannstählen in Kielverankerungen unter statischer Belastung," *Bauingenieur* 56, 1981.
13. Rehm, G., "Kiel und Kammverankerungen für dynamisch beanspruchte Zugglieder aus hochfesten Drähten," *Bauingenieur* 52, 1978.
14. Patzak, M., "Grundlagenuntersuchungen zur statischen und dynamischen Belastbarkeit von metallischen Drahtseilvergüssen (Vergussverankerungen)," *Mitteilungen* 45, 1978, SFB 64, Universität Stuttgart.
15. Köhler, W., *Ermüdungsverhalten von Stahl und Betonbauten*, IABSE, Lausanne, 1982.
16. Fischer, G., "The Severin Bridge at Cologne (Germany)," *Acier-Stahl-Steel* (English version), No. 3, March 1960.
17. Hess, H., "Die Severinsbrücke Köln," *Der Stahlbau*, No. 8, August 1960.
18. Brown, C. D., "Design and Construction of the George Street Bridge over the River Usk, at Newport, Monmouthshire," *Proceedings of the Institution of Civil Engineers*, Vol. 32, September 1965.
19. Schöttgen, J. and Wintergerst, L., "Die Strassenbrücke über den Rhein bei Maxau," *Der Stahlbau*, No. 2, February 1968.
20. Wenk, H., "Die Strömsundbrücke," *Der Stahlbau*, No. 4, April 1954.
21. Leonhardt, F. and Andrä, W., "Fussgängersteg über die Schillerstrasse in Stuttgart," *Die Bautechnik*, No. 4, April 1962.
22. Jarosz, E. S., "Luling Bridge," *Cable-Stayed Bridges*, Structural Engineering Series No. 4, June 1978, Bridge Division, Federal Highway Administration, Washington, D.C.
23. Demers, J. G. and Marquis, P., "Le Pont a Haubans de la Riviere-des-Prairies," *L'Ingenieur*, June 1968.
24. Taylor, P. R. and Demers, J. G., "Design, Fabrication and Erection of the Papineau-Leblanc Bridge," *Canadian Structural Engineers Conference*, 1972, Canadian Steel Industries Construction Council, Toronto, Ontario, Canada.

# 11

## Structural Behavior of Cables

|      |                                  |     |
|------|----------------------------------|-----|
| 11.1 | INTRODUCTION                     | 227 |
| 11.2 | CATENARY CURVE                   | 227 |
| 11.3 | PARABOLIC CURVE                  | 228 |
| 11.4 | CATENARY VERSUS PARABOLA         | 228 |
| 11.5 | ASSUMPTIONS FOR ANALYSIS         | 230 |
| 11.6 | GENERAL CABLE THEOREM            | 231 |
| 11.7 | CABLE WITH INCLINED CHORD        | 232 |
| 11.8 | EQUIVALENT MODULUS OF ELASTICITY | 234 |
|      | REFERENCES                       | 236 |

### 11.1 Introduction

The purpose of this brief discussion of the structural behavior of cables is to provide a basic understanding of the characteristics of cable action under varying load conditions. Unlike structural steel, structural cables are flexible members and, therefore, do not respond to the usual principles applied to the stiffer components.

Detailed technical derivations are not presented because they are available from many other sources on the theory and analysis of structures and/or structural systems. The intent here is to provide an elementary understanding of cables and their behavior as an introduction to the analysis of a complete cable-stayed bridge in Chapter 12. Therefore, only those equations considered to be basic to the understanding of the analysis of cable-stayed bridges are presented.

A fundamental problem encountered in cable structures of all types is the nonlinear behavior of the cable system as a result of the changes in sag and corresponding axial tension. A method for overcoming the nonlinear effect has been proposed; it substitutes an equivalent modulus of elasticity to include the normal modulus together with the effect of change of sag and tension loads. This aspect of cable behavior is discussed in a later section. The usual behavior of cable systems is presented as a prelude to the more meaningful discussion of the several suggestions for the equivalent modulus of elasticity.

### 11.2 Catenary Curve

A freely hanging cable supporting its own uniformly distributed weight and connected at the ends to stable anchorages will take the shape of a catenary curve, Fig. 11.1. The equilibrium of the catenary system is maintained by the anchorage forces at the supported ends. These forces are: the cable tension,  $T$ , with its horizontal component,  $H$ , and vertical component,  $V$ . The vertical components,  $V$ , balance the total weight of the catenary. The horizontal component,  $H$ , is equal and opposite in direction and, therefore, balanced. Stability is achieved by the general static equilibrium of all the forces.

To determine the forces acting on a catenary curve, it is essential to define the shape of the draped cable. This may be accomplished by considering the equilibrium of a segment of the cable such as  $OB$  of Fig. 11.2. The weight of the cable per unit length along the cable axis is denoted by  $w$ , and the length of the arc  $OB$  is denoted by  $S$ . For a horizontal cable chord, when the support points  $A$  and  $B$  are at the same elevation, the low point  $O$  at the center of the span may be taken as the origin of the coordinate system. However, it is also expedient to assume,  $O'$ , at a distance of  $a$  from the low point  $O$ , as a convenient origin of the coordinate axes.

The equation for the catenary elastic curve are stated below without derivation.

$$\tan \theta = \frac{V}{H} = \frac{wS}{H}$$

Let

$$a = \frac{H}{w}$$

then

$$\tan \theta = \frac{S}{a}$$

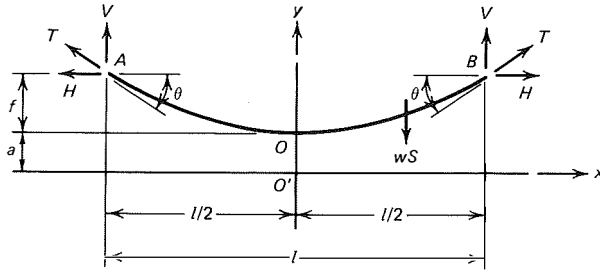


FIGURE 11.1 Catenary curve.

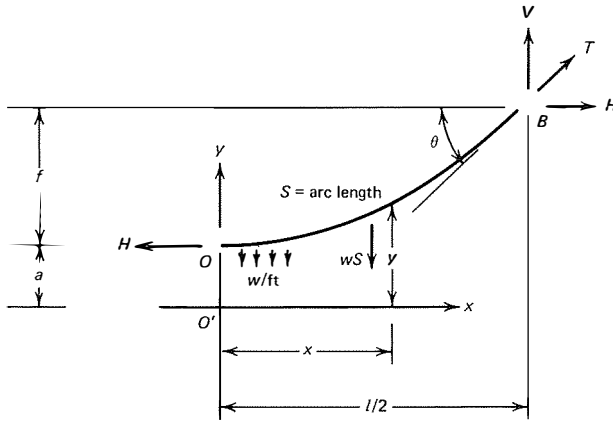


FIGURE 11.2 Segment of catenary.

The equation for a catenary can be shown to be<sup>1,2,3,4</sup>

$$y = a \cosh \frac{x}{a}$$

In order to compare the catenary curve with a corresponding parabolic curve, it is convenient to express the elastic curve in nondimensional terms.

The sag,  $f$ , may be expressed as

$$f = a \left( \cosh \frac{1}{2a} - 1 \right)$$

When the sag ratio  $n = fl/l$ , and  $m = 2a/l$  then

$$n = \frac{m}{2} \left( \cosh \frac{1}{m} - 1 \right) \quad (11.1)$$

which is an expression for the catenary curve in nondimensional terms of  $n$  and  $m$ , which will be referred to in Section 11.4.

### 11.3 Parabolic Curve

The mathematical expression for a parabolic curve is simple when compared with the equation for a catenary curve. Therefore, it is advantageous to compare

the two expressions to determine the range for which a parabolic curve may be substituted for a catenary curve with minimal or insignificant error. Therefore, an equation for a parabolic curve in nondimensional terms will be compared to a similar equation for a catenary curve.

The basic equation for a parabolic cable with a horizontal cable chord supporting a uniformly distributed horizontal load and using the general configuration of Fig. 11.3 is stated as

$$y = \frac{wx^2}{2H}$$

with the origin at point  $O$ .

If the origin is considered to be at  $O'$  to agree with the catenary coordinate system, the equation is expressed as

$$y = a + \frac{x^2}{2a}$$

when cable sag  $f = l^2/8a$ , then at the support point  $B$

$$y_b = f + a = a + \frac{l^2}{8a}$$

substituting the terms  $n$  and  $m$  as previously defined to convert to a nondimensional equation, the following expression for the parabolic curve is obtained

$$n = \frac{1}{4m} \quad (11.2)$$

### 11.4 Catenary Versus Parabola

To compare the parabolic curve with the catenary curve, a full logarithmic plot of equations 11.1 and 11.2 is developed with  $n = fl/l$  as the abscissa, and  $m = 2a/l$  as the ordinate, Fig. 11.4.<sup>6</sup>

The plot indicates that the two curves begin to diverge at a sag ratio  $n = fl/l$ , of approximately 0.15. Therefore, it can be concluded that for sag ratios less than 0.15, the parabolic curve may be substituted for the catenary curve with a reasonably small percentage of error.

The comparison of the parabolic and catenary curves has been computed for a horizontal cable chord with supports at the same elevation and symmetrical about a vertical axis through the low point of the sag of the cables. For an inclined cable chord, Fig. 11.5, which is the usual configuration for cable-stayed bridges, the substitution of a parabolic curve for the

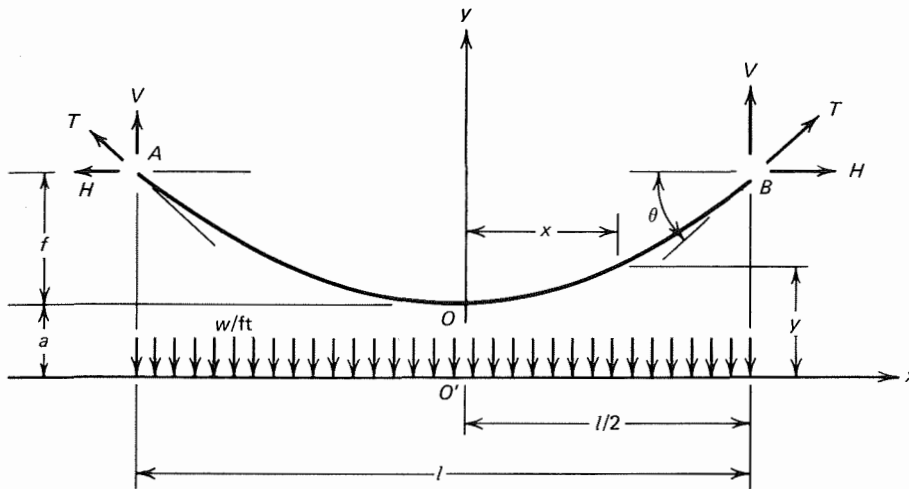


FIGURE 11.3 Parabolic curve.

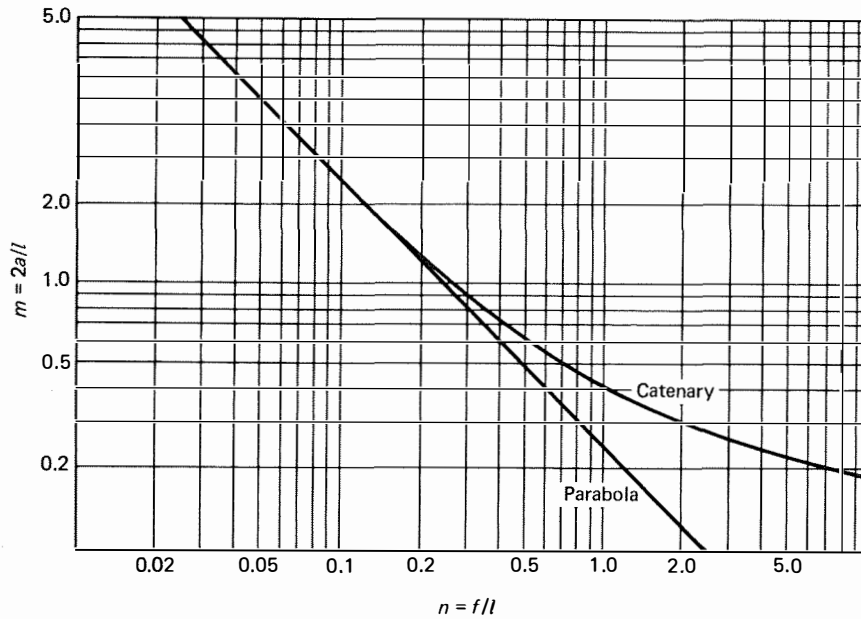


FIGURE 11.4 Catenary versus parabola.

catenary curve may also be made. This substitution is based on a comparison of the lengths of the two cables as indicated below.

In a cable-stayed bridge, the inclined cable takes the shape of a catenary because it simply supports its own weight between anchorages with no other intermediate loads, Fig. 11.5. The length of the catenary cable may be expressed as<sup>7</sup>

$$L^2 = b^2 + 4a^2 \sinh^2 \frac{1}{2a}$$

and letting  $a = H/w$ , the expression may be written as

$$L^2 = b^2 + 4\left(\frac{H}{w}\right)^2 \sinh^2 \frac{lw}{2H} \quad (11.3)$$

Similarly the length of a parabolic cable is stated as (Fig. 11.5)<sup>8,9,10</sup>

$$L = c \left[ 1 + \frac{8}{3} \left( \frac{f}{c} \right)^2 \right]$$

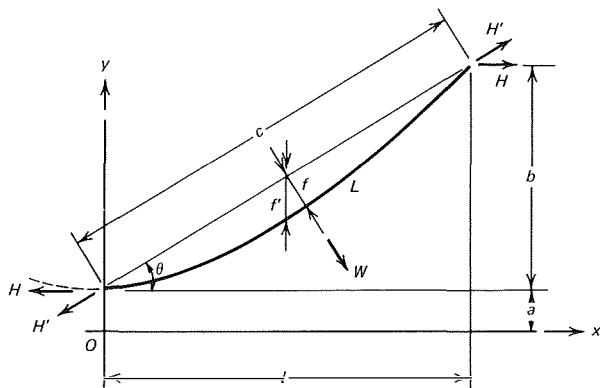


**FIGURE 11.5** Inclined cable chord,  $w$  is the weight per unit cable length, catenary  $w$  is the weight per unit horizontal projected length (parabola).

$$c = \frac{l}{\cos \theta}$$

$$f = f' \cos \theta$$

$$f' = \frac{wl^2}{8H}$$

and substituting in the above equation

$$L = \frac{l}{\cos \theta} \left[ 1 + \frac{8}{3} \left( \frac{wl}{8H} \cos^2 \theta \right)^2 \right] \quad (11.4)$$

In order to compare the two curves, a typical situation for which a comparison of the cable lengths has been investigated is assumed. For convenience of calculation and to represent an inclined cable for a cable-stayed bridge, a typical cable application is assumed with a span of 300 ft and a tower of 125 ft, Fig. 11.6

The difference in length between a catenary and parabolic curve is calculated using equations 11.3 and 11.4,<sup>3</sup> for various values of the horizontal cable component  $H$ . The results are tabulated in Table 11.1, which indicates that the parabolic curve approaches the catenary curve as the value of  $H$  increases.<sup>4</sup> The accompanying percentage error decreases from

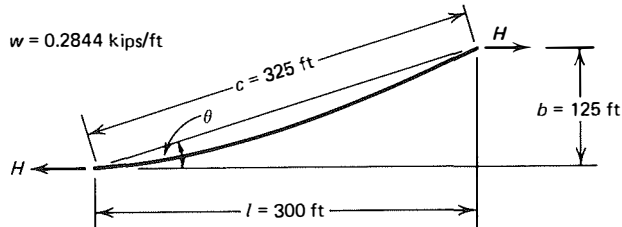


**FIGURE 11.6** Typical cable application. See Fig. 11.5.

0.0289% for a value of  $H$  equal to 100 kips to 0.0165% for a value of  $H$  equal to 500 kips.

### 11.5 Assumptions for Analysis

Although the actual shape of a cable as used in a cable-stayed bridge is a true catenary curve, it has been determined that an assumption of a parabolic curve is within the range of acceptable minimum engineering error for design calculations. Therefore, for analysis and design of cable-stayed bridges with nominal proportions of span to tower height, a parabolic curve will be assumed for the shape of the inclined cable.

Section 11.4 has indicated that for a horizontal cable chord, the parabola may be substituted for the catenary curve below a sag ratio,  $n = f/l$ , of 0.15 with very little error, Fig. 11.4

A study of length comparisons tabulated in Table 11.1 indicates that a parabola may be substituted for a catenary with very little error for reasonably large values of the horizontal component.

For the application of a horizontal cable chord, Shaw<sup>5</sup> has indicated that if the angle  $\theta$ , Fig. 11.1 is small (denoting a sag ratio,  $n = f/l$ , of approximately 1/6 or less), it is sufficiently accurate to assume the weight of the cable to be distributed as a uniform load per unit length of horizontal projection of the cable.

For the usual application of an inclined cable chord in cable-stayed bridges, Fig. 11.5, Francis<sup>7</sup> has shown that the assumption of a parabola replacing the catenary is valid when  $H'/W$  exceeds unity and the angle

**TABLE 11.1** Percentage Error, Catenary vs. Parabola

| $H$ (kips) | Catenary, $L_c$ (ft) | Parabola, $L_p$ (ft) | $\Delta L = (L_c - L_p)$ (ft) | $\Delta L/L_c$ (%) |
|------------|----------------------|----------------------|-------------------------------|--------------------|
| 50         | 360.1257             | 358.5975             | 1.5282                        | 0.4244             |
| 100        | 333.4958             | 333.3993             | 0.0965                        | 0.0289             |
| 150        | 328.7727             | 328.7328             | 0.0399                        | 0.0121             |
| 200        | 327.1328             | 327.0998             | 0.0330                        | 0.0101             |
| 500        | 325.3896             | 325.3359             | 0.0537                        | 0.0165             |

of inclination of the cable chord to the horizontal does not exceed 70 degrees.

11.6 General Cable Theorem

The basic principles of static equilibrium are sufficient to determine the cable forces that develop from the application of gravity loads to the cable system. These cable tension forces may be calculated from the general cable theorem for various configurations of the cable.

The general theory of cables is reviewed in most textbooks on structural analysis and, therefore, only a summary of the theory and a general expression are stated below.<sup>2</sup>

Consider the general case of a cable supported at two points *A* and *B*, which are at different elevations acted upon by any number of loads,  $P_1, P_2, P_3, \dots, P_m$  as indicated in Fig. 11.7. Since it is assumed that the cable is perfectly flexible, the bending moment at any point on the cable must be zero. Because the loads are gravity loads and, therefore, vertical, the horizontal component of the cable tension stress, denoted

$H$ , must have the same value at any point on the cable and at reaction points *A* and *B*.

The general cable theorem states that:

At any point, such as *n*, on a cable which is acted upon by vertical loads (gravity), the product of the horizontal component of the cable stress  $H$  and the vertical distance from that point to the cable chord  $y_n$  equals the moment that would occur at that section if the same loads were acting on an end-supported beam of the same span as that of the cable<sup>2</sup>

The theorem is valid and applicable to any set of vertical loads whether the cable chord is horizontal or inclined. Mathematically the theorem may be expressed as

$$Hy_n = \frac{x}{L} \sum M_B - \sum M_n$$

where  $H$  = horizontal component of cable stress

$y_n$  = vertical distance from cable to inclined chord

$x$  = distance from origin at *A*

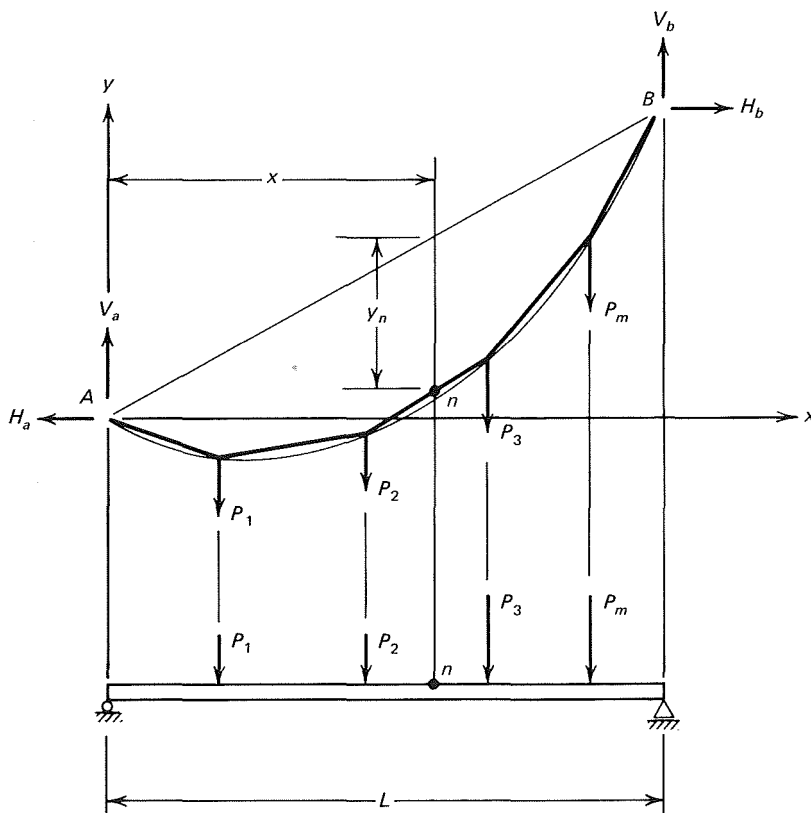


FIGURE 11.7 General cable system.



$L$  = span, horizontal distance between supports

$\sum M_B$  = the algebraic sum of the moments about support  $B$  of all the loads on the cable

$\sum M_n$  = the algebraic sum of the moments about any point  $n$  on the cable of those loads  $P_1, P_2, \dots, P_m$  that act on the cable to the left of point  $n$ .

The above equation is the basic expression for the determination of the horizontal component of the cable stress.

### 11.7 Cable with Inclined Chord

In cable-stayed bridges the cable is always in the inclined chord position, and, as a consequence, the expression to determine the various forces and geometrical changes will be stated for that condition without derivation. For details on the development of the expressions the reader is referred to textbooks on cable structural analysis.<sup>8</sup>

The forces to be determined for analysis and design considerations are:

$H$  = the horizontal component of cable stress

$T_{\max}$  = the maximum tension stress in the cable

$V$  = the vertical component of cable stress

The geometrical quantities to be determined for design and erection considerations are, Fig. 11.8:

$L$  = total span length of cable between supports

$S$  = cable length

$\Delta S_s$  = cable elongation due to cable tension stress

$\Delta S_t$  = cable elongation due to temperature change  $t$  in  $^{\circ}\text{F}$ .

$y$  = vertical distance from cable to inclined cable chord.

The equations for the determination of the forces and geometrical effects are based on the notation of Fig. 11.8.<sup>2,8,9</sup>

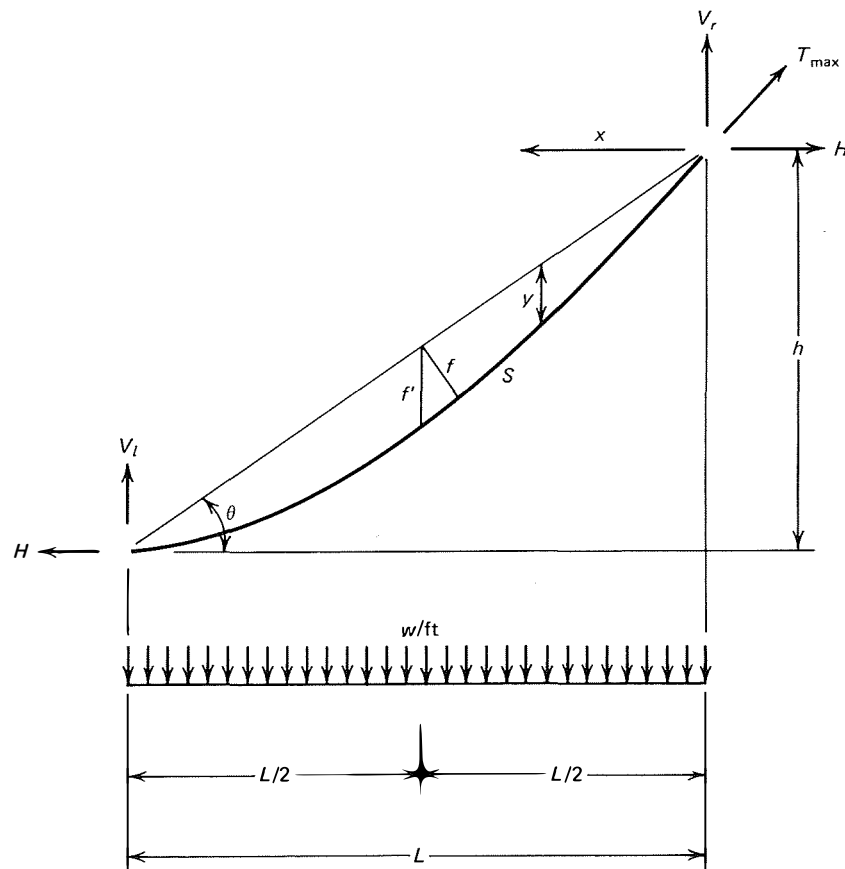


FIGURE 11.8 Inclined cable chord.

$$H = \frac{wL^2}{8f'}$$

$$T_{\max} = H \left[ 1 + \left( \frac{h}{L} + 4n \right)^2 \right]^{1/2}$$

$$V_r = \frac{Hh}{L} + \frac{wL}{2}$$

$$S \approx L \sec \theta \left( 1 + \frac{8n^2}{3 \sec^4 \theta} \right)$$

$$\Delta S_s \approx \frac{HL}{AE} \sec \theta \left( 1 + \frac{16n^2}{3 \sec^4 \theta} \right)$$

$$\Delta S_t = \xi t L \sec \theta \left( 1 + \frac{8n^2}{3 \sec^4 \theta} \right)$$

$$y = \frac{4f'}{L^2} (Lx - x^2)$$

- where  $w$  = uniform load per unit length of horizontal projection
- $f'$  = cable sag
- $n = f'/L$ , sag ratio
- $L$  = span
- $S$  = length of cable curve
- $\xi$  = thermal coefficient of linear expansion, 0.0000065 in./in./( $^{\circ}$ F)
- $t$  = temperature change in  $^{\circ}$ F

The inclined cable in a cable-stayed bridge is assumed to be a straight line between supports in the analysis of the structure. Although the cable is not actually along the chord line, because of the sag produced by its own weight, the tension force thus calculated is assumed to be the tension in the cable. The validity and accuracy of this assumption was investigated by Podolny.<sup>4</sup> He concluded that for design purposes the tension force acting along the inclined chord may be considered as the cable stress.

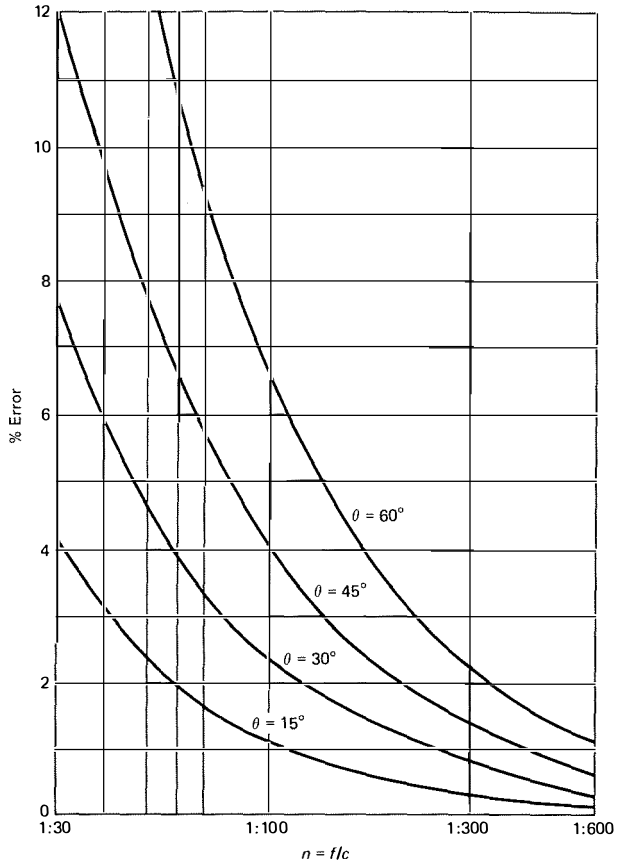


FIGURE 11.10 Percentage error of cable tension versus sag component along inclined chord.

To arrive at this conclusion, Podolny compared the maximum tension stress in the cable to the tension stress along the chord. His study was made by assuming the cable to have a horizontal chord and then comparing the value for the horizontal component  $H$  to the maximum tension force  $T_{\max}$ , Fig. 11.9.

The results are plotted, Fig. 11.10, as percentage error versus the sag ratio  $n$  for various angles of inclination of the chord.

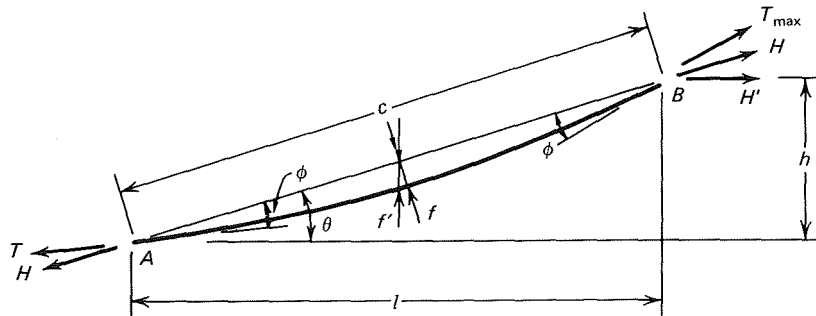


FIGURE 11.9 Maximum tension, inclined cable chord.

It can be seen that for large sag ratios of 1/30 to 1/100 and large angles of chord inclination, the percentage error is quite large, but for smaller sag ratios the error is within acceptable limits. If it is assumed, for discussion purposes, that an initial sag ratio of 1/60 is present and the order of magnitude of tension increases tenfold from initial cable weight only to final tension, then a final sag ratio under load may be of the order of 1/600 or more, and the percentage error decreases to a value of less than 2%.

Therefore, on the basis of this study, the maximum tension in the cable may be taken as the calculated tension assuming the cable as a straight member between supports.

### 11.8 Equivalent Modulus of Elasticity

The analysis of a cable-stayed bridge is based on elastic considerations for the materials and, therefore, elastic

theories of structural analysis are used to determine the forces acting on each member of the system. As stated previously, the cable force is considered to act along the inclined chord even though it sags slightly under its own dead weight. As a result of the flexibility of the cable and the changes in length and sag, it is necessary to adopt a corrective technique to account for these nonelastic features. Several methods have been proposed by various authors who suggest the use of an equivalent modulus of elasticity for the cable. This approach is similar to assuming a straight member with a varying modulus of elasticity that depends on the magnitude of the tension force. The basic principle for analysis is that the behavior of a straight substitute member with an equivalent modulus of elasticity is identical to that of the curved cable.

Although several investigators (Gimsing,<sup>10</sup> Goschy,<sup>11</sup> and Tung and Kudder<sup>12</sup>) have studied the problem of the equivalent modulus of elasticity each approach results in the solution provided by Ernst,<sup>3</sup> which will be considered herein as the fundamental method.

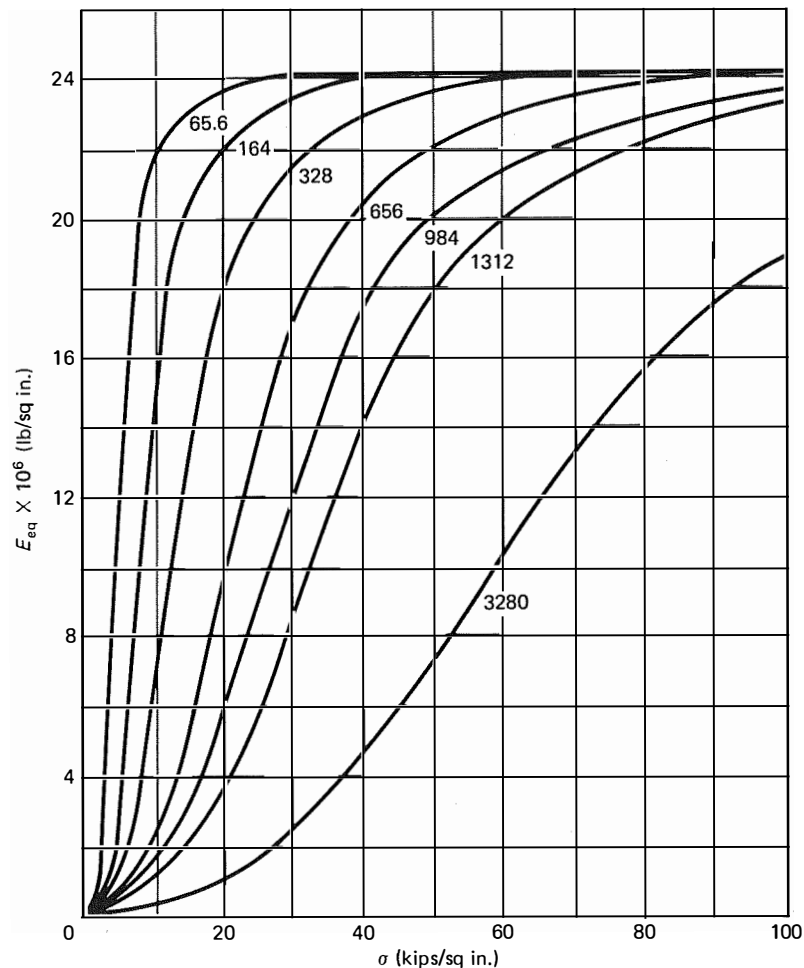


FIGURE 11.11 Ernst's equivalent modulus of elasticity, from reference 3.

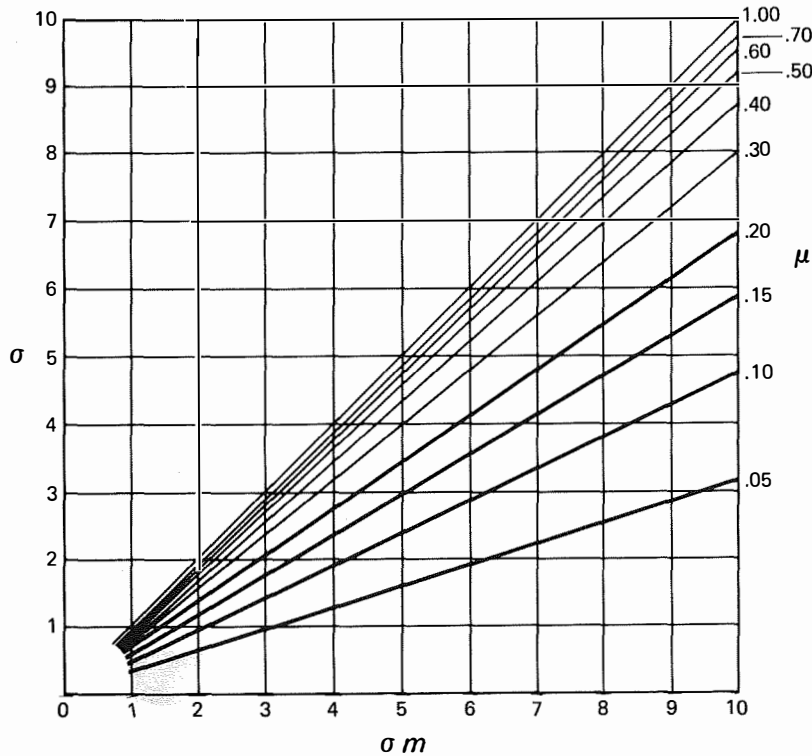


FIGURE 11.12 Ernst's modified stress for equivalent modulus of elasticity, from reference 3.

Ernst developed the following expression for the equivalent modulus of elasticity:

$$E_{eq} = \frac{E}{1 + \frac{(\gamma l)^2}{12\sigma^3} E}$$

- where  $E_{eq}$  = equivalent modulus of elasticity
- $E$  = modulus of elasticity of the cable
- $\gamma$  = specific weight of the cable, weight per unit volume
- $\sigma$  = unit tension stress in the cable

Ernst presented the results of solving his equation as a plot, Fig. 11.11, of several curves representing different values of the span lengths  $L$ . The curves are plotted for an  $E$  equal to 24,180 kips/in.<sup>2</sup> and a specific weight of cable equal to  $3.035 \times 10^{-4}$  kips/in.<sup>3</sup> The plot indicates the equivalent modulus of elasticity to be used for a particular cable stress and span length. However, it is to be noted that the values of  $E_{eq}$  are for a locked-coil strand<sup>3</sup> and for a constant stress in the cable.

The actual action of the cable is such that a change in stress level takes place as the cable forces are in-

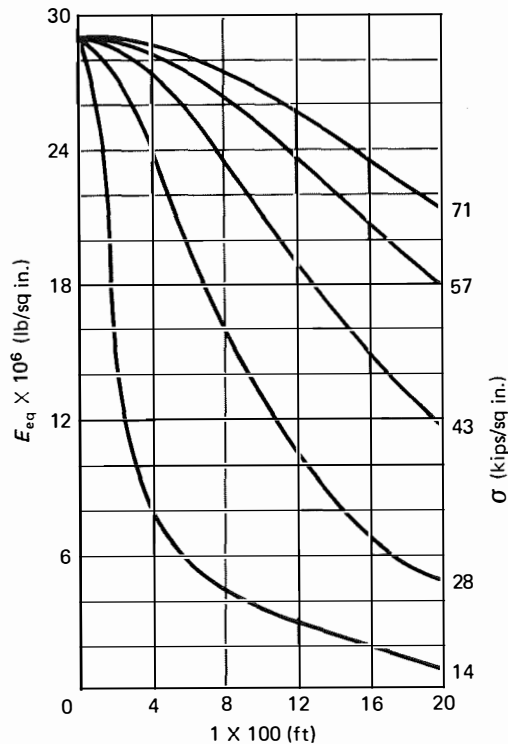


FIGURE 11.13 Equivalent modulus of elasticity. (Courtesy of Fritz Leonhardt, from reference 13.)

creased and the sag decreases. To account for this non-linear changing stress condition, Ernst modified his basic expression. The modification is based on a mean stress of the cable tension for various values of the parameter  $u$ , which is the ratio of the final stress to the original stress in the cable, Fig. 11.12. The plot indicates a revised value of  $\sigma$  for a mean value of  $\sigma_m$  and a specific value of  $u$ . With the revised value of  $\sigma$  from Fig. 11.12 and the plot of Fig. 11.11, an improved value of  $E_{eq}$  is determined.

Leonhardt<sup>13</sup> has presented similar data for parallel wire strands, Fig. 11.13, with the span length as abscissa and the equivalent modulus of elasticity as the ordinate for a family of cable stress levels.

Therefore, in the analysis for the cable tension force, the cable is considered to be a straight member between points of anchorage with an equivalent modulus of elasticity. It is apparent that the analysis becomes an iterative process requiring several determinations of cable stress and the corresponding equivalent modulus of elasticity until a convergence of the values is achieved.

### References

1. Seely, F. B. and Ensign, N. E., *Analytical Mechanics for Engineers*, Wiley, New York, 1948, pp. 104-111.
2. Scalzi, J. B., Podolny, W., Jr., and Teng, W. C., "Design Fundamentals of Cable Roof Structures," ADUSS 55-3580-01, United States Steel Corporation, Pittsburgh, 1969.
3. Ernst, J. H., "Der E-Modul von Seilen unter Berücksichtigung des Durchhanges," *Der Bauingenieur*, Vol. 40, No. 2, February 1965, pp. 52/55.
4. Podolny, W., Jr., "Static Analysis of Cable-Stayed Bridges," Ph.D. Thesis, University of Pittsburgh, 1971.
5. Shaw, F. S., "Some Notes on Cable Suspension Roof Structures," *Journal of the Institution of Engineers*, Australia, Vol. 36, April-May 1964.
6. Odenhausen, H., "Statical Principles of the Application of Steel Wire Ropes in Structural Engineering," *Acier-Stahl-Steel* (English version), No. 2, February 1965.
7. Francis, A. J., "Single Cables Subjected to Loads," *Civil Engineering Transactions*, Institution of Engineers, Australia, Vol. CE7, October 1965, pp. 173-180.
8. Maugh, L. C., *Statically Indeterminate Structures*, Wiley, New York, 1964.
9. *Manual for Structural Applications of Steel Cables for Buildings*, American Iron and Steel Institute, Washington, D.C., 1973.
10. Gimsing, N. J., "Anchored and Partially Stayed Bridges," *Proceedings of the International Symposium on Suspension Bridges, Lisbon*, Laboratorio Nacional De Engenharia Civil, 1966, pp. 475-484.
11. Goschy, Bela, "Dynamics of Cable-Stayed Pipe Bridges," *Acier-Stahl-Steel* (English version), No. 6, June 1961, pp. 277/282.
12. Tung, D. H. H., and Kudder, R. J., "Analysis of Cables as Equivalent Two-Force Members," *Engineering Journal*, American Institute of Steel Construction, January 1968, pp. 12-19.
13. Leonhardt, F. and Zellner, W., "Cable Stayed Bridges: Report on Latest Developments," Canadian Structural Engineering Conference, 1970, Canadian Steel Industries Construction Council, Ontario, Canada.

# 12

## *Design Considerations and Analysis*

|       |   |     |
|-------|---|-----|
| 12.1  | INTRODUCTION  | 237 |
| 12.2  | MULTICABLE-STAY ARRANGEMENT                                     | 238 |
| 12.3  | LONGITUDINAL STAY ARRANGEMENT                                   | 238 |
| 12.4  | TRANSVERSE STAY ARRANGEMENT                                     | 239 |
| 12.5  | SPAN PROPORTIONS  | 239 |
| 12.6  | PROPORTION OF PYLON HEIGHT TO CENTER SPAN                       | 240 |
| 12.7  | LOADS AND FORCES  | 241 |
| 12.8  | STRUCTURE ANCHORAGE   | 242 |
| 12.9  | MULTISPAN STAYED GIRDER BRIDGES                                 | 245 |
| 12.10 | PRELIMINARY MANUAL CALCULATIONS                                 | 249 |
| 12.11 | METHODS OF ANALYSIS   | 252 |
| 12.12 | STIFFNESS PARAMETER   | 252 |
| 12.13 | MIXED METHOD OF ANALYSIS—SINGLE PLANE                           | 255 |
|       | 12.13.1 Cable-Stayed Bridge Behavior                            | 255 |
|       | 12.13.2 Fundamental Analysis                                    | 256 |
|       | 12.13.3 Multicable Structure—Radiating System                   | 259 |
|       | 12.13.4 Multicable Structure—Harp System                        | 259 |
|       | 12.13.5 Axial Force in the Girder                               | 261 |
|       | 12.13.6 Fixed Base Tower  | 261 |
|       | 12.13.7 Multitower Continuous Girder Cable-Stayed Bridge        | 262 |
|       | 12.13.8 Cables Attached to Rigid Supports                       | 262 |
| 12.14 | MIXED METHOD OF ANALYSIS—DOUBLE PLANE                           | 263 |
|       | 12.14.1 Structural Behavior                                     | 263 |
|       | 12.14.2 Basic Analysis  | 264 |
|       | 12.14.3 Effects of Other Actions                                | 266 |
|       | 12.14.4 Double-Plane Structure with an A-Frame Tower            | 267 |
|       | 12.14.5 Double-Plane Structure with a Portal Tower              | 267 |
|       | 12.14.6 Multitower Continuous Girder—Double-Plane Configuration | 268 |
| 12.15 | SUMMARY OF THE MIXED METHOD                                     | 269 |
| 12.16 | NONLINEARITY  | 269 |
| 12.17 | INFLUENCE LINES   | 269 |
| 12.18 | LIVE LOAD STRESSES  | 281 |
| 12.19 | OTHER METHODS OF ANALYSIS                                       | 282 |
|       | REFERENCES  | 283 |

### *12.1 Introduction*

Chapter 11 presented basic assumptions, cable theory, and equations. This chapter discusses general design

and analysis considerations. Aerodynamic considerations are discussed in Chapter 13.

Once the decision is made to build a bridge structure on a given site, the type of bridge must be selected. Generally, because of the number of considerations to be taken into account (e.g., vertical and horizontal clearances for navigation, terrain conditions at the site, environmental factors, and foundation problems), the geometry of the structure will be dictated by these requirements. Normally, several types of bridge structures will be investigated to meet the various parameters imposed, with each type having its own advantages and disadvantages for the particular site.

We do not intend to discuss the decision-making process in bridge type selection, but will mention a few of the factors that must be considered in the selection of a specific bridge type. Bridge selection is more of an art than a science because there are no universally accepted hard and fast rules. What may be a valid, rational decision in one case may have no validity at all in another case.

We will assume that a cable-stayed bridge is to be built and will proceed to present design and analysis considerations for it. However, at this point the reader should be aware that the cable-stayed bridge is not simply one bridge type, but many different individual types evolving from an extremely versatile concept of bridge design. In selecting a bridge type, bridge engineers should not limit their thinking to just a cable-stayed bridge; they should consider a number of geometrical variations of cable-stayed bridges.

A complete design and analysis methodology, criteria, code, or specification is obviously beyond the scope of this book. However, we do present some of the design considerations that are pertinent to this type of structure. Furthermore, wherever possible current design "rules of thumb" and general proportions of existing structures that may prove useful in a trial de-

sign are presented. Because the cable-stayed bridge is affected by a wide range of factors, design and analysis considerations will be presented in a general manner. A particular structure would, of course, be subject to the dictates of its design environment. Many of the design considerations that follow have been discussed in previous chapters and we will attempt to avoid duplication by appropriate cross references. However, we do repeat some of these considerations in order to provide the proper synthesis and continuity of presentations.

### 12.2 *Multicable-Stay Systems*

Economy of construction and degree of difficulty of structural details are greatly affected by the number and spacing of the cable stays. Initial contemporary cable-stay bridges had only one or two stays on each side of the pylon (Strömsund Bridge in Sweden and Morandi's Lake Maracaibo Bridge in Venezuela). Later bridges had only two to six stay supports in the center span at a spacing of 100 to 200 ft (30 to 60 m) at deck level (see top and center of Fig. 2.8). This then required relatively large bending-moment capacity in the girder resulting in girder depths of 10 to 13 ft (3 to 4 m). Stay forces were so large that they had to be built up of a number of cables producing complex and difficult stay attachment details. Also, because of the span between stay attachment points at the girder, a considerable amount of auxiliary erection equipment was required to erect the bridge. In many cases temporary erection stays had to be utilized.<sup>1,2</sup>

Subsequent development of cable-stayed bridges in Germany led to the utilization of a greater number of stays (bottom of Fig. 2.8) with spacing at the deck level of 25 to 50 ft (8 to 15 m). Although more stays are used, the additional cost is more than offset by simpler connection details for the smaller cables and lesser force in the stays. Erection is simplified because the deck structure can be constructed by cantilever method from stay connection point to stay connection point without any auxiliary means. Further, the girder, instead of being primarily a flexural member, now acts primarily as a compressive chord member of a cantilever structure suspended from the pylon by the inclined stays. Therefore, it does not require as large a bending stiffness and, consequently, can be of shallower depth. Longitudinal bending stiffness is governed by the following:<sup>2</sup>

1. Buckling due to the large compressive forces induced by the inclined stays.

2. The necessity to limit local deformations under concentrated live load with respect to the curvature of the deflection line. Dead load bending is kept small by the relatively short spacing of the stays.

In summary, fewer cable stays result in larger cable forces which in turn require massive and complicated anchorage systems and, consequently, reinforcement of the girder to transfer shear, moment, and axial load. A relatively deep girder is required to span the large distance between stay attachments. A large number of cable stays, approaching a continuous supporting elastic media, simplifies the anchorage and distribution of forces to the girder and permits the use of shallower-depth girders.<sup>3</sup>

### 12.3 *Longitudinal Stay Arrangement*

The stay geometry of cable-stayed bridge systems varies greatly. The arrangement of stays is subject to numerous considerations, including highway requirements, site conditions, and aesthetic preferences. Chapter 2 presented an extensive discussion of the advantages and disadvantages of the several geometrical variations.

The three primary longitudinal stay arrangements are the radiating, harp, and fan configurations (see Fig. 2.6). In the radiating configuration all stays converge at the head of the pylon. Cable stays in the radiating system are at a maximum angle of inclination to the girder and take the maximum component of dead and live load. Thus, the axial component to the girder is a minimum.<sup>4</sup> For the harp configuration the stays are parallel to each other and, therefore, are distributed over the height of the pylon. The harp arrangement requires more steel in the stays, produces higher compressive forces in the longitudinal girder, and produces bending moments in the pylon. For these reasons the harp system is not as structurally efficient as the radiating system. However, the harp arrangement may be preferred aesthetically over the radiating system; when a double plane is employed the visual intersection of cables when viewed from an oblique angle is eliminated. Also, with the stay attachments distributed over the entire height of the tower, the structural attachment of the stays to the pylon is greatly simplified compared to the case of a large number of stays converging at the top of the pylon for the radiating arrangement.

The visual disharmony of different directions of stay cables in the radiating configuration can be minimized

if a large number of relatively small stays are used such that they appear as a fine network against the sky with no dominance of single lines.<sup>2</sup>

A compromise between the radiating and harp configurations is achieved in the fan configuration, whereby the stays are distributed over a portion of the pylon at the top. In this manner the complexity of all the stays converging at a single (theoretical) point at the pylon head is avoided. The distribution of stay anchorages at the top portion of the pylon facilitates the replacement of a stay in case of an accident or some unforeseen situation. Stay replacement is a requirement on all federally aided cable-stayed bridges in the United States.

### 12.4 Transverse Stay Arrangement

An extensive discussion of transverse cable-stay geometry is presented in Section 2.2. For the case of a single plane of stays located on the longitudinal centerline, a box girder with high torsional rigidity is required to accommodate the resulting unsymmetrical loading of the deck. Examples are Brotonne Bridge, Fig. 4.32; the Sunshine Skyway Bridge, Fig. 4.44; the Papineau-Leblanc Bridge, Fig. 5.26; and the West Gate Bridge, Fig. 5.55. A relatively wide median strip is required to accommodate a single-shaft pylon and the stays, which must be protected by traffic barriers. Anchorage of the stays may be internal to the box at a single node-point as in the Brotonne Bridge, Fig. 4.32, and the Sunshine Skyway Bridge, Fig. 4.44. In some cases the stay is split into two cables anchoring on each side of a central web as in the Papineau-Leblanc Bridge, Figs. 5.26 and 10.37.

Where the cable-stay system consists of two transverse planes (vertical or sloping) very little torsional rigidity is required in the deck structure because the stays provide a stiff support along each edge and the load deflections are small. Only unsymmetrical loading produces a very small transverse inclination of the deck. Therefore, for a deck width of approximately 50ft (15 m) a simple concrete deck slab with longitudinal edge girders is required, Fig. 2.14(f). For deck widths in excess of 50 ft (15 m), transverse floor beams are required at a spacing of approximately 10 to 16 ft (3 to 5 m).<sup>2</sup>

### 12.5 Span Proportions

In any type of bridge structure, one of the first design considerations to be evaluated is the proportioning of

the spans. Cable-stayed bridges, for the most part, have been utilized to cross navigable rivers where navigation requirements have dictated the dimensions of the principal spans. Because the girder is supported from above by cable stays, cable-stayed bridges are ideal for spanning natural barriers such as wide rivers, Figs. 1.30, 1.41, and 4.43, and deep gorges Figs. 1.28 and 4.4. Similarly, for vehicular or pedestrian bridges crossing interstate highways or areas of heavy urban development, they can provide long spans unobstructed by piers, Figs. 4.2, 7.6, and 7.31.

Span arrangements are of three basic types: two spans, symmetrical or asymmetrical, Fig. 2.1(a); three spans, Fig. 2.1(b); or multiple spans, Fig. 2.1(c). A partial tabulation of two-span asymmetrical structures is presented in Table 2.1, which indicates that the longer span is in the range of 60 to 70% of the total length, or stated in another manner, a ratio of minor span to major span of 0.43 to 0.67. Exceptions are the Batman and Bratislava Bridges, Fig. 2.2, which have ratios of 80% (ratio of minor span to major span of 0.25). However, these two structures do not have the back-stays distributed along the short span; they are concentrated into a single back stay anchored to the abutment. A similar tabulation of three-span structures is presented in Table 2.2, which indicates that the ratio of center span to total length is approximately 55% (ratio of side span to center span of 0.4). In multiple-span structures, the spans are of equal length (although there are exceptions such as the Polcevera Viaduct Table 4.1) with the exception of flanking spans that connect to the approach spans or abutments.

The ratio of side span (s.s.) to center span (c.s.) influences the live load stress range primarily in the back stay cables which fix the pylon head to the anchor pier. Live load in the center span increases these stresses and live load in the side spans decreases them. Where long side spans are used ( $s.s./c.s. > 0.4$ ) the back stays could approach a near-slack condition. Back stays are subject to the largest stress range amplitudes which must be kept below the fatigue capacity of the stays. The ratio of side span to center span also influences the magnitude of the vertical component of the back stays at the anchor pier and thus the anchor pier capacity requirements. This anchor force decreases with increasing ratio of  $s.s./c.s.$

The preceding considerations are with respect to a three-span symmetrical structure. When an asymmetrical structure with a single pylon is used, a comparison can be made to a three-span symmetrical structure where the center span of the three-span bridge is approximately 1.8 times the major span of the asymmetrical structure.



Experience has indicated that in relatively short-span structures, 400 to 600 ft, a three-span cable-stayed bridge will generally be within 3 to 5% of preliminary estimates of other bridge types. Because this comparison is considered within the accuracy of preliminary estimates the economic advantage of the cable-stayed bridge is not clear-cut, although it may be said to be competitive. Where feasible, the designer might consider a two-span asymmetrical cable-stayed structure with perhaps the longer span in a range of 800 to 1000 ft (245 to 305 m). In this type of design, the river piers may be eliminated. If viaduct approach spans are considered then perhaps the approach piers could be used to anchor the backstays and thus stiffen the longer or center span. The cost of the superstructure may increase, but this may be offset by the decreased substructure cost. To reiterate, the designer must be aware that a cable-stayed bridge is not one bridge type but a number of types.

### 12.6 Proportion of Pylon Height to Center Span

The height of the pylons influences the amount of cable-stay steel material and the longitudinal compressive forces in the bridge deck. Leonhardt<sup>5</sup> has developed a relationship for suspension and cable-stayed bridges in which the amount of cable steel required for a given cable force is considered to be a function of the ratio of the tower height to the center span. The effect of the weight of the cable and any load concentrations are neglected. The equation for the resulting weight of the cable required to support a given tensile force is

$$W = \frac{q\lambda L^2}{\sigma} C \quad (12.1)$$

where  $W$  = weight of steel in cables in lbs

$q$  = total load (dead load plus live load)

$\lambda$  = specific weight of cable steel

$\sigma$  = allowable cable stress in psi

$L$  = length of main span in ft

$C$  = dimensionless coefficient depending on bridge type

The cable weight equation is applicable to the classical suspension bridge and the cable-stayed harp and radiating types. The constant,  $C$ , varies for each type and takes the following forms:

For the suspension bridge

$$C_S = \frac{2L_1 + L}{2L} \left[ \sqrt{16 + \frac{1}{u^2} \left( \frac{1}{4} + \frac{2u^2}{3} \right)} + \frac{2u}{3} \right] \quad (12.2)$$

where  $L$  = center span length

$L_1$  = side span length

For the cable-stayed harp

$$C_H = u + \frac{1}{4u} \quad (12.3)$$

For the cable-stayed radiating

$$C_R = 2u + \frac{1}{6u} \quad (12.4)$$

Where  $u$  is the ratio of tower height above the deck to the length of the center span expressed as  $h/L$ .

To provide comparative cable weights, it was necessary to assume the hanger weights were included in the total weight of cable for the suspension system, but to exclude the quantity of cable steel from the ends of the side spans to the anchorages.

In a comparative study of the cable weights for different systems, the only variable term in equation 12.1 is the constant  $C$ . Therefore, the variation of the constant will also be indicative of the comparison of the steel weight in the cables. A plot of the coefficients  $C$  for varying values of  $u$  (the ratio of tower height to center span length  $h/L$ ) is illustrated in Fig. 12.1, for the three types of structures to be discussed.

The end spans are assumed to be 0.4 times the center span for each of the three types of bridges. The lowest point of each curve indicates the optimum minimum value for the coefficient  $C$ , which is also indicative of the minimum cable steel weight. The value of  $u$  for both the suspension bridge and cable-stayed radiating type is approximately equal to 0.28, and the cable-stayed harp type has a minimum value of  $u$  equal to 0.5. These values do not include the weight of the towers and the stiffening girders. When these additional weights are included, the most economical ratio of  $h/L$  for the cable-stayed bridges is approximately 0.2 or 1/5, while that for the suspension type is 0.125 or 1/8. However, to obtain greater stiffness from the cables for suspension bridges, a value of  $u$  of 0.111 or 1/9 is preferred.

The corresponding values of  $C$  are:

|                              |              |
|------------------------------|--------------|
| Suspension system, $u = 1/9$ | $C_S = 2.36$ |
| Suspension system, $u = 1/5$ | $C_S = 1.71$ |

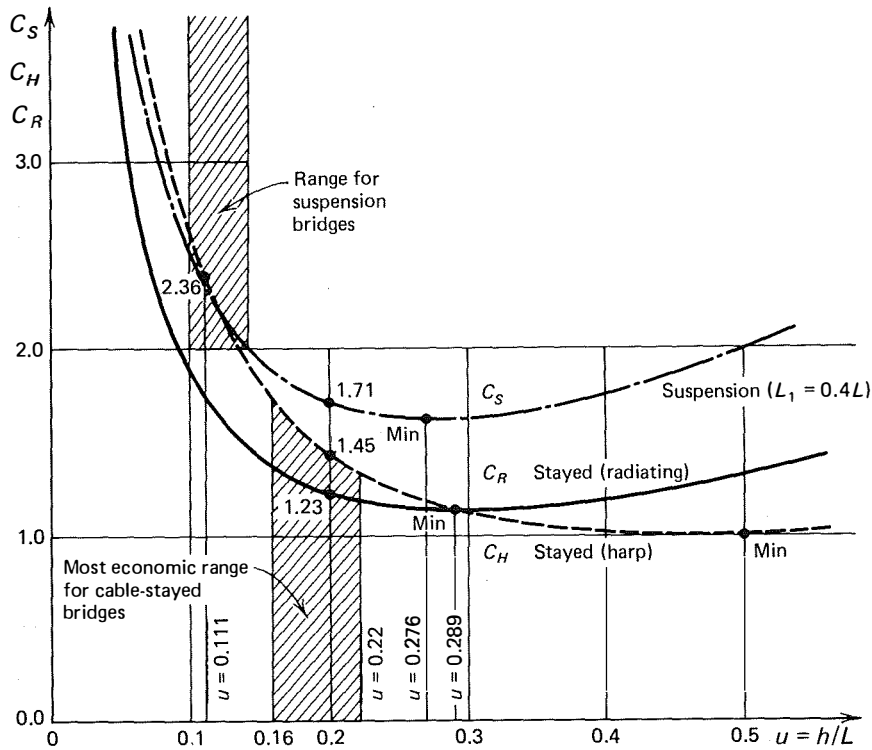


FIGURE 12.1 Economic Comparison—Suspension versus cable-stay, from reference 5.

Cable-stayed radiating type,  $u = 1/5$   $C_R = 1.23$   
 Cable-stayed harp type,  $u = 1/5$   $C_H = 1.45$

12.7 Loads and Forces

Design loadings, their combinations and applications, should be consistent with appropriate specifications, either AASHTO or AREA. These loadings may be modified to suit local conditions and spans in excess of the specification's jurisdiction. It should be noted that AASHTO specifications are only applicable to spans up to 500 ft and, therefore, do not include the long-

span structures. For spans in excess of 500 ft, reductions recommended by Ivy<sup>6</sup> et al (summarized in Table 12.1), are generally accepted criteria.

There is no universally accepted standard for conditions, loadings, and factors of safety to be used for proportioning the cable sizes. In the past, consultants and cable manufacturers have used one-third the ultimate breaking strength of the cable (structural strand ASTM A586) as the allowable design value to arrive at a cable size. The design factor is predicated on the assumption of elastic behavior of the structure and the cable. The range of stress in the cable is calculated to be less than the prestretched elastic limit.

TABLE 12.1. Equivalent Lane Loadings

| Loaded Length (ft) | Uniform Live Loads (lb/ft) | Concentrated Live Load |            |
|--------------------|----------------------------|------------------------|------------|
|                    |                            | Moment (lb)            | Shear (lb) |
| 0-600              | 640                        | 18,000                 | 26,000     |
| 601-800            | 640                        | 9,000                  | 13,000     |
| 801-1000           | 640                        | 0                      | 0          |
| 1001-1200          | 600                        | 0                      | 0          |
| 1201-over          | 560                        | 0                      | 0          |

Where fatigue effects are likely to occur some designers have used one-fifth the ultimate breaking strength of the cable for the design allowable load of the cable.

Current design criteria in the United States for cable stays is based upon the working stress design method. For parallel wires (ASTM A421, Type BA) and parallel strands (ASTM A416) the maximum allowable stress is 0.45 GUTS (guaranteed ultimate tensile strength) for AASHTO Group I loading and 0.50 GUTS for all other AASHTO Group loadings. Where a stay is used in erection, the maximum allowable temporary erection stress is limited to 0.56 GUTS.

The designer and contractor should bear in mind that when saddles are used, the effective design breaking strength of the cable should be reduced based on the ratio of the saddle radius to the strand diameter. A cable manufacturer or cable specialist should be consulted for specific values for particular applications.

### 12.8 Structure Anchorage

The manner in which structure loads are transmitted to the foundation affects the response of stiffness of the structure and the magnitude of axial force in the girder. For long cable-stayed bridges, it may be desirable and practical to consider the effect of expansion joints and their location in the structure. The effect of structure anchorage and expansion joint location has been investigated to some degree by Gimsing.<sup>7</sup>

Consider the structure illustrated in Fig. 12.2(a) under the action of a uniformly distributed load. Because there is no restraint at the supports to the horizontal component of cable force, the axial force distribution in the girder will be as illustrated, zero force or nearly so in the center of the main span and maximum compression at the pylons. The principal axial forces in the girder are compression loads, thus the system is defined as a self-anchored system.

If, in this system, a horizontal restraint is added at the abutments and expansion joints are added at the pylon, the axial force distribution is altered, Fig. 12.2(b). The system now has maximum tension at the center of the main span and zero forces at the pylons. All axial forces in the girder are in tension, consequently, this system is defined as fully anchored externally to abutments or piers.

With expansion joints at the pylon, the center span is only fixed horizontally by the cables and its own lateral flexural stiffness. With live load placed in one-

half the center span a horizontal displacement occurs, and because the uniformly distributed dead load has a stabilizing effect, the magnitude of the displacement, aside from stiffness, is a function of the ratio between dead load and live load. If only one expansion joint were used at one of the pylons, the system would act as fully anchored under dead load. Under live load, that portion of the girder containing one side span and the center span would act as a partially self-anchored system. However, symmetry would be destroyed and undesirable bending moments and distortions might result.

To reduce the magnitude of the axial force, either compression or tension, it may be desirable to combine the self-anchored and fully anchored systems as a partially anchored system. This may be accomplished by providing horizontal restraint at the abutments with no expansion joints, if the induced thermal forces can be accommodated, or with expansion joints located in the end spans, Fig. 12.1(c). In this system, the type of girder axial force varies throughout the length, with maximum compression at the pylon and maximum tension in the center of the main span.

Because only the top cable in the end spans are anchored to the abutments, the flexural deformation of the center span will be influenced not only by the deformation of the cables, but also by the flexural deformation in the end spans. The stiffness of the center span can be increased by piers or abutments supporting the end spans at the points of cable attachments. This has been done on the Kniebrücke, Fig. 2.11(j), and the Düsseldorf-Oberkassel structures, Fig. 5.44, and others. In this manner the vertical component of cable force is resisted by the girder. If the pier is not hinged the horizontal force distribution is a function of the relative stiffness between girder and piers with the result of introducing bending in the pier.

The deflection of the girder, in a harp configuration with live load in the center span (illustrated in Fig. 12.3(a) and Fig. 12.3(b), indicates the deflection for live load in one end span and on one-half the main span. As may be assumed, the structure with the supported side spans has the greatest stiffness.

Piers in the end spans are normally acceptable because only the center span width is required for navigation purposes and the piers in the end span will normally be located on land or in relatively shallow water. Economically, the choice should be justified by a comparison of cost savings in the girder stiffness requirements versus the increased pier costs.

When a vertical restraint (bearing) is provided at

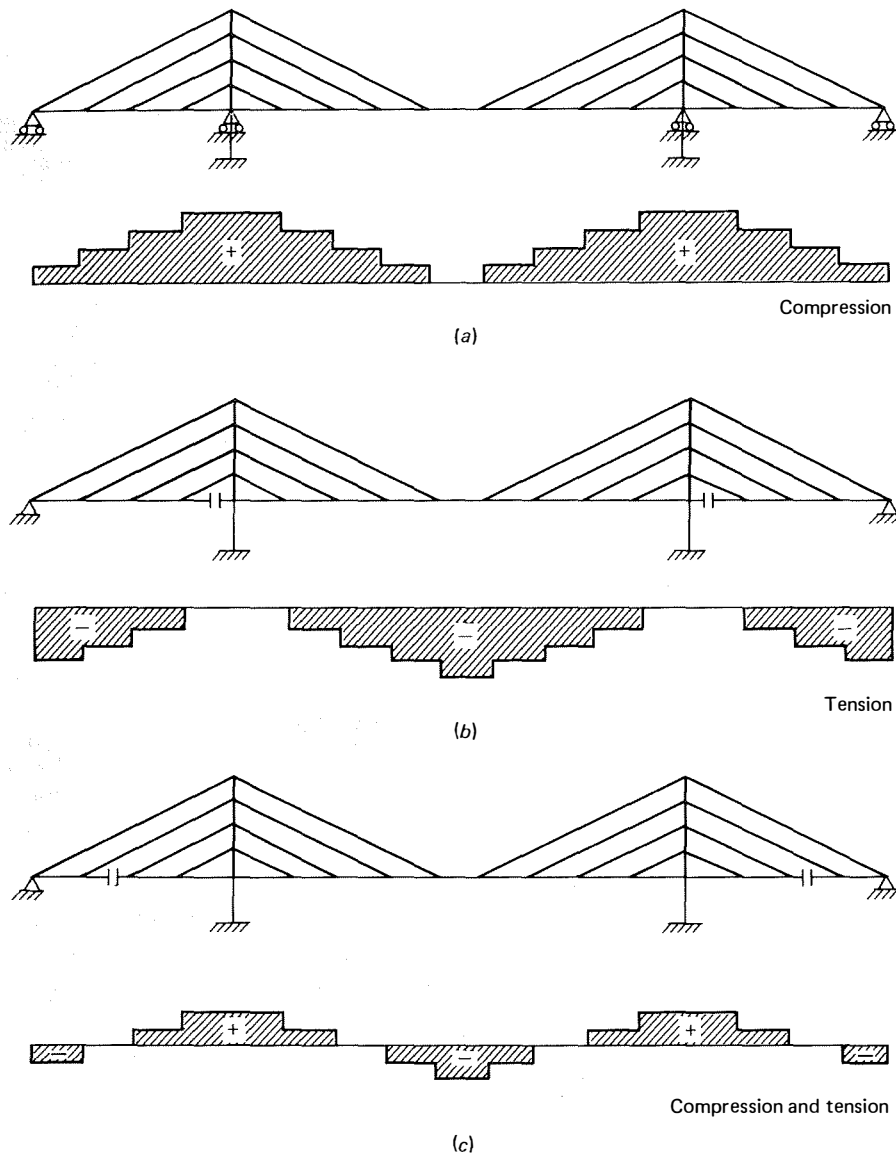


**FIGURE 12.2** Axial forces in stiffening girder: (a) self-anchored, (b) fully-anchored, and (c) partially anchored, from reference 7.

the pylons to support the girder, a relatively large negative bending moment will occur in the girder. In order to minimize this moment and smooth out the overall support moments of the girder this bearing is omitted, and support is provided to the girder by additional cable stays at or in close proximity to the pylon. In this manner the elastically deformable support condition provided by the cable stays is continued at the pylons.

Bearings for horizontal transverse loads (wind) are positioned such that they act directly on the pylon leg.

These bearings must allow angular change of the wind girder in the horizontal plane. They should have an open gap of approximately  $\frac{1}{8}$  in. (3 mm) to allow vertical and longitudinal movement of the girder. A wind bearing or wind lock is provided at the end spans to allow longitudinal movement of the girder and rotation in the vertical and horizontal plane. These bearings or wind locks are usually positioned on the longitudinal centerline of the bridge.

To accommodate longitudinal forces (braking), fixed bearings may be provided at one or two points

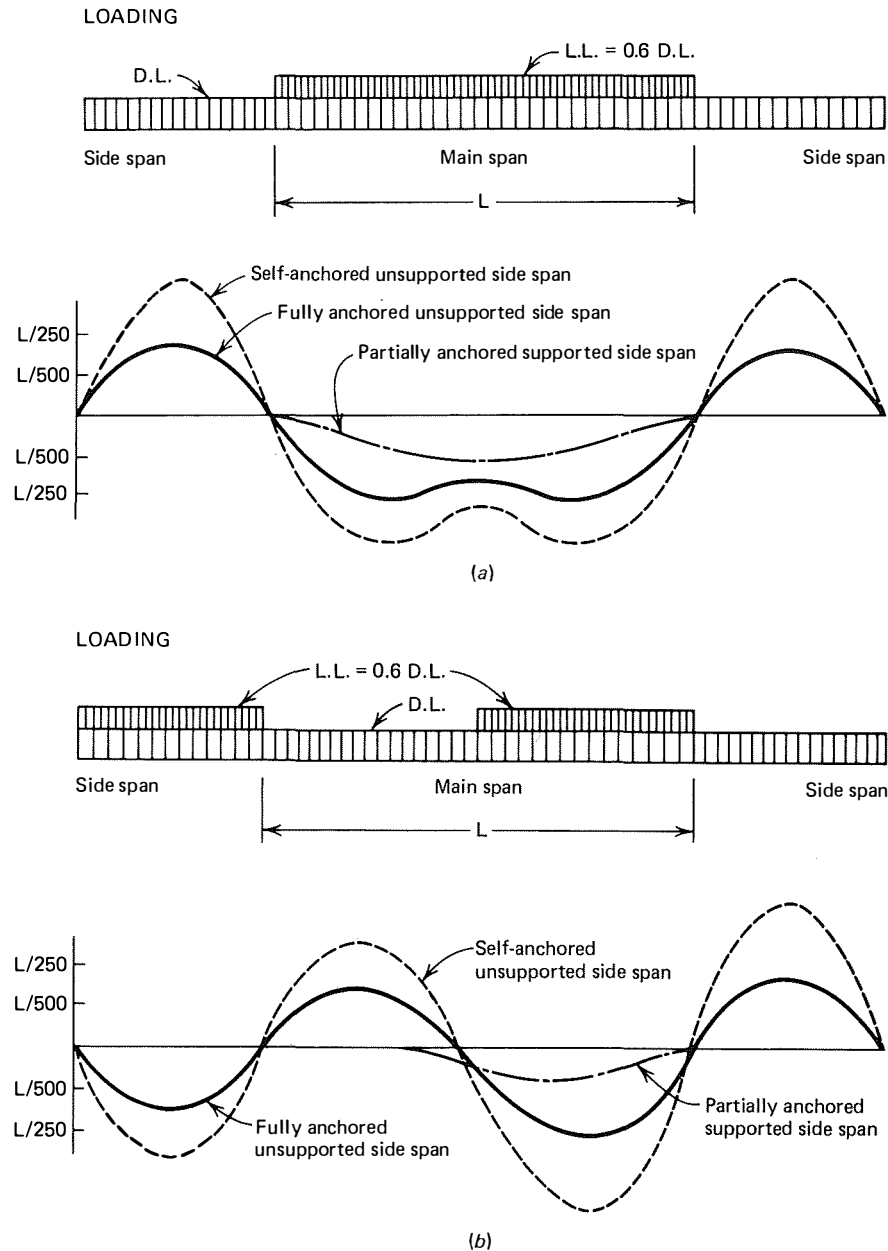


FIGURE 12.3 (a) and (b) Girder deflections, from reference 7.

in the structure, either at the end span or at the pylon. Positioning of bearings for longitudinal loads must take into account thermal expansion and contraction. In seismic areas the bearing should be designed to limit movements under service conditions and to break away if extreme seismic action occurs. In this manner damage to the pylons and piers can be minimized or avoided.

Near the ends of the side span a condition exists whereby the back stays anchor to the girder, the girder

is anchored to the pier, large angular changes of the girder deflection line occur, and, possibly, an expansion joint is placed at the same location. As a result, there is not only the detail problem of congestion at this location but also a major concern that if the expansion joint allows water to pass through, a potentially dangerous situation of corrosion of the anchoring devices may occur.

A solution to this problem is to allow the stay girder to be continuous across the anchor pier incorporating

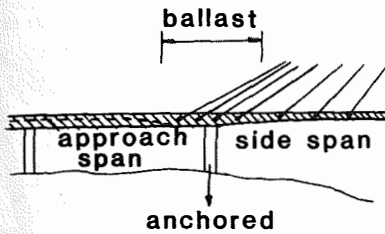


FIGURE 12.4 Girder continuity at anchor pier, from reference 2.

the first approach span, Fig. 12.4, (as in the Luling Bridge) or to provide a hinge joint in the first approach span.<sup>2</sup> In this manner the uplift forces of the back stay can be counteracted by the weight of the adjoining span and by concrete ballast within the depth of this girder which extends to both sides of the anchor pier. This continuity also allows distribution of the back stays over a length of girder behind the anchor pier. Then, the expansion joint can be relocated a distance from the centerline of the anchor pier and away from any linkage devices to the anchor pier.

12.9 Multispan Stayed Girder Bridges

The majority of cable-stayed bridges that have been constructed are of the three-span symmetrical or two-span asymmetrical types. These structures were built with the three- or two-span arrangements because, for the most part, they have been over navigable waterways where only one major navigation span is required. Normally, where two cable planes are utilized the pylon is a portal or an A-frame, which is oriented transversely to the bridge. Occasionally a situation will arise where several large spans or a viaduct structure may be considered. In this type of structure two A-frames or two portal frames may be oriented in the plane of the cables as in most of Morandi's structures, such as the Maracaibo Bridge with its distinctive A-frames, Fig. 4.1, or as in one of the proposed bridges for the Danish Great Belt Bridge with portal frames, Fig. 2.5. The logic for this orientation of the pylon was excellently documented by Gimsing in reference 8 and is presented in the following discussion.

In the usual two- or three-span cable-stayed bridge the displacement of the top of the pylon is controlled by the back stay(s), which are anchored to the stiffening girder, and the vertical component of this stay force is resisted by an anchor pier. This arrangement stiffens the center or major span. In a multispan bridge with several equal main spans the displacement of the top of the interior pylons cannot be restrained or con-

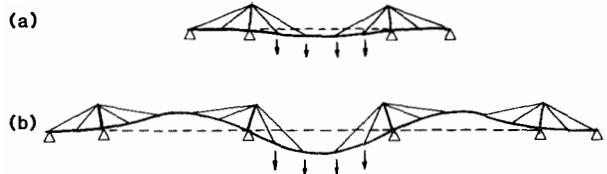


FIGURE 12.5 Deflection of stayed girder bridge with: (a) one main span, and (b) three main spans, from reference 8.

trolled because there is no back stay or anchor stay. The stiffness of a span depends upon the stiffness or deformation of the adjacent spans and pylons. For an unsymmetrical loading pattern with respect to an interior pylon, that is, one span loaded and an adjacent span underloaded, a rotation occurs at an inner cable-stay system which produces an undesirable deflection in the loaded span, Fig. 12.5.

Two radiating-stay systems are illustrated in Fig. 12.6 with loading on the left side of the pylon. The system in Fig. 12.6(a) has a vertical support at the right end and thus, a fixed back stay. The system in Fig. 12.6(b) has a moment-resisting pylon which is assumed to have a constant cross section for its total height. Deflection of the top of the pylon for the system depicted in Fig. 12.6(a) is designated as  $\Delta_1$  and that for the pylon in Fig. 12.6(b) is designated as  $\Delta_2$ . The magnitude of these deflections are determined by the following equations

$$\Delta_1 = \frac{h}{\sin \phi \cos \phi} \frac{\sigma_{fc}}{E_c} \tag{12.5}$$

$$\Delta_2 = \frac{2h^2 + 6sh + 3s^2}{3b} \frac{\sigma_{pb}}{E_p} \tag{12.6}$$

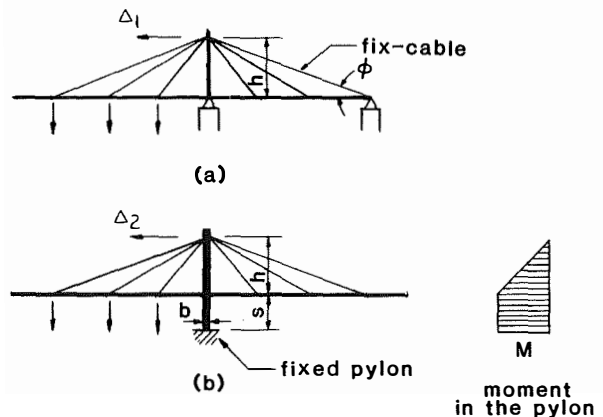


FIGURE 12.6 Stay system with one-sided loading: (a) system with a fixed cable (back stay), and (b) system with a fixed pylon, from reference 8.

where:  $\sigma_{fc}$  = tensile stress in fixed back stay  
 $E_c$  = modulus of elasticity of the stay  
 $\sigma_{pb}$  = bending stress in the bottom of the pylon  
 and  $E_p$  = modulus of elasticity of the pylon

To produce the same stiffness in both systems, for comparison purposes, requires that  $\Delta_1$  equal  $\Delta_2$ . Setting these two equations equal to one another leads to an expression for the width,  $b$ , of the moment resistant pylon as follows:

$$b = \frac{2h^2 + 6sh + 3s^2}{6h} \sin 2\phi \frac{E_c \sigma_{pb}}{E_p \sigma_{fc}} \quad (12.7)$$

Assuming some realistic values, such as, the height of the pylon below the deck,  $s$ , equal to one-half the height of the pylon above the deck,  $h$ ; the angle of the fixed back stay with the horizontal,  $\phi$ , equal to 20 degrees; and the ratio of modulus and stress indicated in the last term as 0.5; a value of  $b = 0.31h$  is obtained.

If a three-span structure is assumed with a fixed back stay and a main span length of 1000 ft (305 m), the height of the pylon above deck level would be about 170 ft (52 m) and the pylon width would be on the order of 7 to 10 ft (2 to 3 m). If the back stay is not fixed then the pylon width would have to be increased to approximately 50 ft (15 m) to obtain the same degree of stiffness. In other words, to compensate for an unanchored or "not-fixed" back stay requires a drastic and aesthetically unacceptable increase in the pylon dimension. The only way to obtain reasonable member dimensions and achieve sufficient stiffness in a fixed pylon structure appears to be the use of a portal frame in the plane of the stays, as indicated in the Danish Great Belt Structure, or by applying an A-frame similar to the Maracaibo Bridge.

In contrast to the Maracaibo Bridge, where there is no connection between the A-frame and the stiffening girder, it is preferable to transmit forces between the stiffening girder and the pylon. In the configuration illustrated on the left side of Fig. 12.7, the moments acting on the entire pylon structure induce only normal forces in the individual members. At the same time, flexural deformations of the vertical members assure a certain horizontal flexibility of the lower part of the pylon structure. This feature allows the application of continuous stiffening girders, which in most cases is preferable. If large horizontal movements of the stiffening girder occur, it is possible to apply movable bearings between the stiffening girder and the vertical legs of the lower part of the pylon structure as shown at the right of Fig. 12.7. These horizontal mov-

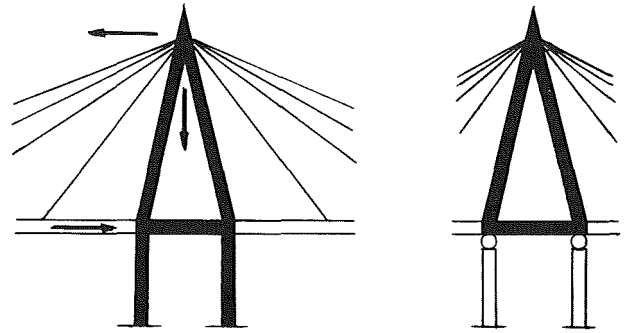


FIGURE 12.7 Triangular pylon structure, from reference 8.

able bearings do not influence the transmission of the primary forces as long as the upper portion of the pylon is still horizontally fixed to the stiffening girder. However, it should be noted that these bearings while permitting mutual rotations and longitudinal movements must also be capable of transferring compressive as well as tensile forces in the vertical direction.

The importance of having a connection capable of transmitting horizontal forces from the stiffening girder to the pylon structure is illustrated in Fig. 12.8. In System I there is no direct connection between the pylon and the stiffening girder, while in System II a connection is effected between the pylon and the stiffening girder, allowing the transmission of the horizontal force in the stiffening girder. In both systems the

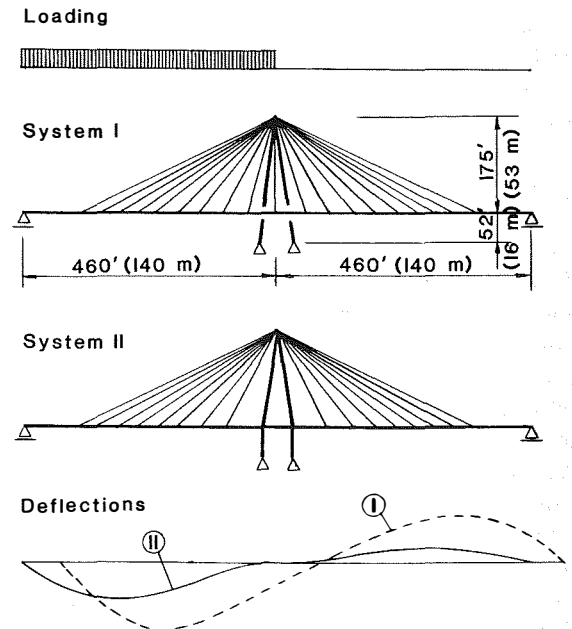


FIGURE 12.8 Deflections of two different stayed systems under one sided loading, from reference 8.

ends of the stiffening girder are supported on bearings that allow longitudinal movements.

For a symmetrical load with respect to the pylon the two systems will have almost identical deflections, but for an unsymmetrical loading a significant difference is observed.

In System I the stiffening girder will move longitudinally toward the unloaded span, thus reducing the action of the stays, and consequently relatively large deflections will occur. In System II the stiffening girder is fixed horizontally to the A-frame and this minor modification of the structural system reduces the vertical deflection to less than one-half those of System I. Further, the bending moments of the stiffening girder and variations of cable forces in the stays are more favorable in System II than in System I.

Gimsing has also suggested another method of reducing the horizontal deflections of intermediate pylons. He suggests using a horizontal fixed cable between all pylon tops, Fig. 12.9. This solution has been used on several French suspension bridges of the nineteenth century. However, it has yet to be used in connection with cable-stayed bridges. It is doubtful whether this solution would be aesthetically acceptable to the general public.

Gimsing also presented a comparison of the deflection of several different multispan systems, Fig. 12.10. System A is the conventional three-span bridge with a radiating cable system and hinged connections between the superstructure and the substructure. The dimensions and cross-sectional properties of the individual members correspond to those required for typical European highway loadings. It is further assumed in this study that the steel in the stiffening girder and pylons is 50 ksi (345 MPa) and the cable wires have an ultimate stress of 220 ksi (1517 MPa).

System B corresponds closely to system A regarding the size of members and type of connections between the superstructure and substructure. Section properties for corresponding members are assumed equal in order to allow a direct comparison.

Systems C and D have a fixed connection between the pylons and substructure. The pylons are the conventional column type. In System C the section properties of the pylon correspond to that of System A and

B, whereas in System D the moment of inertia of the pylon is increased by an order of magnitude of 10.

System E is the same as B except for the addition of the horizontal cable between pylons.

System F contains four triangular pylon structures supported on bearings that allow longitudinal movement but are fixed in relation to the vertical movement.

The deflection diagrams illustrated in Fig. 12.10 are for the central span under a uniformly distributed load. The deflection of the usual three-span bridge, System A, is used as a base reference. It should be kept in mind that the deflections for System A are close to the allowable limits for bridge structures of the actual size. Similar results are found for uniform load and deflections in a span flanking the center span.

Conclusions to be drawn from these deflection curves are as follows:

1. Fixing of the pylons with common flexural stiffness does not reduce the deflection significantly. Compare System B, the hinged pylon with System C the fixed pylon.
2. Even when the pylon is fixed and its flexural stiffness is increased by an order of magnitude of 10, the deflection is not reduced sufficiently. Compare System B with System D.
3. A horizontally fixed cable between the pylon tops, System E, will reduce the deflection of the bridge to an allowable limit.
4. A triangular pylon structure supported on proper bearings, System F, will also produce deflections within allowable limits.

During a structure type design investigation for the Great Belt Bridge in Denmark, three loading conditions were investigated: highway traffic only, railway traffic only, or both road and rail traffic on the same bridge, with the emphasis on the combined traffic situation. For the main spans, two designs were studied, one having three truss spans, each approximately 1200 ft (370 m) and another with two 1970-ft (600-m) stayed girder spans.

The investigation showed that for the combined

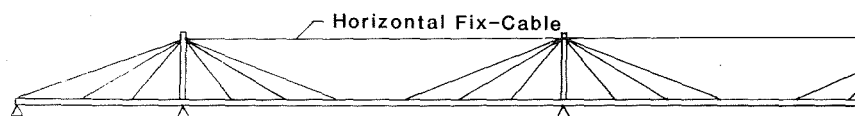
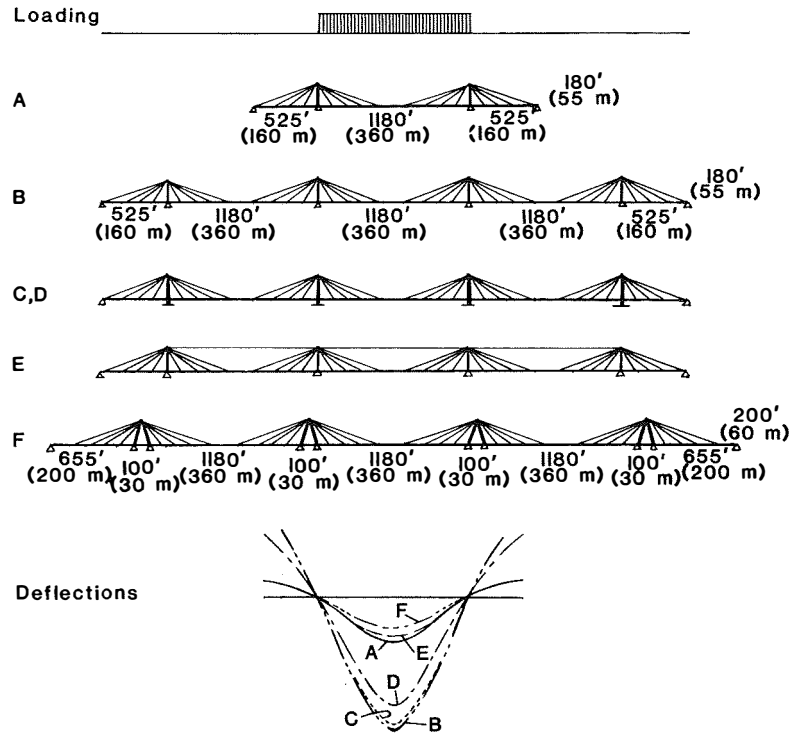


FIGURE 12.9 Stayed girder bridge with horizontal fixed-cable between pylon tops, from reference 8.





**FIGURE 12.10** Relative deflections of different stayed girder systems with loading in central main span, from reference 8.

road and railway bridge with 1970 ft (600 m) main spans only a stayed girder solution would be realistic. A truss bridge would be extremely uneconomical and a suspension bridge would be too flexible to allow railway traffic.

When investigating the longitudinal layout of the main spans it was determined that the application of a horizontal fixed cable above the 1970-ft (600-m) main spans would not be advantageous for the actual bridge, which supports heavy railway traffic. However, as the two navigation spans could be separated by smaller spans, several possibilities of fixing the tops of the inner pylons presented themselves.

Some of the cable-stay systems investigated during this preliminary investigation are illustrated in Fig. 12.11.

System A is essentially composed of two three-span cable-stayed bridges placed side by side. Each stayed bridge has a 1970-ft (600-m) main span and two 690-ft (210-m) side spans. This ratio of main to side spans is required to ensure that the back-stay cable will always be in tension. This concept of two-stayed-girder bridges separated by an anchor pier with double shafts has the advantage of utilizing four identical cable planes supported by vertical pylons subjected to primarily axial forces. However, this system has the dis-

advantage of requiring three piers in the central portion of the structure where water depths are at a maximum. This arrangement can be regarded as a cable-stayed version of the San Francisco-Oakland Bay suspension bridge.

In System B, the central anchor pier is eliminated by placing the two central pylons so closely together that the fixed or back-stay cable from one pylon can be attached to the stiffening girder at the other pylon, and vice versa. However, a number of structural difficulties present themselves at the intersection of the cables. In addition, the axial force in the stiffening girder between the two central pylons is considerably increased due to the fact that this portion of the girder forms a part of both the left and right stayed girder bridges. Further, the intersecting cables at the center portion are not aesthetically appealing.

In System C the intersecting cables at the central portion of the bridge is avoided and the two central pylons differ from A and B by being triangular in shape. To exclude the unbalanced horizontal forces resulting from gravity loads the tops of the two central pylons are connected by a horizontal cable. This cable will also provide a distribution of the horizontal forces from live loads on the two pylons.

Instead of using triangular pylons, it was also found

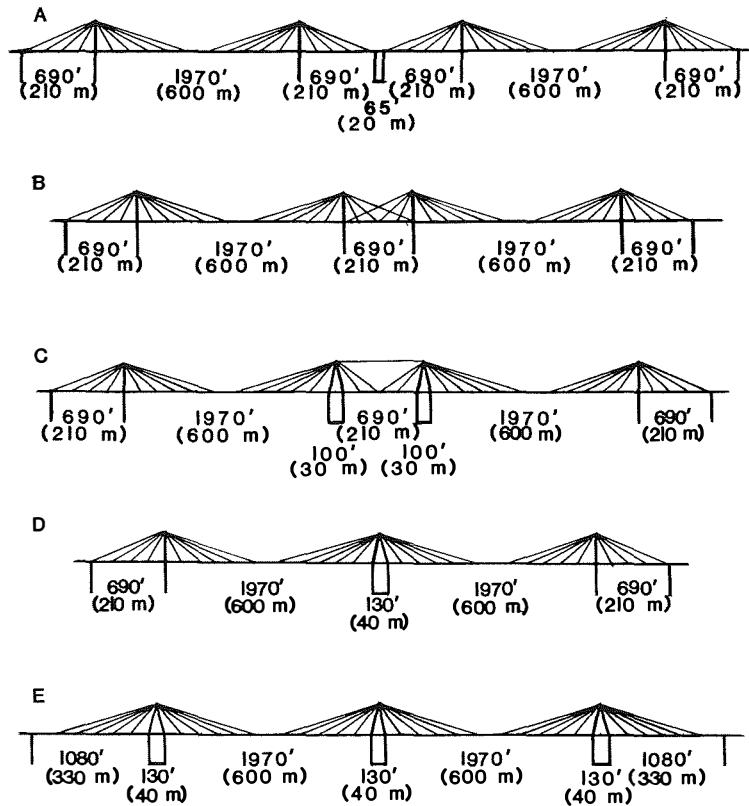


FIGURE 12.11 Cable stay systems investigated for a bridge with two 1970-ft (600-m) navigation spans, from reference 8.

possible to have just one triangular pylon between the two 1970-ft (600-m) spans as indicated in System D. For this case only one pier is required to be in deep water. As a result, this pier must be considerably stiffer than the piers in either System A or B.

In Systems C and D the bridge contains two different types of pylon, the single vertical outer pylon and the triangular central pylon.

A consistent application of triangular pylons is obtained in System E. In this case the bridge has three identical and symmetrical cable systems. Because the outer pylons are triangular in shape there is no need for a fixed back stay. The side span length can be increased from 690 ft (210 m) to 1080 ft (330 m).

After an economical and aesthetic evaluation, Systems B, C, and D were discarded. Systems A and E were both regarded as acceptable.

### 12.10 Preliminary Manual Calculations

Because of the large degree of indeterminateness of cable-stayed bridge structures, exact calculation by

manual procedures is virtually an impossible task. The many parameters involved present a formidable hurdle to manual calculations. The purpose of this section is to present a simplified manual procedure so that reasonable initial values may be obtained in order to enter into an electronic computer solution. The procedure presented will in general follow the methodology presented in reference 9. The reader should keep in mind that this is not an accurate solution. The calculations provide a means of determining first-trial values of required cable-stay areas. By using the analogy of a continuously elastically supported beam, influence lines for stay forces and bending moments in the bridge girder can be simply determined. From these results, stress variations in the stays and the girder resulting from concentrated loads can be estimated.

If the cable forces acting under gravity (dead) loads are such that all deformations in the girder and pylon are zero, the condition corresponds to that of a continuous girder supported on rigid supports. Therefore, the vertical components of the stays due to dead load are known. If, as a first-trial approximation, live load is applied to the same system, the stay forces  $P_i$  in Fig.

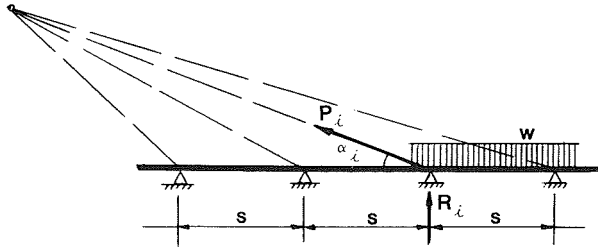


FIGURE 12.12 Cable force  $P_i$ , from reference 9.

12.12 can be determined by equation 12.8.

$$P_i = \frac{R_i}{\sin \alpha_i} \quad (12.8)$$

As stay cables are usually designed for the working load condition, the cross-sectional area of stay ( $i$ ) is determined by:

$$A_i = \frac{R_i}{\sin \alpha_i \sigma_{\text{allow}}} \quad (12.9)$$

Guaranteed ultimate tensile strength,  $f_{pu}$ , for 0.6-in. (15.24-mm) diameter 7-wire ASTM A416 prestressing strand is 270 ksi (1860 MPa) and for  $\frac{1}{4}$ -in. (6.35-mm) diameter ASTM A421 wire is 240 ksi (1655 MPa). Allowable working stress,  $\sigma_{\text{allow}}$ , is equal to 0.45  $f_{pu}$ , therefore, the allowable stress is 121.5 ksi (837 MPa) for strand and 108 ksi (745 MPa) for wire.

The reaction,  $R_i$ , at each cable-stay node may simply be determined as  $R_i = sw$  (see Fig. 12.12). However, at the ends of the girder  $R_i$  may have to be determined by other means.

To determine the force,  $P_o$ , in the back-stay cable, the horizontal force at the pylon top,  $F_h$ , must first be calculated, Fig. 12.13. Maximum force in the back-stay cable will be produced with dead plus live load in the center span and dead load only in the side span. If the pylon head is assumed to be immovable, then  $F_h$  can be determined from the following equation

$$F_h = \sum \frac{R_i^l}{\tan \alpha_i^l} - \sum \frac{R_i^r}{\tan \alpha_i^r} \quad (12.10)$$

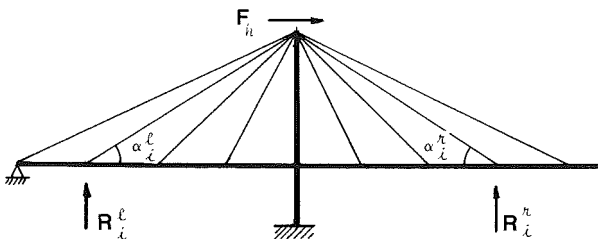


FIGURE 12.13 Pylon horizontal force, from reference 9.

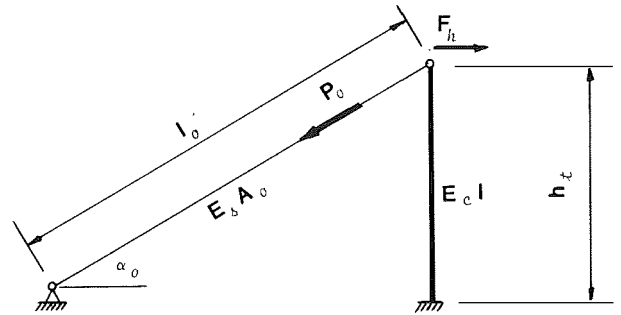


FIGURE 12.14 Back stay force diagram, from reference 9.

If in Fig. 12.14 the change in the angle  $\alpha_o$  is assumed negligibly small as the pylon deflects under the load  $F_h$ , then the load in the back stay cable can be determined as

$$P_o = \frac{F_h h_t^3 \cos \alpha_o}{3 l_o (E_c I / E_s A_o)} \quad (12.11)$$

If the bending stiffness of the pylon is neglected, then  $P_o$  becomes

$$P_o = \frac{F_h}{\cos \alpha_o} \quad (12.12)$$

Using the structure illustrated in Fig. 12.15 as an example, values were obtained for a few select stays by equations 12.8, 12.9, 12.10, and 12.12. These values are tabulated in the left half of Table 12.2. Actual values in the final design based on a computer solution are tabulated in the right half of Table 12.2.

In this example, as cable stays 1, 2, and 3 are distributed to either side of the anchor pier, they are combined into a single back-stay for purposes of manual calculations. The edge girders of the deck at the anchor pier were deepened in the actual design, but this increase in dead weight was ignored in the manual solution. Further, the simplified manual solution does not take into account other load cases such as, temperature, shrinkage, and creep.

The quantity of steel for the stay cables can be estimated from equation 12.1.

Influence lines for stay forces and girder moments are determined on the basis of a continuous, elastically supported beam.<sup>10,11</sup> Referring to Fig. 12.16, the following relationships are obtained:

$$P_i = \frac{1}{\sin \alpha_i}, \quad \Delta l_{si} = \frac{P_i l_{si}}{A_i E_s}, \quad \Delta l_{si} = a_i \sin \alpha_i$$

which lead to

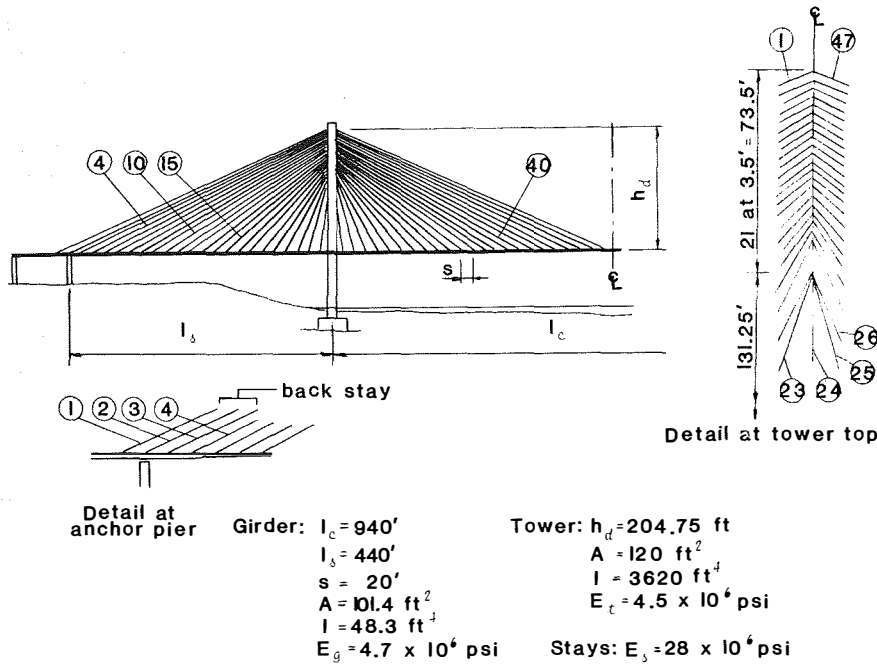


FIGURE 12.15 Example structure.

TABLE 12.2. Comparison of Manual to Final Computer Solution

| Stay Number            | According to Equations 12.8, 12.9, 12.10, and 12.12 |                 |                    |                    |                         | Computer Solution |                                 |  |  |
|------------------------|---|-----------------|--------------------|--------------------|-------------------------|-------------------|---------------------------------|--|--|
|                        | $R_{DL}$ (kips)                                     | $P_{DL}$ (kips) | $R_{DL+LL}$ (kips) | $P_{DL+LL}$ (kips) | $A$ (in. <sup>2</sup> ) | $P_{DL}$ (kips)   | $P_{DL+LL}$ (kips) <sup>b</sup> | Number of 0.6-in. Strands <sup>c</sup> | Strand Area (in. <sup>2</sup> ) <sup>c</sup> |
| back stay <sup>a</sup> | —   | 2596            | —                  | 3969               | 32.667                  | 2775              | 3579                            | 110                                    | 23.87  |
| 4                      | 360   | 824             | 400                | 916                | 7.539                   | 851               | 1049                            | 30                                     | 6.510  |
| 10                     | 360   | 684             | 400                | 760                | 6.255                   | 695               | 797                             | 18                                     | 3.906  |
| 15                     | 360   | 550             | 400                | 611                | 5.029                   | 558               | 654                             | 16                                     | 3.472  |
| 40                     | 360   | 734             | 400                | 815                | 6.708                   | 756               | 878                             | 20                                     | 4.340  |

<sup>a</sup>Stays No. 1, 2, and 3 combined into one back stay.

<sup>b</sup>Maximum live load.

<sup>c</sup>Per plane of a two plane structure.

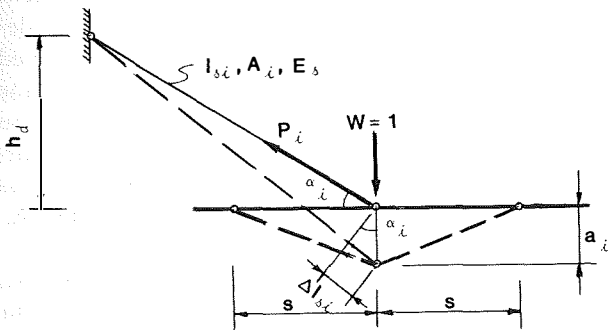


FIGURE 12.16 Spring stiffness notation, from reference 9.

$$a_i = \frac{l_{si}}{A_i E_s \sin^2 \alpha_i}$$

With equation 12.9 and  $l_{si} = h_d / \sin \alpha_i$ , the settlement (deflection) at point  $i$  becomes:

$$a_i = \frac{h_d \sigma_{allow}}{R_i E_s \sin^2 \alpha_i} \quad (12.14)$$

Using  $R_i = s(w_{DL} + w_{LL})$ , see Fig. 12.12, the spring stiffness of cable stay  $i$  is obtained as

$$k_i = \frac{1}{a_i s} = \frac{(w_{DL} + w_{LL}) E_s \sin^2 \alpha_i}{h_d \sigma_{allow}} \quad (12.15)$$

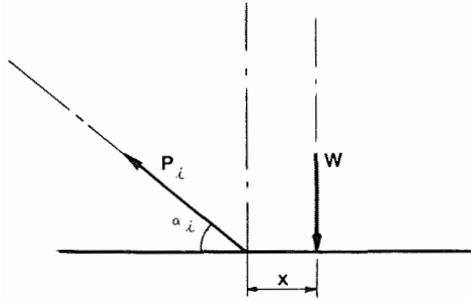


FIGURE 12.17 Cable force  $P_i$ , from reference 9.

The equation for the cable force  $P_i$ , Fig. 12.17, then becomes<sup>11</sup>

$$\begin{aligned} P_i &= \frac{\xi W}{2} \frac{s}{\sin \alpha_i} e^{-\xi x} (\cos \xi x + \sin \xi x) \\ &= \frac{\xi W s}{2 \sin \alpha_i} \eta_p \end{aligned} \quad (12.17)$$

where

$$\eta_p = e^{-\xi x} (\cos \xi x + \sin \xi x)$$

and

$$\xi = \sqrt[4]{\frac{k_i}{4E_c I}} \quad (12.18)$$

which is the degree of flexibility and has the dimension  $\text{ft}^{-1}$  ( $\text{m}^{-1}$ ). For the bending moment  $M_i$  at point  $i$ , the following equation applies

$$M_i = \frac{W}{4\xi} e^{-\xi x} (\cos \xi x - \sin \xi x) = \frac{W}{4\xi} \eta_m \quad (12.19)$$

where

$$\eta_m = e^{-\xi x} (\cos \xi x - \sin \xi x)$$

### 12.11 Methods of Analysis

In order to analyze a cable-stayed bridge an appropriate idealization, or modeling of the structure must be made. The restraints, if any, present at each joint in the structure should be determined in order to mathematically model the structure. The stiffness or flexibility of each member must be known or be determined by the analysis. Connections between the cables, girders, and towers are idealized at their points of intersection. For a single-plane system the structure may

be idealized as a two-dimensional plane frame, and torsional forces acting on the girder would have to be superimposed on the girder. A two-plane system may be idealized as a three-dimensional space frame with torsional forces included in the analysis.

Several methods have been employed in the analysis of cable-stayed bridges. A mixed method of analysis, where the unknowns in the matrix formulation include displacements and forces, has been developed by Stafford Smith.<sup>12,13</sup> A transfer matrix method has been developed in West Germany.<sup>14</sup> Troitsky and Lazar<sup>15</sup> used the flexibility approach while Podolny and Fleming<sup>16,17</sup> used a stiffness approach. Several general computer programs, such as FRAN, STRESS, or STRUDL, are available which use either the stiffness or flexibility approach. However, most of these programs assume linearity and must be modified to accommodate the nonlinear problem inherent in flexible structures. A stiffness approach incorporating an iterative procedure was used by Podolny and Fleming<sup>16,17</sup> to compensate for the nonlinearity of the cables and Tang<sup>18</sup> applied the transfer matrix to the nonlinearity of cable-stayed bridges. The only published material concerning the static behavior analysis of two-plane structures known to us is that of Stafford Smith,<sup>13</sup> Kajita and Cheung,<sup>19</sup> and Baron and Lien,<sup>20,21</sup> the latter also considered dynamic effects in their solution.

### 12.12 Stiffness Parameters

The total stiffness of a cable-stayed bridge is subject to the interrelationship of the individual stiffnesses of the girder, the cables and the pylon. To determine the influence of individual stiffnesses with respect to moments in the girder and pylon and to the tension in the cables, a linear study has been conducted<sup>16</sup> using the radiating and harp configuration in a single-plane arrangement, as shown in Fig. 12.18(a). The girder is rigidly supported vertically at the pylon, but is independent of the pylon so that no moment is transferred between the girder and the pylon. The girder and the pylon are assumed to have a constant cross section throughout the span and height, respectively. It is further assumed that the cable has an initial prestress capable of resisting a possible compression load by releasing the compression force accordingly.

The STRUDL program was used in the analysis with no correction for the nonlinear behavior of the cables. A modulus of  $24 \times 10^6$  psi was used for the cables and a uniform load was applied on all spans of

the structure. It is important to note that the type of loading or magnitude of tension in the cables or moment in the girder or pylon is not important for the purpose of this study, because the relative difference in the values due to changes in various stiffness parameters is the prime concern. The parameters investigated for these configurations were as follows: (1) ratio of moment to inertia of the pylon to girder,  $\alpha = I_p/I_g$ ; (2) stiffness ratio of outside cable to girder,  $\beta = (E_c A_c / l_a) / (E I_g / L^3)$ ; and (3) stiffness ratio of inside cable to outside cable,  $\gamma = (A_a l_b / A_b l_a)$ .

The effect of the parameter  $\alpha$  ratio of moment of inertia of the pylon to girder is indicated in Fig. 12.18(b). As the bending stiffness in the tower increases the tension in the back-stay cable  $a$  decreases and the moment in the pylon increases. There is very little effect on the tension in the other cables or moments in the girder.

The influence of  $\beta$  is indicated in Fig. 12.18(c). As  $\beta$  increases, the tension in the cables increases, and there is a decrease in the moments in the girder and pylon.

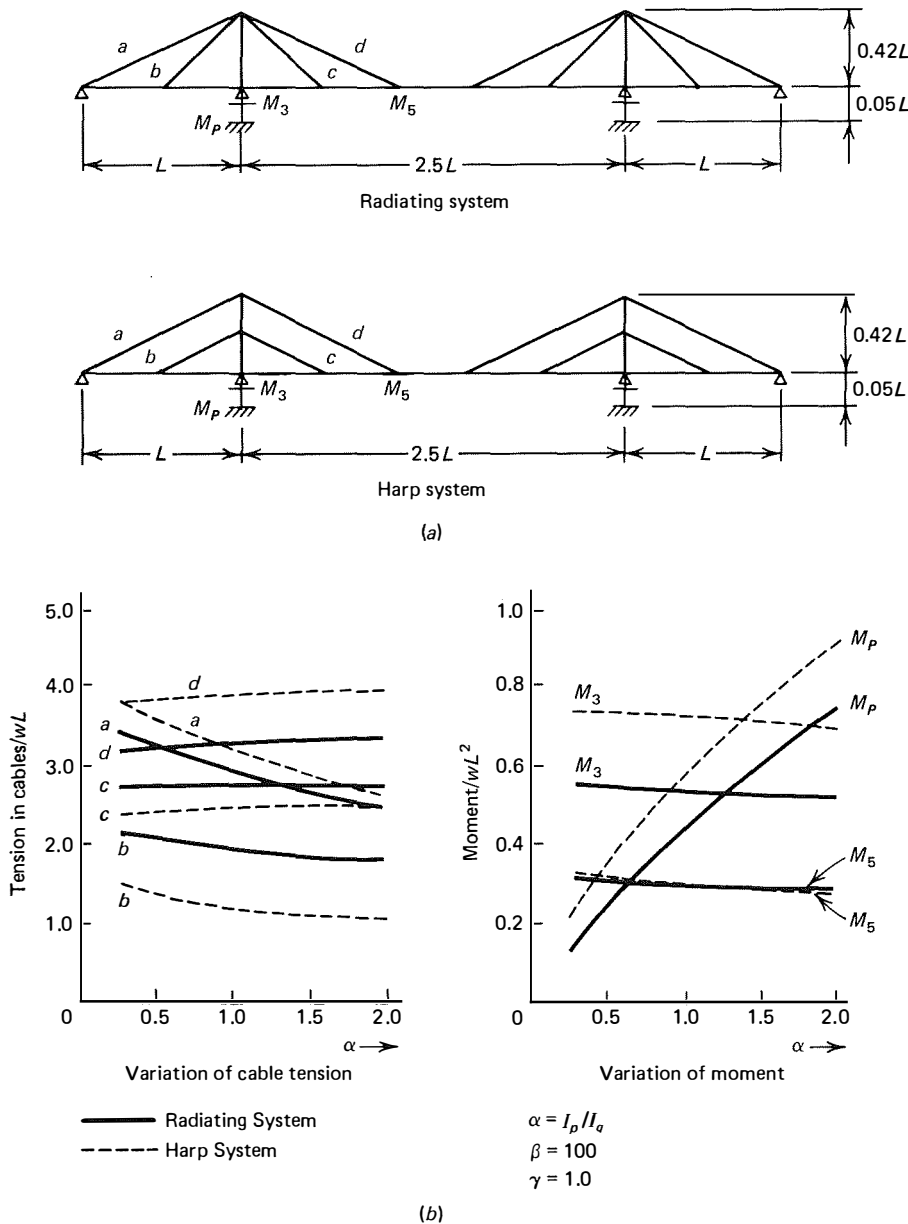


FIGURE 12.18 (a)-(d) Effect of stiffness parameters, from reference 14.

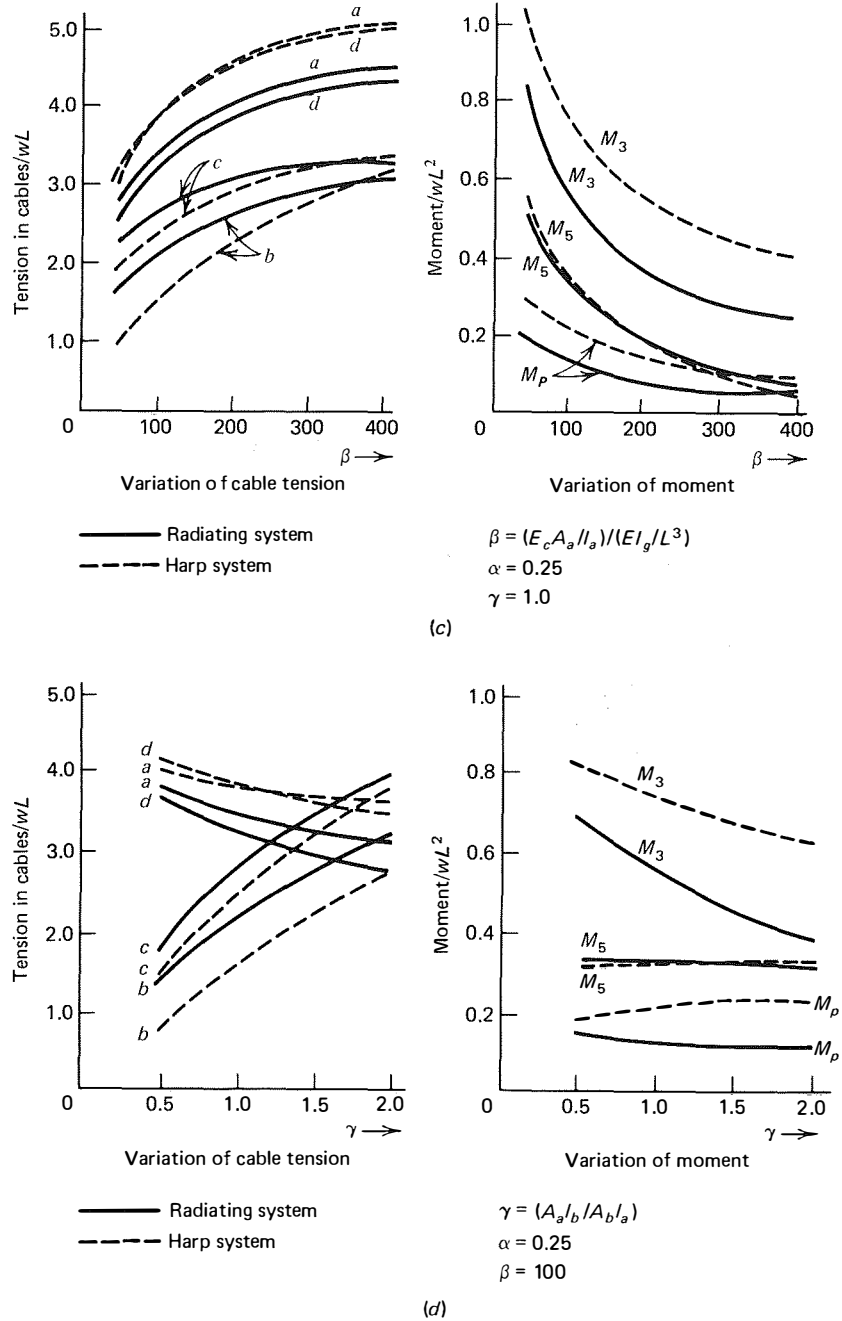


FIGURE 12.18 (Continued)

As the parameter  $\gamma$ , Fig. 12.18(d), increases, the tension in the outside cables decreases, while that of the inside cables increases. There is very little effect upon the pylon and girder midspan moment. However, there is a marked effect on the girder moment at the tower, but not to the same degree as produced by  $\beta$ . These conclusions generally confirm those of Okau-

chi, Yabe, and Ando.<sup>22</sup> The curves are not intended for design purposes, but merely represent a study of the effect of some of the variables involved in the analysis of a cable-stayed bridge.

The significance of the above conclusions may be illustrated as follows. Assuming that in a given trial analysis the overall structure stiffness is inadequate,

and that all other design criteria are satisfied by the trial structure, the designer can either increase overall stiffness or adjust the stiffness of the girder, the pylon or the stays. We would submit that from the above discussion, increasing the stiffness of the stay is the most efficient choice to increase the stiffness of the structure as a whole.

### 12.13 Mixed Method of Analysis—Single Plane

The following procedure and that of the subsequent section have been developed by B. Stafford Smith,<sup>12, 13</sup> and are presented here through the courtesy of the Institution of Civil Engineers.

#### 12.3.1 CABLE-STAYED BRIDGE BEHAVIOR

Before determining a method of analysis for a cable-stayed bridge, it is advantageous to study and understand the behavior of the total structure. A study indicates that the cables support the deck in a vertical direction only, and that torsion due to eccentric loading or wind forces is transmitted to the piers through

the deck structure. The overall behavior of the stayed girder is best understood if the various contributing factors are considered separately. Total behavior will then be determined by super-position of all factors influencing the action of the structure.

Consider the single-plane, two-span stayed girder in Fig. 12.19(a). The girder is simply supported at  $A$ ,  $B$ , and  $C$  with rigid supports and elastically supported at points  $D$  and  $E$  by the cables. The cables are pinned at the top of the tower, and the tower is hinged at the base. If the cables were omitted and a load were to be applied in the left span of the continuous girder, the point  $D$  would drop and point  $E$  would lift up, Fig. 12.19(b), and the displacement at  $D$  becomes greater than that at  $E$ .

First consider the structure to be supported by rigid cables attached at points  $D$  and  $E$  on the girder and at  $F$  at the top of the rigid tower, Fig. 12.19(a). Assuming that the cables and the tower are axially rigid, the triangular geometry of  $DBF$  and  $EBF$  remains equal. With a load in the left span and a hinge at the base of the tower, the tower will rotate in a counterclockwise direction through a rotation  $\phi$ , and the displacement at  $D$  equals that at  $E$ , Fig. 12.19(c). Thus, the first action occurs when a hinge is introduced at the base

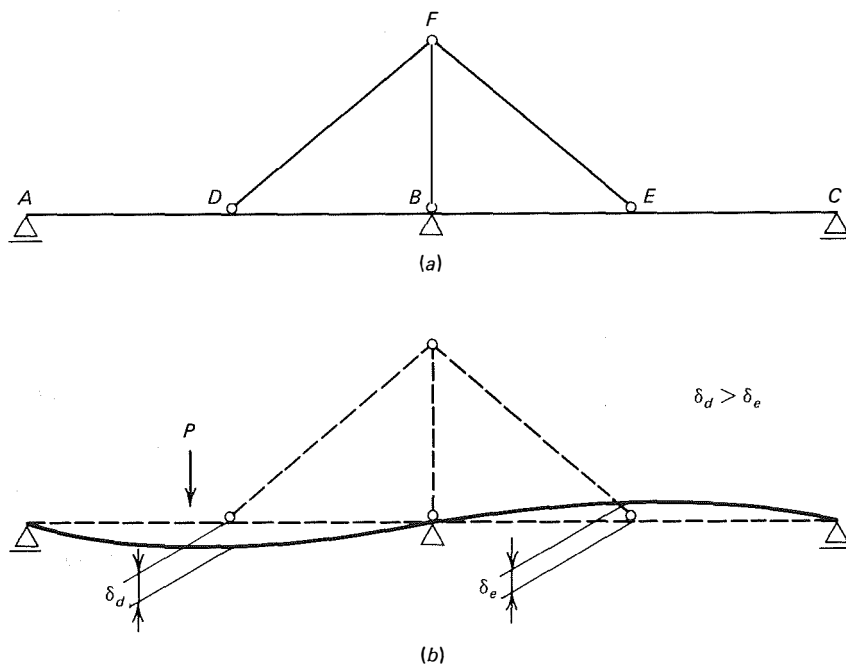


**FIGURE 12.19** (a) and (b) Deflection of girder as a continuous beam, (c) deflection of girder due to applied load, (d) deflection of girder due to elastic elongation of cables, and (e) deflection of girder due to elastic shortening of tower. (Courtesy of the Institution of Civil Engineers, from reference 10.)



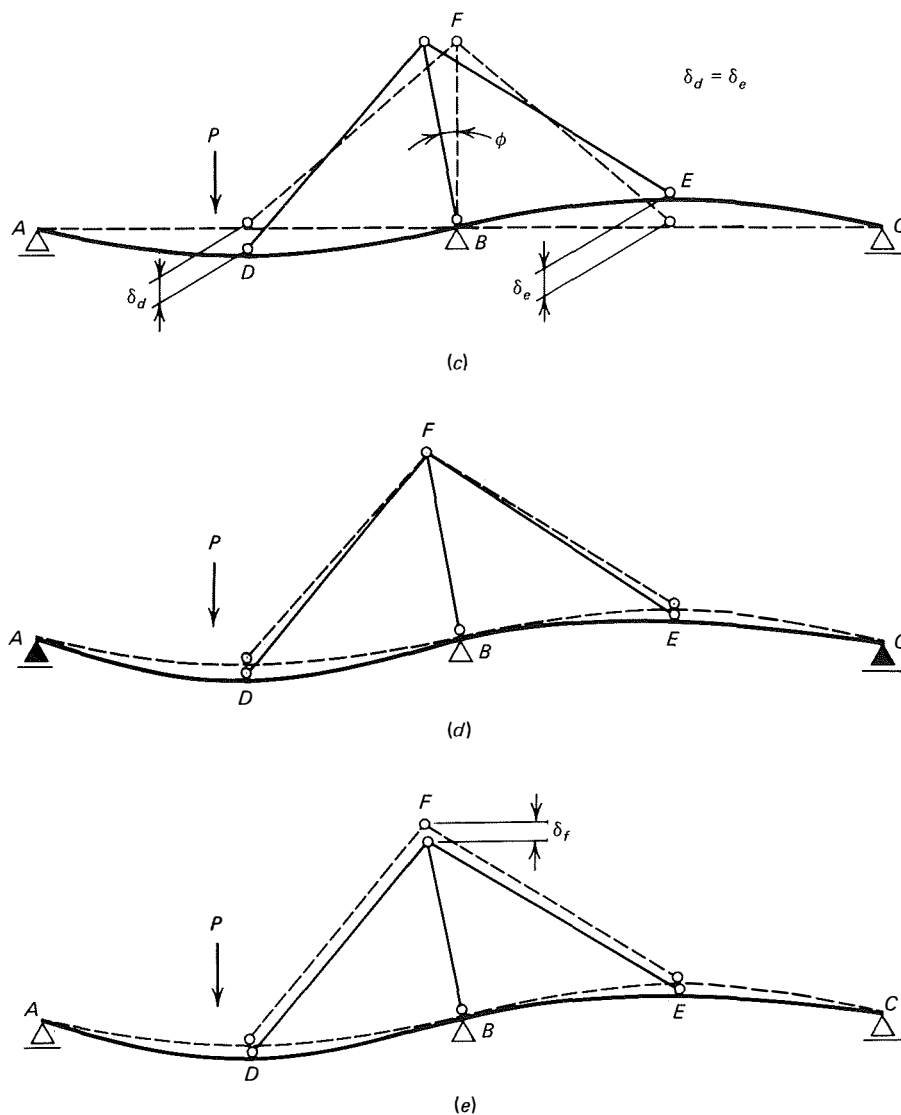


FIGURE 12.19 (Continued)

of the tower and the cables and tower remain axially rigid.

A second action occurs as a result of the elastic stretching of the cables due to the tension created by the first action. Because of the elastic stretch of the cables, the tension in the cables is relieved, increasing the deflection in the girder at  $D$  and decreasing the deflection in the uplift at  $E$ , Fig. 12.19(d).

The third action is the axial shortening of the tower due to the compressive load from the stays. This shortening of the tower causes point  $F$  at the top of the tower to move lower, further relieving the tension in the cables and thus continuing to increase the deflection at  $D$  and decrease the uplift at  $E$ , Fig. 12.19(e).

### 12.3.2 FUNDAMENTAL ANALYSIS

A cable-stayed bridge is a statically indeterminate structure in which the girder acts as a continuous beam supported elastically at the points of cable attachments.

The method of consistent displacements or consistent distortions, also known as the general method,<sup>23</sup> may be used in the solution of the indeterminate cable-stayed bridge. The first mathematical operation consists of removing the redundant stresses and/or reaction components, thus reducing the initial indeterminate structure to a determinate and stable structure. Any combination of redundant stresses and/or reactions may be used. Condition equations are then writ-

ten for the deflection at the point of application of each redundant. On one side of the equation is the summation of all deflection components at the points of application of the redundants (e.g., applied load, redundant load, and temperature), and taken in the direction of the redundant. The other side of the equation is the predetermined sum of all the deflection components. There will be as many equations as there are redundancies.

The general equations for a structure with  $n$  redundants are<sup>24</sup>

$$\begin{aligned} \delta'_a + X_a \delta_{aa} + X_b \delta_{ab} + \dots + X_n \delta_{an} &= \Delta_a \\ \delta'_b + X_a \delta_{ba} + X_b \delta_{bb} + \dots + X_n \delta_{bn} &= \Delta_b \quad (12.20) \\ \delta'_n + X_a \delta_{na} + X_b \delta_{nb} + \dots + X_n \delta_{nn} &= \Delta_n \end{aligned}$$

where  $X_a, X_b, \dots, X_n$  = the equivalent redundant forces

$\delta'_a, \delta'_b, \dots, \delta'_n$  = the displacements due to the applied loads at the points  $A, B, \dots, N$ , in the direction of  $X_a, X_b, \dots, X_n$

$\delta_{aa}, \delta_{bb}, \dots, \delta_{nn}$  = displacements at  $A, B, \dots, N$ , due to  $X_a, X_b, \dots, X_n$  equal to unity, no other loads acting

$\delta_{ab}$  = displacement at  $A$  (in the direction of the action of the force  $X_a$ ) due to  $X_b$  equal to unity acting alone

$\delta_{ba}$  = displacement at  $B$  in the direction of  $X_b$  due to  $X_a$  equal to unity acting alone

$\delta_{ba} = \delta_{ab}$ , from Maxwell principle of reciprocal deflections

$\Delta_a, \Delta_b, \dots, \Delta_n$  = total deflection at  $A, B, \dots, N$

Consider the cable-stayed bridge shown in Fig. 12.20(a), which is simply supported at  $A, B$ , and  $C$  and elastically supported by the cables at  $D$  and  $E$ .<sup>12</sup> The cables are pinned at point  $F$ , the top of the mast, and the mast is pinned at the base. The structure is statically indeterminate to the third degree. The three redundancies may be conveniently taken as the vertical components of tension in the cables and the reaction at the support  $B$ .

If the indeterminate structure is "cut back" to a determinate one, that is, the redundancies removed, it reverts to a simple beam spanning from  $A$  to  $C$  with deflections  $\delta'_d, \delta'_b$ , and  $\delta'_e$  due to the applied loading, Fig. 12.20(b).

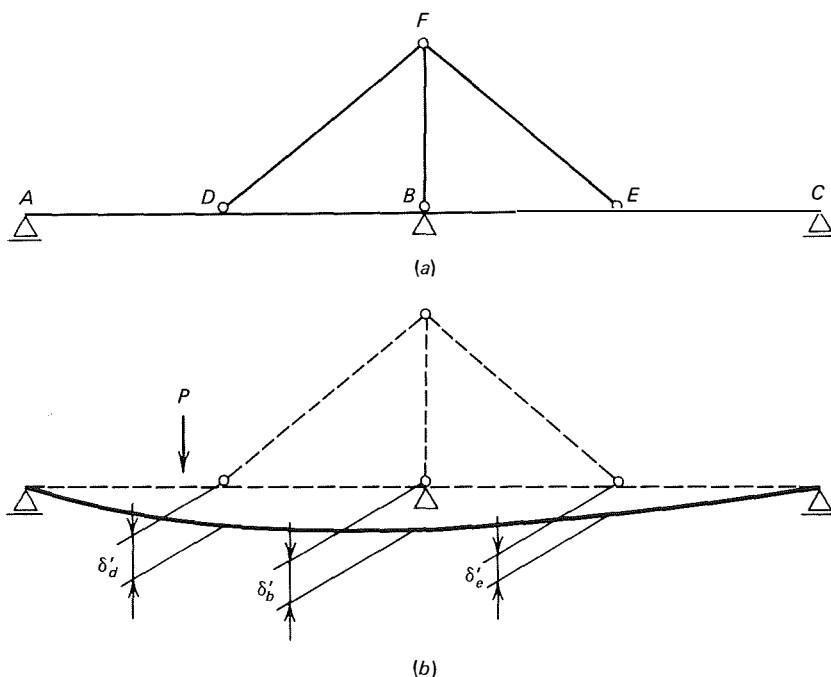


FIGURE 12.20 Deflection of determinate structure with redundants removed. (Courtesy of the Institution of Civil Engineers, from reference 10.)

The deflections of the girder at points  $D$ ,  $B$ , and  $C$  will be considered separately from the deflections of the cables at points  $D$  and  $E$ . Compatibility will require that the girder deflection at  $B$  be zero and the girder deflections at  $D$  and  $E$  be equal to the cable deflection at these points.

Consider the compatibility of the girder deflection at  $D$  in the vertical direction:

$$\delta'_d - f_{dd}X_d - f_{db}X_b - f_{de}X_e = \Delta_d \quad (12.21a)$$

where  $X_d$  and  $X_e$  = vertical components of cable forces at  $D$  and  $E$

$X_b$  = support reaction at  $B$

$f_{dd}$  = flexibility coefficient for the deflection at  $D$  due to a unit load at  $D$  for the simple beam  $AC$

$f_{db}$  = flexibility coefficient for the deflection at  $D$  due to a unit load at  $B$

$f_{de}$  = flexibility coefficient for the deflection at  $D$  due to a unit load at  $E$

$\delta'_d$  = deflection at  $D$  due to the applied loads

$\Delta_d$  = predetermined total deflection at  $D$

In similar manner, girder compatibility equations may be written for the girder deflection at  $B$  and  $E$ .

$$\delta'_b - f_{bd}X_d - f_{bb}X_b - f_{be}X_e = \Delta_b \quad (12.21b)$$

$$\delta'_e - f_{ed}X_d - f_{eb}X_b - f_{ee}X_e = \Delta_e \quad (12.21c)$$

For a conventional bridge on piers only, the deflections  $\Delta_d$ ,  $\Delta_b$ , and  $\Delta_e$  for the girder would be equal to zero because of the fixed supports. However, in a cable-stayed girder the points  $D$  and  $E$  are elastically supported and they do not remain at the same elevation as the rigid supports  $A$ ,  $B$ , and  $C$ . They deflect as a result of the three previously described actions and must, therefore, be modified as follows:

1. The rotation of the tower causes the position of the cable anchorages at  $D$  and  $E$  to change by the amount  $\phi BD$  and  $-\phi BE$ , Fig. 12.19(c). The magnitude of  $\phi$  is assumed such that  $\phi = \tan \theta$ . These additional deflection terms must be added to equations 12.21(a) and 12.21(c) to maintain compatibility.

2. The elastic stretch of the cables will cause further displacement at points  $D$  and  $E$ . For a unit vertical component in the cable tension this displacement becomes,

$$c_d = \frac{l_d}{A_d E_d \sin^2 \theta_d} \quad (12.22a)$$

$$c_e = \frac{l_e}{A_e E_e \sin^2 \theta_e} \quad (12.22b)$$

the deflection for the total force in the cables is thus,

$$c_d X_d$$

$$c_e X_e$$

and equations 12.21(a) and 12.21(c) must be modified accordingly.  $A$ ,  $E$ ,  $l$ , and  $\theta$  are the cross-sectional area, Young's modulus, length, and slope to the horizontal, respectively, of the cables.

3. Because of axial shortening of the tower the deflections at  $D$  and  $E$  must be modified by

$$(X_d + X_e) f_T \quad (12.23)$$

where  $f_T$  represents the unit shortening of the tower. This modification must also be included in equations 12.21(a) and 12.21(c). Therefore, to account for the actions of tower rotation, cable stretch, and axial shortening of the tower, the right side of the equations of compatibility 12.21(a), 12.21(b), and 12.21(c) may be written as:

$$\Delta_d = \phi BD + c_d X_d + (X_d + X_e) f_T \quad (12.24a)$$

$$\Delta_b = 0 \quad (12.24b)$$

$$\Delta_e = -\phi BE + c_e X_e + (X_d + X_e) f_T \quad (12.24c)$$

Because we have interjected an additional variable  $\phi$ , the rotation of the tower, an additional equation becomes necessary for solution. This condition equation can be readily determined by taking moments for the tower about its hinge.<sup>12</sup>

$$X_d BD - X_e BE = 0 \quad (12.24d)$$

Therefore, by collecting terms and rearranging, the compatibility equations may be rewritten in the following form:

$$(f_{dd} + c_d + f_T) X_d + f_{db} X_b + (f_{de} + f_T) X_e + \phi BD = \delta'_d \quad (12.25a)$$

$$f_{bd} X_d + f_{bb} X_b + f_{be} X_e = \delta'_b \quad (12.25b)$$

$$(f_{ed} + f_T) X_d + f_{eb} X_b + (f_{ee} + c_e + f_T) X_e - \phi BE = \delta'_e \quad (12.25c)$$

$$BD X_d - BE X_e = 0 \quad (12.25d)$$

Because of the high order of redundancy in most cable-stayed bridges and, therefore, the number of simultaneous equations, the problem is conducive to a computer solution. When the structure is to be sub-

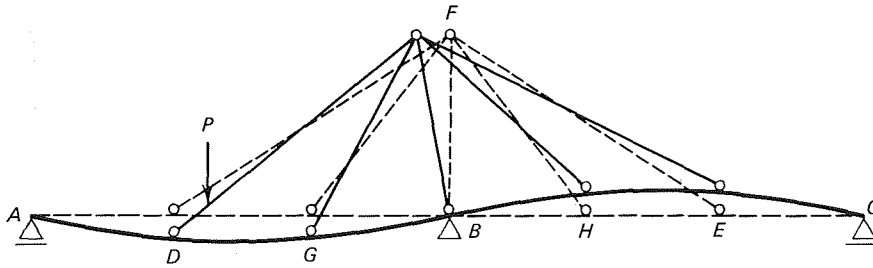


FIGURE 12.21 Deflection of girder for multicable system. (Courtesy of the Institution of Civil Engineers, from reference 10.)

jected to repeated adjustments a computer program is essential to avoid tedious computations.

The simultaneous equations presented in equations 12.25 are conveniently arranged such that they may be expressed in matrix form as shown in equation 12.26.

$$\begin{bmatrix} (f_{dd} + c_d + f_T) & (f_{db}) & (f_{de} + f_T) & BD \\ (f_{bd}) & (f_{bb}) & (f_{be}) & 0 \\ (f_{ed} + f_T) & (f_{eb}) & (f_{ee} + c_e + f_T) & -BE \\ BD & 0 & -BE & 0 \end{bmatrix} \begin{bmatrix} X_d \\ X_b \\ X_e \\ \phi \end{bmatrix} = \begin{bmatrix} \delta'_d \\ \delta'_b \\ \delta'_e \\ 0 \end{bmatrix} \quad (12.26)$$

consideration of the stability of the tower. Because the unknowns in the  $X$  matrix include a displacement along with forces, the method is considered to be of a mixed category.<sup>12</sup>

12.13.3 MULTICABLE STRUCTURE—RADIATING SYSTEM

A radiating cable system, Fig. 12.21, has actions similar to those described above. The structure is statically indeterminate to the fifth degree. The vertical components of cable forces and the interior support reaction may be taken as the redundants. The rotation of the tower affects the displacement at each cable attachment on the girder in proportion to its distance from the base of the tower. Axial shortening of the tower affects each point equally. In the manner described above, a similar set of simultaneous equations may be derived and expressed in matrix form (see equation 12.27).

$$\begin{bmatrix} (f_{dd} + c_d + f_T) & (f_{dg} + f_T) & (f_{db}) & (f_{dh} + f_T) & (f_{de} + f_T) & BD \\ (f_{gd} + f_T) & (f_{gg} + c_g + f_T) & (f_{gb}) & (f_{gh} + f_T) & (f_{ge} + f_T) & BG \\ (f_{bd}) & (f_{bg}) & (f_{bb}) & (f_{bh}) & (f_{be}) & 0 \\ (f_{hd} + f_T) & (f_{hg} + f_T) & (f_{hb}) & (f_{hh} + c_h + f_T) & (f_{he} + f_T) & -BH \\ (f_{ed} + f_T) & (f_{eg} + f_T) & (f_{eb}) & (f_{eh} + f_T) & (f_{ee} + c_e + f_T) & -BE \\ BD & BG & 0 & -BH & -BE & 0 \end{bmatrix} \begin{bmatrix} X_d \\ X_g \\ X_b \\ X_h \\ X_e \\ \phi \end{bmatrix} = \begin{bmatrix} \delta'_d \\ \delta'_g \\ \delta'_b \\ \delta'_h \\ \delta'_e \\ 0 \end{bmatrix} \quad (12.27)$$

The solution of this matrix results in the determination of the vertical components of cable tension  $X_d$  and  $X_e$ , the vertical reaction at the support  $X_b$ , and rotation of the mast  $\phi$ . Other loading conditions may be easily determined by changing the  $\delta'$  matrix. The upper left-hand part of the coefficient matrix is the flexibility matrix for the structure if it were fixed against rotation of the tower. The right-hand column arises from the deflection of the girder caused by the rotation of the tower. The bottom row results from the

12.13.4 MULTICABLE STRUCTURE—HARP SYSTEM

In a harp structure, Fig. 12.22, at least one pair of cables will be pinned or clamped to the tower and possibly all pairs. The first case will normally have the outer pair of cables pinned to the top of the tower so that horizontal movement, with respect to each other, is not permitted. The interior pairs of cables will be supported on saddles in the tower and are free to move

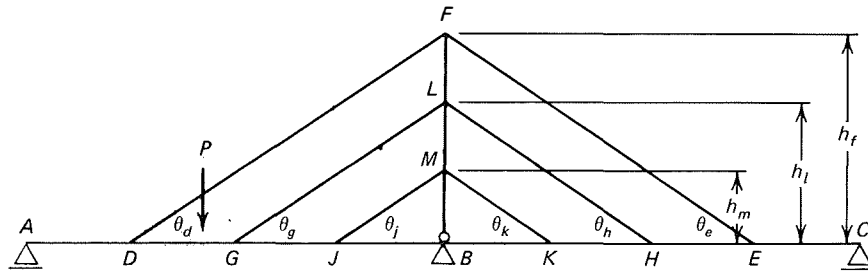


FIGURE 12.22 Multicable structure, harp system. (Courtesy of the Institution of Civil Engineers, from reference 10.)

horizontally. As a result, the tower is subjected to axial forces only.

Where the rotation of the tower  $\phi$  is small, so that the level of the tower supports for the unclamped cables can be assumed not to change, the cables will not contribute to the deflection caused by the rotation of the tower or to the tower's rotational stability. Therefore, terms are not required in the bottom row and right-hand column of the flexibility matrix for the tower stability and vertical deflection, respectively, for the unclamped cables. Nonzero terms in the bottom row and right-hand column will only be required for those points relating to clamped cables only.

In the event that a pair of unclamped cables has unequal slopes on either side of the tower, the saddle that is free to move horizontally will shift when there is a change in load. This action will cause a drop in the cable girder connection toward the side of the shift and an uplift on the other side. If in Fig. 12.22 the cable  $GLH$  is considered to be supported by a saddle on rollers at  $L$  and  $\theta_g$  and  $\theta_h$  are unequal, then the drop at  $G$  and the rise at  $H$  can be determined as,\*

$$\Delta'_g = \left( X_g \frac{\cot^2 \theta_g}{A_g E} \right) \left( \frac{l_h}{\cos^2 \theta_h} - \frac{l_g}{\cos^2 \theta_g} \right) \quad (12.28a)$$

$$\Delta'_h = \left( X_h \frac{\cot^2 \theta_h}{A_h E} \right) \left( \frac{l_g}{\cos^2 \theta_g} - \frac{l_h}{\cos^2 \theta_h} \right) \quad (12.28b)$$

If  $\theta_g$  equals  $\theta_h$  and  $l_g$  equals  $l_h$  the vertical drop at  $G$  and the rise at  $H$  can be determined as

$$\Delta'_g = \frac{X_g l_g}{A_g E \sin^2 \theta_g} \quad (12.28c)$$

$$\Delta'_h = \frac{X_h l_h}{A_h E \sin^2 \theta_h} \quad (12.28d)$$

\*The original equations presented in reference 12 were incorrect, they have been corrected here by private correspondence with B. Stafford Smith.

Therefore, the right side of the appropriate compatibility equation for  $G$  and  $H$  would have to be modified (refer to equations 12.21 and 12.24) by the addition of equations 12.28. The appropriate flexibility matrix coefficients would also be modified.

When all the cable pairs are clamped to the tower, Fig. 12.22, there is the added action of tower bending as a simple beam, between  $F$  and  $B$ , as well as tower rotation. The resulting lateral deflections at  $L$  and  $M$  will influence the tension in the cables as well as the moments in the girder.

The isolated action of bending in the tower is illustrated in Fig. 12.23. The lateral deflection of  $M$  caused by the bending in the tower is determined by:

$$\Delta'_m = (X_j \cot \theta_j - X_k \cot \theta_k) f_{mm} + (X_g \cot \theta_g - X_h \cot \theta_h) f_{ml} \quad (12.29)$$

where

$$f_{mm} = \frac{h_m^2 (h_f - h_m)^2}{3EI_T h_f}$$

and

$$f_{ml} = \frac{h_m (h_f - h_l) [h_f^2 - (h_f - h_l)^2 - h_m^2]}{6EI_T h_f}$$

Thus the deflection at  $J$  due to bending of the tower may be determined as

$$\begin{aligned} \Delta'_j = & X_j \frac{(h_f - h_m)^2}{3EI_T h_f} BJ - X_k \frac{(h_f - h_m)^2}{3EI_T h_f} BK \\ & + X_g \frac{(h_f - h_l) [h_f^2 - (h_f - h_l)^2 - h_m^2]}{6EI_T h_f h_l} BJ \\ & - X_h \frac{(h_f - h_l) [h_f^2 - (h_f - h_l)^2 - h_m^2]}{6EI_T h_f h_l} BH \end{aligned} \quad (12.30)$$

Therefore, to account for the bending in the tower, equation 12.30 would have to be added to the com-

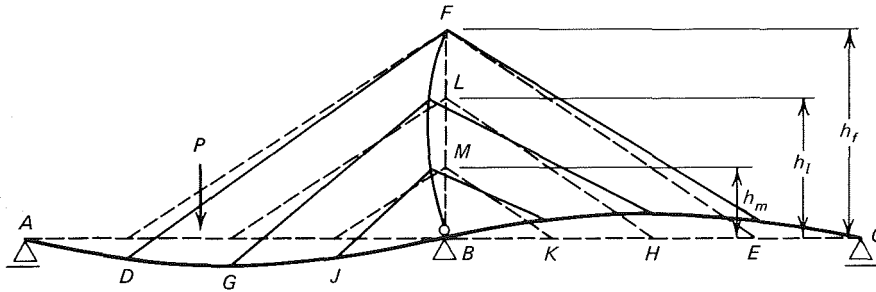


FIGURE 12.23 Bending of tower, multicable system. (Courtesy of the Institution of Civil Engineers, from reference 10.)

patibility equation for  $J$  and similar modifications would have to be made for the compatibility equations of  $G$ ,  $K$ , and  $H$ . It is also to be noted that the value of the unit shortening of the tower,  $f_T$ , will vary for each pair of cables because of the different heights of connection to the tower.

12.13.5 AXIAL FORCE IN THE GIRDER

In long spans where the angle of the cable inclination to the horizontal girder is shallow, the cable tension will be relatively large when compared with the cable tension for a short span where the slope of the cable is greater. Consequently, when the cable has a shallow slope, the horizontal component of force along the axis of the girder will also be high. If in addition the cross section of the girder is relatively light, the axial shortening of the girder should be taken into account in the design calculations.

If the girder is free to move at  $A$ , Fig. 12.19(a), the axial force in  $DB$  is  $X_d \cot \theta_d$  and the girder shortening is  $X_d \cot \theta_d l_{db} / A_G E_G$ . This girder shortening produces an increase in the slope of the cable  $FD$ , which results in a deflection at the cable anchorage  $D$  amounting to:

$$\Delta'_d = X_d \frac{\cot^2 \theta_d l_{db}}{A_G E_G} \quad (12.31)$$

This additional deflection must be taken into account in equation 12.24(a) and therefore the coefficient of  $X_d$  in equation 12.25(a) and also the flexibility matrix equation 12.26 must be modified by adding

$$f_{bd}^G = \frac{I_{db} \cot^2 \theta_d}{A_G E_G} \quad (12.32)$$

When the support at  $A$  is fixed in position and resists the axial force in the girder, the horizontal component of tensile force in the cable must be distributed as a tensile force component in  $AD$  and a compressive force component in  $DB$ . The magnitude of the axial

girder force is proportional to the inverse ratio of the lengths over which they act. Therefore, the axial shortening of  $DB$  would be:

$$\frac{l_{ad} X_d \cot \theta_d l_{db}}{l_{ab} A_G E_G}$$

and the deflection at  $D$  then becomes

$$\Delta'_d = \frac{l_{ad} X_d \cot^2 \theta_d l_{db}}{l_{ab} A_G E_G} \quad (12.33)$$

and the flexibility equation is modified by

$$f_{bd}^G = \frac{l_{ad} l_{db} \cot^2 \theta_d}{l_{ab} A_G E_G} \quad (12.34)$$

In the case of a multicable system as in Fig. 12.21 the deflection of  $D$  and  $G$  due to axial shortening of the girder is

$$\Delta'_d = (X_g \cot \theta_g + X_d \cot \theta_d) \frac{\cot \theta_g l_{gb}}{A_G E_G} \quad (12.35)$$

$$\Delta'_g = (X_g \cot \theta_g l_{gb} + X_d \cot \theta_d l_{db}) \frac{\cot \theta_d}{A_G E_G} \quad (12.36)$$

and the flexibility coefficient would require modification in the compatibility equations of  $G$  and  $D$ .

12.13.6 FIXED BASE TOWER

In a bridge with a tower fixed at the base, the rotation of the tower is prevented. Therefore, the right-hand column and the bottom row of the flexibility matrix, which accounts for the girder deflection and column stability normally caused by tower rotation, may be omitted.

The horizontal movement of point  $L$ , caused by forces in the cables on either side of point  $L$ , Fig. 12.24,

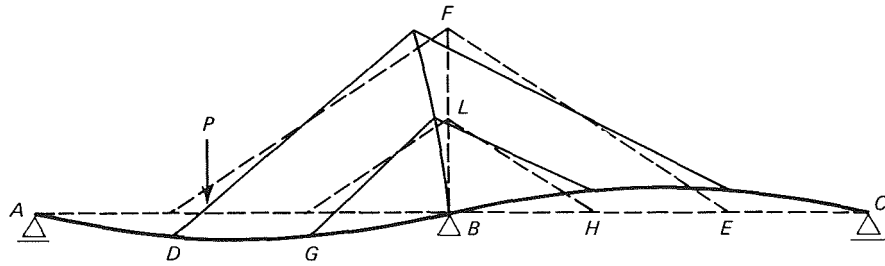


FIGURE 12.24 Deflection of tower due to applied load,  $P$ . (Courtesy of the Institution of Civil Engineers, from reference 10.)

may be determined as:

$$\Delta'_i = (X_g \cot \theta_g - X_h \cot \theta_h) f_{ll} + (X_d \cot \theta_d - X_c \cot \theta_c) f_{ly} \quad (12.37)$$

and for a cantilever of uniform cross section

$$f_{ll} = \frac{h^3}{3EI_T} \quad (12.38)$$

and

$$f_{ly} = \frac{2h_f^3 - 3h_f^2(h_f - h_i) + (h_f - h_i)^3}{6EI_T} \quad (12.39)$$

Therefore, the vertical deflection at  $G$  due to the bending of the tower is:

$$\begin{aligned} \Delta'_g &= X_g \frac{h_f BG}{3EI_T} BG - X_h \frac{h_i BH}{3EI_T} BH \\ &+ X_d \frac{[2h_f^3 - 3h_f^2(h_f - h_i) + (h_f - h_i)^3] GB}{6EI_T h_f h_i} BD \\ &- X_c \frac{[2h_f^3 - 3h_f^2(h_f - h_i) + (h_f - h_i)^3] GB}{6EI_T h_f h_i} BE \end{aligned} \quad (12.40)$$

and the flexibility coefficients in the row representing compatibility at  $G$  must be modified accordingly. Similarly the rows representing compatibility of points  $D$ ,  $H$ , and  $E$  must also be modified.

12.13.7 MULTITOWER CONTINUOUS GIRDER CABLE-STAYED BRIDGE

Where large crossings are required, the normal procedure is to require two towers at either end of a large central span, Fig. 12.25. The analysis of a continuous girder system involving several towers and cables may be performed by initially releasing all girder connections between the end supports  $A$  and  $D$ . As a result, a single coefficient matrix may be constructed and modified as previously outlined. The size of the coefficient matrix will be equal to the total sum of the number of cables, the interior rigid supports, and the number of hinged towers.

12.13.8 CABLES ATTACHED TO RIGID SUPPORTS

When a cable is attached to a fixed support as at  $A$  and  $D$ , Fig. 12.25, the terms  $f_{aa}$  and  $f_{dd}$  of the coefficients of  $X_a$  and  $X_d$  in the coefficient matrix are zero. The coefficients of these two forces will consist only of appropriate modifications. The forces  $X_a$  and  $X_d$  are the vertical components of the force in the cables at  $A$  and  $D$ ; they are not the abutment reactions at  $A$  and  $D$ . The abutment reactions may be evaluated after the cable forces and interior support reactions are determined by considering the equilibrium of the girder as a whole.<sup>12</sup>

Consider the structure, illustrated in Fig. 12.26, wherein the back-stay cable is attached to the girder

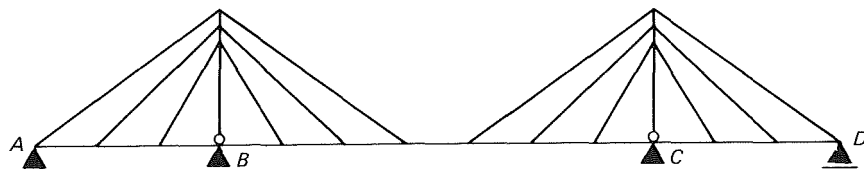


FIGURE 12.25 Long span multitower continuous girder bridge. (Courtesy of the Institution of Civil Engineers, from reference 10.)

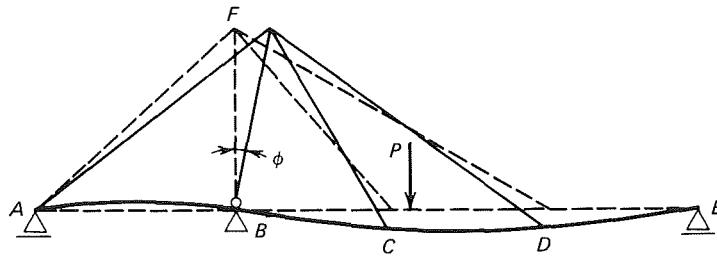


FIGURE 12.26 Single tower, cable attached to rigid support. (Courtesy of the Institution of Civil Engineers, from reference 10.)

at  $A$  and the fore-stay cables are attached to the girder at  $C$  and  $D$ . The continuous girder is supported at  $A$ ,  $B$ , and  $E$ . The tower is pinned at its base at  $B$ , and all cables are pin connected to the tower at  $F$ .

As previously indicated, the number of equations required for a solution is equal to the sum of the number of cables, the interior supports, and the number of hinged towers. Therefore, for this structure, five equations are required.

Four deflection compatibility equations may be written as:

$$\begin{aligned} \delta'_a - f_{aa}X_a - f_{ab}X_b - f_{ac}X_c - f_{ad}X_d &= \Delta_a \\ \delta'_b - f_{ba}X_a - f_{bb}X_b - f_{bc}X_c - f_{bd}X_d &= \Delta_b \\ \delta'_c - f_{ca}X_a - f_{cb}X_b - f_{cc}X_c - f_{cd}X_d &= \Delta_c \\ \delta'_d - f_{da}X_a - f_{db}X_b - f_{dc}X_c - f_{dd}X_d &= \Delta_d \end{aligned} \quad (12.41)$$

It may be seen that terms  $\delta'_a$ ,  $f_{aa}$ , and  $f_{na}$  are equal to zero, and the term  $X_a$  used here denotes the vertical component of tension in the cable at  $A$ . The term  $\Delta_a$  will reflect appropriate modifications as they affect  $X_a$ .

Because of a tower rotation of  $\phi$  there will be a reduction of tension in cables  $C$  and  $D$ , with corresponding deflections at  $C$  and  $D$ . There will also be an increase in the tension of cable  $AF$ . These changes may be represented as

$$\begin{aligned} \Delta'_a &= -\phi BA \\ \Delta'_c &= \phi BC \\ \Delta'_d &= \phi BD \end{aligned} \quad (12.42)$$

Similarly the cable elongation may be represented by

$$\begin{aligned} \Delta'_a &= c_a X_a \\ \Delta'_c &= c_c X_c \\ \Delta'_d &= c_d X_d \end{aligned} \quad (12.43)$$

Elastic shortening of the tower is given by

$$(X_a + X_c + X_d) f_T \quad (12.44)$$

Because the unknown term  $\phi$  representing tower rotation has been introduced, a stability equation for the tower must be formulated by summing moments about the base,

$$-X_a BA + X_c BC + X_d BD = 0 \quad (12.45)$$

By rewriting the deflection compatibility equations and taking into account the tower stability equation, the simultaneous equations may be represented in matrix form as follows:

$$\begin{bmatrix} (c_a + f_T) & 0 & f_T & & & -BA \\ 0 & f_{bb} & f_{bc} & & & 0 \\ f_T & f_{cb} & (f_{cc} + c_c + f_T) & & & BC \\ f_T & f_{db} & (f_{dc} + f_T) & & & BD \\ -BA & 0 & BC & & & 0 \end{bmatrix}$$

$$\begin{bmatrix} X_a \\ X_b \\ X_c \\ X_d \\ \phi \end{bmatrix} = \begin{bmatrix} 0 \\ \delta'_b \\ \delta'_c \\ \delta'_d \\ 0 \end{bmatrix} \quad (12.46)$$

The redundants are the vertical components of cable force and the tower rotation.

## 12.14 Mixed Method of Analysis—Double Plane

### 12.14.1 STRUCTURAL BEHAVIOR

The primary difference in single-plane and double-plane cable-stayed bridge structures is that in the former only vertical actions of the continuous girder are



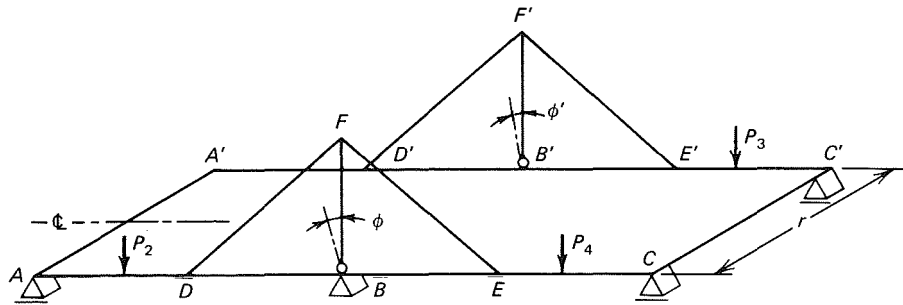


FIGURE 12.27 Double-plane system, eccentric load,  $P_2$  (Courtesy of the Institution of Civil Engineers, from reference 11.)

restrained by the cables, and torsional forces are transmitted through the deck section into the piers. In the latter, the cables assist in restraining both vertical and torsional forces. Double-plane structures require a three-dimensional analysis whereby the deflections of the two cable planes are considered in conjunction with the bending and rotation of the girder.

In the basic structure, illustrated in Fig. 12.27, the continuous girder is supported by pairs of rigid supports at  $AA'$ ,  $BB'$ , and  $CC'$  and by pairs of elastic cable supports at  $DD'$  and  $EE'$ . The cables are pinned or clamped at the top of the masts at  $F$  and  $F'$ . The cables are attached such that the ends are restrained from a relative displacement to the mast, which are hinged at their bases at  $B$  and  $B'$ . The girder is assumed to be completely restrained against torsion at each of the rigid supports.

If a load is placed at any point other than on the longitudinal center line of the bridge as  $P_2$ , Fig. 12.27, the two systems of the towers and cables undergo different displacements, causing different values of tension in the adjacent parallel cables of each system. Therefore, each adjacent pair of parallel cables must assist in restraining the torsion and vertical displacement of the girders.

The amount of restraint provided by the tower cable system is a function of several factors, such as, the tower and cable stiffness, type of connection at the base of the tower, and whether structural connection exists between the towers to resist relative rotation of the towers.

As an illustration of the last factor, consider the structure in Fig. 12.27 in which the towers have no structural connection between them, i.e., no portal frame. If a single eccentric load,  $P_2$  is applied to one of the girders, both towers will rotate in a counterclockwise direction. However, because of the eccentricity of the load,  $P_2$ , there will be a differential ro-

tation  $\phi$  and  $\phi'$  of towers  $BF$  and  $B'F'$ , respectively. As a consequence of the differential rotation, the deflection of  $D$  will be larger than that of  $D'$ , causing a torque in the girder at section  $DD'$ . If the towers were connected to each other to restrain a relative rotation between them, there would be less torque action and the system would be torsionally stiffer.

In the extreme case, when the structure is loaded with equal and antisymmetrically placed loads,  $P_2$  and  $P_3$ , tower  $BF$  rotates in a counterclockwise direction and tower  $B'F'$  rotates in a clockwise direction. Therefore, the torque loads due to applied loads  $P_2$  and  $P_3$ , are cumulative for each position of load. If the structure is loaded with  $P_2$  and  $P_4$  symmetrically placed with respect to the transverse center line of the bridge, the towers will be parallel and remain in their original position, thus providing maximum torsional restraint to the girder.

#### 12.14.2 BASIC ANALYSIS

The analysis of a double-plane, cable-stayed structure is similar to that developed for single-plane, cable-stayed structures. Like single-plane structures, all interior rigid and elastic supports of the girder are released and a set of deflection compatibility equations is formulated for each support and for the stability of the tower. The double-plane structure, in addition, requires that the torque at each interior support be released and additional equations of compatibility be formulated for the torsion at each interior support.

If all redundant releases are applied to the structure, Fig. 12.28, and the external loads are applied to the simple span,  $AA'CC'$ , the center line deflections and twists,  $\delta'_d$ ,  $\delta'_b$ ,  $\delta'_e$ ,  $\psi'_d$ ,  $\psi'_b$ , and  $\psi'_e$ , may be determined by conventional methods. Assuming the restraints provided by the cables at points  $D$ ,  $D'$ ,  $E$ , and  $E'$  are completely rigid against deflection and torque,

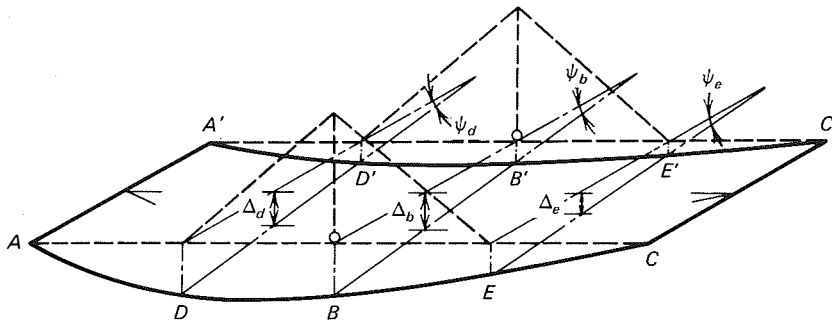


FIGURE 12.28 Deflections and rotations of primary structure. (Courtesy of the Institution of Civil Engineers, from reference 11.)

the compatibility equations are

$$\delta'_d - (X_d + X'_d) f_{dd} - (X_b + X'_b) f_{db} - (X_e + X'_e) f_{de} = \Delta_d$$

$$\delta'_b - (X_d + X'_d) f_{bd} - (X_b + X'_b) f_{bb} - (X_e + X'_e) f_{be} = \Delta_b$$

$$\delta'_e - (X_d + X'_d) f_{ed} - (X_b + X'_b) f_{eb} - (X_e + X'_e) f_{ee} = \Delta_e$$

$$\psi'_d - \frac{(X_d - X'_d) r \psi_{dd}}{2} - \frac{(X_b - X'_b) r \psi_{db}}{2} - \frac{(X_e - X'_e) r \psi_{de}}{2} = \psi_d \quad (12.47)$$

$$\psi'_b - \frac{(X_d - X'_d) r \psi_{bd}}{2} - \frac{(X_b - X'_b) r \psi_{bb}}{2} - \frac{(X_e - X'_e) r \psi_{be}}{2} = \psi_b$$

$$\psi'_e - \frac{(X_d - X'_d) r \psi_{ed}}{2} - \frac{(X_b - X'_b) r \psi_{eb}}{2} - \frac{(X_e - X'_e) r \psi_{ee}}{2} = \psi_e$$

where  $X_d$  = the vertical component of cable tension at  $D$

$f_{dd}$  = the center line deflection at  $D$  due to a unit load at  $D$

$f_{db}$  = the center line deflection at  $D$  due to a unit load at  $B$

$\delta'_d$  = the center line deflection at  $D$  due to the applied loads

$r$  = distance between sets of cables

$\psi_{dd}$  = twist of the girder at  $D$  due to a unit torque applied at  $D$

$\psi_{db}$  = twist of the girder at  $D$  due to a unit torque applied at  $B$

$\psi'_d$  = twist of the girder at  $D$  due to the applied loads

$\Delta_d$  = predetermined total center line deflection at  $D$

$\psi_d$  = predetermined total twist at  $D$

However, the restraints at  $D$  and  $E$  are not rigid because of the rotation of the tower, cable elongation, and elastic shortening of the tower. As before, the compatibility equations 12.47, must be modified to account for these actions.

Assuming that the towers  $BF$  and  $B'F'$  rotate counterclockwise  $\phi$  and  $\phi'$ , respectively, with the application of load, the center line deflection at  $D$  will be  $(\phi + \phi') l_{bd}/2$  and the uplift at  $E$  will be  $-(\phi + \phi') l_{be}/2$ , when the magnitude of  $\phi$  is such that the  $\tan \phi = \phi$ . Corresponding twist at  $D$  and  $E$  will be  $(\phi - \phi') l_{bd}/r$  and  $-(\phi - \phi') l_{be}/r$ , assuming a positive twist sign convention such that an upward movement normal to the deck moves out of the paper toward the reader.

The elongation of the cables will cause the center line of the girder at  $D$  and  $E$  to deflect by  $(X_d + X'_d) c_d/2$  and  $(X_e + X'_e) c_e/2$  respectively, where the vertical flexibility of the cable is formulated as before for the single-plane, cable-stayed girder. The twist then becomes  $(X_d - X'_d) c_d/r$  and  $(X_e - X'_e) c_e/r$  at  $D$  and  $E$  respectively.

Similarly the elastic shortening of the tower will produce a center line deflection of

$$\frac{[(X_d + X_e) + (X'_d + X'_e)] f_T}{2} \quad (12.48)$$

at *D* and *E*, where  $f_T$  is the flexibility coefficient of the tower, and a twist

$$\frac{[(X_d + X_e) - (X'_d + X'_e)] f_T}{r} \quad (12.49)$$

at *D* and *E*.

The right-hand side of equations 12.47 may, therefore, be expressed as

$$\begin{aligned} \Delta_d &= \frac{(\phi + \phi') l_{bd}}{2} + \frac{(X_d + X'_d) c_d}{2} \\ &\quad + \frac{[(X_d + X_e) + (X'_d + X'_e)] f_T}{2} \\ \Delta_b &= 0 \\ \Delta_e &= \frac{-(\phi + \phi') l_{be}}{2} + \frac{(X_e + X'_e) c_e}{2} \\ &\quad + \frac{[(X_d + X_e) + (X'_d + X'_e)] f_T}{2} \\ \psi_d &= \frac{(\phi - \phi') l_{bd}}{r} + \frac{(X_d - X'_d) c_d}{r} \\ &\quad + \frac{[(X_d + X_e) - (X'_d + X'_e)] f_T}{r} \\ \psi_b &= 0 \\ \psi_e &= \frac{-(\phi - \phi') l_{be}}{r} + \frac{(X_e - X'_e) c_e}{r} \\ &\quad + \frac{[(X_d + X_e) - (X'_d + X'_e)] f_T}{r} \end{aligned} \quad (12.50)$$

Similar to the single-plane, cable-stayed structures the additional, unknown rotations of the towers  $\phi$  and  $\phi'$  have been introduced, which require two more equations for a solution. These equations are formulated from the equilibrium of the tower by summing moments about the base. Thus

$$X_d l_{bd} - X_e l_{be} = 0 \quad (12.51)$$

$$X'_d l_{bd} - X'_e l_{be} = 0 \quad (12.52)$$

By rewriting the deflection compatibility equations and using the tower stability equations the matrix form can be written as stated in equation 12.53.

The solution of equation 12.53 produces the vertical reactions at each interior support and cable connection, and the rotation of the towers. With these values, the other reactions, moments, shears, and torques can be determined.

### 12.14.3 EFFECTS OF OTHER ACTIONS

The horizontal components of the cable forces will induce an axial compressive force in the girder. This force will cause an elastic shortening of the girder, the extent of which depends on the magnitude of the axial force and area of the cross section. As a result, a modification of the flexibility matrix may be required.

Depending on the geometrical configuration of a particular structure, other actions that may modify the matrix are the bending of the tower when the base is fixed or when the clamped cables are attached to the tower at different heights. A pair of cables that are carried by saddles on rollers at the tower will also affect the flexibility matrix. All of these factors may be ac-

$$\begin{bmatrix} \left(f_{dd} + \frac{c_d}{2} + \frac{f_T}{2}\right) & \left(f_{de} + \frac{c_d}{2} + \frac{f_T}{2}\right) & (f_{db}) & (f_{db}) & \left(f_{de} + \frac{f_T}{2}\right) & \left(f_{de} + \frac{f_T}{2}\right) & \left(\frac{l_{bd}}{2}\right) & \left(\frac{l_{bd}}{2}\right) \\ (f_{bd}) & (f_{bd}) & (f_{bb}) & (f_{bb}) & (f_{be}) & (f_{be}) & 0 & 0 \\ \left(f_{ed} + \frac{f_T}{2}\right) & \left(f_{ed} + \frac{f_T}{2}\right) & (f_{eb}) & (f_{eb}) & \left(f_{ee} + \frac{c_e}{2} + \frac{f_T}{2}\right) & \left(f_{ee} + \frac{c_e}{2} + \frac{f_T}{2}\right) & -\left(\frac{l_{be}}{2}\right) & -\left(\frac{l_{be}}{2}\right) \\ \left(\frac{r\psi_{dd}}{2} + \frac{c_d}{r} + \frac{f_T}{r}\right) & -\left(\frac{r\psi_{dd}}{2} + \frac{c_d}{r} + \frac{f_T}{r}\right) & \left(\frac{r\psi_{db}}{2}\right) & -\left(\frac{r\psi_{db}}{2}\right) & \left(\frac{r\psi_{de}}{2} + \frac{f_T}{r}\right) & -\left(\frac{r\psi_{de}}{2} + \frac{f_T}{r}\right) & -\left(\frac{l_{bd}}{r}\right) & -\left(\frac{l_{bd}}{r}\right) \\ \left(\frac{r\psi_{bd}}{2}\right) & -\left(\frac{r\psi_{bd}}{2}\right) & \left(\frac{r\psi_{bb}}{2}\right) & -\left(\frac{r\psi_{bb}}{2}\right) & \left(\frac{r\psi_{be}}{2}\right) & -\left(\frac{r\psi_{be}}{2}\right) & 0 & 0 \\ \left(\frac{r\psi_{ed}}{2} + \frac{f_T}{r}\right) & -\left(\frac{r\psi_{ed}}{2} + \frac{f_T}{r}\right) & \left(\frac{r\psi_{eb}}{2}\right) & -\left(\frac{r\psi_{eb}}{2}\right) & \left(\frac{r\psi_{ee}}{2} + \frac{c_e}{r} + \frac{f_T}{r}\right) & -\left(\frac{r\psi_{ee}}{2} + \frac{c_e}{r} + \frac{f_T}{r}\right) & -\left(\frac{l_{be}}{r}\right) & -\left(\frac{l_{be}}{r}\right) \\ (l_{bd}) & 0 & 0 & 0 & -(l_{be}) & 0 & 0 & 0 \\ 0 & (l_{bd}) & 0 & 0 & 0 & -(l_{be}) & 0 & 0 \end{bmatrix} \begin{bmatrix} X_d \\ X'_d \\ X_b \\ X'_b \\ X_e \\ X'_e \\ \phi \\ \phi' \end{bmatrix} = \begin{bmatrix} \delta_d \\ \delta'_d \\ \delta_b \\ \delta'_b \\ \psi_d \\ \psi'_d \\ \psi_b \\ \psi'_b \\ 0 \\ 0 \end{bmatrix} \quad (12.53)$$

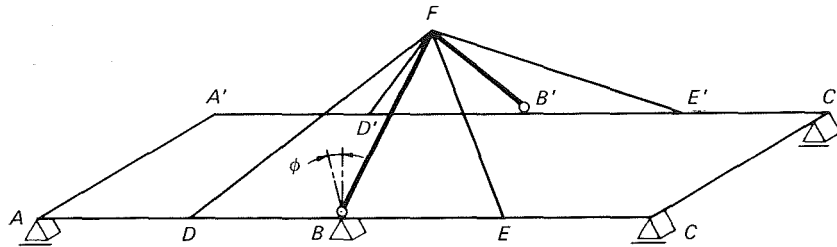


FIGURE 12.29 Bridge with A-frame tower. (Courtesy of the Institution of Civil Engineers, from reference 11.)

commodated by appropriate adjustment of the flexibility matrix as previously outlined for single-plane cable structures, with the exception that the induced torque forces must be taken into account.

12.14.4 DOUBLE-PLANE STRUCTURE WITH AN A-FRAME TOWER

When an A-frame tower is used, Fig. 12.29, and the cables are concentrically connected, the previous separate tower rotations  $\phi$  and  $\phi'$  will become one single value of  $\phi$ . Rotational equilibrium for the combined tower is now dependent on the horizontal components of all cables in the total system, requiring only one equation instead of two and equation 12.53 reduces to equation 12.54. Because of the elimination of the relative rotation of the towers, the structure becomes torsionally stiffer.

$$\begin{bmatrix}
 l_{bd} & l_{bd} & 0 & 0 & -l_{bc} & -l_{bc} & 0 \\
 0 & 0 & -l_{bc} & 0 & 0 & 0 & 0 \\
 X_d & X_d & X_b & X_b & X_e & X_e & \phi \\
 \delta_d & \delta_b & \delta'_e & \psi'_d & \psi'_b & \psi'_e & 0
 \end{bmatrix} = \begin{bmatrix} \delta_d \\ \delta_b \\ \delta'_e \\ \psi'_d \\ \psi'_b \\ \psi'_e \\ 0 \end{bmatrix} \tag{12.54}$$

modified flexibility matrix as in equation 12.53

12.14.5 DOUBLE-PLANE STRUCTURE WITH A PORTAL TOWER

An example of a portal tower arrangement, Fig. 12.30, has the advantage of limiting the relative rotation of the tower and thus increasing the torsional resistance of the system. However, it is not as effective in limiting the relative rotation as the previously discussed A-frame arrangement. If complete rigidity of the portal frame within its plane were practical it would be as

effective as the A-frame. Because complete rigidity is not possible, it becomes necessary to include the effect of out-of-plane warping of the tower in the analysis.

If a load  $P$  is eccentrically applied to one of the girders as indicated in Fig. 12.30, the resulting differential rotation of the towers will produce a twist in the portal beam, as well as the usual counterclockwise rotation of the towers. The resistance provided by the portal beam to the differential rotation of the towers is partly a function of the bending and torsional stiffnesses of the portal columns and beam, and partly due to the degree of fixity against twist provided at the base of the towers.

If the base of the towers are free to twist, the deformation will be as illustrated in Fig. 12.31, in which the columns are subjected only to bending and the beam only to torsion. For this condition it can be shown that the out-of-plane deflection at the top of the tower is

$$\delta_f = (X_d \cot \theta_d - X_e \cot \theta_e) \bar{X} \tag{12.55}$$

where

$$\bar{X} = \left[ \left( \frac{h^2 r}{2GJ_2} \right) + \left( \frac{h^3}{3EI_1} \right) \right]$$

These warping deflections plus or minus  $\delta_f$  at  $F$  and  $F'$  result in downward deflection at  $D$  and an uplift at  $D'$  equal to  $\delta_f l_{bd}/h$  and producing a twist to the girder at  $D$  given by

$$\psi_{df} = \frac{2(X_d \cot \theta_d - X_e \cot \theta_e) l_{bd} \bar{X}}{hr} \tag{12.56}$$

Similarly at  $E$  the twist is

$$\psi_{ef} = \frac{-2(X_d \cot \theta_d - X_e \cot \theta_e) l_{bc} \bar{X}}{hr} \tag{12.57}$$

The behavior of this structure is the same as that for the double-plane, single tower structure except for the portal warping effect. Therefore, the matrix formulation for this structure is the same as that stated in

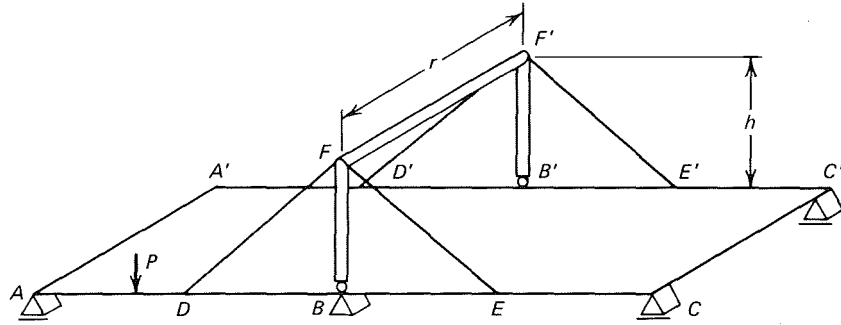


FIGURE 12.30 Bridge with portal tower. (Courtesy of the Institution of Civil Engineers, from reference 11.)

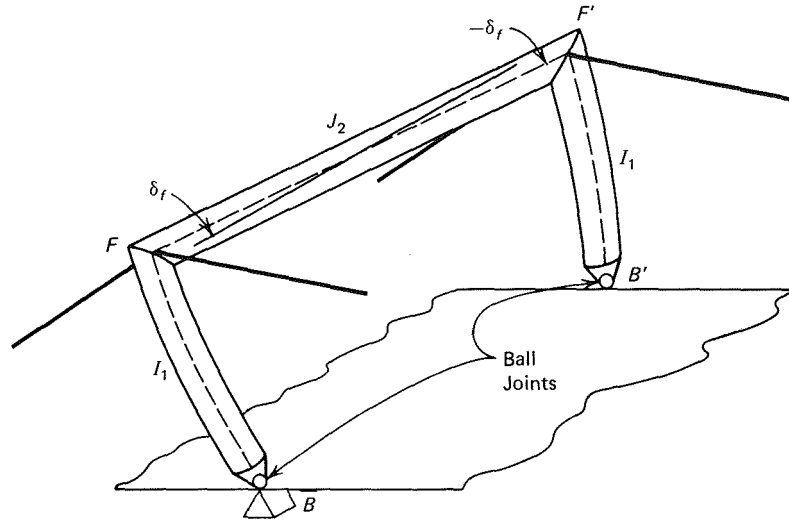


FIGURE 12.31 Portal columns in bending only; portal beam in torsion only. (Courtesy of the Institution of Civil Engineers, from reference 11.)

equation 12.54, provided the coefficients for  $X_d$  and  $X_e$  in the fourth row of the matrix are modified by the addition of  $2l_{bd} \cot \theta_d \bar{X}/hr$  and  $-2l_{bd} \cot \theta_e \bar{X}/hr$ , and modified in the sixth row by  $-2l_{be} \cot \theta_d \bar{X}/hr$  and  $2l_{be} \cot \theta_e \bar{X}/hr$ , respectively. Thus, the torsional compatibility at  $D$  and  $E$  are maintained.

When the base of the towers are restrained against rotation in the horizontal plane, the resulting deformed portal will be as illustrated in Fig. 12.32. In this condition the portal columns and the portal beam are subjected to bending and torsional moments. By an energy analysis, the resulting twist at  $D$  and  $E$ , respectively, may be represented by

$$\psi_{df} = \frac{2(X_d \cot \theta_d - X_e \cot \theta_e) l_{bd}}{hr} \frac{\bar{X}\bar{Y}}{(\bar{X} + \bar{Y})} \quad (12.58)$$

$$\psi_{ef} = \frac{-2(X_d \cot \theta_d - X_e \cot \theta_e) l_{be}}{hr} \frac{\bar{X}\bar{Y}}{(\bar{X} + \bar{Y})} \quad (12.59)$$

where  $\bar{X}$  is as previously defined and

$$\bar{Y} = \left[ \left( \frac{r^2 h}{4GJ_1} \right) + \left( \frac{r^3}{24EI^2} \right) \right]$$

and the coefficient of  $X_d$  and  $X_e$  in the fourth and sixth rows of equation 12.54 must again be modified for the torsional compatibility at  $D$  and  $E$ .

#### 12.14.6 MULTITOWER CONTINUOUS GIRDER—DOUBLE-PLANE CONFIGURATION

In a manner similar to single-plane structures, multi-tower structures may be accommodated by the analysis outlined above. The procedure is to release all interior supports and thereby produce a simple beam for which the “free” deflections and twists may be calculated. Appropriately modified compatibility and stability

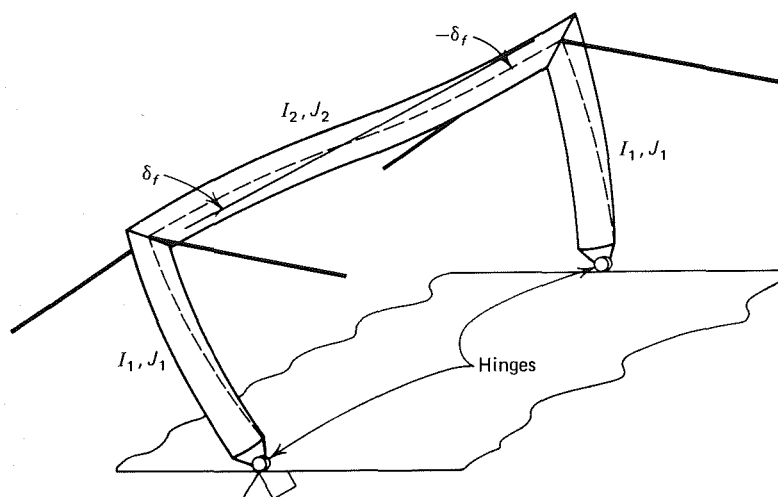


**FIGURE 12.32** Portal columns in bending and torsion; portal beam in bending and torsion. (Courtesy of the Institution of Civil Engineers, from reference 11.)

equations may be formulated to produce a single “mixed” matrix for the entire structure.

### 12.15 Summary of the Mixed Method

The overall behavior of a cable-stayed bridge is determined by superimposing the actions of tower rotation, stay elongation, and tower shortening. Consideration of these actions evolves into a mixed force-displacement analysis in which modifications are made to the coefficients to account for each action. Additional modifications are introduced to accommodate bending of the towers, fixity of the tower at its base, shortening of the girder, twist or torsion of the girder, and so on. The compatibility equations are appropriately modified and the equilibrium equations formulated to produce a single mixed matrix for the total structure.

The mixed method of analysis as presented above is essentially linear. The method assumes that the deflection is proportional to the load at all portions of the structure and for the structure as a whole. The stiffness of the cable can be taken into account by the utilization of an effective modulus for the stays as in Chapter 11. This method does not consider nonlinearity and in that sense is restricted to elastic behavior of the structure. The reader should bear in mind that this methodology was developed when only first-generation computers were available and there were no standard structural framework programs. Today the problem can be solved by standard two-dimensional plane frame or three-dimensional space frame programs that are appropriately modified.

### 12.16 Nonlinearity

Nonlinear considerations in cable-stayed bridges may be classified into three categories: girder, pylon, and cables. Nonlinear behavior in the girder and pylon occurs when they are subjected to compressive loads and bending moments simultaneously. The degree of the nonlinearity depends on the magnitude of the compressive load compared with the Euler load and the magnitude of the deflection produced by the bending action. Normally, it can be assumed that these effects are small. However, for slender girders and pylons this approximation should be verified for extreme loading conditions.

The nonlinear behavior of suspension bridges is well known and is considered in design. It has been assumed by some designers, however, that a cable-stayed bridge is a linear structure since the cables act as direct tension members. This is not the case. Nonlinearity in the cable member occurs when the load increases, and the cable sag decreases, producing an increase in the cable chord length and thus an apparent elongation of the cable. This phenomenon has been discussed in Chapter 11.

### 12.17 Influence Lines

Shortly after the construction of the Strömsund Bridge, Homberg<sup>25</sup> published the analytical results of several cable-stayed systems proposed for the bidding of the North Bridge at Düsseldorf, and the Rhine Bridge at

Speyer. The result of the studies are extracted from the published reports and reproduced below.<sup>25</sup> Some of the cable-stayed systems studied are illustrated schematically in Fig. 12.33. Influence lines for System 1 are presented in Fig. 12.34. The dimensions are those proposed for the Rhine Bridge at Speyer. The corresponding influence lines for a self-anchored suspension bridge under similar conditions is indicated in Fig. 12.35. Comparing Figs. 12.34 and 12.35, the influence lines for the cable-stayed system are seen to be of a different character than those for the suspension bridge. The influence line for bending moment in the girder at the tower indicates large positive and negative areas for the suspension bridge and the cable-stayed system indicates primarily negative moments. It is also seen that the influence lines for moments in the center span of the cable-stayed bridge vary in magnitude and direction as do those of the suspension bridge.

Influence lines for cable forces and bending mo-

ments in the girder for system 3(a) are depicted in Fig. 12.36. The system indicates truss-like characteristics as a result of the fixed saddle cable supports at the towers. If the two interior sets of cables were supported at the tower by movable saddles the bending moments in the stiffening girder would increase considerably.

The cable tension influence lines for the two cable-stay systems 4(a) and 4(b), of Fig. 12.33, as proposed for the North Bridge at Düsseldorf are illustrated in Fig. 12.37. From a stress point of view, system 4(a) has a better balance in the girder, which is attributed to the fixed saddle supports at the tower for all three sets of stays. However, this condition produces considerably higher bending moments in the towers and differentials of horizontal stresses which must be resisted by the saddle bearings.

O'Connor<sup>26</sup> produced similar influence lines and made comparisons, which are duplicated in the following discussion. Influence lines were constructed for the

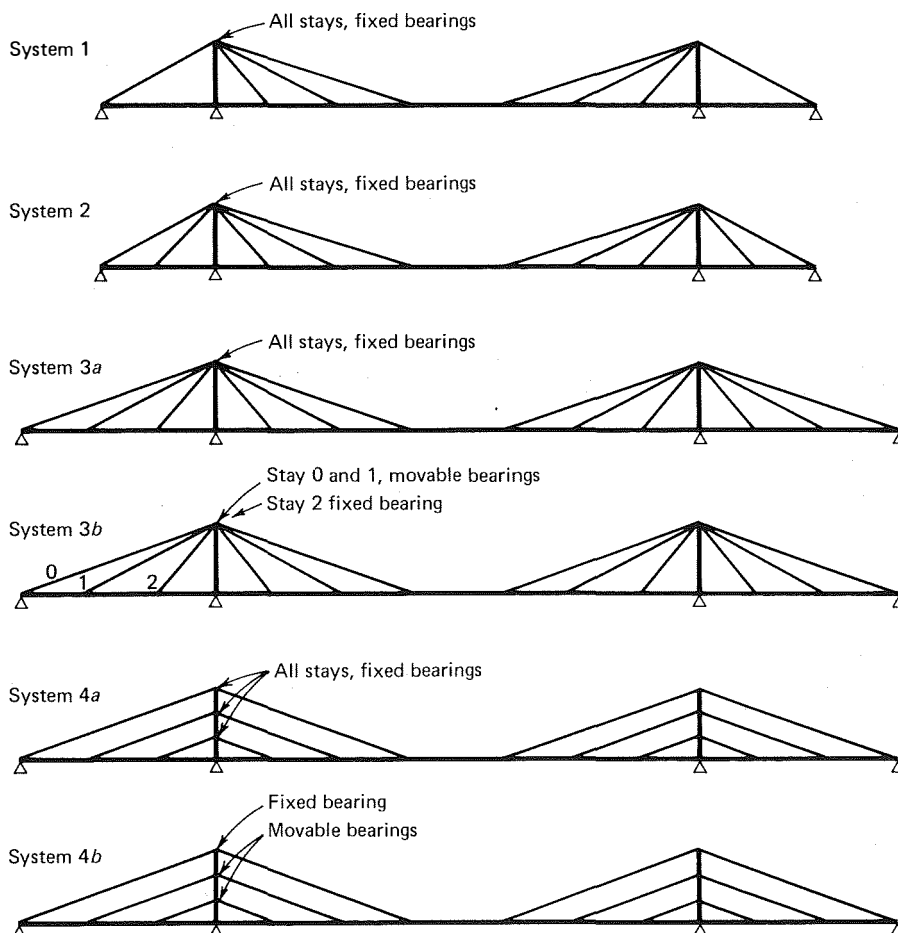
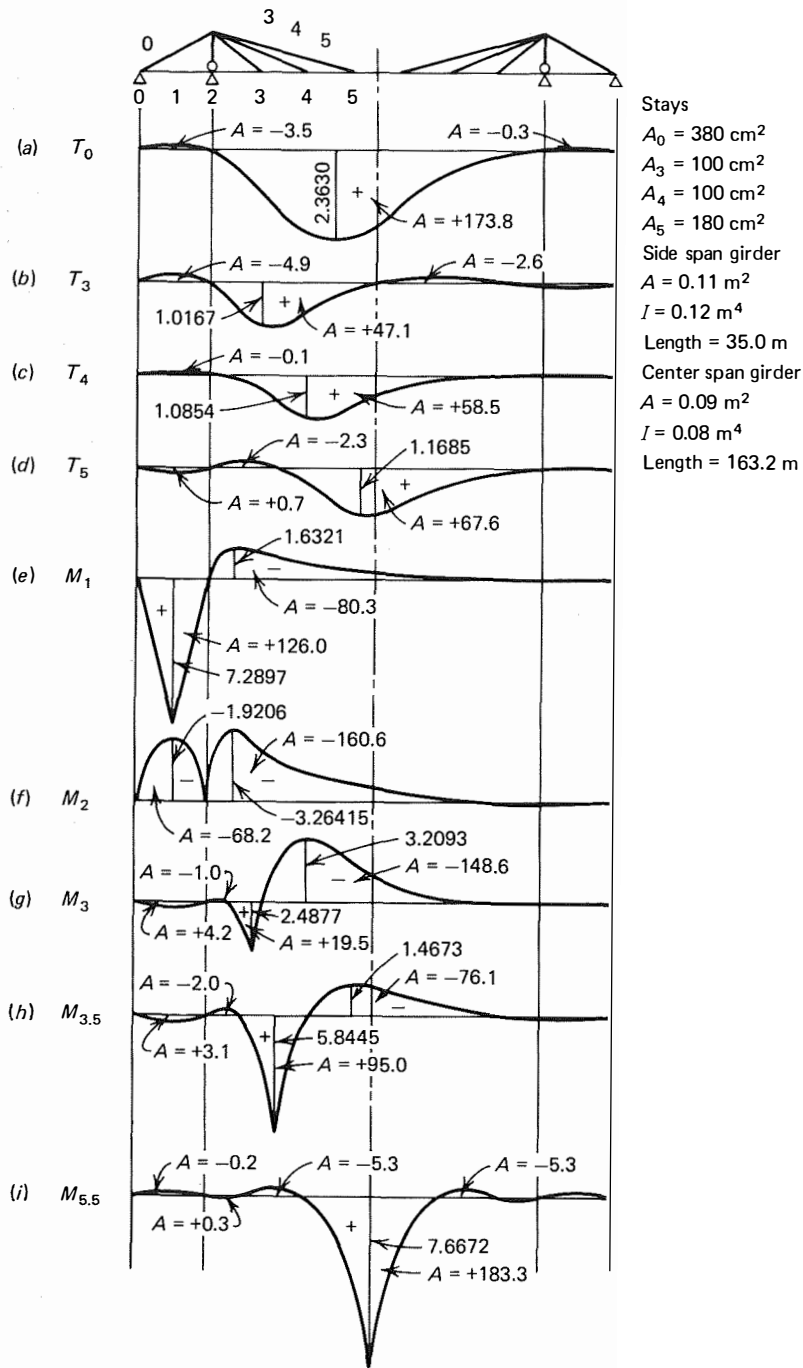
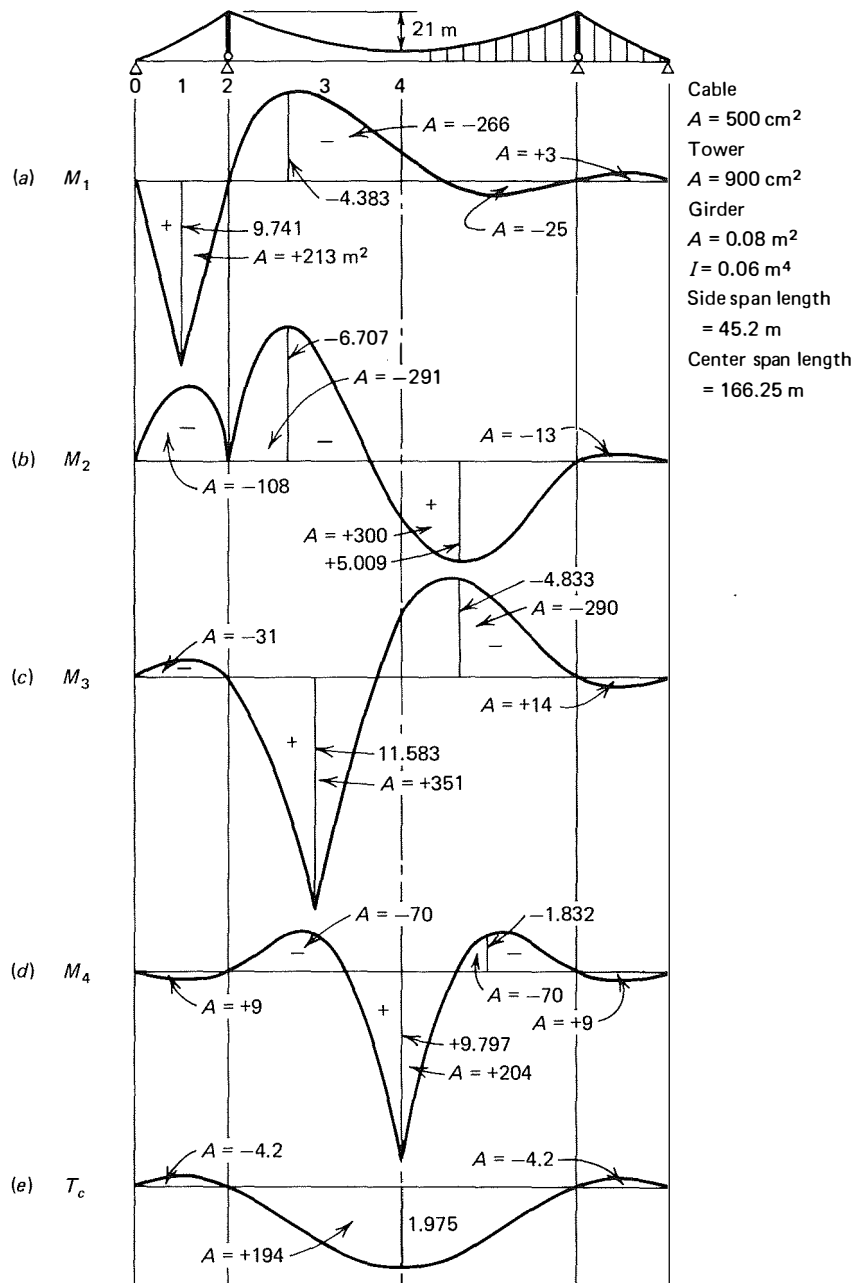


FIGURE 12.33 Schematic representation of cable-stayed bridges. (Courtesy of Der Stahlbau, from reference 24.)



**FIGURE 12.34** Influence line for cable-stayed system 1. (Courtesy of Der Stahlbau, from reference 24.)





**FIGURE 12.35** Influence line for self-anchored suspension bridge. (Courtesy of Der Stahlbau, from reference 24.)

radiating and harp configurations illustrated in Fig. 12.38. The influence lines, shown in Figs. 12.39 through 12.42 do not account for axial strains in the tower and girder and assume that the stay connection at the tower is such that no bending moment is produced in the tower. Cable areas are assumed constant for all stays and the moment of inertia of the girder is constant along the length of the girder.

Cable-stay area is presented as a dimensionless coefficient

$$\frac{E_c A_c L_T^2}{E_G I_G}$$

where  $E_c$  = modulus of elasticity for the cable stay  
 $A_c$  = cross-sectional area of the cable stay

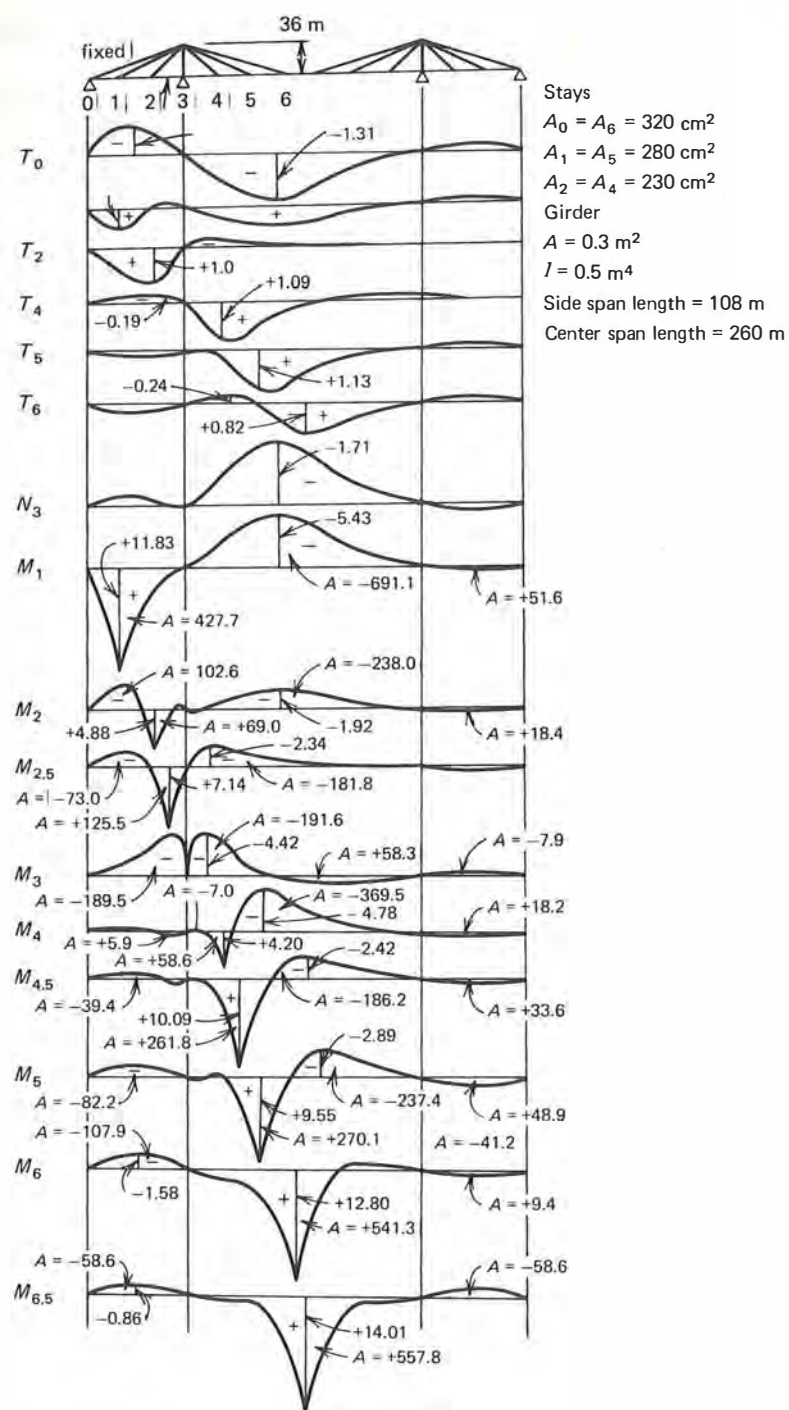


FIGURE 12.36 Influence line for cable-stayed system 3a. (Courtesy of Der Stahlbau, from reference 24.)

$E_G$  = modulus of elasticity for the girder  
 $I_G$  = moment of inertia for the girder  
 $L_T$  = overall length of the structure

Tabulated values for  $E_c A_c L_T^2 / E_G I_G$  range from 250 to 16,000, with practical values ranging from 2,000 to 10,000.

O'Connor's method of analysis for these influence lines is as follows<sup>26</sup>

1. Form a statically determinate base structure by removing the supports at *C* and *H*, and cutting the cables at *B*, *D*, *E*, *F*, *G*, and *I* in the case of the radiating, and at *D*, *E*, *F*, and *G* in the case of the harp, Fig. 12.38. The vertical components of force at these points will be considered as the redundant forces. There are eight such forces in

the case of the radiating system and six for the harp system.

2. Compute deflections corresponding to each of the unit redundant forces. This flexibility matrix is made up of terms from the girder deflections plus terms from the cable extensions.

The matrix of girder deflections can be obtained by a simple standard program, loading the girder with the  $M/EI$  diagram for the particular load and obtaining deflections using moment area methods. The matrix of cable deflections can be computed manually, read as data, and added algebraically to the girder deflections.

3. From the principle of Müller-Breslau, an influence line for bending moment is identical with the deflected shape corresponding to a unit angular rotation across an element at the point in question.

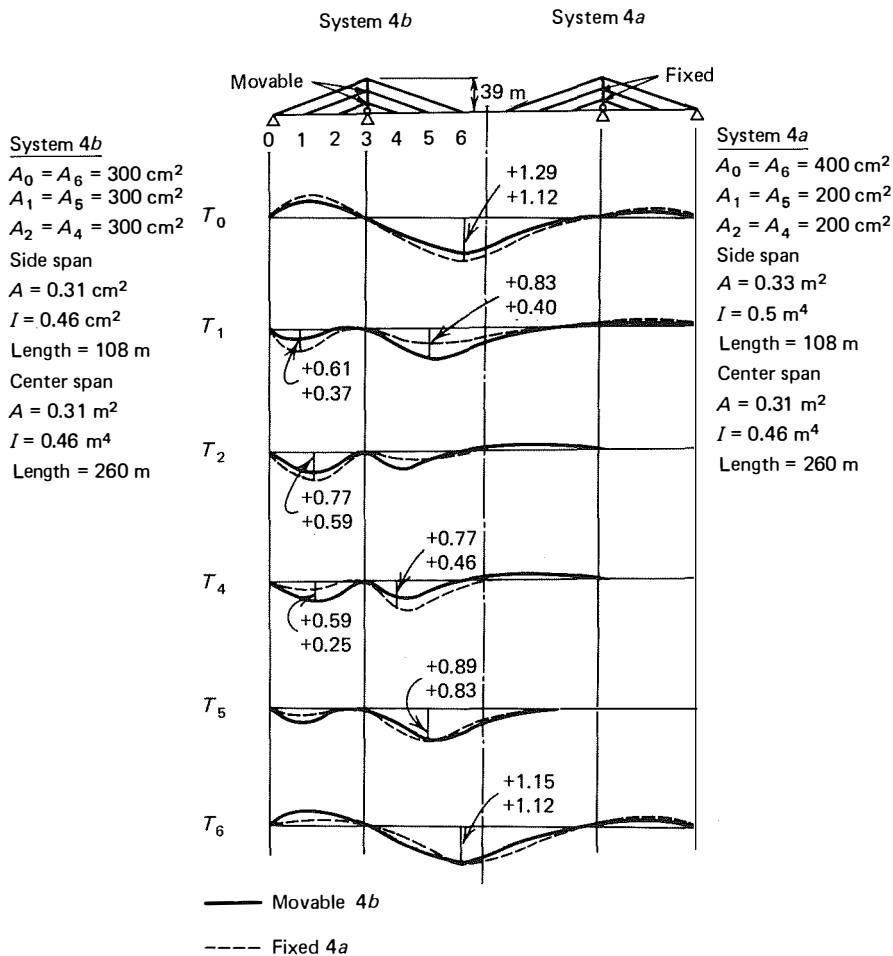


FIGURE 12.37 Influence lines for cable-stayed systems 4a and 4b. (Courtesy of Der Stahlbau, from reference 24.)

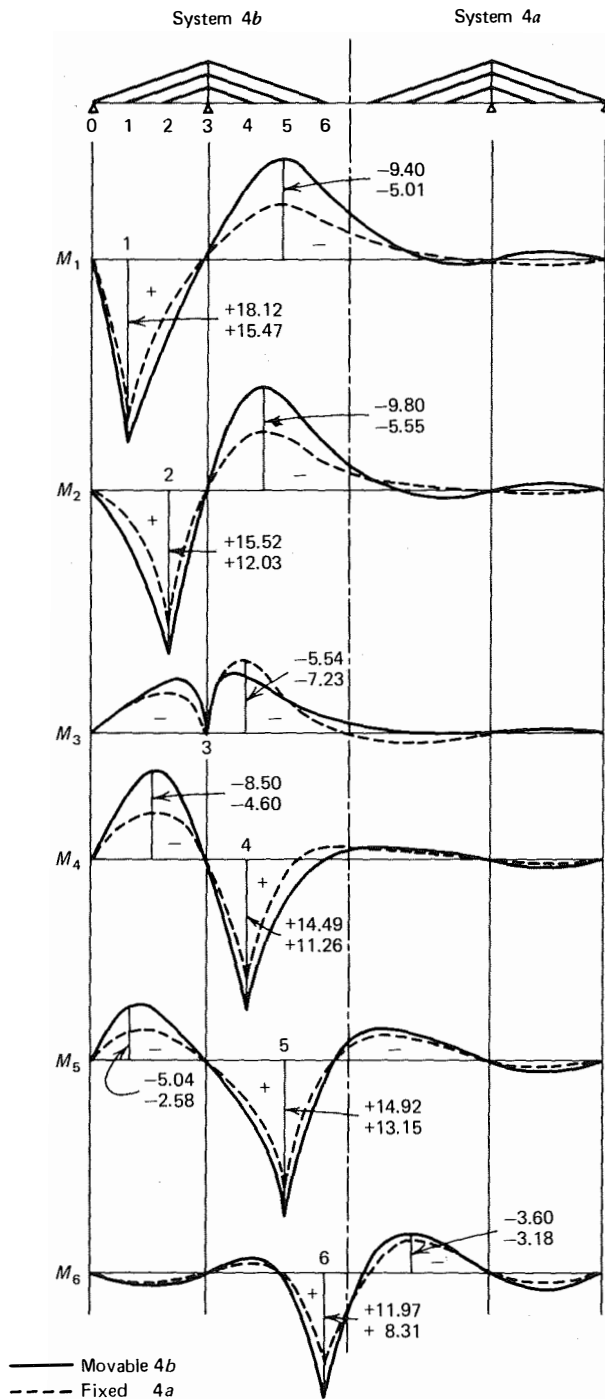


FIGURE 12.37 (Continued)

4. For the base structure, compute the initial deflections of the base structure using the angle-load analogy. Insert these deflections as the constant terms in a set of simultaneous equations with the redundant forces, and the coefficients of the un-

knowns being the flexibility matrix computed previously. Solve for these redundant forces.

5. Apply the redundant forces to the girder alone. Compute its deflected shape. Add this new shape

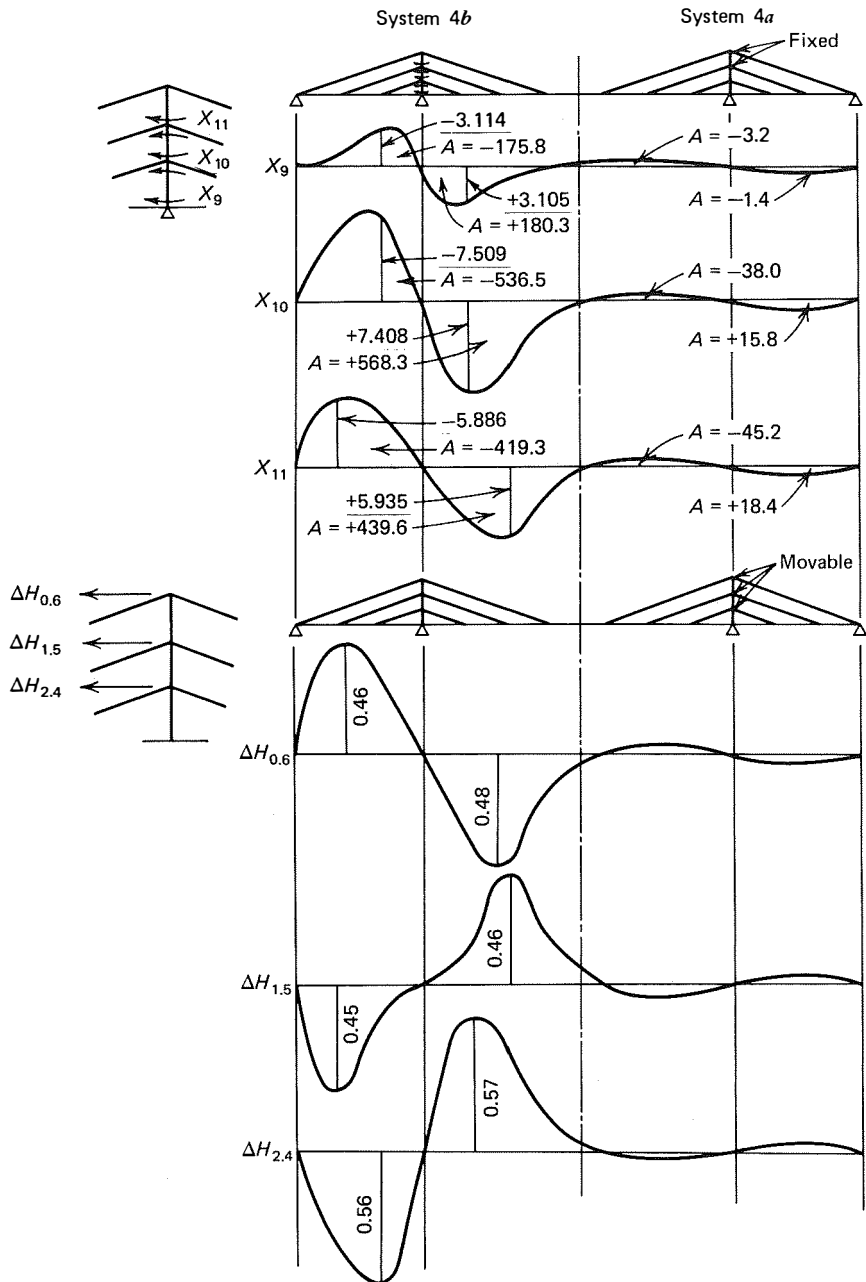


FIGURE 12.37 (Continued)

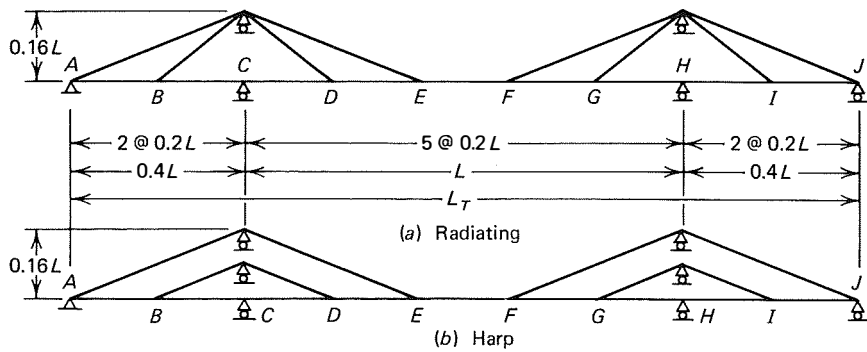
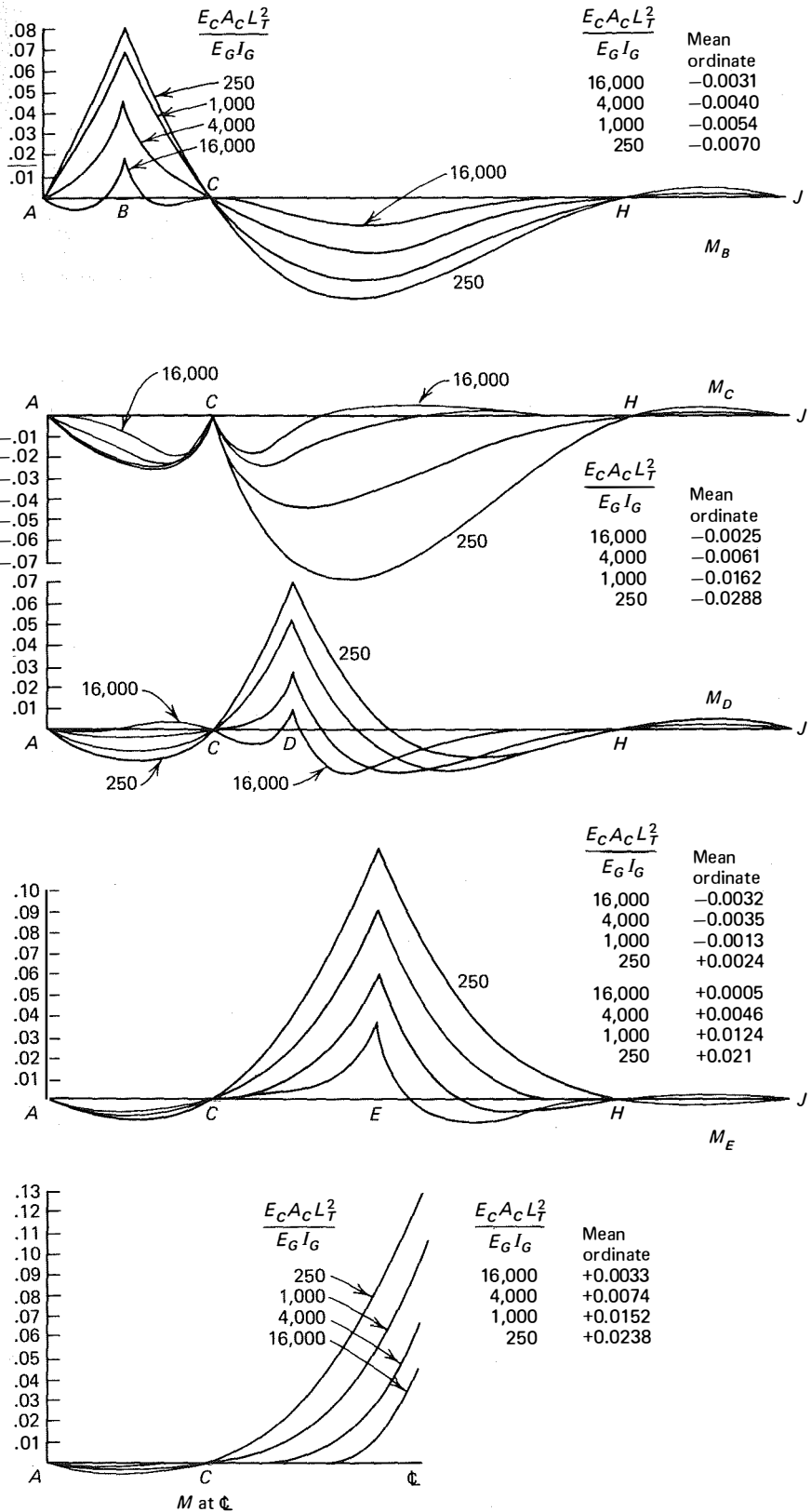


FIGURE 12.38 Bridge geometries used for analysis of radiating and harp types, from reference 25.



**FIGURE 12.39** Influence lines for deck-bending moments, radiating-type bridge; bending moment ordinates times  $L$ ., from reference 25.

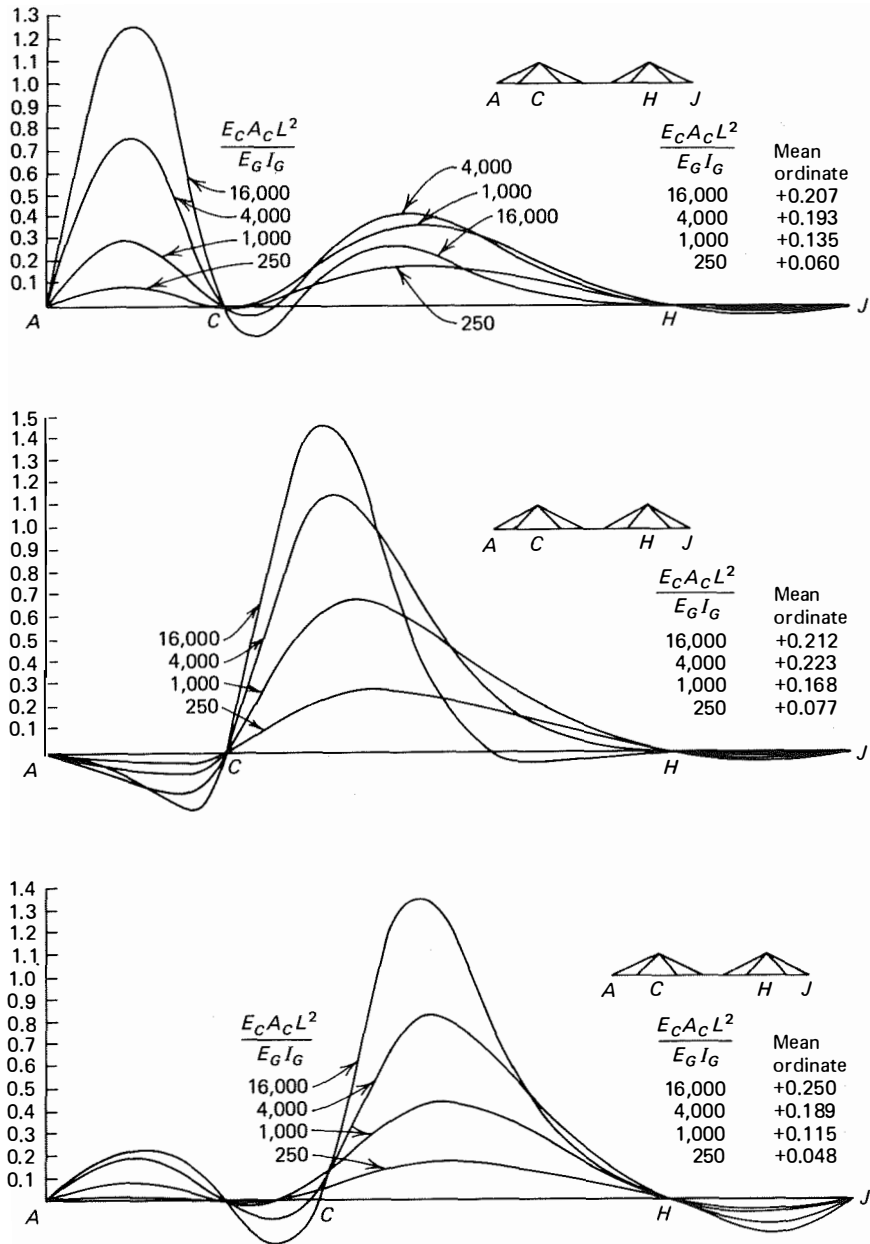


FIGURE 12.40 Influence lines for cable forces, radiating-type bridge, from reference 25.

to the initial deflected shape to determine the required influence line.

- The influence line for the vertical component of a cable force corresponds to a unit relative vertical displacement across the cut in the cable. This unit displacement can be introduced to form a set of simultaneous equations for the redundant forces. The redundant forces may be applied to the girder alone, and the resulting deflected shape is the in-

fluence line for the redundant. The influence line for cable force may be obtained by multiplying each ordinate by  $1/\sin \theta$ , where  $\theta$  is the cable slope from the horizontal.

Based on these influence lines, O'Connor arrived at the following generalized conclusions<sup>26</sup>

- The harp arrangement of cables has larger bend-

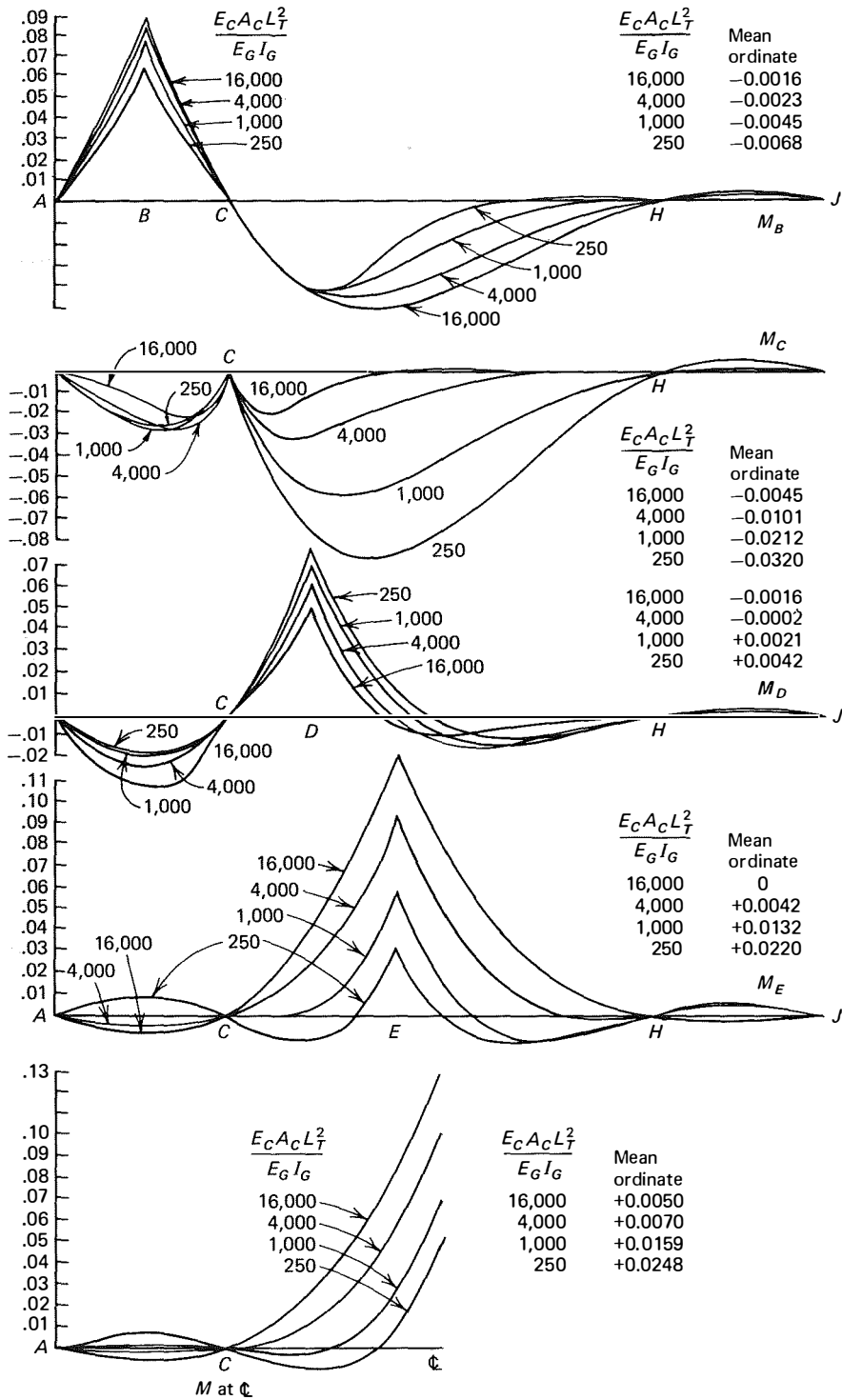


FIGURE 12.41 Influence lines for deck bending moments, harp type bridge; bending moment ordinate times  $L$ , from reference 25.



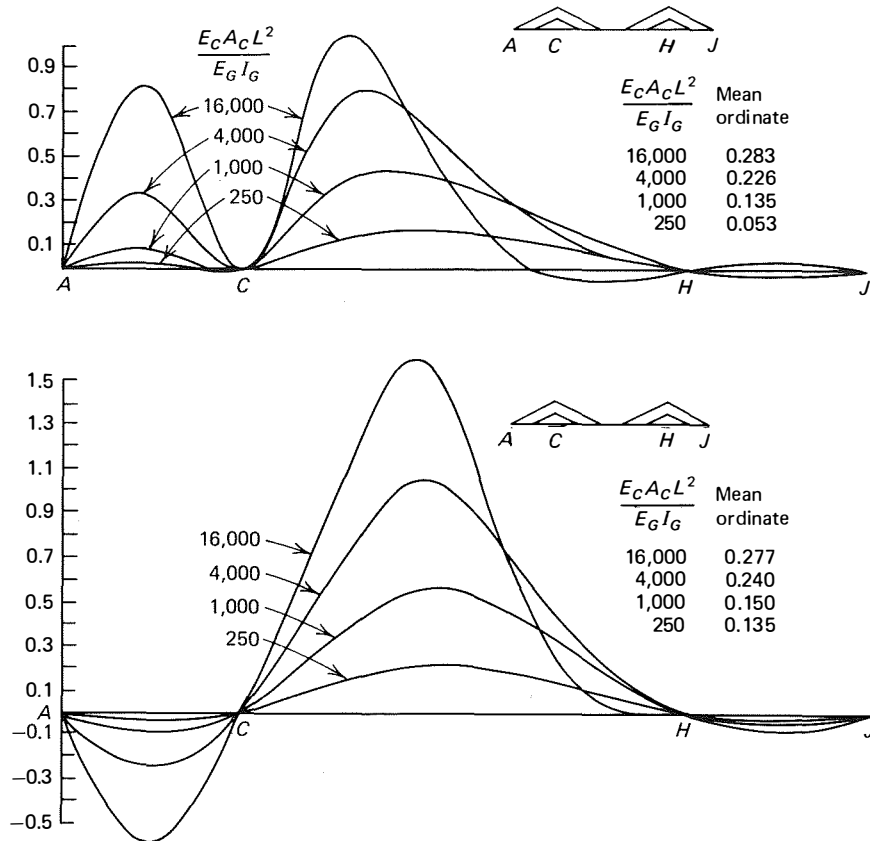


FIGURE 12.42 Influence lines for cable forces, harp-type bridge, from reference 25.

ing moment ordinates and smaller cable force ordinates than the radiating type. This results from the less direct load transfer to the abutments and piers. Consequently, the radiating type configuration is generally to be preferred. However, the difference between the two forms is not as marked as would be expected.

2. For the harp arrangement, the influence lines for bending moments in the girder at the cable connections nearest the towers are hardly affected by the cable stiffness. These bending moments are hardly benefited by the presence of the cables.
3. With this exception, the influence lines for the girders are greatly dependent on the parameter  $E_c A_c L^2 / E_g I_g$ .
4. Plots for: (a) the maximum positive bending moment at the center of the main span; (b) the maximum positive bending moment at the center of the side span; and (c) the maximum negative bending moment at the tower for a moving unit load are illustrated in Fig. 12.43. Observe that

the cable stiffness has a small effect on item b for the harp but a relatively large effect on the other bending moments. This effect of the cable stiffness extends well beyond the normal practical range. Therefore, it would be inaccurate to attempt an analysis that ignored elongations in the cables.

5. The bending moment at the center of the side spans for the harp may become the absolute maximum bending moment as observed in Fig. 12.43. This same conclusion is also evident in the work performed by Homberg.<sup>25</sup>
6. The maximum bending moment at the center of the main span is virtually the same value for the radiating or the harp system.
7. Curves of maximum moment versus location on the girder for a moving unit load are plotted in Fig. 12.44. In general, the negative bending moments are smaller than the positive bending moments in the deck structure. For the harp system,

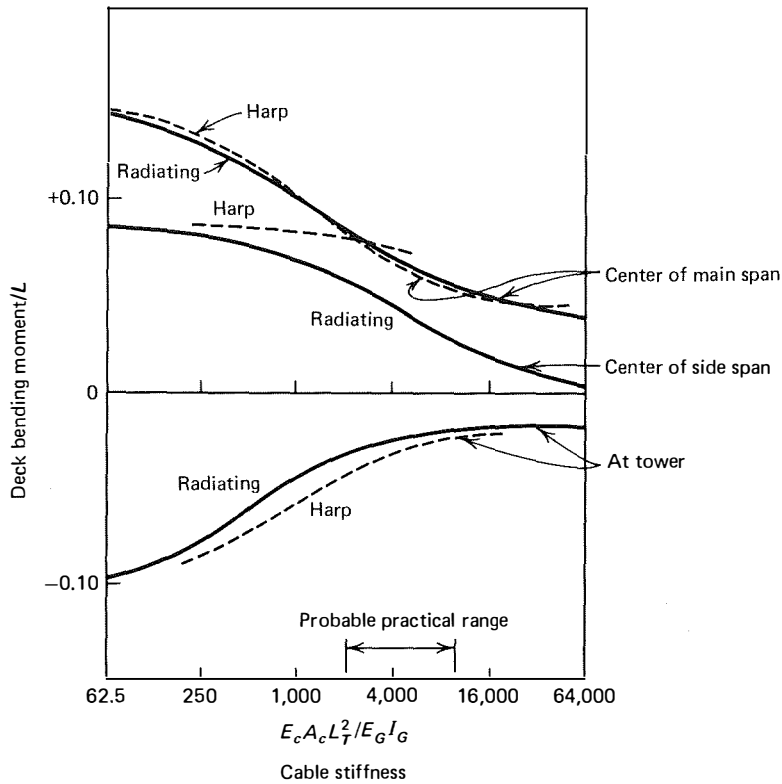


**FIGURE 12.43** Variation of deck bending moment with cable stiffness for a unit moving load, from reference 25.

Fig. 12.44 indicates the relatively high bending moments in the side span and near the towers.

8. The influence lines for cable force have negative ordinates for the radiating and harp arrangements. However, only moderate dead load tensions are necessary to avoid resultant compressive forces, and will prevent the cables from becoming slack. There is little difference between the radiating and harp systems in this respect and, therefore, both are equally acceptable.
9. For the radiating configuration of cables a better distribution of design bending moments in the girder could be achieved with larger side spans and a smaller gap between the central cables.
10. The above comparisons between the harp and radiating arrangements have assumed equal cable areas. In actual fact, this assumption is not valid. The harp would be expected to have smaller cable forces than the radiating system and, therefore, smaller cable areas. As a result, design bending moments for the harp arrangement should be greater than those used in the previous discussion.

### 12.18 Live Load Stresses

In the design of girder bridges an influence line for bending moment is normally sufficient to determine the stress in the girder. The stress at a point  $r$  in section  $i$  is denoted simply by  $f_{i,r} = M_i/S_{i,r}$ , where  $M_i$  is the moment at section  $i$  and  $S_{i,r}$  is the section modulus at point  $r$  in section  $i$ . Thus,  $f_{i,r \max} = M_{i \max}/S_{i,r}$ . However, in cable-stayed bridges, in addition to the bending moment in the girder, there is the effect of axial load and stress concentrations produced by the cable anchorages in the girder and the tower.

Tang<sup>18,27</sup> has suggested the following formulation to obtain the stress at a point  $r$  in section  $i$ :

$$f_{i,r} = a_1 M_i + a_2 N_i + a_3 T_k \quad (12.60)$$

where  $f_{i,r}$ ,  $M_i$ ,  $S_{i,r}$  are as previously designated,  $N_i$  is the axial force at section  $i$ , and  $T_k$  is the cable force of a nearby cable  $k$ . The coefficients are  $a_1 = 1/S_{i,r}$ ,  $a_2 = 1/A_i$ ;  $a_3$  is the effect of nonuniform stress distribution due to the anchorage of cable  $k$ . Note that  $S_{i,r}$  and  $A_i$  are the effective section modulus for point  $r$  at section

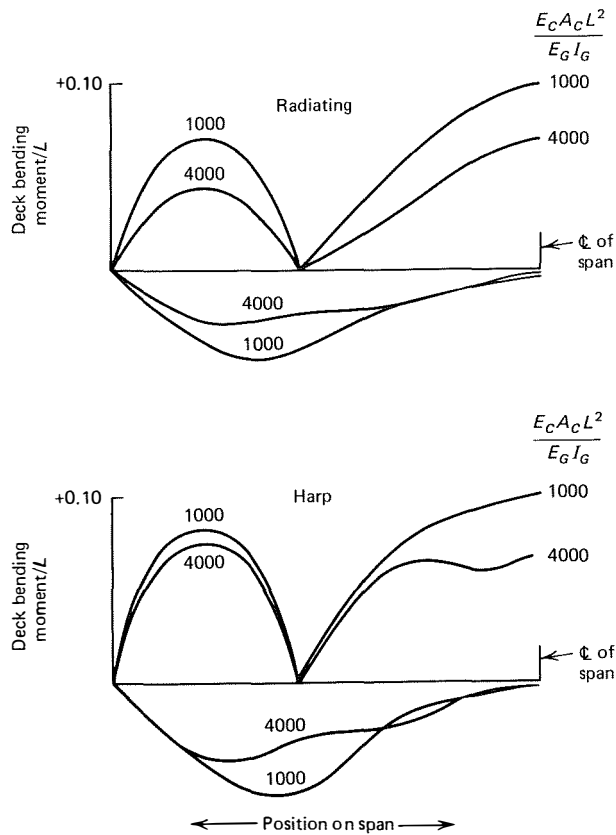


FIGURE 12.44 Curves of maximum deck moment due to a unit moving load, from reference 25.

$i$  and the effective cross-sectional area at section  $i$ , respectively.

The nonuniform bending stress distribution across the bridge deck must be considered when calculating an effective section modulus  $S_{i,r}$ . This is especially true when the girder is slender and wide.

Additionally, at the anchorage point of the cable to the girder or tower a local stress concentration will occur, which is accounted for by the coefficient  $a_3$ . This can be calculated<sup>27</sup> by assuming that a uniform stress distribution is not attained until a distance from the anchorage point equal to the width of the bridge is reached. Between the anchorage point and the point of uniform distribution, the stress may be determined by an approximate analysis, by finite element computer methods, or by some approximate assumption based on sound engineering judgment.

Because the live load that produces a maximum  $M_{i,r}$  or maximum  $N_i$  does not necessarily produce a maximum  $f_{i,r}$  influence lines for the three elements on the right-hand side of equation 12.60 must be evalu-

ated simultaneously, or, as suggested by Tang,<sup>18,27</sup> an influence line in the form of equation 12.60 may be evaluated to obtain a maximum and minimum  $f_{i,r}$ . This can be accomplished by superposition. Instead of the unit deformation  $\Delta\phi_i$  for rotation,  $\Delta u_i$  for horizontal displacement of the girder and vertical displacement of the tower, and  $\Delta l_c$  for change in cable chord length, a combined distortion equal to

$$\Delta\phi_i = a_1, \quad \Delta u_i = a_2, \quad \text{and} \quad \Delta l_c = a_3 \quad (12.61)$$

is applied. The resulting deflection curve of the bridge becomes the influence line of  $f_{i,r}$ .<sup>18,27</sup>

### 12.19 Other Methods of Analysis

Nonlinearity in the bridge structure, other than cable nonlinearity discussed above, involves the girder and tower legs and results from deflections of these components under the combined effect of bending moments and axial forces. Generally, these effects of nonlinearity are negligible unless the girder and/or tower are very slender. In any event, after all details of the design of a cable-stayed bridge are completed, a nonlinear analysis, subject to overload conditions, should be performed to assure the adequacy of the total design. The nonlinear analysis may be necessary to determine stress considerations during erection.

Standard plane frame and space frame computer programs are available, which, when properly modified to account for nonlinearity, can be used for the analyses. Troitsky and Lazar<sup>15</sup> have used a flexibility technique for comparison with models to study the behavior of cable-stayed bridges. Lazar, Troitsky, and Douglass<sup>28</sup> have further proposed a load balancing analysis to partially reduce the effects of loads acting on a structure by applying a prestressing force. Lazar<sup>29</sup> also employed the stiffness method of analysis. The transfer matrix method which was developed in Germany,<sup>14</sup> has been extended by Tang<sup>18,27</sup> to accommodate nonlinearity by using fictitious loads.

Kajita and Cheung<sup>19</sup> employed a finite element method for a linear method of analysis to consider the torsion in the deck for a two-plane, three-dimensional structure. This method was further extended to consider dynamic analysis. Baron and Lien<sup>20</sup> presented static and dynamic analyses of the proposed Southern Bay Crossing Cable-Stayed Bridge, in San Francisco.

References 15, 18, 19, 20, 27, 28, and 29 provide detailed explanations of the various methodologies used for the analysis of cable-stayed bridges.

## References

1. Leonhardt, F., "Latest Developments of Cable-Stayed Bridges for Long Spans," *Saertryk af Bygningsstatistiske Meddelelser*, Vol. 45, No. 4, 1974. Danmarks tekniske Højskole.
2. Leonhardt, F. and Zellner, W., "Cable-Stayed Bridges" IABSE Surveys S-13/80, IABSE Periodica 2/1980, May 1980.
3. Leonhardt, F. and Zellner, W., "Cable-Stayed Bridges: Report on Latest Developments," *Canadian Structural Engineering Conference*, 1970, Canadian Steel Industries Construction Council, Toronto, Ontario, Canada.
4. Simpson, C. V. J., "Modern Long Span Steel Bridge Construction in Western Europe," *Proceedings, The Institution of Civil Engineers*, Supplement (ii), 1970.
5. Leonhardt, F. and Zellner, W., "Vergleiche zwischen Hängebriücken und Shrägkabelbrücken für Spannweiten über 600 m," *International Association for Bridge and Structural Engineering*, Vol. 32, 1972.
6. Ivy, R. J., Lin, T. Y., Mitchell, S., Raab, N. C., Richey, V. J., and Scheffey, C. F., "Live Loading for Long-Span Highway Bridges," *ASCE Transactions*, Vol. 119, Paper No. 2708, 1954.
7. Gimsing, N. J., "Anchored and Partially Anchored Stayed Bridges," *Proceedings of the International Symposium on Suspension Bridges*, Lisbon, Laboratorio Nacional de Engenharia Civil, 1966.
8. Gimsing, N. J., "Multispan Stayed Girder Bridges," *Journal of the Structural Division*, ASCE, Vol. 102, No. ST10, October 1976.
9. Anon., "VSL Stay Cables for Cable-Stayed Bridges," *VSL International*, Losinger Ltd., Berne, Switzerland, January 1984.
10. Hahn, J., *Durchlaufträger, Rahmen, Platten und Balken auf elastischer Bettung*, Werner-Verlag, Düsseldorf, 1976.
11. Orlov, G. and Saxenhofer, H., *Balken auf elastischer Unterlage*, Verlag Leemann, Zürich, 1963.
12. Smith, B. Stafford, "The Single Plane Cable-Stayed Girder Bridge: A Method of Analysis Suitable for Computer Use," *Proceedings of the Institution of Civil Engineers*, May 1967.
13. Smith, B. S., "A Linear Method of Analysis for Double-Plane Cable-Stayed Girder Bridges," *Proceedings of the Institution of Civil Engineers*, January 1968.
14. Protte, W. and Tross, W., "Simulation als Vorgehensweise bei der Berechnung von Schrägseilbrücken," *Der Stahlbau*, No. 7, July 1966.
15. Troitsky, M. S. and Lazar, B. E., "Model Analysis and Design of Cable-Stayed Bridges," *Proceedings of the Institution of Civil Engineers*, March 1971.
16. Podolny, W., Jr., "Static Analysis of Cable-Stayed Bridges," Ph.D. Thesis, University of Pittsburgh, 1971.
17. Podolny, W., Jr. and Fleming, J. F., "Cable-Stayed Bridges—Single Plane Static Analysis," *Highway Focus*, Vol. 5, No. 2, August 1973, U.S. Dept. of Transportation, Federal Highway Administration, Washington, D.C.
18. Tang, M. C., "Analysis of Cable-Stayed Girder Bridges," *Journal of the Structural Division*, ASCE, Vol. 97, No. ST 5, May 1971, Proc. Paper 8116.
19. Kajita, T. and Cheung, Y. K., "Finite Element Analysis of Cable-Stayed Bridges," IABSE, Pub. 33-II, 1973.
20. Baron, F. and Lien, S. Y., "Analytical Studies of a Cable Stayed Girder Bridge," *Computers & Structures*, Vol. 3, Pergamon Press, New York, 1973.
21. Baron, F. and Lien, S. Y., "Analytical Studies of the Southern Crossing Cable Stayed Girder Bridge," Report No. UC SESM 71-10, Vol. I & II, Department of Civil Engineering, University of California, Berkeley, California, June 1971.
22. Okauchi, I., Yabe, A. and Ando, K., "Studies on the Characteristics of a Cable-Stayed Bridge," *Bull. of the Faculty of Science and Engineering*, Chuo University, Vol. 10, 1967 (in Japanese).
23. Kinney, J. S., *Indeterminate Structural Analysis*, Reading, MA, Addison-Wesley, 1957.
24. Scalzi, J. B., Podolny, W., Jr., and Teng, W. C., "Design Fundamentals of Cable Roof Structures," United States Steel Corporation, ADUSS 55-3580-01, Pittsburgh, Pennsylvania, October 1969.
25. Homberg, H., "Einflusslinien von Schagseilbrücken," *Der Stahlbau*, No. 2, February 1955.
26. O'Conner, C., *Design of Bridge Superstructures*, New York, Wiley, 1971.
27. Tang, M. C., "Design of Cable-Stayed Girder Bridges," *Journal of the Structural Division*, ASCE, Vol. 98, No. ST 8, August 1972, Proc. Paper 9151.
28. Lazar, B. E., Troitsky, M. S. and Douglass, M. McC., "Load Balancing Analysis of Cable-Stayed Bridges," *Journal of the Structural Division*, ASCE, Vol. 98, No. ST 8, August 1972, Proc. Paper 9122.
29. Lazar, B. E., "Stiffness Analysis of Cable-Stayed Bridges," *Journal of the Structural Division*, ASCE, Vol. 98, No. ST 7, July 1972, Proc. Paper 9036.

# 13

## *Design Considerations—Wind Effects*

|         |  |     |
|---------|--|-----|
| 13.1    | INTRODUCTION                                       | 284 |
| 13.1.1  | Description of Bridge Failures                     | 284 |
| 13.1.2  | Adverse Vibrations in Other Bridges                | 288 |
| 13.1.3  | Lessons from History                               | 289 |
| 13.2    | WIND ENVIRONMENT                                   | 289 |
| 13.2.1  | The Natural Wind                                   | 290 |
| 13.2.2  | Design Wind Velocity                               | 291 |
| 13.2.3  | Funnelling Factor                                  | 291 |
| 13.2.4  | Design Wind Velocity at Structure                  |     |
|         | Altitude   | 291 |
| 13.2.5  | Effect of Structure Length on Design Wind Velocity | 291 |
| 13.2.6  | Effect of Structure Height on Design Wind Velocity | 292 |
| 13.2.7  | Wind Force and Angle of Attack                     | 293 |
| 13.3    | WIND EFFECTS—STATIC                                | 294 |
| 13.3.1  | Lateral Buckling                                   | 295 |
| 13.3.2  | Torsional Divergence                               | 295 |
| 13.3.3  | Turbulence Effects                                 | 297 |
| 13.4    | VIBRATION  | 297 |
| 13.4.1  | Free Vibrations                                    | 298 |
| 13.4.2  | Forced Vibrations                                  | 298 |
| 13.4.3  | Self-Excited Vibrations                            | 298 |
| 13.4.4  | Damping  | 299 |
| 13.5    | WIND EFFECTS—AERODYNAMIC                           | 300 |
| 13.5.1  | Vortex Shedding                                    | 300 |
| 13.5.2  | Flutter  | 302 |
| 13.5.3  | Turbulence   | 302 |
| 13.6    | WIND TUNNEL TESTING                                | 303 |
| 13.6.1  | Boundary Layer Full Model Test                     | 303 |
| 13.6.2  | Sectional Model Test                               | 303 |
| 13.6.3  | Dynamic Similarity                                 | 303 |
| 13.6.4  | Aerodynamic Similarity                             | 304 |
| 13.7    | STABILITY OF STAYED-GIRDER BRIDGES                 | 304 |
| 13.8    | DECK STABILITY                                     | 305 |
| 13.9    | STABILITY DURING ERECTION                          | 306 |
| 13.10   | WIND TUNNEL INVESTIGATIONS                         | 307 |
| 13.10.1 | Long's Creek Bridge, Canada                        | 307 |
| 13.10.2 | Kniebrücke, West Germany                           | 308 |
| 13.10.3 | Proposed New Burrard Inlet Crossing, Canada        | 308 |
| 13.10.4 | Pasco-Kennewick Intercity Bridge, U.S.A.           | 309 |
| 13.10.5 | The Narrows Bridge, Canada                         | 310 |
| 13.10.6 | Luling Bridge, U.S.A.                              | 313 |
| 13.11   | MOTION TOLERANCE                                   | 313 |
|         | REFERENCES   | 315 |

### *13.1 Introduction*

Because of their flexibility, cable-supported systems may be subject to potentially large dynamic motions induced by wind forces. In the past 16 decades wind oscillations have severely damaged at least 11 suspension structures, including the Tacoma Narrows Bridge in Washington. A popular misconception is that wind forces are only significant for long-span bridges. This is obviously incorrect, as seen from Table 13.1,<sup>1</sup> which lists bridges in a span range from 245 to 2800 ft (75 to 850 m) that have been damaged or destroyed. It has been known for 150 years that suspension bridges are susceptible to serious vibration problems induced by wind forces. Yet on November 7, 1940 the Tacoma Narrows Bridge began to oscillate in a mild gale, Fig. 13.1, and its oscillations increased to a destructive amplitude until, in a final agonizing spasm, the main span broke loose from its supporting cables and crashed into the water 208 ft (63 m) below, Fig. 13.2. This catastrophic failure shocked the engineering profession, and many professionals were surprised to find that such a wind-induced failure of a suspension bridge was not without precedent.

#### *13.1.1 DESCRIPTION OF BRIDGE FAILURES*

In 1817 a 4-ft (13-m) wide, 260-ft (79-m) span foot-bridge was constructed across the Tweed River at Dryburgh Abbey in Berwick County, Scotland. This structure was distinguished by a side parapet, which served as a stiffening member, and by supporting inclined (stay) chains. In 1818, 6 months after completion, it collapsed when the chain stays broke at the joints as a result of wind-induced oscillations.<sup>1,2,3,4,5</sup>

Sir Samuel Brown built the first vehicular suspension bridge (Union) in England in 1820 across the Tweed at Nordham near Berwick. This structure had

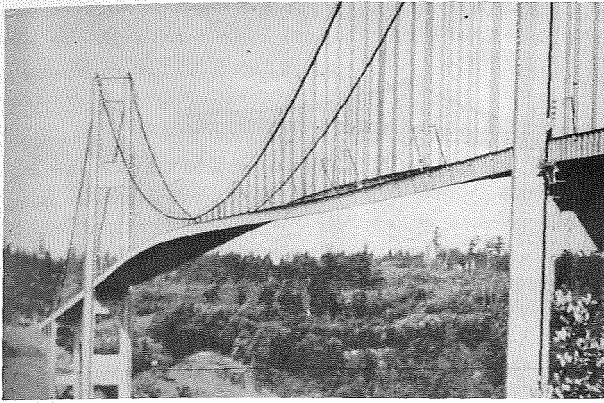


**FIGURE 13.1** Tacoma Narrows Bridge, torsional motion just before failure, November 7, 1940.

a 12-ft (3.7-m) roadway, with 3-ft (1-m) walks on each side, and a span of 449 ft (137 m). It was the first eyebar suspension bridge completed in England and had 12 chains of eyebars, each 2 in. (50 mm) in diameter. Failure occurred in a violent wind 6 months after completion.<sup>1,2,3,4,5</sup>

The Nassau Bridge was constructed with eyebar chains and without stiffening members across the Lahn River in Germany. Twelve chains were broken in a wind storm 4 years after it had been opened to traffic.<sup>1,4</sup>

The four-span Brighton Chain Pier structure was built in 1823 and partially wrecked by a wind storm in 1833. This structure was rebuilt and was destroyed 3 years later. It consisted of four 255-ft (78-m) spans supported by four chains of 2-in. (50-mm) diameter eyebars on each side of a 12-ft 8-in. (3.8-m) roadway. This collapse was witnessed and documented by Lt. Col. William Reid of the British Army.<sup>6</sup> His sketches (Fig. 13.3) and a few paragraphs of his report are reproduced below.<sup>1,2</sup>

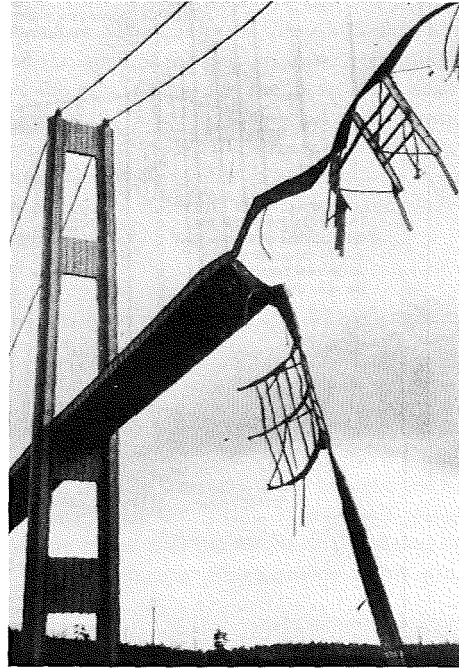


**FIGURE 13.2** Tacoma Narrows Bridge, failure.

The same span of the Brighton chain-pier (the third from the shore) has now twice given way in a storm. The first time it happened in a dark night, and the storm was accompanied by much thunder and lightning; the general opinion of those who do not inquire into the cause of such matters was, that it was destroyed by lightning; but the persons employed about the pier, and whose business it was to repair it, were satisfied that the first fracture was neither caused by lightning nor by the waters, but by the wind.

The fracture this year was similar to the former, and the cause evidently the same. This time, it gave way half an hour after midday, on the 30th of November 1836, and a great number of persons were therefore enabled to see it.

**TABLE 13.1** Bridges Severely Damaged or Destroyed by Wind

| Bridge              | Location | Designer               | Span (ft) | Failure Date |
|---------------------|----------|------------------------|-----------|--------------|
| Dryburgh Abbey      | Scotland | John and William Smith | 260       | 1818         |
| Union               | England  | Sir Samuel Brown       | 449       | 1821         |
| Nassau              | Germany  | Lossen and Wolf        | 245       | 1834         |
| Brighton Chain Pier | England  | Sir Samuel Brown       | 255       | 1836         |
| Montrose            | Scotland | Sir Samuel Brown       | 432       | 1838         |
| Menai Straits       | Wales    | Thomas Telford         | 580       | 1839         |
| Roche-Bernard       | France   | Le Blanc               | 641       | 1852         |
| Wheeling            | U.S.A.   | Charles Ellet          | 1010      | 1854         |
| Niagara-Lewiston    | U.S.A.   | Edward Serrell         | 1041      | 1864         |
| Niagara-Clifton     | U.S.A.   | Samuel Keefer          | 1260      | 1889         |
| Tacoma Narrows      | U.S.A.   | Leon Moisseiff         | 2800      | 1940         |

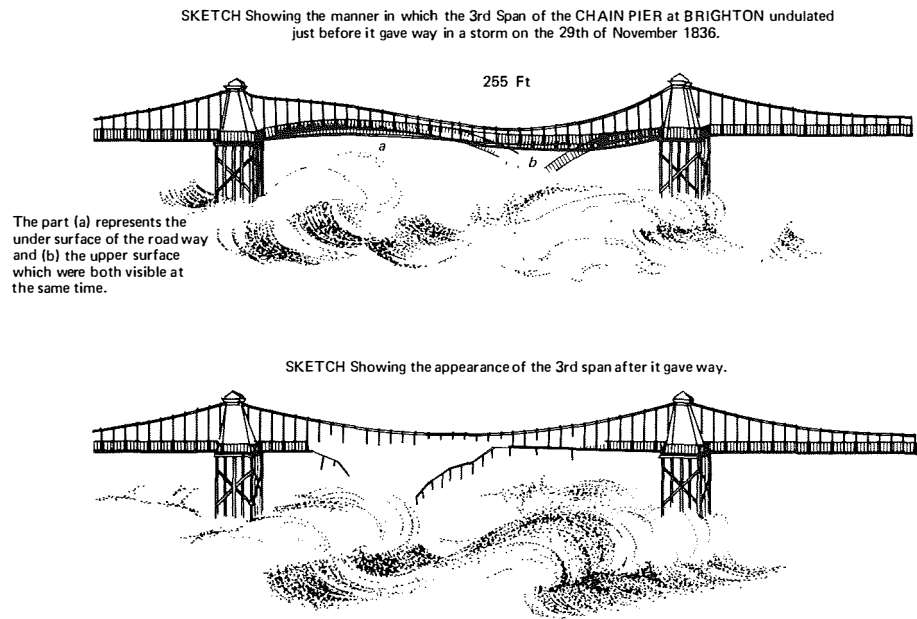


**FIGURE 13.3** Damage to the Brighton Chain Pier. (Lt. Col. Reid's sketches, reference 1.)

The upper one of the two sketches annexed, shows the greatest degree of undulation it arrived at before the roadway broke; and the under one shows its state after it broke; but the great chains from which the road is suspended remained entire.

When this span became relieved from a portion of its load by the roadway falling into the sea, its two piers went a little to one side, and the curve of the chain became less, as in the sketch. The second and fourth spans in these sketches are drawn straight, merely to show better the degree of undulation of the third span.

Those also undulated greatly during the storm, but not in the same degree as the third span. A movement of the same kind in the roadway has always been sensibly felt by persons walking on it in high winds; but on the 29th of November 1836, the wind had almost the same violence as in a tropical hurricane, since it unroofed houses and threw down trees. To those who were at Brighton at the time, the effect of such a storm on the chain-pier was matter of interest and great curiosity. For a considerable time the undulations of all the spans seemed nearly equal. The gale became a storm about eleven o'clock in the forenoon, and by noon it blew very hard. Up to this period many persons, from curiosity, went across the first span, and a few were seen at the further end; but soon after mid-day the lateral oscillations of the third span increased to a degree to make it doubtful whether the work could withstand the storm; and soon afterwards the oscillating motion across the roadway seemed to the eye to be lost in the undulating one, which in the third span was much greater than in the other three; the undulatory motion which was along the length of the road is that which is shown

in the first sketch; but there was also an oscillating motion of the great chains across the work, though the one seemed to destroy the other, as they did not both (at least as far as could be seen) take place in a marked manner at the same time.

At last the railing on the east side was seen to be breaking away, falling into the sea; and immediately the undulations increased; and when the railing on this side was nearly all gone, the undulations were quite as great as represented in the drawing.

Lt. Col. Reid's sketches indicate the characteristic sine-curve oscillations that eventually lead to the classical flutter mode of failure.

The Montrose Bridge over the South Esk River in Forfarshire, Scotland, had a 432-ft (132-m) span and was built in 1829. Shortly after construction, in 1830, approximately 700 people congregated on one side of the structure to witness a boat race. As the boats passed under the bridge the crowd rushed to the other side. The sudden impact snapped the chains on one side resulting in great loss of life. The bridge was repaired but was subsequently destroyed 8 years later by a violent gale. Eyewitness reports indicate the span undulated in two segments.<sup>1,2,4,5</sup>

The world-famous Menai Straits Bridge in Wales was built in 1826 by the renowned British engineer, Thomas Telford, and had, for its day, a record span—580 ft (177 m). It was damaged by wind in 1826, 1836,

and 1839. The following excerpt is from a paper by Mr. W. A. Provis<sup>7</sup> and relates the motion that was observed in the 1826 storm.<sup>2</sup>

It was observed, that the character of the motion of the platform was not that of simple undulation, as had been anticipated, but the movement of the undulatory wave was oblique, both with respect to the lines of the bearers, and to the general direction of the bridge. It appeared, that when the summit of the wave was at a given point on the windward side, it was not collateral with it on the leeward side, but, in relation to the flow of the wave, consistently behind it, and forming a diagonal line of wave across the platform.

This description indicates that the structure was undergoing a torsional oscillation. After necessary repairs were made the structure survived 10 years without any distress until 1836 when an unusually heavy gale caused violent undulations of the deck and fractured several suspenders. A gatekeeper reported waves or undulations of 16-ft (4.9-m) double amplitude. The damage was repaired, but the structure was again subjected to winds of hurricane intensity in 1839. This storm so severely damaged the structure that, with the exception of the pylons, it had to be entirely rebuilt.<sup>1,2</sup>

The Roche-Bernard Bridge over the Vilaine River had, for its day a record span—641 ft (195 m)—and is notable in that it was among the earliest suspension bridges to use wire cable. It was damaged in a hurricane in 1852 and the suspended roadway dropped into the river.<sup>1,2,5</sup>

In 1848, Charles Ellet, Jr., built the record-breaking 1010-ft (308-m) span suspension bridge over the Ohio River at Wheeling, West Virginia. Six years later, in 1854, the structure was destroyed in what was described as a hurricane. The bridge deck was completely destroyed and 10 of its 12 cables were pulled from their anchorages. The following account of the failure appeared in the *Wheeling Intelligencer*.

For a few moments we watched it with breathless anxiety, lunging, like a ship in the storm; at one time it rose to nearly the height of the towers, then fell, and twisted and writhed, and was dashed almost bottom upward. At last there seemed to be a determined twist along the entire span, about one-half of the flooring being nearly reversed, and down went the immense structure from its dizzy height to the stream below, with an appalling crash and roar.

For a mechanical solution of the unexpected fall of this stupendous structure, we must await further developments. We witnessed the terrific scene and saw that it was brought about by the violence of the gale. The great body of the flooring and the suspenders, forming something like a basket swung

between the towers, was swayed to and fro, like the motion of a pendulum. The cables on the south side were finally blown off the apex of the eastern tower, retaining their position on the opposite side of the river. This destroyed the equilibrium of the swinging body; and each vibration giving it increased momentum, the cables, which sustained the whole structure, were unable to resist a force operating on them in so many different directions, and were literally twisted and wrenched from their fastenings.

Steinman commented on the Wheeling newspaper account as follows:

The newspaperman who wrote the foregoing dramatic account unknowingly summarized the crux of the aerodynamic phenomenon he had observed when he used the significant phrase: "Each vibration giving it increased momentum." And when he stated that the mechanical solution of the failure "must await further developments," he wrote better than he knew.

A structure with a span of 1043 ft (318 m) was constructed in 1850 over the Niagara River between Lewistown, New York, and Queenston, Ontario. To partially stabilize the bridge against motion, it was built with guy cables extending from the roadway deck to the sides of the gorge. Because these guys were jeopardized by an ice jam which had formed upstream during the winter of 1863–64, it was decided that they would be temporarily removed in the spring when the ice jam would break up. While the guys were detached, a heavy wind arose and the entire suspended system was destroyed, leaving only the cables which stood for another 34 years but were never used.<sup>2</sup>

The 1268-ft (386-m) Niagara-Clifton Bridge at Niagara Falls was built in 1868 by Samuel Keefer and rebuilt by G. W. McNulty in 1888. Seven months later on the night of January 9, 1889 it was completely destroyed by wind action. An eyewitness described the bridge as rocking "like a boat in a heavy sea," tipping up "almost on its very edge." By morning the structure was destroyed. It lay a crumpled mass of steel and wire bottom side up beneath the waters of the river below.<sup>5</sup>

At the time of its construction the Tacoma Narrows Bridge had the third longest center span of any type bridge constructed. It had a main span of 2800 ft (853 m). It was stiffened by a shallow plate girder and had a narrow roadway width such that the ratio of its length to width was much larger than any similar contemporary structure. Early in the morning of November 7, 1940 a fairly strong wind arose which caused some



movement in the structure. By 7:30 or 8:00 A.M. the wind velocity increased to 38 miles per hour (61 km/h) (verified by an anemometer reading taken at the time). The main span was oscillating in a vertical mode of moderate amplitude at a frequency of approximately 36 cycles per minute. The vibration continued in this manner until about 10:00 A.M. when the velocity increased to 42 miles per hour (67 km/h). At this point there was a drastic change in the motion. The frequency of motion changed from 36 cycles per minute to 12 cycles per minute. The changed motion was in a violent torsional mode with angular distortion reaching an amplitude of approximately 45 degrees from the static position. The vertical acceleration was rapidly approaching that of gravity. The torsional motion of the structure is illustrated in Fig. 13.1. The structure withstood this torsional deformation for about an hour when it finally yielded and a section of deck and laterals near the center of the span dropped out. The motion decreased momentarily and then built up again. In a few minutes the rest of the deck tore away from the cables and fell into the water. As a result of the loss of dead weight in the center span, the center cables rose up and the side spans sagged deeply, causing the towers to deflect shoreward and the motion to die out.<sup>2</sup>

The Tacoma Narrows Bridge was observed to have undesirable motions during and immediately after construction. It was recognized that some correction was necessary, and there were suggestions for stop-gap provisions. However, no one recognized the catastrophic potential. It was assumed there was plenty of time to make laboratory studies and arrive at corrective measures in due course.

The authors wish to emphasize that the designer of the Tacoma Narrows Bridge, Leon Moissieff, was one of the most highly regarded and progressive bridge engineers of his day. At the time, aerodynamic considerations for bridge designs were unheard of. Moissieff was a pioneer in a bridge design concept which

was not yet in the structural research laboratories and certainly not in the average bridge designer's offices.

### 13.1.2 ADVERSE VIBRATIONS IN OTHER BRIDGES

Obviously not all suspended bridge structures have been destroyed or badly damaged as a result of wind forces. However, a few structures have been observed to have undesirable oscillations as a result of wind-induced vibration. They are listed in Table 13.2.<sup>1</sup>

The Fykkesund Bridge in Norway is a rolled I beam stiffened bridge located at a site where high winds are frequent. This structure was reported to have oscillations of 1 to 3 nodes in the center span and amplitudes of plus or minus 2 ft 7½ in. (0.8 m). In 1945 stays were added below the structure and have apparently been effective in controlling the motion.<sup>1</sup>

The Golden Gate Bridge is the only structure listed in Table 13.2 that has a stiffening truss. Motions were observed twice. Vibration was observed on February 9, 1938, but the wind velocity was not recorded. The second occurred during a storm on February 11, 1941 with a recorded wind velocity of 62 mph (99 km/h). On both occasions the amplitude of vibration was estimated at 2 ft (0.6 m).<sup>1,8</sup>

The Thousand Island Bridge project connecting the United States and Canada consists of two suspension bridges. The span on the American side is 800 ft (244 m) while that on the Canadian side is 750 ft (229 m). Both structures are stiffened by plate girders. Frequent mild motion has been reported but apparently has been effectively corrected by the addition of guys.<sup>1,9</sup>

Before the Deer Isle Bridge was completed in 1939 it had to be stabilized against wind-induced vibrations by the addition of diagonal stays, which joined the stiffening girder at the pylon to the main cables in the center and side spans. However, serious damage, including breaking of some of the stays, was incurred during storms occurring during the winter of 1942–1943. A more extensive system of longitudinal cable-

TABLE 13.2. Modern Bridges that Have Oscillated in Wind

| Bridge                    | Year Built | Span (ft) | Type of Stiffening |
|---------------------------|------------|-----------|--------------------|
| Fykkesund (Norway)        | 1937       | 750       | Rolled I beam      |
| Golden Gate (U.S.A.)      | 1937       | 4200      | Truss              |
| Thousand Island (U.S.A.)  | 1938       | 800       | Plate girder       |
| Deer Isle (U.S.A.)        | 1939       | 1080      | Plate girder       |
| Bronx-Whitestone (U.S.A.) | 1939       | 2300      | Plate girder       |
| Long's Creek (Canada)     | 1967       | 713       | Plate girder       |

to-girder diagonals and transverse stays has since been installed and no excessive motions have been reported.<sup>1</sup>

Ever since the new floor system was installed on the Bronx-Whitestone Bridge crossing the East River in New York it has had a tendency for mild vertical motions. The vibrations have not been serious but have been observed by those crossing the structure. A single-stay system was installed to reduce the vibrations, but the structure was not effectively stiffened until truss members in the plane above the existing plate girder were installed in 1946. The plate girder then became the bottom chord of the truss.<sup>1,10,11</sup>

Shortly after its erection in 1967, the Long's Creek Bridge, located 20 miles (32 km) west of Fredericton on the Trans-Canada Highway, was subjected to wind-induced vibrations. This structure is a cable-stayed bridge with a main span of 713 ft (217 m). The deck structure consists of an orthotropic deck forming the top flange for two 8 ft (2.4 m) deep inverted T-plate girders, 33 ft (10 m) on center. The vibration frequency was observed to be 0.6 cycles per second with the amplitude of vibration reaching as much as 8 in. (200 mm) when the handrail was blocked with snow. The vibration was in the shape of a half-sine wave. When wind tunnel tests were undertaken to study the damping of the vibration, ten boxes, 6 by 6 by 1 ft. 6 in. deep (1.8 by 1.8 by 0.45 m) filled with rocks were hung from the bottom flange of the structure and submerged in the water. The addition of a soffit plate on the bottom changed the cross section into a box of increased torsional stability and the vibration was diminished by 40%. The addition of triangular edge fairing on the outside of the structure virtually eliminated the vibration. An interesting fact is that an essentially twin structure, 10 miles (16 km) upstream from the first structure, had no observed motion because the structure is sheltered by a high embankment.<sup>12,13</sup>

### 13.1.3 LESSONS FROM HISTORY

The failure of the Tacoma Narrows in 1940 startled and shocked the engineering profession. As indicated in the preceding section, the phenomenon was not without precedent. However, the failures of the past had been discounted; a later generation of engineers, not recognizing the lessons of history, espoused the virtue of flexibility without careful consideration of its hazards.

In the recent past there have been a number of

innovations in structural analysis, materials, fabrication, and erection procedures. These include the use of high-strength steels, welding, orthotropic decks, box girders, computer technology, cable stays, monocable suspension, transverse as well as inclined hangers, cantilever construction, prestressed concrete, parallel wire strands, and many other technological advances. As a result, recent bridge structures have larger dimensions and increased flexibility and decreased dead weight and damping characteristics. Reduction of dead weight produces a magnification of wind effects relative to the inertia of the structure; increased flexibility decreases the natural frequency of vibration. Thus, modern fabrication techniques have decreased the structure's ability to absorb energy by sliding friction between component parts and thus less energy is required to initiate and maintain vibration.<sup>14</sup>

Therefore, recently constructed structures are more sensitive not only to static wind effects but to dynamic effects as well. Some existing and relatively recent structures have been so affected by wind oscillations that they required additional reinforcement. As a consequence, wind forces have taken on an increased significance and can be a major problem in cable-supported bridge systems. Serious consideration of these forces is required of the designer. If we, as a new generation of engineers, do not take cognizance of these forces then history will repeat its cycle and we will suffer another series of disasters culminating in future disasters as shocking and as dramatic as the Tacoma Narrows failure.

## 13.2 Wind Environment

Before wind instability studies are conducted for a particular bridge, it is important to estimate the wind environment at the particular site. It is desirable, in the determination of wind action on a suspended bridge structure, to obtain information of strong wind activity at the site over a period of years. Required are the wind velocity, direction, and frequency. This type of data is generally obtainable from meteorological records of the U.S. Weather Bureau and similar local weather records. However, these data are generally recorded at an airport or federal building at a nearby city which may be some distance from the bridge site. These records should be carefully used because the effects of the terrain at the instrument location may be somewhat different from those at the bridge site.

From meteorological data it is possible to plot high

wind speeds and probability of occurrence. With this information, statisticians can estimate the highest expected winds, their expected direction, and their recurrence interval.

### 13.2.1 THE NATURAL WIND

The composition of the wind in the atmosphere is a complex subject which is beyond the scope of this text. However, it is important for the bridge engineer to have a basic knowledge of the nature of wind. Wind may be defined in an elementary manner as air movement caused by atmospheric pressure differentials which occur over the earth's surface. Pressure differentials are produced by complex atmospheric processes from temperature differentials resulting from solar radiation. Solar radiation is strongest at the equator and weakest at the poles along with radiation away from the earth. Pressure differences are indicated on weather maps by isobars or contour lines of equal barometric pressure. Differences in pressure produce acceleration of air particles. Additional accelerators are geostrophic acceleration, resulting from the curvature and rotation of the earth, and centripetal acceleration. The sum of these accelerations is a movement in the free air unaffected by friction at the ground surface. The velocity of this free air is referred to as a gradient velocity,  $\bar{V}_G$ . The height above the earth's surface at which the gradient velocity is attained, usually between 1000 and 2000 ft, is referred to as the gradient height,  $z_G$ . At heights above this value the wind velocity is regarded as constant with height.<sup>15, 16, 17</sup>

The concern of structural engineers is with wind velocity at or near the earth's surface. At this level the wind velocity is affected by the surface friction, which is a function of surface roughness or terrain conditions.

Davenport<sup>16, 17</sup> has suggested that the mean wind speed  $\bar{V}_z$  at a height  $z$ , less than  $z_G$  may be related to the gradient velocity  $\bar{V}_G$  by a power law relationship of the form

$$\frac{\bar{V}_z}{\bar{V}_G} = \left(\frac{z}{z_G}\right)^a \quad (13.1)$$

where the gradient height  $z_G$  and the exponent  $a$  are a function of the surface roughness. Suggested values are presented in Table 13.3.<sup>16, 17</sup> The term "mean wind speed" is generally assumed to be an average of the wind speed over a given time period which may vary from one hour to ten minutes duration.

The above discussion is applicable to relatively flat terrain. The wind velocity can be significantly modified by hilly or mountainous terrain or by abrupt changes in terrain roughness. These effects are discussed in detail by Davenport.<sup>16</sup> The terrain roughness is also significant when trying to assess the wind environment at a bridge site from records made some distance away.

The interaction of the natural wind with the surface roughness or friction of the earth's surface produces a wind character that is gusty or turbulent as opposed to being smooth and uniform. Turbulence or gusts produce velocity fluctuations that are spatial and temporal in character. That is, the wind force acting on a structure will vary in direction as well as magnitude in a vertical as well as horizontal direction at any point in time and will also vary with time.

Terrain conditions may also significantly effect the design wind considerations for a particular site, depending on the structure's exposure. A bridge spanning a large river may be exposed to strong steady winds in a direction perpendicular to its longitudinal axis and turbulent winds parallel to the structure.

TABLE 13.3 Surface Roughness Influence on Gradient Height and Power Law Exponent

| Surface Condition  | Gradient Height<br>$z_G$ (ft) | Power Law<br>Exponent $a$ |
|--|-------------------------------|---------------------------|
| Open water surface   | 900                           | 0.12                      |
| Open flat land<br>(open grass, prairie or farm land<br>with few obstacles; shores, desert) | 900                           | 0.16                      |
| Forest and suburban<br>(uniformly covered with obstacles<br>30-50 ft. in height)           | 1300                          | 0.28                      |
| Urban areas<br>(large and irregular objects, centers<br>of cities)                         | 1700                          | 0.40                      |

13.2.2 DESIGN WIND VELOCITY

In the structural design for wind resistance of any structure a fundamental problem is the estimation of the expected wind velocity. It has been previously mentioned that from a statistical interpretation of meteorological records it is possible to determine wind velocity, direction, and frequency. From this meteorological information, a local mean velocity or fundamental wind velocity,  $V_f$ , is obtained, with reference to some arbitrary datum or height,  $z_f$ , which is often at 33 ft (10 m). The structure may then be designed for this fundamental wind velocity recurring at a specified time interval with proper modification to account for spacial distributions as functions of the dimensions of the structure.

The value of the time interval is the expected life span of the structure. For bridge structures it is recommended that the fundamental wind velocity be determined for a minimum time interval of 100 years.

Contours showing the fastest mile of wind, in miles per hour, 30 ft (10 m) above ground, at a 100-year period of recurrence for the United States are presented in Fig. 13.4.<sup>18</sup>

13.2.3 FUNNELLING FACTOR

A funnelling factor should be applied to the design wind velocity where a structure is located in a valley

where local funnelling of the wind occurs, or where the site is to the leeward side of a range of hills causing local acceleration of wind. This factor should not be less than 1.1.

13.2.4 DESIGN WIND VELOCITY AT STRUCTURE ALTITUDE

Design conditions at a particular site will require that the altitude of the structure (bridge deck elevation) be set at some predetermined value, for example, the height above water for navigation clearance. The design wind velocity at the specified height may be determined by the power law relationship given by equation 13.1, where the fundamental wind velocity and height,  $V_f$  and  $z_f$ , are substituted for the gradient velocity and height,  $\bar{V}_G$  and  $z_G$ , respectively.

$$\frac{V_z}{V_f} = \left(\frac{z}{z_f}\right)^a \tag{13.2}$$

The power law exponent  $a$  should be determined from observations at the bridge site; however, where this is impossible, the values presented in Table 13.3 may be used.

13.2.5 EFFECT OF STRUCTURE LENGTH ON DESIGN WIND VELOCITY

In the previous section, a design wind velocity was determined for some datum elevation or height of the

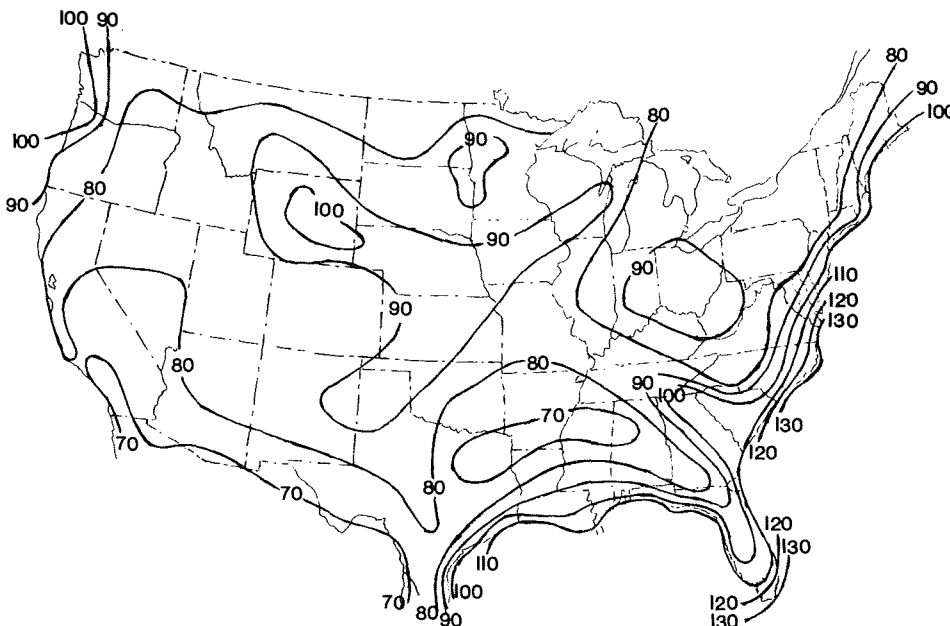


FIGURE 13.4 Basic wind speed in miles per hour. Annual extreme mile 30 ft above ground, 100-year mean recurrence interval, from reference 18.

structure, such as the elevation of the bridge deck. If it is assumed that the direction of the wind is perpendicular to the longitudinal axis of the bridge, then the wind velocity will vary from point to point along the length of the bridge and will further vary with time.

The wind speed  $V_z$  is the mean or average speed over some time period, say 10 minutes. As a result of surface roughness, a turbulence or gust effect is produced in the natural wind such that for some interval of time  $S$  within this 10 minutes, the actual wind velocity  $V_s$  will be larger than the mean velocity  $V_z$ . The mean wind velocity may be considered as a constant wind velocity uniformly distributed across the length of the bridge. Because of the gust effect of the wind, an increased velocity is randomly dispersed and superimposed on the mean velocity along the structure length.

Hirai and Okubo<sup>19</sup> have reported the following empirical formula of Ishizaki and Mitsuda,<sup>20</sup> based upon observations of Sherlock<sup>21</sup> and Deacon<sup>22</sup>

$$\frac{V_s}{V_z} = \left(\frac{S}{600}\right)^{-r}; \quad r = 0.09 \left(\frac{z}{12.2}\right)^{-0.42} \quad (13.3)$$

where  $V_s$  and  $V_z$  are wind velocities at a height  $z$  (in meters) for the time duration  $S$  in seconds. If the value of  $z$  is expressed in feet in the equation for  $r$  above, then the term  $z$  should be divided by the constant 3.72 instead of 12.2

The width of the turbulence  $L$  in the direction of the wind is stated as the product of  $V_s$  and  $S$ . If the horizontal width of the turbulence along the length of the bridge and perpendicular to the wind direction is taken as  $B$ , then  $L$  may be related to  $B$  by some factor  $k$  such that

$$L = kB = V_s S \quad (13.4)$$

then from equations 13.3 and 13.4

$$M_1 = \frac{V_s}{V_z} = \left(\frac{kB}{600V_z}\right)^{-r(1-r)} \quad (13.5)$$

Assuming that the duration  $S$  is determined by equating  $B$  to the horizontal length of the structure, the modification factor  $M_1$  for the design wind velocity can be evaluated. Thus the design wind velocity along the length of the bridge can be determined as the product of the modification factor and the  $V_z$  term determined from equation 13.2

Hirai and Okubo<sup>19</sup> assumed a value of 7.0 for  $k$  in equation 13.5 and a value of 40 m/sec for  $V_f$  and 0.16 for  $a$  in equation 13.2. The value of  $z_f$  was taken as 10 m. Based on these values, corresponding values for  $M_1$  are shown in Table 13.4. From this table it can be seen that the effect of the spatial distribution of gusts decreases as the length and elevation or height of the structure increases.

13.2.6 EFFECT OF STRUCTURE HEIGHT ON DESIGN WIND VELOCITY

In the same manner that the wind velocity varies along the length of the deck of a bridge structure, it will also vary along the height of the pylon. However, the determination of a modification factor for height,  $M_h$ , is considerably more complex than that for the length of the structure. Empirically, Hirai and Okubo<sup>19</sup> have suggested that a height modification factor may be determined in the same manner as for length by substituting the height  $H$  of the structure for the length  $L$  (equating  $H$  to  $B$  in equation 13.5) and  $H/2$  for the structure altitude  $z$ . In this manner the modification factor for height can be determined similarly to that determined for length. Values for the height modification factor are given in Table 13.5, for the same

TABLE 13.4 Modification Factors  $M_1$  for Horizontal Lengths of Structures

| $z(m)$ | $B(m)$ |       |       |       |       |       |       |       |       |       |
|--------|--------|-------|-------|-------|-------|-------|-------|-------|-------|-------|
|        | 150    | 300   | 450   | 600   | 750   | 900   | 1050  | 1200  | 1350  | 1500  |
| 10     | 1.400  | 1.300 | 1.244 | 1.206 | 1.177 | 1.155 | 1.136 | 1.119 | 1.105 | 1.093 |
| 30     | 1.240  | 1.186 | 1.155 | 1.133 | 1.117 | 1.104 | 1.093 | 1.083 | 1.075 | 1.068 |
| 50     | 1.196  | 1.153 | 1.129 | 1.112 | 1.099 | 1.088 | 1.080 | 1.072 | 1.065 | 1.059 |
| 70     | 1.168  | 1.132 | 1.112 | 1.097 | 1.086 | 1.078 | 1.070 | 1.064 | 1.058 | 1.053 |
| 100    | 1.144  | 1.114 | 1.097 | 1.085 | 1.076 | 1.069 | 1.062 | 1.057 | 1.052 | 1.048 |

TABLE 13.5. Modification Factors  $M_h$  for Vertical Heights of Structures

| $H(m)$ | 30    | 40    | 60    | 80    | 100   | 120   | 140   | 160   | 180   | 200   | 220   | 240   |
|--------|-------|-------|-------|-------|-------|-------|-------|-------|-------|-------|-------|-------|
| $M_h$  | 1.500 | 1.432 | 1.316 | 1.256 | 1.221 | 1.192 | 1.171 | 1.157 | 1.144 | 1.132 | 1.121 | 1.114 |

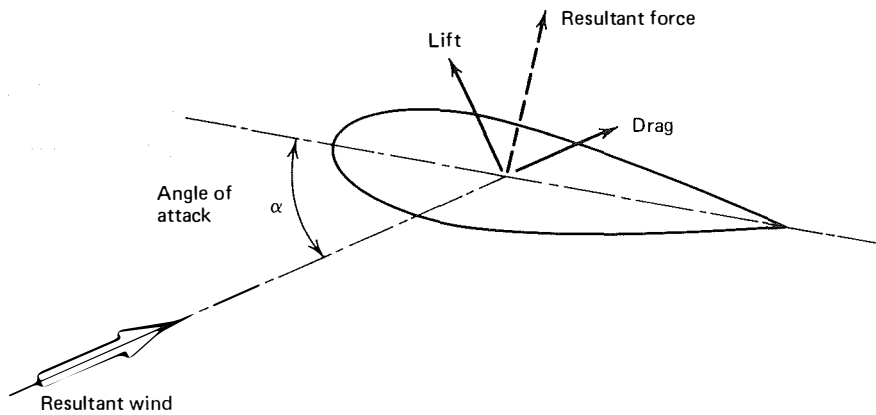


FIGURE 13.5 Force components on an airfoil section.

conditions as those evaluated for length in Table 13.4. From this tabulation it can be seen that the effect of spatial distribution of gusts decreases as height increases.

### 13.2.7 WIND FORCE AND ANGLE OF ATTACK

The wind force assumed on an object is normally not in the same line as the direction of the actual wind. In conventional aerodynamic analysis (e.g., airfoil design), the wind force is divided into components: drag and lift parallel and perpendicular to the wind direction (Fig. 13.5). This same convention may be applied to a bridge deck (Fig. 13.6), wherein the resultant wind is oriented to the structure by the angle of attack  $\alpha$  assumed to be positive when striking the section from the underside. It is convenient in considering wind effects on bridge structures to consider lift acting perpendicular to the normal position of the bridge deck and drag to be acting parallel to the normal position of the bridge deck (Fig. 13.7). The application of the orientation criteria requires the conversion of the wind

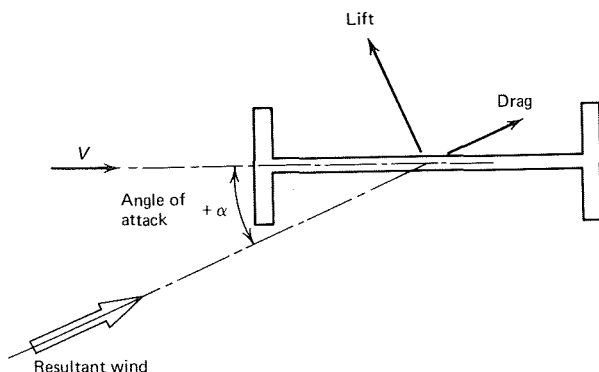


FIGURE 13.6 Force components on a bridge section.

tunnel test data to the changed orientation of the lift and drag forces. The wind also produces an angular motion or torsional moment force acting on the cross section.

When evaluating wind forces on a structure, the possible direction of critical wind velocity should be determined. In plan it is generally assumed that the critical wind direction is perpendicular to the longitudinal axis of the bridge. An obvious question arises as to the maximum value of the angle attack  $\alpha$  that should be considered on the deck cross section. The angle of attack is a function of wind velocity and site conditions. Data for the relationship between maximum observed angle of attack and wind velocity were made at the site of the Severn Bridge<sup>23</sup> and are plotted in Fig. 13.8. Preliminary data obtained by the Federal Highway Administration on the Newport Suspension Bridge during hurricane Doria is also plotted for maximum and minimum values in Fig. 13.8. From these curves it can be seen that the angle of attack decreases with increasing wind speed. Therefore, at lower wind speeds the structure must be made stable for larger values of the angle of attack. The curves shown in Fig. 13.8 may serve as a guide, but are not necessarily applicable to other sites and possibly may impose unnecessary constraints to the analysis.

Wind forces are dynamic considerations because they represent the effect of a moving fluid around a cross section. A common design assumption is to separate wind effects into two major classifications, static and dynamic effects. Under an idealized condition which never occurs in practice, an object subjected to a wind stream of constant velocity and direction that does not vary with time may be thought of as being subjected to static effects. Dynamic effects of flow around an object arise from turbulence in the natural wind, vortex separation, and changes in the flow pattern as a result of the movement of the object. Thus,

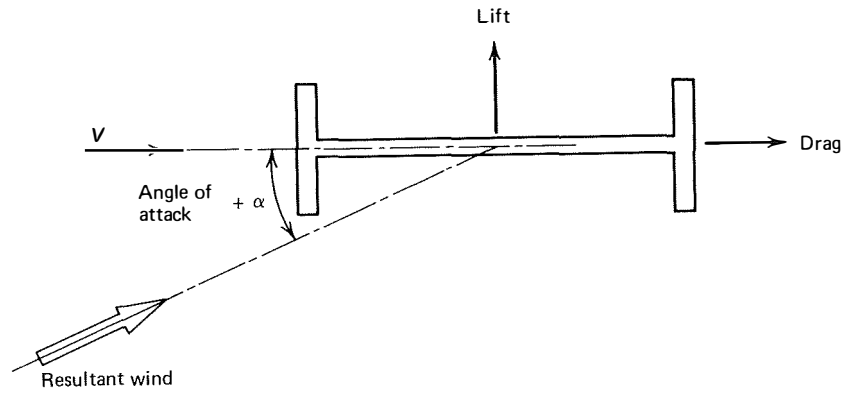


FIGURE 13.7 Reoriented force components on a bridge section.

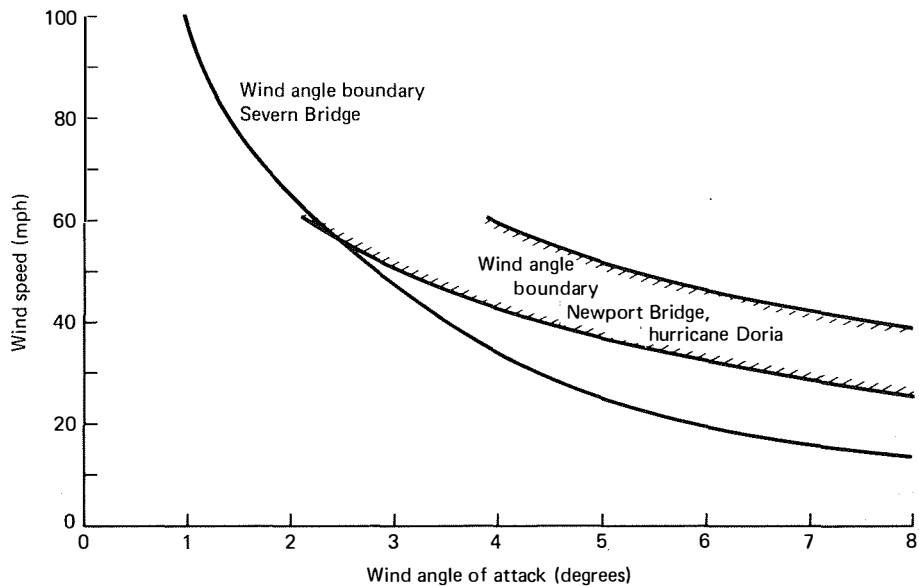


FIGURE 13.8 Angle of attack versus wind speed.

these mechanisms cause time-dependent variations of the wind force.

### 13.3 Wind Effects—Static

The bridge structure should be designed for static as well as dynamic wind effects. Static wind loads are derived from an assumption of a steady, uniform wind, and the lift, drag, and moment forces may be determined from the following basic equation

$$F = \frac{1}{2} \rho V^2 C A \tag{13.6}$$

where  $F$  is the lift or drag force,  $C$  is a dimensionless lift or drag coefficient as a function of the angle of

attack  $\alpha$ ,  $A$  is the projected (frontal) area exposed to the wind,  $V$  is the wind speed normal to the bridge, and  $\rho$  is the density of air (mass per unit volume assumed to be 0.002378 slugs/ft<sup>3</sup> or 0.0766 lb/ft<sup>3</sup> at sea level and at 15°C). Thus, the lift and drag forces are stated as:

$$L = \frac{1}{2} \rho V^2 C_L A \tag{13.7}$$

$$D = \frac{1}{2} \rho V^2 C_D A \tag{13.8}$$

and for a unit length of span, equations 13.7 and 13.8 become

$$L = \frac{\rho V^2 C_L A}{2S} \tag{13.9}$$

$$D = \frac{\rho V^2 C_D A}{2S} \quad (13.10)$$

where  $S$  is the span length.

Under steady conditions, the lift force will generally be displaced from the axis of rotation of the section and cause a moment or torque about the axis of rotation. This moment can be expressed as

$$M = \frac{1}{2} \rho V^2 C_M AB \quad (13.11)$$

and for a unit span length

$$M = \frac{\rho V^2 C_m AB}{2S} \quad (13.12)$$

where  $B$  is the deck width.

The magnitude of these forces will vary with changes in the angle of attack and with the cross-sectional shape. Because the effect of shape generally can be determined only by wind tunnel tests, the actual effects are usually not subject to control at the design stage. Empirical values, based on previous tests for similar cross sections, are normally used in design and then verified in wind tunnel tests. By testing properly scaled models in a wind tunnel, it is possible to obtain scaled forces of lift, drag, and torsional moment. Typical nondimensional plots of lift, drag, and moment coefficients for varying angles of attack are shown in Fig. 13.9.<sup>24,25</sup>

### 13.3.1 LATERAL BUCKLING

The lateral out-of-plane buckling of a bridge deck may be visualized as a simple beam loaded by the wind force. The wind force acts approximately along the beam's centroidal axis in the direction of the drag force; it has a lateral bending stiffness  $EI_l$  and torsional stiffness  $GJ$ .<sup>26</sup> A solution for the critical lateral uniform buckling load based on the above assumptions is attributed to Prandtl and is given as

$$q_{cr} = \frac{28.3[EI_l GJ]^{1/2}}{S^3} \quad (13.13)$$

where  $S$  is the span. Equation 13.13 presents a first estimate of the uniform load  $q_{cr}$ , that will produce a lateral buckling of the bridge deck. From equation 13.10 the corresponding critical wind velocity, normal to the section, can be determined as:

$$V_{cr} = \left[ \frac{2q_{cr}}{\rho C_D (A/S)} \right]^{1/2} \quad (13.14)$$

### 13.3.2 TORSIONAL DIVERGENCE

The cross section of a bridge deck may twist under the wind action as a result of excessive lift and/or drag loads, which increase the angle of attack causing an increased twisting moment in the deck.<sup>26</sup> On a truss bridge, this phenomenon is analogous to an overturning moment such as that which caused the failure of the Chester, Illinois, bridge over the Mississippi River (July 29, 1944).<sup>5</sup>

A simplified analysis of torsional divergence may be derived by considering an element of the bridge deck at midspan.<sup>26</sup> The twisting moment per unit length of span due to wind is determined by equation 13.12 as

$$M = \frac{\rho V^2 C_M AB}{2S}$$

The value of  $C_M$  as a function of the angle of attack may be approximated from a moment plot (Fig. 13.9) as

$$C_M = a\alpha + b \quad (13.15)$$

where  $a$  is the slope of the moment curve and  $b$  is the intercept of  $C_m$  at  $\alpha$  equal to zero.

$$a = \frac{dC_M}{d\alpha} \quad b = C_{M_0}$$

substituting equation 13.15 into 13.12 results in

$$M = \frac{1}{2} \rho V^2 \left( \frac{dC_M}{d\alpha} \alpha + C_{M_0} \right) \frac{AB}{S} \quad (13.16)$$

and represents the moment force acting on the section. The resisting moment per unit span is related to the twist angle  $\alpha$  by

$$M_r = k\alpha \quad (13.17)$$

where  $k$  is the structural stiffness coefficient obtained from the torsional stiffness properties of the deck structure.

Equating equations 13.16 and 13.17 results in a linear relationship in  $\alpha$  given by

$$k\alpha = \frac{1}{2} \rho V^2 \left( \frac{dC_M}{d\alpha} \alpha + C_{M_0} \right) \frac{AB}{S} \quad (13.18)$$

which can be rewritten in the form

$$\alpha = \frac{\frac{1}{2} \rho V^2 C_{M_0} AB/S}{k - \frac{1}{2} \rho V^2 (dC_M/d\alpha) (AB/S)} \quad (13.19)$$



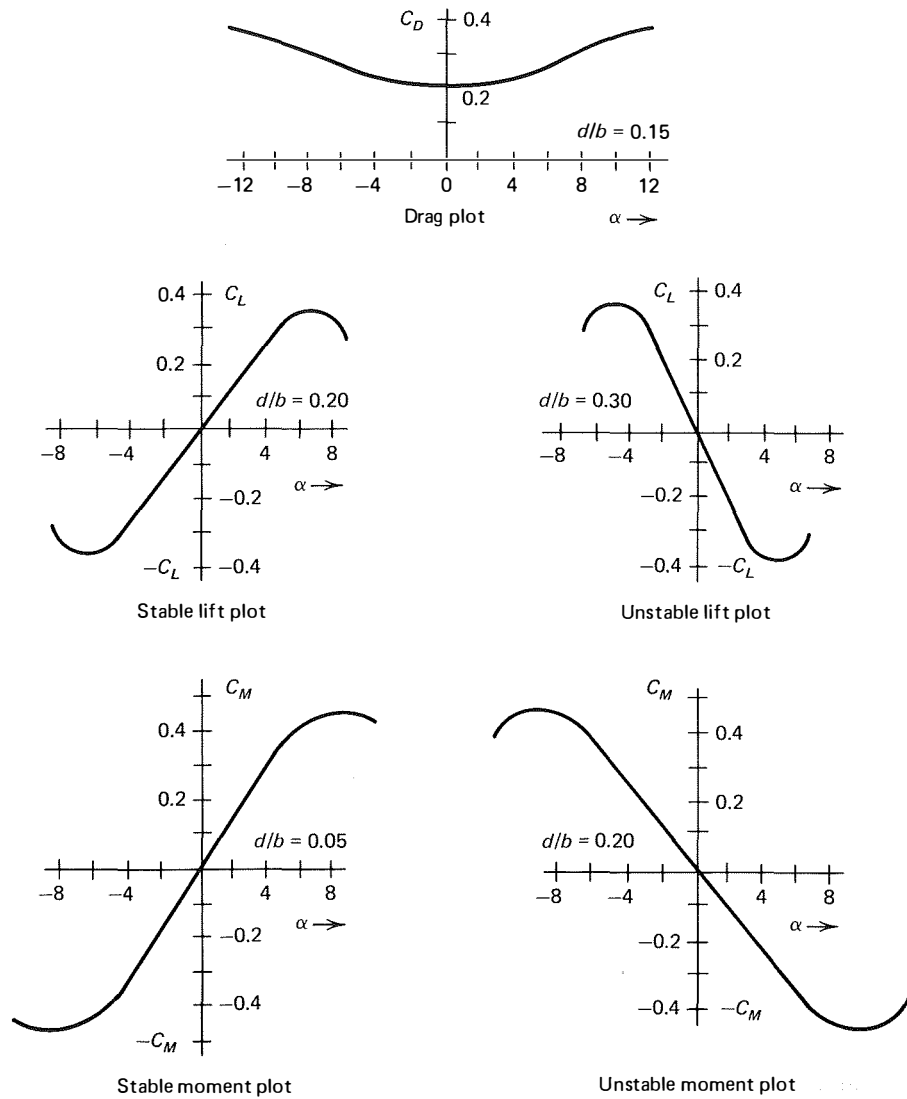


FIGURE 13.9 Lift, drag, and moment plots, from reference 24.

In equation 13.19, as the denominator approaches zero the value of  $\alpha$  approaches infinity. The torsional divergence velocity can thus be defined as

$$\frac{1}{2} \rho V^2 \frac{dC_M}{d\alpha} \frac{AB}{S} = k$$

$$V = \left( \frac{2k}{(dC_M/d\alpha)(AB/S)} \right)^{1/2} \quad (13.20)$$

The above derivation considered only an element at the midspan of the structure. For an actual structure the solution must consider each element along the span simultaneously. Scanlan<sup>26</sup> has presented the following solution.

When assuming a uniform wind velocity across the deck section and along the span, the twisting moment force applied by the wind to all elements of the deck is given by equation 13.16. The torsional resisting moment (equation 13.17) for the total span is given by

$$\{M_r\} = [K] \{\alpha\} \quad (13.21)$$

where  $[K]$  is a symmetrical torsional stiffness matrix and  $\{\alpha\}$  is a column matrix of torsional deformation (angle of attack) for  $N$  positions along the span.

By equating equations 13.16 and 13.21 and letting

$$\lambda = \frac{1}{2} \rho V^2 \left( \frac{dC_m}{d\alpha} \right) \frac{AB}{S} \quad (13.22)$$

the following matrix relationship is obtained

$$[K]\{\alpha\} = \lambda\{\alpha\} + \left(\frac{1}{2}\rho V^2 C_{M_0} \frac{AB}{S}\right)\{1\} \quad (13.23)$$

where  $\{1\}$  is a column matrix of ones.

Equation 13.23 may be rewritten as

$$([K] - \lambda I)\{\alpha\} = \lambda\{\alpha_0\} \quad (13.24)$$

where

$$\alpha_0 = \frac{C_{M_0}}{dC_M/d\alpha}$$

By substituting  $\beta = \alpha + \alpha_0$ , equation 13.24 may be rewritten as

$$([K] - \lambda I)\beta = [K]\{\alpha_0\} \quad (13.25)$$

To solve for  $\beta$  the evaluation of  $([K] - \lambda I)^{-1}$  is required. However, as before, the value of  $\beta$  grows without bound as the determinate  $([K] - \lambda I)^{-1}$  approaches zero. By setting this determinate to zero the critical values of  $\lambda$  can be determined. Thus, the smallest root  $\lambda$ , which is a solution to

$$([K] - \lambda I)^{-1} = 0 \quad (13.26)$$

results in the determination of critical wind velocity for torsional divergence

$$V_{cr} = \left[ \frac{2\lambda_r}{\rho(dC_M/d\alpha)(AB/S)} \right]^{1/2} \quad (13.27)$$

Normally, torsional divergence is not a problem because the deck structure usually has adequate torsional stiffness as a result of other structural design considerations. However, for conventional suspension or cable-stayed structures that are very slender and have low torsional stiffness, the torsional divergence may manifest itself.

### 13.3.3 TURBULENCE EFFECTS

In the previous two sections the presentation was based on the assumption that the wind was uniform in intensity along the length of the structure. In fact, as previously pointed out (Section 13.2.1), natural wind is not steady but turbulent in character. Consequently, the wind pressure at all points along the span will not be constant at any given moment. As a result, some authorities assume that the average pressure is less than that of the mean. Thus, as discussed above, the static phenomenon wherein the wind pressure is considered uniform is assumed to be a conservative approach. However, as discussed in Sections 13.2.5 and 13.2.6, tentative specifications require an increase in the mean velocity (Tables 13.4 and 13.5).

### 13.4 Vibration

A vibration is a reciprocating or oscillating motion that repeats itself after an interval of time, Fig. 13.10. This interval of time is referred to as the *period* of vibration and is measured as a unit of time per cycle, such as seconds per cycle. The *frequency* of vibration is numerically equal to the reciprocal of the period and is measured as the number of cycles per unit of time, cycles per second. The maximum ordinate of the curve of Fig. 13.10 represents the maximum displacement of the vibrating body from its position of equilibrium and is referred to as the *amplitude* of vibration.

All structures have a *natural frequency* such that when an external dynamic force acting on the structure comes within the natural frequency range, a state of vibration may be reached whereby the driving force frequency and the body's natural frequency are in

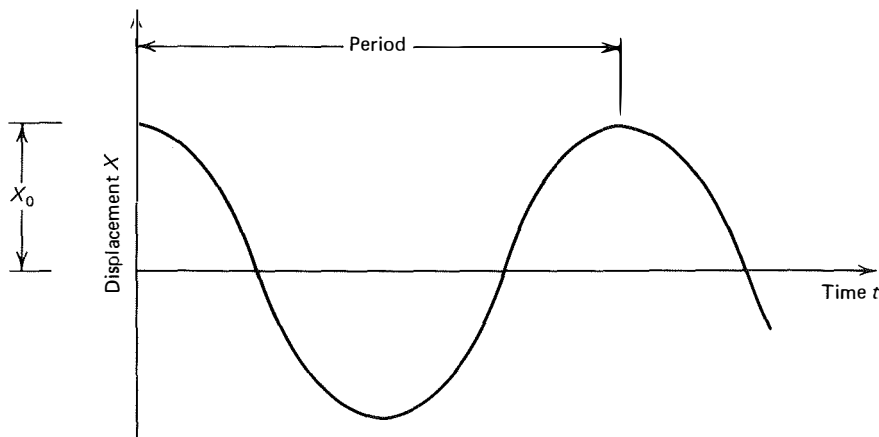


FIGURE 13.10 Undamped free vibration starting from an initial displacement.

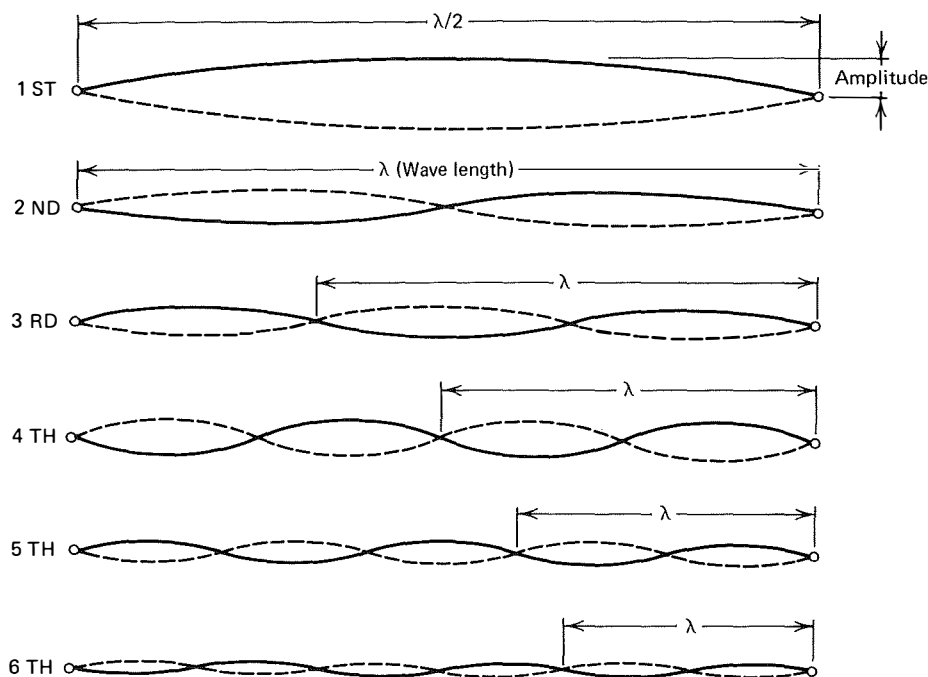


FIGURE 13.11 Modes of vibration.

tune, a condition referred to as *resonance*. At resonance the structure undergoes violent vibration, often resulting in major structural damage. A familiar example of resonance is the shattering of a glass by a particular musical note or sonic vibration.

When an external dynamic force (wind) is applied to a mass, such as a cable or bridge deck, the mass will be set into a vibratory motion. This vibratory motion can be represented by an infinite number of superimposed modes of vibration, Fig. 13.11. If one of these modes coincides with the natural frequency of one of the lower modes, and if the imposed force has a periodic component of the same frequency, then resonance will occur. The amplitude or displacement will be increased and the effect of the pulsating force may also increase. This is why marching troops break step when crossing a bridge. The two dynamic response phenomena associated with flexible systems are forced vibrations and self-induced vibrations, which are discussed in subsequent sections.

#### 13.4.1 FREE VIBRATIONS

When an externally applied disturbance acting on a structure is removed, the structure will respond to the removal of the excitation by vibrating. When a mass is displaced and then released, for example, as a result

of an initial velocity produced by an impulse or impact such as a moving load, motion will occur as the result of the initial displacement.

#### 13.4.2 FORCED VIBRATIONS

Forced vibrations are those produced by a time-dependent externally applied force that is impressed on the structure; examples are wind, or displacements caused by earthquakes. The magnitudes of these forces or externally applied displacements are independent of the motion of the structure. The response of the structural system diminishes with time as a result of damping. While the excitation force is active, there is a forced vibration. When the excitation is removed the response is a free vibration.

#### 13.4.3 SELF-EXCITED VIBRATIONS

Self-excited vibrations are those caused by forces produced by the displacements or deformations of the system. Forces causing these vibrations cease when the motion stops, whereas in forced vibrations the external force is independent of the motion. In this type of vibration, the structure's own movement is exerting an additional energy to that of the exciting force, Fig. 13.12.

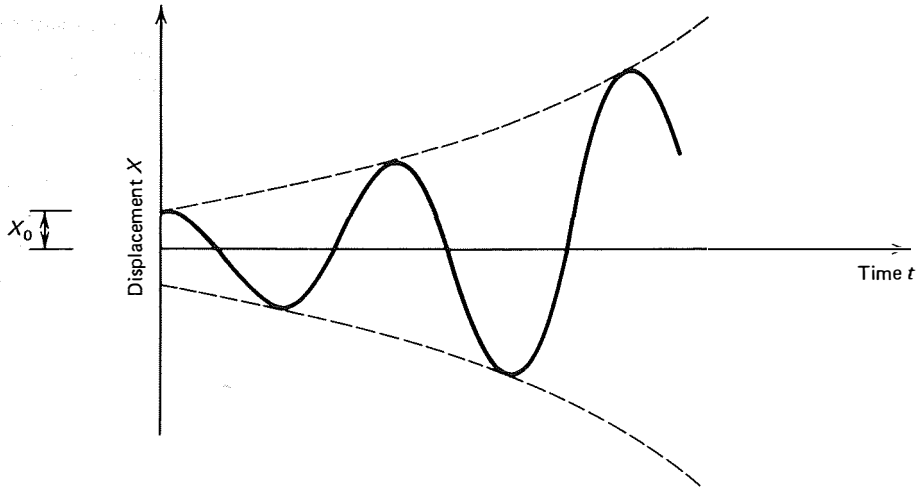


FIGURE 13.12 Self-excited vibration.

13.4.4 DAMPING

The vibratory motion indicated in Fig. 13.10 is classified as undamped vibration and theoretically would continue indefinitely. Vibrations can be diminished if a damping force can be provided that will act in a direction opposite to the movement of the structure. In aerodynamic vibration, the wind is exerting energy into the structure. This energy is then dissipated by the internal frictional resistance of the molecules of the material, the drag effect of the medium surrounding the structure, or dry frictional resistance resulting from the slippage of structural connections between members or between the structure supports. When the cause of vibration is removed from a vibrating structure, the vibration will decay or damp as a result of the dissi-

ipation of energy within the structure, Fig. 13.13. A piano string that has been set to vibrating by the striking of a hammer will gradually stop due to air resistance and internal friction.

The degree of structural damping is expressed as the logarithmic decrement  $\delta$ . It can be defined as the logarithm of the ratio of two consecutive peaks (amplitudes).<sup>13,27</sup>

$$\delta = \log \left( \frac{X_{n-1}}{X_n} \right) \quad (13.28)$$

see Fig. 13.13

Lack of available data prevents estimation of damping in a bridge. The impracticability of exciting a large bridge prohibits the measurement of damping of existing structures. However, any slipping motion be-

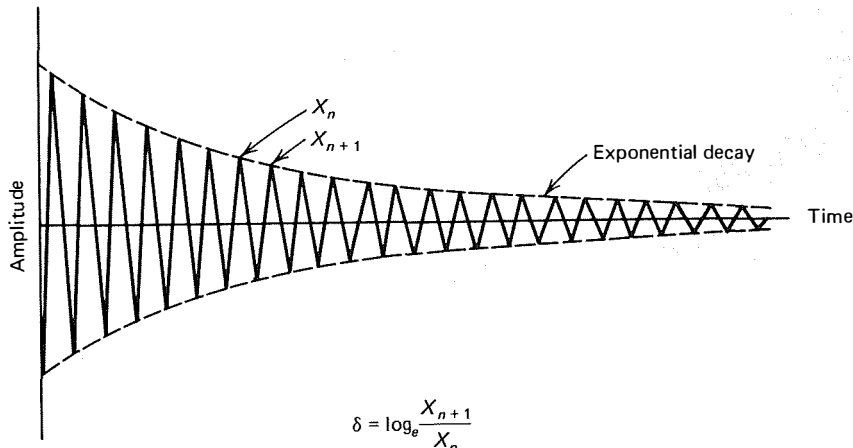


FIGURE 13.13 Exponential decay of a free vibration with viscous damping.

tween component parts of a structure will increase the damping value because it helps to dissipate the energy. Thus, bolted connections which may slip a little will have better damping characteristics than welded connections. The friction developed by stringers sliding on transverse floor beams will develop a higher damping value than an orthotropic plate deck. From observations of movements on the shop welded, field bolted cable stayed Long's Creek Bridge, the logarithmic decrement  $\delta$  was estimated to be 0.065.<sup>12</sup> Model tests of the Golden Gate Bridge were compatible with the prototype if a value  $\delta = 0.031$  were assumed.<sup>28</sup> The logarithmic decrement was assumed as zero for the deck of the all-welded Severn Bridge; however, the diagonal hangers were estimated as having a value of  $\delta = 0.052$ . The actual damping value for the deck was used as "insurance" or taken as a bonus.<sup>23</sup> Damping devices are not normally built into bridges. However, as a temporary measure, weighted boxes were suspended from the deck of the Long's Creek Bridge and im-

mersed in the water below as a means of damping the oscillations until permanent corrective measures could be applied (Section 13.1.2).

### 13.5 Wind Effects—Aerodynamic

There are several mechanisms of interaction between wind and structure that produce a vibration in the structure, but only three of the mechanisms are important to bridge design. They are vortex shedding, flutter, and turbulence.

#### 13.5.1 VORTEX SHEDDING

If a steady wind blows against a cylinder or other obstruction, the wake consists of a special turbulence termed the Von Karman vortex street or, for brevity vortex shedding, Fig. 13.14. Vortexes are formed as a result of air flowing around a cross section and sepa-

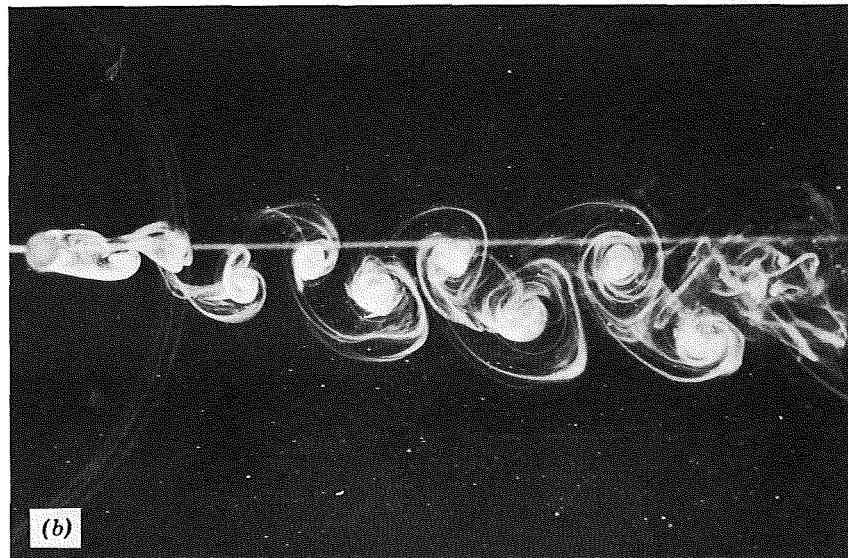
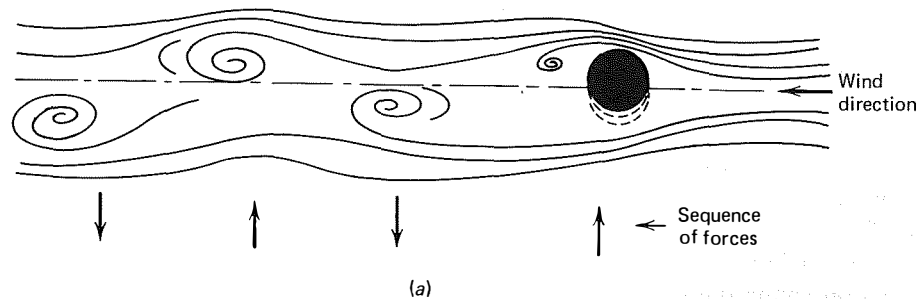


**FIGURE 13.14** (a) Schematic vortex street and (b) vortex shedding behind a cylinder in water using fluorescein dye at a very low Reynolds number (between 2000 and 3000). (Courtesy of R. L. Wardlaw).

rating from the boundary of that section. The shedding of these vortexes on the leeward side is representative of forces acting on the cross section at right angles to the direction of the wind in an alternating and periodic fashion.

It is important to note, that the oscillations of the section are not produced by the vortexes. They are merely a convenient physical and mathematical indication from which the air flow around the cross section, and the resulting forces that are acting, may be inferred, formulated, and computed.<sup>24, 25, 29</sup>

Any bluff object will shed vortexes when placed in a wind stream. If a bridge deck represents a solid section, such as a plate girder or box girder, the entire deck, as a unit, will shed vortexes. Bridge towers, cables, and hangers will also produce a vortex trail.

The unsteadiness of forces produced by the wind flow around an object can be separated into three components: the time-dependent fluctuation of force resulting from the separation of the wind flow around the section, even in a steady flow; the unsteadiness due to the structure's own movement; and the unsteadiness or turbulence of the wind itself. These components are not necessarily independent and they frequently occur simultaneously.

Although the vortex shedding is a complicated phenomenon in fluid mechanics, the frequency of shedding can be expressed by the simple equation

$$S = \frac{fD}{V} \tag{13.29}$$

where  $f$  is the frequency of vortex formation on one side of the wake,  $D$  is the dimension of the body normal to the wind flow,  $V$  is the wind velocity, and  $S$  is the dimensionless Strouhal number. The value of the Strouhal number is a function of the geometry of the section and a nondimensional Reynolds number defined as

$$R_e = \frac{\rho VD}{\mu} \tag{13.30}$$

where  $\rho$  is the mass density of the fluid (air),  $V$  is the wind velocity,  $D$  is the dimension normal to the flow, and  $\mu$  is the viscosity of the air. The ratio  $\mu/\rho$  is defined as the kinematic viscosity of air  $\nu$ ; thus the Reynolds number becomes

$$R_e = \frac{VD}{\nu} \tag{13.31}$$

The value of the Strouhal number for a given shape is reasonably constant over large ranges of the Reynolds number. The Strouhal number for circular cylinders

has been experimentally established for a Reynolds number range of  $10^2$  to  $10^5$  as approximate values of 0.2 in a smooth flow and 0.25 in a turbulent flow. Experimental work at the Fairbank Highway Research Station wind tunnel by Robert A. Komenda has established a value of 0.22 for the Strouhal number of a helical strand cross section (thesis is unpublished at this writing). For square cross sections in natural wind,  $S \approx 0.11$ .

The frequency of the vortex trail is representative of the oscillatory force on the section. When the wind velocity is such that the frequency of the vortex trail corresponds to the natural frequency of the structure or member, it is possible for large amplitudes of vibration to occur. The magnitude of the amplitude will depend on the structural damping and geometry of the section. Slenderness and streamlining of a deck section reduces the tendency of the air flow to separate from the section and will, in effect, narrow the vortex wake, reducing the intensity of the vortexes and thus the magnitude of the oscillatory forces.<sup>13</sup>

The motion response of the structure will occur over a narrow band of wind velocity near the critical resonant value. After passing through resonance, increasing velocity will cause the exciting or vortex frequency to be larger than the natural frequency and the amplitude will decrease.

Wind tunnel tests on a model of the Long's Creek Bridge were conducted by Wardlaw<sup>12, 27</sup> in Canada, Fig. 13.15, and show that vortex shedding is limited

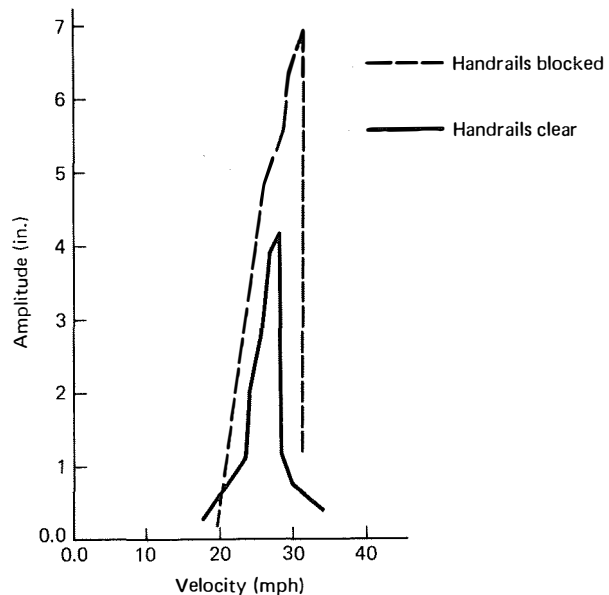


FIGURE 13.15 Long's Creek Bridge, wind tunnel observation on vertical motion, from reference 13.

in amplitude and is confined to narrow velocity ranges. It should be noted, however, that for flexible structures in a natural wind environment, the periodic vortex shedding frequency may be slightly altered by turbulence in the air stream and the structure's own motion. Therefore, there is a tendency to arrive at the structure's natural frequency over a wide range of wind speeds.<sup>14</sup>

A contributing factor to the collapse of the original Tacoma Narrows Bridge was an approximately 39-ft-long Karman vortex which occurred during a steady 42-mph wind. Oscillations had occurred for two hours during a 38-mph wind velocity. When the wind increased to 42 mph, the structure entered a torsional vibration mode, which had an angular rotation of about 45 degrees with the deck in each direction. This continued for another hour until failure finally occurred.

Analytical solutions for the elimination of vortex excitations are not available. Wind tunnel tests can indicate the type of cross sections which cause minimal excitations. Desirable cross sections are those that allow a laminar flow pattern around them.

### 13.5.2 FLUTTER

A self-induced vibration is produced by a change in the wind force as a result of the structures' own motion. If this vibration opposes the motion, then it is said to have a damping effect. If it adds to the motion, the oscillations can build up to dangerous amplitudes. Only a few sectional shapes are sensitive to this condition. However, all shapes develop a simultaneous aerodynamic coupling of torsional and vertical motion known as flutter, which lies between the natural frequencies of the structure for vertical flexure and torsion. As wind velocity increases, a critical velocity will be reached whereby flutter is incipient. As described for the Tacoma Bridge, flutter is characterized by a rapid buildup in amplitude with little or no increase in wind speed, and there is a distinct possibility that a catastrophic amplitude may be produced in a few cycles of motion.

Mass and ratio of torsional to vertical bending natural frequencies are the factors that govern the wind speed that will cause flutter. No analytical methods are available to predict critical velocity of bridge deck structures. Bleich<sup>30</sup> has presented a method whereby critical velocities can be achieved for a flat plate, which might be considered an idealization of a bridge deck. Experience has indicated that bridge decks will have a lower critical velocity than a flat plate.

German<sup>31</sup> wind tunnel tests on various types of cross

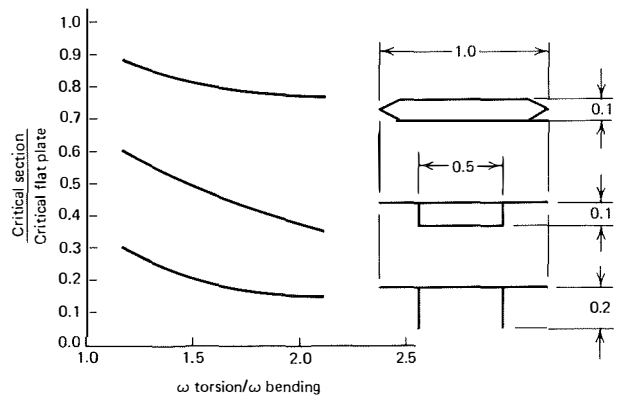


FIGURE 13.16 Flutter speeds for various bridge cross sections. (Taylor, Engineering Journal (Canada), November 1969, from reference 14.)

sections have produced sufficient data to experimentally determine shape factors in some instances and obtain a bridge critical velocity. This velocity is a function or percentage of the value for a flat plate with an equivalent inertia and elastic properties. Taylor<sup>14</sup> has published flutter speeds for various bridge cross sections, Fig. 13.16. They indicate that the percentage variation approaches 100 for streamline shapes and decreases to 20 for bluff, open shapes. However, some care must be exercised when generalizing these results. Where there is doubt, model tests should be used.<sup>32</sup>

### 13.5.3 TURBULENCE

The natural wind is turbulent or gusty rather than smooth and uniform in character. Thus turbulence results in velocity fluctuations in both vertical and horizontal directions. These fluctuations are random in nature because they do not occur at a particular frequency but are distributed over a band of frequencies. The structure will respond to these random fluctuations when they occur at or near frequencies of the bridge. Wind acting on a structure will always have spatial variations; that is, distribution along the height and length of the structure will not be uniform. At any instant in time, the velocity will not be constant in direction or magnitude.

As a consequence of turbulence, vortex shedding excitation becomes more difficult to determine than that in smooth flow. Critical flutter velocities for vortex shedding are higher than those in smooth flow. The combined effects of vortex shedding and higher critical flutter velocities have a greater influence on the longer spans.

### 13.6 Wind Tunnel Testing

Because of nonexistent or cumbersome analytical procedures, wind tunnel tests are a convenient and economical method to establish aerodynamic characteristics and stability of a structure. There are two types of wind tunnel tests, the full model test simulating the atmospheric boundary layer, and the so-called static section model test. These will be discussed separately in the following sections.

#### 13.6.1 BOUNDARY LAYER FULL MODEL TEST

A full model is a scaled down, 1/200 or higher, reproduction of a structure with suitably scaled dimensions, moments of inertia, and elastic characteristics. There is some doubt by engineers concerning the validity of testing at greatly reduced scales. There are scale effects within limits which cannot be ignored. Usually in this type of testing the terrain, as well as the structure, is usually modeled.

Often the exposure of a structure to aerodynamic effects is significantly different for different wind directions. A bridge crossing a wide river may be exposed to strong steady winds perpendicular to the bridge, but turbulent winds may occur parallel to the bridge. The question of terrain roughness becomes important when attempting to assess the wind strength at the site of a structure from weather data recorded at a distance from the site. Davenport<sup>33</sup> has indicated in a recent investigation of the Narrows Bridge in Halifax that sectional model tests are not a reliable representation of the total stability of the structure. However, tests of this type may be useful to determine general stability under conditions of partial erection. Full model tests of the Narrows Bridge will be discussed in Section 13.10.5.

#### 13.6.2 SECTIONAL MODEL TEST

In a sectional model test only a representative portion of the bridge suspended structure is tested. The scale may be in the range of 1/30 to 1/50. The scale test specimens are larger and modeling costs are lower than for the full model method. The model is mounted on springs to have the appropriate scaled mass, moment of inertia, and frequencies.

In a static wind tunnel test, the sectional model of the deck is subjected to various wind velocities at various angles of attack. The reaction forces of lift, drag, and moment are carefully measured. Static drag, lift, and moment curves are obtained by plotting the di-

mensionless coefficients  $C_D$ ,  $C_L$ , and  $C_M$ , for various angles of attack, Fig. 13.9.

These plots are significant because the slope of the lift and moment curves indicate stability or instability of the section. The steeper the positive slope in the central range, the greater the stability, and, conversely, the steeper the negative slope, the greater the instability.<sup>24</sup>

In full model testing it is possible to test with a properly simulated turbulent flow. Techniques have not been developed as yet to properly simulate turbulent flow for the larger sectional model tests. It is normal practice to test sectional models in a steady flow on the assumption that the results are conservative for turbulent flow. The assumption of conservatism is based on the fact that turbulent flow reduces the susceptibility to vortex excitation and raises the critical flutter speed. However, this assumption is questioned by the writers of the tentative Japanese specifications for wind<sup>19</sup> (Sections 13.2.5 and 13.2.6).

#### 13.6.3 DYNAMIC SIMILARITY

So that the prototype structure and the model agree, there must be an equality of the several nondimensional parameters between prototype and model<sup>12,13,34</sup> indicated below by category, such as

$$\frac{V}{N_y D}, \quad \frac{V}{N_\theta D} \quad (13.32)$$

where  $N_y$  and  $N_\theta$  are the natural frequencies in vertical flexure and torsion respectively

$$\frac{m}{\rho D^2}, \quad \frac{J}{\rho D^4} \quad (13.33)$$

where  $m$  and  $J$  are the mass per foot of span and mass moment of inertia per foot of span, respectively, and  $\rho$  is the air density, and

$$\delta_y, \quad \delta_\theta \quad (13.34)$$

are the logarithmic decrement in vertical flexure and torsion, respectively.

In addition to the above parameters for agreement, there must be agreement of the center of gravity and the axis of torsional movement between prototype and model. The wind velocity scale is established from equation 13.32 such that

$$\frac{V_p}{V_m} = \frac{D_p N_p}{D_m N_m} \quad (13.35)$$

where the subscripts  $p$  and  $m$  refer to the prototype and model, respectively.



### 13.6.4 AERODYNAMIC SIMILARITY

The parameter that establishes the equivalency between prototype and model is the Reynolds number,  $VD/v$ . It is impractical, in wind model tests, for the Reynolds number of the model to achieve similarity to that of the prototype. However, it has been shown<sup>35</sup> in model tests conducted for the Severn Bridge that, for commonly used cross sections of sharp-edged bluff bodies, the flow similarity can be practically achieved even with large variations between model and prototype parameter values. In the Severn Bridge investigations it was found that the forces on the model are sensitive to Reynolds number below  $R_e = 2 \times 10^6$ .

However, at larger values it was found that the forces were virtually independent of the Reynolds number. The above investigations were conducted on sectional models. Therefore, the validity of aerodynamic testing of full models at greatly reduced scales is questioned by some engineers because there are some limits for which the scaling effects can no longer be safely ignored.<sup>13</sup>

### 13.7 Stability of Stayed-Girder Bridges

Having established some degree of understanding of wind forces and their effects, let us now investigate and compare the aerodynamic capabilities of a cable-stayed system with that of a conventional suspension system. The modes of vibration of a suspension system are the symmetric and antisymmetric modes, Fig. 13.17.<sup>27</sup> In the symmetric mode, the towers are deflecting toward each other, causing the center span to deflect while the end spans are cambering. In the antisymmetric mode, the towers are deflecting in the same direction, resulting in the antisymmetric deformation pattern with respect to the midspan.<sup>27</sup>

In a suspension bridge, the most dangerous mode of oscillation is the antisymmetric flutter mode, Fig. 13.18(a). This type of oscillation caused the destruc-

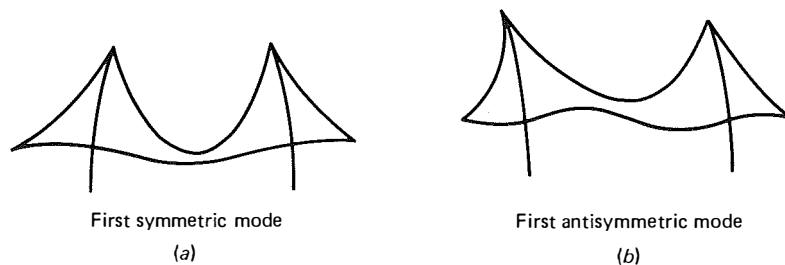


**FIGURE 13.17** Longitudinal modes of vibration: (a) first symmetric mode and (b) first antisymmetric mode, from reference 27.

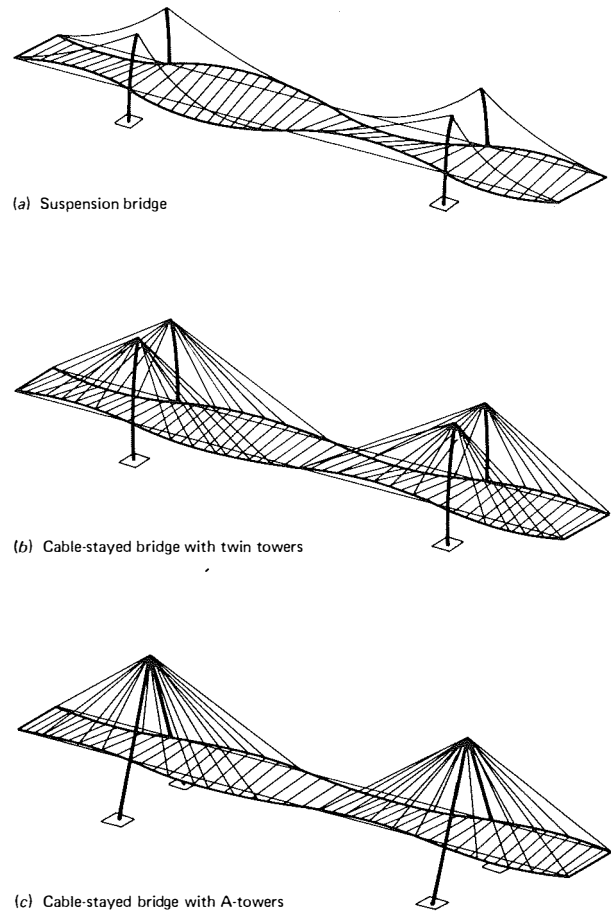


**FIGURE 13.18** Relative deformations: (a) suspension bridge, (b) cable-stayed bridge with twin towers, and (c) cable-stayed bridge with A-towers. (Leonhardt and Zellner. By permission of the Canadian Steel Industries Construction Council, from reference 3.)

tion of the Tacoma Narrows Bridge. This specific mode is easily developed by the pitching moment of wind forces; the two cables move in opposite directions in half the span length—one goes up while the other goes down. Since the cable system provides no resistance to the induced torsional deformation of the deck, a

relatively high torsional and bending restraining deck system is required.<sup>3,36</sup> This mode of oscillation can be restricted if the cables are attached to the girder or truss at the center of the structure, because the cable at this point is attempting to move in opposite directions simultaneously. This method was used in an effort to stabilize the Tacoma Narrows Bridge, but the connection broke and the structure reverted into the first antisymmetric mode and was consequently demolished within an hour.<sup>27</sup>

It is relatively more difficult to provide and maintain a resonant oscillation with attendant large amplitudes in a multicable stayed structure. The cables of different lengths and different frequencies tend to disturb the formation of the first or second mode of oscillation by interfering with smaller wave lengths of higher order. Thus, the inherent system damping of the cable-stayed structure produces relatively smaller amplitudes compared with the suspension system. The difference in deflection of the girders in the two cable planes of a cable-stayed system results primarily from the different deflections of the pylons in each plane, Fig. 13.18(b). For an A-frame tower, the differential deflection of the towers in each cable plane is negated, and the resistance of the cable-stay system to torsional oscillations of the roadway deck is further enhanced, Fig. 13.18(c).<sup>3,36</sup>

As a result of the inherent system stiffness and damping, the cable-stayed bridge is not as sensitive to wind oscillations as the suspension bridge. Therefore, the cable-stayed bridge requires less torsional stiffness in its suspended deck system. However, this conclusion is only qualitative. The difference in response of the two systems has yet to be demonstrated by wind tunnel tests of sectional models.

### 13.8 Deck Stability

Numerous wind tunnel tests by investigators in several countries have indicated that bluff cross sections have characteristics that produce intense Karman vortex shedding and large fluctuating vertical forces, which result in vertical bending coupled with a torsional response. These tests have led to the development of a cross-sectional shape that is considered to have favorable aerodynamic characteristics. Aerodynamic stability of suspension and cable-stayed bridges can be achieved by shaping the cross section such that.<sup>3,36</sup>

1. The wind eddies that produce the Karman vortex shedding effect will be diminished or eliminated.

2. A minimum of lift and pitching moments will be produced to minimize the bending and torsional oscillation.

Additional studies and tests have tended to validate this conclusion. Therefore, it can be stated that the conventional stiffening truss of the Verazzano Narrows suspension bridge, Fig. 13.19 is designed for increased flexural and torsional stiffness to resist the effect of wind forces. Whereas the aerodynamically "streamlined" cross section used on the Severn suspension bridge in England, Fig. 13.20 is designed to minimize the excitation force and motion which cause aerodynamic instability. As a result, the streamlined cross section seeks to eliminate the cause rather than totally resist the effect. A secondary improvement to some designers is the aesthetics of the structure.

Leonhardt first reported this concept of streamlining the cross section for cable-stayed bridges in 1968,<sup>37</sup> although aerodynamic tests were conducted in 1959 for a monocable suspension structure that was unsuccessful in the Tagus River Bridge competition at Lisbon. This same concept was again proposed unsuccessfully for the Rheinbrücke-Emmerich bridge.

The first modern structure to use the aerodynamically shaped cross section in its deck structure was the Severn Bridge in England, designed by Freeman, Fox and Partners. Christen Ostfeld of Copenhagen used the streamlined concept on the Lillebelt Bridge in Denmark, although the original design was made with the conventional stiffening girder concept. Freeman, Fox and Partners have also used the streamlined cross section in the Bosphorus Bridge. Therefore, aerodynamic stability can be attained even for extremely long spans with a sufficiently wide aerodynamically-shaped girder that is continuous at the pylons. Although the previous discussion has indicated a relatively favorable response for cable-stayed structures compared to the conventional suspension structure, disturbing aerodynamic oscillations can and do occur in cable-stayed bridges.

It has been illustrated that the cable-stayed system is not as sensitive to wind oscillations as a suspension bridge because of the inherent system stiffness and damping. Further, it has been shown that vortex shedding, bending and torsional oscillations can be minimized with streamlined deck cross sections. However, the reader is cautioned that these conclusions are generalizations based on data available from limited tests conducted on relatively few structures. It is suggested that wind tunnel tests be performed for any major cable-stayed structure.

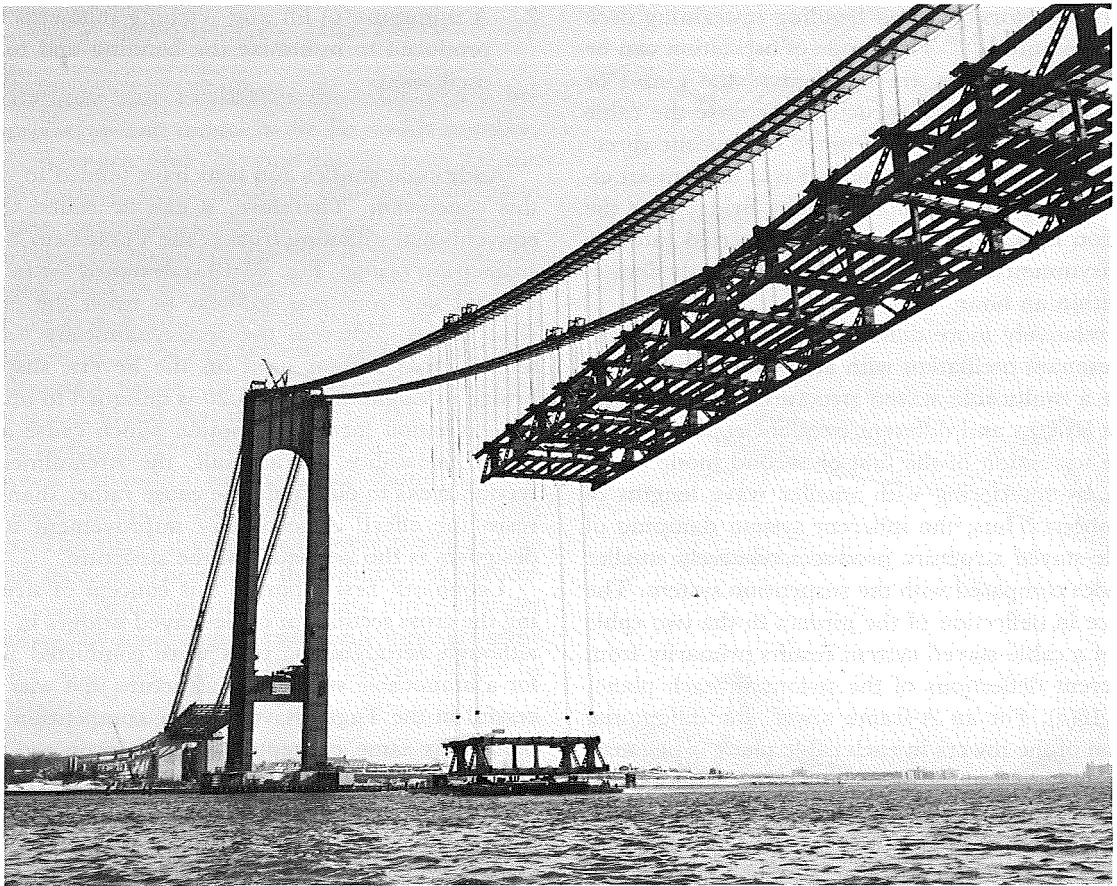


FIGURE 13.19 Verrozano Narrows Bridge, New York.

### 13.9 Stability During Erection

It is most important to note that the validation of stability of the completed structure for expected wind speeds at the site is mandatory. However, this does not necessarily imply that the most critical stability condition of the structure occurs when the structure is fully completed. A more dangerous condition may occur during erection, when the joints have not been fully connected and, therefore, full stiffness of the structure has not yet been realized. In the erection stage, the frequencies are lower than in the final condition and the ratio of torsional frequency to flexural frequency may approach unity. Various stages of the partially erected structure may be more critical than the completed bridge. The use of welded components in towers has contributed to their susceptibility to vibration during erection.

The erection method used in the Severn Bridge,<sup>38</sup> Fig. 13.20 was to hoist 60 ft long segments of the deck

structure from barges on the river to their connection to the suspender ropes. With only a moderate structural connection between segments, the critical flutter speed was established at less than 50 mph. By introducing a more effective torsional connection, the critical speed was raised to 100 mph for all stages of erection, Fig. 13.21. Scruton also noted that while the individual components were being erected, they were subject to violent yawing and pitching oscillations at low wind speeds unless a system of check ropes was operative.<sup>38</sup> Contractors must assure themselves that the structure will be aerodynamically stable during erection.

Component parts of the structure are also in themselves susceptible to wind excitation, either during erection or in the final condition. The cables of cable-stayed bridges, the hangers of suspension and arch bridges, and the towers of suspension and cable-stayed<sup>39</sup> bridges have been known to exhibit oscillations, usually from vortex excited vibrations.

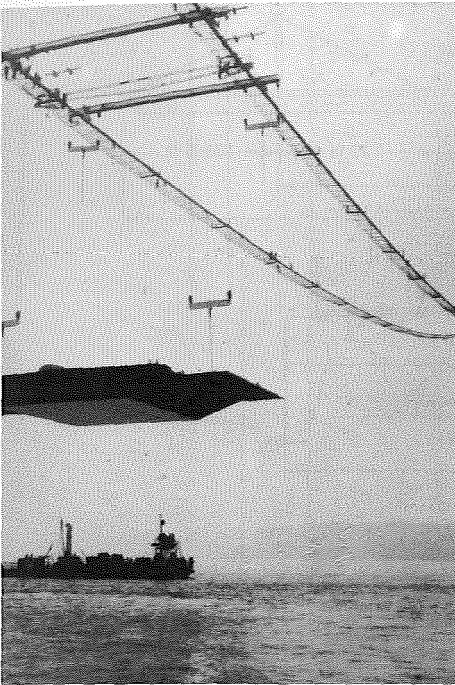


FIGURE 13.20 Severn Suspension Bridge, England.

### 13.10 Wind Tunnel Investigations

Because no other analytical procedures are yet available, wind tunnel tests are used to evaluate the aerodynamic characteristics of the cross section of an existing or proposed bridge deck, tower, or total bridge. More importantly, the wind tunnel tests may be used during the design process to evaluate the performance of a number of proposed cross sections for a particular project. In this manner, the wind tunnel investigations become a part of the design decision process and not a postconstruction corrective action. The following dis-

cussion of specific structures that have been investigated by wind tunnel tests has been extracted from reference 13 unless otherwise noted.

#### 13.10.1 LONG'S CREEK BRIDGE, CANADA

The Long's Creek Bridge in New Brunswick, Canada, has a center span of 713 ft, with two vertical cable planes in cross section and only one pair of radiating stays from each pylon, Fig. 13.22(a). At wind speeds of 30 mph, the structure was observed to have a vibration frequency of 0.6 cps and an amplitude reaching 4 in., or 8 in. when snow fills the railing openings,<sup>12,27</sup> (Fig. 13.15). The bluff cross section produces an unfavorable aerodynamic section, Fig. 13.22(b). The single pair of stays in each plane has a natural low resonant oscillation. If three to five stays had been used, the system damping as a whole would have been increased.<sup>36</sup> As a result of wind tunnel tests, a soffit, or bottom plate, was installed to produce a closed box section, thus increasing torsional stiffness, Fig. 13.22(c). The addition of the soffit plate decreased the amplitude of motion by as much as 40%, Fig. 13.23.

Additional streamlining of the cross section by the addition of triangular edge fairings further reduced amplitude. The values indicated in Fig. 13.23 are for a height of structure 15 ft above water. The structure was 100 ft above water level before the reservoir in the valley below the bridge was filled. Further tests established that had the structure been maintained at an elevation of 100 ft, symmetrical edge fairings would have been required, Fig. 13.24.

A study was also conducted to determine the effect of girder perforations, Fig. 13.25. A 30% perforation would have been required to reduce the motion to an acceptable level. However, this condition would have had serious effects on other aspects of the design.

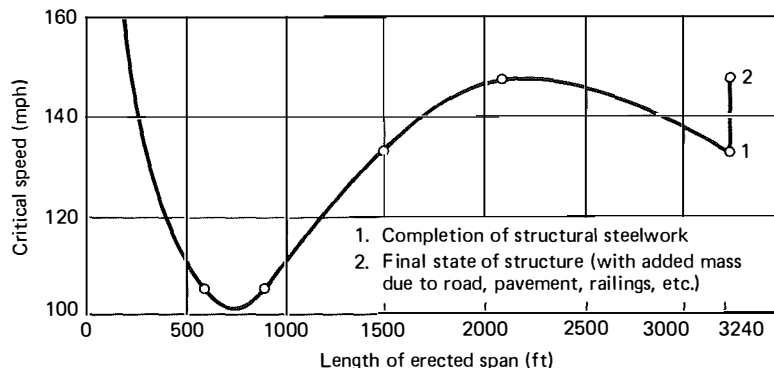
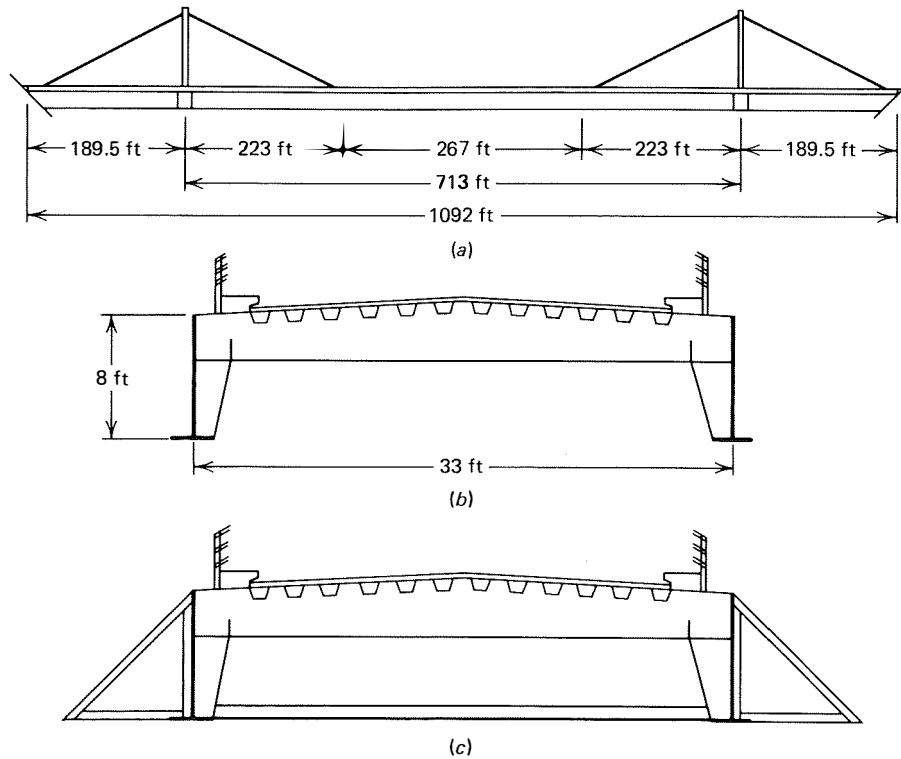


FIGURE 13.21 Severn Suspension Bridge, variation of critical wind speed with length of erected center span, from reference 38.



**FIGURE 13.22** Long's Creek Bridge, from reference 13, (a) elevation, (b) original cross section, and (c) section after fairing.

### 13.10.2 KNIEBRÜCKE, WEST GERMANY

The usual wind tunnel tests of a section model of the Kniebrücke Bridge in Düsseldorf indicated instability at high wind speeds. The instability was thought to be due to the sensitivity to torsional oscillation attributed to the omission of the bottom plate, which would have formed a closed box section.<sup>3</sup> Because of the width of the structure, this bottom plate was deliberately omitted as an economy measure, Fig. 13.26(a). The reason the bridge has not shown any signs of disturbing oscillations has been attributed to its low elevation above the water level and to turbulence caused by the urban terrain.

Further studies were performed to determine whether remedial measures could be undertaken should undesirable wind oscillations develop in the prototype bridge. These studies indicated that an additional lining outside of the main girders would be sufficient to produce stability, Fig. 13.26(b). As a consequence, Leonhardt<sup>3,36</sup> has proposed that a cross sectional configuration with triangular boxes at the edges and an open bottom deck be used on subsequent structures. He has further suggested that the slope of the soffit

plate of the outside edge boxes should not exceed an angle of 35 degrees.<sup>3</sup>

### 13.10.3 PROPOSED NEW BURRARD INLET CROSSING, CANADA

Wind tunnel tests were conducted at the National Physical Laboratory in Ottawa<sup>13,40,41,42</sup> on a proposed structure with an approximately 2500-ft main span in Vancouver, B.C., on Canada's Pacific Coast. The deck of this bridge is to have an elevation of 208 ft above mean sea level at the towers.

Section model tests were conducted on six basic bridge configurations: (1) plate girder suspension bridge, (2) stiffening truss suspension bridge, (3) box girder suspension bridge, (4) trapezoidal box girder cable stay, (5) twin edge triangular box girder cable stay, and (6) box section cable stay. A number of variations were also studied that considered edge geometry, deck perforations, and girder perforations.

The trapezoidal box section was found to exhibit a degree of instability at low angles of attack that made it unacceptable, Fig. 13.27(a). Edge modifications provided a high degree of stability, Fig. 13.27b. Water

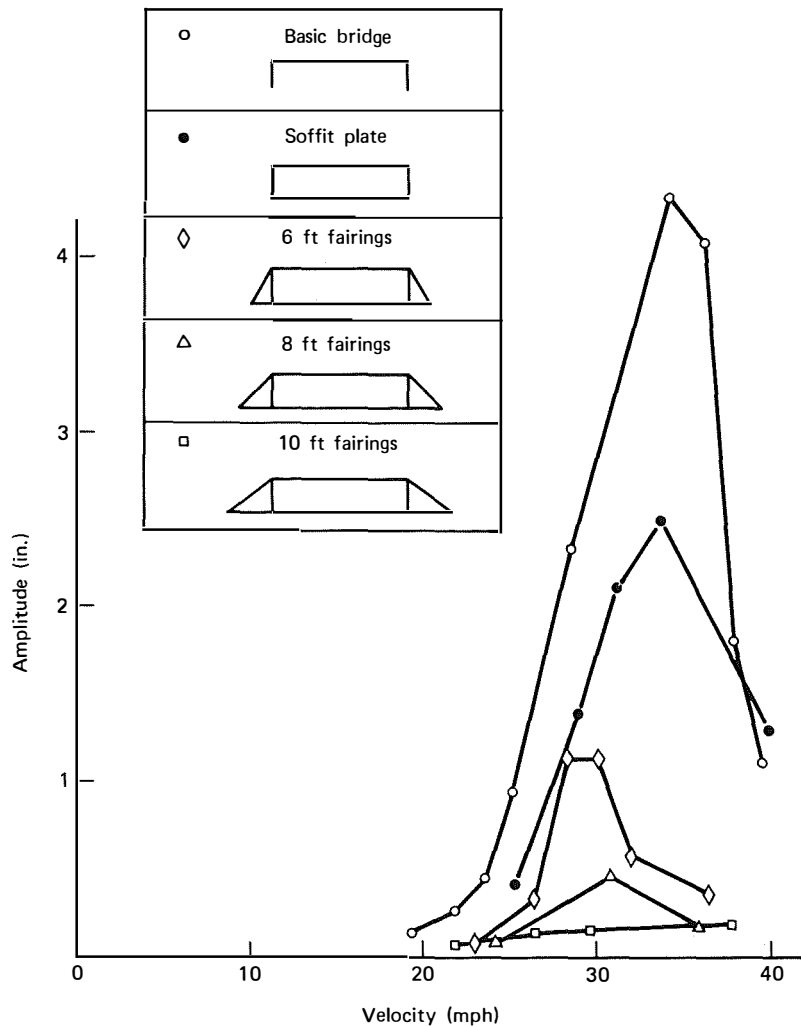


FIGURE 13.23 Long's Creek Bridge, vertical amplitude with asymmetric fairings, effect of fairing width (bridge height = 15 ft), from reference 13.

tunnel flow test at an angle of attack of +4 degrees show a large separated flow with no reattachment and a wide wake for the initial section, compared with the reattachment at the upper and lower surfaces and a narrower wake for the modified section, Fig. 13.28. These comparison features were evident at angles of attack as high as plus or minus 10 degrees.

Wind tunnel tests were conducted for a twin triangular edge box girder section to determine the necessity for torsional stiffness and requirements for extremely wide bridges with a streamlined cross section, Fig. 13.28. These tests indicated that aerodynamic stability could be achieved on the deck cross section without the enclosing bottom plate and without consideration of the favorable system damping provided by

cable stays. The performance of the section is due to the incorporation of a downward sloping wind nose at the top outside edges.

13.10.4 PASCO-KENNEWICK INTERCITY BRIDGE, U.S.A.

The concrete girder of this structure has a much higher mass than that of other structures considered in the design studies. The superstructure cross section is a twin triangular edge box configurations with a depth to width ratio of 11, Fig. 4.25. The deck streamlining provided a highly favorable aerodynamic response despite the low value of the ratio of torsional frequency to vertical bending frequency of  $(N_\theta/N_y) = 1.4$ .

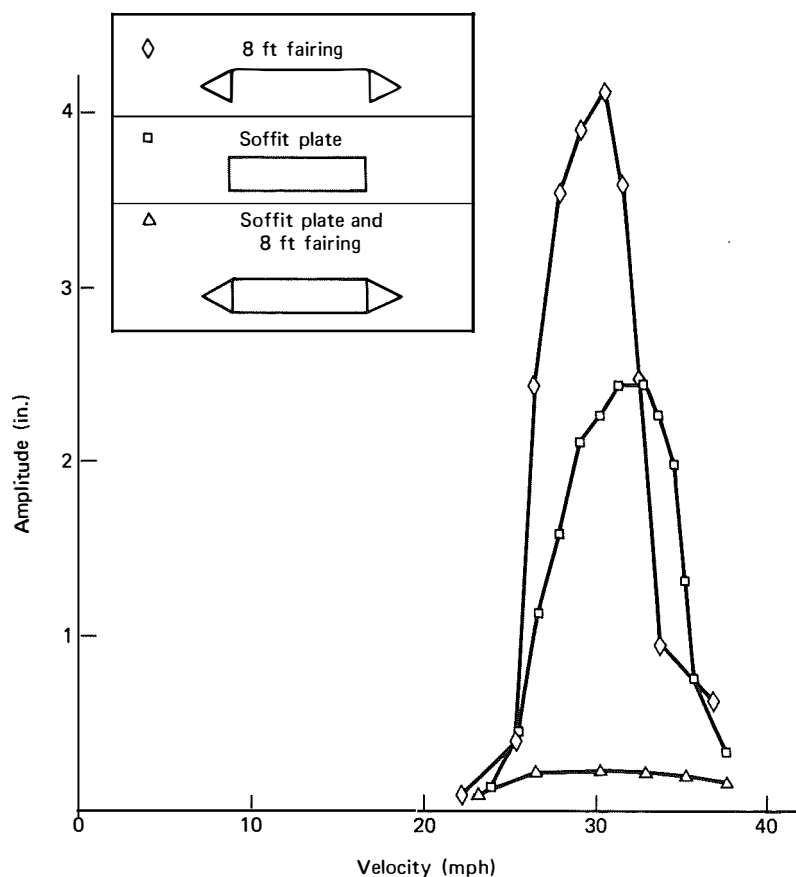


**FIGURE 13.24** Long Creek Bridge, vertical amplitude with soffit plate and 8 ft symmetric edge fairings (bridge height = 100 ft), from reference 13.

A number of damping coefficients and edge configurations were investigated, and a typical result for a bridge height above water of 57 ft is shown in Fig. 13.29. As indicated, flutter and vortex excitation oscillations were found to exist at large angles of attack and velocities of the wind that are above those assumed for design at the site.

#### 13.10.5 THE NARROWS BRIDGE, CANADA

The Narrows Bridge, Halifax, Canada, is a suspension bridge with a center span of 1400 ft, end spans of 513 ft 10 in., and a vertical navigation clearance of 165 ft at midspan. This structure is important because it is one of a few bridges that has been tested using not only a section model but also a full model test in both uniform flow and turbulent boundary layer flow.<sup>33,43</sup>

Comparisons of test results were made in this study for a 1/40 and 1/320 scale section model and a 1/320 full bridge model in both uniform flow and turbulent boundary layer flow. Based on wind normal to the

longitudinal axis of the bridge, the following observations were made: (1) the section models exhibited a coupled vertical-torsional oscillatory instability at critical wind velocity; (2) a divergent instability was noted for the full model in a uniform flow at velocities well above the critical velocity observed for the sectional model; (3) for the full model in turbulent flow, random vertical oscillations were observed to increase in amplitude with increased wind velocity and turbulence but no instability or torsional motion was recorded.

The results are very dissimilar, especially between the section model and full model tests in uniform flow. They are also contrary to previous conclusions derived from the work of Farquharson et al.<sup>1</sup> and Frazer and Scruton<sup>44</sup> whose data formed the basis for the validity of the procedure for section model testing. At first it was felt that the difference in scale of 1/40 for the section model compared to the scale of 1/320 for the full model accounted for the dissimilarity of results. However, comparison of the results for the 1/40 and 1/320 sectional models were in fairly good agreement, which

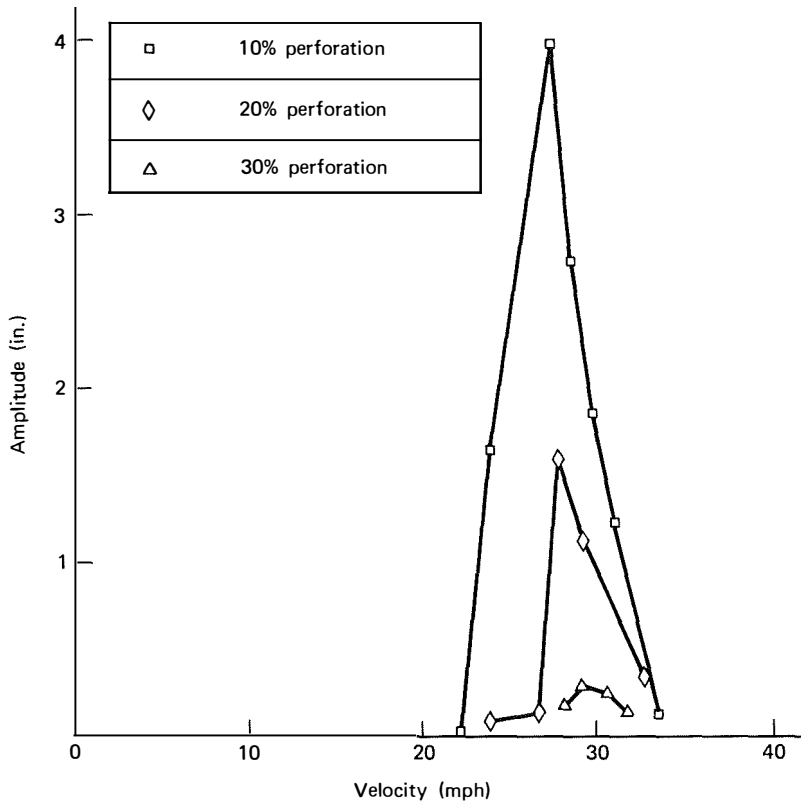


FIGURE 13.25 Long's Creek Bridge, vertical amplitude with girder web perforations (bridge height = 100 ft), from reference 13.

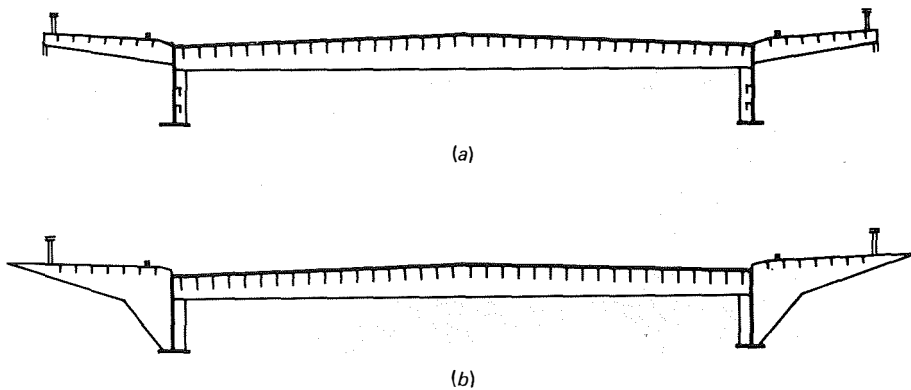


FIGURE 13.26 Kniebrücke, (a) and (b) cross sections, Düsseldorf, from reference 36.

would appear to discount the scaling problem explanation.

Davenport<sup>33</sup> suggests the following explanation for the variation of results: (1) The orthotropic deck structure is relatively light compared to more conventional structures that have been tested. Therefore, aerodynamic and mechanical parameters, including participation of the towers and cables in responding to the

wind, which are generally ignored in section model tests were exerting their influence. (2) The possibility of static deformations interfering with the instability mechanisms which are observed in the full model but not in the section model. Leonhardt has also commented on the system stability of the total structure, with special reference to the effect of the cables in a cable-stayed structure, (Section 13.7).



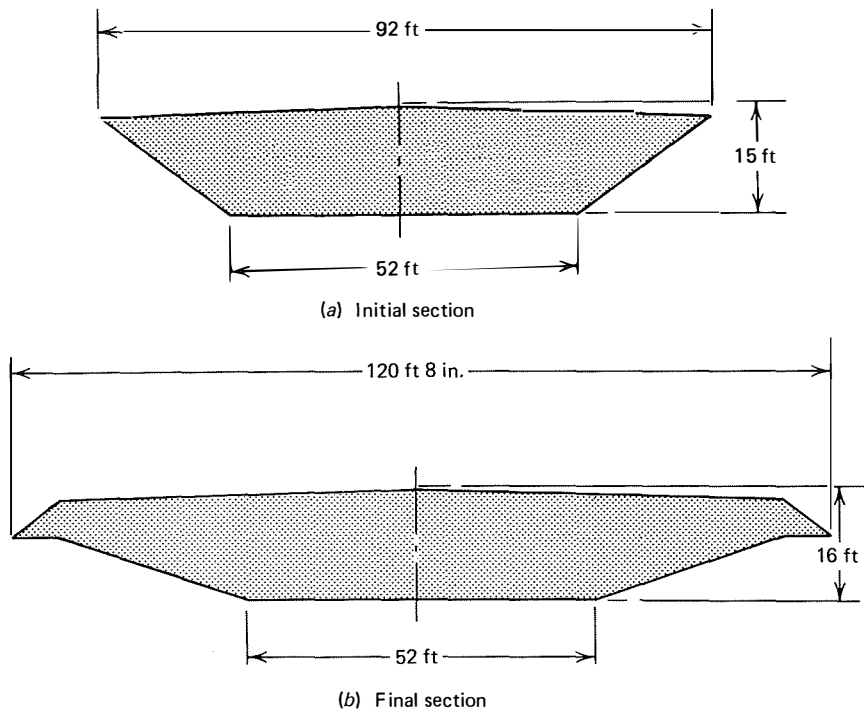


**FIGURE 13.27** New Burrard Inlet Crossing Bridge, the initial and final road deck sections for the proposed: (a) initial section and (b) final section, from reference 13.

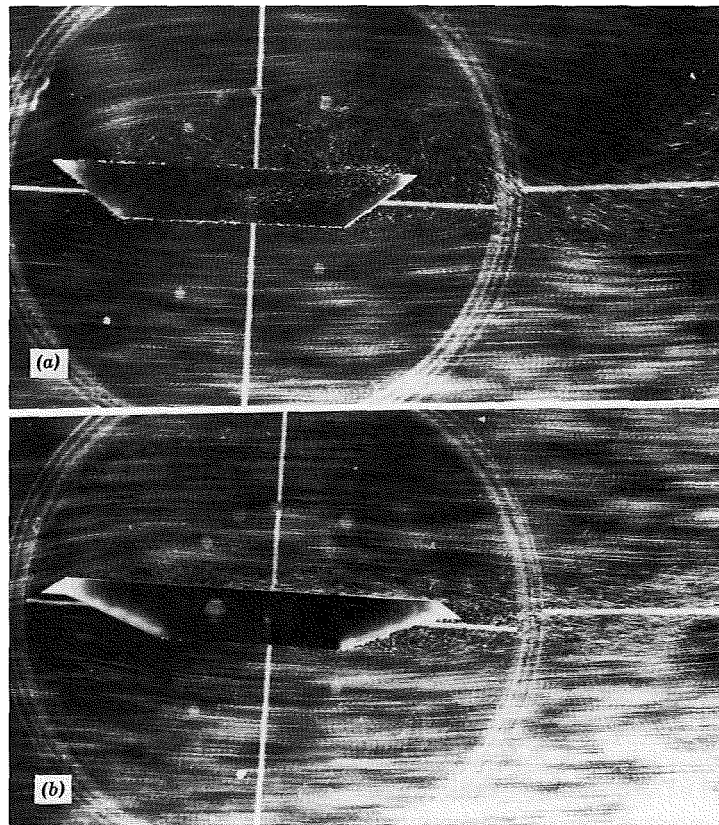


**FIGURE 13.28** New Burrard Inlet Crossing Bridge, flow visualization: (a) original section, (b) improved section (edge extension), from reference 13.

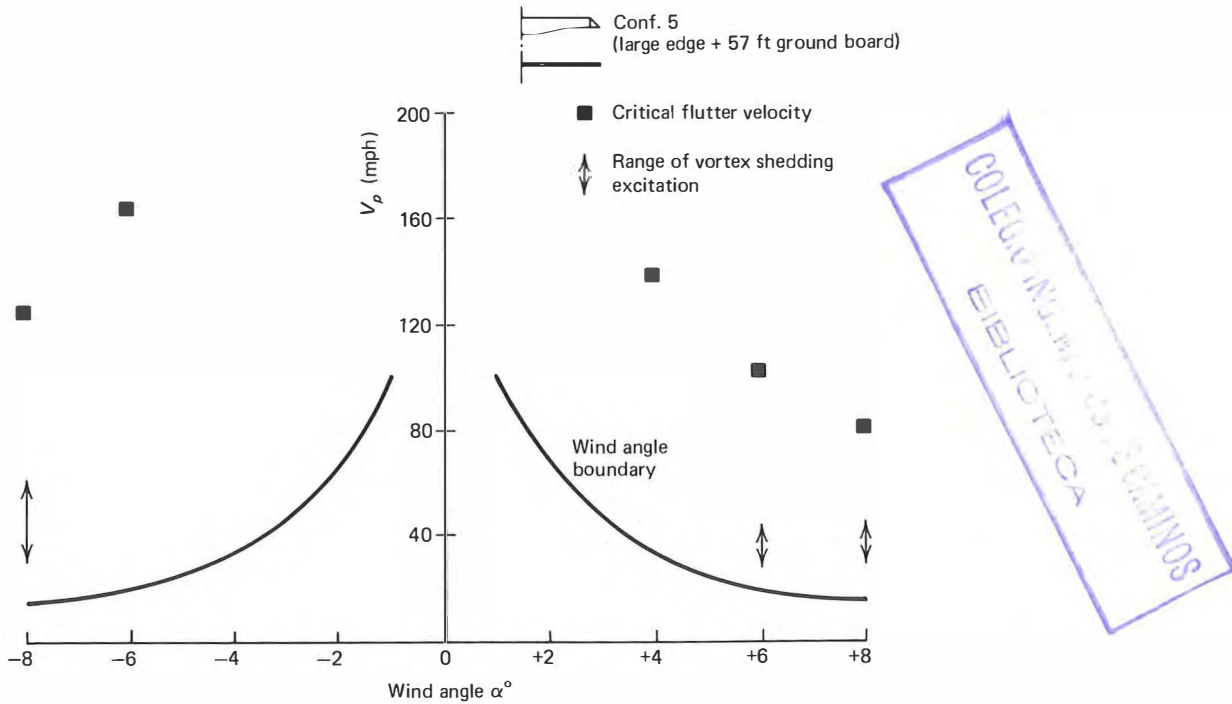


**FIGURE 13.29** Critical flutter velocity and range of vortex shedding excitation, from reference 13.

13.10.6 LULING BRIDGE, U.S.A.

Wind tunnel tests were conducted on a 1/60-scale section model for the bridge deck superstructure cross-sectional shapes of the Luling, Louisiana cable-stayed bridge over the Mississippi River. Seven superstructure configurations were considered, all having a centerline median barrier. Cross-sectional configurations and model dimensions are shown in Fig. 13.30 and Table 13.6. Initial wind tunnel tests suggested that the double trapezoidal box girder design with an orthotropic deck modified by nonstructural fascia plate (C-2C-A) would exhibit a marked improvement in aerodynamic response.

All model shapes indicated freedom from self-excited divergent vertical flutter oscillation. Torsional flutter occurred at wind speeds well above the design value of 150 mph (240 km/hr), or at unlikely wind angles. However, all models responded, variously, to vortex shedding response. This is an amplitude limited response whereby the periodic shedding of vortices in the wake of the structure is resonant with the vertical or torsional modes, or both, of the structural system. This amplitude-limited oscillation can be an unacceptable characteristic of the design when it occurs at moderate wind speeds and the resulting acceleration of the oscillating structure is disturbing to the user.

A small-scale (1/150) sectional representation of the cross-section model. C-2C-C was placed in an air flow containing smoke filaments for purposes of flow visualization. Flow separation tripped by the leading parapet railing, and again by the median barrier is illustrated in Fig. 13.31(a). The trailing vortex is captured in Figs. 13.31(b) and (c).

A more complete report of the test can be found in references 45 and 46.

13.11 Motion Tolerance

Consideration of an acceptable level of motion falls into two categories: (1) structurally damaging motion, and (2) human response motion. The first relates to violent motion that may be catastrophic or motion that over a period of time may lead to related fatigue failures. The second relates to motion that may not be structurally damaging but may be objectionable from the standpoint of user acceptance, such as vibrations that are noticeable to pedestrians or occupants of standing or moving vehicles.

The critical wind velocity level at which structural damage begins to occur is defined as that velocity which causes violent flutter motions. Velocities below the flutter speed will not produce structural damage. Very

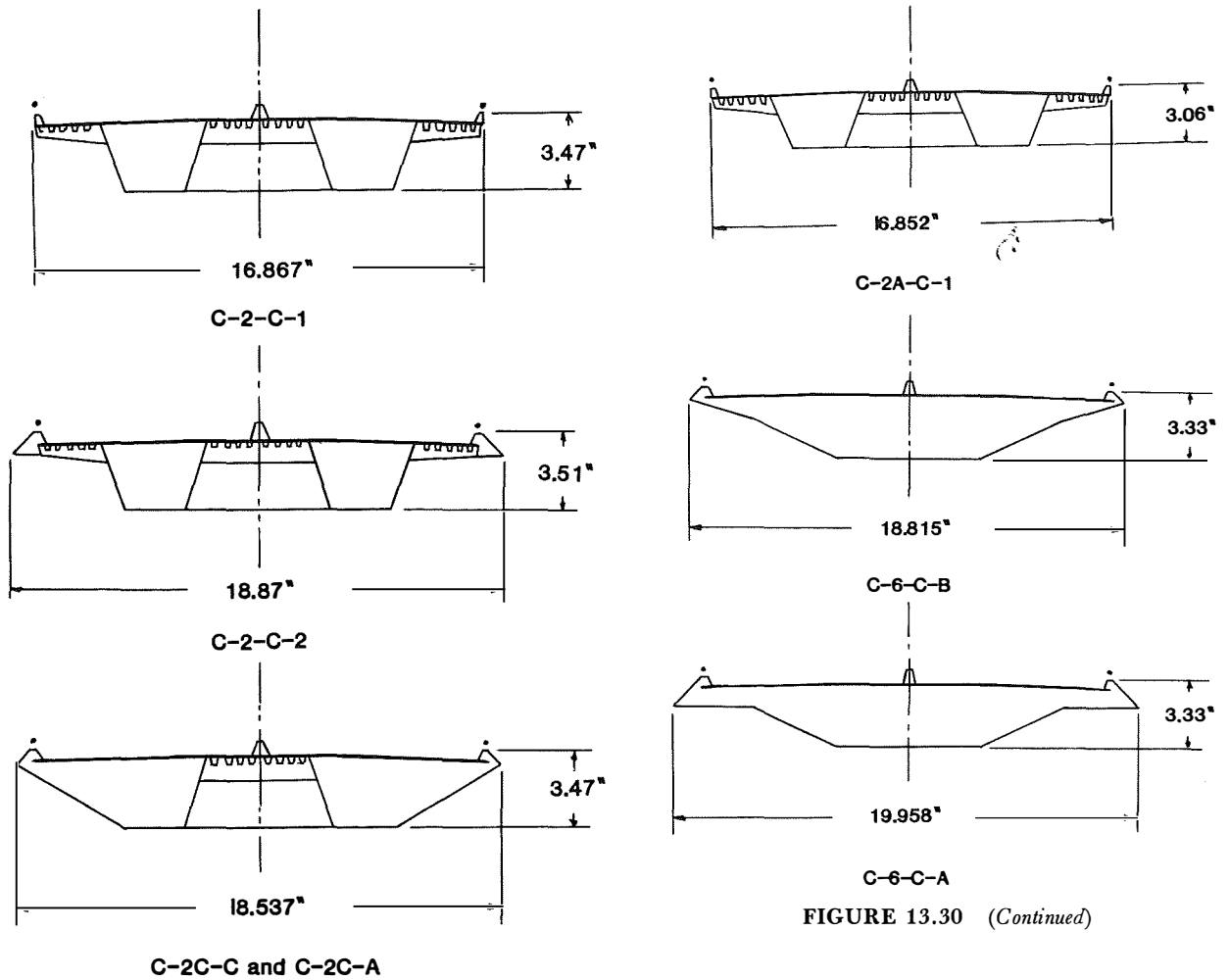


FIGURE 13.30 (Continued)

FIGURE 13.30 Luling Bridge, 1/60 scale section models.

little information on the subject of flutter of bridges is presented in the literature; however, Buckland and Wardlaw<sup>27</sup> have suggested a design approach which is presented below.

A bridge is designed for static wind loads at a cer-

tain wind speed. This is not a collapse condition, but usually produces an allowable overstress. From this design condition the wind speed at which failure or yield would be expected to occur can be calculated.

With a flutter type of motion, the onset of oscillations is sudden and violent; and occurs at the critical flutter speed. It is suggested that as long as the flutter speed is greater than that calculated to cause failure,

Table 13.6 Cross-Sectional Data on Luling Bridge Models

| Section Model Designation | Prototype Section Depth, in Feet | Roadway Surface | Vertical Natural Frequency $N_v$ , in Cycles per Second | Torsional Natural Frequency $N_t$ , in Cycles per Second |
|---------------------------|----------------------------------|-----------------|---|--|
| C-2-C-1                   | 14                               | Concrete        | 2.62  | 5.29   |
| C-2-C-2                   | 14                               | Concrete        | 2.56  | 5.20   |
| C-2C-C                    | 14                               | Concrete        | 2.56  | 5.35   |
| C-2C-A                    | 14                               | Asphalt         | 2.80  | 5.25   |
| C-2A-C-1                  | 12                               | Concrete        | 2.53  | 5.24   |
| C-6-C-B                   | 14                               | Concrete        | 2.49  | 5.33   |
| C-6-C-A                   | 14                               | Concrete        | 2.48  | 5.24   |

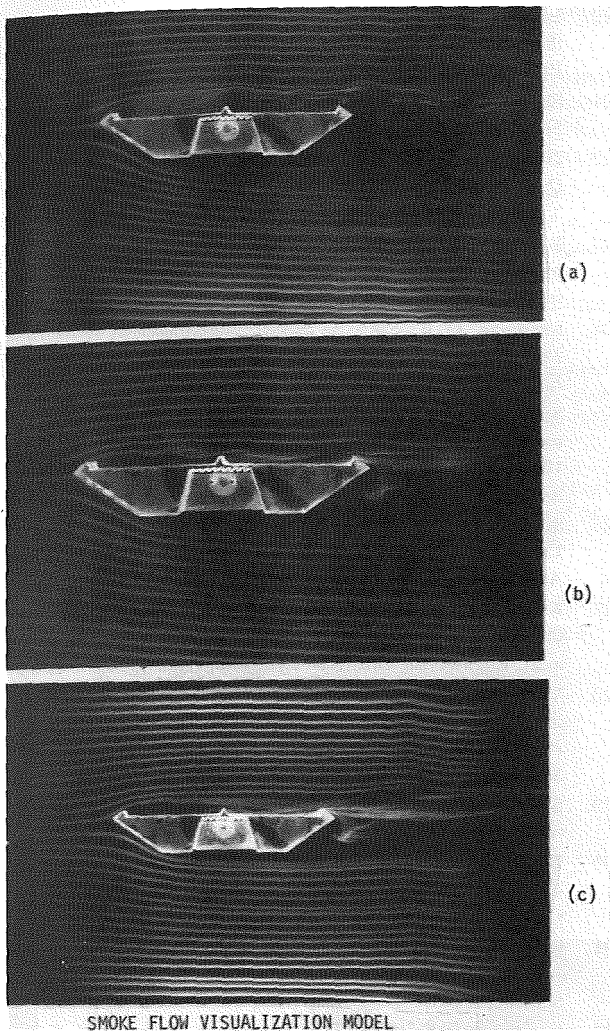


FIGURE 13.31 Smoke flow visualization model.

the same degree of safety against failure is obtained as for other design conditions. This is best demonstrated by an example:

Assume a bridge designed for a maximum wind gust speed of 90 mph, for which the basic allowable stress is  $f$ . Assume also that:

|                                       |          |
|---------------------------------------|----------|
| Dead load + Live load produce         | 1.00 $f$ |
| Dead load only produces               | 0.80 $f$ |
| Dead load + 90 mph wind load produces | 1.25 $f$ |
| Failure occurs at                     | 1.70 $f$ |

Because the wind load is proportional to the square of the velocity:

$$\text{the stress due to a 90 mph wind} = K \times 90^2 = (1.25 - 0.8) f$$

$$\text{the stress due to wind at failure} = K \times V^2 = (1.7 - 0.8) f$$

where  $V$  is the wind velocity that could cause failure and  $K$  is a constant of proportionality.

Therefore,

$$V^2 = (90)^2 \left( \frac{1.7 - 0.8}{1.25 - 0.8} \right)$$

and  $V = 127$  mph. In this case we would expect a gust of 127 mph to be the maximum that the bridge can withstand. It follows then that if the "flutter speed" is greater than 127 mph, flutter is less likely to cause destruction of the bridge than what structural engineers refer to as "wind pressure." This is correct, but still unduly conservative.

It must be remembered that "wind pressure" is based upon a gust of wind—the greatest gust velocity which can be expected to occur at least once during a period of several years. But a gust is not of sufficient duration or spatial extent to build up flutter, so we should also calculate the mean wind velocity which corresponds to a gust of 127 mph. The National Building Code<sup>47</sup> of Canada suggests a formula

$$V_{\text{mean}} = \frac{V_{\text{gust}} - 5.8}{1.29}$$

The result is that wind with a mean velocity of 94 mph could be expected to gust to 127 mph, which could destroy the bridge. Consequently, if the flutter speed is greater than 94 mph, flutter should not be a cause of failure.

Some vibrations that do not damage a structure may be unacceptable to the user of the bridge. Little data is available with respect to peoples' reaction to motion while standing, walking, or in automobiles. This subject is also discussed by Buckland and Wardlaw<sup>27</sup> and their suggested tentative criteria for motions affecting people is presented below:

1. For wind speeds up to 30 mph, 2% of  $g$
2. For wind speeds from 30 to 70 mph, 5% of  $g$
3. Over 70 mph, effects on observers may be disregarded in design considerations.

In the above  $g$  is the acceleration of gravity in ft per sec<sup>2</sup>.

### References

1. Farquharson, F. B., Smith, F. C., and Vincent, G. S., "Aerodynamic Stability of Suspension Bridges," *University of Washington Bull.*, 116, parts I through V, 1949-1954.

2. Bleich, F., McCullough, C. B., Rosecrans, R., and Vincent, G. S., "The Mathematical Theory of Vibration in Suspension Bridges," Bureau of Public Roads, U.S. Department of Commerce, Government Printing Office, Washington, D.C., 1950.
3. Leonhardt, F. and Zellner, W., "Cable-Stayed Bridges: Report on Latest Developments," Canadian Structural Engineering Conference, 1970, Canadian Steel Industries Construction Council, Toronto, Ontario, Canada.
4. Jakkula, A. A., "A History of Suspension Bridges in Bibliographical Form," *Texas A. & M. College of Engineering Experimental Station Bulletin* No. 57, July 1, 1941.
5. Steinman, D. B., "Design of Bridges Against Wind," *Civil Engineering*, ASCE, October, November, and December 1945 and January and February 1946.
6. Reid, W., "A Short Account of the Failure of a Part of the Brighton Chain Pier in the Gale of the 30th of November, 1836," *Professional Papers of the Corps of Royal Engineers*, Vol. 1, 1844, p. 99.
7. Provis, W. A., "Observations on the Effect of Wind on the Suspension Bridge over Menai Straits," *Minutes of Proceedings of the Institution of Civil Engineers*; Vol. 1, 1837-41, Session of 1841, p. 74.
8. Vincent, G. S., "Golden Gate Bridge Vibration Studies," *Journal of the Structural Division*, ASCE, Proc. Paper 1817, October 1958.
9. Steinman, D. B., "Aerodynamics of Suspension Bridges," *Proceedings of the Thirty-Second Annual Roads School*, Purdue University, January 1946.
10. Anon., "Stays and Brakes Check Oscillation of Whitestone Bridge," *Engineering News-Record*, December 5, 1940.
11. Ammann, O. H., "Additional Stiffening of Bronx-Whitestone Bridge," *Civil Engineering*, ASCE, Vol. 16, No. 3, March 1946.
12. Wardlaw, R. L. and Ponder, C. A., "Wind Tunnel Investigation on the Aerodynamic Stability of Bridges," Canadian Structural Engineering Conference, 1970, Canadian Steel Industries Construction Council, Toronto, Ontario, Canada.
13. Wardlaw, R. L., "A Review of the Aerodynamics of Bridge Road Decks and the Role of Wind Tunnel Investigation," U.S. Department of Transportation, Federal Highway Administration, Report No. FHWA-RD-73-76.
14. Taylor, P. R., "Cable-Stayed Bridges and Their Potential in Canada," *Engineering Journal* (Canada), Vol. 52, No. 11 (November, 1969).
15. Davenport, A. G., "Rationale for Determining Design Wind Velocities," *Journal of the Structural Division*, ASCE, paper 2476, Vol. 86, No. ST 5, May 1960.
16. Davenport, A. G., ed., "New Approaches to Design Against Wind Action," Course notes, ASCE Wind Seminar, Cleveland, Ohio, April 1972, Boundary Layer Wind Tunnel, University of Western Ontario, London, Canada.
17. Davenport, A. G., "The Application of Statistical Concepts to the Wind Loading of Structures," *Proceedings of the Institute of Civil Engineers*, Vol. 19, Paper No. 6480, August 1961.
18. Thom, H. C. S., "New Distribution of Extreme Winds in the United States," *Journal of the Structural Division*, ASCE, Vol. 94, No. ST7, July 1968.
19. Hirai, A. and Okubo, T., "On the Design Criteria Against Wind Effects for Proposed Honshu-Shikoku bridges," Paper No. 10, *Symposium on Suspension Bridges*, Lisbon, November 1966.
20. Ishizaki, H. and Mitsuda, Y., "On the Extent of Gusts and the Gust Factors of Strong Wind (in Japanese), *Ann. Disas. Prev. Res. Inst. Kyoto Univ.* No. 5A, 1962.
21. Sherlock, R. H., "Variations of Wind Velocity and Gusts with Height," *Proceedings ASCE*, Vol. 78, No. 126, 1952.
22. Deacon, E. L., "Gust Variations with Height up to 150 m," *Quarterly Journal of the Royal Meteorological Society*, Vol. 81, Ab. 350, 1955.
23. Roberts, G., "Severn Bridge—Design and Contract Arrangements," *Proceedings of the Institute Civil Engineers*, Vol. 41, September 1958.
24. Steinman, D. B., *Suspension Bridges: The Aerodynamic Problem and Its Solution*, International Association for Bridge and Structural Engineering, Volume 14, 1954.
25. Steinman, D. B., "Problems of Aerodynamic and Hydrodynamic Stability," *Proceedings Third Hydraulics Conference*, June 10-12, 1946, University of Iowa, Studies in Engineering, Bulletin 31.
26. Scanlan, R. H., "Aeroelastic Stability of Long-Span Bridges," U.S. Department of Transportation, Federal Highway Administration, Report No. FHWA-RD-73-75.
27. Buckland, P. G. and Wardlaw, R. L., "Some Aerodynamic Considerations in Bridge Design," *Engineering Journal* (Canada), Engineering Institute of Canada, April 1972.
28. Vincent, G. S., "A Summary of Laboratory and Field Studies in the United States on Wind Effects on Suspension Bridges," *Proceedings of Symposium No. 16, Wind Effects on Buildings and Structures*, National Physical Lab., England, 1963.
29. Steinman, D. B., "Aerodynamic Theory of Bridge Oscillation," *Transactions*, ASCE, Vol. 115, 1950.
30. Bleich, F., "Dynamic Instability of Truss-Stiffened Suspension Bridges Under Wind Action," ASCE, *Proceedings* Vol. 74, October 1948.
31. Kloppel, K. and Thiele, F., "Modellversuche im Windkanal zur Bemessung von Brücken gegen die Gefahr widerregter Schwingungen," *Der Stahlbau*, No. 12, December, 1967.
32. Scanlan, R. H., "Studies of Suspension Bridge Deck Flutter Instability," American Institute of Aeronautics and Astronautics, Paper No. 69.744, July 1969.
33. Davenport, A. G. et al., "A Study of Wind Action on a Suspension Bridge During Erection and on Completion," Research Report of University of Western Ontario, Canada, BLWT, 3, 69.
34. Walshe, D. E. J., "The Use of Models to Predict the Oscillatory Behavior of Suspension Bridges in Wind," National Physical Laboratory, Teddington, England, *Proceedings of Symposium No. 16, "Wind Effects on Buildings and Structures,"* 1963.
35. Walshe, D. E. J. and Rayner, D. V., "A Further Aerodynamic Investigation for the Proposed River Severn Bridge," National Physical Laboratory, England, NPL Aero Report 1010, March 1962.
36. Leonhardt, F. and Zellner, W., "Vergleiche zwischen Hängebrücken und Schrägkabelbrücken für Spannweiten über 600 m," *International Association for Bridge and Structural Engineering*, Vol. 32, 1972.
37. Leonhardt, F., "Zur Entwicklung aerodynamisch stabiler Hängebrücken," *Die Bautechnik* 45 (1968), Nos. 10 and 11.
38. Scruton, C., "Aerodynamics of Structures," *Wind Effects on Buildings and Structures, Proceedings of the International Research Sem-*

- inar held at the National Research Council, Ottawa, Canada on 11-15 September 1967, University of Toronto Press.
39. Gade, R. H., "Status of the Investigation of Aerodynamic Behavior of the Sitka Harbor Cable-Stayed Bridge," presented at the Symposium on Full Scale Measurements of Wind Effects on Tall Buildings and Other Structures, London, Ontario, Canada, June 1974.
  40. Wardlaw, R. L., "A Preliminary Wind Tunnel Study of the Aerodynamic Stability of Four Bridge Sections for Proposed New Burrard Inlet Crossing," National Research Council of Canada, National Aeronautical Establishment, Tech. Report LTR-LA-31, July 14, 1969.
  41. Wardlaw, R. L., "Some Approaches for Improving the Aerodynamic Stability of Bridge Road Decks," *Proceedings of the Third International Conference on Wind Effects on Buildings and Structures*, Tokyo, 1971.
  42. Wardlaw, R. L., "Static Force Measurements of Six Deck Sections for the Proposed New Burrard Inlet Crossing," National Research Council of Canada, National Aeronautical Establishment, Tech. Report LTR-LA-53, June 4, 1970.
  43. Davenport, A. G., Isyumov, N., and Miyata, T., "The Experimental Determination of the Response of Suspension Bridges to Turbulent Wind," *Proceedings of the Third International Conference on Wind Effects on Buildings and Structures*, Tokyo, 1971.
  44. Frazer, R. A. and Scruton, C., "A Summarized Account of the Severn Bridge Aerodynamic Investigation," Report NPL/Aero/222, H.M.S.O., 1952.
  45. Gade, R. H., Bosch, H. R., and Podolny, W. Jr., "Recent Aerodynamic Studies of Long-Span Bridges," *Journal of the Structural Division*, ASCE, Vol. 102, No. ST7, July 1976.
  46. "Aerodynamic Investigations of the Luling, Louisiana Cable-Stayed Bridge," Report No. FHWA-RD-77-161, Offices of Research and Development, Federal Highway Administration, Washington, D.C., July 1978.
  47. National Building Code of Canada, 1965 Edition, Supplement No. 1, "Climatic Information for Building Design in Canada, 1965" NRC No. 8329.

# APPENDIX A

## Chronological Bibliography

1. Fidler, T. C., "Straight Link Suspension Bridges," *Engineering* (London), Vol. 31 (March 25, 1881), pp. 297-300, 373-374, 584-585.
2. Mehrrens, *Eisenbrückenbau [Steel Bridge Construction]*, Vol. I, (Verlag Engelmann, Leipzig, 1908).
3. "New Type Bridge Proposed by Germans," *Engineering News-Record* (September 2, 1948), pp. 86-87.
4. Dischinger, F., "Hängebrücken für schwerste Verkehrslasten," *Der Bauingenier* (March 1949), pp. 65, 107.
5. Wenk, H., "Die Strömsundbrücke [The Strömsund Bridge]," *Der Stahlbau*, Vol. 23, No. 4 (April 1954), pp. 73-76.
6. Beyer, E. and Tussing, F., "Nordbrücke Düsseldorf," *Der Stahlbau*, Vol. 24, No. 2, 3, and 4 (February, March, April, 1955), pp. 25-33, 63-67, 79-88.
7. Homberg, H., "Einflusslinien von Schrägseilbrücken," *Der Stahlbau*, Vol. 24, No. 2 (February 1955), pp. 40-44.
8. Klingenberg, W. and Plum, "Versuche an dem Drähten und Seilen der neuen Rheinbrücke in Rodenkirchen bei Köln," *Der Stahlbau*, Vol. 24, No. 12 (December 1955), pp. 265-272.
9. Sievers, H. and Görtz, W., "Der Wiederaufbau der Strassenbrücke über den Rhein zwischen Duisburg Ruhort and Homberg," *Der Stahlbau*, Vol. 25, No. 4 (April 1956), pp. 77-88.
10. Ernst, H. J., "Montage eines seilverspannten Balken im Gross-Brückenbau," *Der Stahlbau*, Vol. 25, No. 5 (May 1956), pp. 101-108.
11. Godfrey, G. B., "Post-War Development in Germany: Steel Bridges and Structures," *Structural Engineer*, Vol. 35, No. 2 (February 1957), pp. 53-68.
12. Godfrey, G. B., "Post-War Development in Germany Steel Bridges and Structures (Discussion)," *Structural Engineer*, Vol. 35, No. 10 (October 1957), pp. 390-398.
13. Kunz, R., Trappmann, H. and Tröndle, E., "Die Büchener Brücke, eine neue Schrägseilbrücke der Bundesstrasse 35 in Bruchsal," *Der Stahlbau*, Vol. 26, No. 4 (April 1957), pp. 98-102.
14. Beyer, E. and Ernst, H. J., "Erfahrungen und Seilversuche an einer seilunterspannten Verbundkonstruktion," *Der Stahlbau*, Vol. 26, No. 7 (July 1957), pp. 117-183.
15. Schüssler, K. and Braun, F., "Wettbewerb 1954 zum Bau einer Rheinbrücke oder eines Tunnels in Köln im Zuge Klappergasse-Gotenring," *Der Stahlbau*, Vol. 26, No. 8, 9, 10, and 11 (August, September, October, and November, 1957), pp. 205-217, 253-274, 294-312, and 326-348.
16. *Denkschrift über die Nordbrücke Düsseldorf* (Springer-Verlag, Berlin-Göttingen-Heidelberg, 1958).
17. Beyer, E., "Nordbrücke Düsseldorf I. Theil: Gesamtanlage und Montage der neuen Rheinbrücke," *Der Stahlbau*, Vol. 27, No. 1 (January 1958), pp. 1-6.
18. Hadley, H. M., "Tied Cantilever Bridge—Pioneer Structure in U.S.," *Civil Engineering*, ASCE, January 1958.
19. Lewenton, G., "Die deutschen Pavillonbauten auf der Weltausstellung Brüssel 1958," *Der Stahlbau*, Vol. 27, No. 4 (April 1958), pp. 1-91.
20. Fuchs, D., "Der Fussgängersteg auf der Brüsseler Weltausstellung 1958," *Der Stahlbau*, Vol. 27, No. 4 (April 1958), pp. 91-97.
21. Wintergerst, L., "Nordbrücke Düsseldorf III. Theil: Statik und Konstruktion der Strombrücke," *Der Stahlbau*, Vol. 27, No. 6 (June 1958), pp. 147-158.
22. Schreier, G., "North Bridge at Düsseldorf: Analysis, Design, Fabrication and Erection of the Bridge Spanning the River," *Acier-Stahl-Steel* (English version), Part 1, No. 9 (September 1958), Part 2, No. 11 (November 1958).
23. Fischer, G., "Die Severinsbrücke in Köln" ["The Severin Bridge at Cologne"], *Acier-Stahl-Steel*, Vol. 25, No. 3 (March 1960), p. 101 (pp. 97-107, English version).
24. Vogel, G., "Erfahrungen mit geschweissten Montaggestossen beim Bau der Severinsbrücke in Köln," *Schweissen und Schneiden*, Vol. 12, No. 5 (May 1960), pp. 189-194.
25. Hess, H., "Die Severinsbrücke Köln, Entwurf und Fertigung der Strömbrücke," *Der Stahlbau*, Vol. 29, No. 8 (August 1960), pp. 225-261.
26. Vogel, G., "Die Montage des Stahlüberbaues der Severinsbrücke Köln," *Der Stahlbau*, Vol. 29, No. 9 (September 1960), pp. 269-293.
27. Michalos, J. and Birnstiel, C., "Movements of a Cable due to Changes in Loading," *Journal of the Structural Division*,

- ASCE, Vol. 86, No. ST 12, Proc. Paper 2674 (December 1960), pp. 23-38.
28. Goschy, Bella, "Dynamics of Cable-Stayed Pipe Bridges," *Acier-Stahl-Steel*, Vol. 26, No. 6 (June 1961), pp. 277-282.
  29. Dotzauer, H. K. and Hess, H., "Belastungsprobe der Severinsbrücke Köln," *Der Stahlbau*, Vol. 30, No. 10 (October 1961), pp. 303-311.
  30. Leonhardt, F. and Andrä, W., "Fussgängersteg über die Schillerstrasse im Stuttgart," *Die Bautechnik*, Vol. 39, No. 4 (April 1962), pp. 110-116.
  31. Appelbaum, G. and Rokicki, K., "Wesentliche Merkmale der Vorfertigung und Montage der Autobahn-Norderelbbrücke bei Hamburg," *Schweissen und Schneiden*, Vol. 14, No. 6 (June 1962), pp. 255-258.
  32. Havemann, H. K., "Die Seilverspannung der Autobahnbrücke über die Norderelbe-Bericht über Versuche zur Daverfestigkeit der Drahtseile," *Der Stahlbau*, Vol. 31, No. 8 (August 1962), pp. 225-232.
  33. Jennings, A., "The Free Cable," *The Engineer* (December 28, 1962), pp. 1111-1112.
  34. *Design Manual for Orthotropic Steel Plate Deck Bridges* (New York: American Institute of Steel Construction, 1963), pp. 7-10.
  35. "The Bridge Spanning Lake Maracaibo in Venezuela, The General Rafael Urdaneta Bridge" (Bauverlag GmbH Weisbaden, Berlin, 1963).
  36. Klöppel and Weber, "Teilmodellversuche zur Beurteilung des aerodynamischen Verhaltens von Brücken," *Der Stahlbau*, Vol. 32, No. 3 and 4 (March and April, 1963), pp. 65-79, 113-121.
  37. Poskitt, T. J. and Livesley, R. H., "Structural Analysis of Guyed Masts," *Proceedings of the Institution of Civil Engineers*, Vol. 24 (March 1963), pp. 373-386.
  38. Brotton, D. M., Williamson, N. W. W. and Millar, M., "The Solution of Suspension Bridge Problems by Digital Computers—Part I," *Structural Engineer*, Vol. 41, No. 4 (April 1963).
  39. Poskitt, T. J., "The Application of Elastic Catenary Functions to the Analysis of Suspended Cable Structures," *Structural Engineer*, Vol. 41, No. 5 (May 1963).
  40. Reimers, K., "Fussgängerbrücke über die Glacischaussee in Hamburg für die Internationale Gartenbau-Ausstellung 1963," *Schweissen und Schneiden*, Vol. 15, No. 6 (June 1963), pp. 262-264.
  41. Braun, F. and Moors, J., "Wettbewerb zum Bau einer Rheinbrücke im Zuge der Inneren Kanalstrasse in Köln (Zoo-Brücke), *Der Stahlbau*, Vol. 32, No. 6, 7, and 8 (June, July, and August, 1963), pp. 174-183, 204-213, 248-254.
  42. Havemann, H. K., "Die Brücke über die Norderelbe im Zuge der Bundesautobahn Südliche Umgehung Hamburg, Teil I: Ideen- und Bauwettbewerb," *Der Stahlbau*, Vol. 32, No. 7 (July 1963), pp. 193-198.
  43. Brotton, D. M. and Arnold, G., "The solution of Suspension Bridge Problems by Digital Computers—Part II," *Structural Engineer*, Vol. 41, No. 7 (July 1963.)
  44. Aschenberg, H. and Freudenberg, G., "Die Brücke über die Norderelbe im Zuge der Bundesautobahn Südliche Umgehung Hamburg, Teil II: Konstruktion des Brückenüberbaus," *Der Stahlbau*, Vol. 32, No. 8 (August 1963), pp. 240-248.
  45. Aschenberg, H. and Freudenberg, G., "Die Brücke über die Norderelbe im Zuge der Bundesautobahn Südliche Umgehung Hamburg, Teil III: Statische Berechnung des Brückenüberbaus," *Der Stahlbau*, Vol. 32, No. 9 (September 1963), pp. 281-287.
  46. Poskitt, T. J. and Livesley, R. H., "Structural Analysis of Guyed Masts (Discussion)," *Proceedings of the Institution of Civil Engineers*, Vol. 26 (September 1963), pp. 185-186.
  47. Havemann, H. K. and Freudenberg, G., "Die Brücke über die Norderelbe im Zuge der Bundesautobahn Südliche Umgehung Hamburg, Teil IV: Bauausführung der stählernen Überbauten," *Der Stahlbau*, Vol. 32, No. 10 (October 1963), pp. 310-317.
  48. "Norderelbe Bridge K6: A Welded Steel Motorway Bridge," *Acier-Stahl-Steel*, Vol. 28, No. 11 (November 1963), pp. 499-500.
  49. *Stahlbau, Ein Handbuch für Studium und Praxis* (Vol. II, 2nd ed.; Cologne: Stahlbauverlag GmbH, 1964), "Seilverspannte Balken," p. 584.
  50. Leonhardt, F., "Aerodynamisch stabile Hängerbrücke für grosse Spannweiten," International Association for Bridge and Structural Engineering, Preliminary Publication, Seventh Congress, Rio de Janeiro (1964), pp. 155-167.
  51. Leonhardt, F., "Kabel mit hoher Ermüdungsfestigkeit für Hängebrücken," International Association for Bridge and Structural Engineering, Preliminary Publication, Seventh Congress, Rio de Janeiro (1964), pp. 1055-1060.
  52. Homberg, H., "Fortschritt im deutschen Stahlbrückenbau [Progress in German Steel Bridge Construction]," *Report on Steel Congress 1964 of the High Authority of the European Economic Community*.
  53. Feige, A., "Steel Motorway Bridge Construction in Germany," *Acier-Stahl-Steel*, Vol. 29, No. 3 (March 1964), pp. 113-126.
  54. Shaw, F. S., "Some Notes on Cable Suspension Roof Structures," *Journal of the Institution of Engineers (Australia)* (April-May 1964), pp. 105-113.
  55. O'Brien, W. T. and Francis, A. J., "Cable Movements under Two Dimensional Loads," *Journal of the Structural Division, ASCE*, Vol. 90, No. ST 3 (June 1964), pp. 89-123.
  56. Havemann, H. K., "Spannungs- und Schwingungsmessungen an der Brücke über die Norderelbe im Zuge der Bundesautobahn Südliche Umgehung Hamburg," *Der Stahlbau*, Vol. 33, No. 10 (October 1964), pp. 289-297.
  57. Lohmer, G., "Brückenbaukunst," *Der Stahlbau*, Vol. 33, No. 11 (November 1964).
  58. Beyer, E. and Ernst, H. J., "Brücke Jülicher Strasse in Düsseldorf," *Der Bauingenieur*, Vol. 39, No. 12 (December 1964), pp. 469-477.
  59. Ernst, H. J., "Der E-Modul von Seilen unter Berücksichtigung des Durchhanges," *Der Bauingenieur*, Vol. 40, No. 2 (February 1965), pp. 52-55.
  60. Daniel, H., "Die Bundesautobahnbrücke über den Rhein bei Leverkusen. Planung, Wettbewerb und seine Ergebnisse," *Der Stahlbau*, Vol. 34, No. 2, 3, 4, 5, and 12 (February, March, April, May, and December 1965), pp. 33-36, 83-86, 115-119, 153-158, 362-368.
  61. "Montreal Hosts a Double Bridge Spectacular in the St. Lawrence," *Engineering News Record* (August 5, 1965), pp. 24-27, 31.



62. Brown, C. D., "Design and Construction of the George Street Bridge over the River Usk, at Newport, Monmouthshire," *Proceedings of the Institution of Civil Engineers*, Vol. 32 (September 1965), pp. 31-52.
63. Francis, A. J., "Single Cables Subjected to Loads," *Civil Engineering Transactions*, Institution of Engineers, Australia (October 1965), pp. 173-180.
64. Klöppel, K., Esslinger, M. and Kollmeier, H., "Die Berechnung eingespannter und fest mit dem Kabel verbundener Hängebrückenpylonen bei Beanspruchung in Brückenlängsrichtung," *Der Stahlbau*, Vol. 34, No. 12 (December 1965), pp. 358-361.
65. Poskitt, T. J., "The Structural Analysis of Suspension Bridge," *Journal of the Structural Division*, ASCE, Vol. 92, No. ST 1, Proc. Paper 4664 (February 1966), pp. 49-73.
66. Brown, C. D., "Design and Construction of the George Street Bridge over the River Usk, at Newport, Monmouthshire (Discussion)," *Proceedings of the Institution of Civil Engineers*, Vol. 33 (March 1966), pp. 552-561.
67. Thul, H., "Stählerne Strassenbrücken in der Bundesrepublik," *Der Bauingenieur*, Vol. 41, No. 5 (May 1966), pp. 169-189.
68. Daniel, H. and Urban, J., "Die Bundesautobahnbrücke über den Rhein bei Leverkusen," *Der Stahlbau*, Vol. 35, No. 7 (July 1966).
69. Protte, W. and Tross, W., "Simulation als Vorgehensweise bei der Berechnung von Schragseilbrücken," *Der Stahlbau*, Vol. 35, No. 7 (July 1966).
70. Freudenberg, G. and Ratka, O., "Die Zoobrücke über den Rhein in Köln," *Der Stahlbau*, Vol. 38, No. 8, 9, and 11 (August, September, and November 1966).
71. Thul, H., "Cable Stayed Bridges in Germany," *Proceedings of the Conference on Structural Steelwork* held at the Institution of Civil Engineers (September 26-28, 1966), The British Constructional Steelwork Association, Ltd., London, pp. 69-81.
72. "The Slender Severn Suspension Bridge," *Engineering*, Vol. 202, No. 5238 (September 9, 1966), pp. 449-456.
73. "Continuing the Severn Crossing: The Wye Viaduct," *Engineering*, Vol. 202, No. 5239 (September 16, 1966).
74. Gimsing, N. J., "Anchored and Partially Anchored Stayed Bridges," Symposium on Suspension Bridges, Paper No. 30, Lisbon, Laboratorio Nacional De Engenharia Civil, November, 1966.
75. Feige, A., "The Evolution of German-Stayed Bridges: An Overall Survey," *Acier-Stahl-Steel* (English version), Vol. 31, No. 12 (December 1966), pp. 523-532.
76. *Steel Footbridges*, British Constructional Steelwork Association, Ltd., 16M/623/1266.
77. Goschy, B., "The Torsion of Skew-Cable Suspension Bridges," *Space Structures*, edited by R. M. Davies (Oxford and Edinburgh: Blackwell Scientific Publications, 1967), pp. 213-220.
78. Okaucki, I., Yabe, A. and Ando, K., "Studies on the Characteristics of a Cable-Stayed Bridge," *Bulletin of the Faculty of Science and Engineering*, Chuo University, Vol. 10 (1967).
79. "Bridge May Hang Like a Roof," *Engineering News-Record* (January 26, 1967), p. 56.
80. Heeb, A., Gerold, W. and Dreher, W., "Die Stahlkonstruktion der Neckarbrücke Untertürkheim," *Der Stahlbau*, Vol. 36, No. 2 (February 1967), pp. 33-38.
81. "Great Belt Bridge Award Winner," *Consulting Engineer* (England) (March 1967).
82. "Another Cable-Stayed Bridge Conquers the Rhine," *Engineering News-Record* (May 25, 1967), pp. 102-103, 107.
83. Smith, B. S., "The Single Plane Cable-Stayed Girder Bridge: A Method of Analysis Suitable for Computer Use," *Proceedings of the Institution of Civil Engineers*, Vol. 37 (May 1967), pp. 183-194.
84. Feige, A., "The Evolution of German Cable-Stayed Bridges: An Overall Survey," *Engineering Journal*, American Institute of Steel Construction (July 1967), pp. 113-122.
85. Daniel, H. and Schumann, H., "Die Bundesautobahnbrücke über den Rhein bei Leverkusen," *Der Stahlbau*, Vol. 36, No. 8 (August 1967), pp. 225-236.
86. Klöppel, K. and Thiele, F., "Modellversuche im Windkanal zur Bemessung von Brücken gegen die Gefahr winderegter Schwingungen," *Der Stahlbau*, Vol. 36, No. 12 (December 1967), pp. 353-365.
87. Payne, R. J., "The Structural Requirements of the Batman Bridge as They Affect Fabrication of the Steelwork," *Journal of the Institution of Engineers* (Australia), Vol. 39, No. 12 (December 1967).
88. Bresler, B., Lin, T. Y. and Scalzi, J. B., *Design of Steel Structures*, Chapter 15, Gilespie, J. W., McDermott, J. F. and Podolny, W., Jr., "Special Structures" (2nd ed.; New York: Wiley, 1968), pp. 752-754.
89. Heckel, R., "The Use of Orthotropic Steel Decks in Austria," *Proceedings of the Conference on Steel Bridges*, The British Constructional Steelwork Association, Ltd., London (1968), pp. 143-150.
90. Schor, R. J., "Steel Bridges in Holland," *Proceedings of the Conference on Steel Bridges*, The British Constructional Steelwork Association, Ltd., London (1968), pp. 161-168.
91. Allen, J. S., Leeson, J. and Upstone, M. P., "River Severn Pipe Bridge and Road Crossing for the South Staffordshire Waterworks Company," *Proceedings of the Conference on Steel Bridges*, The British Constructional Steelwork Association, Ltd., London (1968), pp. 169-176.
92. Elliott, P., "Can Steel Bridges Become More Competitive?," *Proceedings of the Conference on Steel Bridges*, The British Constructional Steelwork Association, Ltd., London (1968), pp. 199-210.
93. Foucriat, J. and Sfintesco, M., "Steel Bridges in France," *Proceedings of the Conference on Steel Bridges*, The British Constructional Steelwork Association, Ltd., London (1968), pp. 217-227.
94. Troitsky, M. S., *Orthotropic Bridges Theory and Design* (Cleveland, Ohio: The James F. Lincoln Arc Welding Foundation, 1968), pp. 46-52.
95. *Suspended Structures*, British Constructional Steelwork Association, Ltd., 16M/842/68.
96. Tung, D. H. H. and Kudder, R. J., "Analysis of Cables as Equivalent Two-Force Members," *Engineering Journal*, American Institute of Steel Construction (January 1968), pp. 12-19.
97. Smith, B. S., "A Linear Method of Analysis for Double-

- Plane Cable-Stayed Girder Bridges," *Proceedings of the Institution of Civil Engineers*, Vol. 39 (January 1968), pp. 85-94.
98. Schottgen, J. and Wintergerst, L., "Die Strassenbrücke über den Rhein bei Maxau," *Der Stahlbau*, Vol. 37, No. 1 (January 1968), pp. 1-9.
  99. Morandi, R., "Ill viadotto—dell' Ansa della Magliana—per la Autostrada Roma—Aeroporto di Fiumicino," *L'Industria Italiana del Cemento*, No. 38 (March 1968), pp. 147-162.
  100. Feige, A., "Fussgängerbrücken aus Stahl," *Merkblatt 251*, Beratungsstelle für Stahlverwendung, Düsseldorf, 3 Auflage 1968.
  101. "The Expo Bridge: Study in Steel Quality (Canada)," *Acier-Stahl-Steel*, Vol. 33, No. 5 (May 1968), pp. 238-240.
  102. "Opening Batman Bridge 18th May 1968," Department of Public Works, Tasmania, Australia.
  103. Demers, J. G. and Marquis, P., "Le Pont a Haubans de la Riviere-des-Prairies," *L'Ingenieur*, Vol. 54, No. 231 (June 1968), pp. 24-28.
  104. Tesár, A., "Das Projekt der neuen Strassenbrücke über die Donau in Bratislava/CSSR," *Der Bauingenieur*, Vol. 43, No. 6 (June 1968), pp. 189-198.
  105. Klingenberg, W. and Thul, H., "Ideenwettbewerb für einen Brückenschlag über den Grossen Belt," *Der Stahlbau*, Vol. 37, No. 8 (August 1968).
  106. Moser, K., "Der Einfluss des zeitabhängigen Verhaltens bei Hänge und Schrägseilbrückensystemen," *International Association for Bridge and Structural Engineering, Final Report*, Eighth Congress, New York (September 9-14, 1968), pp. 119-129.
  107. Murakami, E. and Okubo, T., "Wind Resistant Design of a Cable-Stayed Girder Bridge," *International Association for Bridge and Structural Engineering, Final Report*, Eighth Congress, New York (September 9-14, 1968), pp. 1263-1274.
  108. Leonhardt, F., "Zur Entwicklung aerodynamisch stabiler Hängerbrücken," *Die Bautechnik*, Vol. 45, No. 10 and 11 (1968), pp. 1-21.
  109. Morandi, R., "Some Types of Tied Bridges in Prestressed Concrete," *First International Symposium, Concrete Bridge Design*, ACI Publication SP-23, Paper SP 23-25 (1969).
  110. Tamms and Beyer, "Kniebrücke Düsseldorf," Beton-Verlag GmbH, Düsseldorf, 1969.
  111. Balbachevsky, G. N., "Study Tour of the A.F.P.C.," *Acier-Stahl-Steel*, Vol. 34, No. 2 (February 1969), pp. 73-82.
  112. Pflüger, A., "Schwingungsverhalten der Schwebelahnbrücke Alter Markt Wuppertal," *Der Stahlbau*, Vol. 38, No. 5 (May 1969), pp. 140-144.
  113. "Erskine Bridge," *Building with Steel*, Vol. 5, No. 4 (June 1969), pp. 28-32.
  114. Wardlaw, R. L., "A Preliminary Wind Tunnel Study of the Aerodynamic Stability of Four Bridge Sections for Proposed New Burrard Inlet Crossing," National Research Council of Canada, National Aeronautical Establishment, Tech. Report LTR-LA-31 (July 14, 1969).
  115. Andrä, W. and Zellner, W., "Zugglieder aus Paralleldrahtbündeln und ihre Verankerung bei hoher Dauerschwellbelastung," *Die Bautechnik*, Vol. 46, No. 8 and 9 (1969), pp. 1-12.
  116. Rooke, W. G., "Papineau Bridge Steel Erected in Record Time," *Heavy Construction News* (September 1, 1969).
  117. Tschemmerneegg, F., "Über die Aerodynamik und Statik von Monokabelhängebrücken," *Der Bauingenieur*, Vol. 44, No. 10 (October 1969), pp. 353-362.
  118. Scalzi, J. B., Podolny, W., Jr., and Teng, W. C., "Design Fundamentals of Cable Roof Structures," United States Steel Corporation, ADUSS 55-3580-01 (October 1969).
  119. Taylor, P. R., "Cable Stayed Bridges and Their Potential in Canada," *Engineering Journal (Canada)*, Vol. 52, No. 11 (November 1969), pp. 15-21.
  120. Simpson, C. V. J., "Modern Long Span Steel Bridge Construction in Western Europe," *Proceedings of the Institution of Civil Engineers* (1970), Supplement (ii).
  121. Leonhardt, F. and Zellner, W., "Cable-Stayed Bridges: Report on Latest Developments," Canadian Structural Engineering Conference, 1970, Canadian Steel Industries Construction Council, Toronto, Ontario, Canada.
  122. Wardlaw, R. L. and Ponder, C. A., "Wind Tunnel Investigation on the Aerodynamic Stability of Bridges," Canadian Structural Engineering Conference, 1970, Canadian Steel Industries Construction Council, Toronto, Ontario, Canada.
  123. "Der Fussgängersteg Raxstrasse in Wien 10," *Stahlbau Rundschau*, 34 (February 1970), pp. 2-3.
  124. "Japanese Try Shop Fabricated Bridge Cables," *Engineering News-Record* (February 26, 1970), p. 14.
  125. Bachelart, H., "Pont de la Bourse, Footbridge over the Bassin du Commerce Le Havre (France)," *Acier-Stahl-Steel*, Vol. 35, No. 4 (April 1970), pp. 167-169.
  126. Tamhankar, M. G., "Design of Cable-Stayed Girder Bridges," *Journal of the Indian Roads Congress*, Vol. XXXIII-1 (May 1970).
  127. "The Paris-Masséna Bridge: A Cable-Stayed Structure," *Acier-Stahl-Steel*, Vol. 35, No. 6 (June 1970), pp. 278-284.
  128. Wardlaw, R. L., "Static Force Measurements of Six Deck Sections for the Proposed New Burrard Inlet Crossing," National Research Council of Canada, National Aeronautical Establishment, Tech. Report LTR-LA-53 (June 4, 1970).
  129. "Record All-Welded, Cable-Stayed Span Hangs from Pylons," *Engineering News-Record* (September 3, 1970), pp. 20-21.
  130. Freudenberg, G., "Die Stahlhochstrasse über den neuen Hauptbahnhof in Ludwigshafen/Rhein," *Der Stahlbau*, Vol. 39, No. 9 (September 1970), pp. 257-267.
  131. Wardlaw, R. L., "Some Approaches for Improving the Aerodynamic Stability of Bridge Road Decks," *Proceedings of the Third International Conference on Wind Effects on Buildings and Structures*, Tokyo (1971).
  132. O'Conner, Colin, *Design of Bridge Superstructures* (New York: Wiley-Interscience, John Wiley & Sons, Inc., 1971).
  133. "Bridge Bidder Leaves \$21 Million on the Table," *Engineering News-Record* (January 7, 1971), p. 11.
  134. Podolny, W., Jr. and Fleming, J. F., "Cable-Stayed Bridges—A State of the Art," Preprint Paper 1346, ASCE National Water Resources Engineering Meeting, Phoenix, Arizona (January 11-15, 1971).
  135. Seim, C., Larsen, S. and Dang, A., "Design of the Southern Crossing Cable Stayed Girder," Preprint Paper 1352, ASCE National Water Resources Engineering Meeting, Phoenix, Arizona (January 11-15, 1971).

136. Troitsky, M. S. and Lazar, B. E., "Model Analysis and Design of Cable-Stayed Bridges," *Proceedings of the Institution of Civil Engineers* (March 1971).
137. Seim, C., Larsen, S. and Dang, A., "Analysis of Southern Crossing Cable-Stayed Girder," Preprint Paper 1402, ASCE National Structural Engineering Meeting, Baltimore, Maryland (April 19-23, 1971).
138. Tang, Man-Chung, "Analysis of Cable-Stayed Girder Bridges," *Journal of the Structural Division*, ASCE, Vol. 97, No. ST 5 (May 1971), pp. 1481-1496.
139. Feige, A. and Idelberger, K., "Long-Span Steel Highway Bridges Today and Tomorrow," *Acier-Stahl-Steel* (English version), No. 5 (May 1971).
140. Donnelly, J. A., "Beauty of Steel Footbridges," *Acier-Stahl-Steel* (English version), No. 6 (June 1971).
141. Baron, F. and Lien, S. Y., "Analytical Studies of the Southern Crossing Cable-Stayed Girder Bridge," Report No. UC SESM 71-10, Vols. I and II, Department of Civil Engineering, University of California, Berkeley, California (June 1971).
142. Podolny, W., Jr., "Static Analysis of Cable-Stayed Bridges," Ph.D. thesis, University of Pittsburgh, 1971.
143. "River Foyle Bridge," *Civil Engineering and Public Works Review*, Vol. 66, No. 780 (July 1971), p. 753.
144. "Longest Concrete Cable-Stayed Span Cantilevered over Tough Terrain," *Engineering News-Record* (July 15, 1971), pp. 28-29.
145. "Feasibility Study of Mississippi River Crossings Interstate Route 410," Report to Louisiana Department of Highways in Cooperation with Federal Highway Administration, Modjeski and Masters, Consulting Engineers, Harrisburg, Pennsylvania (July 1971).
146. Demers, J. G. and Simonsen, O. F., "Montreal Boasts Cable-Stayed Bridge," *Civil Engineering*, ASCE (August 1971).
147. Lazar, B. E., "Analysis of Cable-Stayed Girder Bridges (Discussion)," by Man-Chung Tang, *Journal of the Structural Division*, ASCE, Vol. 97, No. ST 10 (October 1971), pp. 2631-2632.
148. Gee, A. F., "Cable-Stayed Concrete Bridges," *Developments in Bridge Design and Construction*, edited by Rockey, Bannister, and Evans (London: Crosby Lockwood & Sons, Ltd., October 1971).
149. Scalzi, J. B. and McGrath, W. K., "Mechanical Properties of Structural Cables," *Journal of the Structural Division*, ASCE, Vol. 97, No. ST 12 (December 1971), pp. 2837-2844.
150. "Der Bau der 2. Mainbrücke der Farbwerke Hoechst AG." New York: Dickerhoff and Widemann, Inc., 1972).
151. Leonhardt, F. and Zellner, W., "Vergleiche zwischen Hängerbrücken und Schrägseilbrücken für Spannweiten über 600 m [Comparative Investigations Between Suspension Bridges and Cable-Stayed Bridges for Spans Exceeding 600 m], *IABSE Publication 32-I*, 1972.
152. "Dywidag-Spannverfahren, Paralleldrahtseil," Bericht Nr. 14, Herausgegeben von der Abteilung für Entwicklung (New York: Dickerhoff and Widemann, Inc., June 1972).
153. Taylor, P. R. and Demers, J. G., "Design, Fabrication and Erection of the Papineau-Leblanc Bridge," Canadian Structural Engineering Conference, 1972, Canadian Steel Industries Construction Council, Toronto, Ontario, Canada.
154. Dubrova, E., "On Economic Effectiveness of Application of Precast Reinforced Concrete and Steel for Large Bridges (USSR)," *IABSE Bulletin*, 28 (1972).
155. Daniel, H., "Die Rheinbrücke Duisburg-Neuenhamp," *Der Stahlbau*, Vol. 41, No. 1 (January 1972), pp. 7-14.
156. "Die Erskine-Brücke-eine 1321 m langes Schrägseilbrücke in Schottland," *Der Stahlbau*, Vol. 41, No. 1 (January 1972), pp. 26-29.
157. Daniel, H., "Die Rheinbrücke Duisburg-Neuenkamp," *Der Stahlbau*, Vol. 41, No. 3 (March 1972), pp. 73-78.
158. Jonatowski, J., "Analysis of Cable-Stayed Girder Bridges (Discussion)," by Man-Chung Tang, *Journal of the Structural Division*, ASCE, Vol. 98, No. ST 3 (March 1972), pp. 770-774.
159. Lin, T. Y. and Kulka, F., "Basic Design Concepts for Long Span Structures," Preprint Paper 1727, ASCE National Structural Engineering Meeting, Cleveland, Ohio (April 24-28, 1972).
160. Kerensky, O. A., Henderson, W. and Brown, W. C., "The Erskine Bridge," *Structural Engineer*, Vol. 50, No. 4 (April 1972).
161. Buckland, P. G. and Wardlaw, R. L., "Some Aerodynamic Considerations in Bridge Design," *Engineering Journal* (Canada), Engineering Institute of Canada (April 1972).
162. Finsterwalder, U. and Finsterwalder, K., "Neue Entwicklung von Parallel-drahtseil für Schrägseil und Spannbandbrücken," Preliminary Report, Ninth IABSE Congress, Amsterdam (May 1972), pp. 877-883.
163. ERRATA, "Analysis of Cable-Stayed Girder Bridges," by Man-Chung Tang, *Journal of the Structural Division*, ASCE, Vol. 98, No. ST 5 (May 1972), p. 1191.
164. Schreier, G., "Bridge over the Rhine at Düsseldorf: Design, Calculation, Fabrication and Erection," *Acier-Stahl-Steel* (English version), No. 5 (May 1972).
165. Leonhardt, F., "Seilkonstruktionen und seil verspannte Konstruktionen," Introductory Report, Ninth IABSE Congress, Amsterdam (May 1972).
166. "Cable-Stayed Bridges with Bolted Galvanized Joints," *Civil Engineering*, ASCE (May 1972), p. 98.
167. Thul, H., "Schrägseilbrücken," Preliminary Report, Ninth IABSE Congress, Amsterdam (May 1972), pp. 249-258.
168. "First U.S. Stayed Girder Span Is a Slim, Economical Crossing," *Engineering News-Record* (June 29, 1972), pp. 14-15.
169. Thul, H., "Entwicklungen im Deutschen Schrägseilbrückenbau," *Der Stahlbau*, Vol. 41, No. 6 (June 1972), pp. 161-171.
170. Kondo, K., Komatsu, S., Inoue, H. and Matsukawa, A., "Design and Construction of Toyosato-Ohashi Bridge," *Der Stahlbau*, Vol. 41, No. 6 (June 1972), pp. 181-189.
171. "Seattle Plans Second U.S. Stayed-Girder Bridge," *Engineering News-Record* (July 27, 1972), p. 10.
172. Lazar, B. E., "Stiffness Analysis of Cable-Stayed Bridges," *Journal of the Structural Division*, ASCE, Vol. 98, No. ST 7 (July 1972), pp. 1605-1612.
173. Weisskopf, F., "World's Longest-Span Cable-Stayed Girder Bridge over the Rhine near Duisburg (Germany)," *Acier-Stahl-Steel* (English version) (July-August, 1972).
174. "Record Stayed-Girder Span Goes Up Amid Controversy," *Engineering News-Record* (August 3, 1972), p. 13.

175. "Repair Work Gives New Lift to Old Bridge," *Engineering News-Record* (August 24, 1972), p. 17.
176. Lazar, B. E., Troitsky, M. S. and Douglas, M. McC., "Load Balancing Analysis of Cable Stayed Bridges," *Journal of the Structural Division*, ASCE, Vol. 98, No. ST 8 (August 1972), pp. 1725-1740.
177. Tang, M. C., "Design of Cable-Stayed Girder Bridges," *Journal of the Structural Division*, ASCE, Vol. 98, No. ST 8 (August 1972), pp. 1789-1802.
178. Birdsall, Blair, "Mechanical Properties of Structural Cables (Discussion)," by Scalzi and McGrath, *Journal of the Structural Division*, ASCE, Vol. 98, No. ST 8 (August 1972), pp. 1883-1884.
179. Borelly, W., "Nordbrücke Mannheim-Ludwigshafen," *Der Bauingenieur*, Heft 8 u. 9 (August and September 1972).
180. Podolny, W., Jr., and Fleming, J. F., "Historical Development of Cable-Stayed Bridges," *Journal of the Structural Division*, ASCE, Vol. 98, No. ST 9 (September 1972), pp. 2079-2095.
181. "Concrete Cable-Stayed Bridge over River Main in Germany," *Civil Engineering and Public Works Review*, Vol. 67, No. 796 (November 1972).
182. Kajita, T. and Cheung, Y. K., "Finite Element Analysis of Cable-Stayed Bridges," *IABSE Publication 33-II*, 1973.
183. Baron, F. and Lien, S. Y., "Analytical Studies of a Cable-Stayed Girder Bridge," *Computers & Structures*, Vol. 3, New York, Pergamon, 1973.
184. Gray, N., "Chaco/Corrientes Bridge in Argentina," *Municipal Engineers Journal*, Paper No. 380, Vol. 59 (Fourth Quarter, 1973).
185. "Schrägelbrücke in Kanada," *Der Stahlbau*, Heft 1 (January 1973).
186. Podolny, W., Jr., "Cable-Stayed Bridges of Prestressed Concrete," *PCI Journal*, Vol. 18, No. 1 (January-February 1973).
187. Anon., "Tiel Bridge," Freyssinet International, STUPP Bulletin, March-April 1973.
188. Podolny, W., Jr., "Cable Connections in Stayed Girder Bridges," Meeting Preprint 1933, ASCE National Structural Engineering Meeting, April 9-13, 1973, San Francisco, California.
189. Gute, W. L., "Design and Construction of the Sitka Harbor Bridge," Meeting Preprint 1957, ASCE National Structural Engineering Meeting, April 9-13, 1973, San Francisco, California.
190. Kealey, R. T., "Feasibility Study of Mississippi River Crossings—Interstate 410," Meeting Preprint 2003, ASCE National Structural Engineering Meeting, San Francisco, California (April 9-13, 1973).
191. Woods, S. W., "Historical Development of Cable-Stayed Bridges (Discussion)," by Podolny and Fleming, *Journal of the Structural Division*, ASCE, Vol. 99, No. ST 4 (April 1973).
192. Volke, E., "Die Strombrücke im Zuge der Nordbrücke Mannheim-Ludwigshafen (Kurt-Schumacher Brücke)," *Der Stahlbau*, Heft 4 u. 5 (April and May 1973).
193. Rademacher, C. H., "Die Strombrücke im Zuge der Nordbrücke Mannheim-Ludwigshafen (Kurt-Schumacher Brücke), Teil II: Werkstattfertig und Montage," *Der Stahlbau*, Heft 6 (June 1973).
194. Kavanagh, T. C., Discussion to "Historical Development of Cable-Stayed Bridges," by Podolny and Fleming, *Journal of the Structural Division*, ASCE, Vol. 99, No. ST 7 (July 1973).
195. Podolny, W., Jr. and Fleming, J. F., "Cable-Stayed Bridges—Single Plane Static Analysis," *Highway Focus*, Vol. 5, No. 2 (August 1973), U.S. Dept. of Transportation, Federal Highway Administration, Washington, D.C.
196. Podolny, W., Jr., "Economic Comparisons of Stayed Girder Bridges," *Highway Focus*, Vol. 5, No. 2 (August 1973), U.S. Dept. of Transportation, Federal Highway Administration, Washington, D.C.
197. Podolny, W., Jr., "Cable-Stayed Bridges and Wind Effects," *Highway Focus*, Vol. 5, No. 2 (August 1973), U.S. Dept. of Transportation, Federal Highway Administration, Washington, D.C.
198. Podolny, W., Jr., Readers Comment, "Cable-Stayed Bridges of Prestressed Concrete," *PCI Journal*, September-October, 1973.
199. Naruoka, M. and Sakamoto, T., "Cable-Stayed Bridges in Japan," *Acier-Stahl-Steel* (English version), No. 10 (October 1973).
200. "Seattle Plans Cable-Stayed Bridge," *Engineering News-Record* (November 29, 1973), p. 13.
201. Gute, W. L., "First Vehicular Cable-Stayed Bridge in the U.S.," *Civil Engineering*, ASCE, Vol. 43, No. 11 (November 1973).
202. Burgholzer, L., Garn, E., Schimetta, O., "Die 2. Donau-Brücke Linz," *Der Stahlbau*, Heft 11 (November 1973).
203. Podolny, W., Jr., "Cable-Stayed Bridges," *Engineering Journal*, American Institute of Steel Construction (First Quarter 1974).
204. "Cable-Stayed Span Will Set U.S. Record," *Engineering News-Record* (January 3, 1974), p. 10.
205. "Cable-Stayed Bridge Will Have Record 981 ft. Span," *Engineering News-Record* (March 21, 1974), p. 39.
206. "First Stayed Swing Span Cuts Costs," *Engineering News-Record* (March 28, 1974), p. 11.
207. Rothman, H. B. and Chang, F. K., "Longest Precast-Concrete Box-Girder Bridge in Western Hemisphere," *Civil Engineering*, ASCE (March 1974).
208. "Chaco/Corrientes, Latin America's Longest Cable-Supported Bridge," *World Construction* (English version), Vol. 27, No. 3 (March 1974).
209. Burns, C. A. and Fotheringham, W. D., "Deck Panels for West Gate Bridge (Australia)," *Acier-Stahl-Steel* (English version) (June 1974).
210. Mohsen, H., "Trends in the Construction of Steel Highway Bridges," *Acier-Stahl-Steel* (English version) (June 1974).
211. Gade, R. H., "Status of the Investigation of Aerodynamic Behavior of the Sitka Harbor Cable-Stayed Bridge," presented at the Symposium on Full Scale Measurements of Wind Effects on Tall Buildings and Other Structures, London, Ontario, Canada (June 1974).
212. "Rigid Stays Slim Box Girder Bridge and Reduce Deflection," *Engineering News-Record* (June 20, 1974), p. 58.
213. "Cable-Stayed Crossing Bids Top Estimate by 40%," *Engineering News-Record* (July 4, 1974), p. 13.
214. Andrä, W. and Saul, R., "Versuche mit Bündeln aus parallelen Drähten und Litzen für die Nordbrücke Mannheim-

- Ludwigshafen und das Zeltdach München," *Die Bautechnik*, Heft 9, 10 u. 11 (September, October, and November 1974).
215. "Site Conditions Turn Bridge Tower Upside Down," *Engineering News-Record* (October 17, 1974), p. 25-26.
216. Podolny, W., Jr., "Design Considerations in Cable-Stayed Bridges," *Proceedings of the Specialty Conference on Metal Bridges*, ASCE, St. Louis, Missouri (November 12-13, 1974).
217. Podolny, W., Jr., "Cable Connections in Stayed Girder Bridges," *Engineering Journal*, American Institute of Steel Construction (Fourth Quarter, 1974).
218. Leonhardt, F., "Latest Developments of Cable-Stayed Bridges for Long Spans," *Saertryk af Bygningsstatiske Meddelelser*, Vol. 45, No. 4, Denmark, 1974. Danmarks tekniske Højskole.
219. Beyer, E. and Ramberger, G., "Die Franklinbrücke in Düsseldorf," *Der Stahlbau*, Heft 5 (May 1975).
220. Schwab, R., "Die Köhlbranddreuzung, Überbrückung einer Seeschiffsstrasse im Hamburger Hafen," *Strasse und Autobahn* (May 1975).
221. Schwab, R. and Homann, H., "Der Bau der Köhlbrandbrücke," *Die Bautechnik*, Heft 5 (May 1975).
222. Warolus, L., "Cable-Stayed Bridge over the Meuse at Heer-Agimont (Belgium)," *Acier-Stahl-Steel* (English version) (May 1975).
223. Anon., "The Danube Canal Bridge (Austria)," *Freysinet Bulletin*, (May-June 1975).
224. Boué, P. and Höhne, K. J., "Der Stromüberbau der Köhlbrandbrücke," *Der Stahlbau*, Heft 6 (June 1975).
225. Rabe, J. and Baumer, H., "Die Gründungen und Pfeiler der Köhlbrandbrücke," *Die Bautechnik*, Heft 6 (June 1975).
226. Schwab, R., "Die Köhlbrandbrücke im Hamburger Hafen—ein Beispiel für eine Montage mit mobilen Schwerlastkränen," *Strasse Brücke Tunnel*, Heft 7 (July 1975).
227. Homberg, H., "Schrägseilbrücken, Vielseilsysteme—Le Pont de Brotonne," *Der Stahlbau*, Heft 8, (August 1975).
228. Anon., "Contractor rides the tides to construct record stayed girder," *Engineering News-Record*, October 16, 1975.
229. Schaaf, T. and Spoelstra, J. S., "Cable-Stayed Bridge over the Waal near Ewijk (Netherlands)," *Acier-Stahl-Steel* (English version), (January 1976).
230. Casado, D. F., Montercia, J., and Troyano, L. F., "Cable-Stayed Foot-bridge in Barcelona (Spain) (E.C.C.S. Prize 1975)," *Acier-Stahl-Steel* (English version), (February 1976).
231. Scheuch, G., "Moving the 'Oberkasseler Brücke' at Düsseldorf," *Acier-Stahl-Steel* (English version), (February 1976).
232. Sanson, R., "Saint-Nazaire-Saint-Brévin Bridge over the Loire Estuary (France)," *Acier-Stahl-Steel* (English version), (May 1976).
233. Podolny, W. Jr., "Cable-Stayed versus Classical Suspension Bridge," *Transportation Engineering Journal*, ASCE, Vol. 102, No. TE2, (May 1976).
234. Gade, R. H., Bosch, H. R., and Podolny, W. Jr., "Recent Aerodynamic Studies of Long-Span Bridges," *Journal of the Structural Division*, ASCE, Vol. 102, No. ST7, (July 1976).
235. Hatano, Y., Okamoto, T., and Yamaguchi, K., "Suchiro Bridge, Japan's Longest Cable-stayed Bridge," *Acier-Stahl-Steel* (English version), (July-August 1976).
236. Tang, Man-Chung, "Buckling of Cable-Stayed Girder Bridges," *Journal of the Structural Division*, ASCE, Vol. 102, No. ST9, (September 1976).
237. Anon., "Cable-stayed bridge goes to a record with hybrid girder design," *Engineering News-Record*, (October 28, 1976).
238. Gimsing, Niels J., "Multispan Stayed Girder Bridges," *Journal of the Structural Division*, ASCE, Vol. 102, No. ST10, (October 1976).
239. Pauser, A. and Beschoner, K., "Betrachtungen über seilverspannte Massivbrücken, ausgehend vom Bau der Schrägseilbrücke über den Donaukanal in Wein," *Beton- und Stahlbetonbau*, Heft 11, (November 1976).
240. Weitz, F. R., "Überspannungen aus Stahlseilen—Konstruktionskomponenten für den modernen Grossbrückenbau," *Bauingenieur* 51 (1976).
241. Anon., "Twin stayed girders to carry eccentrically placed railroad," *Engineering News-Record*, (February 10, 1977).
242. Anon., "Concrete stayed girder for trains," *Engineering News-Record*, (March 3, 1977).
243. Komatsu, S. and Torii, Y., "Cable-stayed Bridge 'Rokko Ohhashi' at Kobe (Japan)," *Acier-Stahl-Steel* (English version), (March 1977).
244. Beyer, E., Volke, E., Gottstein, F., and Ramberger, G., "Neubau und Querverschub der Rheinbrücke Düsseldorf-Oberkassel," *Der Stahlbau*, Heft 3, 4, 5 u. 6, (March, April, May and June 1977).
245. Firmage, D. A., "The querverschub of the 2,000 ft Oberkassel Bridge," *Civil Engineering*, ASCE, (May 1977).
246. Podolny, W. Jr., Chmn., "Tentative Recommendations for Cable-Stayed Bridge Structures," *Journal of the Structural Division*, ASCE, Vol. 103, No. ST5, (May 1977).
247. Podolny, W. Jr., Chmn., "Commentary on the Tentative Recommendations for Cable-Stayed Bridge Structures," *Journal of the Structural Division*, ASCE, Vol. 103, No. ST5, (May 1977).
248. Grant, A., "Pasco-Kennewick Bridge—The longest cable-stayed bridge in North America," *Civil Engineering*, ASCE, (August 1977).
249. Dehard, J., "Foot-bridge at Tilff (Belgium)," *Acier-Stahl-Steel* (English version), (September 1977).
250. Yiu, C. S. C., Chmn., "Bibliography and Data on Cable-Stayed Bridges," *Journal of the Structural Division*, ASCE, Vol. 103, No. ST10, (October 1977).
251. Epple, G., Rössing, E., Schaber, E., and Wintergerst, L., "Die neue Rheinbrücke für die Bundesautobahn bei Speyer," *Der Stahlbau*, Heft 10, 11 u. 12 (October, November and December 1977).
252. Troitsky, M. S., "Cable-Stayed Bridges, Theory and Design," Crosby Lockwood Staples, London, (1977).
253. Ichter, L. L., Discussion, "Commentary on the Tentative Recommendations for Cable-Stayed Bridge Structures," *Journal of the Structural Division*, ASCE, Vol. 104, No. ST1, (January 1978).
254. Ito, M. and Maeda, Y., Discussion, "Commentary on the Tentative Recommendations for Cable-Stayed Bridge Structures," *Journal of the Structural Division*, ASCE, Vol. 104, No. ST2, (February 1978).
255. Isyumov, N. and Tschanz, T., Discussion, "Commentary on the Tentative Recommendations for Cable-Stayed Bridge

- Structures," *Journal of the Structural Division*, ASCE, Vol. 104, No. ST3, (March 1978).
256. Anon., "Pont à haubans sur le canal Albert à Godsheide (B) Cable-stayed Bridge," *Acier-Stahl-Steel* (English version), (March 1978).
257. Hajdin, N. and Jevtović, Lj., "Eisenbahnschrägseilbrücke über die Save in Belgrad," *Der Stahlbau*, Heft 4 (April 1978).
258. Bacher, A. E., Kirkland, D. E., and Klein, E. G., Jr., "The Sacramento River Bridge at Meridian—A Cable Stayed Swing Span," *Cable-Stayed Bridges*, Structural Engineering Series No. 4, (June 1978) Bridge Division, Federal Highway Administration, Washington, D.C.
259. Bridges, C. P., "Erection Control Pasco-Kennewick Intercity Bridge," *Cable-Stayed Bridges*, Structural Engineering Series No. 4, (June 1978) Bridge Division, Federal Highway Administration, Washington, D.C.
260. Castellow, T., Frank, K., and Campbell, M., "Fatigue Design Characteristics and Fatigue Testing of Prescon Stay Cable Anchorages," *Cable-Stayed Bridges*, Structural Engineering Series No. 4, (June 1978) Bridge Division, Federal Highway Administration, Washington, D.C.
261. Clark, J. H., "Relation of Erection Planning to Design," *Cable-Stayed Bridges*, Structural Engineering Series No. 4, (June 1978), Bridge Division, Federal Highway Administration, Washington, D.C.
262. Cutler, E. and Castellow, T., "Manufacture of Stay Cables for the Pasco-Kennewick Bridge," *Cable-Stayed Bridges*, Structural Engineering Series No. 4, (June 1978), Bridge Division, Federal Highway Administration, Washington, D.C.
263. Firmage, D. A., "The Final Positioning of the Oberkassel Cable-Stayed Bridge," *Cable-Stayed Bridges*, Structural Engineering Series No. 4, (June 1978), Bridge Division, Federal Highway Administration, Washington, D.C.
264. Fleming, J. F. and Egeseli, E. A., "Dynamic Response of Cable-Stayed Bridge Structures," *Cable-Stayed Bridges*, Structural Engineering Series No. 4, (June 1978), Bridge Division, Federal Highway Administration, Washington, D.C.
265. Graham, H. J., "Dame Point Bridge," *Cable-Stayed Bridges*, Structural Engineering Series, No. 4, (June 1978), Bridge Division, Federal Highway Administration, Washington, D.C.
266. Grant, A., "Intercity Bridge: A Concrete Ribbon over the Columbia River, Washington," *Cable-Stayed Bridges*, Structural Engineering Series No. 4, (June 1978), Bridge Division, Federal Highway Administration, Washington, D.C.
267. Grant, A., "Special Features of the Pasco Project," *Cable-Stayed Bridges*, Structural Engineering Series No. 4, (June 1978), Bridge Division, Federal Highway Administration, Washington, D.C.
268. Jarosz, S. E., "Luling Bridge," *Cable-Stayed Bridges*, Structural Engineering Series No. 4, (June 1978), Bridge Division, Federal Highway Administration, Washington, D.C.
269. Knudsen, C. V. and Kozy, W. R., "Proposed Cable-Stayed Bridge over Ohio River Between Weirton, West Virginia and Steubenville, Ohio," *Cable-Stayed Bridges*, Structural Engineering Series No. 4, (June 1978), Bridge Division, Federal Highway Administration, Washington, D.C.
270. Lenglet, C., "Brottonne Bridge Longest Prestressed Concrete Cable-Stayed Bridge," *Cable-Stayed Bridges*, Structural Engineering Series No. 4, (June 1978), Bridge Division, Federal Highway Administration, Washington, D.C.
271. Leonhardt, F., "Future of Cable-Stayed Bridges," *Cable-Stayed Bridges*, Structural Engineering Series No. 4, (June 1978), Bridge Division, Federal Highway Administration, Washington, D.C.
272. Lin, T. Y., Yang, Y. C., Lu, H. K., and Redfield, C. M., "Design of Ruck-A-Chucky Bridge," *Cable-Stayed Bridges*, Structural Engineering Series No. 4, (June 1978), Bridge Division, Federal Highway Administration, Washington, D.C.
273. Pavlo, E. L. and Yiu, C. S. C., "East Huntington Bridge," *Cable-Stayed Bridges*, Structural Engineering Series No. 4, (June 1978), Bridge Division, Federal Highway Administration, Washington, D.C.
274. Schambek, H., "The Construction of the Main Bridge-Hochst to the Design of the 365 m Span Rhein Bridge in Duesseldorf-Flehe," *Cable-Stayed Bridges*, Structural Engineering Series No. 4, (June 1978), Bridge Division, Federal Highway Administration, Washington, D.C.
275. Egeseli, E. A. and Alarcon, E., Discussion, "Bibliography and Data on Cable-Stayed Bridges," *Journal of the Structural Division* ASCE, Vol. 104, No. ST8, (August 1978).
276. Podolny, W., Jr., "Concrete Cable-Stayed Bridges," *Transportation Research Record* 665, Bridge Engineering, Vol. 2, *Proceedings, Transportation Research Board Conference*, September 25-27, 1978, St. Louis, Mo., National Academy of Sciences, Washington, D.C.
277. "Bibliography and Data on Cable-Stayed Bridges," Closure Discussion, *Journal of the Structural Division*, ASCE, Vol. 104, No. ST9, (September 1978).
278. Brunner, J., Schönagel, R., and Feder, D., "Die Donau-Brücke Deggenau," *Der Stahlbau*, Heft 10 u. 11 (October and November 1978).
279. Idelberger, K., "Die Schrägseilbrücke mit A-Pylon über den Rhein bei Neuwied," *Der Stahlbau*, Heft 10 (October 1978).
280. "Tentative Recommendations for Cable-Stayed Bridge Structures and Commentary on the Tentative Recommendations for Cable-Stayed Bridge Structures," Closure Discussion, *Journal of the Structural Division*, ASCE, Vol. 104, No. ST11, (November 1978).
281. Godden, W. G. and Aslam, M., "Dynamic Model Studies of Ruck-A-Chucky Bridge," *Journal of the Structural Division*, ASCE, Vol. 104, No. ST12, (December 1978).
282. Gossow, K., "Seilverspannte Pylon im Sport-, Freizeit- und Erholungsgebiet 'Salzgittersee'," *Der Stahlbau*, Heft 4 (April 1979).
283. Roil, K. and Haensel, J., "Die Entwurfsüberarbeitung der West Gate Brücke in Melbourne," *Der Stahlbau*, Heft 7 (July 1979).
284. Leonhardt, F., Zellner, W., and Saul, R., "Zwei Schrägkabelbrücken für Eisenbahn- und Strassenverkehr über den Rio Paraná (Argentinien)," *Der Stahlbau*, Heft 8 u. 9 (August and September 1979).
285. Firmage, D. A. and Goodwin, R. J., "The Economics of Various Parameters of Cable-Stayed Bridges," Preprint Paper 3721, *ASCE Convention & Exposition*, Atlanta, Georgia, October 23-25, 1979.
286. Lu, Zung-Au, "Dynamic Analysis of Cable-Hung Ruck-A-

- Chucky Bridge," *Journal of the Structural Division*, ASCE, Vol. 105, No. ST10, (October 1979).
287. Haensel, J., "Die Montage der West Gate Brücke, Melbourne," *Der Stahlbau*, Heft 1 (January 1980).
288. Komatsu, S., Kato, T. and Matsumura, H., "Design and Construction of Kawasaki-Bashi Foot-Bridge," *Der Stahlbau*, Heft 3 (March 1980).
289. Podolny, W. Jr., "Cable-Stayed Bridges—present and future," *World Construction*, Vol. 33, No. 4, (April 1980).
290. Leonhardt, F. and Zellner, W., "Cable-Stayed Bridges," *IABSE Surveys* S-13/80, *IABSE Periodica* 2/1980, (May 1980).
291. Birkenmaier, M., "Fatigue Resistant Tendons for Cable-Stayed Construction," *IABSE Proceedings* P-30/80, *IABSE Periodica* 2/1980, May 1980.
292. Rajaraman, A., Loganathan, K., and Raman, N. V., "Non-linear Analysis of Cable-Stayed Bridges," *IABSE Proceedings* P-37/80, *IABSE Periodica* 4/1980, November 1980.
293. Podolny, W. Jr., "Cable-Stayed Bridges: A Current Review," O. H. Ammann Centennial Conference, Long-Span Bridges, *Annals of the New York Academy of Sciences*, Vol. 352, 1980.
294. Fischer, M. and Hildenbrand, P., "Entwurf und Konstruktion eines Fussgängerstiges über den Neckar in Ludwigsburg," *Der Stahlbau*, Heft 3 (March 1981).
295. Podolny, W. Jr., "The Evolution of Concrete Cable-Stayed Bridges," *Concrete International*, ACI, Vol. 3, No. 8, (August 1981).
296. Sofronie, R., "The V-Shaped Cable-Stayed Bridges," *Mécanique Appliquée*, Tome 26, No. 5, (September–October 1981), Académie De La République Socialiste De Roumainie, Bucarest.
297. Anon., "Stayed-girder span sets U.S. record," *Engineering News-Record*, (April 8, 1982).
298. Sofronie, R., "Equal Stay Cable Bridge System," *Mécanique Appliquée*, Tome 27, No. 3, (May–June 1982), Académie De La République Socialiste De Roumainie, Bucarest.
299. Kovács, I., "Zur Frage der Seilschwingungen und der Seildämpfung," *Die Bautechnik*, Heft 10 (October 1982).
300. Gilsanz, R. E. and Biggs, J. M., "Cable-Stayed Bridges: Degree of Anchoring," *Journal of the Structural Division*, ASCE, Vol. 109, No. 1, January 1983.
301. Hajdin, N., "Strassenbrücke 'SLOBODA' über die Donau in Novi Sad," *Der Stahlbau*, Heft 4 (April 1983).
302. Mathivat, J., "Evolution of Concrete Cable-Stayed Bridges," *IABSE Proceedings* P-63/83, *IABSE Periodica* 2/1983, (May 1983).
303. Koger, E., "Aerodynamische Untersuchungen an der neuen Tjörnbrücke," *Der Stahlbau*, Heft 5 (May 1983).
304. Khalil, M. S., Dilger, W. H., and Ghali, A., "Time Dependent Analysis of PC Cable Stayed Bridges," *Journal of the Structural Division*, ASCE, Vol. 109, No. 8, August 1983.
305. Anon., "Japanese builders lift 358 ft bridge towers to speed construction," *Engineering News-Record*, (December 8, 1983).
306. Anon., *VSL Stay Cables for Cable-Stayed Bridges*, VSL International, Losinger Ltd., Berne, Switzerland, (January 1984).
307. Nakayama, Y., "Cable-Stayed Bridge with New Vierendeel-Type Girder," *IABSE Proceedings* P-71/84, *IABSE Periodica* 1/1984, (February 1984).
308. Saul, R., Svensson, H., Andra, H. P., and Selchow, H. J., "Die Sunshine-Skyway Brücke in Florida, USA—Entwurf einer Schrägkebelbrücke mit Verbundüberbau," *Die Bautechnik*, Heft 7 u. 9 (July and September 1984).
309. Anon., "Hybrid girder in cable-stay debut," *Engineering News-Record*, (November 15, 1984).
310. Castillo, E., Canteli, A. F., Esslinger, V., and Thürliman, B., "Statistical Model for Fatigue Analysis of Wires, Strands and Cables," *IABSE Proceedings* P-82/85, *IABSE Periodica* 1/1985, (February, 1985).
311. Zellner, W. and Saul, R., "Über Erfahrungen beim Umbau und Sanieren von Brücken," *Bautechnik*, Heft 2 (February 1985).

# APPENDIX B

## *Author Vitae*

WALTER PODOLNY, JR. has served as a structural engineer for the Federal Highway Administration for the last 14 years. In his present capacity he is actively involved in the design review and approval of cable-stayed as well as prestressed concrete segmental bridges for the Federal Highway Administration. Formerly, he was a design engineer with Marketing Technical Services of the United States Steel Corporation, in private consultant practice, and Chief Engineer for two prestressed precast concrete firms.

Dr. Podolny received his Ph.D. from the University of Pittsburgh, an M.S. from Case-Western Reserve University and earned a Bachelor of Structural Engineering and a Bachelor of Civil Engineering from Cleveland State University. He has authored or co-authored over 50 technical publications or articles including *Construction and Design of Prestressed Concrete Segmental Bridges* (Wiley, 1982). He is a fellow in the American Concrete Institute and the American Society of Civil Engineers; holds membership in the Prestressed Concrete Institute, Reinforced Concrete Research Council, International Association for Bridge and Structural Engineering; and is a member of the Federation Internationale de la Precontrainte (FIP) Commission on Practical Construction, as well as numerous other technical committees.

He is the recipient of the Outstanding Engineering Alumnus Award from Cleveland State University

(1983), the National Society of Professional Engineers Engineer of the Year Award (Federal Highway Administration) for 1983, and is co-recipient of the Secretary of Transportation award for Cost Avoidance, Reduction and Efficiency (CARE). He holds professional engineering registration in four States.

JOHN B. SCALZI is currently a Program Director in the Engineering Directorate at the National Science Foundation, Washington, D.C. He also served at the U.S. Department of Housing and Urban Development. Prior to his government affiliation, Dr. Scalzi was Director of Marketing Technical Services for U.S. Steel Corporation at Pittsburgh. He was formerly professor of structural engineering at Case-Western Reserve University at Cleveland, Ohio. He also was a lecturer at Carnegie-Mellon University, Pittsburgh, Pa., and The George Washington University, Washington, D.C.

Dr. Scalzi received his Sc.D. and S.M. degrees in Civil and Structural Engineering at the Massachusetts Institute of Technology, Cambridge, Mass. He earned his B.S. degree at Worcester Polytechnic Institute, Worcester, Mass. Dr. Scalzi has authored many papers on the analysis and design of buildings and bridges, and co-authored three other books. His professional experience includes the design of many buildings and bridges of steel, reinforced concrete, and prestressed concrete.





## *Index of Bridges*

- Airport Hotel, 52, 53  
 Albert Bridge, 67  
 Annacis, 50, 117  
 Arakawa River, 24, 34, 100
- Barranquilla, 52, 53, 55, 56  
 Barrios De Luna, 52, 53, 57, 75-77, 84  
 Barwon River, 52, 53, 135, 138  
 Batman, 21, 22, 23, 29, 101, 102, 118, 163-165, 185, 186, 188, 190, 239  
 Benton City Bridge, 10, 51, 52, 53  
 Bering Straits, *see* Inter-Continental Peace Bridge  
 Bonn, 24, 29, 34. *See also* Friedrich-Ebert Bridge  
 Bosphorus Bridge, 305  
 Bratislava, 21, 22, 23, 29, 102, 103, 104, 118, 239  
 Brighton Chain Pier, 285, 316  
 Bronx-Whitestone, 288, 289, 316  
 Brooklyn Bridge, 4, 6  
 Brotonne, 34, 52, 53, 56, 66-70, 73, 84, 239  
 Brucksal, 34
- Canal du Centre, pedestrian bridge, 52, 53, 134, 138  
 Captain William Moore Bridge, 12, 13, 21, 49  
 Carpineto, 52, 53, 55, 56  
 Chaco/Corrientes, 52, 53, 56, 59, 60, 77, 84, 174-176, 190  
 Chester, Illinois Bridge, 295  
 Cincinnati Bridge, 4, 5  
 Cochrane Bridge, 18  
 Cooper River Bridge, 19, 20, 33, 83, 84  
 Coos River Bridge, 9
- Dame Point Bridge, 16, 18, 24, 33, 34, 49, 50, 52, 53, 56, 78, 79, 84  
 Danube Canal, 52, 53, 70-72, 84  
 Deer Isle, 288  
 Dnieper River, 52, 53  
 Dryburgh-Abbey, 3, 284, 285  
 Duisburg-Neuenkamp, 24, 29, 94, 95, 96  
 Dusseldorf-Flehe, 84
- East Huntington, 15, 16, 22, 32, 34, 49, 50, 119, 122, 180-184  
 Ebro River, 21, 23, 52, 53  
 Elbe River, 7  
 Erskine, 100, 101, 118
- Freemont Bridge, 10, 11  
 Friedrich-Ebert Bridge, 93. *See also* Bonn  
 Fyksesund, 288
- Ganga, 29  
 General Manuel Belgrano Bridge, *see* Chaco/Corrientes  
 General Rafeal Urdaneta Bridge, *see* Maracaibo  
 George Street Bridge, 217, 218, 226  
 Gisclard-Arnodin type bridge, 6  
 Glacischaussee pedestrian bridge, 131, 133, 134, 135, 142  
 Golden Gate, 288, 300, 316  
 Great Belt Crossing (Denmark), 10, 11, 22, 25, 28, 54, 56, 60, 77, 78, 245, 246, 247
- Hale Boggs Memorial Bridge, *see* Luling Bridge
- Hatley chain bridge, 6  
 Hawkshaw, 29  
 Honshu-Shikoku, 316  
 Hooghly River Bridge, 117  
 Horikoshi, 52, 53, 140, 141  
 Houston Ship Channel (Baytown Bridge), 20
- Inter-Continental Peace Bridge, 13, 14, 20  
 Ishikari, 34
- James River Bridge, 18, 32, 33, 82-84, 119, 127, 128  
 John O'Connell Memorial Bridge, *see* Sitka Harbor Bridge  
 Jülicherstrasse, 34, 146-149, 189
- Kaiseraugst (Liebrüti), 52, 53, 139, 140  
 Karlsruhe, 22, 29  
 King's Meadow footbridge, 3  
 Kniebrücke, 22, 29, 34, 41, 96-98, 105, 118, 152, 165-169, 188, 190, 242, 308, 311  
 Köhlbrandbrücke, 28, 105, 106, 107, 108, 109  
 Kurt-Schumacher, *see* Nordbrücke Mannheim-Ludwigshafen  
 Kwang Fu, 52, 53
- Leverkusen, 24, 29, 34  
 Liebrüti, *see* Kaiseraugst  
 Lillebelt Bridge, 305  
 Lodemann pedestrian bridge, 132, 135  
 Long Island Sound, 12, 13  
 Long's Creek, 288, 289, 300, 301, 307, 308, 309, 310, 311

- Löscher timber bridge, 3  
 Ludwigshafen, 29, 34, 93, 94  
 Luling Bridge, 1, 2, 3, 14, 15, 20, 24, 34, 46, 113–115, 118, 221, 224, 226, 245, 313, 314, 317
- M-25 Overpass, 52, 53  
 M-30 Motorway, 141, 142  
 Magliana Viaduct, 52, 53, 55, 56  
 Mainbrücke (Main Bridge), 52, 53, 56, 60, 61, 62, 84, 197  
 Mannheim, 22, 29  
 Maracaibo, 22, 28, 29, 51, 52, 53, 54, 57, 58, 59, 77, 84, 169–174, 190, 238, 245, 246  
 Maxau, 34, 89, 90, 91, 118, 144, 145, 189, 219, 226  
 Maya, 22, 34  
 Menai Straits, 285, 286, 316  
 Menomonee Falls, 11, 12, 24, 136, 139  
 Meridian swing bridge, California, 12, 14, 49. *See also* Sacramento River Bridge  
 Montrose, 285, 286  
 Mount Street, 52, 53, 136, 138
- Nagoya Harbor Bridge, 117  
 Narrows Bridge in Halifax, 303, 310, 311  
 Nassau, 285  
 Neches River Bridge, 16, 17, 24, 33, 34, 52, 53, 74, 75  
 New Burrard Inlet, 308, 309, 312, 317  
 Newport Suspension Bridge, 293  
 Niagara-Clifton, 285, 287  
 Niagara Falls, 4  
 Niagara-Lewiston, 285, 287  
 Nienburg, 3  
 Nordbrücke Mannheim-Ludwigshafen, 103–105, 106, 118, 226  
 Norderelbe, 24, 26, 27, 29, 34, 89, 90, 118  
 North Bridge at Dusseldorf, 22, 24, 29. *See also* Theodor Heuss Bridge
- Oberkassel, 29, 105, 106, 109, 118, 144, 152–156, 189, 242  
 Old St. Clair Bridge (Pittsburgh), 4, 5
- Onomichi, 24, 29, 34, 94
- Papineau-Leblanc, 24, 29, 34, 98, 99, 118, 158, 159, 186, 187, 188, 189, 223, 226, 239  
 Paris-Masséna, 149–152, 189  
 Pasco-Kennewick Bridge, 12, 14, 24, 33, 34, 46, 47, 49, 50, 52, 53, 56, 64, 65, 66, 84, 176–180, 221, 222, 225, 226, 309, 310  
 Penang Bridge, 197  
 Polcevera Viaduct, 52, 53, 54, 239  
 Pont de la Bourse pedestrian bridge, 133, 137, 142  
 Poyet type bridge, 4  
 Pretoria, 52, 53  
 Prince's Island pedestrian bridge, 139
- Quinault River, 9, 10  
 Quincy Bridge, 15, 17, 24, 34, 50, 125–128
- Raxstrasse pedestrian bridge, 132, 136, 137  
 Rees, 24, 29, 34, 92, 93  
 Rheinbrücke-Emmerich, 305  
 Roche-Bernard, 285, 287  
 Ruck-a-Chucky Bridge, 13, 15, 20, 79–82, 83, 84
- Saale River, 3  
 Sacramento River Bridge, 108, 109, 110, 113, 118. *See also* Meridian swing bridge, California  
 Saint Florent, 29  
 Saint Nazaire Bridge, 117, 118  
 Salazar Bridge, *see* Tagus River  
 San Francisco-Oakland Bay, 248  
 Schillerstrasse pedestrian bridge, 131, 132, 133, 142, 219, 220, 226  
 Severin (Germany), 22, 29, 34, 88, 118, 159–163, 165, 189, 190, 216, 217, 219, 226  
 Severn Suspension Bridge (England), 90, 100, 293, 300, 304, 305, 306, 307, 316, 217
- Shinno, 34  
 Sitka Harbor Bridge, 12, 24, 34, 44, 45, 50, 119–121, 219, 220, 224, 225, 317
- South Myrtle Creek, 9  
 Southern Crossing (San Francisco), 10, 12, 20, 28, 35, 282, 283  
 Speyer, 270  
 Strömsund Bridge, 7, 8, 9, 24, 29, 34, 85, 86, 117, 156, 157, 189, 219, 222, 224, 226, 238, 269  
 Suehiro, 24  
 Sunshine Skyway, 15, 17, 24, 33, 34, 50, 52, 53, 72–74, 119, 122–124, 125, 128, 239
- Tacoma Narrows Bridge, 284, 285, 287, 288, 289, 302, 304, 305  
 Tagus River, 7, 8, 305  
 Talmadge Memorial Bridge, 18, 19, 33, 119  
 Tancarville, 66  
 Tempul Aqueduct, 51, 52, 53, 54, 56  
 Theodor Heuss Bridge, 86, 87, 269, 270. *See also* North Bridge at Dusseldorf  
 Thousand Island, 288  
 Tiel Bridge, 61–63, 84. *See also* Waal River  
 Toyosata-Ohashi, 24, 34, 99, 118, 145, 146, 189, 226
- Union, 284, 285
- Verazzano Narrows, 305, 306  
 Volta-Steg pedestrian bridge, 130, 131
- Waal River, 52, 53. *See also* Tiel Bridge  
 Wadi Kuf, 52, 53, 55, 59, 77  
 Weirton-Steubenville, 15, 16, 22, 33, 34, 49, 50, 119, 124, 125, 126  
 West Gate Bridge, 116, 117, 118, 187, 190, 239  
 West German Pavilion pedestrian bridge (Duisburg), 129, 130, 131  
 West Seattle Freeway, 12, 13  
 Wheeling, West Virginia, 5, 6, 285, 287  
 Whitewater River, 9, 20  
 Wye River Bridge, 90, 91, 92, 100
- Zarate-Brazo Largo, 107, 108, 110, 111, 112

## *Index of Personal Names*

- Aeberhard, H. U., 139, 140, 141  
Albert, A., 192  
Ammann, O. H., 316  
Ando, K., 254, 283  
Andrä, W., 128, 142, 226  
Arnberg, J. E., 13  
Arnodin, 6  
Aschenberg, H., 118
- Bachelart, H., 142  
Bacher, A. E., 118  
Balbachevsky, G. N., 189  
Bannister, J. L., 142  
Baron, F., 252, 282, 283  
Beyer, Edwin, 118, 152, 189, 190  
Birdsall, B., 200  
Bleich, F., 302, 316  
Borelly, Wolfgang, 105, 106, 107, 108, 109, 118  
Bosch, H. R., 317  
Brown, C. D., 226  
Brown, Samuel, 284, 285  
Brown, W. C., 118  
Buckland, P. G., 314, 316  
Burns, C. A., 190
- Castellaw, T., 226  
Chang, F. K., 84, 190  
Cheung, Y. K., 252, 282, 283  
Chilstrom, Joseph A., 139  
Cutler, E., 226
- Dang, W., 20, 35  
Davenport, A. G., 290, 303, 311, 316, 317  
Deacon, E. L., 292, 316  
Demers, J. G., 118, 189, 226
- Dischinger, F., 7, 8, 20  
Douglass, M. McC., 282, 283  
Dubrova, E., 41, 42, 44, 50
- Ellet, Charles, Jr., 5, 6, 285, 287  
Ensign, N. E., 236  
Ernst, H. J., 118, 128, 189, 234, 235, 236  
Evans, H. R., 142
- Farquharson, F. B., 310, 315  
Feige, A., 20, 35, 142, 189  
Finsterwalder, Ulrich, 56, 60, 77  
Firmage, D. A., 118, 189  
Fischer, G., 118, 190, 226  
Fleming, J. F., 20, 34, 142, 200, 252, 283  
Fotheringham, W. D., 190  
Francis, A. J., 230, 236  
Frazer, R. A., 310, 317  
Freudenberg, G., 118  
Fuchs, D., 142
- Gade, R. H., 317  
Garren, John H., 9, 10, 103, 120, 121  
Garrido, L. A., 55  
Gee, A. F., 142  
Gimsing, N. J., 234, 236, 242, 245, 247, 283  
Gischlard, 6  
Gomez, Juan B. Ripoll, 226  
Goschy, Bela, 234, 236  
Graham, H. J., 84  
Grant, Arvid, 10, 14, 16, 64, 65, 66, 84, 177, 180  
Gray, Normer, 56, 84, 190  
Gute, William L., 12, 20, 45, 50, 128
- Hadley, Homer M., 10, 20, 51, 84  
Hahn, J., 283  
Halsted, Donald, 13  
Hatley, 6  
Havermann, H. K., 118  
Heinen, Richard, 62  
Henderson, W., 118  
Hess, H., 226  
Hirai, A., 292, 316  
Homburg, H., 269, 280, 283  
Hopkins, H. J., 20
- Iffland, Jerome S. B., 13  
Inoue, H., 118, 189, 226  
Ishizaki, H., 292, 316  
Isyumov, N., 317  
Ivy, R. J., 241, 283
- Jakkula, A. A., 316  
Jarosz, Stanley E., 2, 20, 118, 226
- Kajita, T., 252, 282, 283  
Kavanagh, T. C., 20  
Kealey, T. Robert, 46, 50  
Keefer, Samuel, 285, 287  
Kerensky, O. A., 118  
Kinney, J. S., 283  
Kirkland, D. E., 118  
Klein, E. G., Jr., 118  
Kloppel, K., 316  
Köhler, W., 212, 226  
Komatsu, S., 118, 189, 226  
Kondo, K., 118, 189, 226  
Kudder, R. J., 234, 236  
Kulicki, John M., 17
- Larsen, S., 20, 35

- Lawing, Wendell B., 19  
 Lazar, B. E., 252, 282, 283  
 Le Blanc, 285  
 Lenglet, C., 84  
 Leonhardt, F., 20, 29, 35, 41, 44, 50,  
     57, 65, 84, 142, 205, 226, 235, 236,  
     240, 283, 304, 305, 308, 311, 316  
 Lien, S. Y., 252, 282, 283  
 Lin, T. Y., 14, 15, 20, 84, 283  
 Löscher, C. J., 3  
 Lossen, 285  
 Lu, H. K., 20, 84  
  
 Marquis, Paul, 159, 187, 226  
 Matsukawa, A., 118, 146, 189, 226  
 Maugh, L. C., 236  
 McCullough, C. B., 316  
 McGrath, W. K., 200  
 McNulty, G. W., 287  
 Milward, Frank, 10  
 Mitchell, S., 283  
 Mitsuda, Y., 292, 316  
 Miyata, T., 317  
 Mohsen, H., 118  
 Moisseiff, Leon, 285, 288  
 Morandi, Riccardo, 51, 54, 55, 56, 59,  
     77, 84, 245  
 Muller, J. M., 84, 190  
  
 Naruoka, M., 118  
 Navier, 4, 5  
 Nurnberger, U., 212, 226  
  
 O'Connor, C., 270, 274, 278, 283  
 Odenhausen, H., 26, 93, 96, 236  
 Okauchi, I., 254, 283  
 Okubo, T., 292, 316  
 Orlov, G., 283  
 O'Shea, Albert W., 121  
 Ostefeld, Christen, 305  
  
 Patzak, M., 212, 226  
 Payne, R. J., 118, 190  
 Phoenix, S. L., 226  
 Podolny, Walter, Jr., 20, 34, 50, 84,  
     142, 190, 200, 226, 233, 236, 252,  
     283, 317  
 Poleynard, Sidney L., 9  
 Polivka, J. J., 84  
 Polivka, Milos, 84  
 Ponder, C. A., 316  
 Poyet, 3, 4  
 Prandtl, 295  
 Protte, W., 283  
 Provis, W. A., 287, 316  
  
 Raab, N. C., 283  
 Rademacher, C. H., 118  
 Rayner, D. V., 316  
 Redfield, C. M., 20, 84  
 Redpath, 3  
 Rehm, G., 212, 226  
 Reid, William, Lt. Col., 285, 286, 316  
 Reimers, K., 142  
 Richey, V. J., 283  
 Roberts, G., 316  
 Rockey, K. C., 142  
 Roebing, John, 4, 5, 7  
 Rooke, W. G., 189  
 Rosecrans, R., 316  
 Rothman, H. B., 84, 190  
  
 Sakamoto, T., 118  
 Sanson, R., 118  
 Saul, R., 128, 226  
 Saxenhofer, H., 283  
 Scalzi, J. B., 200, 226, 236, 283  
 Scanlan, R. H., 296, 316  
 Schambeck, H., 84  
 Scheffey, C. F., 283  
 Scheuch, G., 189  
 Schöttgen, J., 118, 189, 226  
 Schreier, G., 118, 190  
 Scruton, C., 306, 310, 316, 317  
 Seely, F. B., 236  
 Seim, C. F., 12, 20, 35  
 Selchow, H. J., 128  
 Serrell, Edward, 285  
 Shaw, F. S., 230, 236  
 Sherlock, R. H., 292, 316  
 Sherwood, W. C., 75, 76, 77, 142  
  
 Shookhov, V. G., 192  
 Simonsen, O. F., 118, 189  
 Simpson, C. V. J., 35, 226, 283  
 Smith, B. Stafford, 252, 255, 283  
 Smith, F. C., 315  
 Smith, John, 285  
 Smith, William, 285  
 Sofronie, Ramiro, 25, 35  
 Steinman, D. B., 7, 287, 316  
 Svensson, H., 128  
  
 Tamms, F., 118, 190  
 Tang, M. C., 252, 282, 283  
 Taylor, P. R., 41, 50, 118, 189, 226,  
     302, 316  
 Telford, Thomas, 285, 286  
 Teng, W. C., 200, 226, 236, 283  
 Tesár, A., 118  
 Thiele, F., 316  
 Thom, H. C. S., 316  
 Thul, H., 20, 40, 50, 118, 226  
 Torroja, E., 51, 54, 56, 84  
 Troitsky, M. S., 252, 282, 283  
 Tross, W., 283  
 Tung, D. H. H., 234, 236  
  
 Verantius, 3  
 Vincent, G. S., 315, 316  
 Vogel, G., 189  
 Volke, E., 118  
  
 Walshe, D. E. J., 316  
 Wardlaw, R. L., 300, 301, 314, 316,  
     317  
 Weisskopf, Friedrich, 95, 118  
 Wenk, H., 117, 189, 226  
 Wilson, 192  
 Wintergerst, L., 118, 189, 226  
 Wolf, 285  
 Woods, Stanley W., 11, 20, 142  
  
 Yabe, A., 254, 283  
 Yang, Y. C., 20, 84  
  
 Zellner, Wilhelm, 20, 29, 35, 50, 84,  
     226, 236, 283, 304, 316

## *Index of Firms and Organizations*

- Alaska Department of Highways, 121  
AlJohnson Construction Company, 15  
Aloha Lumber Company, 9, 10  
American Association of State Highway and Transportation Officials (AASHTO), 50, 113, 241  
American Concrete Institute, 56, 84  
American Institute of Aeronautics and Astronautics, 316  
American Institute of Steel Construction, 11, 20, 34, 136  
American Iron and Steel Institute, 200, 203, 226  
American Railway Engineers Association (AREA), 241  
American Road and Transportation Builders Association (ARTBA), 50  
American Society of Civil Engineers (ASCE), 11, 20, 34, 50, 59, 60, 98, 118, 120, 128, 142, 174, 175, 176, 189, 190, 200, 283, 316, 317  
American Society for Testing and Materials (ASTM), 194, 196, 197, 198, 204  
Arvid Grant and Associates, Inc., 10, 12, 14, 15, 16, 47, 50, 66, 122, 176, 177, 180  
Associated Engineers and Contractors, Inc., 121  
Association of General Contractors (AGC), 50  
Bauverlag, GmbH., 190  
Beratungsstelle für Stahlverwendung, 26, 93, 96, 131, 132, 135  
Bethlehem Steel Corporation, 193, 194, 199, 200  
Beton-Verlag, GmbH., 96, 98, 166, 167, 168, 169, 189, 190  
British Constructional Steelwork Association, Ltd., 3, 4, 6, 7, 20, 40, 50, 91, 92, 94, 101, 118, 130, 132, 133, 134, 135, 142  
Bureau BBR, Ltd., 205  
Bureau of Public Roads, 316  
California Department of Transportation, 108  
California State Division of Bay Toll Crossings, 10  
Campenon Bernard, 66  
Canadian Steel Industries Construction Council, 20, 29, 35, 158, 186, 189, 226, 283, 304, 316  
Carswell Engineering, Ltd., 139  
Chu University (Japan), 283  
City of Seattle Department of Engineering, 13  
Cornell University, 226  
Corps of Royal Engineers, 316  
Danish Government, 10  
Demag, 8  
Department of Public Works, Tasmania, 102, 118, 164, 165, 190  
Department of Transportation, Division of Highways, State of California, 14  
Dominion Bridge, 186  
Dyckerhoff & Widmann, 56, 77, 78  
Engineering Institute of Canada, 316  
Fabwerke Hoechst, 60  
Federal Highway Administration (FHWA), 9, 10, 20, 38, 39, 50, 84, 103, 118, 120, 121, 122, 139, 189, 214, 226, 283, 293, 316, 317  
Figg and Muller Engineers, Inc., 15, 16, 17, 18, 19, 73  
Frankland and Lienhard, 2  
Freeman, Fox and Partners, 305  
Freyssinet International, 84  
Gendron Lefebvre Associates, 159, 187  
General Services Administration (GSA), 38  
Georgia DOT, 19  
Greiner Engineering Sciences, Inc., 20, 123, 128  
Gutehoffnungshütte Sterkrade AG, 95  
Hein, Lehmann AG, 156, 189  
Howard Needles Tammen and Bergendoff, 18, 78, 79, 80, 81, 84  
ICPB, Inc., 20  
Iffland Kavanagh Waterbury, P.C., 13  
Institution of Civil Engineers, 20, 35, 50, 118, 218, 226, 257, 259, 260, 261, 262, 263, 264, 265, 267, 268, 269, 283, 316  
Institution of Engineers, Australia, 118  
International Association for Bridge and Structural Engineering (IABSE), 35, 50, 84, 226, 283, 316  
Julius Berger-Bauboag Aktiengesellschaft, 54, 57, 58, 169, 170, 171, 172, 173

- Knoerle, Bender, Stone & Associates, Inc., 12  
 Kyoto University, 316
- Laboratorio Nacional de Engenharia Civil, 283  
 Leonhardt and Andra, 13, 15, 47, 66, 108, 122, 123, 152, 176  
 L'Industria Italiana del Cemento, 55  
 Louisiana Department of Highways, 1, 50  
 Lower Yarra Crossing Authority, 116
- Maddigan and Prager, 12  
 Massman Construction Company, 15  
 Melbourne Brothers Construction Company, 15  
 Michael Baker, Jr., Inc., 15, 16, 125  
 Mitchell Bridge Company, 9  
 Modjeski and Masters, 15, 16, 17, 46, 50, 125
- National Academy of Sciences, 84  
 National Aeronautical Establishment (Canada), 317  
 National Physical Laboratory (Ottawa), 308  
 National Physical Laboratory, (Teddington, England), 316
- National Research Council of Canada, 316
- Parsons Brinkerhoff Quade & Douglas, 10  
 Prescon Corporation, 65, 66  
 Purdue University, 316
- Raymond Technical Facilities, Inc., 9  
 Royal Meteorological Society, 316
- Shinko Wire Company, Ltd., 207  
 Society of American Value Engineering, 37  
 State of Alaska Department of Highways, 12, 13  
 State of California Division of Highways, 12  
 Steel Structures Painting Council, 199  
 Stronghold International, Ltd., 75, 76, 77, 84, 142, 210, 212, 213, 214  
 Stuttgart University, 213, 226  
 Sverdrup & Parcel and Associates, Inc., 10
- T. Y. Lin International, 13, 79  
 Texas A & M College of Engineering, 316
- U. S. Army Corps of Engineers, 38  
 U. S. Bureau of Reclamation, 38  
 U. S. Department of Commerce, 316  
 U. S. Department of Defense, 37  
 U. S. Department of Transportation, 38, 50, 283, 316  
 U. S. Navy Bureau of Yards and Docks, 38  
 United States Steel Corporation, 192, 193, 196, 200, 204, 226, 283  
 U. S. Weather Bureau, 289  
 University of California, Berkeley, 283  
 University of Iowa, 316  
 University of Pittsburgh, 283  
 University of Washington, 315  
 University of Western Ontario, 316
- VSL International, Losinger, Ltd., 139, 140, 141, 142, 192, 200, 206, 207, 208, 209, 210, 211, 226, 283
- Waagner-Biro Aktiengesellschaft, 136, 137  
 White Young & Partners, 25, 56, 77  
 Williams Brothers Construction Company, 15  
 Wisconsin Division of Highways, 11, 12, 136, 139

## Index of Subjects

- Aerodynamic, studies, 100, 117
- Analysis:  
  fundamental, 256  
  methods, 252  
  nonlinearity, 227  
  Strudl, 252
- Anchorage:  
  BBRV, 220  
  blocks, 21, 70  
  cable, 46, 65  
  end, 202  
  HiAm, 114, 122, 123, 205, 206  
  systems, 26
- Bar, high strength, 3
- Box girder, 1, 57, 62, 63, 70, 73, 82, 84,  
  85, 89, 91, 93, 95, 96, 100, 116,  
  122, 139, 145, 146, 149, 150, 174
- Bridge, swing span, 108
- Bridge failures, *see* Collapse
- Cable, definition, 191
- Cable arrangements:  
  configurations, 21, 29  
  double plane, 21, 25, 27, 31, 85  
  fan, 25, 26, 27, 90, 93, 125, 140  
  harp, 25, 74, 86, 88, 92, 96, 100,  
  103, 122, 123  
  longitudinal, 25  
  multiple spans, 56  
  oblique, 31  
  parallel planes, 65, 74, 77  
  radiating (converging), 25, 26, 27,  
  85, 99, 103, 105, 133, 135, 156  
  single plane, 21, 22, 23, 31, 84, 89,  
  90, 98, 100
- sloping, 6  
  star, 25, 26, 27  
  summary, 29  
  three plane, 25, 77  
  three spans, 15, 51, 100, 119  
  two planes, 92  
  two span, 21
- Catenary, 5, 6
- Collapse, 3, 5, 7, 10, 63, 116
- Computer Programs, 252
- Configurations, *see* Cable arrangements
- Construction, *see* Erection
- Corrosion, 31, 66, 94, 198
- Cost, 42, 99
- Deck:  
  composite, 15, 16, 18, 33, 34, 50,  
  119, 120, 122, 123, 124, 128, 150  
  orthotropic, 8, 15, 33, 45, 47, 49, 85,  
  87, 89, 92, 94, 96, 99, 100, 101,  
  103, 105, 107, 114, 116, 119, 122,  
  132, 139, 145, 146, 150, 158, 162  
  precast, 16  
  segmental, 77
- Deflection:  
  live load, 54, 113, 242, 246, 247, 255  
  pylon, 245  
  vertical, 7, 56, 63, 157
- Dywidag bars, 59, 61, 77, 79
- Economy, 36, 44, 184, 202, 240
- Epoxy Resin, 65, 66, 175, 199
- Erection:  
  cantilever method, 42, 49, 88, 90, 92,  
  94, 96, 99, 143, 144, 158, 159,  
  162, 165, 168, 238
- cost, 36  
  pushout method, 143, 147, 148, 151  
  segmental method, 61  
  staging method, 143
- Expansion joints, 62, 79, 82, 242
- Fabrication, 36, 184, 189
- Fatigue, 204, 205
- Flutter, *see* Oscillation
- Frequency, *see* Oscillation
- Geometry, *see* Cable arrangements
- Girder:  
  drop-in (suspended), 56, 60  
  multiple, 33  
  segmental concrete, 33
- Loads, live, 42
- Locked coil strands, *see* Strand
- Longitudinal forces, 243
- Materials, 7  
  ASTM A354, 223  
  ASTM A416, 198, 242, 250  
  ASTM A421, 197, 198, 205, 242,  
  250  
  ASTM A441, 99  
  ASTM A514, 221  
  ASTM A586, 110, 194, 198, 204,  
  241  
  ASTM A588, 114  
  ASTM A603, 194, 198, 204  
  ASTM A722, 197  
  ASTM C469, 189  
  ASTM C512, 189  
  ASTM D3035, 199



- Modulus of elasticity, 195, 196, 227
- Oscillation:  
 aeolian, 176  
 aerodynamic, 54  
 natural frequency, 64, 65  
 vibration, 121
- Pier, *see* Pylon
- Prestressing, longitudinal, 48
- Prestretching, *see* Strand
- Pylon:  
 A-frame, 11, 27, 28, 56, 57, 59, 85, 88, 89, 93, 99, 101, 102, 103, 114, 132, 133, 137, 145, 169, 170, 245  
 cantilever, 86  
 cellular, 28  
 concrete, 12, 28, 107, 119, 122  
 delta, 105  
 diamond, 123  
 H-shaped, 128  
 portal frame, 12, 27, 56, 63, 85, 94, 140  
 triangular, 248, 249  
 wide-flange, 10  
 X-frame, 56, 57, 169, 170  
 Y-frame, 125, 132
- Ratio:  
 center span to length, 40  
 drop-in span length to total span length, 10, 21, 51  
 girder depth to span, 3, 34, 54, 56, 86, 89, 92, 93, 95, 100, 105, 113, 117, 125, 128  
 material cost to fabrication cost, 184  
 moment of inertia of pylon to girder, 253  
 side span to center span, 239  
 stiffness of inside cable to outside cable, 253  
 stiffness of outside cable to girder, 253  
 tower height to span length, 28, 54, 117, 122, 125, 240
- Resin, synthetic, 99
- Reynolds number, 300
- Rope, 191, 192, 193, 194, 197
- Saddle, 71, 75, 90, 95, 96, 99, 100, 149, 151, 152, 202
- Safety factor, 63
- Similarity:  
 arrangements, 21  
 curved, 13
- Specifications, ASTM, *see* Materials
- Strand:  
 allowable design strength, 194, 198  
 bars, 197  
 curved, 146  
 galvanized, 12, 119  
 high tensile strength, 75  
 locked coil, 85, 95, 96, 102, 117, 175, 191, 197, 222, 223  
 parallel wire, 47, 104, 145, 146, 197, 198  
 prefabricated parallel wire, 99, 198  
 prestretching, 195
- Strouhal number, 301
- Superstructure:  
 bridge, 4  
 concrete, 51, 52, 53  
 orthotropic, *see* Deck  
 segmental, 59, 61, 64, 66  
 solid web, 31  
 steel, 51  
 stiffening truss, 31, 101, 164  
 suspension bridge, 1, 4, 5  
 types, 31
- Teflon, bearings, 62, 64, 147, 152
- Torsion, stiffness, 114
- Towers, *see* Pylon
- Vibrations, *see* Oscillation
- Weight:  
 cable, 240  
 structural steel, 40, 100, 159, 162, 164  
 structure, 92
- Welding, 185
- Wind:  
 forces, 26  
 loads, 113
- Wire, 3, 99, 117, 191
- Working stress design, 242
- Zinc:  
 coatings, 199  
 methods, 204, 205

COLEGIO INGENIEROS DE CAMINOS  
BIBLIOTECA